The Development and Applications of a System Designed to Quantify Coronary Arterial Stenosis

by

Mark Jackson

A Doctoral Thesis

Submitted in partial fulfilment of the requirements for the award of Doctor of Philosophy of the Loughborough University of Technology

May 1988

Abstract

The Development and Applications of a System Designed to Quantify Coronary Arterial Stenosis.

Mark Jackson, May 1988.

The objective analysis of coronary artery stenosis is required for the assessment of interventions in the management of Coronary Artery Disease (CAD). This thesis presents a microcomputer based system designed to meet this requirement which is easy to use and relatively cheap.

The hardware consists of a standard 35mm cine projector (International General Electric Company), a rear projection graphics tablet (GTCO Corporation) and microcomputer (Vector Graphic Limited) with printer (Epson Limited). The graphics tablet and projector are mounted into a steel framework which allows an arteriographic image to be cast from the rear of the projector and focused, parallax free, onto the centre of the tablet. The tablet in turn communicates with the computer via a RS232 link.

Arterial contours are outlined directly onto the tablet surface using a fine nibbed water soluble pen. These contours are then digitized at 25 coordinates per second by retracing with the graphic tablet cursor. All coordinates are held in computer memory until digitization is complete, converted to ASCII and stored on disk.

A suite of programs manipulate these raw data producing absolute and relative measures which characterize stenotic morphology, including maximal and minimal artery diameter, percent diameter stenosis and various measurements of artery eccentricity.

The Quantitative Angiographic Mensuration System (QAMS) has been found to be repeatable and objective over a series of repeated trials, with standard errors of measurement for maximal artery diameter being 0.015mm and 0.14mm respectively. On validation, dimensional results were not significantly different from test objects.

Longitudinal data have been collected from 62 patients undergoing Percutaneous Transluminal Coronary Angioplasty (PTCA) using QAMS. Significant differences at the 0.01% level are evident in parameters reflecting stenotic severity post PTCA, correlating strongly with improved patient exercise tolerance. Failure of the PTCA technique in the right coronary artery was significantly related to small pre PTCA dimensions and high eccentricity at the minimum diameter. Visual overestimation of stenotic severity was common in high grade lesions compared to objective quantification.

Myocardial function, quantified using a modified exercise multiple gated radionuclide angiocardiography (MUGA RNA) technique, was related to stenotic severity measured using QAMS in 28 patients receiving arteriography or PTCA.

Significant relationships were few and of low probability, however, global diastolic function exhibited increasing compromise with increasing stenotic severity when represented by a weighted factor of percent diameter stenosis.

Exercise MUGA RNA was repeated in 5 patients following successful PTCA of the LAD artery where significant differences in stenotic morphology were reciprocated by significant improvement in global diastolic function.

In conclusion, QAMS has proved to be of clinical use and therefore warrants further development.

Keywords: Anatomy, Physiology, Coronary, Artery, Disease, Quantification, Computer, Angioplasty, Radionuclide, Angiography, Clinical.

Dedication

This thesis is dedicated to my late Grandmother, Mrs Dorothy Louise Macklin, affectionately known as "Span", who sadly did not live to witness its completion.

This is for you Span!

Acknowledgements

Grateful thanks are extended to my Director of Research and Departmental Supervisor, Dr P.R.M. Jones (Reader in Human Functional Anatomy, Department of Human Sciences, Loughborough University), who gave his time willingly and unselfishly throughout the course of my research. His enthusiasm and dedication is something I should wish to emulate throughout the rest of my career.

Many thanks also go to my two external Supervisors, Dr. P.J.B. Hubner (Consultant Cardiologist, The Groby Road Hospital, Leicester) and Mr M.Y. Early (Principal Physicist, Department of Medical Physics, Leicester Royal Infirmary) who between them provided me with the opportunity, funds, material and background knowledge necessary for carrying out this work.

I am greatly indebted to Mr N.C.S. Smith (Computing Technician, Department of Human Sciences, Loughborough University) whose knowledge of mathematics and the Fortran programming language was a constant source of help throughout the development of the Quantitative Angiographic Mesuration System (Q.A.M.S.). Similar thanks are due to Mr D.V. Palmer, (Information Technology Technician, Department of Human Sciences, Loughborough University of Technology) who provided the interfacing routines necessary for communication between the graphics tablet and computer. General thanks are also extended to staff and students of the Department whose background support provided me with motivation throughout the course of my studies.

A great debt is also due to Mr T.J. Heard (Senior Technician, The Radioisotope Imaging Unit, The Groby Road Hospital, Leicester) who provided all programming skills necessary to transform all my ideas regarding the measurement of left ventricular function into reality. Special thanks also go to the staff of the above; Mrs H. Williams, Mrs A. Shepard and Dr M.N. Khalil, their

assistance was invaluable. Thanks also to all the patients who allowed themselves to be submitted to my investigations.

I am also grateful to Messrs. Gibson and Swain (International General Electric Company, Daventry, Northamptonshire) who provided me with free use of the CAP-35B cine projector throughout the development and applications of Q.A.M.S. Thanks are also due to the Leicester Area Health Authority who funded the cost of my travel between Loughborough University and the Groby Road Hospital throughout my research.

Last, but by no means least, an enormous debt of gratitude, thanks and love are extended to my wife, Mrs Dawn Angela Jackson, who not only typed this thesis, but has suffered my moans, groans, lack of money and lack of time (I'll do the D.I.Y. from now on, promise!) for the last four and a half years - is this just the beginning?

CONTENTS

SECTION 1

DEVELOPMENT

CHAPTER ONE

GENERAL INTRODUCTION

1.1 The Need for Quantification

Medicine is an inherently subjective and qualitative science. Most often, a physician works on symptom history and visual inspection of his patient, making decisions on the investigative parameter based on accumulated experience and some ill defined and usually personal "feel" for what constitutes normality and abnormality. For the majority of the time, this approach is adequate, with the patient receiving the correct treatment for his complication despite the imprecise origin of the decision. There are however, many areas in medicine where quantification would not only be a useful additional tool, but also a tremendous aid in the routine decision making regarding everyday care, culminating in maximal benefit to the patient. One such area is Cardiology and, more precisely, Coronary Artery Disease (CAD).

Coronary arteriography, first introduced by Sones in 1959 is still regarded as the gold standard for the assessment of CAD, and forms the basis of much of the decision making in its medical and surgical management. The arterial images are produced after the advancement of one of a number of specially designed catheters from the arterial entry point (femoral and brachial) into the right or left coronary ostia. Iodine containing radiopaque contrast media is injected directly into the cannulated artery via the catheter. The cine angiogram is produced as a sequence of images formed when the moving X-ray shadow of a transiently opacified arterial lumen is cast upon the input phosphor screen of the image intensifier. This electronic tube converts the

energy of incident X-radiation into light, and produces an amplified, focused optical image of the coronary luminal shadow which is then recorded on 35mm cine film.

Quantification of such images could prove useful in the evaluation of the efficacy of modern therapeutic procedures, in the effects of short term intervention on the size of coronary arterial segments, on the selection of patients for coronary artery bypass grafting and on the effects of long term intervention studies on the regression and progression of the disease state.

Currently, visual inspection forms the basis of the clinical interpretation of these angiograms. Whilst the eye is an exceptional system for resolving very small differences, it has limited quantification capabilities. Clearly there exists a need for an objective and reproducible technique for the assessment of coronary atherosclerosis. Over the past 15 years, this need has been met to some extent by various systems with varying degrees of success. Generally speaking however, existing systems tend to be either simple extensions of subjective assessment (eg. vernier calipers) or involve large amounts of computer hardware and software (eg. edge detection) and as such have not enjoyed worldwide use. This thesis presents a system capable of providing objective quantification whilst being self contained, easy to use and simple to understand.

1.2 **The Problem**

CAD is the most frequent cause of death and premature adult death in Britain today (Wharton et al 1986).

Specifically, CAD annually produces considerable absence of the British workforce; 23,900,000 lost man days in the period 1978/79, a figure which had risen steadily since 1969 when absence due to other conditions tended

to show a fall. This level puts considerable demands on our hospitals at a time of great economic stringency in health care. In the year 1980, 154,358 deaths in England and Wales were attributable to CAD alone, some 30% of all male deaths. Mortality in Britain due to CAD has seen a steady increase since 1950 which plateaued in the early 70's and recently appears to be undergoing a slight decline (Wharton 1980). However, these changes, less than 1% on average, still fall well behind the changing pattern of the USA. During the period 1969 to 1977, they recorded a 22.6% decline in the incidence of mortality rate due to CAD in men aged 35 - 64 years (Wharton, 1986). Various theories have been put forward to explain why there has been a fall in some countries, including a growing public awareness to the harm of smoking (Cook et al 1986), the harm of poor diet that is high in saturated fats and dairy produce (Keys et al 1970, Shaper 1987), and to the benefits of adequate exercise (Kannel et al 1986, Paffenberger et al 1986). These changes are in part due to government funded national health education programs and in part due to what is and is not currently socially acceptable.

Cigarette smoking has been shown to double the mortality from CAD. Vigorous physical activity that induces breathlessness is beneficial and the diet should be adjusted so that dietary energy provided by fat is at the level of 25 - 30% of the total with increased consumption of foods rich in fibre. Other environmental factors include raised blood pressure, obesity and stress. All these factors may be amenable to assault and control, but after taking these so called "risk factors" into account and examining the mortality figures for different countries, it is difficult to explain their marked statistical variation. Clearly there are genetic factors which are as yet beyond our control, evident from the significant association of incidence of CAD and parental CAD history, even in the absence of all other risk factors (Rosenman et al 1975).

Type A behavior pattern alone has been proved to be strongly related to CAD incidence (Rosenman et al 1975). This association could not be explained by the relation of behavior pattern with any other single or multiple predictive risk factors.

It is CAD that provides one of the greatest current challenges in modern day epidemiological studies.

1.3 The Aetiology of Chronic CAD

This section deals with the evolution of atherosclerosis and briefly discusses the two popular theories of the time. It is not the intention of this text to comprehensively review this area of the literature, but merely introduce it as a platform for future reference.

Atherosclerosis is the most important of the degenerative diseases of all arteries and consists of focal accumulation in the intimal lining of a variable combination of lipids, complex carbohydrates, blood and blood products, fibrous tissue and calcium deposits. In common with other diseases, atherosclerosis establishes itself over a period of time and consequently, there are notable stages of progression.

Early atherosclerosis is manifest as short, thin, slightly raised yellow lines which run longitudinally along the internal surface of the artery. These are known as fatty streaks and consist of intracellular accumulation of lipids within the smooth muscle cells of the intima. At this stage the disease appears to be reversible, in that some fatty streaks may progress to plaques whilst others may recede and disappear.

Plaques represent established atherosclerosis and are characterised as raised focal, circumscribed lesions up to one centimetre in diameter, consisting of various amounts of fibrous tissue and lipid. Depending on which

of these constituents is predominant leads to further classification. Where extracellular lipid is most evident, the plaques are termed soft or atheromatous, whilst when fibrous tissue is most abundant, the plaques are known as hard of fibrous. The former are common in early established atherosclerosis which with time slowly reverts to the latter. Both types of plaque however have the same effect, namely increased thickness of the intima with encroachment into the lumen of the vessel. With the passage of time individual plaques will grow in size and tend to coalesce.

These well established lesions may be further complicated according to the following mechanism. First, loss of endothelium may occur resulting in surface ulceration and consequent exposure of the lesions fatty contents to the bloodstream. Secondly, as a result of the roughened ulcerated surface, fibrin is commonly deposited with accompanying thrombosis which in time becomes incorporated into the plaque. Free blood may also enter a lesion at this stage. The plaque may then eventually become covered by endothelium. Finally, calcification may occur.

The pathogenesis of atherosclerosis is still a contestable issue, with the following two theories being most popular of late. However, they are not mutually exclusive.

THE FILTRATION THEORY. This theory postulates that lipids necessary for establishing atheromatous plaques reach the intima by filtering through defects in the endothelium, aided by transportation on low density lipoproteins (LDL). Once inside, the reverse passage of the LDL is somehow retarded. This may be due to the mucopolysaccharides of the ground substance, some of which have been shown to be able to precipitate LDL in vitro.

THE THROMBOGENIC THEORY. This theory maintains that minute lesions may occur in the intimal surface as a result of some mechanical trauma. These defects then act as focal points for platelet aggregation, resulting in thrombosis formation and its adherence to the vessel wall. The fibrin in the thrombus then becomes organized, fibrous tissue is formed, eventually becoming covered with endothelium. The lipid within the thrombus then becomes the lipid of the atherosclerotic lesion.

Whichever theory is correct the consequences to the patient are the same; a progressively narrowing arterial lumen which causes pain and imposes physiological constraints with concomitant reduction in the quality of life.

1.4 **The Treatment**

Once the patient has presented with the physiological consequences of CAD, be it chest pain due to the ischaemic myocardium (angina), myocardial infarct, heart failure or arrhythmia, the role of the physician is to treat the symptoms. The aim of treatment is twofold:

1) To prolong life.
2) To improve the quality of life by freeing the patients from the restriction of their condition.

Currently, three avenues are open to the physician, the one of choice being the option that best suits the patients condition in the light of all available information. What follows is a short review of each treatment group discussing only the mechanism of action. It is not the intention of this text to give comprehensive pharmacological and/or surgical insight.

1.4.1 Medical Management

This is the option of choice in the patient with relatively mild symptoms or in the more elderly patient where the mortality risk of an operation contradicts this action. Drug regimes are usually made up of compounds from one or more of the following three groups:

1) Nitrates.
2) Beta - adrenergic blocking agents (β blockers).
3) Calcium antagonists.

1) NITRATES: The principal pharmacologic effect of nitrates is direct relaxation of smooth muscle, including that of the vascular walls. Accordingly, administration of nitrates has been shown experimentally to produce dilation of the arteries (Brown et al 1981), veins and capillaries (Doorey et al 1985) leading to improved muscle perfusion and enhanced exercise tolerance.

2) BETA BLOCKERS: Beta adrenergic blockers are pharmacologically similar to the normal neural transmitters and work by blunting the increased sympathetic drive concomitant with stress and/or exercise, the primary effect being decreased heart rate and cardiac output (Strait et al 1965). These effects reduce cardiac workload and myocardial oxygen consumption resulting in anginal relief. However, due to the distribution of the two (β_1 and β_2) adrenergic receptors around the body, the so called non selective blockers are prone to contradictory side effects, one of which is vasoconstriction which will lead to increased central circulating volume with corresponding increased cardiac workload, the exact opposite of the intention. Recently, these problems have been overcome with the advent of "cardioselective"

adrenergic blockers which act only on the β_1 receptors conveniently situated almost exclusively in the nervous system of the heart.

3) CALCIUM ANTAGONISTS: This group of drugs are specific arterial vasodilators and achieve their effects by the inhibition of the movement of calcium across cell membranes, thus causing relaxation of the arterial smooth muscle (Wharton et al 1986).

Hence, following calcium antagonist administration, there is improved coronary blood flow as a direct result of increased coronary artery dimensions, and decreased afterload as a result of decreased peripheral arterial tone. Due to their coronary specificity they are the regime of choice when coronary artery spasm is suspected as being causative of exercise related pain with normal coronary arteries.

1.4.2 Coronary Artery Bypass Grafting (CABG)

As the name suggests this technique employs various vessels harvested from elsewhere in the body to bypass diseased segments of coronary arteries, thereby improving distal myocardial blood flow and perfusion.

Typically, vessels from either the thorax or lower limb tend to be used as those employed from the upper limb have questionable patency (Raess et al 1986). Hence common conduits of choice are the internal mammary artery and the greater saphenous vein, although the lesser saphenous vein is becoming popular when the extent of myocardial revascularisation is extensive and/or recurrent (Raess et al 1986). The technique requires extensive surgery both at the "donor site" and the thorax, but incurs a mortality rate of only 1% in uncomplicated cases with consequent 80 - 90% cure of

angina (Wharton et al 1986). In some lesions, typically those of the left main stem, patients do better in terms of survival than those who are medically managed when matched for stenotic severity.

Recently, myocardial function pre and post operatively has been examined by Shearn et al 1986. Utilizing a radionuclide ventriculogram technique, he demonstrated significant improvements in resting global ejection fraction from 32% to 37% with 55% of previously akinetic segments regaining some function. This was concomitant with an improvement of two functional classes of angina and one functional class of heart failure in patients occupying the higher functional classes preoperatively.

1.4.3 Percutaneous Transluminal Coronary Angioplasty (PTCA)

Classified as non surgical intervention, the procedure uses a guide wire system to advance and position at the coronary stenosis a small calibre balloon tipped catheter. The balloon is then simply inflated to various pressures and for various durations until the operator judges that he has effected enough deformation of the atheromatous plaque to restore adequate distal myocardial blood flow and therefore perfusion.

Exercise electrocardiography and thallium scintigraphy were utilized by Scholl et al 1982 in a serial follow up study of patients pre and post PTCA. One month following PTCA, 61% were a asymptomatic, with the frequency of abnormal ECGs dropping from 56% to 19% and positive thallium scans from 58% to 17%. Of the initial asymptomatic group, follow up coronary arteriography was carried out at 6 months on 20 patients: 18 had the initial PTCA result preserved with normal stress tests and 2 with partial restenosis had abnormal stress tests.

However, the technique may not be applied to all factions of CAD. Typically only 10% of all those suitable for CABG are suitable for PTCA, the decision resting on fulfillment of the following criteria:

1) Good left ventricular function.
2) Short history of angina (therefore stenosis predominantly atheromatic - section 1.3).
3) One short proximal discrete concentric subtotal lesion.
4) No ostial or side branch involvement.

Consequently, single vessel disease has received the majority of benefit from PTCA, although, as is the case with the Groby Road Hospital, Leicester, continued practice and the constant improvements in PTCA equipment design has led to increased usage in double and triple vessel disease (particularly in the USA, and not without increased risk - Ellis et al 1988) and the more complex one vessel case (eg. left main stem stenosis - Stertzer et al 1985 and even bypass grafts - Ford et al 1981). However, rate of restenosis, currently between 25% and 30% (Black and King 1987) continues to be an important limitation in the usefulness of PTCA.

Golding et al 1986 highlighted the case for rigorous selection when he studied the need for emergency CABG in patients following unsuccessful PTCA. From a group of 81 primary failures, 52 had 75 major complications following CABG, by far the most common being myocardial infarct (46% incidence). Clearly, emergency surgery following failed PTCA carries a high incidence of major postoperative complications, the like of which can be minimized if stringent conditions dictate selection. However, one must bear in mind the relative costs of the CABG and PTCA procedures. Kelly et al 1985 carried out a study in which even after allowing for the additional cost of CABG following unsuccessful PTCA and

representation with restenosis etc, the total cost of care per patient was still 43% lower on average in those patients receiving PTCA as an initial procedure for single vessel coronary artery disease. The lower morbidity risks, reduced cost, prompt recovery (median time to return to work 14 days in patients for whom PTCA is successful - Holmes et al 1983) and rapid return to full activity favour PTCA as an alternative therapy to bypass surgery in those candidates for whom it is suitable.

The ability to quantify the nature, extent and severity of CAD would be of use in all of the three described treatment regimes.

CHAPTER TWO

LITERATURE REVIEW

2.1 **Aims**

In order to understand the decisions made regarding the choice of type of quantification system presented in this thesis, the aims for its performance are presented below. Section 2.3 will state the approach of choice in the light of these aims and the current literature.

AIM 1 - To involve no extra work in the catheterisation procedure or film processing.

AIM 2 - To be accurate, repeatable and valid.

AIM 3 - To be microcomputer based. The speed of larger (mainframe) machines suffer proportionately with the number of users. However, a microcomputer, when presented with the same information will always run at the same speed. Also, a microcomputer based system has the added benefit of being portable.

AIM 4 - To be easy to use, utilizing a familiar and conceptually easy to understand mode of data entry.

AIM 5 - To be easy to develop further. This involves the use of generically applicable hardware and software written in a portable high level language. These criteria will allow the transfer of the system to another host microcomputer enabling the system to "keep up" with technology and have scope for manipulation of the basic data for the derivation of new parameters.

AIM 6 - To produce quantitative information on parameters routinely used by Cardiologists at the Groby

Road Hospital. These include percent diameter stenosis, absolute diameters and lengths.

AIM 7 - To produce other less well known parameters which characterize stenotic morphology. eg. Eccentricity and atheromal quantification.

AIM 8 - To be as automated as possible. Once a relevant frame has been selected, the system should rely on operator input as little as possible, thereby minimizing subjective bias.

AIM 9 - To be flexible in its use. This aim is focused primarily at the option of submitting data to be analysed individually eg. when a result is urgently required or as a batch, when a large number of cases are being studied.

AIM 10 - Last, but by no means least, the system should be relatively cheap, both in terms of initial outlay for hardware and in routine maintenance (service contracts, technician time, consumables, etc).

2.2 **Literature Review**

All mensuration systems rely on good quality images, for derived data can only be as accurate as the original and is usually less so. Therefore, for the purposes of discussion, it is assumed that images selected for quantification under the systems outlined in this text are worthy of further study. A generic review of the potential factors which may negate against quantification of an image are discussed in section 3.1, however, specific factors which disadvantage one approach in comparison with others are discussed here.

2.2.1 Subjective Quantification

This is by far the most common form of assessment of the clinical angiogram. The procedure usually involves the

projection of the film at two to three times normal size with visual comparison of the "normal" and usually proximal diameter to the more distal stenotic diameter in any particular artery. The results are then usually expressed as a percentage narrowing calculated thus:

$$\% \text{ Stenosis} = 100 \times \left(\frac{\text{Normal diameter - Stenotic diameter}}{\text{Normal diameter}} \right)$$

Stenoses visible in other views may be treated in the same way, with the final result being the expression of the most severe stenosis in any one view (usual case) or an average of all collated values.

This technique has high intra and interobserver variability. De Rowen et al 1977 recorded an average variability of +/- 25% when he asked 11 experienced cardiac angiographers to estimate the severity (in terms of percent stenosis) of the worst lesion in 10 different standard arterial segments in each of 10 angiograms. Koh et al 1979 removed the errors in locating the lesions by specifying the stenosis to be graded. Average variability was reduced to +/- 12% when compared to a computer assisted method (Brown Dodge method - section 2.2.3) with substantial overestimation occurring in the 60% to 90% range. However, one must be very careful when evaluating the worth of the subjectively assessed percent stenosis estimate from the literature as inconsistent and misleading methodology is common. One example of this occurred in a paper by Shub et al 1981 who reported remarkably small inter and intraobserver differences (mean differences of less than 5%) for stenoses of less than 20% or greater than 80%; findings in direct conflict with the overestimation evident in the previous report. For stenoses between 20 and 80%, the differences were slightly greater at 8 to 14%; still most acceptable when compared to the **average** for the whole range described in the previous reference. These anomalies are soon explained on scrutiny of the experimental design when one discovers that they based their assessment of intra and

interobserver variability on differences recorded by the same subjects re-reading 25 randomly selected angiograms three months later. It is obvious that subjective bias present at the initial reading will still be in evidence on the second occasion. Therefore, to present an adequately designed study, it is important to use some means of quantification which may be held as a "gold standard" and allow comparisons to be made. However, researchers employing this strategy do not always utilize the full power of their new technology.

Trask et al 1984 exemplified this when he compared computerized planimetric measurements of luminal cross-sectional area from histological sections to visual interpretation, concluding that 'eyeballing' can be used to evaluate coronary anatomy with a high degree of accuracy and minimal interobserver variability. In order to arrive at this statement, he had firstly visually graded the stenoses by percent diameter reduction into the following discontinuous intervals, normal, 25%, 50%, 75%, 95% or occluded. Secondly, he visually graded the same stenoses as pathological sections by percent cross-sectional area involvement (figure 2.1) thereby mixing his parameters. A random sample of these were checked using a computerized planimeter and found to be in good agreement (estimate deviation mean 4.6% +/- 5.8%). Finally, he reduced this semi-quantitative data down to whether the lesion was considered significant or not based on 75% or greater diameter reduction or 90% or greater reduction in cross-sectional area. Agreement between the two observers was considered to exist when both classified a lesion as either significant or not significant. Exact agreement on the already crudely subdivided estimated of percent stenosis (by either method) was not required. It is therefore not surprising that mean accuracy of correct identification was 93% for both angiographers. Moreover, he fails to comment on the potential hazards of comparing living anatomy with processed pathology (section 2.2.3).

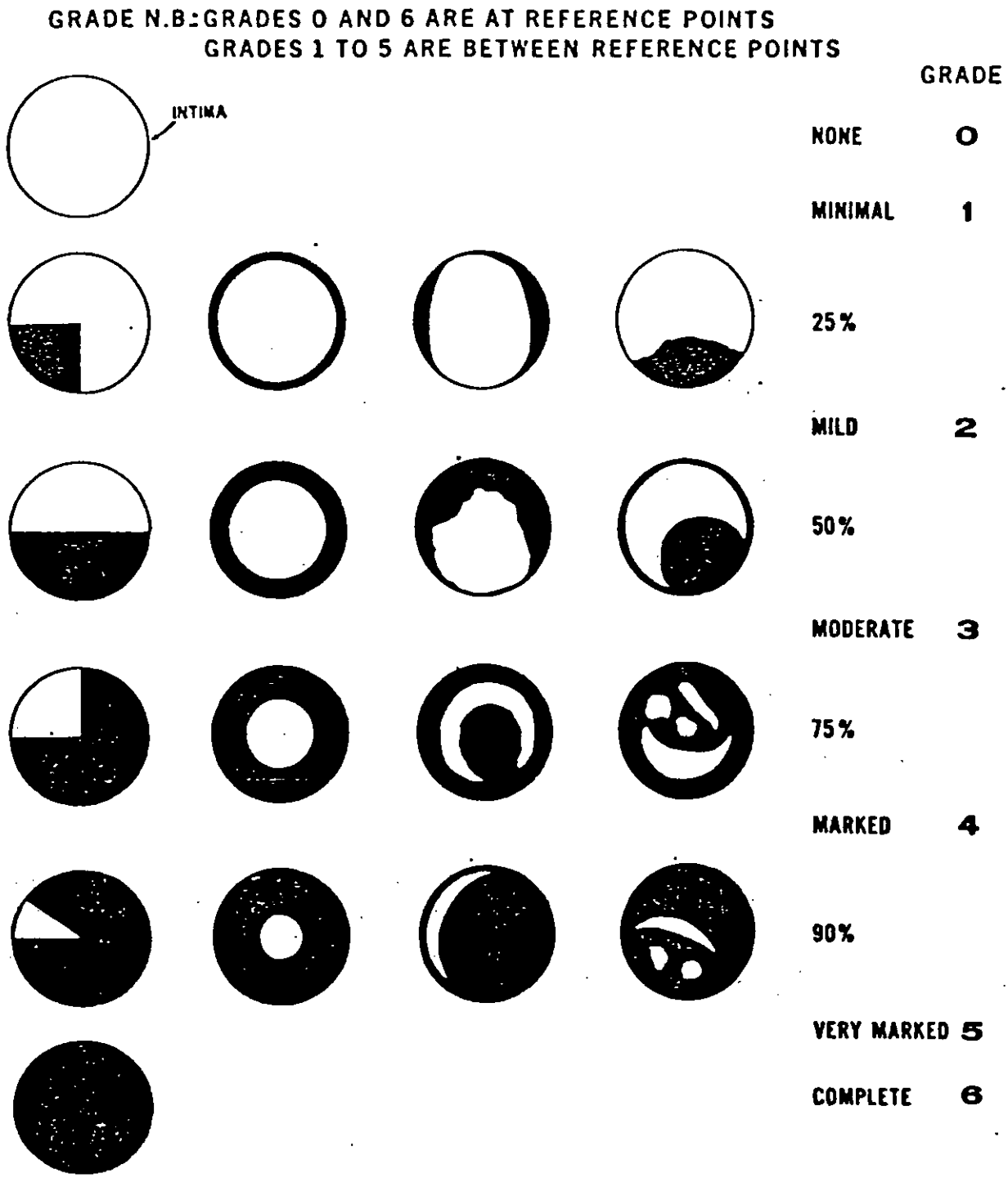

Figure 2.1 Chart of coronary artery lumens of different shapes and different degress of narrowing

Trask N, Califf RM, Conley MJ, Kong Y, Peter R, Lee KL, Hackel DB and Wagner GS, 1984, J. Am. Coll. Cardiol., 3, 5, 1145-1154.

In their study Trask et al 1984 have made objective measures of an important stenotic parameter but were successful in using them for no more than a checking procedure.

The most widely used application of subjective quantification of coronary stenoses is documented in a paper by Brandt et al 1977. Here he presents the "Green Lane system", a myocardial scoring system which not only takes into account the degree of visualized stenosis in any number of arterial branches, but also their importance in terms of the amount of myocardium supplied. The most severe stenosis in any artery is graded as below:

Grade	% cross-sectional area loss (extrapolated from percent diameter reduction)
A	100
B	90 - 99
C	75 - 89
D	50 - 74
E	$\leqslant$ 50

The facility for increased haemodynamic significance is provided in increasing the grade by one unit (except to grade A) if two similar stenoses are present in series, or if the stenosis in question is more than one centimetre long. Using the grade of the stenosis and the myocardial value (the total number of previously designated arbitrary units of myocardium supplied by the artery distal to the stenosis), each artery is given a myocardial score. The score serves as a reflection of the physiological significance of the disease in that artery, thereby allowing logical numerical expression of it severity.

Without exception, all the subjective methods of quantification of coronary artery disease rely on the parameter percent diameter stenosis (or its natural extension percent CSA stenosis). However, is this an

appropriate measure of atherosclerotic severity? Apparently not. If one examines the classical equations of pressure loss in a fluid dynamic situation (figure 2.2), one will appreciate that it is absolute minimum stenosis diameter (d_{min}) that is the greatest single determinant of the haemodynamic impact of any coronary narrowing (fluid mechanics and coronary stenoses are considered in greater detail in section 6.1). The inverse powered function of d_{min} which appears in both terms of the formulae is mathematically very powerful. Thus, one weakness of the percent diameter (or CSA) stenosis parameter is that it is a relative estimate of luminal narrowing, whilst haemodynamic impact depends upon the absolute value of the minimum lumen diameter. Also, the "normal" portion of the vessel lumen, whose diameter forms the denominator of the percent stenosis estimate is very seldom normal. It may be dilated by the aging process or, as a result of turbulence caused by the stenosis, may even be substantially narrowed by diffuse atherosclerotic thickening of the intima.

Yet, the simplicity of the percent stenosis estimate and the force of tradition (especially clinical) will undoubtedly compel its continued use, but clearly some method of obtaining absolute measurements of coronary stenoses would be the natural progression, particularly so for use in the more "scientific" studies.

2.2.2 Simple Visually Assisted Quantification

Estimates of absolute coronary dimensions require the presence of some form of calibration object in the same frontal plane as the lesion to be measured. A typical and convenient choice is that of the catheter despite the fact that due to initial positioning and motion throughout the cardiac cycle it seldom meets the above criteria (section 2.2.3). Gensini et al 1971 employed projected dimensions taken from the catheter tip to scale to absolute size measurements taken from across the arteriographic lumen. This was achieved using a special projector fitted with

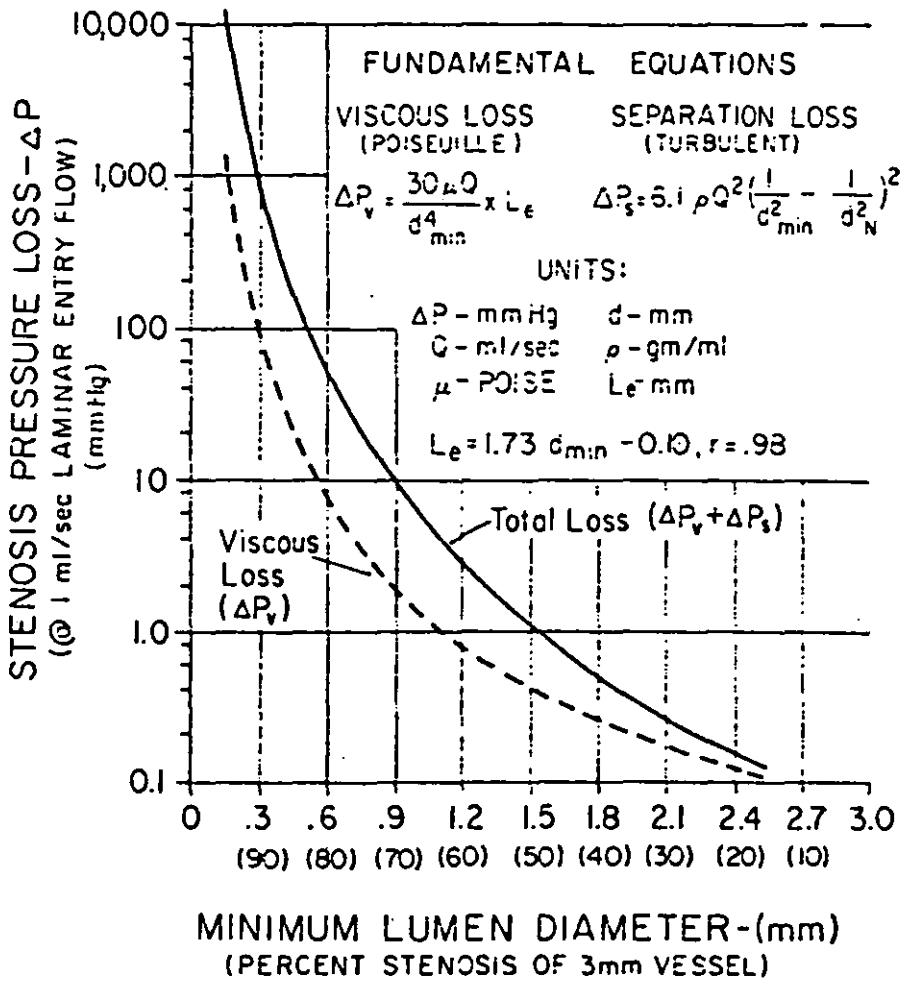

Figure 2.2 The fundamental equations of fluid mechanics

Brown BG, Bolson EL and Dodge HT, 1982, Arteriosclerosis, 2, 2-15

movable cursors which were subjectively positioned at the minimum diameter and at the normal. Projected dimension was electronically calculated and corrected for magnification using the ratio of projected catheter width to known catheter width. Variability in the estimates of known dimensions using this approach was as little as 0.08mm.

MacAlpin et al 1973 was aware of the limitations in using the catheter and instead employed an object of known dimensions placed external to the body, filmed at the level of the atrioventricular groove and the left ventricular apex (previously determined by fluoroscopy). Although the object may not be in exactly the same plane as the stenosis, he reasoned that application of the magnification factor derived from the atrioventricular groove position would serve to correct dimensions taken from the right coronary and left circumflex arteries when viewed in the left anterior oblique (LAO) projection, whereas the magnification factor derived from the left ventricular apex position would adequately reflect the degree of correction necessary for the left anterior descending and posterior descending coronary arteries in the right anterior oblique (RAO) projection. When employing the same single plane view, he was able to make direct hand held divider measurements of projected arterial diameter to an accuracy of +/- 0.2mm when reduced to true scale. This discrepancy in accuracy (2.5 times larger than Gensini et al 1971) considering his refined technique is explained by the fact that this system is hand held and therefore suffers from "hand tremor". Also the reported accuracy values are based on measurements from coronary arteries in this study and objects of known dimension in the former (problems encountered in measuring dimensions from coronary arteries is covered in section 3.1).

Reliance on the one view only as the method for stenotic quantification are in itself erroneous, as severe overestimation or underestimation can occur if the lesion has anything but concentric geometry (section 2.2.3). It is

therefore better to use multiple views, and indeed this usually results in even less variation in results as Meier et al 1983a demonstrated. Comparing estimates of relative percent stenosis estimate taken from angiograms using a calibrated magnifying glass, three observers showed a decrease in interobserver variability from 7% when only one view (the view demonstrating the stenosis at greatest severity) was considered to 6.4% when a mean of three views was used. Intraobserver variability was also significantly reduced from 16% to 10.5% under these conditions.

From the above section it can be seen that it is possible to get accurate, reproducible and absolute results with very simple equipment. The method employed by Gensini et al 1971 may possibly be the most reproducible due to its unreliance on motor dexterity. However, the simple corrections employed for magnification discussed here are not all that are required for the attainment of true absolute dimensions (see following section).

2.2.3 Computer Assisted Image Reconstruction

The introduction of a computer based quantification system brings with it many advantages over the previously described methods. Namely quantification is usually more objective (removing subjective bias in the positioning of cursors, dividers, etc), capable of producing more information than just percent diameter stenosis and in some cases has graphic facilities for the production of hard copy reports for patient notes etc.

The system introduced by Brown and Dodge et al 1977 was the first attempt to overcome the errors inherent in the previously cited systems using computer assisted reconstruction. This system has seen application by various centres the United States over the last 10 years with no change in the original calculations.

The system works by constructing a three dimensional true scale representation of the diseased arterial segment from two single plane projections. As mentioned earlier (section 2.2.2), the diseased coronary lumen is seldom circular, ie. stenotic dimension in one view differs from that seen in another, hence complementary (orthogonal) pairs of views are used, for example 60 degrees LAO and 30 degrees RAO. However, following histological studies, pathologists raised the question whether the results from any view or combination of views from an arteriogram represent the true state of the coronary arteries. Their studies show that histological sections cut through atheromatous plaque often display a strikingly irregular cross section. Since the arteriogram is a two dimensional representation of a three dimensional object, single or indeed multiple views will seldom allow the arteriographer comprehensive insight into the true state of the artery in cross-section. For example, postmortem specimens often display a residual lumen which is cresenteric in shape. This cross section may give the two dimensional appearance of **not** being severely narrowed in any arteriographic view (figure 2.3), and may explain the frequent underestimation of mild stenosis severity by angiographers (Wright et al 1984). However, justification for a two view approach is given by these authors in a later paper (Brown et al 1982) which states that "such lumen usually occur as artifacts of postmortem arterial fixation in the unpressurised state. Those who raise the non regular lumen argument have simply ignored the physical principle that an elastic chamber under pressure will adopt a regular configuration which can be easily visualized with the combination of two views". Indeed, a study was carried out by Liu et al 1976 where arterial segments were fixed at physiological pressures. He concluded that cresenteric lumen or indeed the simpler truly slit like lumen did not exist in the living state.

Selected cine frames are projected at approximately five times magnification onto a large screen. The selected arterial segment and a portion of the catheter, of known

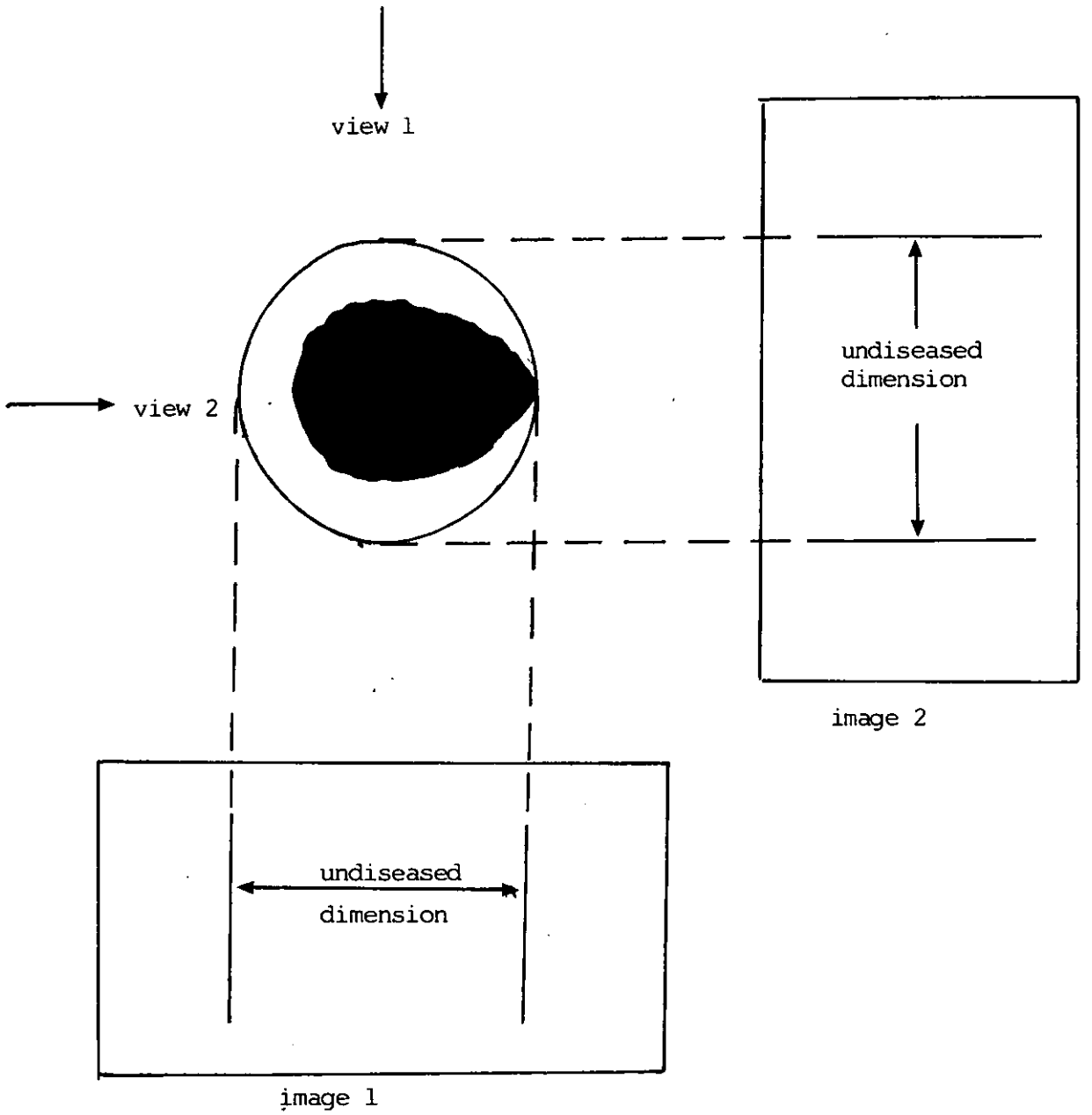

Figure 2.3 Projected appearance of cresenteric lumen

dimension, are manually traced onto paper from this view and its 90 degree complementary at the same point in the cardiac cycle.

The traced vessel and catheter segments are then converted to digital information in the form of cartesian coordinates by retracing the original traces on a commercially available graphics tablet (Autotrol 3400-B, resolution 0.1mm). This has the potential of doubling the error in the data due to the retracing, yet these authors have shown retracing repeatability to be as low as +/- 0.03mm, suspiciously low when considering the resolution of the graphics tablet. They believe the image processing capabilities of the human eye and brain which integrate to locate and trace the border of the lumen image provide the most accurate method for data entry. Other methods which work by edge detection (section 2.2.4) commonly require very sophisticated hardware and software and are still capable of making gross errors.

The digital information is then transmitted via modem to a remote mainframe computer which allows visual interaction via a graphics terminal. The data is then reduced to true scale by two correction processes. The first removes distortion resulting from the convex curvature of the input phosphor vacuum tube. This so called pincushion distortion effect results in selective magnification of objects near to the edge of the cine frame compared with their size at the centre of the field. This distortion, if left uncorrected, can account for 5% to 8% error in directly scaled dimensional estimates like those commonly employed with a visually assisted quantification system. The pincushion effect is theoretically radially symmetric about the central X ray beam, a fact confirmed by these authors who proposed the following empirically determined analytical function to characterize the distortion:

$$R^1 = \frac{1}{\sqrt{C}} . \tan^{-1} (R . \sqrt{C})$$

Where: R^1 is the true radial distance from the centre of the image to the projected image point.

R is the projected radial distance from the centre of the image to the projected image point.

C is an empirically determined coefficient which characterizes the distortion.

Each coordinate point of the digitized image is thus corrected for pincushion distortion using the following transformation:

$$X \text{ corrected} = (R^1/R)X$$
$$Y \text{ corrected} = (R^1/R)Y$$

The second correction removes distortion of the image due to divergence of the X-ray beam, which, left untreated, results in selective magnification of objects closest to the X-ray source. This accounts for errors of up to 1.5% of estimate cm^{-1} separating the scaling object (eg. the catheter) and the measured object (eg. the stenosis) along the X-ray beam axis (section 2.2.2). A correction factor, CF, is determined for each view such that the product of the CF and the projected dimension result in the actual dimension according to the following formulae:

$$CF_R = \frac{CW}{CW_R^1} + (M_R . D_L^1) \frac{CW}{CW_L^1}$$

$$CF_L = \frac{CW}{CW_L^1} + (M_L . D_R^1) \frac{CW}{CW_R^1}$$

Where: CF_R and CF_L are the correction factors in the respective RAO and LAO views.

CW is the known catheter diameter at its point of measurement.

CW_R^1 and CW_L^1 are the pincushion corrected dimensions of the traced catheter segments in their respective views.

D_R^1 and D_L^1 are pincushion corrected horizontal distances separating the lesion centre P (entered as separate information during the digitization process) and the traced catheter segment C in the respective views.

M_R and M_L are empirically defined coefficients characteristic of the X-ray system reflecting the rate of change of correction factor with distance along the axis of the divergent X-ray beam.

The initial terms of the above formulae reduce the projected dimensions to approximately true scale by using the dimension of the projected catheter tip as a scaling device. The fine correction for axial displacement is achieved by the second term, resulting in the derivation of a correction factor for the view in question. Multiplication of each coordinate by the appropriate CF yields data scaled to true size. The overall correction procedure is summarized in figure 2.4.

Following the derivation of true scale, error free data, a centre line is mathematically defined such that its perpendicular at any point intersects both vessel edges at equal distances from itself. Resultant data describing the centreline and projected diameters (between 40 and 80 in number depending on segment length) are computed for both views. The two views are then matched with the point of maximal constriction, considered to represent the origin of a newly defined three dimensional coordinate system. This results in a representation of the arterial segments as paired diameters crossing at 90 degrees with midpoints running through a common centreline coordinate. Hence three dimensional reconstruction is complete.

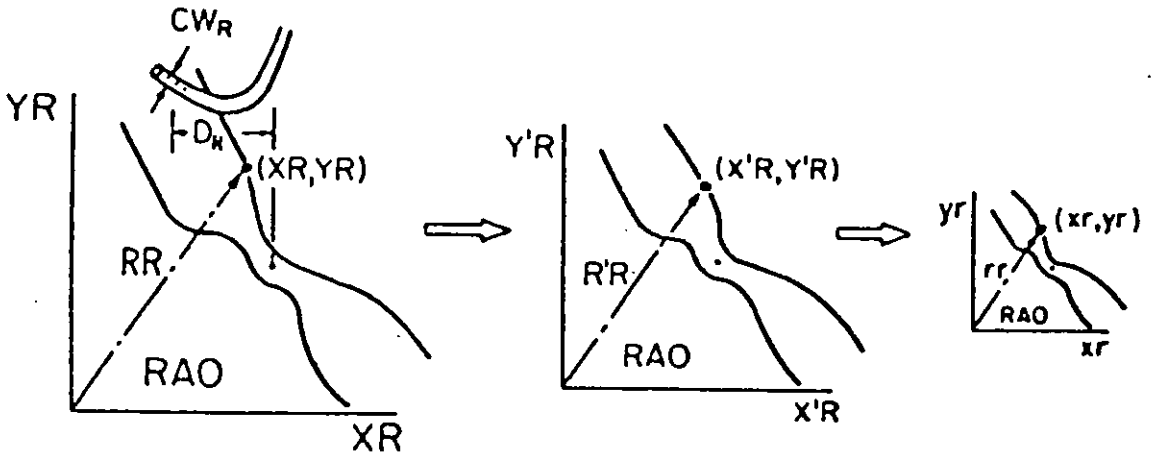

BASIC RELATIONSHIPS:

PINCUSHION DISTORTION: $R'R = \frac{1}{\sqrt{C}} \tan^{-1}(RR\sqrt{C})$

RADIAL SYMMETRY: $\frac{R'R}{RR} = \frac{X'R}{XR} = \frac{Y'R}{YR}$

MAGNIFICATION: $CF_R = \frac{xr}{X'R} = \frac{yr}{Y'R} = \frac{CW}{CW'_R} + (m_R D'_L)\frac{CW}{CW'_L}$

$$xr = XR \frac{\tan^{-1}\sqrt{RR^2 C}}{\sqrt{C}\, RR} \cdot CF_R$$

$$yr = YR \frac{\tan^{-1}\sqrt{RR^2 C}}{\sqrt{C}\, RR} \cdot CF_R$$

Figure 2.4 Overall correction procedure for the Brown-Dodge system

Brown BG, Bolson E, Frimer M and Dodge HT, 1977, Circulation, 55, 2, 329-337

From this basic raw information, the system produces a number of familiar stenotic parameters, eg. absolute maximal and minimal diameter and percent diameter stenosis as well as a number of new parameters. Amongst these are absolute and relative cross- sectional areas based on an elliptical model (thereby utilizing the two views), atheroma mass based on linear interpolation of undiseased vessel above to undiseased vessel below and segmental resistance of the stenosis assuming various hypothetical coronary artery flow rates.

Whilst seemingly cumbersome to apply, the system is relatively quick taking on average four minutes in frame selection, three minutes in tracing and three minutes for computer processing. It is also remarkably accurate. In processing information resulting from cine angiograms of a dummy brass lesion of known size, computer dimensions were exact to within 0.08mm of the known value. Diseased arteries were removed from postmortem human hearts and injected at 100 mmHg pressure with contrast containing gelatin. Cine angiograms of these segments were made in two views and quantified in the normal manner. The segments were then sectioned appropriately and lumen cross-sectional area independently planimetered by the resident pathologist. Browns paper graphically represents very good correlation between the computer estimation and the planimetered result yet omits to cite the correlation coefficient.

A very comprehensive repeatability study was also carried out which yielded standard deviations of minimal diameter estimate in the range +/- 0.027mm to +/- 0.28mm depending on the experimental design. Accuracy in studies carried out at other centres utilizing the Brown - Dodge system are comparable - +/- 0.103mm (McMahon et al 1979), and +/- $0.11mm^2$ for the minimum cross-sectional area standard error of measurement (Wilson et al 1986).

Using this system, it would appear that trained observers can re-measure absolute vessel dimensions to an accuracy

(standard deviation) of +/- 0.1 - 0.15mm. This represents the equivalent of about 3-8% of the normally sized coronary artery and is of a magnitude of error tolerable in clinical situation. The system is reasonably easy to use and conceptually easy to understand, producing a host of useful parameters previously unavailable from earlier discussed quantification systems. Its only disadvantage would seen to be the necessity to collect stenotic data twice - once in paper tracing and again in digitization.

A analogous system proposed by Owen et al 1983 produces similar stenotic parameters but is much more difficult to use. The system has the option of creating data from 35mm spot films or videotape images, in either case data entry is achieved by movements of a keypad cursor upon a back-lit graphics tablet.

Following image selection, empirically derived calibration constants depending on employed X-ray geometry are entered into the computer. Next the operator defines the arterial segment by digitizing its proximal and distal end points either from the spot film, directly mounted on to the graphics tablet, or by positioning on the TV screen a generated video cursor again controlled by the keypad on the graphics tablet. The user then digitizes a rough arterial centreline between the two previously entered points. Spatial derivatives are next calculated by the program at fixed increments (typically 1mm) along the arterial centreline in order to generate tangent vectors which are later used to define diameters perpendicular to the centreline. Following establishment of the said vectors, the centreline is then shifted to a new location outside of the constraints of the artery in order to avoid mathematical instability when calculated diameters approach zero.

The user then proceeds to digitize the arterial edges using one of the previously described methods depending on the image origin. Random variations in edge identification are eliminated using a re-digitization and averaging approach.

The artery outline is then displayed on a graphics terminal. The plot is checked for acceptability and either discarded or stored. Subsequent analysis of the image results in the production of similar parameters to those of the Brown - Dodge system.

The system was firstly validated by digitization of test objects. A comparison of calculated versus actual measurements yielded a correlation coefficient of 0.998 and a standard error of estimate of +/- 0.025mm; a more realistic figure than that quoted by Brown and Dodge. Repeatability was calculated to be +/- 0.05mm which represents an error of 1.6% in a 3mm diameter artery. Further validation was achieved by the filming and digitization of images from the coronary arteries of dogs containing previously placed hollow plastic cylinders of known dimensions. The relationship describing the calculated to the actual size had a correlation coefficient of 0.986 and a standard error of estimate of +/- 0.062mm.

Despite the increased versatility (spot film and/or video medium) of this method above that of the Brown - Dodge system, it has been less readily accepted into routine use in other centres throughout the United States. The system is conceptually more difficult to understand, lacks the capability of 3D construction and requires much more operator interaction.

2.2.4 Edge Detection Methods

These methods have attempted to reduce operator interaction to a minimum by employing very sophisticated computer software to "recognize" the arterial borders. Basically this is achieved by examining the brightness in each pixel along the scanline in question and comparing it to its two adjacent neighbours. Maximal differences between the pixels denotes the vessel edge (figure 2.5). The accumulation of successive scanline brightness profiles depict the arterial morphology (figure 2.6).

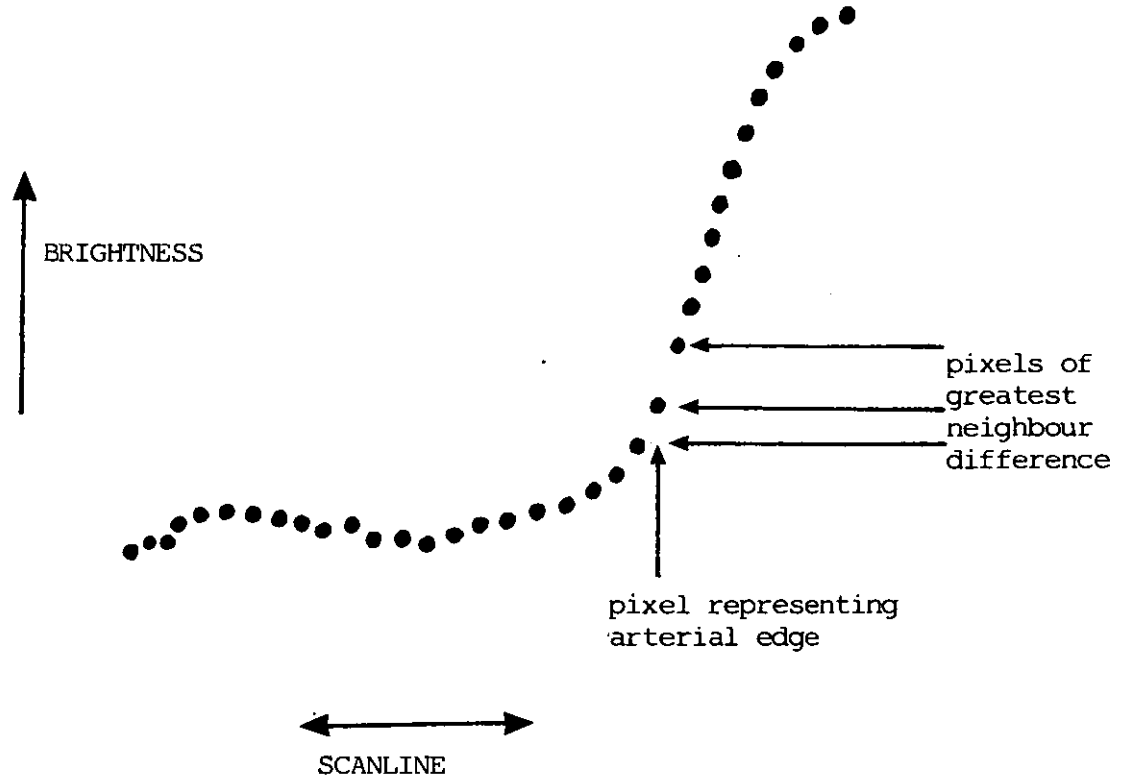

Figure 2.5 Edge detection procedure

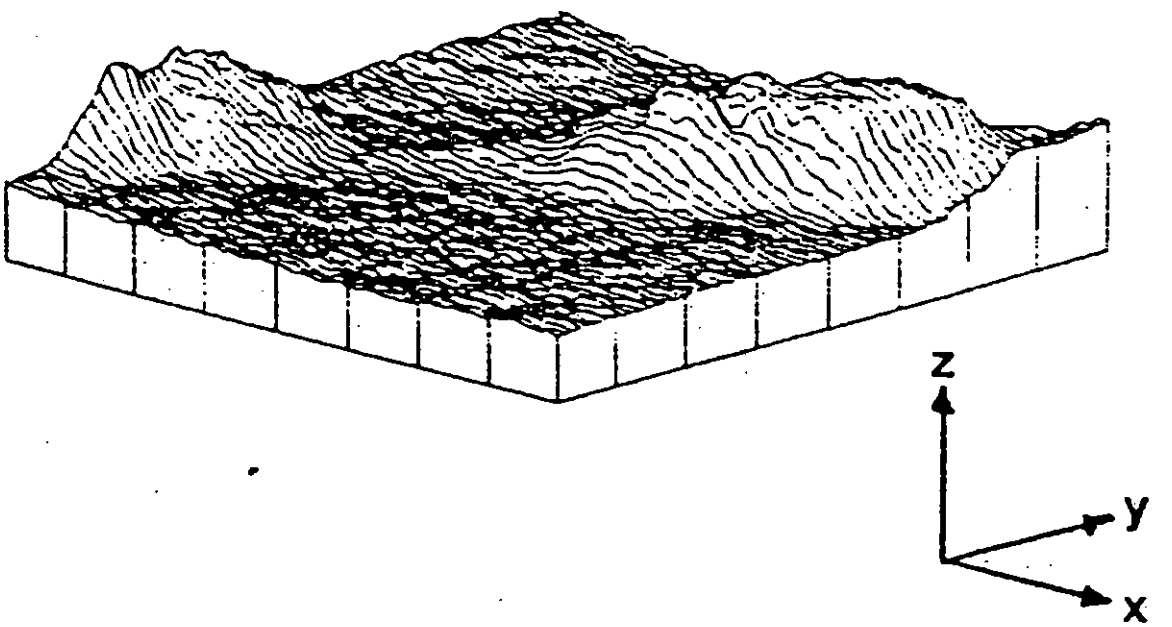

Figure 2.6 Arterial morphology represented by successive brightness profiles

Booman F, Reiber JHC, Gerbrands JJ, Slager CJ, Schuurbiers JCH, and Meester GT, 1979, Proc. Computers in Cardiology, 177-180.

One such system was presented by Reiber et al 1978. Magnified portions of the cineframe are converted to a digital image via a high resolution video camera, such that the pixel size referred to actual size at the level of the heart equals approximately 0.1mm for a 15.25cm (6 inch) image intensifier. Unfortunately this has the effect of limiting the systems resolution, making estimates of small diameters (those seen routinely in clinically significant coronary artery disease) more inaccurate.

In order to determine the positions of the arterial edges, the system requires a centreline to be defined by the user. This is achieved through communication via a graphics tablet. The user digitizes a number of centreline positions within the arterial segment such that straight lines joining these points remain within the artery. The sharp inflections encountered where one segment meets another are then smoothed by means of a first degree polynomial function. A new more accurate centreline will be generated following subsequent contour detection and the procedure reiterated for improved accuracy and reduction of error due to user bias in the selection of the centre points.

Starting at the top centre point, a 64 x 64 pixel matrix is established within which scanlines are constructed at 90 degrees to the centreline. For each scanline, 2 contour positions are determined from the maximum rate of change of pixel brightness as previously described. Also, a new centreline position is derived as the pixel with the maximum brightness along the scanline in question, provided it does not deviate from the original tentative position by more than 5 pixels (the expectation window). If it should, the tentative position is retained as being an accurate estimation of true centre point position. Scanlines continue to be processed in this manner until either a new centreline segment (and therefore direction) is detected or the end of the current matrix is encountered. A new matrix is established which allows the processing of scanlines perpendicular to the new centreline if the former condition

was operative, or, perpendicular to an average centreline computed from the direction of the previous centreline and the next if the latter condition prevails. The complete procedure repeats itself until the end of the centreline is reached.

Where one matrix changes in direction in comparison to another, contour position density suffers accordingly, with discontinuities occurring on one side and clustering occurring at the other. Missing contour positions are established using linear interpolation between existing adjacent points, whereas clusters are reduced using a thinning operator. The effect of these functions on data integrity when rapid changes in artery direction are encountered are not reported, but it seems reasonable to assume that a 90 degree curvature (which often occurs in the right coronary artery at the acute margin) cannot be adequately modelled using a linear interpolation approach (figure 2.7). Each contour position is the then finally smoothed using a second degree polynomial function by basing the equation on the location of the ten previous and the ten following contour positions.

The final contours are then superimposed on the original video image for user refinement. This is commonly required when the arterial segment of interest includes a side branch and the calculations based on brightness lead the computer to believe the artery is wider than it actually is. Also, background structures such as bones may lead to slight stretching of the edge position if the brightness is of similar intensity to that encountered at the less densely opacified arterial lumen edge (section 3.1). Seemingly, the so called automated approach is struggling to mimic the image processing capabilities of the human eye and brain which were utilized in the systems reviewed in section 2.2.3. Interpolation across small changes in brightness function (grey scale) are beyond this type of approach since the system has no concept of the structure of the image as a whole.

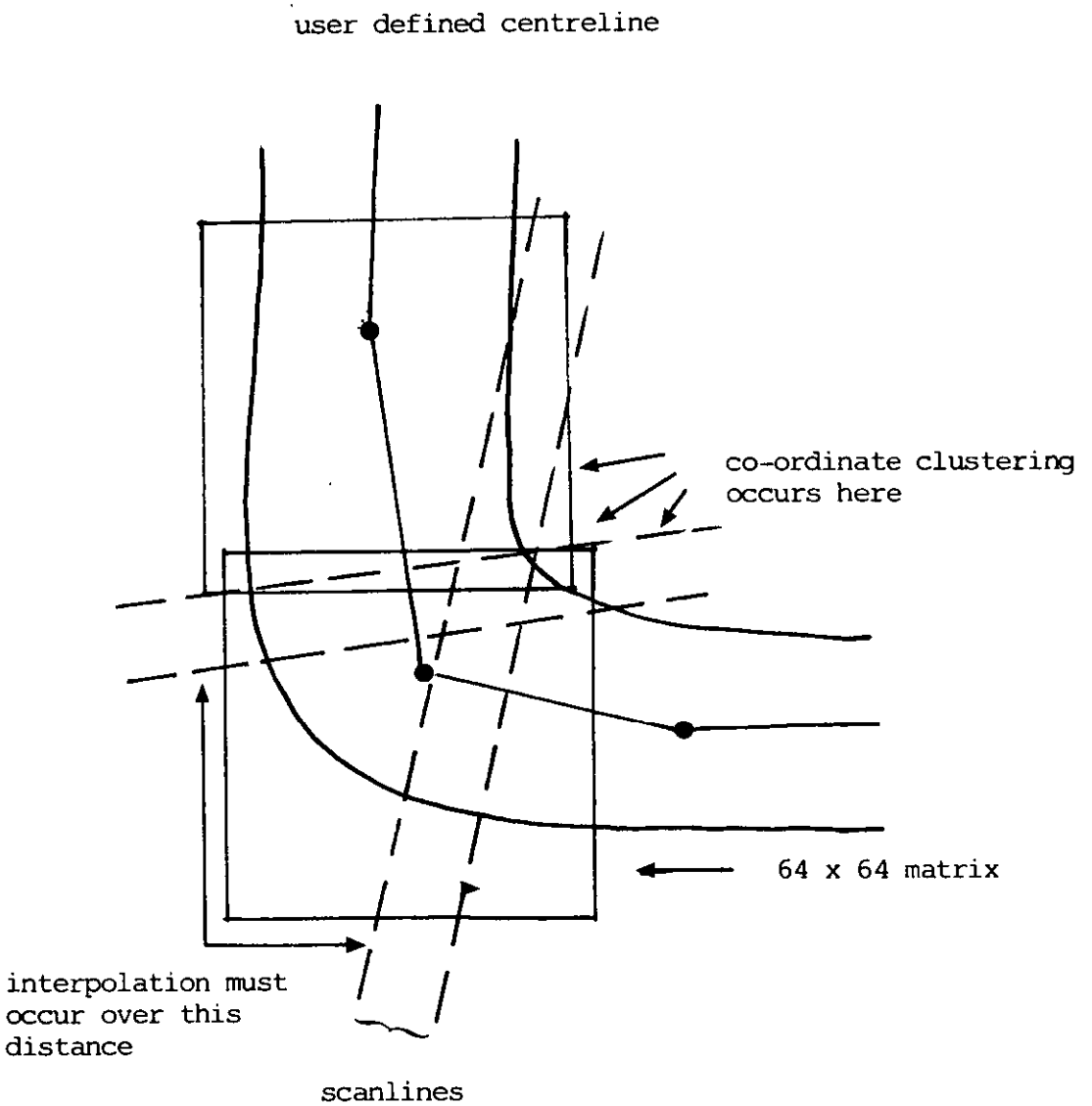

Figure 2.7 Diagram showing inability of edge detection method to cope with rapidly changing artery profile

Once the user is satisfied that the computed contour positions fit the artery reasonably well, the system goes on to correct for pincushion distortion. This involves applying a correction based on calibration grids filmed at the time of the angiogram, therefore prolonging catheter study time. Analysis of the images of the grids yields information pertaining to the discrepancy of any one point in the image from its original (unfilmed) position. Calibration for reduction of images to true size is obtained from a repeat edge detection operation on the catheter. These authors utilized only a single plane approach for this part of the image correction, thereby accepting the 1.5% error cm^{-1} axial displacement. This fact is rather surprising considering the complex approach employed to achieve accurate artery edge data.

Contour analysis is then performed by determining the distances between corresponding contour points to the right and left of the centreline, with the calculation of variables akin to those encountered in the Brown and Dodge system in section 2.2.3.

The system was tested for accuracy using machined brass cylinders of various simulated percent diameter stenosis. The correlation coefficient between the actual and measured values was very favourable at 0.99 with a standard error in the estimate of percent diameter stenosis of +/- 2.33%. However, as alluded to earlier, the authors recommend that this approach is really only suitable for quantification of lumen diameters of 0.8mm or greater due to less dependency on pixel size, and as a consequence, may be better suited to quantification of femoral or even cerebral vessels.

Although this method has been employed in various studies on coronary artery quantification (Reiber et al 1979, Serruys 1980, Serruys et al 1984, Wijns et al 1985ab) further data regarding its validation is not evident. The fact the system has only been validated under "laboratory conditions" on test items leaves the system open to question. The high

content of complex mathematics and the prolific use of smoothing in order to produce artery edges which more often then not still require user interaction is poor methodology from the outset. Overall, this system is difficult to understand, requires many computer manipulations and much costly hardware (approximate cost, £90,000 - personal visit, the Hammersmith Hospital) and has poorly documented validation both in terms of accuracy and operator time.

Alderman et al 1981 proposed a similar system to that outlined above with the exception that the two arterial borders are roughly approximated as digital input from the user rather than the centreline. Both borders are then refined by perpendicular brightness scans akin to the Reiber method. In their review article, Brown et al 1986 state that Alderman has yet to report the dimensional accuracy of this method, but he has demonstrated very low variability in repeated dimensional estimates, nearly equalling that obtained with manual tracing. It seems obvious that this category of quantification system has tried to tread the totally automatic analysis approach and failed. Not only is user interaction necessary to initiate the system and correct it when it goes wrong, but the combination of said interaction with automation produces results which are inferior to direct tracing.

2.2.5 Photodensitometry

In the previously discussed computer aided methods of quantification, the major emphasis has been on locating the vessel edge. However, if one were able to subtract background noise from an image and apply the Beer - Lambert law which states that a homogenous bolus (section 3.1) of contrast filling a vessel will attenuate the intensity of transmitted X-ray in proportion to length of the X-ray path through the vessel, then it is theoretically possible to avoid precise lumen border definition altogether. Integration of the resultant background subtracted attenuation profile will provide a direct estimate of lumen

cross-sectional area (figure 2.8). This is the approach of photodensitometry.

The typical system is composed of a video camera receiving a projected cine frame as input (figure 2.9). The signal produced by the camera is then digitized using an analogue to digital converter prior to being transmitted to the computer.

The approach of the system proposed by Nichols et al 1984 digitized the image into a 512 x 512 matrix such that each pixel represented 0.011mm in absolute dimensions. The image is then analysed quantitatively by positioning rectangular regions of interest (ROIs) across the artery long enough to extend across its full width. Two smaller ROIs two pixels square are positioned adjacent to the ends of the above regions of interest for determining background videodensity. In order to determine percent cross-sectional area stenosis, the ROIs were positioned across a normal arterial segment and the visually assessed most severe stenotic segment (figure 2.10). Brightness profiles reflecting the density of the luminal contrast are then acquired along with values from the background areas. The final videosensiometric volume for either ROI is corrected thus:

$$\begin{matrix}\text{Corrected} \\ \text{videodensitometric volume}\end{matrix} = \begin{matrix}\text{Total} \\ \text{videodensitometric volume}\end{matrix} - ub$$

where u = number of pixels in sample ROI
b = average background density per pixel.

This approach separates the videodensitometric signal representing the column of contrast from the background density without requiring identification of the margins of the arterial lumen. Hence percent cross-sectional area stenosis may be calculated in a manner akin to the calculations of percent diameter stenosis.

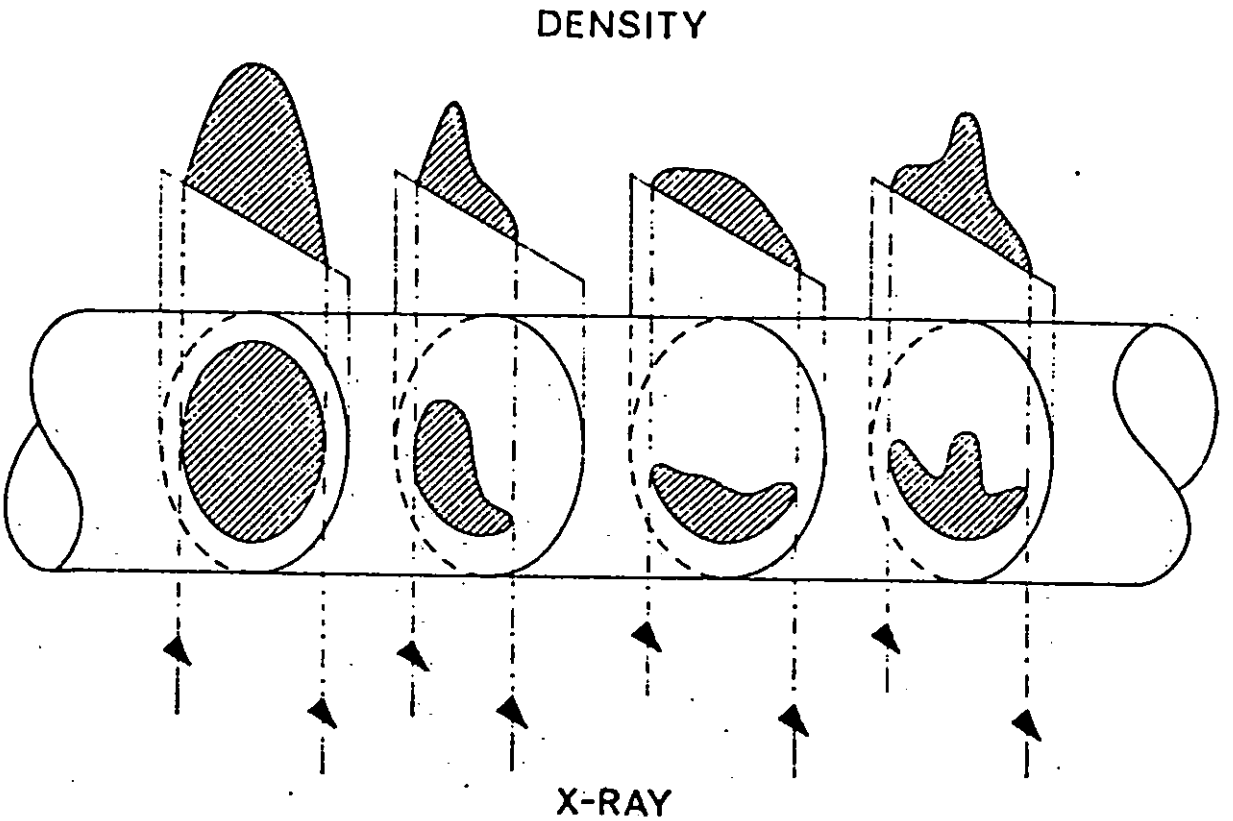

Figure 2.8 Diagram shows relationship between the irradiated object thickness and the density of the angiographic image

Reiber JHC, Kooijman CJ, Slager CJ, Gerbrands JJ, Schuurbiers JCH, Den Boer A, Wijns W and Surruys PW, 1984, Automedica, 5, 219-238.

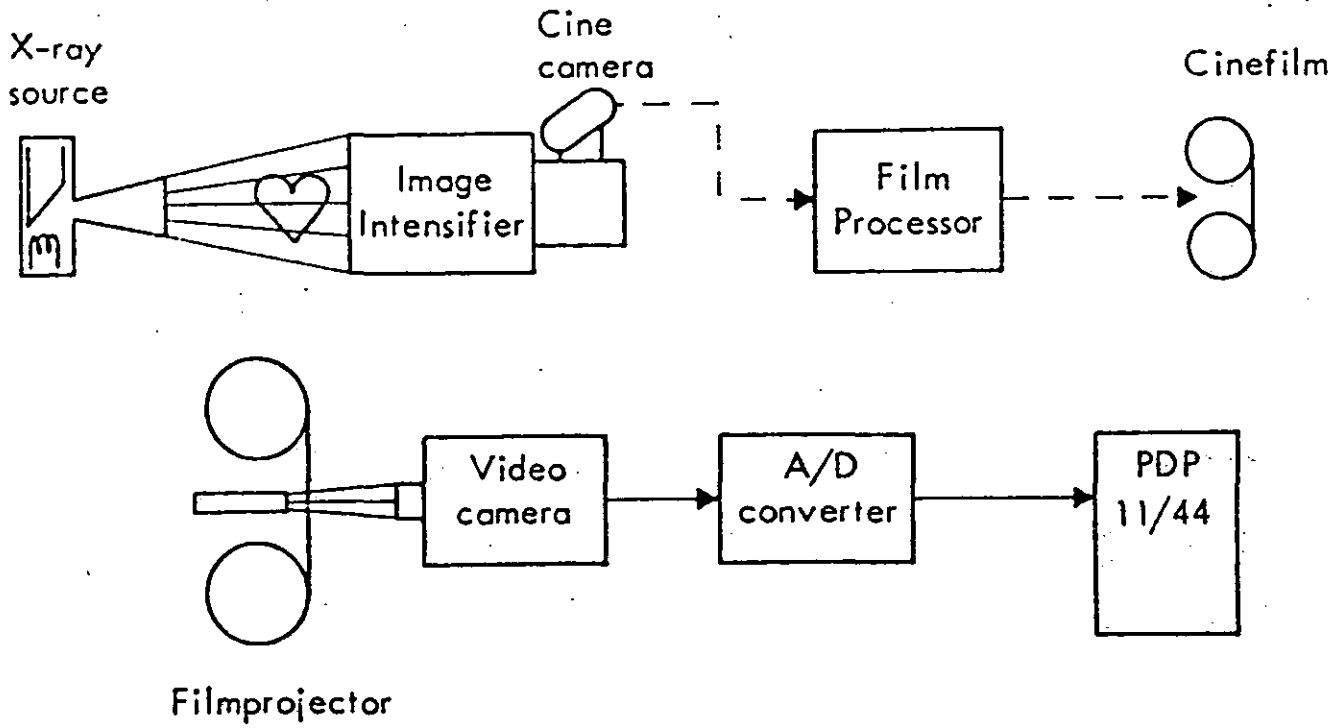

Figure 2.9 Diagrammatic representation of a videcdensitometric quantification system

Reiber JHC, Kooijman CJ, Slager CJ, Gerbrands JJ, Schuurbiers JCH, Den Boer A, Wijns W and Serruys PW, 1984, Automedica, 5, 219-238

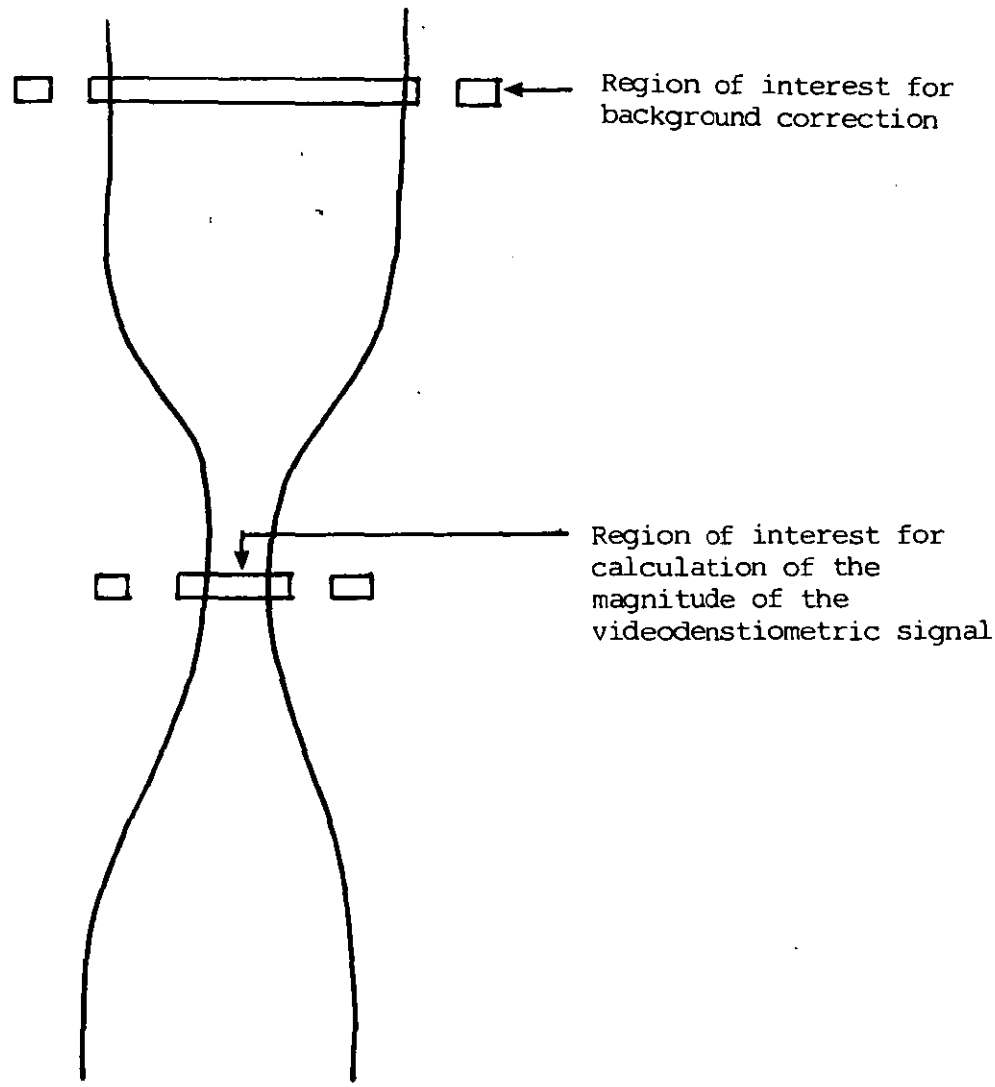

Signals from the normal (Vn) and the stenotic (Vs) portions allows the calculation of percent stenosis thus:

percent stenosis = 100 x (Vn-Vs)/Vn

Figure 2.10 Nichols method for the relative quantification of coronary arteries

The system was validated firstly using test objects ranging in diameter from 1.00 to 4.00mm. Even when the concentration of contrast medium was varied from 100% to 25%, the relationship describing the cross-sectional area and the integrated background subtracted videodensitometric values was still highly linear ($r >= 0.98$). Test object stenoses in the range 5% to 79% (1.78 to 4.16mm) were well predicted by this method too ($r = 0.99$, SEE = 3.9%). Measurements of undiseased coronary artery area estimate validated against intraoperative high frequency epicardial echocardiography compared well ($r = 0.86$ - Johnson et al 1988). However, like edge detection, diameters of less than 1mm are avoided.

Postmortem studies comparing planimetered artery cross section with the videodensitometric method compared well ($r = 0.97$, SEE = 7.0%). Intraobserver and interobserver variability are acceptably low at 7.7% and 4.3% respectively. As yet, absolute measurements are unavailable on this system.

Serruys et al 1984 proposed a perhaps more elegant system which utilized a combination of edge detection and videodensitometry. Centreline detection and contour recognition are firstly performed according to the method of Reiber et al 1978. The errors inherent in the transfer of the image from its analogue to digital form are monitored and corrected for by measurement (on a pixel by pixel basis) of 21 calibrated density frames which are processed simultaneously with the rest of the cine film. His article declines to report the consequences of this procedure in terms of additional time spent in the catheterisation laboratory. Analysis of the calibration frames permits the calculation of a transfer function which is applied to the sequential video brightness profiles. These result from integration along scanlines perpendicular to the centreline in a previously defined ROI encompassing the whole stenosis. Background contribution is estimated by an interpolative method from all pixels adjacent to the detected contours and

removed from profiles in the normal way allowing the expression of percent cross-sectional area reduction at every scanline, and maximal percent cross-sectional area reduction using operator selected positions. Validation data is again conspicuous by its absence.

Sandor et al 1979 proposed a system whereby digital magnification and grey scale "thresholding" of the image may be used to enhance its visual quality. He specifies an analyzing window using operator controlled cursors within which the computer determines multiple density profiles by scanning the vessel roughly perpendicular to its long axis. Each profile is then smoothed by a three point weighted digital filter and background corrected. User positioned cursors dictate the position of the reference and stenotic scanlines which allow the expression of maximal percent cross sectional area stenosis. A careful and detailed evaluation of their method reveals variability in area estimates of phantoms filmed against a background of a dog thorax of 20% of the mean for tubes of the size of the left coronary artery, but more than 30% for tubes of $1mm^2$ area or less. The authors conclude that high precision densitometry has potential utility, but its failure to be able to produce an absolute measurement, coupled with increased measurement variability for small lumen negate routine application with coronary arteries.

Other potential limitations of this method not discussed by any of the authors include:

1. Superimposition of a vessel of interest directly on top of a underlying smaller vessel. On this occasion the arterial borders are correctly preserved but contrast density with the vessels is falsely elevated.

2. Obliquely placed reference cursors causing overestimation of the area values.

3. Errors in background subtraction. For example, if the areas sampled overlie a dense structure such as bone. This will lead to generalized enhancement of the videodensitometric profiles with concomitant magnification of the relative percent cross-sectional area estimate.

Consequently, this method has found better application in the quantification of larger more solitary vessels, for example the femoral artery.

2.2.6 Conclusion

The widely used clinical tool of arteriography is currently limited by imprecise and, to a certain extent, inappropriate subjective methods of interpretation. More objective methods for the analysis of the arteriographic image have become available over the past 10 years and have found application particularly in the United States and to a lesser extent, Europe, with Great Britain being somewhat left behind. Results pertaining to the use of the objective methods discussed in this review have resulted in considerable increases in the understanding of the pathogenic mechanisms of CAD. Surely the increased use of objective quantification is warranted in the light of these findings.

2.3 **Statement of Approach**

Considering the initial aims and the current review of the literature presented from this chapter, it was felt that a digitization system involving manual tracing of the arterial borders (section 2.2.3) most suited our purpose. Below are presented the reasons behind this decision listed for ease of comparison as complements to the previously stated aims.

REASON 1 Characterization of the X-ray system for the corrections required to remove pincushion distortion and selective magnification can be

performed as a self contained experiment separate to routine catheterisation. Once completed it need never be repeated providing there are no changes to the X-ray system. By adopting this approach, all that is required for image quantification is the image itself. The various corrections are made by reference to derived empirical coefficients, therefore no unnecessary film need be processed or additional time incurred.

REASON 2 Visually assisted methods of quantification are quick and quite repeatable, but results are invalid and lack correction for image distortion. Edge detection and videodensitometry are only accurate for dimensions of 1mm and above and are poorly validated in the clinical environment. The digitization methods discussed in the review are highly accurate, repeatable and valid - the Brown and Dodge system, perhaps, suspiciously so.

REASON 3 Edge detection and videodensitometric methods of quantification require large amounts of computer memory to allow their software to run. This has necessitated the use of the larger, less versatile minicomputers as the host machine. Visually assisted methods require no computerization, whereas the digitization methods have required mainframe links. Therefore basing a digitization system on a microcomputer would be an improvement to the systems currently in existence.

REASON 4 Of all the systems reviewed, the visually assisted methods are easiest to understand since the user performs all the calculations. Videodensitometry and edge detection are easy to use but use much complex mathematics in order to produce results. This makes the "mechanics" of the system less easy

to understand. This is not so with digitization, as the user "instructs" the computer where the arterial borders are and what is their shape. ie. he is responsible for entry of the raw data, not a mathematical routine.

REASON 5 Further development may be possible with all the systems discussed, though this is never mentioned. However, a graphics tablet is a common peripheral item unlikely to undergo the degree of change perhaps expected of a system based on the popular video medium. Software compatibility may be preserved by using a language for which international standards have been set, for example Fortran. This will allow the system to advance with new computer technology.

REASON 6 Routinely used parameters are capable of being produced by all the quantification systems except videodensitometry, which produces a more haemodynamically significant variable, though less widely employed. However, a digitization based system produces the best validated results in terms of accuracy.

REASON 7 Videodensitometry produces the only true estimate of percent cross-sectional area stenosis, whereas the other methods can only infer this parameter and other area/volume results based on information derived from a combination of views. However, edge detection and digitization methods are also capable of interpolating the normal vessel morphology from the diseased state. This may aid in the quantification of an infrequently used yet important parameter, that of eccentricity (chapter 7).

REASON 8 All the systems discussed require some form of user interaction, firstly for data entry (and/or

correction) and secondly for position identification of various parameters, eg. minimum diameter. Digitization is the only method quoted capable of identifying these positions automatically, therefore reducing user input and subjective bias to a minimum.

REASON 9 Batching information for processing may be available on all the computer based systems, though this is never discussed in the literature above. However, it is particularly easy in the dedicated microcomputer environment.

REASON 10 A visually assisted method would be the cheapest system when viewed from all facets, but the derivation of accurate absolute dimensions remains a problem. The introduction of computers and other hardware necessitates some expenditure, although this can be kept to a minimum if for example the choice of computer is popular (ie. microcomputer, which may also be put to other uses in the Department apart from dedicated mensuration) and the software is self generated rather than bought. Peripherals can also be expensive, so one may be advised to choose a peripheral combining greatest accuracy with least maintenance; this is perhaps true of a high resolution graphics tablet.

CHAPTER THREE

METHOD

3.1 Image Quality Considerations

As discussed briefly in section 2.2, not all arteriographic images are suitable for quantification. This section will discuss factors affecting image quality and outline the image selection criteria adopted and recommended for use with the Quantitative Arteriographic Mensuration System (QAMS).

The sharpness of an arteriographic image is dependent on many factors.

1. Intraluminal contrast concentration. This in itself is dependant on volume, velocity and density of the injected bolus. In order to produce an acceptable image, the volume must be sufficient to fill the coronary artery, be delivered at a speed which allows a complete fill of the said artery and be dense enough to sufficiently attenuate the X-ray radiation. Typically volumes of between 4 and 8ml are injected manually over a period of 6 to 10 seconds using a 70% mixture; maximum opacification being towards the middle third of the injection phase. Use of inadequate volumes produces proximal segmental opacification of the coronary artery with subsequent distal dilution by the blood, resulting in inadequate image density for visual inspection or quantification. Slow injection velocity results in streaming (contrast medium confined to areas of highest blood flow) of the contrast medium with consequent failure to demonstrate the full arterial dimensions. In particular, the true edges are not demonstrated due to the reduced blood flow and added frictional forces present in these areas. Adoption of an over diluted contrast medium results in poor image definition as a result of low X-ray attenuation. However, adequate

intraluminal contrast concentrations are usually achieved by an experienced angiographer.

2. The difference in attenuation coefficients between the contrast medium and the surrounding biological material. Obviously, superimposition of the opacified artery up on a material of similar attenuation coefficient (eg. another opacified vessel) results in loss of image sharpness. This is a particular problem at the arterial border since the physical amount of contrast at these locations is least and therefore attenuation is diminished. For this reason, images must be selected which are free from interference by any surrounding objects. Typically other opacified vessels and vertebrae present the most common occurrence of this problem.

3. Radiation energy. Increased radiation energy improves penetration power which results in less attenuation by interfering structures and their subsequent deduction from the final image. However, this practice results in less of the true image being recorded, particularly the vessel edges. Also there are practical safety limits governing the use of radiation energy which must be adhered to for both the angiographers and patients wellbeing.

4. The penumbra effect. The focal spot of all X-ray sources are of finite size, not a point source. Irradiation of an object by such a source causes the penumbra effect (figure 3.1), an area of less defined attenuation around the object, causing blurring of the arteriographic border. This factor is inherent in the X-ray system employed for the catheterization procedure and is unavoidable. However, it should be noted that the smaller the focal spot, the smaller the penumbra effect and the sharper will be the resultant image.

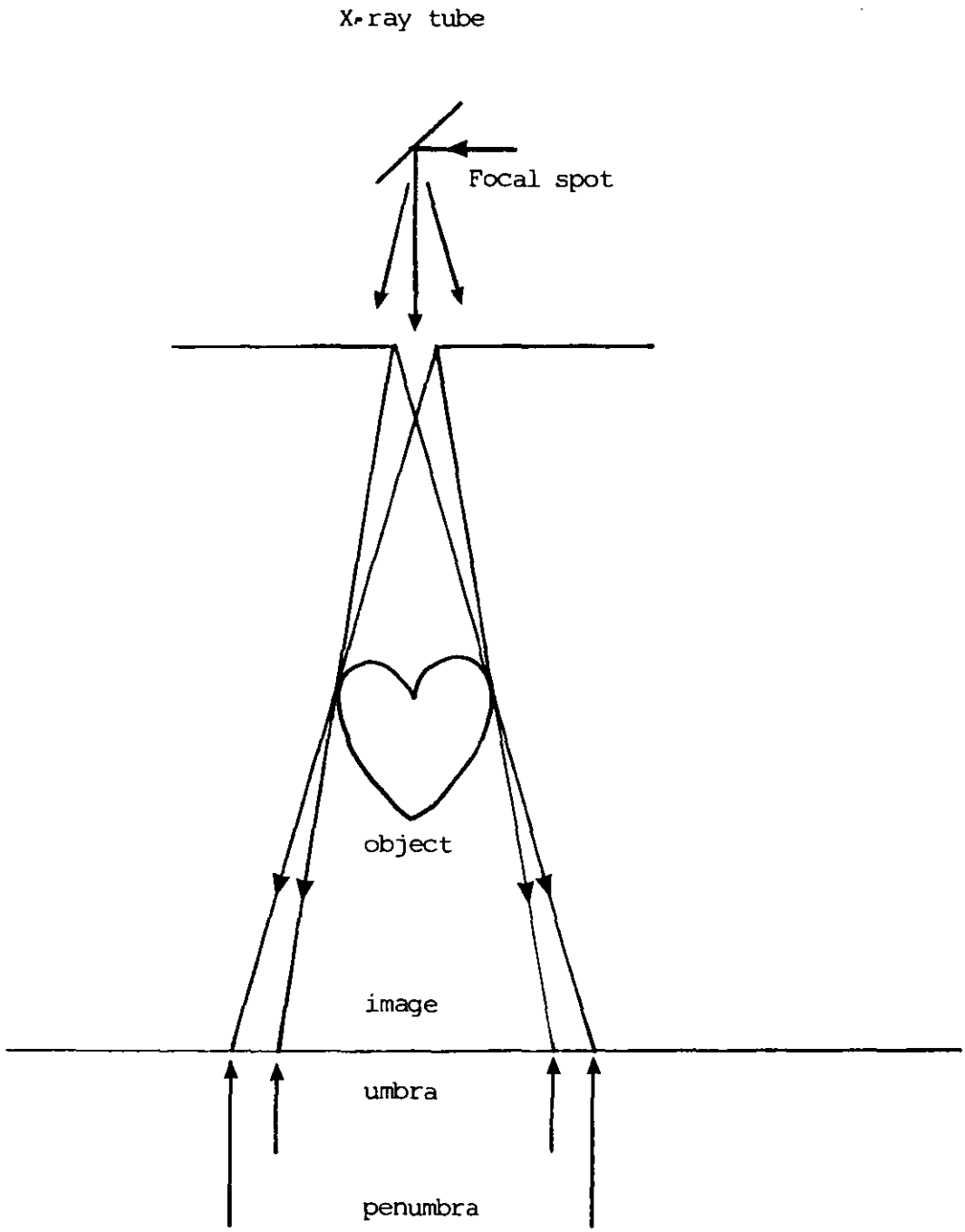

Figure 3.1 The penumbra effect

5. Motion blur. The opacified coronary artery is irradiated by pulses of X-rays typically lasting between 4 and 7 milliseconds. However, throughout this small duration, the heart and therefore the artery is in motion; this leads to additional blurring of the image. Conversely maximal image definition occurs at periods of least heart motion, generally end systole, late diastole and at the peak of atrial contraction. It is therefore advisable to select images coincident with these stages of the cardiac cycle for quantification.

6. Non linear magnification effects. Blurring of one section of artery in comparison to another can occur if the course of the artery runs across one half of the field of view, or more. This is due to pincushion distortion and peripheral unfocusing equivalent to spherical aberration in optical systems. Arteries of this type are best avoided and seldom occur in the coronary arterial tree.

7. Quantum mottle. Low levels of transmitted X-radiation have high statistical variation of energy. This can result in focal irregularities in the final representation of image contrast (quantum mottle), leading to poor definition of the vessel edge. Therefore it is advisable to use medium range energies which have the effect of slightly reducing the actual size of the arteriographic lumen (ie. very low contrast densities are not recorded) but avoids quantum mottle without excessive degradation of the image.

8. Film characteristic. When the image is recorded on film, the exposure must be such that the image of interest is filmed in the linear range of the film characteristic curve (figure 3.2), otherwise the vessel edge may be "burned away" or "whited out". Enhanced image quality is available by use of the recently developed Digital Subtraction Angiography. The initial

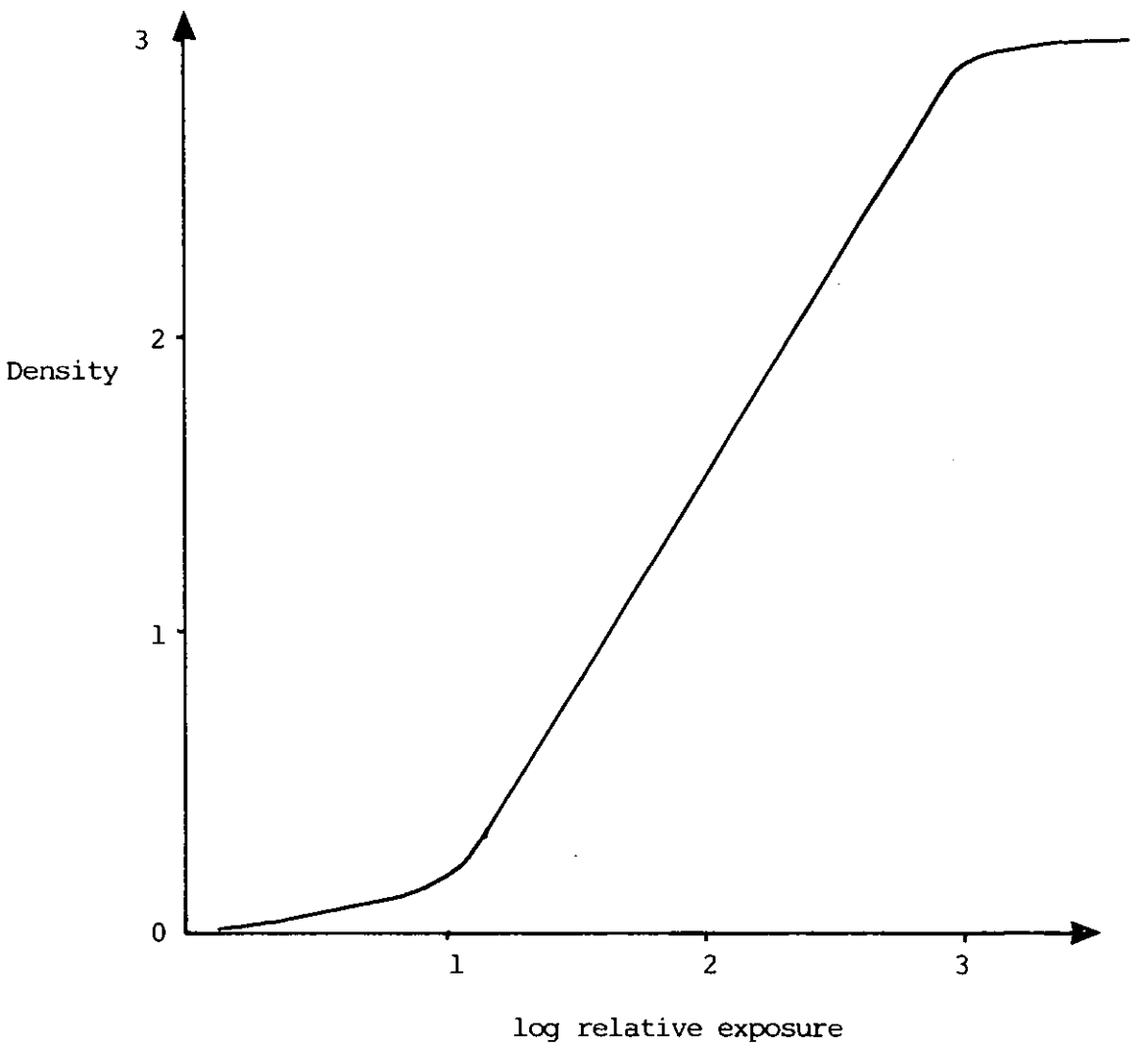

Figure 3.2 X-ray film characteristic curve

fluoroscopic image is firstly logarithmically amplified - this allows the use of lower concentrations of contrast medium which has been proven to have a cardiodepressive effect (Bonoron - Adele et al 1984). It then undergoes analogue to digital conversion before being stored in computer memory where it may be accessed allowing immediate playback. Interfering objects other than those which are directly opacified are removed from the final image by the creation of a mask - an image recording the field of view prior to contrast injection. This is converted in a similar fashion and subtracted from the contrast image data; however the motion of the heart can cause some misregistration of the mask on the original image (Tobis et al 1983). Therefore the technique is better suited to peripheral angiography although the above laboratory has taken on digital recording as its primary storage medium of all arteriograms (Tobis et al 1984).

True anatomical representation of the arteriographic image is dependent upon:

1. View. As reviewed in section 2.2.3, arterial cross-section is seldom symmetrical. Therefore, in order to exemplify true stenotic morphology by quantification or otherwise, one must utilize at least two views. Perpendicularly matched views are most desirable due to the potential for three dimensional reconstruction. The image which depicts the stenosis of greater severity is usually utilized as one view as many artifacts, some beyond the arteriographers control, can serve to increase apparent lumen diameter eg. motion blur, superimposition or foreshortening (see later). But few, usually within angiographer control, can cause the lumen to appear narrower than reality eg. streaming and inadequate contrast injection. Therefore the most severe view is usually the most accurate, and should be quantified.

In addition, the views used for quantification must represent as far as is possible a true long axis view of the artery. Without meeting the criteria, the artery runs in the Z plane of the arteriographic image to some extent (the foreshortening effect). This leads to misrepresentation of the true anatomical state of the artery, usually manifest as increased dimensions and diminished length. The presence or absence of this foreshortening effect in an image to be quantified is entirely a subjective decision. However, as part of the image selection procedure a chart was employed which highlighted areas of potential foreshortening for every routinely used view in coronary artery catheterization (May and Baker Ltd). If a stenotic segment being considered for quantification fell into one of these "potentially hazardous" areas in any particular view, it was rejected, and another view was selected with the segment of interest in a "safe" location.

Whilst the chart is based on "average" coronary anatomy, it was found a useful guide in avoiding the foreshortening problem and its continued use is recommended until superseded by a more elegant approach.

2. Magnification variation. Pincushion distortion and selective magnification, qualities discussed in section 2.2.3, distort the object in an arteriographic image relative to where it appears in the field of view (X and Y axes for pincushion distortion and in the Z axis for selective magnification). These parameters are to be quantified so that their effect may be removed from the image data (section 3.6).

3. Presence of a scaling factor. As discussed in chapter 2, if absolute dimensions of the lesion are required, a scaling factor must be present in the same image as the

object (eg. the stenosis) to be quantified. The typical choice is that of the catheter.

4. Superimposition. Superimposition of the arterial segment of interest upon a neighbouring opacified artery is to be avoided, as interpolation of stenotic artery borders is impossible due to their varied nature.

By adhering to the above guidelines, it became possible to select images suitable for quantification in less than one minute following loading of the film.

3.2 **Catheterization**

This section states the equipment and current practices employed by staff at Groby Road Hospital. It is not intended to be an exhaustive review of catheter procedure.

3.2.1 Tube-Image Intensifier Equipment

Groby Road Hospital has two X-ray systems currently in operation. Room A contains the single plane Thomson-CGR system composed of an Angix 80 arm, CPG 20 generator, Angiomax 80 catheterization table, Nuvicon TV system, Arritechno 35mm camera and SP11 image intensifier (16 and 23cm in diameter). Room B has the biplane Siemens system with the Cardioskop-U arm, Pondoras optimatic generator, CU catheterization table, Videomed3 TV system, Arritechno 35mm camera with Sirecon2 image intensifier (15 and 25cm in diameter). Both systems are "C" arm based and allow full X-ray tube - image intensifier rotation and angulation, as well as the more commonplace ability to alter focal spot (anode) to film distance. These capabilities avoid branch superimposition, in particular allowing for better definition of the left coronary artery main stem and its proximal branches.

3.2.2 Current Technique of Selective Arteriography

Cardiologists and Radiologists at the Groby Road Hospital currently use a retrograde percutaneous transfemoral technique for selective catheterization of the coronary vessels. The guidewire of choice is commonly 145cm in length, 0.89mm (0.035 inches) wide with a 3mm J tip as opposed to a straight tip, used to reduce the likelihood of dissection of atheromatous plaque and easing the passage through tortuous iliac arteries. Both Judkins and Amplatz catheters are used, the basic difference being secondary arm configuration and are available in polyurethane and polyethylene with a metal braid incorporated into the wall of the shaft for better "torque" control.

The catheters are usually a standard 100cm length and vary in external diameter according to the commonly used French system, where each French number is the external diameter of the catheter multiplied by three. In adults, commonly used sizes are the number 7 and 8 French with the tip tapering to a number 5 French in both cases. For contrast medium, a non-ionic preparation is preferred due to induction of lower osmolality than ionic counterparts, resulting in less cardiodepressive action during the use of the transiently high concentrations employed for coronary arteriography (Bonoron - Adele et al 1984). Iopamidol (Niopam), Merck Ltd) an Iodine based compound at 300mg ml^{-1} or 370mg ml^{-1} is the frequent choice.

Following injection of the contrast media with radiography, the resultant images are recorded on Agfagevaert film (Agfa Ltd.) and developed using standard film processing techniques. Routinely, films are available for viewing within the day although exceptions can be made for emergencies (typically, half an hour from catheterization to viewing).

3.3 **The Equipment**

The basic equipment forming the Quantitative Arteriographic Mensuration System (QAMS) is assembled according to figure 3.3.

3.3.1 The Rig

A steel framework (figure 3.4) of dimensions three feet long by three feet high by two feet wide was constructed which allowed the image projection side of the mensuration system to be housed as one functional unit. At the lower end was constructed a lift in/lift out cradle which secured the cine projector. This allowed the image origin to be fixed whilst the weight of the projector gave stability to the system. The projector could also be quickly released from the cradle if it were required elsewhere. At the upper end of the rig was built a slotted wooden framework which housed the graphics tablet. As with the projector, removal of the graphics tablet was a simple matter of withdrawing it through the top access slot. Hence both units of the projection side of the system could be used independently for other applications, ie. this equipment is by no means dedicated to the system, unlike in previous systems (Chapter 2). This allows very expensive equipment to be utilized to the full, rather than being tied to one application for perhaps only two hours per week.

The steel framework is inclined at 45 degrees to the horizontal and the graphics tablet at 45 degrees to the vertical (figure 3.4) thus providing a good ergonomic surface from which to mark the artery tracings. The rig is further constructed such that the plane of the graphics tablet, when housed, is exactly parallel to the plane of the image, thus removing any possible errors in the image due to parallax.

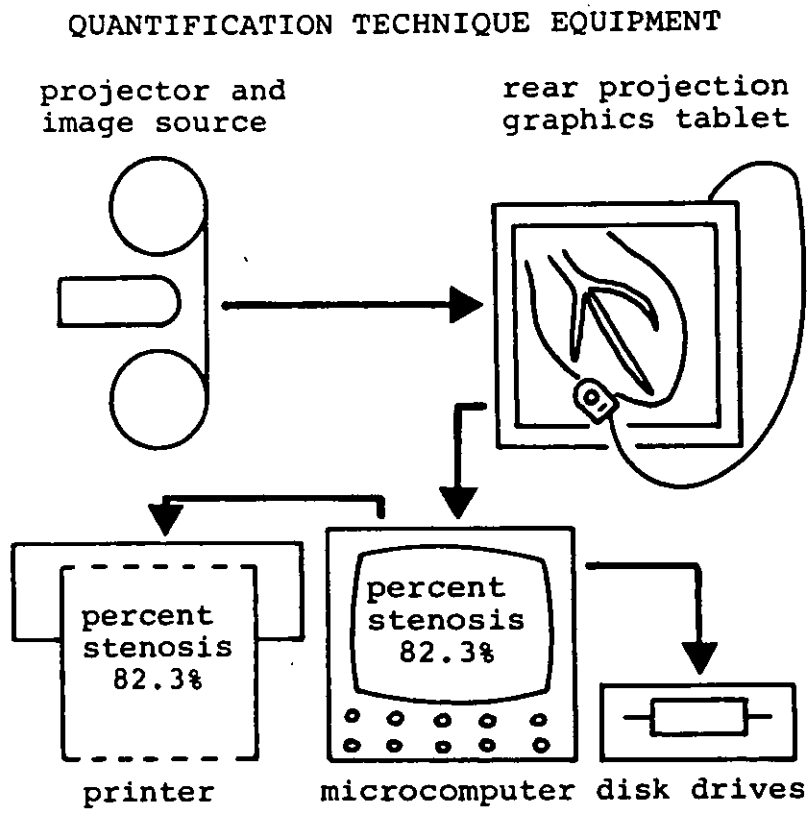

Figure 3.3 Assembly of the Quantitative Angiographic Mensuration System (Q.A.M.S.) equipment

Figure 3.4 Steel framework used for housing of projector and graphics tablet (graphics tablet shown)

3.3.2 The Cine Projector

The projector of choice was the CAP-35B 35mm cine projector (figure 3.5a and 3.5b) manufactured by the International General Electric Company (IGE - Daventry, Northamptonshire). This projector is unique in that it could be readily converted into a back projection system by merely altering the position of the internal reflecting mirror via two external controls.

Noiseless, flickerless projection is achieved through a 16 facet rotary prism; the resultant image may be magnified up to 1.6 times using the built in zoom lens (f 4.5) facility. In addition, easy to use frame trimming, single frame advance and auto stop mechanisms are provided as standard. The projector also had the necessary electronics for video display, polaroid stills and X-ray duplication.

At a weight of 55kg, it was a simple two man task to transfer the projector from its mobile stand and into the rig cradle.

3.3.3 The Computer

As it was the intention of this work to develop the software at the Department of Human Sciences, Loughborough University and apply it to cines at the Groby Road Hospital, Leicester, it seemed wise to use a computer which was common to the two establishments. For this reason the twin disk drive Vector3 (Vector Graphic inc. L.A.) was chosen (figure 3.6). The computer is based on the Z80 8 bit microchip running at 2 megahertz for the Loughborough machine and 6 megahertz (a later version) at Groby Road. Unfortunately, when the software development was complete, the Groby Road machine broke down and was judged too costly to repair. Hence the software did not receive the benefit of the extra 4 megahertz of speed. However, as this version of the QAMS is essentially a prototype, provided the system works well

Figure 3.5a Anterior view of CAP35B Cine Projector (International General Electric Company) showing loading spools and controls.

Figure 3.5b Posterior view of CAP35B Cine Projector showing rear projection aperture.

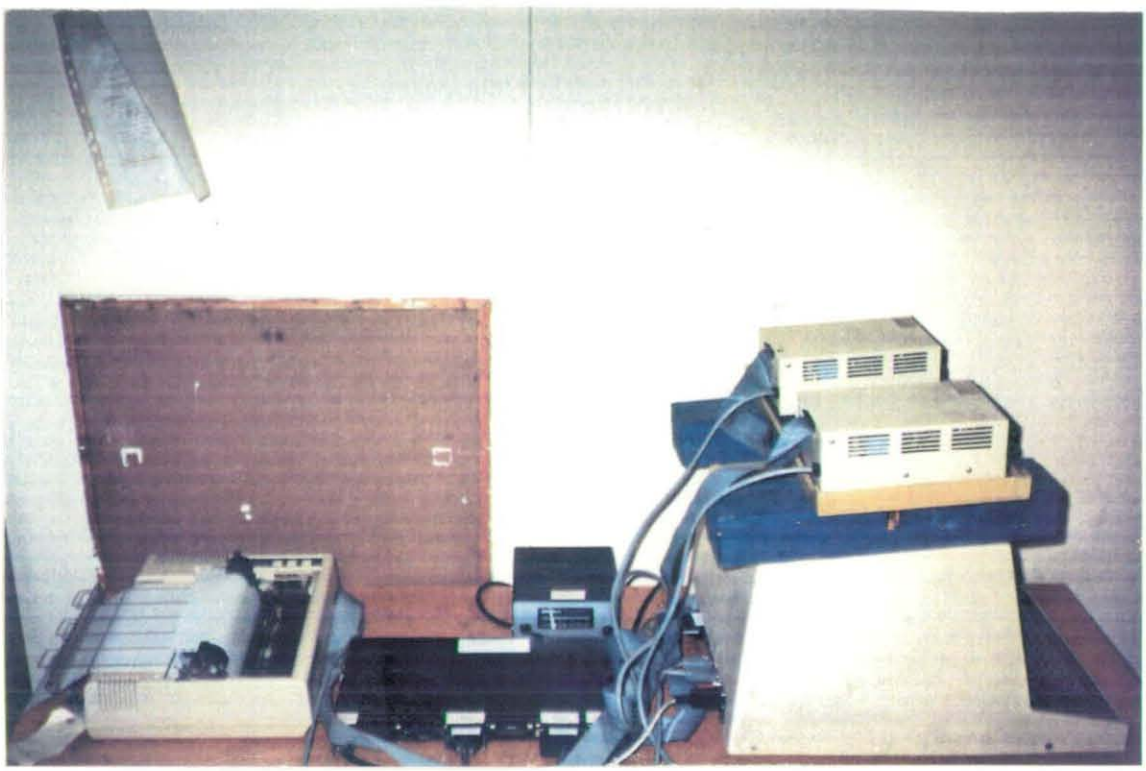

Figure 3.6 Vector 3 microcomputer (Vector Graphic Inc), printer (Epson Ltd) and graphic tablet controller with power supply (GTCO Corp).

(chapter 4), running speed may be enhanced by transferring the system to a new host microcomputer.

The computer runs the familiar CP/M (Digital Research, California) operating system version 2.2, which allows a memory configuration of 56K and data disks to be created of 560K capacity - sufficient for approximately 75 image files.

With portability and speed in mind, the Fortran programming language was employed. The two pass compiler, produced by Microsoft Ltd (Bellvue W.A.) was compatible with 1966 standards which made it slightly less flexible to use than its successor, the 1977 standard. These problems were generally overcome by use of extra programming code eg. in DO loops and IF statements, but character handling remained a problem. For this reason, it was necessary to make the initial filename acted upon by the first program common, ie. a standard filename, and either copy or rename a data file to this standard prior to processing.

The Vector3 has two ports for peripheral communication. The serial port was attached an 80 column FX80 Epson printer for hardcopy of results etc whilst the graphics tablet was connected to the RS232 port. Communications software for the transmission of data between the graphics tablet and the computer was written by the Departmental Information Technology Technician. This consisted of two programs (appendix 1 for digitization procedure):

1. A machine code routine BITPADB which allowed the graphics tablet to transmit hexadecimal coordinate information in real time at baud rate 9600 to the computer where it was written to disk under the common filename DATA.DAT.

2. A conversion program BITPADC written in the compiled BASIC language which converted the hexadecimal file DATA.DAT into denary cartesian coordinates prior to

rewriting the information to disk under a user defined filename and erasing the original DATA.DAT file.

These listings are not included in the body of this thesis as they are generic graphic tablet utilities and not specific to the QAMS (although they were originally written for this application).

As can be appreciated, this reading, writing, re-reading, rewriting sequence naturally incurred the addition of extra time to the data acquisition procedure. However, the only way the computer could process the data at the speed it was being delivered from the graphics tablet, and for it to remain reasonably error free (section 3.5), was to accept it in the hexadecimal form and reconvert it later. Indeed, many problems were encountered during this interfacing stage due to equipment failure and the exceptionally poor after sales service received from the company who provided the graphics tablet. In fact, the time from acquisition of the graphics tablet to successful interfacing measured eighteen months in total, which caused delays to improvements of the system and further work discussed in Chapter 9.

3.3.4 Graphics Tablet

In order to reduce tracing errors to a minimum, direct projection onto the graphics tablet was required. This could be achieved in one of two ways:

1. The image could be reflected from the surface of several mirrors, eventually being projected from above onto the surface of an opaque graphics tablet. However, several problems exist in using this approach. Firstly, the intensity of the light source must be powerful enough so as to produce a sufficiently bright image on the graphics tablet. Standard projectors (including the CAP-35B) use bulbs of 250-300 watt rating which was sufficient only for projection over relatively short distances. Secondly the mirrors used

in reflection process must be of high optical quality in order not to distort the projected image. These are usually very expensive. Thirdly, the angles of these mirrors relative to the source, themselves and the projection surface must be carefully aligned in order to avoid parallax errors. This would require cumbersome fixing equipment and much time spent in checking by the operator. Lastly, accurate digitization from an overhead projection is extremely difficult if not impossible due to the fact that as your hands and cursor enter the field of projection, they become the projection surface themselves, resulting in gross image distortion.

2. The image could be projected directly onto a rear projection graphics tablet, ie. a graphics tablet whose surface is translucent.

As the system was being designed to be as flexible, compact and easy to use as possible, the second option seemed to suit the requirements of the system best.

Rear projection graphic tablets are a rare commodity. However, a suitable one was selected from Dicol Ltd, Reading who are the UK repairing outlet for the GTCO corporation, Rockville, MD. The tablet (the Digi-Pad-5 - figure 3.4) has an 11" x 11" active area and was provided complete with a controller (Z80A microchip, 4 megahertz clock, RS232I/O), 5 button dual bulb cursor and power supply (figures 3.6 and 3.4).

The graphics tablet operates on an electromagnetic principle producing absolute coordinate information based upon measuring the time taken for an electromagnetic (EM) wave front to travel down an axis. The EM wave front is created by sequentially pulsing a d.c. current down consecutive copper conductor gridlines set into the tablet, spaced at half inch intervals. This induces a complex signal in the cursor coil which provides a means of measuring cursor

position by using the linear relationship between distance and time of arrival of the field at the coil. Scanning in the horizontal plane gives X axis position and the vertical plane Y axis position. Resultant cursor position information is transmitted to the controller where it is organized and packed, prior to being transmitted to the computer via the RS232 interface.

The graphics tablet has an intrinsic resolution of 0.001 inches and can operate in three modes - point, continuous and stream where it is capable of producing coordinates at a rate of 200 points per second depending on set up configuration and computer baud rate. This was judged to be far to fast for our purposes, so the lower rate of 25 coordinates per second was chosen.

The system also hosts a four tone alarm mechanism which allows immediate fault diagnosis and audible feedback on correct operation. Graphics tablet configuration, mode selection, alarm control and data handling are all dictated through the machine code program BITPADB.

3.4 **Routine Identification**

Now that the creation of a file containing X,Y ASCII coordinate data describing the digitized stenosis (appendix 1) is possible, it becomes necessary to consider how the system will transform this information into meaningful results.

3.4.1 Initial Considerations

The overriding consideration is, of course, accuracy. Coordinate output rate from the graphics tablet is fixed at 25 points per second and computer memory is fixed at 56K. Timed trials (tracing of a stenosis) revealed that it was necessary to spend 30 to 40 seconds in the digitization procedure (appendix 1) for accurate results to be achieved. Each coordinate is an integer number which requires two

bytes of storage space in computer memory. Therefore, by simple calculations, the maximum data storage area required for one tracing is 4K:

2 (X,Y coordinates) x 2 (No. bytes per coordinate) x 40 (tracing time) x 25 (rate per second)

equals 4000, approximately equal to 4K

The compiler required to transform the object code into runnable code consumes another 16K of memory. Therefore, total source program size must not exceed 36K maximum for successful compilation.

After identification of the areas required for transformation of the raw data into meaningful results (section 3.4.2), it was decided that 36K was not enough space to accommodate a program with all the recognized potential; each section should therefore be written and run as a separate entity, with the full suite of programs assembled in a batch formation allowing automatic concurrent implementation. This would also allow each program to be fully documented within the source code to facilitate use and change by other users in the future. However, this "building block" approach must be traded off against the extra running time carried in re-reading the data for every program . In the future, transfer of the system to a larger machine will allow combination of some if not all these programs, therefore removing this problem.

The effects of pincushion distortion are to be removed from the data prior to any handling or calculations, whereas the reduction to true scale is to be left until all processing is complete. This will allow the data to be preserved in its integer format, thereby keeping memory requirements for data to the minimum. The reference for magnification is to be the injecting catheter as with previous systems (Brown et al 1977), so that no additional work need be done at the time of catheterization (MacAlpin et al 1973).

The system is to work initially in single plane format, thereby accepting the documented error of 1.5% of estimate per centimetre axial displacement between the location of the stenosis and the catheter. Whilst no error in a system is most desirable, it was judged that this level of discrepancy was acceptable, especially in the light of this systems major application in this thesis (chapter 7), where proximally situated lesions are most frequent, therefore axial displacement is at a minimum. It was the intention to write a program capable of matching coordinate data from two views once the initial single plane programs had proven themselves. Unfortunately, due to the excessive time required to produce a working software interface between the graphics tablet and the computer, and concern over memory limitations, this was never achieved. However, an algorithm for a matching program is presented in appendix 1. This is by far the most important aspect of future work (chapter 9) for continued use of this system.

3.4.2 Algorithm Identification

This section divides the problem of the production of meaningful information from a tracing into its constituent parts. These parts are discussed under the program titles they eventually became focusing mainly on what the program does and what files are produced as a consequence. The mathematical basis of each program is discussed in the following section.

PROGRAM PNTED

The raw data exists as a file on disk arranged as sequential X and Y coordinates according to the program BITPADC (section 3.3.3 and appendix 1). Information on demarcation between the relevant sections of the file (appendix 1) is contained in the first 12 lines of the file, the "header". The first task therefore it to read the data from the file and divide it up into its constituent parts so that each may be handled separately. Following this, all data should be

corrected for pincushion distortion according to the catheter room the investigation took place in, so that the system is dealing with data representative of true life in all aspects apart from magnification. The corrected data from the digitized catheter is then written to file under the filename POINTMAG.NIF for use by a later program.

As will be appreciated, when a user is tracing an object at slow speed and coordinates are being delivered at a relatively high rate, it is easy for the same coordinate position to be registered twice, or more. Also, precise control of hand movements is achieved by fine interplay between the forces developed by the wrist extensors and flexors. This invariably leads to slight tremor of the hand during the tracing procedure. Since the graphics tablet used in this application is sensitive to changes of one thousandth of an inch, it is also quite possible to enter coordinates whose location is opposite to the general direction of tracing. Program PNTED removes these coincident points and then the so called reversals by comparing the amount of "reversed" displacement with values derived from a hand tremor experiment (section 3.6.1). Hence the system is then presented with data free from the artifacts of tracing ie. it is said to be "clean". This area of methodology has not previously been discussed or employed by previous systems, although it is fair to say that less accurate graphic tablets have commonly been used, and these corrections to the data may not have been necessary.

The resultant data are written to the files SIDE1POI.NTS and SIDE2POI.NTS for use by the next program.

PROGRAM DIAMAV

Every stenosis morphology is different. Therefore every tracing of stenosis will differ, one of the basic differences being the coordinate density. It is true to say that a user will spend relatively more time digitizing a

stenosis with complex morphology than one of simpler structure. An ideal system will base calculations pertaining to a stenosis specifically to that stenosis, rather than assuming a global factor by which all stenoses should be processed, eg. the use of a 64 x 64 matrix in Reibers edge detection system. Program DIAMAV provides this criterion on the assumption that the artery is unlikely to grossly alter its general direction over a relatively small distance.

An easily calculable parameter which takes into account coordinate density and is specific to each individual tracing is the average diameter of the stenosis. Therefore program DIAMAV calculates this individualistic factor and writes it to disk under the filename AVERAGED.IAM for future use.

PROGRAM DIAMRS

The basic function of the system is to produce serial diameters along the length of a digitized stenosis which are at right angles to its long axis. This is the task achieved by program DIAMRS. The program uses the factor generated by the previous program to limit calculations to overlapping areas (from now on referred to as "the bubble") whose size (parameter bublen) is dictated by individual morphology, where coordinates are generated representing the positions of the ends of the aforementioned diameters. These are sequentially written to the file DIAMETER.EPS for use in the following program.

PROGRAM ANALYZ

Program ANALYZ firstly reads the contents of the file POINTMAG.NIF and derives the apparent size of the catheter for magnification correction. It then reads the file DIAMETER.EPS and calculates the apparent diameters, cross sectional areas and lengths from the X,Y coordinate data contained within (section 3.5). The program lastly reduces

all the parameters to true scale based on the French value of the catheter used (user input), before writing the results to screen and/or printer.

PROGRAM ECCFTR

Lesion eccentricity, defined as degree of offset of the stenotic diameter in comparison to the "normal", has been of interest to various workers in Cardiology (Meier et al 1983b) but as yet has not been quantified, perhaps in part due to inferior techniques used to recreate original artery profile (section 2.2.3). This program amends these shortcomings by producing a file (ARCRADII.EPS) of undiseased diameter points representing the morphology of the artery if disease were absent. However, the user must exercise judgement in selecting stenoses where undiseased morphology construction is valid (section 3.5).

Area calculations are also performed on the undiseased and diseased artery areas, resulting in the quantification of atheromal area. Values for mean eccentricity, maximal eccentricity and eccentricity at minimum diameter are subsequently computed and written to screen and/or printer.

PROGRAM ARTDR

Graphical as well as numeric output is always useful in the assessment of stenotic morphology. This program produces such output allowing the display of the lesion diameters, the undiseased diameters, the artery axis or combinations of these data according to the users choice.

Unfortunately, due to the lack of graphics facilities on the Vector3 microcomputer, this program is only available on the University's Prime Mainframe Computer. However, should the system be transferred to a modern machine, this facility could easily be recreated, allowing the production of permanent pictorial records for patients notes.

Figure 3.7 presents simply the overall schema for the QAMS system.

3.5 Software Theory

It is important to stress at this point that the production of software for a working version of QAMS has been a developmental process, ie. the work presented in this section is only a fraction of the work that was actually required in order to arrive at successful methodology. Many initial ideas have either seen extensive revision or have been superseded by more elegant or practical methodology.

Throughout the development and validation of the QAMS software, all coding and testing was performed on the Prime System as the Fortran compiler was much faster than that on the Vector3 thus allowing small changes to be made much more quickly. Once the programs were complete and running properly, they were downloaded to the Vector3.

As the information provided by the graphics tablet is basically geometric, each X,Y coordinate being considered to be connected to the next by a straight line, it is not surprising that the majority of the theory behind the workings of the system has its foundations in single plane trigonometric geometry. Special emphasis has been placed on keeping the mathematical solutions to problems as simple as possible, since the system is aimed for use by biologists or Doctors, not mathematicians.

A full listing of every program concerned with QAMS can be found in appendix 1. It is not the intention of this section to exhaustively review each routine line by line. Much of the code is simple, either involving the linking of various program sections or performing simple error trapping, with most steps adequately explained within the listing itself - a luxury afforded by the use of several smaller programs rather than one larger one. Therefore each program is presented as a figure depicting a flow diagram or

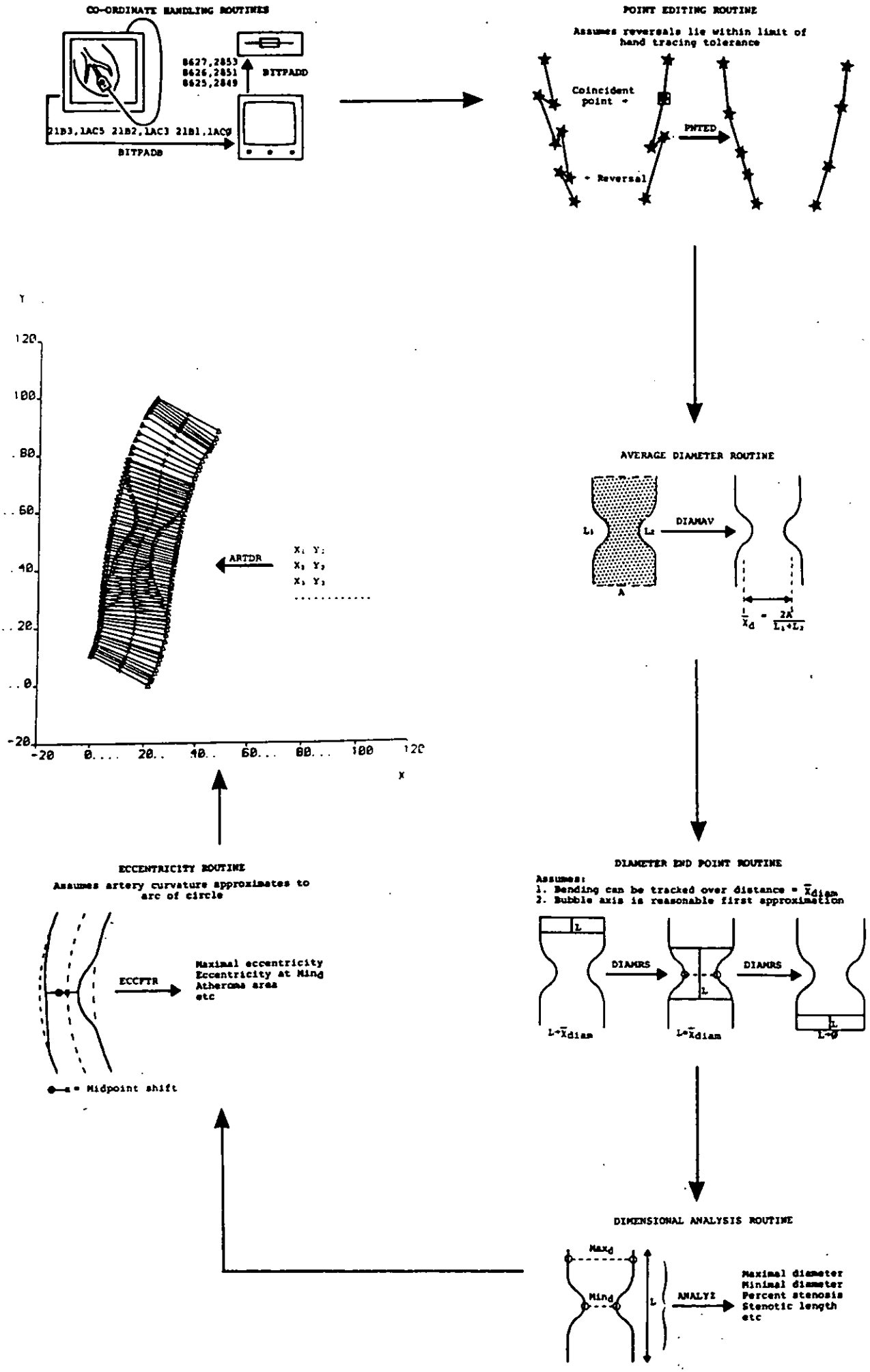

Figure 3.7 Overall schema for the QAMS system

algorithm. However, mathematically more intricate areas (those in the square boxes) require further explanation. This appears as relevant text and separate figures within this section. It is important to note that each derivation of an expression or explanation of a routine subsection will not appear exactly as found in the listing, for it is the proof of the methodology which is important, not its translation into Fortran 66. However symbols and parameter names used by the programs are adhered to in the proof for direct comparison, except when the same program element has been used again in a later program, when the element is simply re-referenced in order to minimize duplication.

PROGRAM PNTED

As per algorithm presented in figure 3.8. The following areas are highlighted for further discussion.

The correction of data for pincushion distortion - SUBROUTINE PCUSH

Location of the 1st and 2nd coordinates outside the tolerance limit.

The reversal check - SUBROUTINE PPSIDE.

SUBROUTINE PCUSH. This subroutine applies a correction to each coordinate point such that the effect of pincushion distortion (section 2.2.3) is removed. The equation used to characterize this distortion was based on the fact that the origin of the distortion is the convexly curved nature of the input phosphor vacuum tube.

If one films a rectilinear grid, the result is a distorted rectangular image (figure 3.9). Grid interval appears to vary as a function of the square of the radial distance from the centre of the image (personal communication, Phillips Medical Systems, Hammersmith, London). This ties in with the fact that the distorting element is quadratic in nature.

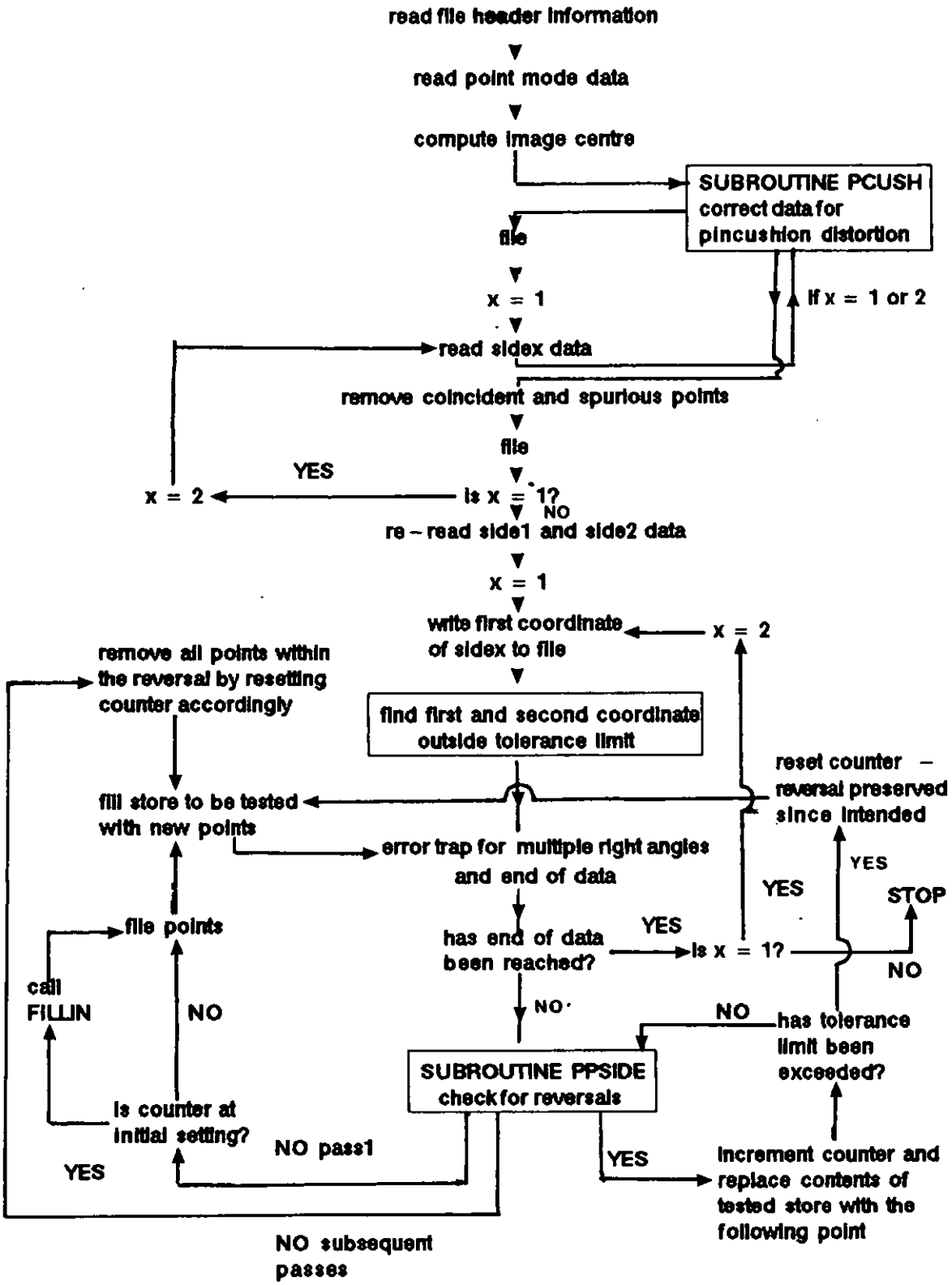

figure 3.8 PNTED algorithm

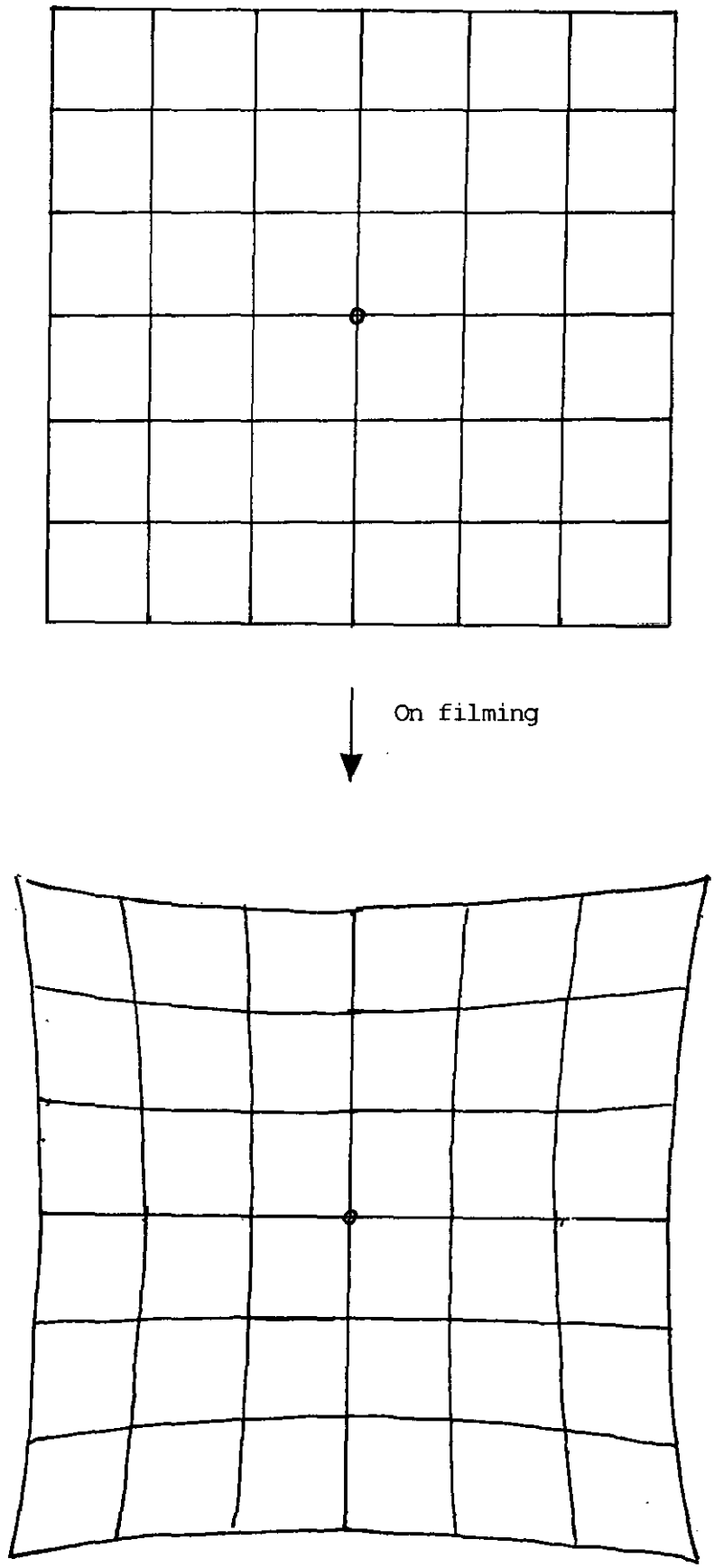

Figure 3.9 The pincushion distortion effect

Since grid interval at the centre of the image is unaffected (ie. unity) the following basic equation may be formulated:

$$\frac{\Delta R}{\Delta R_o} \propto 1 + R^2$$

Where ΔR = The projected grid interval.
ΔR_o = The undistorted grid interval (and for practical purposes that at the centre of the image).
R^2 = The square of the radial distance from the centre of the image.

In order to obtain equality, a constant (C) must be added to the equation which quantifies the amount of distortion for the system from which the image under consideration was obtained.

$$\frac{\Delta R}{\Delta R_o} = 1 + CR^2$$

This equation must be rewritten and integrated in order to arrive at an expression which quantifies pincushion distortion at each and every point at radius R from the centre of the image. Thus:

$$R^1 = \frac{1}{\sqrt{C}} \cdot \tan^{-1} (R.\sqrt{C})$$

Where R^1 is the true radial distance from the centre of the image to the point of interest.

The above equation forms the basis of the correction procedure employed in the SUBROUTINE PCUSH. The derivation of C is reported in the characterization experiments, section 3.6.1.

LOCATING COORDINATES. This area of software has been highlighted in order to present the derivation of the method

for calculating the length of a line joining two distinct coordinate points, as this piece of coding is used repeatedly throughout the suite of QAMS programs. The introduction of the tolerance limit theory is reserved for the validation experiments in section 3.6.

Referring to the diagram in figure 3.10 it can be seen that the length of a line may be resolved using pythagoras theorem ie:

$$C = \sqrt{(X1-X(J))^2 + (Y1 - Y(J))^2}$$

On expansion:

$$C = \sqrt{X1^2-2X1X(J)+X(J)^2+Y1^2-2Y1Y(J)+Y(J)^2}$$

On rearranging:

$$C = \sqrt{(X1^2+X(J)^2+Y1^2+Y(J)^2-2(X1X(J)+Y1Y(J)))}$$

This is the equation found in the software listing for the location of the 1st and 2nd points outside of the tolerance limit.

FUNCTION PPSIDE. This function allows serial detection of the "direction" of the data vector. This is achieved by constructing a circle of uncertainty of radius equal to hand tracing tolerance (section 3.6) with centre at the second of every set of three coordinates. The segment connecting points 1 and 2 dictatesthe direction of the vector, with the dividing line between constant direction and reversal being made from a test of the position of the third coordinate with respect to the perpendicular to the direction segment, a point lying on the perpendicular or on the same side as the direction vector is deemed a reversal, whilst a point on the opposite side of perpendicular to the direction vector has the same direction as the direction vector.

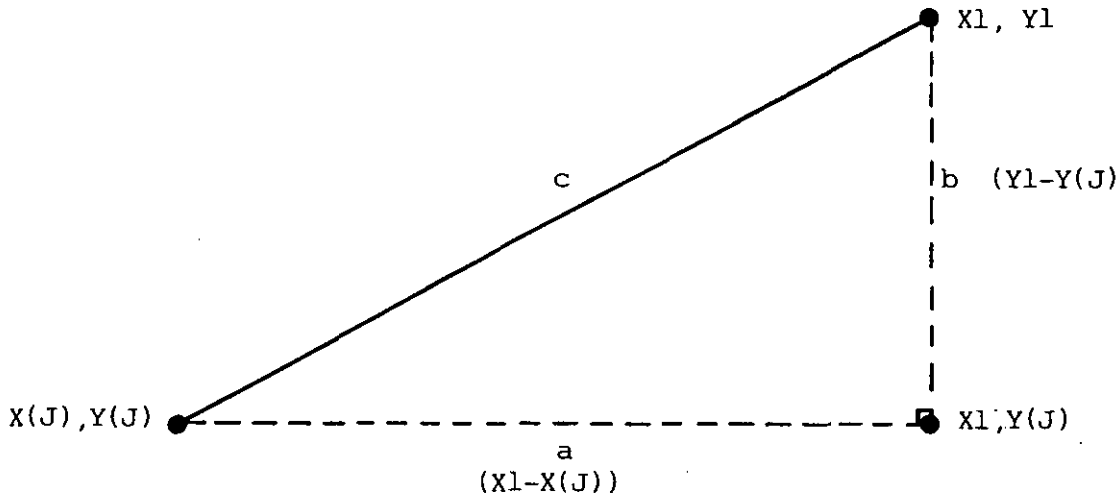

Pythagoras theorem stages:

$$c^2 = a^2 + b^2$$

Therefore $c = \sqrt{a^2 + b^2}$

Substituting above terms:

$$c = \sqrt{(X1-X(J))^2 + (Y1-Y(J))^2}$$

On expanding

$$c = \sqrt{X1^2-2X1X(J) + X(J)^2 + Y1^2 - 2Y1Y(J) + Y(J)^2}$$

Collecting like terms

$$c = \sqrt{X^2 + X(J)^2 + Y1^2 + Y(J)^2 - 2(X1X(J) + Y1Y(J))}$$

Figure 3.10 Calculation of the length of a line using Pythagoras theorem

The physical size of the circle of uncertainty is used by the main program to decide when a reversal test is actually required. ie. points within the circle are to be tested since the reversal may be a function of hand tremor - the effect trying to be removed, whereas points outside the circle are not tested since the reversed direction is assumed to be implied. Figure 3.11 exemplifies the workings of the reversal test with various possibilities.

The test revolves around deriving the equation of the perpendicular to the direction vector and substituting in it the values of the coordinates to be tested. In order to achieve this, one must first calculate the coordinate values of two points which lie on this line. Considering the situation presented in figure 3.12, it can be seen that the gradient angle of the direction vector may be represented in terms of both sine and cosine thus:

$$\text{SINGRA} = \frac{\text{OPPOSITE}}{\text{HYPOTENUSE}} = \frac{y}{R}$$

$$\text{COSGRA} = \frac{\text{ADJACENT}}{\text{HYPOTENUSE}} = \frac{x}{R}$$

These values allow the construction of two similar triangles at right angles to the direction vector with hypotenuse length each equal to the tolerance value, thereby establishing the circle of uncertainty. Using simple trigonometry, distances d_1 to d_4 may be calculated in order to allow translation of the coordinate values of X2,Y2 to points on the perpendicular line at the limits of hand tracing tolerance thus:

$$\text{For } d_1 \quad \text{SINGRA} = \frac{\text{OPPOSITE}}{\text{HYPOTENUSE}} = \frac{d_1}{\text{TOL}} \qquad d_1 = \text{SINGRA X TOL}$$

$$\text{For } d_2 \quad \text{COSGRA} = \frac{\text{OPPOSITE}}{\text{ADJACENT}} = \frac{d_2}{\text{TOL}} \qquad d_2 = \text{COSGRA X TOL}$$

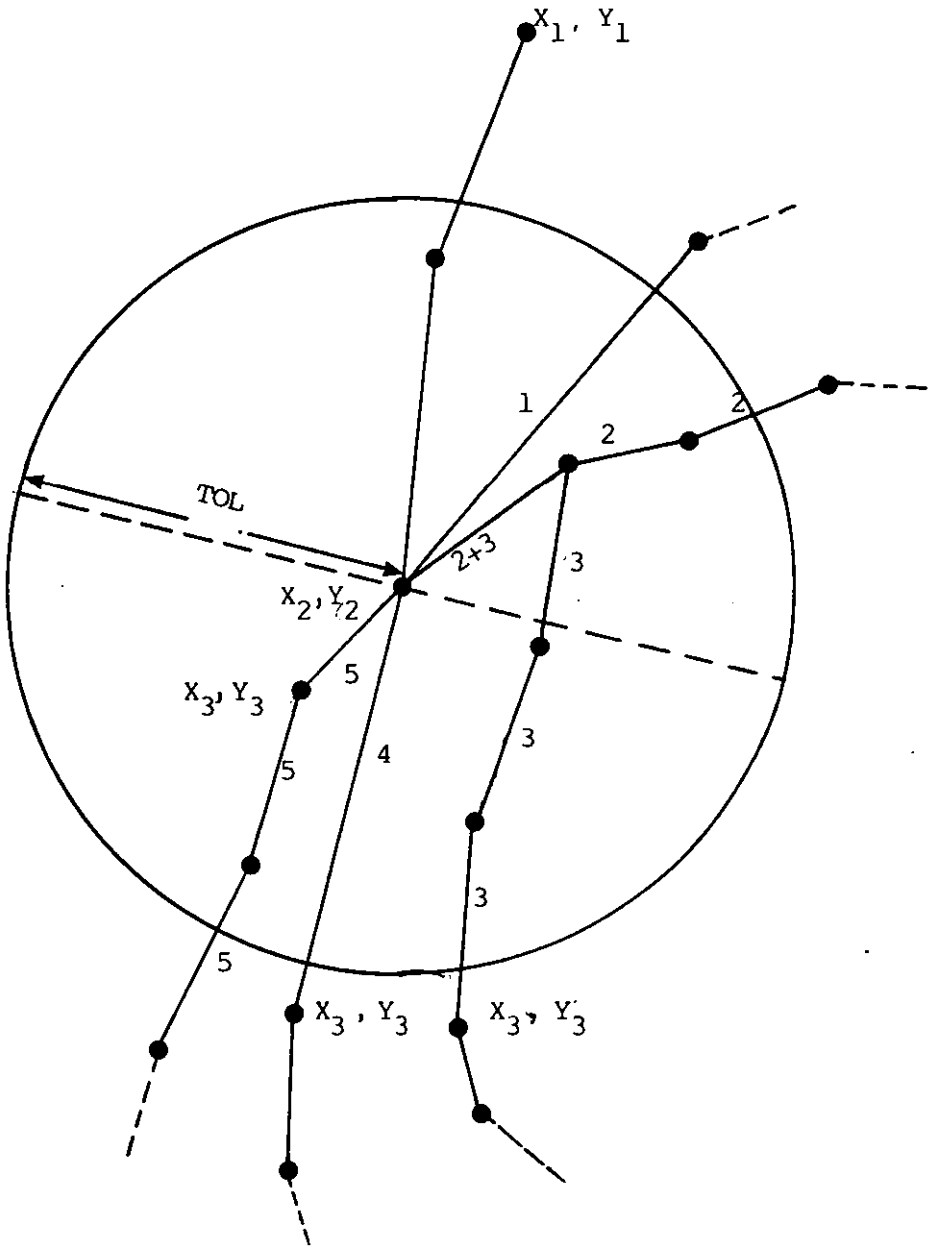

No	Condition	Action
1	Intended reversal	none - Intentional change in direction
2	Intended reversal	none - Intentional change in direction
3	Unintended reversal	Points between X_2Y_2 and X_3Y_3 removed
4	Vector direction maintained	none - Relative coordinate position correct
5	Vector direction maintained	none - Relative coordinate position correct

Figure 3.11 Reversal test possibilities

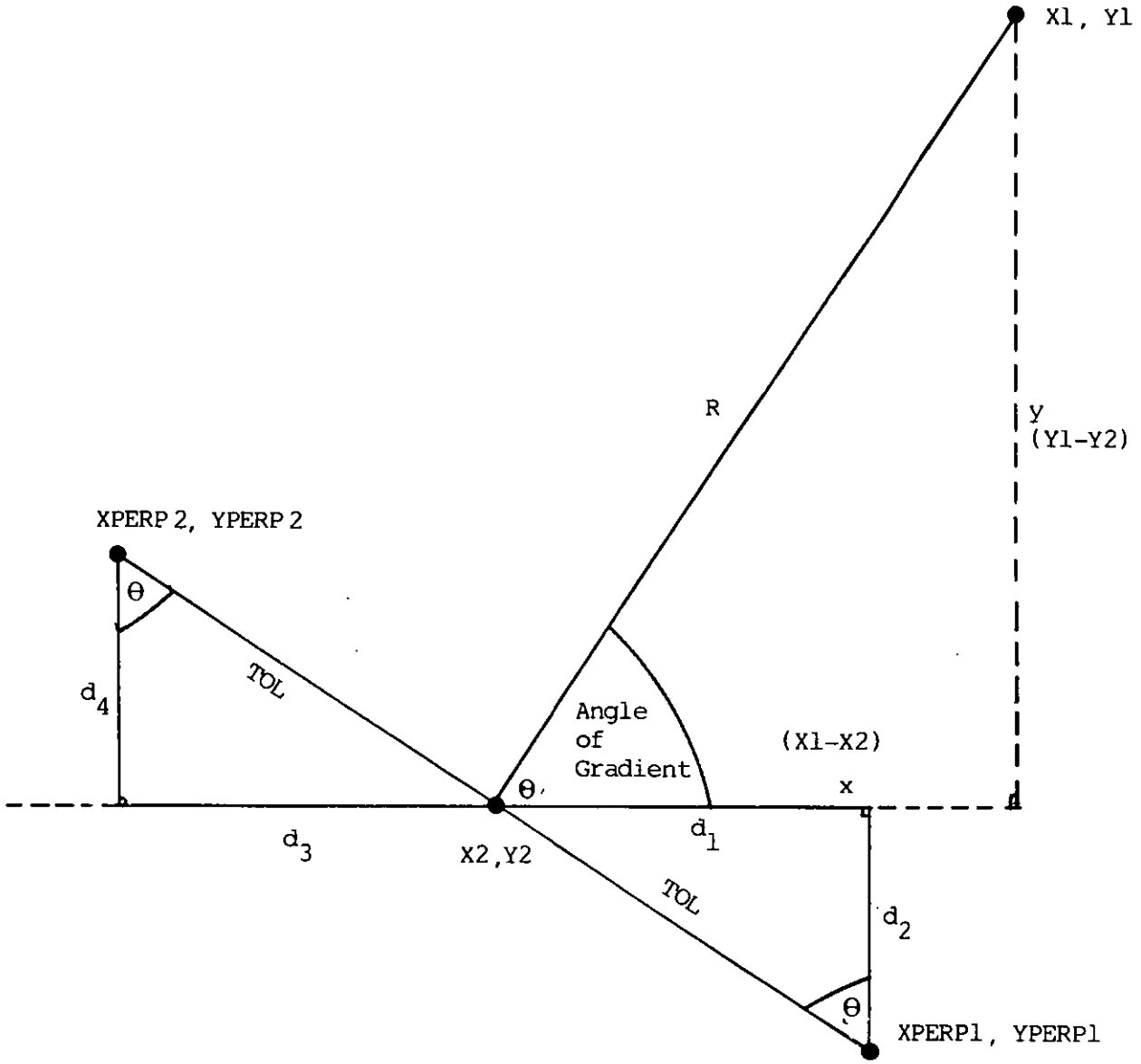

Sine gradient angle = $\frac{y}{R}$

Cosine gradient angle = $\frac{x}{R}$

Using similar triangles:

Sine gradient angle = $\frac{d_1}{TOL}$ $\therefore$ d_1 = Singrad x TOL

Cosine gradient angle = $\frac{d_2}{TOL}$ $\therefore$ d_2 = Cosgrad x TOL

On translation :

XPERP1 = X2 + d_1

YPERP1 = Y2 + d_2

Similar operations are carried out for computing XPERP2 and YPERP2

Figure 3.12 Formation of perpendicular, subroutine PPSIDE

Translating: $XPERP1 = X2 + d_1$

$YPERP1 = Y2 - d_2$

A similar transformation is made for XPERP2,YPERP2. Evaluation of the equation of the line perpendicular to the direction vector may now be made.

It can be seen from figure 3.12 that construction of similar triangles effects a rotation of the parent triangle by 90 degrees in either direction depending on which triangle is considered. Considering just the upper triangle of figure 3.12 for demonstration purposes (figure 3.13), the gradient may be expressed as:

$$\text{Gradient} = \frac{\text{Increase in y}}{\text{Increase in x}} = \frac{YPERP2 - YPERP1}{XPERP2 - XPERP1}$$

The general equation of a straight line may be written as:

$$y = ax + b$$

In order to derive an expression for b, the intercept, we must first consider the equation in its most simple form, ie. with the intercept at 0, that is:

$$y = ax$$

For any point X,Y (figure 3.13):

$$Y - Y2 = \frac{YPERP2 - YPERP1}{XPERP2 - XPERP1} \cdot (X - X2)$$

Rearranging:

$$0 = \frac{YPERP2 - YPERP1}{XPERP2 - XPERP1} \cdot (X - X2) - Y + Y2$$

Multiplying out (NB. Some terms reverse to maintain positivity):

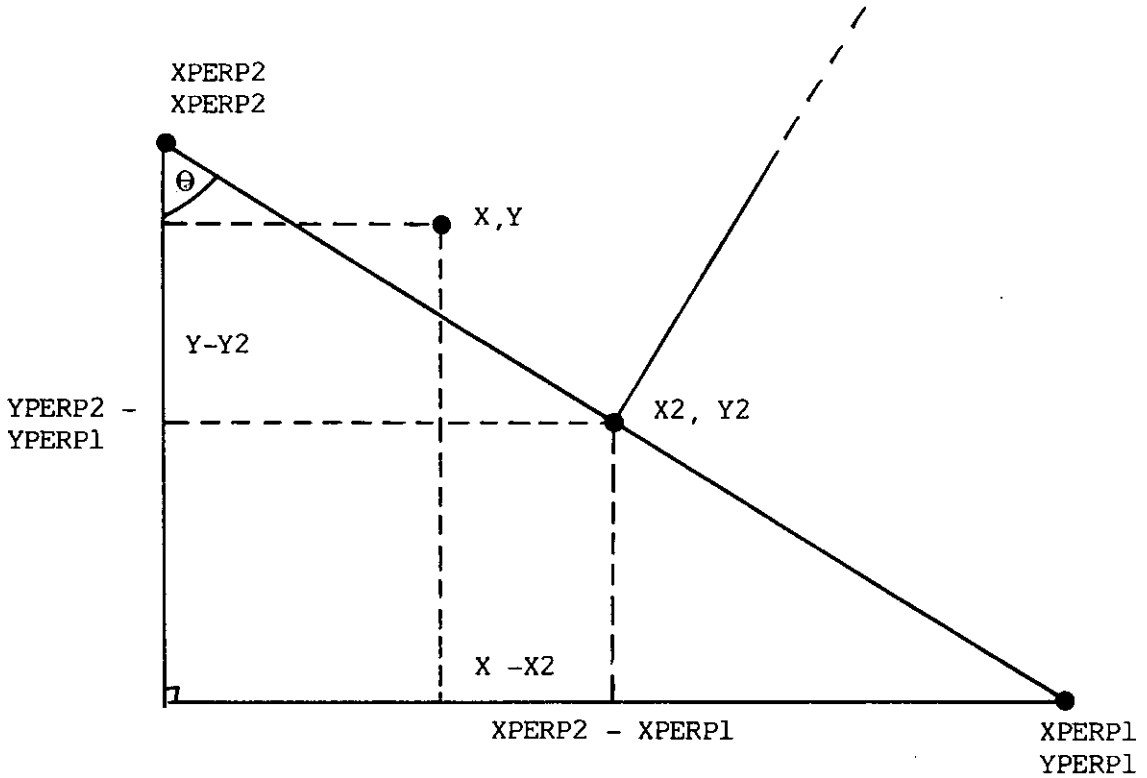

General equation of line for point X, Y

$$Y - Y2 = \frac{YPERP2 - YPERP1}{XPERP2 - XPERP1} (X - X2)$$

Figure 3.13 Computation of the general equation for the perpendicular, subroutine PPSIDE

```
0 =  (YPERP2 - YPERP1)X + (XPERP1 - XPERP2)Y +
      X2(YPERP1 - YPERP2) + Y2(XPERP2 - XPERP1)

0 =  (YPERP2 - YPERP1)X + (XPERP1 - XPERP2)Y +
      X2.YPERP1 - X2.YPERP2 + Y2.XPERP2 - Y2.XPERP1

0 =  (YPERP2 - YPERP1)X + (XPERP1 - XPERP2)Y +
     (X2.YPERP1 + Y2.XPERP2) - (X2.YPERP2 + Y2.XPERP1)
```

The equation is now in the form found in the program listing and has reduced to the coefficient method for the expression of the equation of a straight line, ie. 0 = aX + bY + constant.

The constant evaluates to zero in the simple case (origin at 0,0) but is mathematically correct to return a value of b when the line originates elsewhere.

This equation is then used in the program to test the position of the third coordinate point. This is achieved by considering the perpendicular line in question to be neighboured by many other perpendicular lines of obviously equal gradient, but differing intercept. If the point lies on the perpendicular line, then as proved, the result will be zero. If, however, the point lies above the line, then the result with be negative and vice versa. The resultant discrepancy between the calculated value and zero is a function of the differences in intercept only. As parallel gradients are the same, the difference reflects the shortest distance (Y value to Y value) between the two lines. The implication of this latter point becomes apparent in PROGRAM DIAMRS.

Based on the sign of the difference, the function ascribes a result of either +1, 0 or -1. Within the same line of code in the main program, the function is called again, this time with the 1st point of the three being the coordinate to be tested. The function duly returns a value of +1, 0 or -1 as

before, and the results to the two tested points are compared; if the results are the same, then a reversal has occurred, as point 3 is on the same side of the perpendicular as point 1, whereas if the results are opposite, then point 3 is on the opposite side of the perpendicular to point 1 and constancy of direction is deemed to have been preserved in this particular three point complex.

PROGRAM DIAMAV

Refer to algorithm presented in figure 3.14.

CALCULATION OF AVERAGE ABSOLUTE AREA AND AVERAGE DIAMETER. The artery tracing can be considered to be a continuous loop by simply joining of the two ends. From this loop a centroid may then be calculated by simple averaging of all points within that loop. The total area of the figure may now be obtained from the addition of all the separate triangles which constitute it.

In order to arrive at an expression for the compuation of triangle area one must again return to the simplest case, that of the triangle having a vertex at the origin, or 0,0.

From figure 3.15 it can be seen that the area of the hatched region is a product of the following expression:

$$\text{Area } OP_1P_2 = \text{Area } OA_2P_2 + \text{Area } A_1P_1P_2A_2 - \text{Area } OA_1P_1$$

Now, the area of a simple triangle is equal to the base multiplied by the height divided by two and of a rhombus base multiplied by average height, therefore:

$$\text{Area } OP_1P_2 = \tfrac{1}{2}OA_2 \times A_2P_2 + \tfrac{1}{2}(A_2P_2 + A_1P_1) \times A_2A_1 - \tfrac{1}{2}OA_1 \times A_1P_1$$

The distance O to A_n are displacements in the x direction of n units and A_n to P_n displacements in the y direction again of n units.

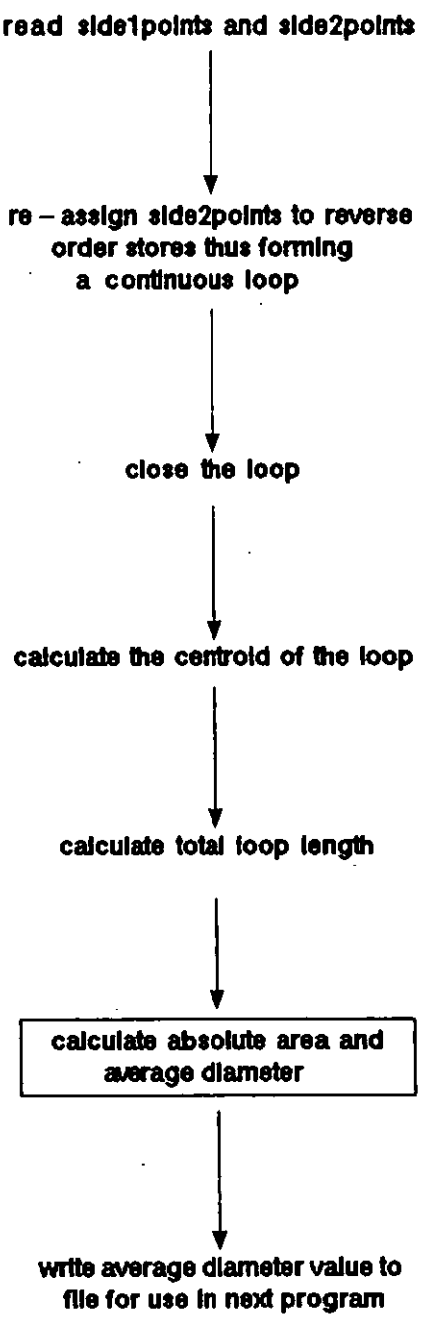

figure 3.14 DIAMAV algorithm

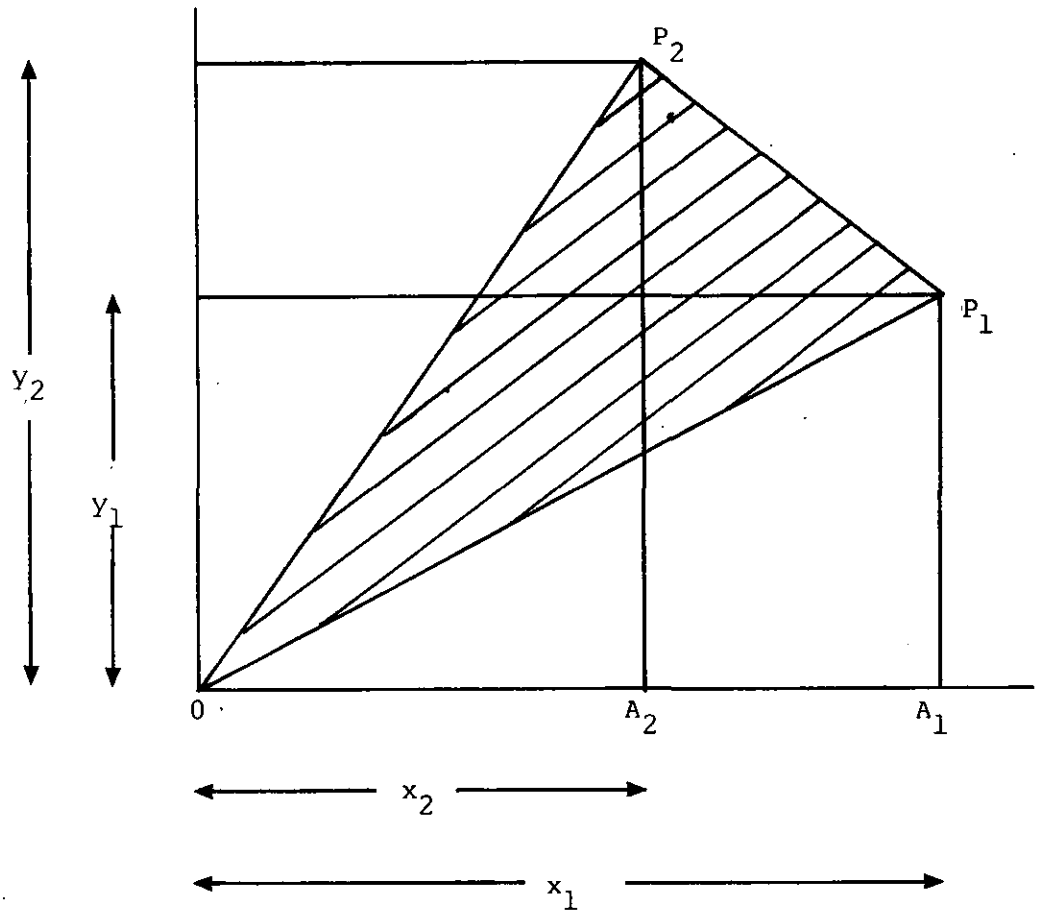

Area $OP_1P_2 = \frac{1}{2}(X_1Y_2 - X_2Y_1)$

Figure 3.15 Area of a triangle with one vertex at the origin

Substituting:

$$\text{Area } OP_1P_2 = \tfrac{1}{2}x_2y_2 + \tfrac{1}{2}(y_2+y_1)(x_1-x_2) - \tfrac{1}{2}x_1y_1$$

Expanding:

$$\text{Area } OP_1P_2 = \tfrac{1}{2}(x_2y_2 + x_1y_2 - x_2y_1 - x_2y_2 + x_1y_1 - x_1y_1)$$

$$\text{Therefore area of triangle } OP_1P_2 = \tfrac{1}{2}(x_1y_2 - x_2y_1)$$

The sign of the resultant area depends upon the direction of rotation. In this example, rotation is from P_1 to P_2 ie. from OX to OY. This is the positive plane of rotation and returns a positive answer. Rotation in the opposite direction would yield an answer numerically equivalent to the previous, yet opposite in sign. The significance of this effect is given later.

If the origin is within the perimeter of the triangle (Figure 3.16a), the total area is the sum of the three component triangles thus:

$$\text{Area } P_1P_2P_3 = OP_2P_3 + OP_3P_1 + OP_1P_2$$

Substituting the above derived expression for the area of a triangle:

$$\text{Area } P_1P_2P_3 = \tfrac{1}{2}(x_2y_3-x_3y_2)+\tfrac{1}{2}(x_3y_1-x_1y_3)+\tfrac{1}{2}(x_1y_2-x_2y_1)$$

However, the more normal case (typical of this work) is for the origin to be removed from the triangle (figure 3.16b). Relating the coordinates of P_1, P_2 and P_3 to the origin reveals that the area of the component triangle is given by:

$$\text{Area } P_1P_2P_3 = \text{Area } OP_2P_3 - \text{Area } OP_2P_1 - \text{Area } OP_1P_3$$

Each constituent area is a triangle in its own right, therefore we may substitute the previously derived expression for their area, ie:

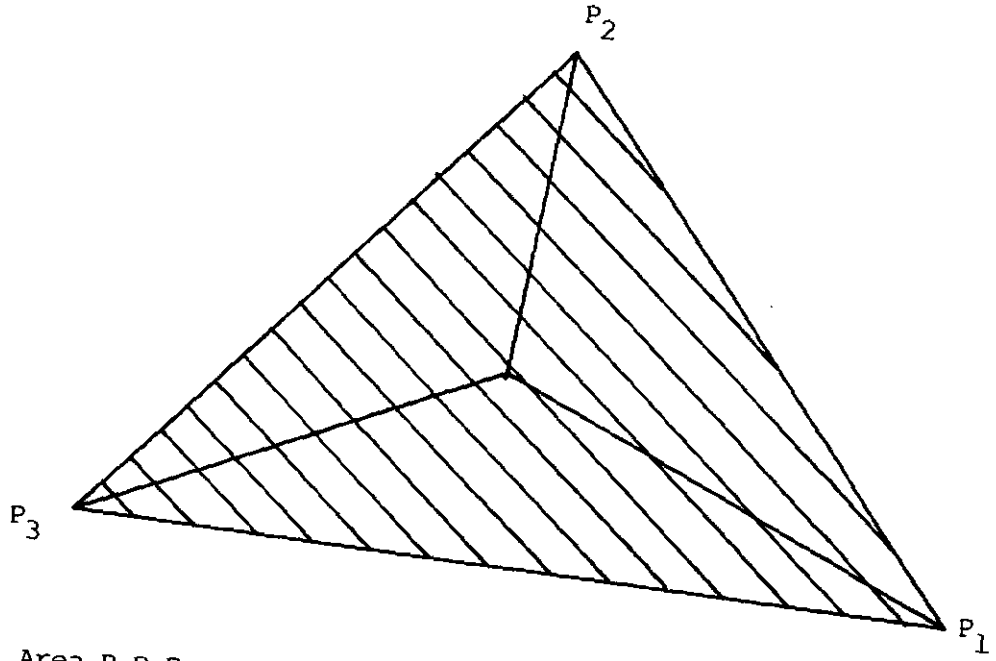

Area $P_1P_2P_3 = OP_2P_3 + OP_3P_1 + OP_1P_2$

Figure 3.16a Area of triangle $P_1P_2P_3$ with enclosed origin

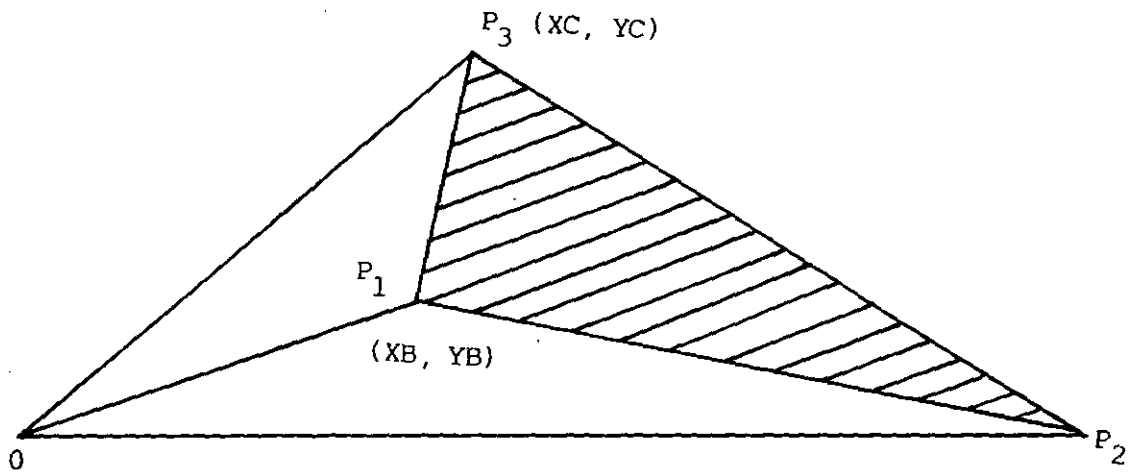

$$\text{Area } P_1P_2P_3 = OP_2P_3 - OP_2P_1 - OP_1P_3$$

$$= \frac{((XBXA + YCXB+YAXC) - (YBXC+YCXA+YAXB))}{2}$$

Figure 3.16b Area of triangle $P_1P_2P_3$ with removed origin

$$\text{Area } P_1P_2P_3 = \tfrac{1}{2}(x_2y_3-x_3y_2) - \tfrac{1}{2}(x_2y_1-x_1y_2) - \tfrac{1}{2}(x_1y_3-x_3y_1)$$

The negative term may now be removed by rearrangement, yielding the expression for area found in the program listing.

$$\text{Area } P_1P_2P_3 = \tfrac{1}{2}(x_2y_3-x_3y_2) + \tfrac{1}{2}(x_1y_2-x_2y_1) + \tfrac{1}{2}(x_3y_1-x_1y_3)$$

By further arrangement:

Constituent Area = ((YBXA+YCXB+YAXC)-(YBXC+YCXA+YAXB))/2

When the tracing shape is complex, ie. the profile folds in on itself (figure 3.17), it is evident that the direction of rotation for the calculation of the area is reversed, hence the result is negative. If all areas, positive or negative are accumulated, then the resultant will be the area only enclosed by the loop, all infolds will have been removed by the reversed direction technique.

If, whilst the areas are accumulated, the segment lengths are computed also (length of line technique, PROGRAM PNTED), total perimeter length of the tracing will be derived. From this, average artery side length may be computed as half the perimeter length. Whilst this is not the **true** average side length due to inclusion of the segments joining the two ends of the data arrays, it is still related to the tracing in question and is therefore specific.

The average side length may then be used to calculate the average diameter of the tracing for use as scan size criterion in the following program as follows:

$$\text{Dimensionally, Average diameter} = \frac{L^2}{L} = \frac{\text{Total tracing area}}{\text{Average artery side length}}$$

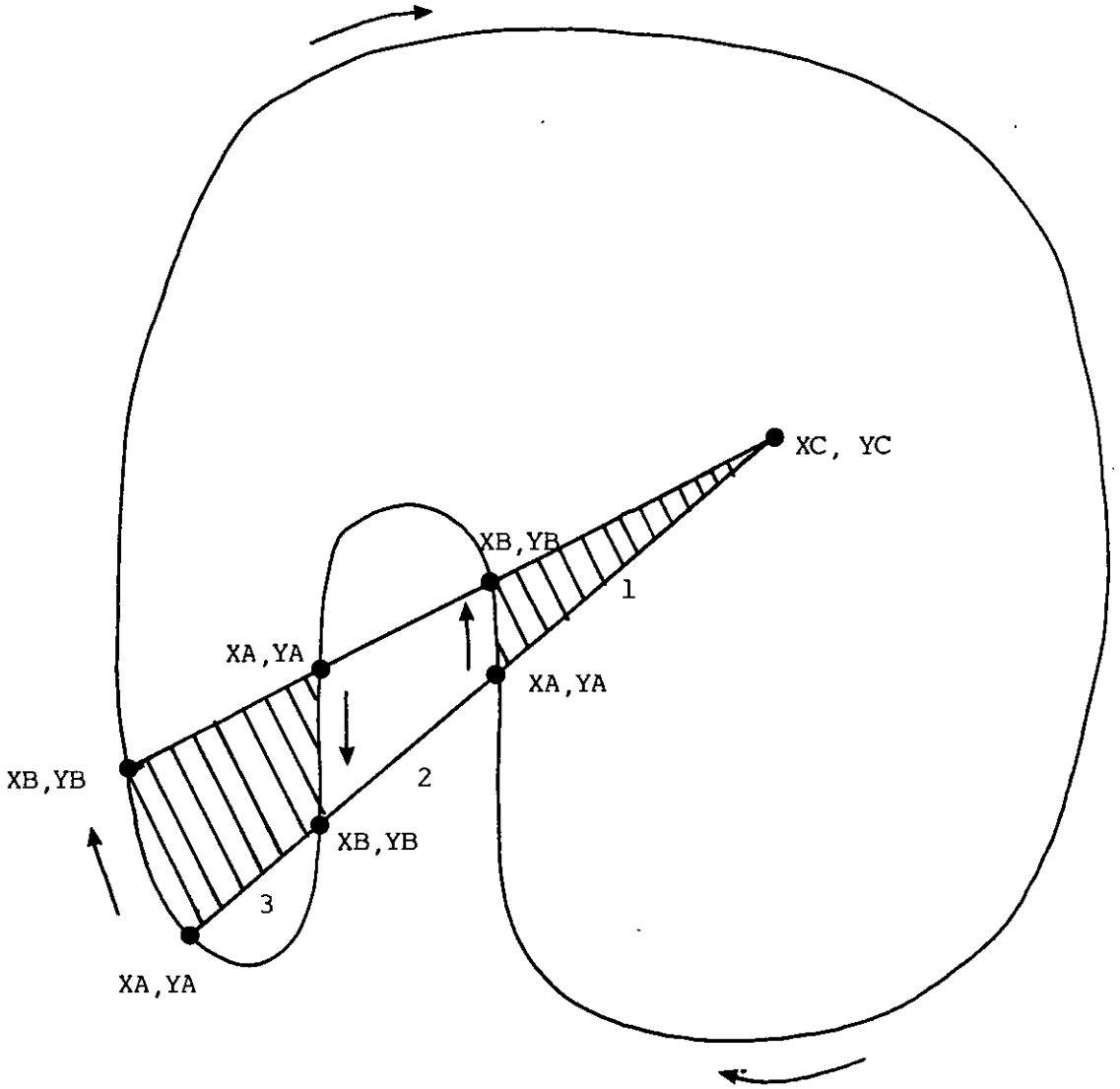

	total triangle area	Running total
Area 1 = 5 units included	5	+5
Area 2 = 10 units removed	15	-10
Area 3 = 15 units included	30	+20

Area 1 + 3 = 20 units

Note: Area removed originates from triangle whose direction of rotation is reversed

Figure 3.17 Computation of the area of an infolded loop

PROGRAM DIAMRS

Refer to the algorithm presented as figure 3.18. Re-reference to figure 3.7 at this point may also make the following explanation more clear.

Areas highlighted for further discussion are the alignment of the data vectors, alteration of bubble subscripts and location of the diameter end points.

DATA VECTOR ALIGNMENT. This is necessary to allow the bubble to grow in an orderly fashion ie. when number of points within the bubble is low, even with the adjustments provided by SUBROUTINE ADJBUB, the possibility of not finding a diameter end point is increased by not performing this correction (see SUBROUTINE ADJBUB).

Whilst the mathematical background to this portion of the program is not new (calculation of length of a line, PROGRAM PNTED), its application requires further explanation.

Pythagoras theorem, which states that the square of the hypotenuse of a triangle in equal to the sum of squares of the other two sides, holds exactly for right angled triangles only. This fact may be used to good effect by sequential calculation of the value of the hypotenuse as the lengths of the other two sides change, with computation terminating when approximation to a right angle is achieved between the two sides, resulting in a calculated hypotenuse value approximating closely to what would be the true hypotenuse. Figure 3.19a illustrates the three possible conditions when data alignment is to be carried out, along with desired placement of the bubble starting position from pythagoras theorem assuming the data were continuous. Of course, this is never the case, since this data set is made up of discrete coordinate points.

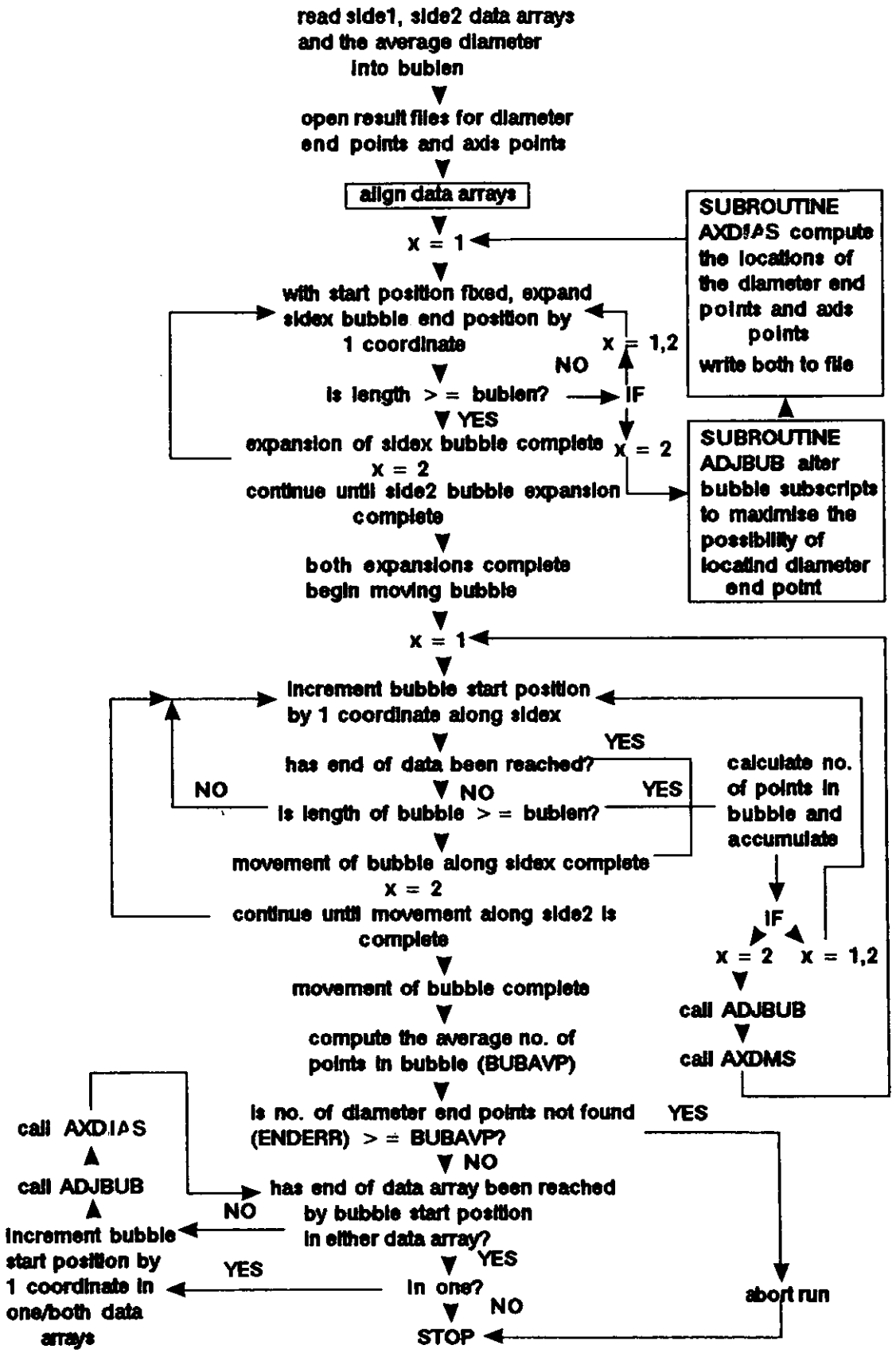

figure 3.18 DIAMRS algorithm

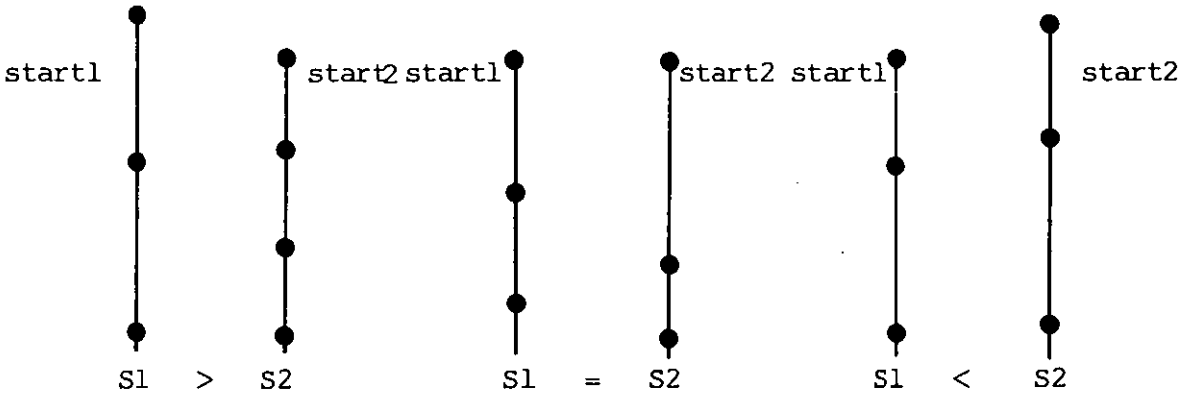

Figure 3.19a Possible conditions for data vector alignment

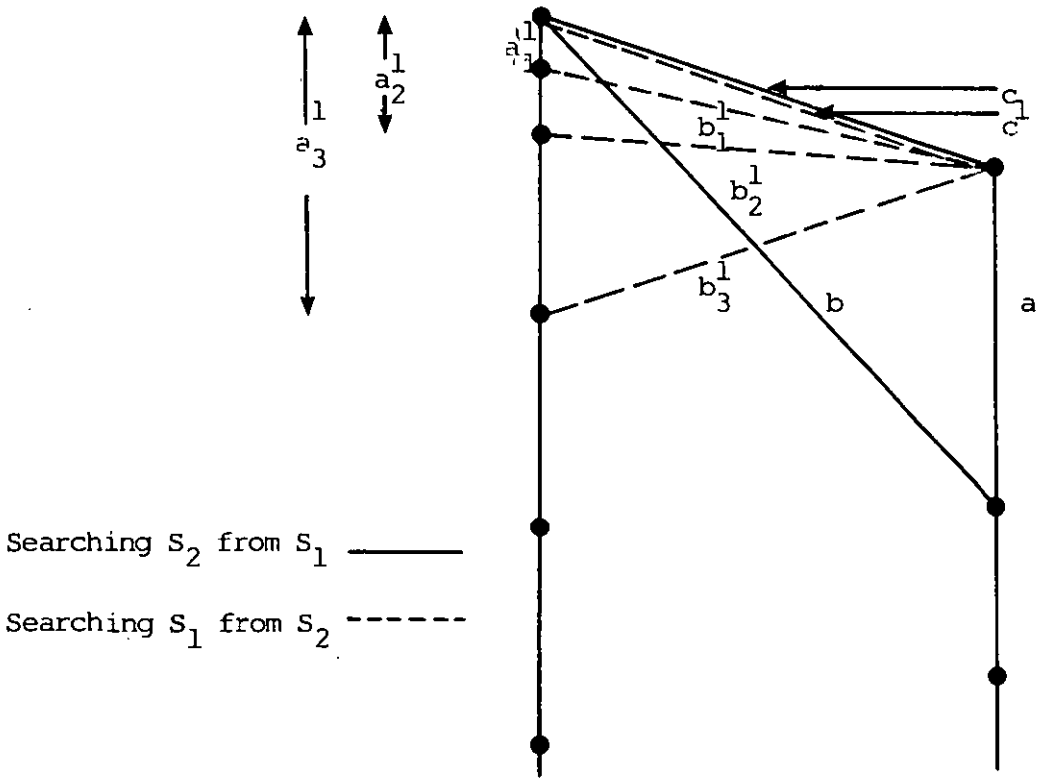

Figure 3.19b Calculation of pythagoras theorem terms

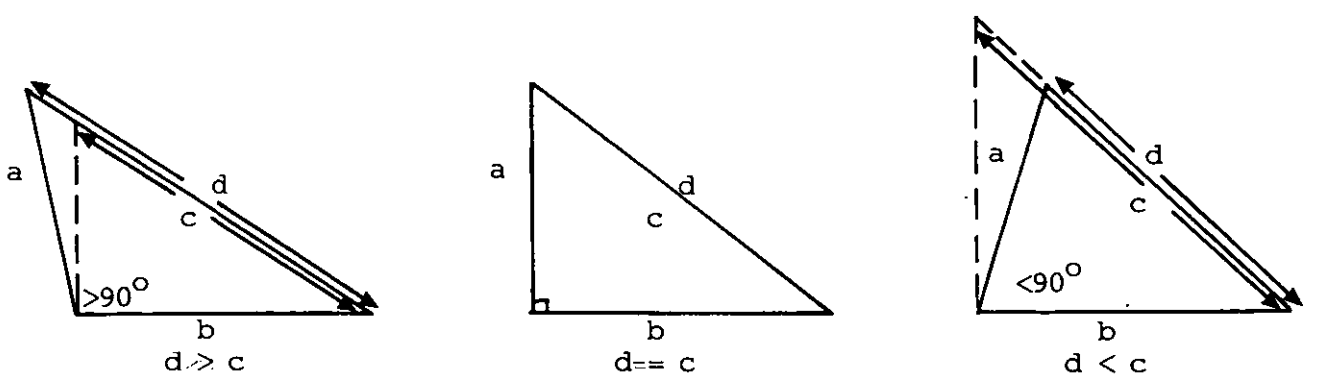

Figure 3.19c Relationship between c and d at various angles

When the position of the start of SIDE1POI.NTS is in exactly the same plane as SIDE2POI.NTS no alignment correction is necessary, however, this is rarely the case. Taking SIDE1POI.NTS being longer than SIDE2POI.NTS as the example, it becomes obvious that SIDE1POI.NTS must be shortened in order for the data vectors to be aligned as closely as possible. Using the test method presented in figure 3.19b, the software first calculates the length of the line connecting the first coordinate points of each vector. This becomes the true hypotenuse, c (figure 3.19c). Next SIDE2POI.NTS is searched from the first coordinate of SIDE1POI.NTS (full lines) with sidea being the length of the segment between points 1 and 2 of SIDE2POI.NTS and sideb the length of the line connecting point 1 SIDE1POI.NTS to point 2 SIDE2POI.NTS. The length of the theoretical hypotenuse, d, for this situation is then calculated and compared with the true value. As the angle between sidea and sideb is less than 90 degrees, (figure 3.19b) the calculated value of the hypotenuse exceeds the true value of c. In this occurrence, the searching of SIDE2POI.NTS stops, since further increments along this vector would only serve to further reduce the angle between sides a and b and therefore further extend the length of d.

The roles are then reversed, with SIDE1POI.NTS being searched from the first coordinate of SIDE2POI.NTS (dotted lines with sub and superscripted letters). The lengths of sides a^1 and b^1 along with the theoretical hypotenuse d^1 are calculated as before, and d^1 compared to c. Since the angle between side a^1 and b^1 is greater than 90 degrees (figure 3.19b), d^1 is less than c. The software thus increments from the second to the third points (figure 3.19b) in SIDE1POI.NTS and the procedure is repeated. Further increments occur until an approximate 90 degree angle is achieved between side a^n and side b^n, with consequent close agreement between d^n and c.

SUBROUTINE ADJBUB. In order to understand how this subroutine works and why it is necessary, the performance of

the nearly identical SUBROUTINE AXDIAS must also be discussed. However SUBROUTINE AXDIAS is also presented as the next section, as this code deals with computing the points of intersection and the angle between the diameter and the data vector, facts not relevant to this subroutine.

Basically, SUBROUTINE ADJBUB corrects for inequalities in coordinate density between the two vectors. The main program is responsible for producing the bubble subscripts (start of bubble in SIDE1, start of bubble in SIDE2, end of bubble in SIDE1 and end of bubble in SIDE2) which dictate the margins of the bubble according to growth towards, attainment of, or contraction below the length set by the previous program. This allows a reasonable first approximation of the artery axis to be constructed as a segment joining the midpoint of lines connecting the top and the bottom coordinates of the bubble (figure 3.20a).

Within the SUBROUTINE AXDIAS the artery axis is then bisected at 90 degrees at its midpoint and the coordinate values of its points of intersection with the data arrays SIDE1POI.NTS and SIDE2POI.NTS are computed. These represent the location of the serial diameters and are written to file for manipulation in the following program. It is evident from the perfect case in Figure 3.20a that there is plenty of distance enclosed within the bubble from both data vectors in order to allow the true diameter end points to be found. This is not the case in figure 3.20b. As before, the sides of the bubble have been adjusted to the correct bubble length and the subscripts of the bubble fixed as shown by the main program. The problem is that due to the rather erratic coordinate density of SIDE2POI.NTS (in actuality, both data vectors are erratic, especially where the user has traced an element of a stenosis more carefully than another, for example, the profile approaching the minimal narrowing. However, for ease of explanation, SIDE2POI.NTS is shown as the only data vector of varying coordinate density), a reasonable approximation to the bubble length in this data vector cannot be achieved. The

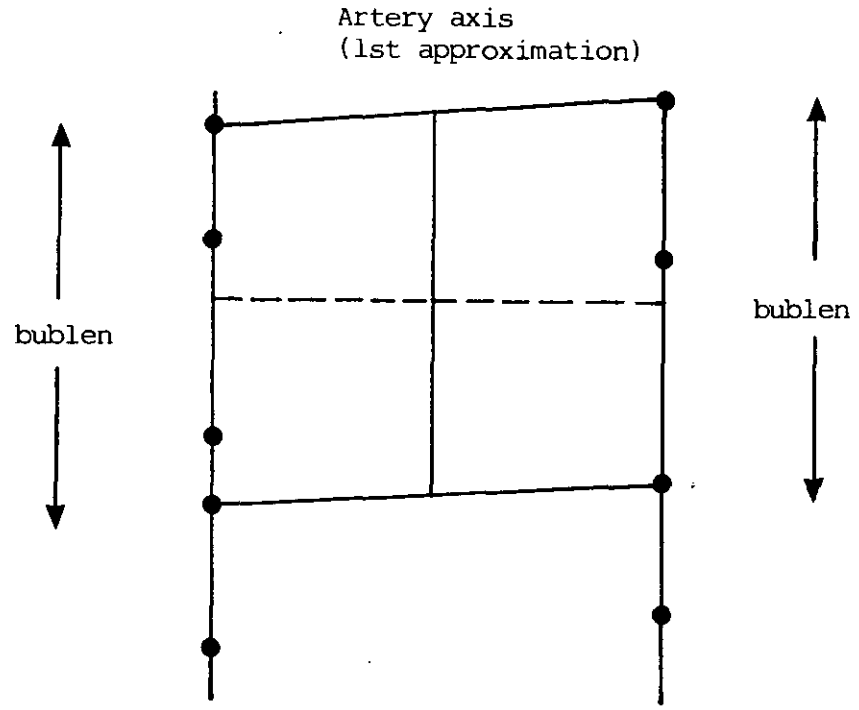

Figure 3.20a Establishment of bubble and bisecting diameter - equal coordinate density, coordinate end points located

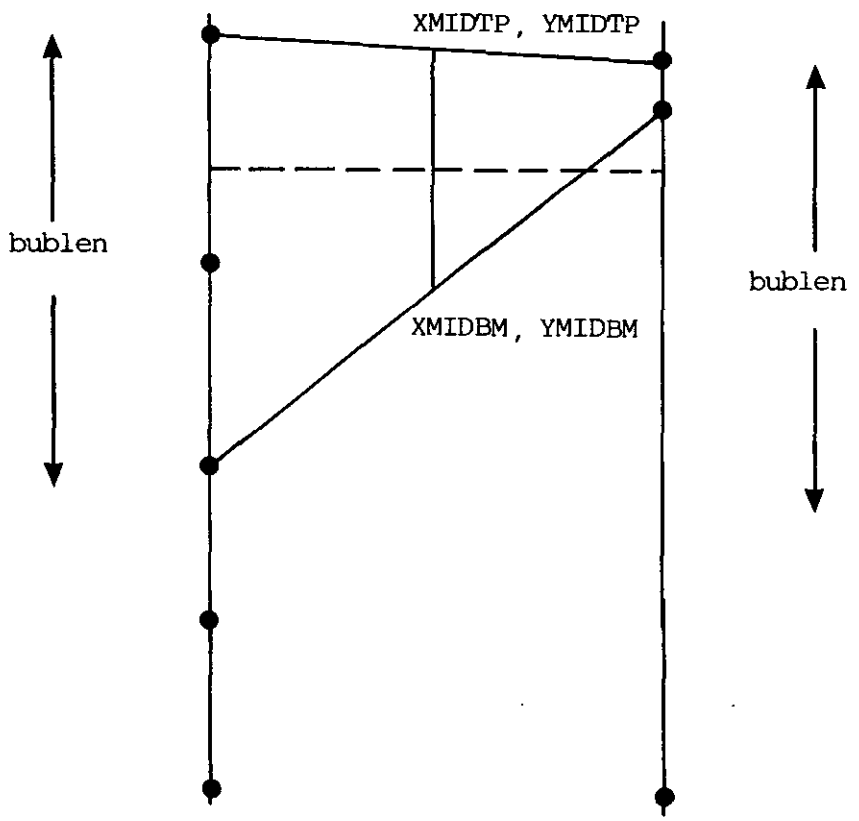

Figure 3.20b Establishment of bubble and bisecting diameter - unequal coordinate density, side2points coordinate end points not located

program is designed to select the point which conforms to a length less than that required, however, in this instance, it would be no better off selecting the next point. As a consequence, the first approximation to the artery axis remains unaffected, but, the distance from which true diameter end points may be located within SIDE2POI.NTS is vastly reduced, and, indeed, as this case illustrates, the diameter end point is actually located outside of the bubble. Since we are using the bubble as a maximal expectation window within which we are searching for diameter end points, this one will remain unlocated and this area of the tracing will remain unsampled. As mentioned earlier, if this problem is left uncorrected, sections of the vector with high coordinate density in comparison to an equivalent position in the complementary data vector (eg. in the tracing of an eccentric stenosis - figure 3.20c) will remain completely unsampled, with a resultant lack of data in the final output commonly located at the point of maximum interest!

So, obviously some transformation of the position of the bubble subscripts is necessary once the artery first approximation is set. This routine achieves this by finding the coordinates nearest to perpendiculars created at the top and bottom of the artery axis. In this way any adjustments are made on the basis of original artery axis length and position, and indeed, these change only minimally following correction. Figure 3.20d demonstrates a situation where correction is necessary; The profile is more complex on side 2 (for simplification, drawn as an angled straight line) leading to non uniform coordinate density. This method is superior to picking the nearest coordinate to give an approximate bublen (smaller or larger) as it involves a degree of averaging between the two sides and maximizes the chances of locating the diameter end points as a consequence of the bubble "shape adjustment".

The basic mathematics surrounding subscript transformation encountered within this subroutine have been described

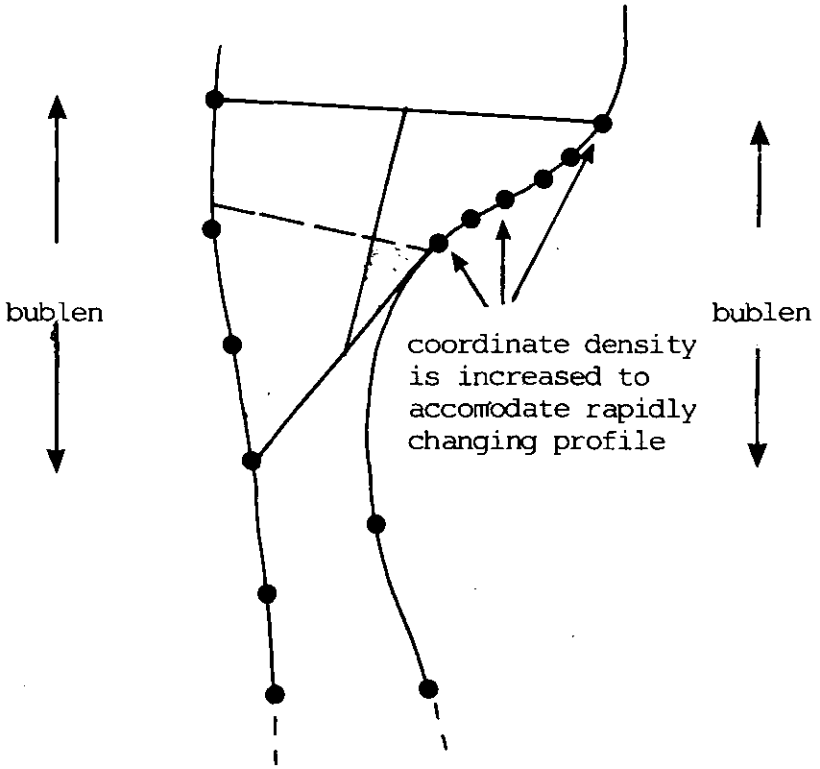

Figure 3.20c Side2points coordinate end points not found due to unequal coordinate density resulting from carefully traced eccentric stenosis

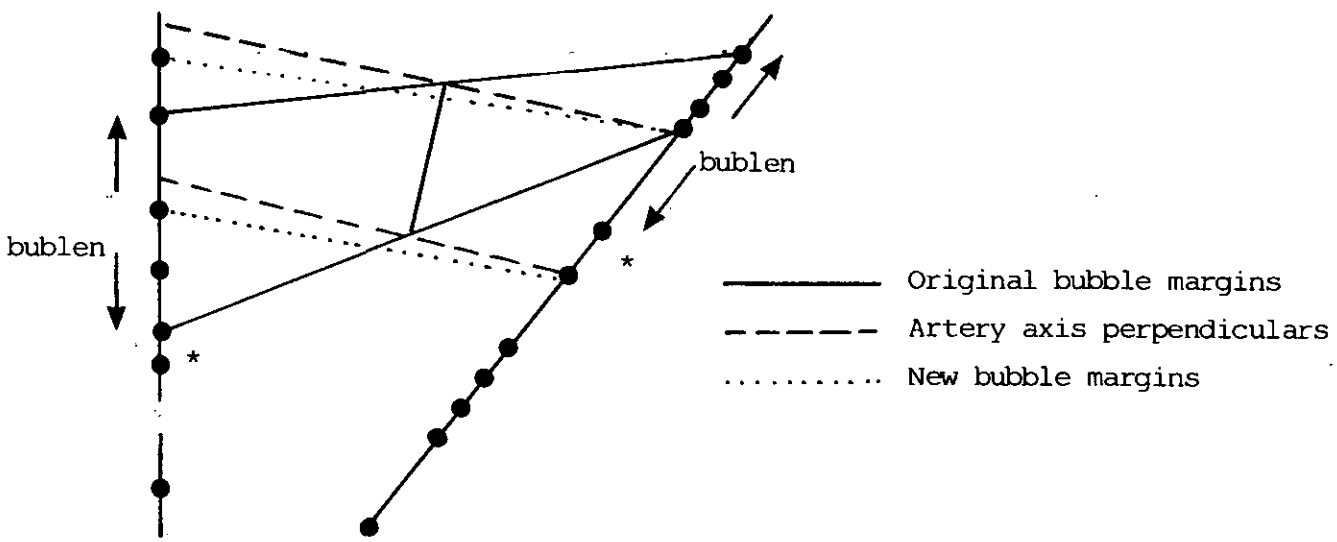

Notice that side 2points has irregular coordinate density. Following the establishment of the original bubble, perpendiculars from the artery axis mark the positions of "maximal expectancy" for locating an artery diameter. This dictates a change in bubble margin location with little effect on original artery axis position or length. Notice also that if the decision regarding bubble manipulation had been made on nearest coordinate above or below bublen, then the coordinates marked with a * would have been picked. This would have resulted in a bottom bubble margin of similar orientation to the original, thus reducing the possibility of locating an artery diameter.

Figure 3.20d Bubble margin change in progress

within program PNTED. The following account is therefore basically descriptive with reference to the required proofs as necessary.

Firstly, the equation of the artery axis must be computed from which perpendiculars at each end may be drawn up. The proof of the equation of a perpendicular line can be located in the section function PPSIDE, PROGRAM PNTED. The following is proof of the equation of a normal line.

From figure 3.20b the gradient of the axis line may be expressed thus:

$$\text{Gradient} = \frac{\text{Increase in y}}{\text{Increase in x}} = \frac{\text{YMIDTP-YMIDBM}}{\text{XMIDTP-XMIDBM}}$$

In its simplest form, for any point x,y on a line, the equation may be expressed as:

$$\text{Y-YMIDTP} = \frac{\text{YMIDTP-YMIDBM}}{\text{XMIDTP-XMIDBM}} \cdot (\text{X-XMIDTP})$$

Rearranging:

$$0 = \frac{\text{YMIDTP-YMIDBM}}{\text{XMIDTP-XMIDBM}} \cdot (\text{X-XMIDTP})-(\text{Y+YMIDTP})$$

Multiplying out:

$$0 = (\text{YMIDTP-YMIDBM})\text{X} + (\text{XMIDBM-XMIDTP})\text{Y} + \text{YMIDTP}(\text{XMIDTP-XMIDMBM}) + \text{XMIDTP}(\text{YMIDBM-YMIDTP})$$

Further multiplication:

$$0 = (\text{YMIDTP-YMIDBM})\text{X} + (\text{XMIDBM-XMIDTP})\text{Y} + \text{YMIDTP.XMIDTP-YMIDTP.XMIDBM+XMIDTP.YMIDBM-XMIDTP.YMIDTP}$$

Overall:

```
0 = (YMIDTP-YMIDBM)X + (XMIDBM-XMIDTP)Y +
    (XMIDTP.YMIDBM) - (YMIDTP.XMIDBM)
```

The equation is now in the familiar form aX+bY+c=0 and is as stated in the program listing.

Following the calculation of the equations of the perpendiculars, the nearest coordinates to their points of intersection must be found and be reassigned as the new bubble margins for use in the following subroutine AXDIAS. This is achieved using the function DISIDE which checks which side of the perpendicular a pair of points (the third point is used for error trapping) are in a fashion identical to the reversal test in the function PPSIDE in program PNTED. The test returns a value of +1, 0 or -1 for each point of the pair which serves as a quick check for location (figure 3.21a). If a solution is not immediate, as with pairs 2 and 3 in figure 3.21b, the routine continues and calculates the shortest displacement (LINE calculations) between the perpendicular line and the point under consideration in a manner again identical to that found in function PPSIDE. This value represents the distance the point is away from the perpendicular line. For pair 2, a flag is raised within the software which indicates that this pair of points is astride the perpendicular. Therefore the smallest absolute displacement reflects the coordinate of choice for appropriate transformation of the bubble margin. For pair 3, the lower displacement for point B instructs the software to increment down the data vector until pair 2 reached, the appropriate coordinate being selected as described. This process of adjusting the bubble subscripts with computation of the diameter end points (SUBROUTINE AXDIAS) continues until the bubble meets the bottom of the two data vectors and contracts to zero.

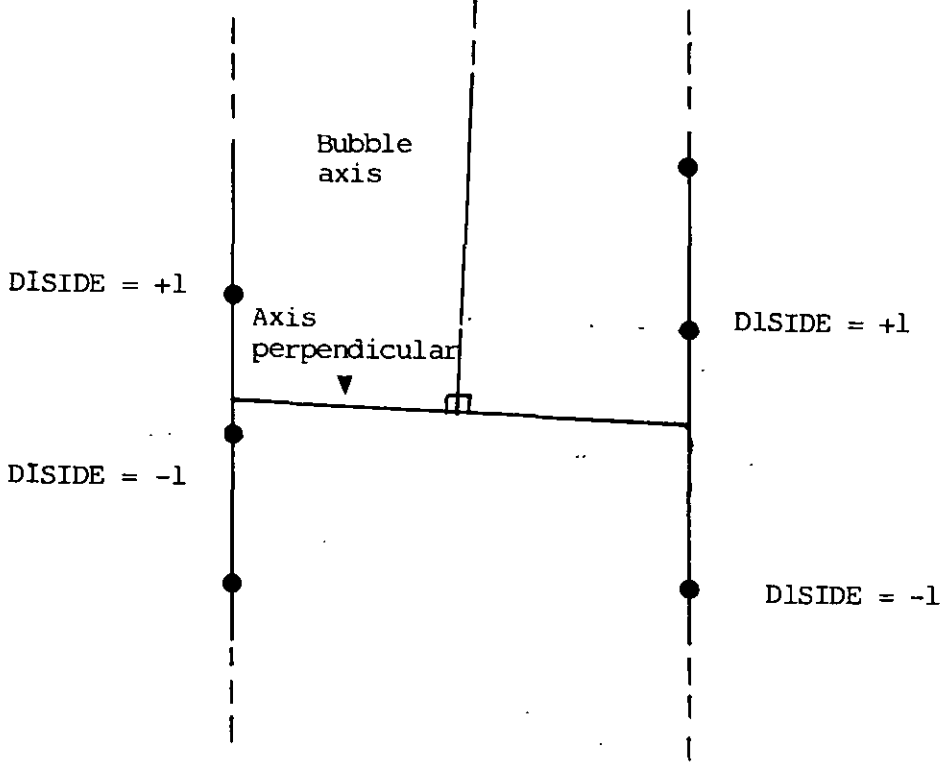

Figure 3.21a locating the relative positions of coordinates using function DISIDE

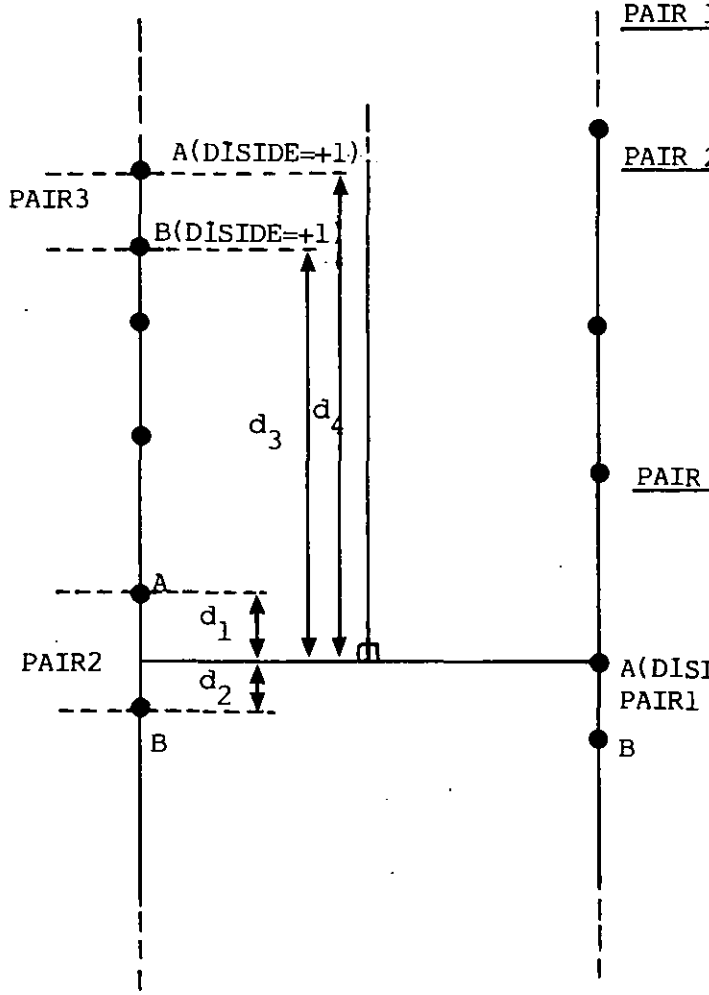

PAIR 1 Point A is on the perpendicular. This point is automatically selected as new subscript

PAIR 2 Flag F3 has been raised indicating points A &B are astride the perpendicular. The line tests compute the distance d_1 and d_2. d_2 is the smaller, therefore point B is assigned to be the new bubble subscript

PAIR 3 Both points are on the same side of the perpendicular. d_3 is less than d_4, therefore search proceeds downwards work until PAIR2 is encountered

Figure 3.21b Locating the closest coordinates to the bubble axis perpendicular using DISIDE and the LINE tests

Due to the simplistic nature of the LINE test, there are two clearly definable conditions where errors in the searching process may occur. These are:

1. When coordinate density is high and artery profile is changing rapidly producing a set of points whose connecting segments are exactly parallel to the bisecting line in question, be it from the SUBROUTINE ADJBUB or AXDIAS. As can be seen from figure 3.22a, the LINE test indicates that all points within the test are an equal distance away from the bisector, ie. there is no convergence or divergence of values present in order to instruct the program in which direction to continue the search. Therefore, to all intents and purposes, the searching process is "stuck".

   This occurrence is dealt with in one of two ways depending on which routine is currently running. For ADJBUB, where the searching is taking place across the whole data vector, once the problem is detected, the current bubble margin is incremented by one unit before being passed to AXDIAS. In this way, although true bubble parallelity is temporarily lost, the solution is quick and resolves itself following the necessary number of unit increments. For AXDIAS however, the situation is somewhat different. Here, the true location of the bisecting line must be located, hence the check for equivalence of the line tests promotes unit increase in the searching counter, with subsequent re-searching one step further down the data vector. This method is best suited to this situation since the number of possible searches is small in comparison to the previous routine, being limited by the bubble margins.

2. When coordinate density is high and artery profile is changing rapidly producing an inflection is the artery profile relative to the bisector. This can occur when the bisecting line has intersected with the data vector

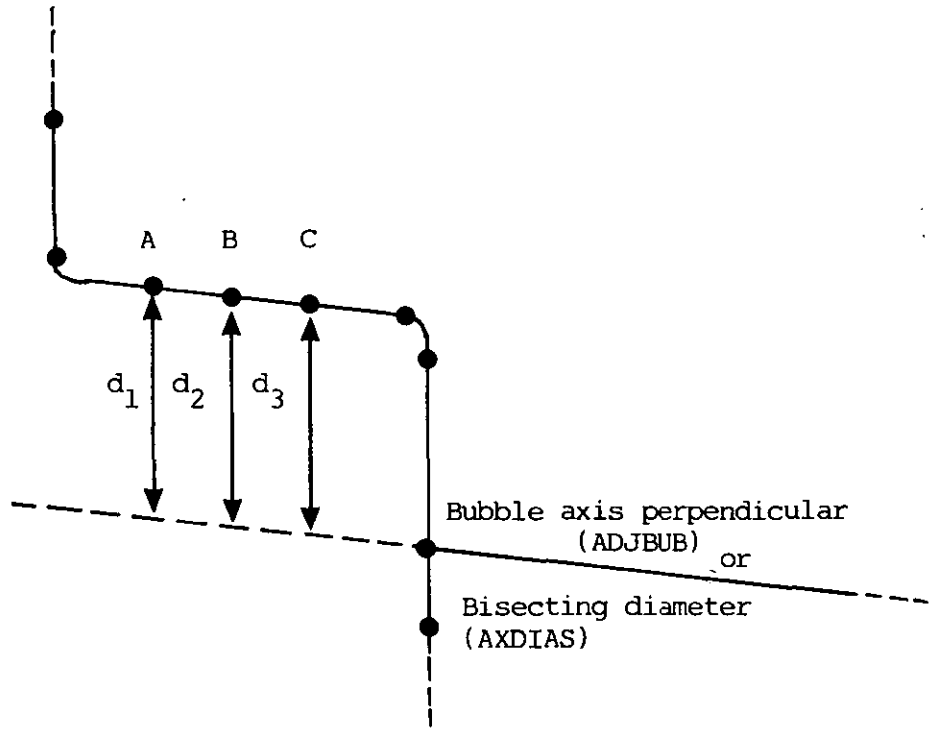

$d_1 = d_2 = d_3$ Therefore bisector and artery contour are parallel

Figure 3.22a "Sticking" of the searching process due to parallelity between artery contour and bisector

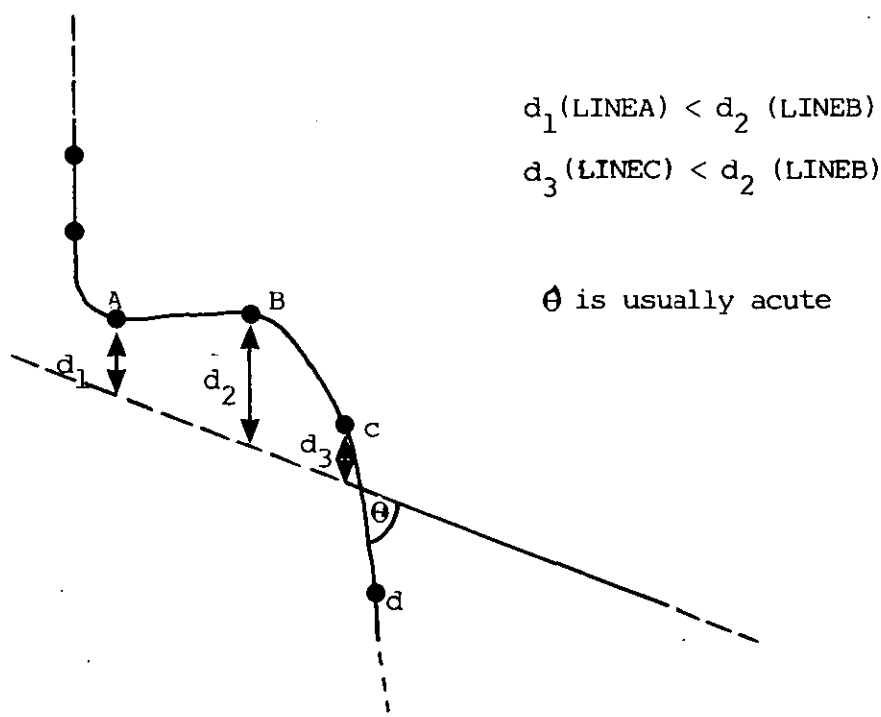

Figure 3.22b Potential problem with the searching process caused by an inflection in the artery profile relative to the bisector

in a normal fashion but at a relatively steep angle. From figure 3.22b, it can be seen that the continuation of bisector runs close to other data points currently being searched in a fashion which, on testing using the LINE method, leaves point B further from the bisecting line than points A and C. This constitutes what was earlier defined as a reversal (PROGRAM PNTED). The search must thus continue in order to locate the point nearest to the axis perpendicular (SUBROUTINE ADJBUB) or the actual point of intersection (SUBROUTINE AXDIAS) as in this example (between points C and D). Hence, the software compares the relative values of LINE A, B and C; a peak at LINE B denotes a false reversal which promotes continued searching of the subsequent data.

Whilst the LINE test has these shortcomings, providing they are appreciated and attended to adequately within the program, the test performs well and maintains the easy to understand approach which is one of the core aims of this work.

SUBROUTINE AXDIAS. As previously mentioned, the bulk of the coding for this routine is essentially the same as the previous, in that bisecting lines are created at 90 degrees to the artery axis and the data vectors are scanned within the recently adjusted bubble in order to find where the intersecting segments lie. The major difference between the two routines is that AXDIAS takes the computation one step further by actually computing the points of intersection, along with the angle between the bisector and the data segment in question. This angle information is then used as a check against the minimum angle obtainable on the graphics tablet following which a decision is made on the credibility of this particular diameter line, whilst computed diameter end points are written to the file DIAMETER.EPS. Presented below is the proof for computation of points of intersection followed by a description of the function ANGLE, which performs the angle calculations.

Point x,y satisfies both equations as in figure 3.23. Using a pivotal method (Davies and Hicks 1978) for the solution of two simultaneous equations, x and y may be expressed in terms of equation coefficients only:

State basic equations:

$$XCOEFDx + YCOEFDy + CONSTD = 0 \quad - 1$$
$$XCOEF1x + YCOEF1y + CONST1 = 0 \quad - 2$$

Calculating x in terms of coefficients only:

Remove y term by first multiplying equation 1 by YCOEF1 and equation 2 by YCOEFD.

$$XCOEFD.YCOEF1x + YCOEFD.YCOEF1y + CONSTD.YCOEF1 = 0 \quad - 3$$
$$XCOEF1.YCOEFDx + YCOEF1.YCOEFDy + CONST1.YCOEFD = 0 \quad - 4$$

Subtract equation 3 from equation 4 thus removing y term.

$$XCOEFD.YCOEF1x + YCOEFD.YCOEF1y + CONSTD.YCOEF1 -$$
$$XCOEF1.YCOEFDx - YCOEF1.YCOEFDy - CONST1.YCOEFD = 0$$

Collect like terms:

$$XCOEFD.YCOEF1.x - XCOEF1.YCOEFDx = - CONSTD.YCOEF1 + CONST1.YCOEFD$$

Solve for x:

$$x = \frac{CONST1.YCOEFD - CONSTD.YCOEF1}{XCOEFD.YCOEF1 - XCOEF1.YCOEFD}$$

Calculating y in terms of coefficients only:

Remove x term by firstly multiplying equation 1 by XCOEF1 and equation 2 by XCOEFD.

$$XCOEFD.XCOEF1x + YCOEFD.XCOEF1y + CONSTD.XCOEF1 = 0 \quad - 5$$

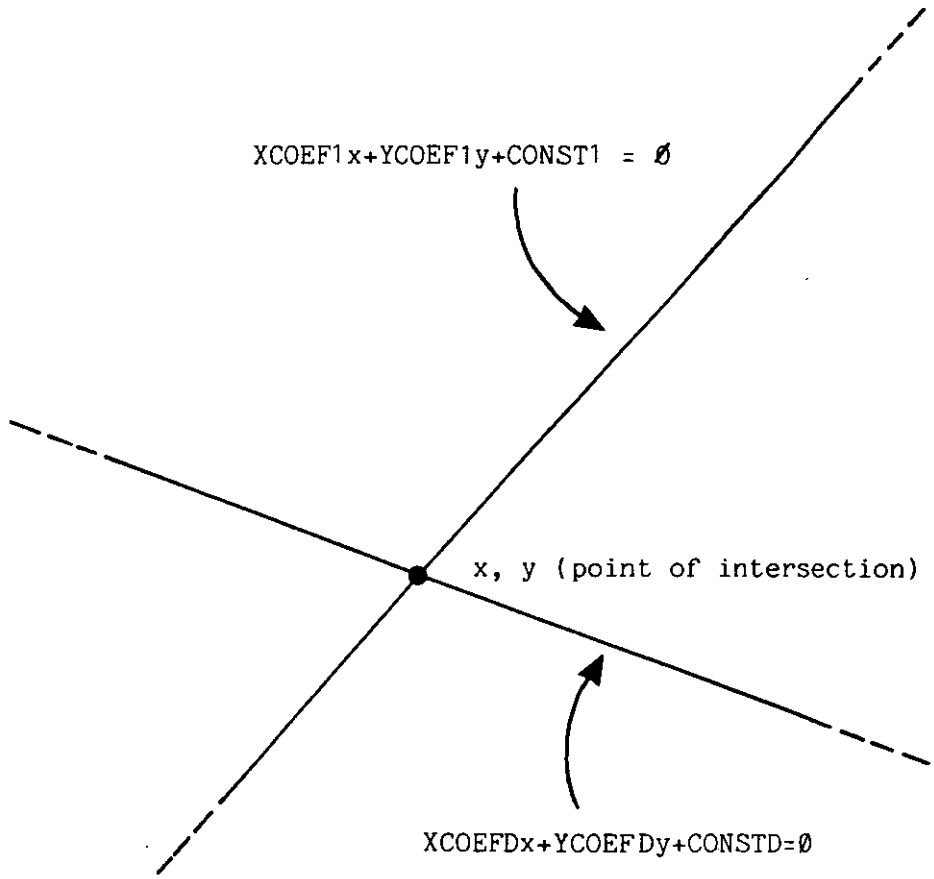

point x, y satisfys both equations.

Figure 3.23 Demonstration of a point intersection

$$XCOEF1.XCOEFDx + YCOEF1.XCOEFDy + CONST1.XCOEFD = 0 \quad - 6$$

Subtract equation 5 from equation 6 thus removing x term.

$$\cancel{XCOEFD.XCOEF1x} + YCOEFD.XCOEF1y + CONSTD.XCOEF1 -$$
$$\cancel{XCOEF1.XCOEFDx} - YCOEF1.XCOEFDy - CONST1.XCOEFD = 0$$

Collect like terms:

$$YCOEFD.XCOEF1y - YCOEF1.XCOEFDy = - CONSTD.XCOEF1 + CONST1.XCOEFD$$

Solve for y:

$$y = \frac{CONST1.XCOEFD - CONSTD.XCOEF1}{YCOEFD.XCOEF1 - YCOEF1.XCOEFD} \text{ or } \frac{CONSTD.XCOEF1 - CONST1.XCOEFD}{YCOEF1.XCOEFD - YCOEFD.XCOEF1}$$

This reversal of terms for y allows the same denominator to be used in both the calculation of x and y, the equations quoted being directly comparable with those in the listing.

The function ANGLE calculates the angle between any line and the right directed horizontal according to figure 3.24a. Considering any line on which lie two known points, (for example the bisecting diameter line) the equation may be calculated (function PPSIDE, PROGRAM PNTED). This allows the equation to be expressed in the form:

$$XCOEFDx + XCOEFDy + CONSTD = 0$$

Rearranging for y (y ax+b format):

$$y = - \frac{XCOEFD}{YCOEFD} x - \frac{CONSTD}{YCOEFD}$$

ie. the gradient of the line may be expressed as:

$$\text{Gradient} = \frac{XCOEFD}{-YCOEFD} \text{ or } Tan\theta \text{ or } \frac{SINE\ \theta}{COSINE\ \theta}$$

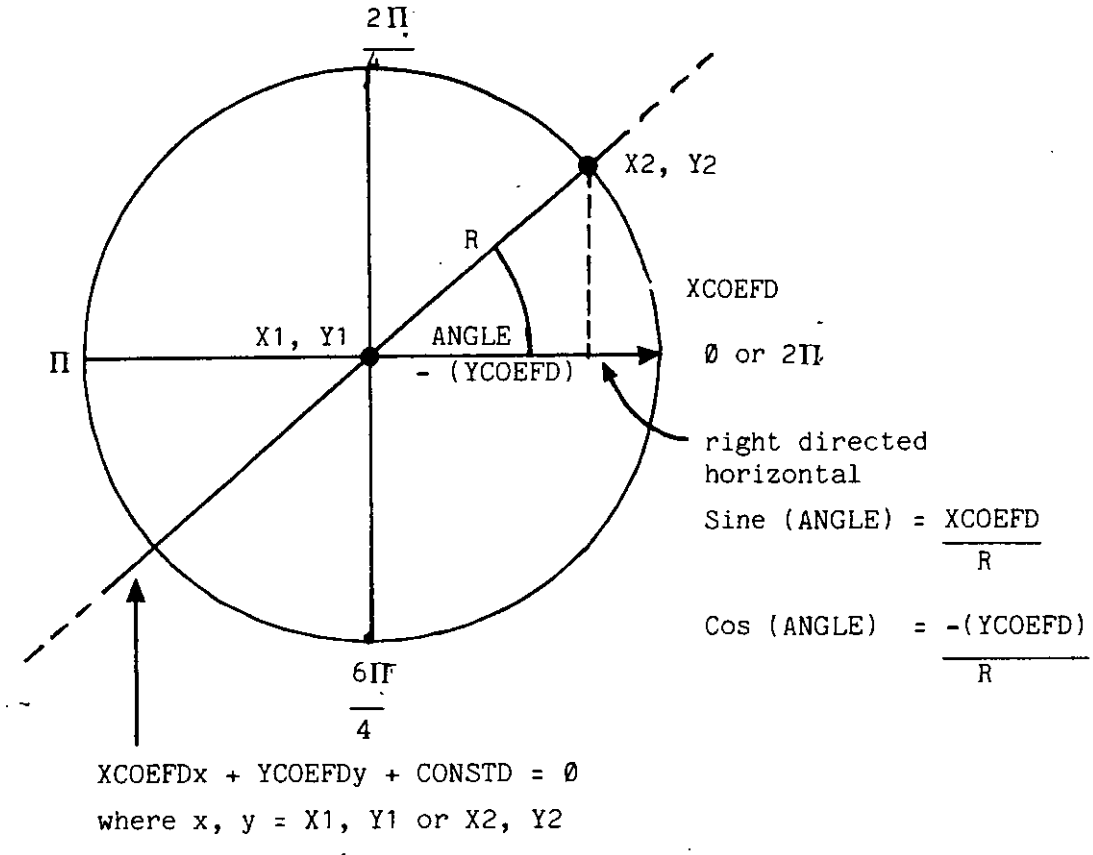

Figure 3.24a Calculating the angle between the right directed horizontal and the bisector using function ANGLE

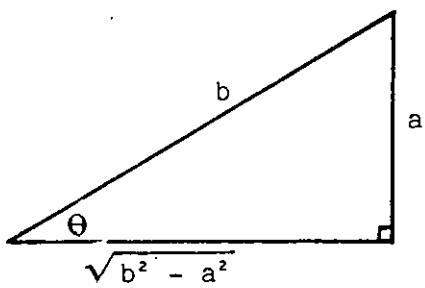

$$\theta = \text{ARCSIN}\ \frac{a}{b}$$

$$= \text{ARCTAN}\ \frac{a}{\sqrt{b^2 - a^2}}$$

$$= \text{ARCTAN}\ \frac{a}{b\sqrt{1 - \frac{a^2}{b^2}}}$$

LET $\frac{a}{b} = X$

$$\frac{a}{b} = \text{ARCTAN}\ \frac{X}{1 - X^2}$$

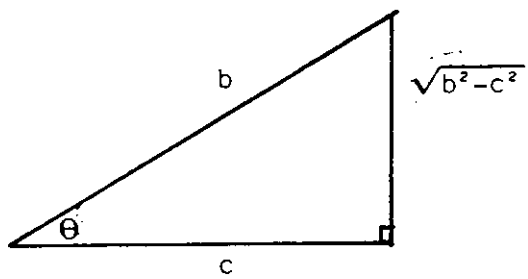

$$\theta = \text{ARCCOS}\ \frac{c}{b}$$

$$= \text{ARCTAN}\ \frac{\sqrt{b^2 - c^2}}{c}$$

$$= \text{ARCTAN}\ \frac{b\sqrt{1 - \frac{a^2}{b^2}}}{c}$$

LET $\frac{c}{b} = X$

$$= \text{ARCTAN}\ \frac{1 - X^2}{X}$$

Figure 3.24 Converting ARCSINE and ARCCOS to ARCTAN

As the tangent function tends to infinity at its limits, it was thought more sensible to base an angle calculation routine on the sine and cosine functions. However once the routine was complete and ready for coding, it was found the version of Fortran running on the Vector3 did not support inverse sine and cosine functions. This was overcome by using inverse tan (see figure 3.24b for derivation). As the angles are initially calculated in terms of sine and cosine, the converted to tan the effects of limits are avoided.

Figure 3.24c presents the two functions mapped across one complete cycle. The dotted areas indicate when there is a non linear response between current angle and returned function value, whilst the solid areas indicate linearity. For accuracy, all calculations of angle are made from the appropriate function depending on the relative position of X2,Y2 to X1,Y1. This is derived from the relative relationships of the previously derived equation coefficients, which are passed directly to the routine.

Hence, this routine begins with the calculation of sine and cosine from the equation coefficient as in figure 3.24a. These figures are then rounded up or down to prevent numerical accuracy problems originating from the computer. There then follows four quadrant traps, within which are two octant traps where the angle between the right directed horizontal and the line in question is computed from the correct function as in figure 3.24c.

The function ANGLE is used again to calculate the angle between the right directed horizontal and data segment with which the diameter intersects. Subtraction of one angle from another gives the angular difference between the two lines (figure 3.24d).

This is then compared to the minimum angle obtainable on the graphics tablet, calculated thus:

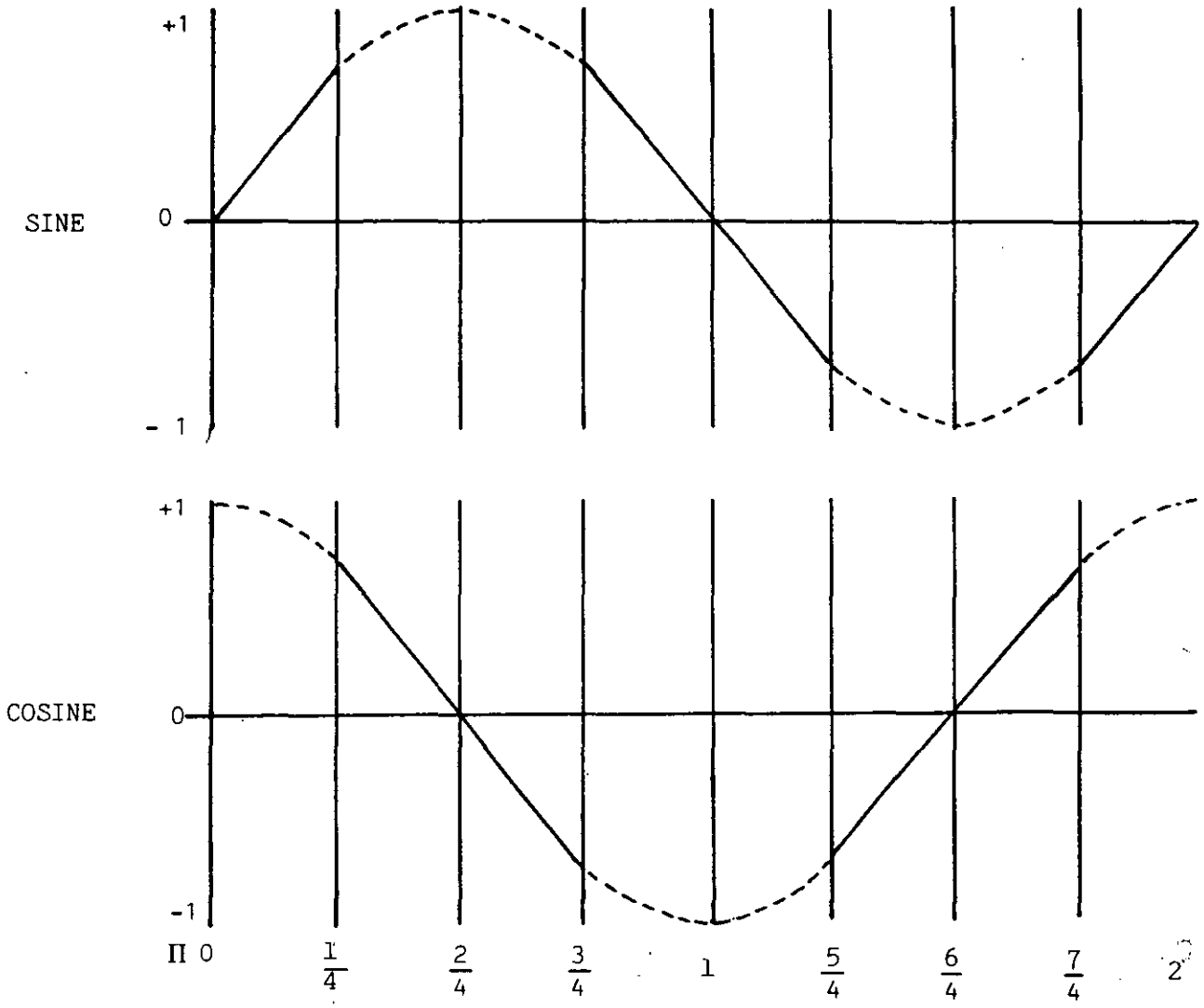

Figure 3.24c Selection of the appropriate function for the computation of ANGLE

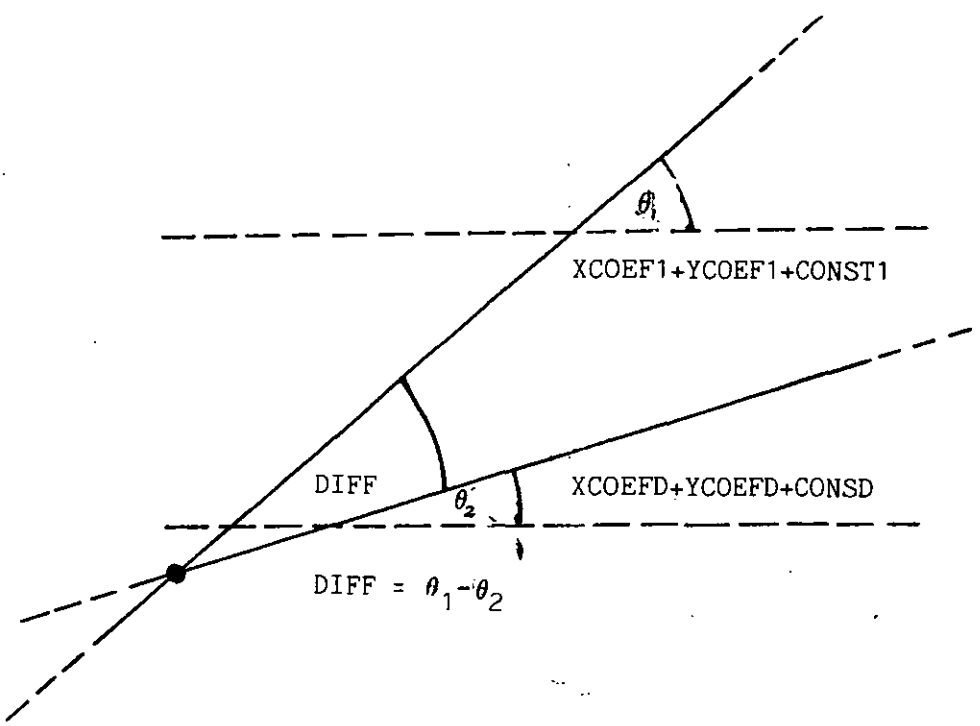

Figure 3.24d Using function ANGLE to calculate angular separation between a diameter line and a data segment

Graphics tablet scale = 0 - 11000 units.

Minimum axis discrepancy = 1
Maximum axis discrepancy = 11000.

$$\text{Minimum gradient} = \frac{1}{11000} = 3.33333321 \times 10^{-4}$$

Any recorded angular difference smaller than this critical angle dictated that the lines are essentially parallel to each other and therefore the diameter line under test should be excluded from the final data set.

PROGRAM ANALYZ

This is basically the "number crunching" program of the set and works according to the algorithm presented as figure 3.25.

The following areas have been highlighted for further discussion:

1. Calculation of diameter lengths, cross-sectional areas (CSA's) and true artery axis.

2. Obtaining number of maxima with hand tracing tolerance (TOL).

3. Searching for the first occurrence of a CSA greater than 90% of the average maximum. This forms the cut off for the calculation of stenotic length, a parameter influencing the fluid mechanics equations presented in chapter 2.

4. Calculation of percent diameter and cross-sectional area stenosis.

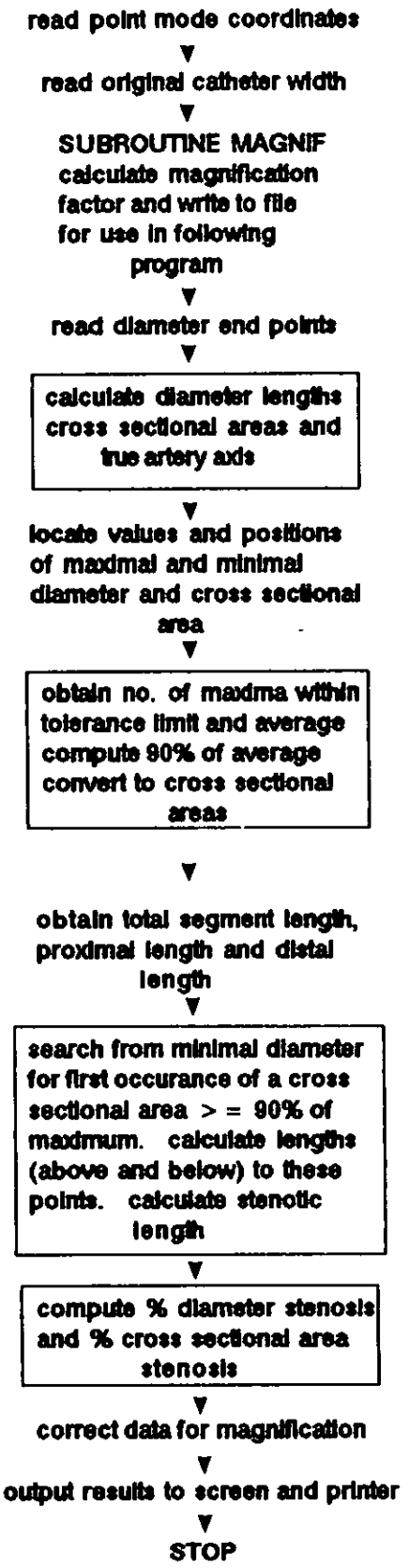

figure 3.25 ANALYZ algorithm

CALCULATION OF DIAMETER LENGTHS ETC. Diameter end point information is read from the file DIAMETER.EPS produced by the previous program and converted into lengths using the technique described in program PNTED. From these lengths, cross-sectional areas are calculated under the assumption that the artery is cylindrical in cross section.

ie: $CSA = PI \cdot (DILENS/2.0)^2$

Whilst this is almost certainly never true, its value provides a better **estimate** of the haemodynamic significance of the current diameter at the location in question (chapter 2).

Now that the locations of the diameters have been fixed, a true artery axis may be computed as a line connecting the midpoints of all artery diameters. These midpoints are then written to the file AXPTS for use in the following graphics program (available on the Prime System only).

OBTAINING THE NUMBER OF MAXIMA WITHIN TOL. Since maximal diameter is the denominator of the percent diameter stenosis parameter (section 2.2.1), it is mathematically powerful. Therefore, it is important that the value used for the maximum represents the true state of artery morphology and is not some spurious value which was entered from the graphics tablet during a period of excessive hand tremor, occurring for example at the onset of tracing. It is for this reason that the denominator for the percent diameter stenosis estimate, and indeed, "the maximum" used in all other applications is formed from an average of all those diameter values falling within the hand tremor tolerance (derivation section 3.6.1). This is achieved by summing all those diameters which are greater than the previously quantified maximum, **less** the tolerance value. The sum is then divided by the number of maxima fulfilling this criteria thus producing an average maximum estimate. In this way no one maxima gives excessive bias to the result at the expense of "shaky tracing".

SEARCHING FOR THE FIRST OCCURRENCE OF A CSA>= 90% OF MAXIMUM. Whilst the code for a search procedure is very simple, the use of a 90th centile value as the cut off for the calculation of stenotic length needs explanation.

When a user digitizes an image, the amount of normal vessel, above or below, included in the tracing is entirely a subjective decision. Therefore, if the stenotic length result were based entirely on total length of tracing, the answer would be somewhat meaningless. So, the method of McMahon et al 1979 was adopted, whereby stenotic lengths were based on the distance between 90% of the average maximal cross-sectional area above to 90% of the average maximal cross-section below. In this way, the result reflects the true length of the stenosis rather than the traced segment length. However, on a fair proportion of the occasions, no lower 90th centile can be detected due to the natural taper of the artery. Therefore, in the results, the length of the traced segment is also reported as a backup, though caution must be drawn to its interpretation.

CALCULATION OF PERCENT DIAMETER AND CROSS SECTIONAL AREA STENOSIS. These are calculated as simple ratios of the difference between average maximal and minimal (diameter and/or CSA)to average maximal(diameter and/or CSA) thus:

$$\text{percent diameter stenosis} = 100 \times \left(\frac{\text{Average maximal diameter} - \text{minimal diameter}}{\text{Average maximal diameter}} \right)$$

$$\text{percent CSA stenosis} = 100 \times \left(\frac{\text{Average maximal CSA} - \text{minimal CSA}}{\text{Average maximal CSA}} \right)$$

These represent the most commonly used (the former more so) clinical parameters in the current literature.

A hard copy of the following parameters are produced as results at the printer for placement in patient notes:

MEAN MAXIMAL DIAMETER 90% MAXIMAL DIAMETER MINIMAL DIAMETER	Absolute
% DIAMETER STENOSIS	Relative
MEAN MAXIMAL CSA 90% MAXIMAL CSA MINIMUM CSA	Absolute
% CSA STENOSIS	Relative
DISTANCE TO UPPER 90TH CENTILE DISTANCE TO LOWER 90TH CENTILE STENOTIC LENGTH SEGMENT LENGTH	Absolute

PROGRAM ECCFTR

Whilst this program draws on a lot of the mathematics presented thus far, the concept is difficult to describe in small sections without the reader having an overall feel for the schema of the program. For this reason, the diagram presented as figure 3.26 provides a global introduction to the workings of this routine which supplements the algorithm in figure 3.27.

The following areas have been highlighted for further discussion:

1. Calculation of diseased area.

2. Calculation of proximal and distal diameter equations plus parallel check.

3. Fitting linear equation between proximal and distal diameters.

4. Calculating the points of intersection between extrapolation of the proximal and distal diameters.

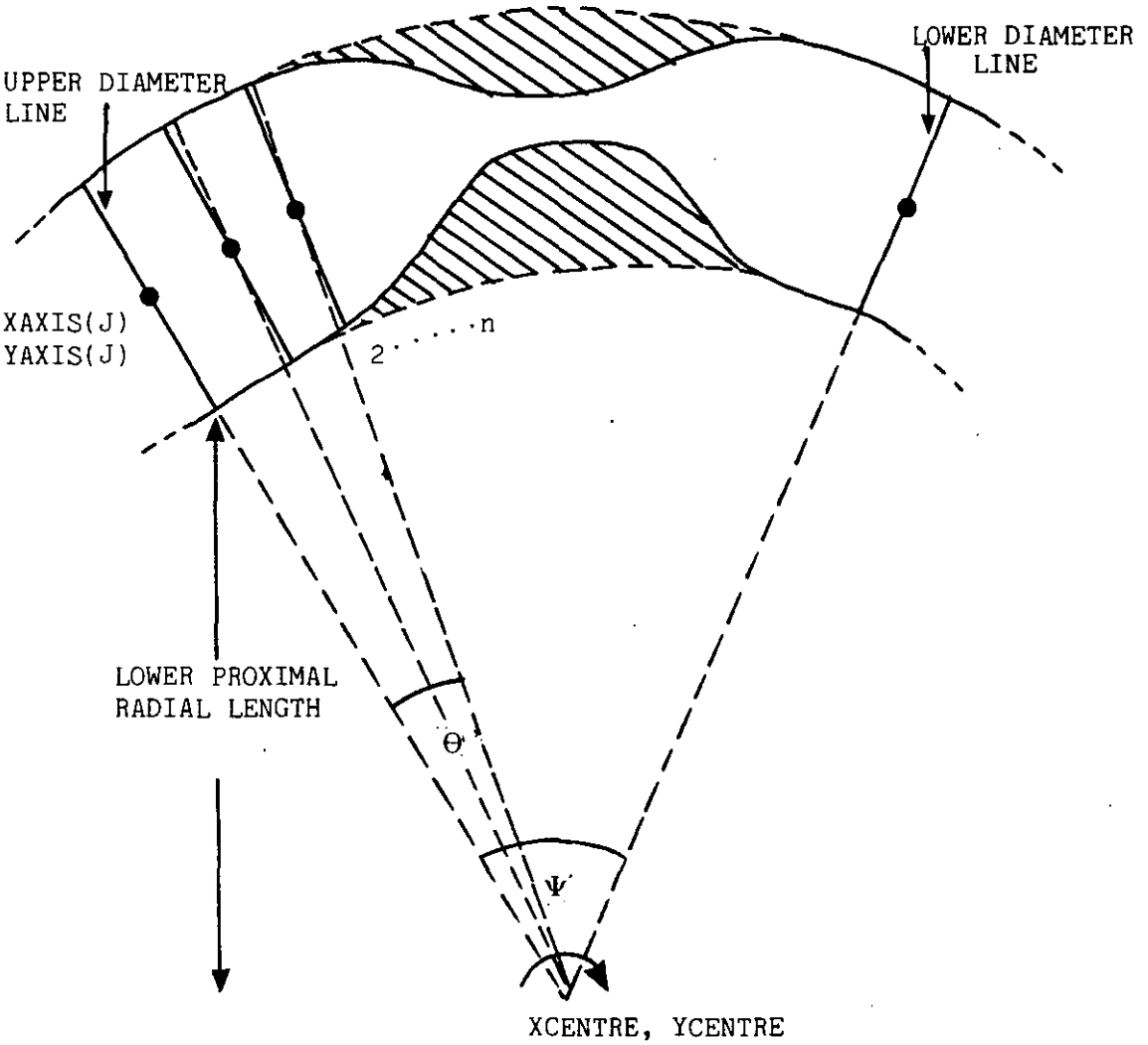

The angular separation between upper and lower boundry diameter lines dictate the curvature of the arc to be fitted (Ψ). Between the artery axis and the arc's centre of rotation, a radii establishes the position of the undiseased diameter line. End point co-ordinates for this diameter are computed from rate of change of radial length with change in angle (Θ).

All diameters are worked through sequentially such that each pair of diseased diameter end point co-ordinates, has a complementary part of undiseased diameter end point co-ordinates.

Atheroma area may now be calculated as the difference between undiseased and diseased artery area.

Figure 3.26 Program ECCFTR - overall schema

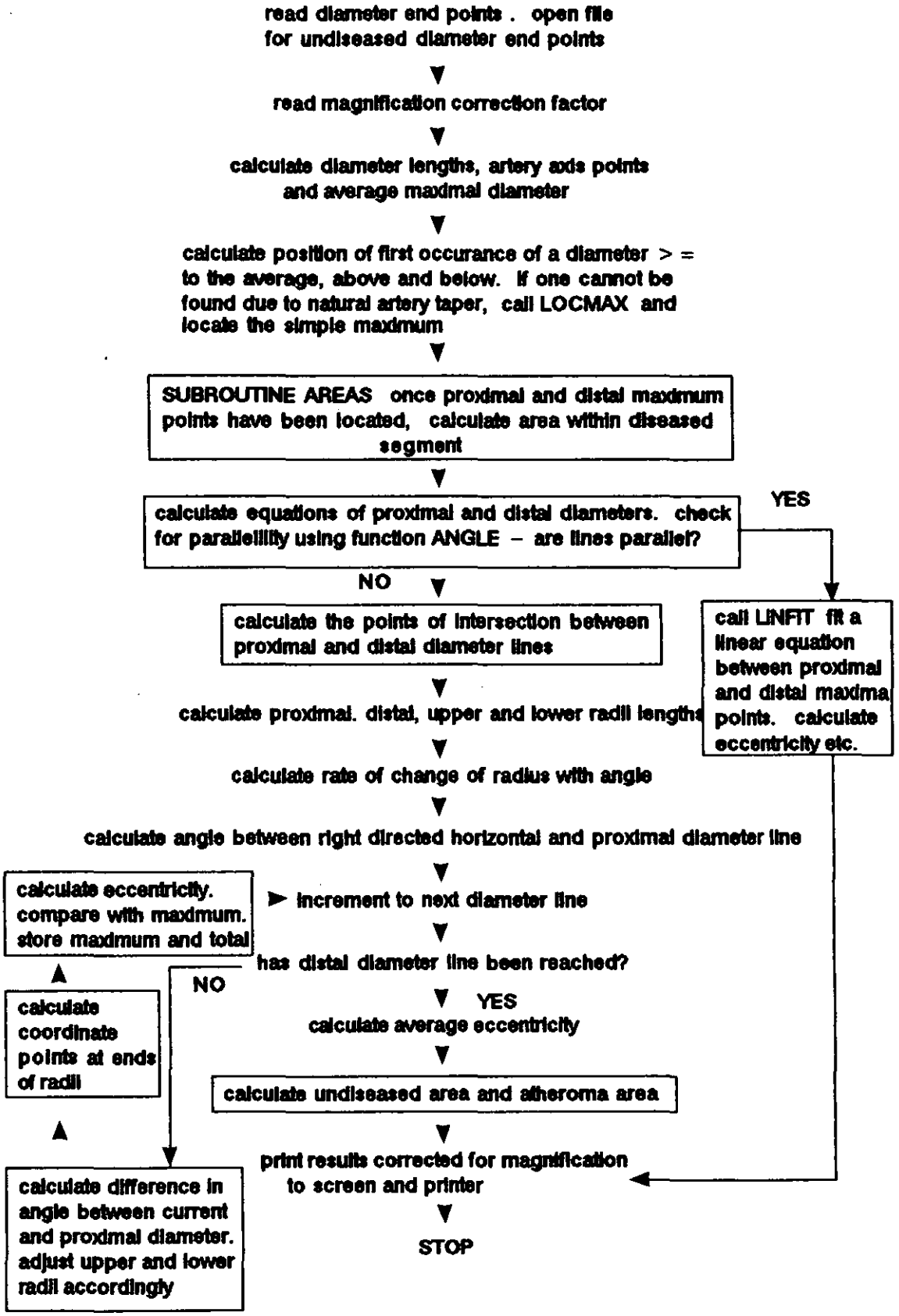

figure 3.27 ECCFTR algorithm

5. Calculating angular difference and radii adjustments.

6. Calculating coordinates of radial end points.

7. Calculation of eccentricity.

8. Calculation of undiseased and atheroma area.

CALCULATING THE DISEASED AREA. This is performed by the subroutine AREAS and is an almost carbon copy of the program DIAMAV.

COMPUTING DIAMETER EQUATIONS AND PARALLEL CHECK. The mathematical proof for calculating the equation of a straight line is presented in PROGRAM PNTED function PPSIDE.

The parallelity check consists of comparing the angles of the upper and lower diameter lines (figure 3.26) with respect to the right directed horizontal (PROGRAM DIAMRS, function ANGLE). If the difference between the lines is less than the smallest angle obtainable on the graphics tablet from direct tracing (3.33×10^{-4}) the lines are judged to be parallel. If this is the case, a linear equation is fitted between the diameters and represents the artery profile if disease were not present (next section). If the lines are not judged to be parallel, then the artery profile is represented by a circular function.

FITTING LINEAR EQUATIONS. Although an artery may taper throughout the course of its traced segment, discernible curvature may not be present. Fulfilment of the parallelity check allows linear equations (PROGRAM PNTED, function PPSIDE) to be fitted between the proximal and distal diameters (figure 3.28) in the subroutine LINFIT. End points of the undiseased diameters are computed as the points of intersection between an extrapolation of the diseased diameter and the fitted equation between the proximal end distal boundaries according to the method described in PROGRAM DIAMRS, SUBROUTINE AXDIAS. Linking of

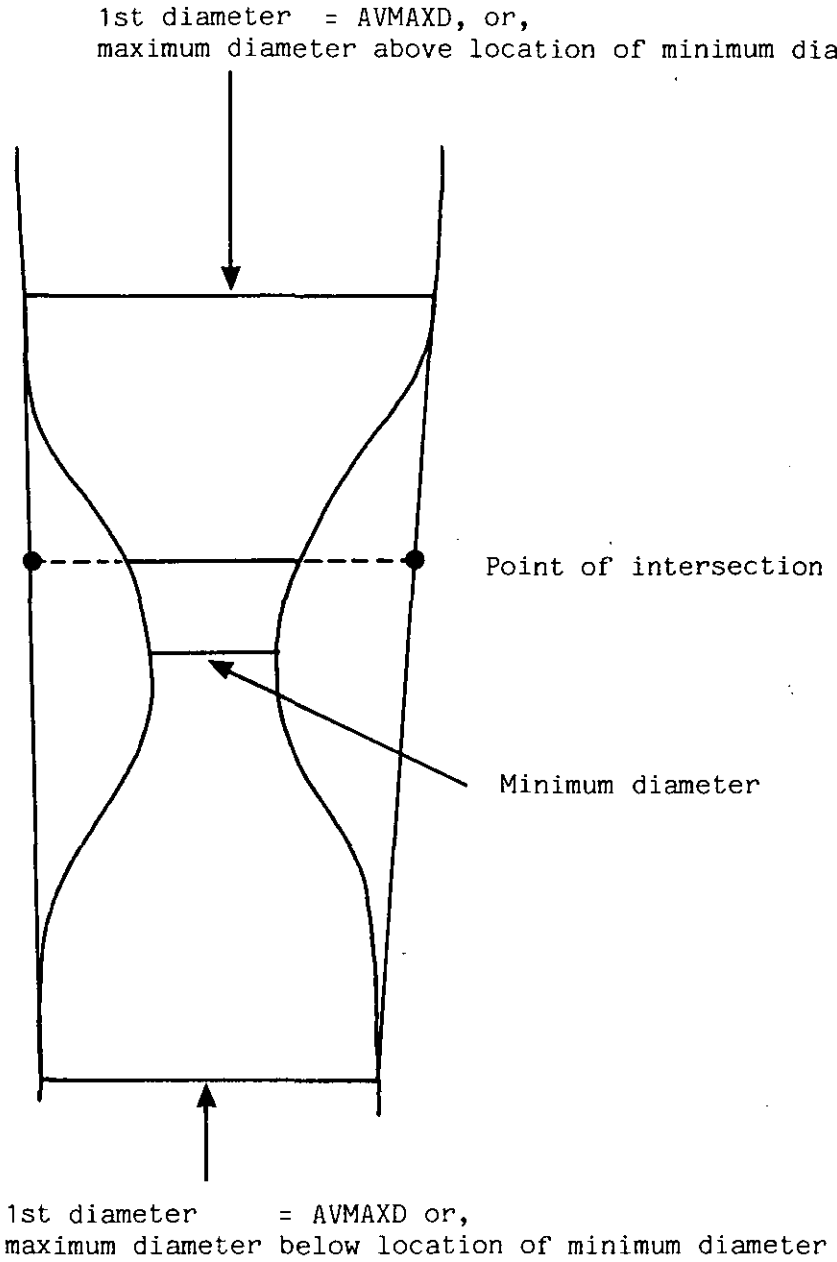

Figure 3.28 Subroutine LINFIT - Rate of change of diameter length between upper and lower boundries determines the degree of interpolation necessary for each sequential diameter

these end points describes the artery profile in the absence of disease.

CALCULATING POINTS OF INTERSECTION. If the parallelity check fails, then significant curvature is present in profile of the artery. This dictates a fit based on a circular function between proximal and distal diameters. A circular function is chosen for two reasons:

1) The data cannot realistically support the fitting of a polynomial equation as all the information for the normal artery fit is located at the "ends" (usually taken to be normal) of the tracing.

2) At large radii, the arc of a circle approximates to an ellipse, a geometric shape commonly fitted to the interior of the left ventricle particularly and the shape of the heart in general. It has been assumed that one may employ this shape to describe the course of an artery accross the external surface of the heart, provided it is viewed at right angles to its long axis.

The centre of the circle is computed as the point of intersection between extrapolation of proximal and distal diameter lines (figure 3.26) following the methodology cited in PROGRAM DIAMRS.

CALCULATING ANGULAR DIFFERENCE AND ADJUSTING RADII. The angular difference between proximal and distal diameters (figure 3.26) is computed by successive use of the function ANGLE in the normal way. Starting radii are calculated as the distances between the circle centre and the lower bound and upper bound points of the diameter lines (figure 3.26). The change in radius between the proximal and distal ends is calculated as a direct difference and the product is divided by the angular difference, resulting in an expression of rate of change of radius for that boundary with angle. For any subsequent diameter under test (figure 3.26), the lengths of the radii for this position may be obtained as:

New radius	= starting radius	+ rate of change of radius	. angular difference between start and current diameter

CALCULATING COORDINATES OF RADIAL END POINTS. Consider the diagram presented as figure 3.29. The program is proceeding to calculate new radial end points in a clockwise direction. The angular difference between the starting diameter (taken as the proximal diameter in all cases) and the current diameter is represented as θ in the figure and the parameter CURANG in the program.

Taking the lower boundary as the example, PLRAD represents the starting radial distance and LRAD the current radial distance for the position of the current diameter line. Two triangles can now be formed between the lower boundary coordinates of the diameter, the x axis and centre point and the lower boundary radial end points currently under computation, the x axis and the centre point. Ψ is used to represent the angle between the starting radius and the x axis, such that θ and Ψ represents the angle between the current radius and the x axis (NB notice that there is a difference in the use of these symbols between this figure and figure 3.26). By referring all displacements to the centre coordinates, XCENTR,YCENTR, expressions for the radial end points may be written thus:

$$LP1X(J) - XCENTR = LRAD \cos(\theta + \Psi)$$

$$LPIY(J) - YCENTR = LRAD \sin(\theta + \Psi)$$

Using trigonometric compound angle formula, these expressions may be written as:

$$LRAD\cos(\theta + \Psi) = LRAD(\cos\theta\cos\Psi - \sin\theta\sin\Psi)$$
$$LRAD\sin(\theta + \Psi) = LRAD(\sin\theta\cos\Psi - \cos\theta\sin\Psi)$$

The above are standard ratios for compound angles. For full derivation, see Davies and Hicks 1978.

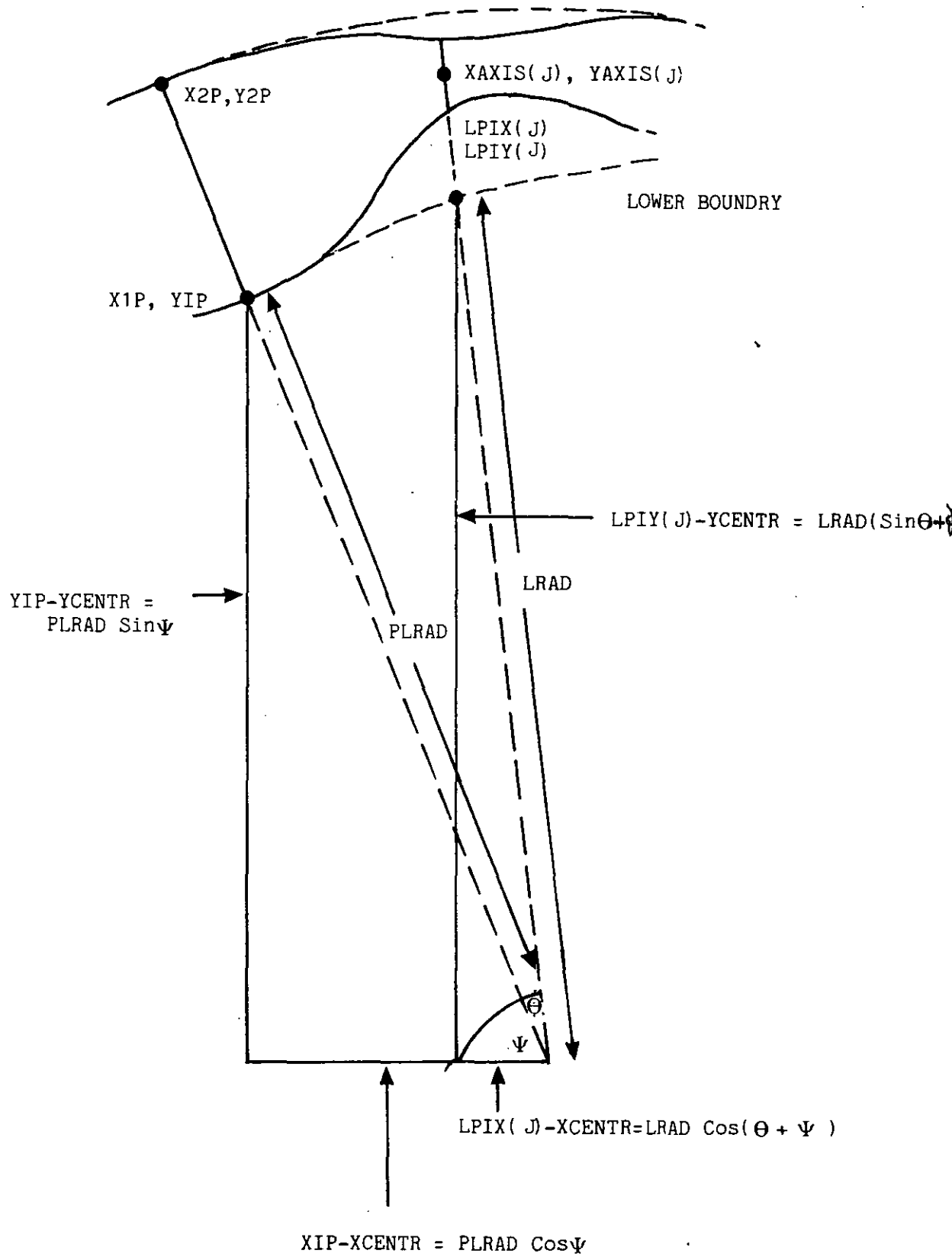

Figure 3.29 Calculation of radial end point position
(lower boundry only)

Expressions for $\sin\Psi$ and $\cos\Psi$ are obtained from the starting diameter triangle thus:

$$X1P - XCENTR = PLRAD\cos\Psi$$

Rearranging:

$$\cos\Psi = \frac{X1P-XCENTR}{PLRAD}$$

$$Y1P - YCENTR = PLRAD\sin\Psi$$

Rearranging:

$$\sin\Psi = \frac{YIP-YCENTR}{PLRAD}$$

Substituting into the radial end point equations:

$$LPIX(J)-XCENTR = LRAD \cdot \left[\left(\frac{X1P-XCENTR}{PLRAD}\right)\cos\theta - \left(\frac{Y1P-YCENTR}{PLRAD}\right)\sin\theta\right]$$

$$LPIY(J)-YCENTR = LRAD \cdot \left[\left(\frac{Y1P-YCENTR}{PLRAD}\right)\cos\theta - \left(\frac{X1P-XCENTR}{PLRAD}\right)\sin\theta\right]$$

Rearranging for radial end points:

$$LPIX(J) = \frac{LRAD}{PLRAD}\left[(X1P-XCENTR)\cos\theta - (Y1P-YCENTR)\sin\theta\right] + XCENTR$$

$$LPIY(J) = \frac{LRAD}{PLRAD}\left[(Y1P-YCENTR)\cos\theta + (X1P-XCENTR)\sin\theta\right] + YCENTR$$

This is the equation found in the listing for computation of lower boundary radial end points. The procedure is repeated for points on the upper boundry.

CALCULATION OF ECCENTRICITY. An object which is described as eccentric is defined as not having its axis placed

centrally. This method of calculating eccentricity hinges entirely on this definition.

Figure 3.30 shows a slightly eccentric lesion with superimposed normal artery profile and axis as calculated earlier in this routine. One diseased and one "normal" diameter line are highlighted as an example. They have had to be separated in order to be drawn. In actuality they sit on top of each other to some extent, crossing at the diseased artery axis as this point has been used for the radii positioning (figure 3.29). Their angles of orientation differ slightly according to the degree to which the position of the diseased artery axis changed within the controlling parameter bublen (section 3.6).

It is evident that the position of the diseased artery axis at this point does not lie on the normal artery axis line. The parameter SHIFT expresses this discrepancy in absolute terms. However, it was decided that this parameter may be better expressed as a relative measure. As absolute concentricity would be indicated by superimposition of diseased and normal artery axis points (0% eccentricity), with eccentricity capable of being measured in either direction ie. diseased axis point on either lower or upper boundry (100% eccentricity), the denominator for eccentricity calculation was taken as half the "normal" diameter. Hence the expression for relative eccentricity becomes:

$$\text{Eccentricity (\%)} = \left(\frac{\text{SHIFT} \cdot 2.0}{\text{undiseased diameter length at this location}} \right) \times 100$$

Eccentricity values at each point are compared with the maximum thus far in order to locate the point of maximal artery axis offset. Eccentricity at the previously located minimal diameter is also stored, along with cumulative eccentricity from which the average may be computed.

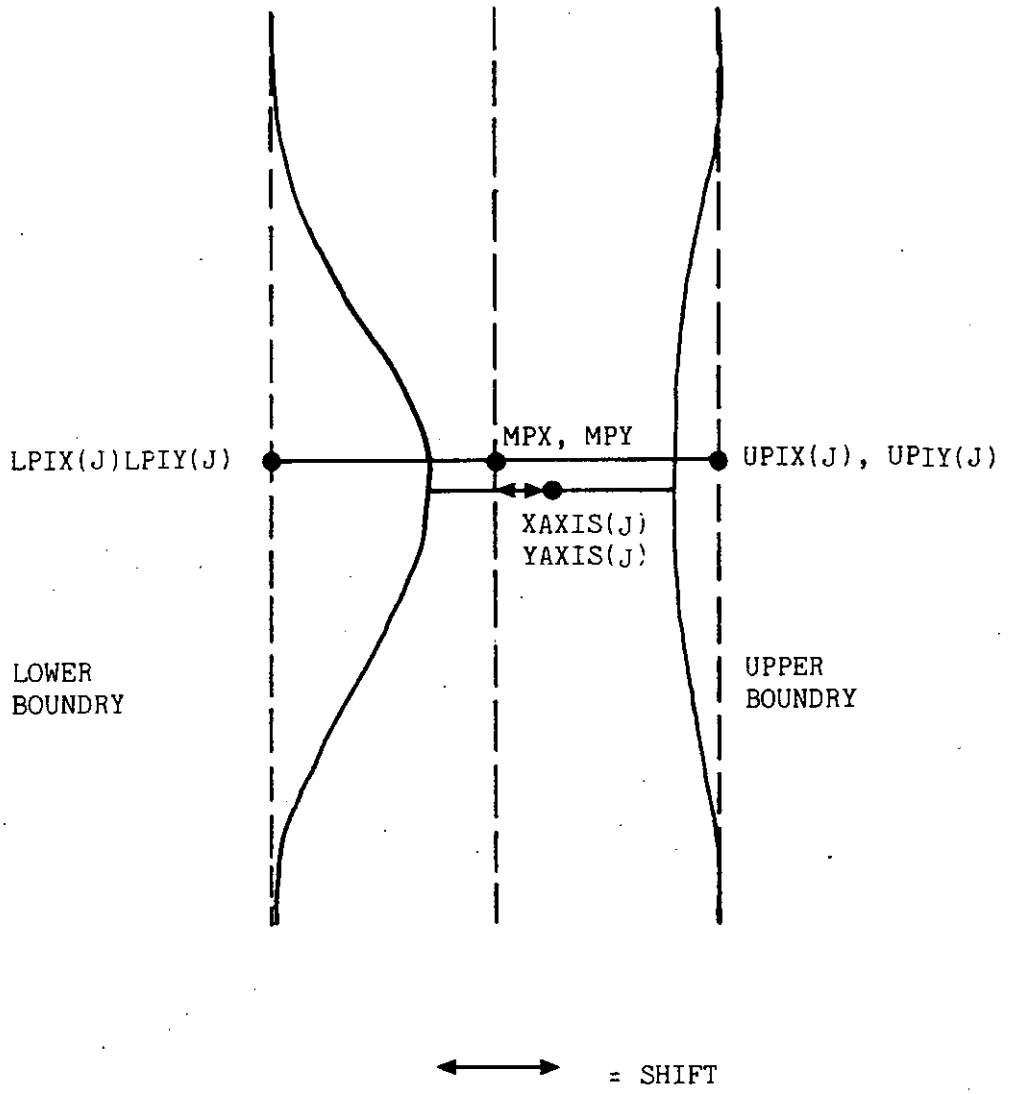

$$\text{ECCENT} = \frac{(2 \times \text{SHIFT})}{\text{UNDISEASED DIAMETER}}$$

Figure 3.30 Calculation of the eccentricity factor

CALCULATION OF UNDISEASED AND ATHEROMA AREA. Following the computation of the lower and upper boundry coordinate positions which describe normal artery profile, these may be passed to the same subroutine AREAS which calculated the diseased artery area earlier in the program. The result is an expression of the area of the normal artery between the fitted circular function limits. Atheroma area is obtained by simple difference between the undiseased and diseased areas (figure 3.26). All areas are expressed in absolute terms following correction for magnification.

Program ECCFTR produces a hardcopy of the following results:

ECCENTRICITY FACTOR AT MINIMUM DIAMETER	Relative
MAXIMAL ECCENTRICITY FACTOR	
MEAN ECCENTRICITY FACTOR	
STENOTIC AREA	Absolute
UNDISEASED AREA	
ATHEROMA AREA	

Whilst the fit of the arc of a circle to the course of the artery is perhaps not the most appropriate method for interpolation of eccentricity, it is mathematically simple and has obvious advantages over visually scored methods (Meier et al 1983b) or a purely linear fit (Wijns et al 1985a) which allows for artery taper, but not for artery curvature.

However, the technique is limited to arteries exhibiting curvature in one direction only. A second (or more) change of curvature direction throughout the course of the traced segment invalidates the circular fit and anomalous results are generated. This is also true in arteries whose direction changes reasonably rapidly eg. the RCA at the acute margin. Such results are usually manifest as negative atheroma areas and/or eccentricity values above 100%.

PROGRAM ARTDR

Whilst quantification is the primary aim of this project, the addition of graphical information can aid in its interpretation. For this reason, PROGRAM ARTDR was written and operates according to the algorithm presented as figure 3.31. No areas are highlighted for further discussion as no complicated mathematics are involved.

Unfortunately, due to lack of graphics facilities on the Vector3, this routine runs on Loughborough University Prime mainframe computer only, employing the dedicated graphics package GINO. However, should the system be transferred to a more modern microcomputer, an equivalent program could be written to allow routine hardcopy generation for placement in the patients notes, supplementing the quantitative information. Direct visualization would also be useful during program ECCFTR as the circular function fit could be directly viewed and its worth assessed prior to being printed. Figure 3.32 displays a plot of diseased artery diameter with quantification output from program ANALYZ. It is important to note that only every eighth diameter has been plotted. Figure 3.33 shows the artery axis and interpolated undiseased artery diameters superimposed upon the previous figure. Quantification data from program ECCFTR the is also included. These figures summarize the present capabilities of QAMS as it stands.

3.6 **Characterization and Validity Experiments**

3.6.1 System characterization

This section describes the methodology behind the derivation of the various constants necessary for the QAMS to run. All experiments in this section were carried out on the QAMS system itself rather than on the Prime System.

HAND TRACING TOLERANCE. As the QAMS system relies on tracing accuracy for data entry, it is important to quantify

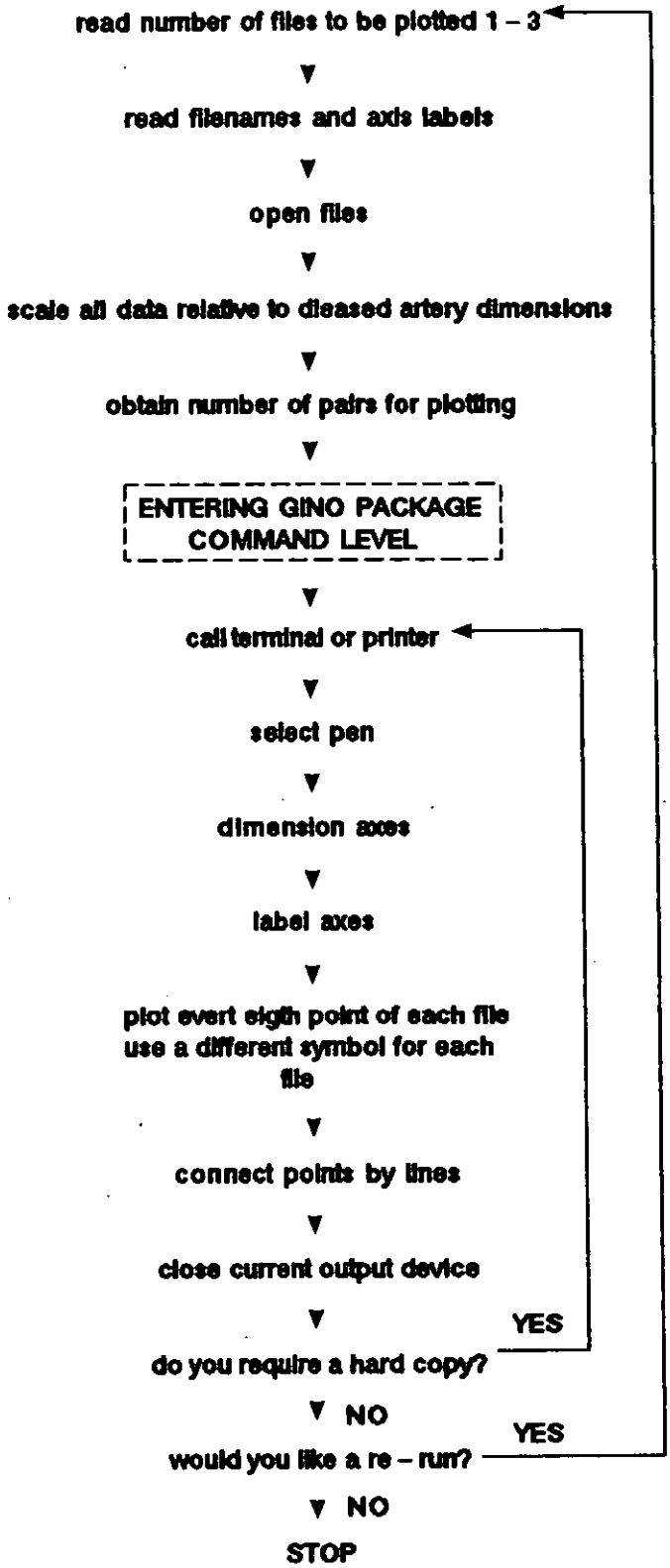

figure 3.31 ARTDR algorithm

Figure 3.32 Graphical representation of sequential artery diameters; program ANALYZ quantification data included

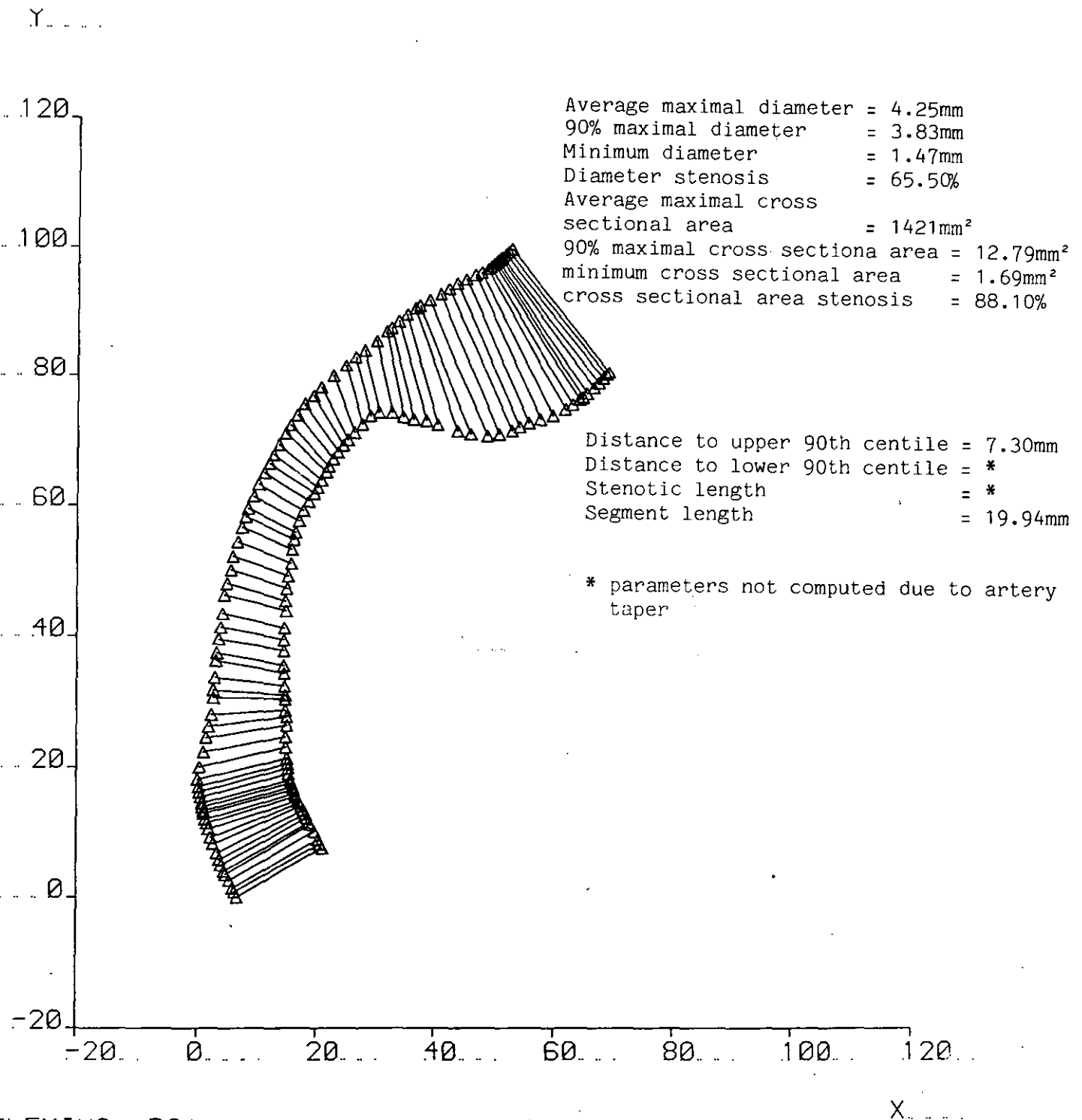

Figure 3.33 Graphical Representation of sequential diseased artery diameters, undiseased artery diameters and artery long axis; program ECCFTR quantification data included

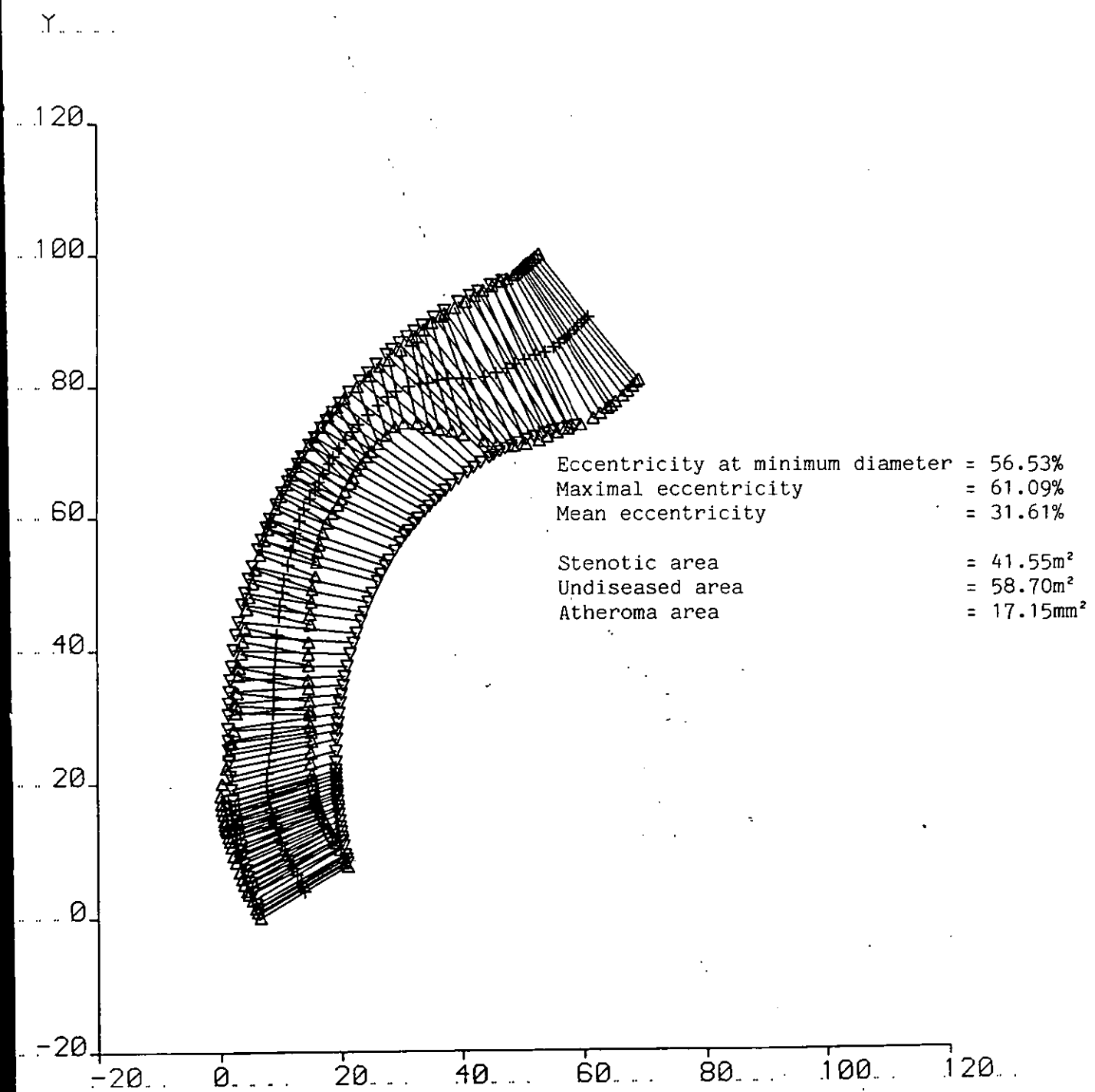

FLEMING, RCA

the extent to which a user fails to digitize to within the resolution accuracy of the graphics tablet. The magnitude of this factor is both of general interest (is it so large as to be unacceptable when digitizing objects of a size to be routinely met in the primary application of QAMS) and specific interest for application in the previously cited software.

Four naive users were each instructed to trace a marked horizontal and vertical line across the graphics tablet in their own time as accurately as possible. The lines taken were those of the wires embedded into the graphics tablet, their course reflecting a constant Y coordinate value for the horizontal and a constant X coordinate value for the vertical. Each user traced each line four times in random order before being allowed at least a one hour rest. The same users were then asked to retrace the four lines, again in random order, so that repeatability of the tolerance factor could be investigated.

Coordinate data files produced where firstly analyzed by the program BPSTAT.BAS (appendix 1) in the presence of the user which computed the number of coordinates accumulated for each trace, the mean coordinate value the standard deviation and the coefficient of variation. This information served as a quick check of data integrity (a wild standard deviation would indicate the accumulation of spurious coordinates from the collection programs) and provided the raw data for further manipulation in the mainframe based statistical package, MINITAB (Ryan,Joiner,Ryan Penn State University). MINITAB was used to calculate the average standard deviation for the whole group, the parameter accepted as the basis for the hand tolerance factor (chapter 4). Standard errors of measurement were also calculated and the data further investigated for interuser and intertest condition variation using analysis of variance and related t tests.

MAGNIFICATION AND PINCUSHION DISTORTION FACTORS. The QAMS system has been originally designed for single plane use only, which unavoidably introduces error as a result of axial displacement between the stenosis and the calibrating object (the catheter - chapter 2). Whilst this displacement cannot be measured on this system as it stands, it is important for the user to be aware of how much error there may be in an absolute measurement of a stenosis with varying axial displacement. Should the user be requiring absolute measurements, the magnitude of the magnification factor may encourage him to combine knowledge of cardiac anatomy with radiological projection in an effort to employ a view where axial displacement is at a minimum. Derivation of the pincushion distortion factor is necessary so that objects to be quantified using the QAMS may have the effects of selective magnification at the frame edges removed as discussed in section 3.5.

The deviation of both factors was combined into one experiment.

Films were taken at the catheter rooms of the Groby Road Hospital, Leicester of a calibration grid composed of crosswires. A custom made grid was not available, so industrial mesh was used instead, with the absolute measurements of all wire separations to be quantified from the film being previously measured with a set of hand held vernier calipers accurate to 0.02mm, the average of three repeat measurements being used. One exposure of the grid was made in each room with the grid centre at that of the image intensifier at five differing but known source - film distances and the two commonly employed image intensifier sizes (section 3.2.1) giving a total of ten exposures per catheter room.

As pincushion distortion is absent at the centre of the image, the magnification factor may be derived from analysis of the rate of change of separation of centrally placed crosswires with increasing source - film distance, and its

comparison to the absolute separation. Characterization of the pincushion distortion factor requires measurement of crosswires separation at increasing radial distances from the centre and comparison to the absolute separation in a manner described in section 3.5.

Hence, using point mode, the 4 corners of a centrally located square of the grid image were digitized, along with other squares in the horizontal and vertical planes at increasing radial distances from the image centre. The resultant data files were processed by a custom written program CUSHCALC.FOR (appendix 1). For every source - film distance and image intensifier size, the program supplied values of current magnification factor, ratio of crossgrid wire separation in the outer field to that in the centre, and radial distance from midpoint of digitized point pairs to image centre. This raw information was further investigated using the MINITAB statistical package where regression analyses were performed.

3.6.2 Software Validity

This section addresses the questions "do the routines perform the tasks they are supposed to, and, are the subsequent results accurate enough to warrant further implementation"? Thus, for every routine which involved any form of computation other than pure "number crunching" (ie. PROGRAM ANALYZ), an experiment was designed and undertaken to put the code to the test. As these experiments were at the heart of the software developmental process, the data for these experiments was collected and processed using the University's graphics tablet and Prime System.

TESTING PNTED. Leaving pincushion distortion aside for the moment, the program basically works by making decisions about the structure of the datafile in question. Competence is assessed on whether the data file is free of any coincident points or reversals. Therefore, in order to

test PROGRAM PNTED, a sample data file was created containing known errors designed to test every facet of the decision making process. The routine was judged accurate when all discrepancies were correctly identified and removed.

Correction of the data for pincushion distortion involves adjustment of the value of each coordinate point in accordance with the value of the earlier derived factor in the form of the equation which characterizes the distortion. Raw datafiles were checked by hand and tested for agreement with their processed equivalents.

TESTING DIAMAV. Program DIAMAV was tested by employing the following two experiments:

Experiment 1. This experiment was conducted in order to establish if the program was capable of accurately measuring areas of the size likely to be encountered during the quantification process. To this end, two sets of test data were created. Firstly, representing undiseased coronary arteries, "tubes" of known area, range $0.5cm^2$ to $5cm^2$ in $0.5cm^2$ increments were drawn on graph paper. Secondly, tracings of actual coronary arteries (exhibiting coronary artery disease) were taken directly from the projected images. The area of the tracings was then calculated using a planimeter (Gerbruder Haff GMBH, Pfronten-1, West Germany), the mean of three tracings taken to be representative of the true area.

Each area was then digitized on the University's Summagraphics graphics tablet (Terminal Display Systems Ltd., Blackburn Lancs.), which allowed the production of a coordinate datafile in the Prime filespace for subsequent area analysis. Each area was digitized three times, with each datafile being separately analyzed by the PROGRAM DIAMAV. The mean of the three tracings was taken to be representative of the true area for analysis (chapter 4). Linear Regression analysis was then carried out on the two

data sets to highlight potential differences. The two data sets were then combined in order to produce a data set representative of all physiological possibilities in the quantification of the dimensions of coronary arteries. Linear regression analysis was performed on this "combined" data set also.

Experiment 2. The ability to measure area accurately from an analogue source is very useful. Indeed, the measurement of area has many applications other than the one found for it in this thesis. Hence, this experiment was conducted in order to establish whether the algorithm which lies at the core of the PROGRAM DIAMAV was capable of measuring areas of any size (limited only the input device, the graphics tablet) and any shape, regular or infolded. Again, two sets of data were created. The first, like before, was constructed as drawings on graph paper. In this instance, a variety of geometrical shapes of varying size were chosen, the area of which was either calculable directly by equation, eg. Πr^2 or obtainable by dividing the more complex shape up into a collection of smaller regular shapes whose individual areas could be calculated from equation. The shapes chosen included the square, circle, triangle, hexagon, horseshoe and sixpointed star. The second data set was taken from planimetered areas of highly complex shapes which were drawn at random, the area of which was not calculable by any form of equation. Again, the mean of three tracings was utilized for analysis in the results.

All areas were digitized and processed according to the previously cited methodology. All data was then analyzed in a similar fashion to that in the previous experiment, both separately and combined.

TESTING DIAMRS. PROGRAM DIAMRS uses the information passed to it from PROGRAM DIAMAV to grow, move and contract a mathematical bubble along the course of the digitized coronary artery, calculating the position of diameter lines perpendicular to the long axis as it goes. It seemed

obvious that the crucial parameter to test as a mark of performance of this program was the perpendicularity of the diameter lines. In order to investigate this, the data files from the tubes in the previous routines validation where re-employed. Note, tubes 1 to 5 had a diameter of 50mm whilst tubes 6 to 10 had a diameter of 100mm. PROGRAM DIAMRS was allowed to run on these files following processing by PROGRAM DIAMAV which provided the relevant bubble information.

In addition to the file of diameter end point information which is normally produced, an additional file containing the angle between the diameter line and the right directed horizontal was created. This latter file could now be analyzed for constancy of angle expressed as mean, standard deviation and coefficient of variation thus describing parallelity between the diameter lines throughout the traced tube. Once the actual diameters had been calculated from the coordinate information in the DIAMETER.EPS file, variability in these dimensions could be expressed as mean, standard deviation and coefficient of variation, their magnitude reflecting the combination of the errors of non-parallelity with those of hand tracing tolerance.

The ability of the routine to work with curvature was also investigated. Three curved tubes of varying radii were drawn and digitized. PROGRAM DIAMRS then processed these files, the diameter lengths expressed again as mean, standard deviation and coefficient of variation. Unfortunately it is not possible to examine variability in angle in the same fashion as was adopted in the previous validation as the angle of the diameter lines relative to the right directed horizontal will be changing as the bubble travels down the axis of the curve.

Whether the value of bublen provided by PROGRAM DIAMAV was producing the best results also came under scrutiny at this point. If the value of bublen were set correctly for the tracing under test, then errors in stenotic parameters would

be at a minimum. Hence, program DIAMRS was allowed to run on data from digitized coronary stenoses (taken from projected tracings, as in PROGRAM DIAMAV validity) and the bubble length from program DIAMAV was altered in the following manner. Taking the original value as 100%, PROGRAM DIAMRS was allowed to run on 50%, 75%, 100%, 150% and 175% of this value with resultant data files examined in the manner previously described.

TESTING ANALYZ. Program ANALYZ is a simple numerical manipulation routine, and therefore did not undergo any extensive validation other than comparison of results from hand worked examples with those of computed ones - this includes the calculation of the magnification factor from the digitized catheter coordinates.

TESTING ECCFTR. The principle behind program ECCFTR involves fitting of an arc of a circle between two previously identified diameter lines. Therefore, in order to validate the routine, the three curved tubes from the previous validation were re-employed. The coordinates representing the proximal and distal diameter lines between which the fit had taken place were obtained, along with all coordinates between these limits. PROGRAM ECCFTR then processed these files in the normal way. As the routine produces a set of coordinates from the fit for every set of initial coordinates, direct comparison of the differences between the two data sets could be made. This was carried out using a two tailed unrelated 't' test at the 5% level of significance.

TESTING ARTDR. Like PROGRAM ANALYZ, PROGRAM ARTDR is merely an numerical manipulation routine, the only difference being that the Fortran code is interfaced through Prime resident GINO routines to the University's Laser Jet printer. The routine was not validated in the true sense, (other than working through), but rather parameters within the code were altered until a "pleasant" graphical result was obtained from the raw data.

3.6.3. Usability

This section describes experiments conducted in order to assess the repeatability, objectivity and validity of the QAMS system and as such all data were collected using the system itself, rather than the University's mainframe computer as in the previous section.

In each of the three sections which follow, the method of data collection is exactly the same as that described in appendix 1.

1. REPEATABILITY. This section addresses the question "to what extent does image selection and preparation interfere with obtaining repeatable results in the digitization of coronary artery stenoses". As group variability for digitization had already been studied (section 3.6.1), this experiment concerned itself with individual variability only.

   The following data was collected in order to investigate repeatability. NB. each test utilized a different film.

   a. 8 times repeated digitization of the same pretraced stenosis (apparently most severe) in the same frame of a given cine angiogram.

   b. 2 sessions of single digitization of eight different pretraced stenoses.

   c. 8 times repeated tracing and digitization of the same stenosis (apparently most severe) in the same frame of a given cine angiogram.

   d. 8 times repeated tracing and digitization of the same stenosis in multi-frame increments over the course of one cardiac cycle (systole - systole)

(NB. the stenosis could only be digitized when adequately visualized).

e. 4 times single tracing and digitization of the same stenosis in the same frame (as judged by left ventricular wall movement) across consecutive cardiac cycles.

Using the above strategy, variability within the results for coronary artery quantification due to digitization, tracing, intracardiac cycle change and intercardiac cycle change could be evaluated. The results for each trial were examined and compared using simple descriptive statistics. Data from experiment b was subjected to computation of the standard error of measurement statistic.

2. OBJECTIVITY. This trial addressed the question,"how well does one individuals measurements of a coronary artery agree with another?". This trial was conducted at Loughborough University using students reading Human Biology as users. Since patient cine films could not be removed from the Groby Road Hospital premises, slides taken from patients films were used as an alternative source of data. As errors introduced by repeat tracing had previously been evaluated, the contours of the stenosis were highlighted prior to commencement of the trial.

Eight users each traced the same artery once, variability amongst the stenotic dimension estimates between the users was examined using descriptive statistics. The same eight users then each traced eight different stenoses twice; the resultant data then afforded computation of a standard error of measurement statistic.

3. VALIDITY. " Do estimates of dimensions obtained using the QAMS system reflect their dimensions true life?".

In order to investigate this question, one must have access to films of material whose true size is known accurately. This is far more difficult to achieve than it sounds. Ideally, this system would have been best validated on comparisons of dimensions of histologically processed human coronary arteries and their equivalents from the QAMS system. However, such a comparison could not be made within the scope of this work for the following reasons:

1. The handling of human postmortem material in a busy catheter laboratory is unethical and hazardous, unless done under completely aseptic conditions, cleaning thoroughly both before and after use. This is costly both in terms of time the catheter laboratory is out of action, and manpower involved.

2. Fresh postmortem material is difficult to acquire. ie. before it is subjected to the routinely used preservatives which tend to distort and alter the structure of the material. Even abbatoir animal material is rendered unusable by the slitting of the heart walls during routine meat inspections.

3. Loughborough University has no histological processing facilities.

As coronary arteries could not be used, objects of known size were substituted. As grid radiographs already taken in both catheter rooms existed (section 3.6.1) it seemed sensible to cut intrusion into the normal workings of the catheter laboratory down to a minimum, and use the separation of the grid wires as the raw data.

Hence, two sections of gridwire were arbitrarily selected across the surface of the grid, one in the horizontal plane and one in a vertical plane for each catheter room and image intensifier size. Each section was carefully measured with

an engineering vernier caliper (accurate to 0.01mm), the mean of three readings being taken to be representative of the true value. Then, each section of grid wire was digitized eight times. Comparisons between the vernier measurements and those provided by the QAMS system where then made using correlation analysis and a two tailed unrelated "t" test with significance set at the 5% level. Repeatability of true wire separation estimate was also examined using simple descriptive statistics.

CHAPTER FOUR

RESULTS

4.1 System Characterization

4.1.1 Hand Tracing Tolerance

Table 4.1a presents the data from the repeatability study described in section 3.6.1. Each individuals data have been averaged across the four re-traces.

Hand tracing tolerance was calculated as twice the average standard deviation (SD) across all users on both trials - the result being 22.04 graphics tablet units (g.t.u - table 4.1a). Thus, in the PROGRAM PNTED, there is 95% confidence that any reversals of magnitude equal to or less than 22.04 g.t.u are due to "hand tremor". Reversals exceeding this criterion are treated as intended and **not** removed from the final data set.

Standard errors of measurement (Smeas) for the three parameters of total coordinate number, mean coordinate value and SD were also calculated as the SD of the differences in any one parameter, divided by the square root of two (table 4.1a). The results indicate that variability incurred in the digitization of a constant X or Y value is very small (coefficients of variation (CV) for each re-trace less than 0.3%) over a wide range of total coordinates collected (Smeas 60.13) both in absolute terms, and relative to the previously calculated hand tracing tolerance (SD only).

Variability across the users (subjects) and between the two test conditions was then examined in order to exclude the possibility that the magnitude of the hand tracing tolerance factor had not been unduly influenced by any one users results. This was achieved using two way analysis of variance (table 4.1b). The analysis demonstrated only three significant results at the 1% level, all due to between

Table 4.1a Group repeatability (mean of 4 runs), standard error of measurement and computation of hand tracing tolerance

gtu = graphic tablet units (thousands of an inch)

		RUN 1				RUN 2			
		N	$\bar{X}$(gtu)	SD(gtu)	CV(%)	N	$\bar{X}$(gtu)	SD(gtu)	CV(%)
X CONSANT	MJ	327.7	5294.95	8.58	0.162	268.2	5295.52	8.70	0.164
	VWM	277.0	5292.17	9.51	0.181	143.7	5293.95	11.42	0.216
	PSB	300.0	5292.37	13.10	0.248	369.7	5294.55	9.74	0.184
	DB	341.7	5296.10	8.53	0.161	283.7	5299.75	9.64	0.182
Y CONSANT	MJ	280.0	5806.65	9.64	0.166	281.5	5804.85	8.28	0.143
	VWM	239.2	5810.62	13.60	0.234	146.2	5810.82	16.94	0.293
	PSB	454.2	5810.90	14.46	0.249	469.7	5810.12	11.76	0.203
	DB	296.0	5808.85	9.43	0.162	239.0	5805.50	13.07	0.225

Standard errors of measurement (Run 1 - Run 2)
(Subject and X, Y data combined)

N = 60.13
X = 4.19
SD = 2.88

Average standard deviation (whole group) = 11.02 : Hand tracing tolerance = 2 x SD = 22.04 gtu

Table 4.1b Intersubject and intertest variability. Two way analysis of variance $\alpha = 0.01$ (Run 1 vs Run 2 and MJ vs VWM vs PSB vs DB)

	Between Subjects		Between test conditions		Interaction	
X CONSTANT	df	F obs	df	F obs	df	F obs
N	3,24	7.04 $p \leqslant 0.01$	1,24	4.87	3,24	4.22
X(gtu)	3,24	4.12	1,24	3.51	3,24	0.80
SD(gtu)	3,24	2.42	1,24	0.05	3,24	2.01
Y CONSTANT						
N	3,24	74.30 $p \leqslant 0.01$	1,24	6.29	3,24	3.66
X(gtu)	3,24	2.81	1,24	0.95	3,24	0.26
SD(gtu)	3,24	6.65 $p \leqslant 0.01$	1,24	0.49	3,24	2.41

subject variation; those of total number of coordinates collected for both X and Y constant, plus SD for Y constant.

Although no significant differences were encountered for between test condition variation, it was thought wise to examine this parameter on an intrasubject level using a battery of related t tests (table 4.1c). Such testing allows examination of individual repeatability of the tolerance factor and change in the magnitude of the SD as a result of accumulated experience from the first run.

All results are non significant at the 1% level (table 4.1c) confirming that the tolerance factor is individually repeatable and the magnitude of the SD shows no training effect.

These facts establish the conclusion that the current setting for the hand tracing tolerance factor is appropriate even after allowing for familiarization.

4.4.2 Magnification and Pincushion Distortion Factors

a. Magnification factors (MF's). Data, following initial processing by the program CUSHCALC.FOR is presented in table 4.2. The upper half of the table documents the MFs at increasing source to film distances (relative displacement) whilst the bottom half of the table deals with rate of change of MF using regression analyses.

   The two variables of MF and distance were regressed against each other for each of the four conditions (figure 4.1), the resulting gradient from each analysis representing the rate of change of MF with distance.

   Rate of change of MF varied from $0.0158cm^{-1}$ in Room A, small image intensifier size to $0.0251cm^{-1}$ in Room B, large image intensifier size (section 3.2.1). Transferring these two extremes to a practical condition where a 3.5mm lesion may be displaced from

Table 4.1c Intrasubject variability between test conditons
2 tailed related t tests (Run 1 vs Run 2) $\alpha = 0.01$

		N	X(gtu)	SD(gtu)
X CONSANT	MJ	2.75	-0.26	-0.54
	VWM	3.03	-0.41	-1.32
	PSB	-1.04	-1.48	3.22
	DB	2.24	-2.33	-0.98
Y CONSANT	MJ	-0.23	0.91	0.91
	VWM	4.41	-0.06	-0.83
	PSD	-0.63	0.23	1.79
	DB	4.45	0.71	-2.90

All results are non significant

Table 4.2 Rate of change of magnification factor (MF)

	MF			
Relative distance (cm)	Room A, SmallII	Room A, LargeII	Room B, SmallII	Room B, Large II
0	1.66192	2.59103	1.42231	2.16513
5	1.70076	2.60222	*	2.25376
10	1.76831	2.76197	1.57891	2.41854
15	1.86133	2.89800	1.66559	2.50377
20	1.98098	2.97607	1.79799	2.66696
Gradient (rate of change of MF cm^{-1})	0.015848	0.021317	0.018303	0.025073
SE gradient	0.001761	0.002684	0.001650	0.001526
r	0.98 $p \leqslant 0.01$	0.97 $p < 0.01$	0.99 $p < 0.01$	0.99 $p \leqslant 0.01$
SEE	0.028	0.042	0.024	0.024

II = Image intensifier

* indicates missing value

figure 4.1 Rate of change of magnification factor.

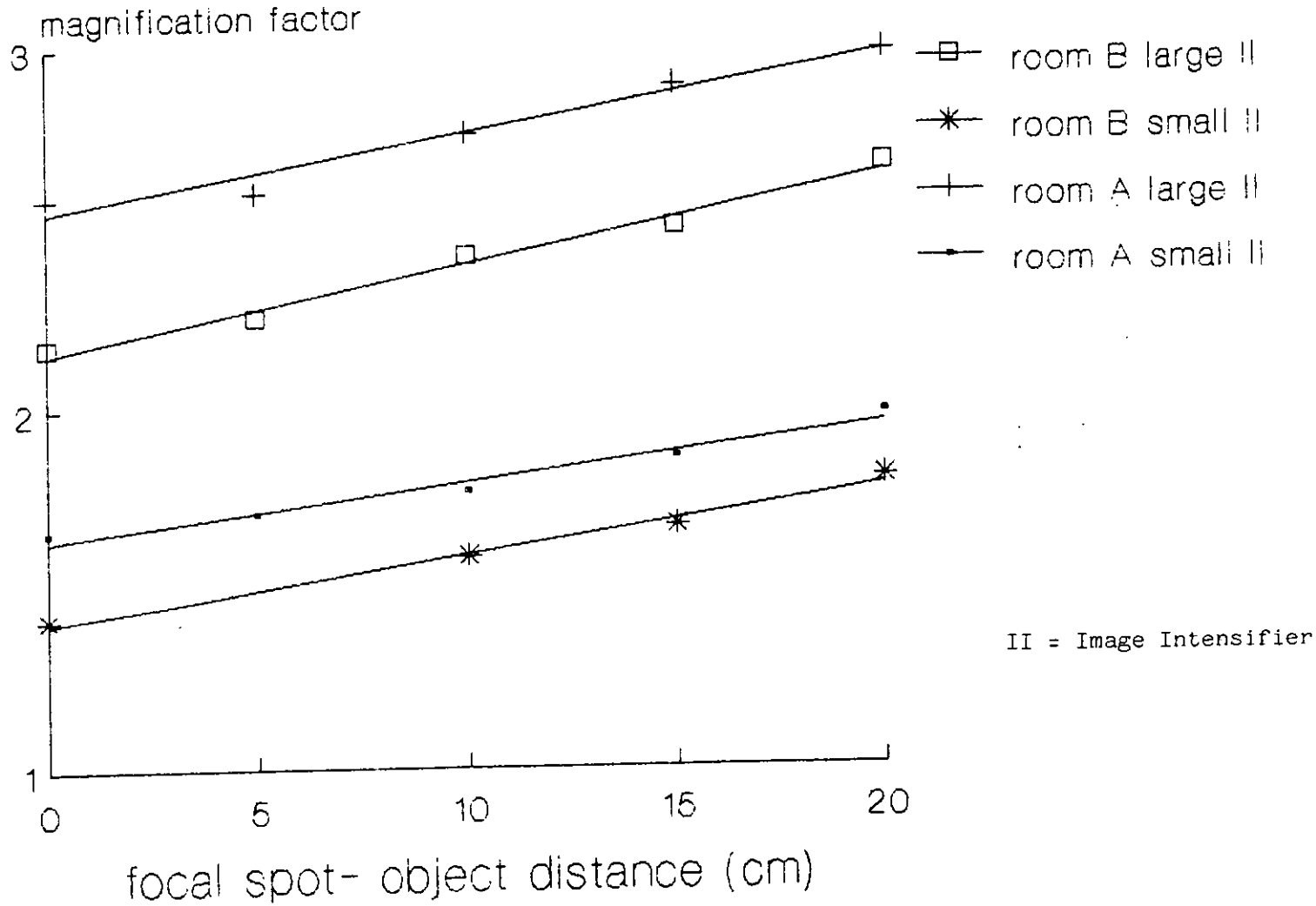

II = Image Intensifier

the catheter by for example, as much as 3cm, rates of change of MF of this order would incur errors in the estimation of maximal diameter of 4.7% and 7.5% respectively. However, 3cm represents a theoretical maximal displacement; it is envisaged that the working discrepancy in the major application of the QAMS in this thesis would be much smaller than this.

All correlation coefficients describing the relationship between MF and distance were compared against a critical value at the 1% level of significance in the one tailed condition, as the regressed relationship was expected to be positive. All correlation coefficients were significant under these conditions, confirming the highly linear relationship between MF and distance.

b. Pincushion distortion factors. As presented in section 3.5, magnification factor at increasing distances from the centre of the image intensifier is related to the square of this distance according to the general equation $Y = aX^2+b$. Therefore regression analysis was performed between the square of the radial distance and magnification factor at these increasing radii.

The upper portion of table 4.3 documents the regression results describing the rate of change of pincushion distortion factor with the square of increasing radial distance. Graphical representation of the relationships is presented as figure 4.2. All relationships are highly linear ($r >= 0.88$) with low variability about the regression line (standard error of the estimate - SEE $<= 0.045$). All gradients (equivalent to 'C', the coefficient characterizing the pincushion distortion in this and the Brown - Dodge method) agree reasonably well apart from that in room A with the small image intensifier. This particular relationship also has the largest standard error of the gradient (SEgrad).

Table 4.3 Pincushion distortion factors

General equation: $Y = aX^2 + b$

	Room A, SmallII	Room A, LargeII	Room B, SmallII	Room B, LargeII
N	39	28	29	33
Gradient (cm^{-2})	0.0020136	0.00062484	0.0006513	0.00053700
SE gradient (cm^{-2})	0.0001486	0.00005607	0.00006559	0.00004235
r	0.91 $p \leqslant 0.01$	0.91 $p \leqslant 0.01$	0.88 $p \leqslant 0.01$	0.91 $p \leqslant 0.01$
SEE	0.045	0.015	0.021	0.017
Intercept	1.00479	1.00614	1.01232	1.01260
SE intercept	0.01240	0.00434	0.00551	0.00417
t ratio	0.37	1.41	2.23	3.02 $p \leqslant 0.01$

figure 4.2 Rate of change of pincushion distortion factor.

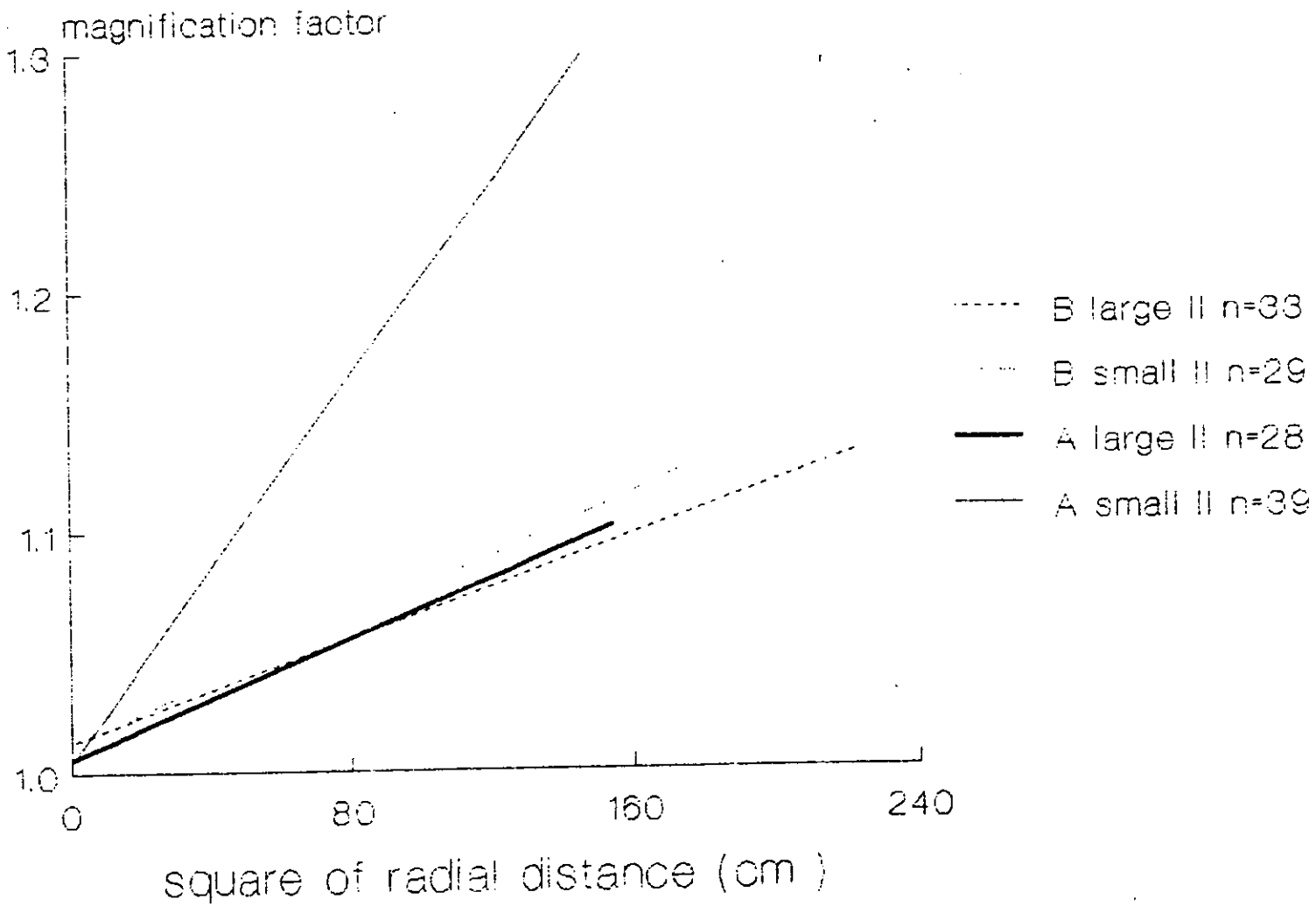

As pincushion distortion is theoretically absent at the centre of the image intensifier, all regression relationships should intercept with the y axis at a magnification factor of 1. This theory was put to the test applying a criterion t test to the intercept data calculated thus:

$$t\ Ratio = \left(\frac{\text{true intercept} - \text{expected intercept(ie1.0)}}{\text{SEIntercept}}\right)$$

The theory is confirmed in three of the four cases, with the intercept in room B, large image intensifier being significantly different from 1.0 at the 1% level.

4.2 Software Validity

4.2.1 PROGRAM PNTED

Figure 4.3a presents the test datafile containing both coincident points and reversals. Note the metric equivalent of the hand tracing tolerance factor was used. This enabled coordinate separation to be kept small and easy to handle during testing.

As a validation procedure, PROGRAM PNTED was allowed to process this datafile and the resultant file was checked for errors. PROGRAM PNTED was not implemented until detection rate was 100%. The objective data file is presented as figure 4.3b and was produced both by hand and the current version of PROGRAM PNTED.

4.2.2 PROGRAM DIAMAV

Table 4.4 documents the results to a series of related t tests performed on the six sets (4 individual, 2 combined) of data collected for the validation of the routine DIAMAV. The 5% level of significance was chosen for these tests as this reduces the possibility of a type II error, ie. failing to reject the null hypothesis when it is actually false.

figure 4.3a Test data file - pre program PNTED processing.

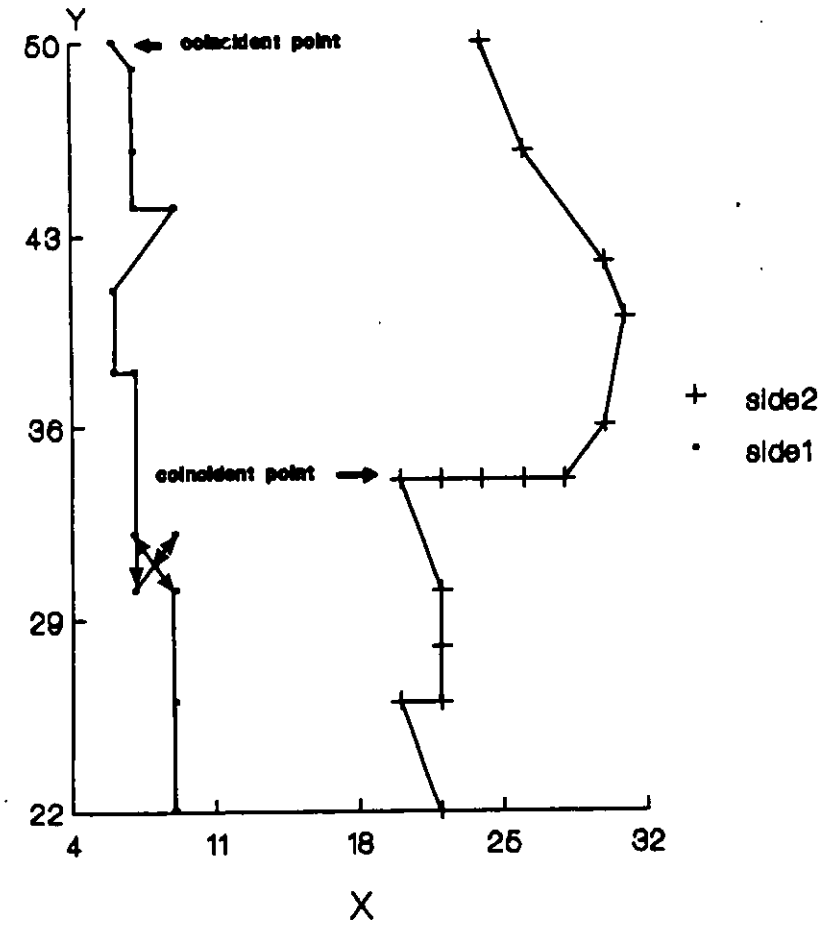

In this example, hand tracing tolerance has been set to metric equivalent: i.e. 0.056 cm (5.6 bitpad units)

figure 4.3b Test data file - post program PNTED processing.

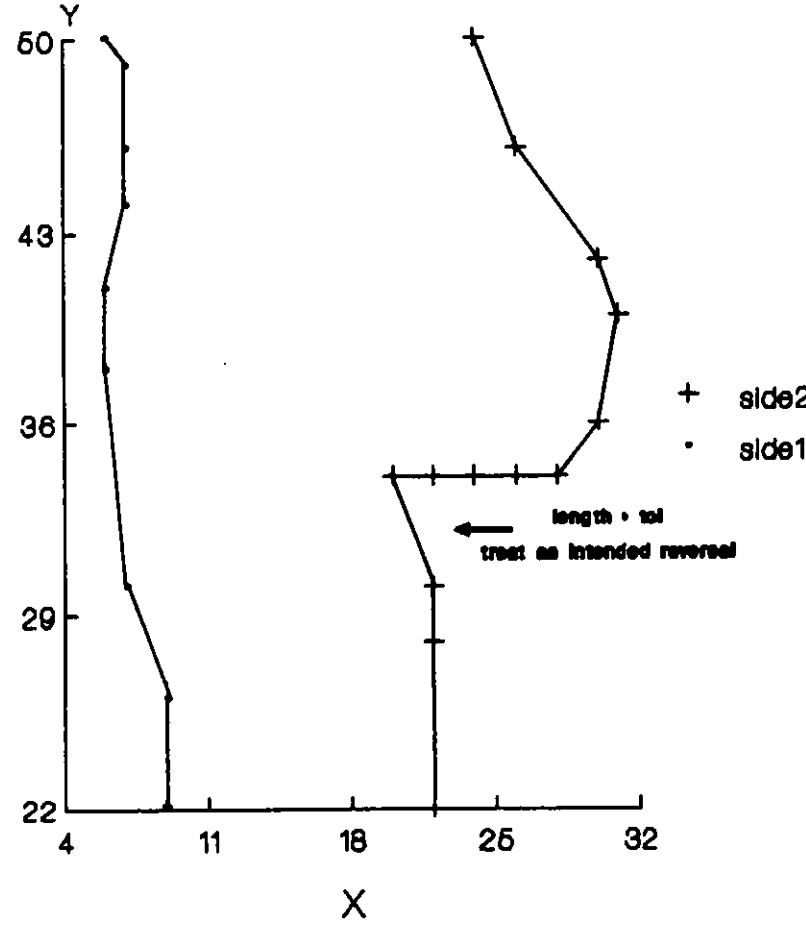

In this example, hand tracing tolerance has been set to metric equivalent: i.e. 0.056 cm (5.6 bitpad units)

Table 4.4 2 tailed related t test results, $\alpha = 0.05$, DIAMAV evaluation

	t observed	d.f.	t critical	decision
Tubes in the physiological range	0.6851	9	3.250	NS
Digitised arteries	1.4895	9	3.250	NS
Tubes and arteries combined	1.6299	19	2.861	NS
Geometric shapes	0.3648	13	3.012	NS
Convoluted areas	-0.2652	9	3.250	NS
Shapes and areas combined	-0.1532	23	2.807	NS

NS = Not significant

This level of significance seemed most appropriate as even small discrepancies are important in the measurement of area due to its two dimensional nature.

From the evidence of the validation results, the routine performs well as there are no statistically significant differences detected in any of the individual or combination groups.

The validity of area measurement using PROGRAM DIAMAV was further examined by regressing true area against computed area (table 4.5 and figures 4.4a,4.4b). If the routine computes true area, the regression relationship should show no significant differences from the line of identity. All SEgrads are low, with those in the geometric shape and convoluted area groups being relatively smaller than those in the tubes and arteries groups. All t tests performed to detect significant differences from the line of identity (t ratio formula presented in section 4.1.2) are non significant, confirming that the routine does indeed compute area accurately over a wide range of shapes and sizes. Intercepts are all approximately zero reinforcing this statement. All SEEs are low and correlation coefficients equal to unity. The significance of the regression relationship has also been tested using analysis of variance (Fregr) yielding highly significant results.

Overall, this routine is sufficiently accurate to be used in the QAMS system.

4.2.3 PROGRAM DIAMRS

Analysis of the tube data for variation in diameter length and angle (with respect to the right directed horizontal) from the previous sections experiments resulted in the data presented in table 4.6. Regarding the results of variability in diameter length firstly, all mean diameters approximate to the criterion values (50mm and 100mm), however, there is increased disparity in tubes 1 to 5 (CV

Table 4.5 Regression analyses results for DIAMAV evaluation

	N	Gradient	SEgrad	t regr	Intercept (cm)	SEE	r	F regr
Tubes in physiological range	10	1.0005	0.0140	0.036	0.0118	0.0636	1.00 $p \leqslant 0.05$	5077.82 $p \leqslant 0.05$
Digitised arteries	10	1.0157	0.0503	0.312	0.0152	0.0915	0.99 $p \leqslant 0.05$	408.56 $p \leqslant 0.05$
Tubes and arteries combined	20	0.9973	0.0144	-0.188	0.0349	0.0763	1.00 $p \leqslant 0.05$	4789.20 $p \leqslant 0.05$
Geometric shapes	14	1.0025	0.00138	1.812	-0.1505	0.3510	1.00 $p \leqslant 0.05$	 $p \leqslant 0.05$
Convoluted areas	10	1.0027	0.0068	0.397	-0.2973	1.5787	1.00 $p \leqslant 0.05$	21696.30 $p \leqslant 0.05$
Shapes and areas combined	24	1.0027	0.0029	0.931	-0.2168	0.9890	1.00 $p \leqslant 0.05$	122015.51 $p \leqslant 0.05$

figure 4.4a Relationship between true and computed areas in the physiological range - program DIAMAV validation.

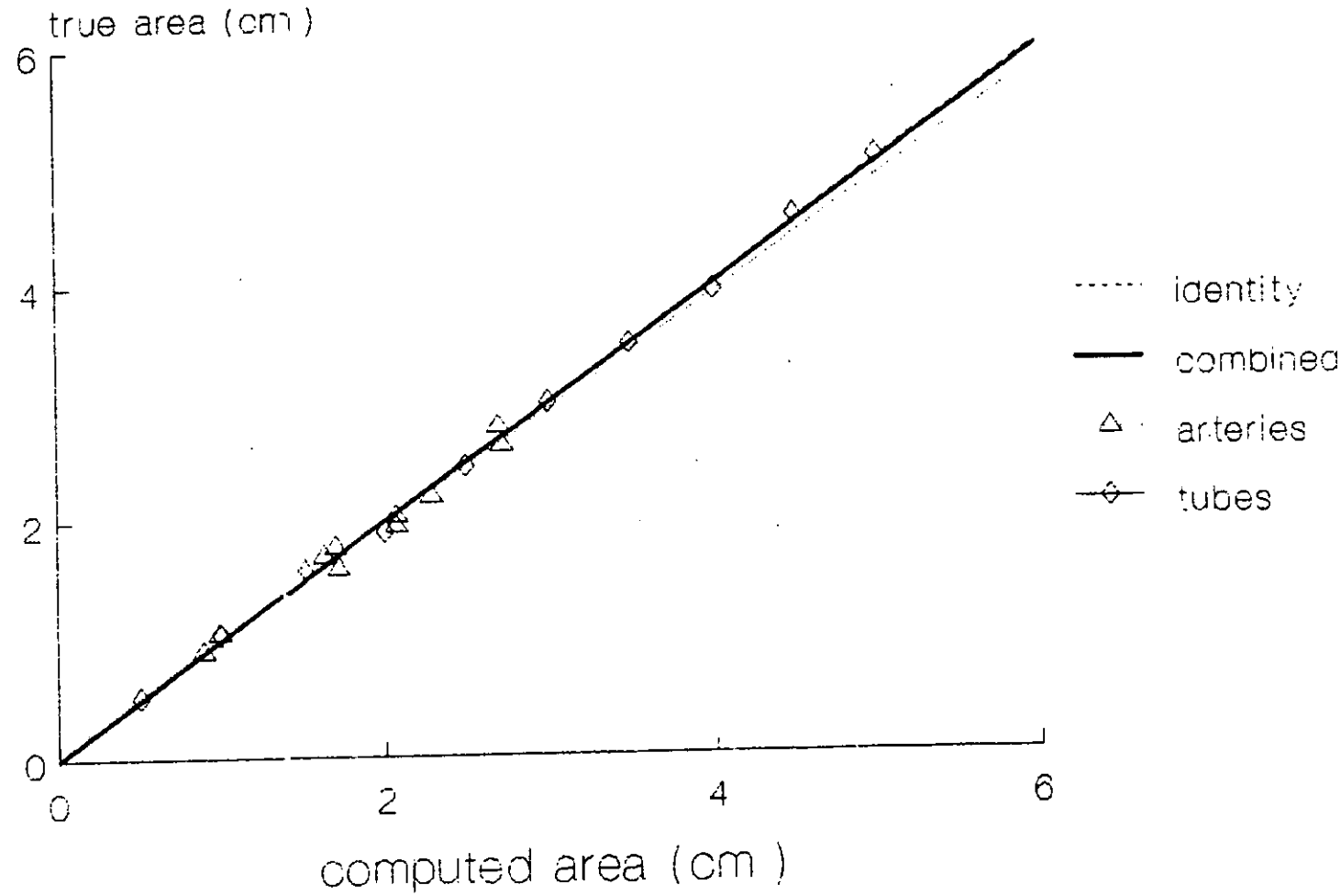

figure 4.4b Relationship between true and computed areas in the general range program DIAMAV validation.

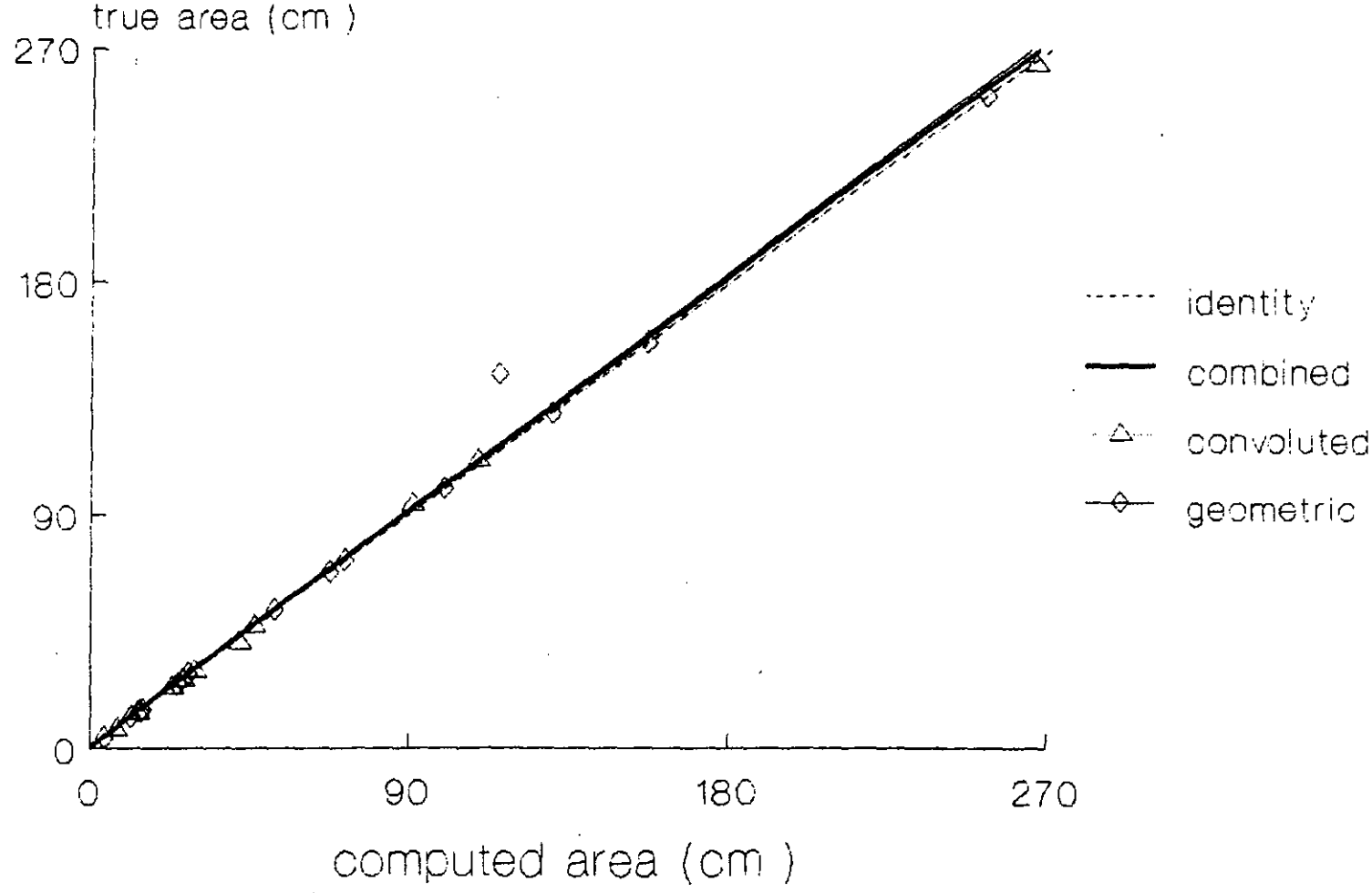

Table 4.6 Variability in diameter length and angle (with respect to the right directed horizontal) of digitised tubes. DIAMRS validation

Tube No	Length (cm)	DIAMETER			ANGLE		
		$\bar{X}$(mm)	SD(mm)	CV(%)	$\bar{X}$(rad)	SD(rad)	CV(%)
1	1	50.67	0.83	1.6	3.13	0.029	0.9
2	2	51.73	1.43	2.8	3.13	0.026	0.8
3	3	52.58	1.17	2.2	3.12	0.029	0.9
4	4	47.58	1.54	3.2	3.13	0.029	0.9
5	5	50.39	1.32	2.6	3.12	0.021	0.6
6	3	100.18	1.62	1.6	3.12	0.029	0.9
7	3.5	99.36	1.54	1.5	3.12	0.020	0.6
8	4	99.24	1.70	1.7	3.13	0.013	0.4
9	4.5	*	*	*	*	*	*
10	5	101.28	1.41	1.4	3.12	0.020	0.6

* Datafile corrupted by mainframe to microcomputer transfer

1.6% to 3.2%). SDs are, on the whole, relatively constant regardless of mean diameter length. CVs are all low suggesting homogeneity of diameter lengths, although lower in tubes 6 to 10 (see above). There appears to be no linear trend between CV and increasing tube length.

Angle results however are remarkably constant in both subsections, inferring very good parallelity between successive diameters.

These data were processed sometime after it was collected by a microcomputer statistical package. Unfortunately, the transfer between mainframe and microcomputer (using MOVE - IT and GETFILE, appendix 1) lead to the loss of the data for tube 9.

Table 4.7 presents data regarding variability of the diameter length in three digitized curves of varying radii. SD of the diameter length, like those earlier are relatively constant and apparently independent of mean diameter length. However, variability is generally higher than that encountered in a straight tube, and highest in the curved tube with the smallest radii. On reflection, it is unlikely that artery segments will have morphology with radius of curvature as small as 18.0mm with mean diameter 41.6mm. Therefore the normal case is perhaps better represented by curves 1 and 3.

Table 4.8 presents results to a similar experiment performed on actual tracings of coronary stenoses of varying severity. In this instance bubble length (section 3.6) was allowed to vary also. The data show that varying the bubble length between 50% of normal and 150% of normal has little effect on the variation in the diameter lengths, although there is a tendency for average diameter length to increase as bubble length increases.

However, on the whole, the number of diameter end points not found by the program tends to decrease as bubble length

Table 4.7 Variability in diameter length of digitised curves of varying radii, DIAMRS validation

	DIAMETER		
Curve No.	X(mm)	SD(mm)	CV(%)
1 radius 28mm	80.45	2.02	2.5
2 radius 18mm	41.57	2.45	5.9
3 radius 34mm	122.16	3.53	2.9

Percentage bublen (%)	PAT254, % stenosis = 40%				PAT214, % stenosis = 57%				PAT223, % stenosis = 80%				PAT312, % stenosis = 70%				PAT51, % stenosis = 84%			
	No. DEPNF	$\bar{X}$ (mm)	SD (mm)	CV (%)	No. DEPNF	$\bar{X}$ (mm)	SD (mm)	CV (%)	No. DEPNF	$\bar{X}$ (mm)	SD (mm)	CV (%)	No. DEPNF	$\bar{X}$ (mm)	SD (mm)	CV (%)	No. DEPNF	$\bar{X}$ (mm)	SD (mm)	CV (%)
50	9	255.0	40.9	16.03	11	226.3	55.4	24.48	*	*	*	*	15	219.6	80.8	36.79	12	226.7	105.7	46.63
75	9	256.2	40.9	15.96	10	227.3	55.5	24.41	12	130.5	36.4	27.89	16	220.9	80.7	36.53	12	229.7	107.4	46.76
100	9	260.1	39.2	15.07	9	228.0	55.6	24.39	11	131.7	37.2	28.25	15	222.8	80.7	36.22	11	234.2	107.4	45.86
125	9	260.3	39.4	15.13	9	229.2	55.9	24.39	11	131.9	37.2	28.20	16	226.6	81.6	36.01	12	238.9	106.3	44.50
150	9	260.6	39.5	15.15	9	230.6	56.2	24.37	11	131.8	36.7	27.85	16	229.4	81.9	35.66	12	243.6	104.1	42.73

No. DEPNF = Number of diameter end points not found

* program aborted due to too many diameter end points not found.

Bubble length normally used by Q.A.M.S. shown as 100 percent

Table 4.8 Variation in diameter lengths of coronary stenoses with changing bubble length

increases up to the average (ie. 100% bublen), and increase again with increasing bubble length. Indeed, for PAT223 at 50% bubble length, the program aborted due to too many diameter end points not found. The implications of varying bubble length will be considered in the following discussion.

4.2.4 PROGRAM ECCFTR

When ECCFTR was allowed to run on the curve data from the previous validation, and diameter end point coordinates compared with radial end point coordinates using an unrelated t test, all combinations of complementary coordinate position were non significant (table 4.9). This leads to the conclusion that PROGRAM ECCFTR produces a set of coordinates which are essentially equivalent in position to where the diameter end points are, or would be if the segment digitized had been normal. Information regarding midpoint shift and eccentricity is not provided as the true diameters and radial diameters are essentially equivalent, and therefore shift is zero.

4.3 **Usability**

For this section of the results, 8 parameters from the 18 normally produced have been selected in order to demonstrate repeatability and objectivity. The other 10 parameters are either products of a selected variable or combine in some way to produce a selected variable and therefore do not warrant individual discussion.

4.3.1 Repeatability

Table 4.10 documents the results to the four factor repeatability trial (data from experiment b was used for Smeas computation).

As expected, repeated digitizing generally shows the lowest variability across the selected parameters, with minimal

Table 4.9 Comparision of diameter end point and radial end point position using a two tailed unrelated t test $\alpha = 0.01$ ECCFTR validation

	CURVE 1			CURVE 2			CURVE 3		
	t obs	df	t crit	t obs	df	t crit	t obs	df	t crit
X_{1d} vs X_{1r}	-0.35	186	2.57	-0.11	60	2.66	0.26	62	2.66
Y_{1d} vs Y_{1r}	-0.12	186	2.57	0.13	60	2.66	-0.12	62	2.66
X_{2d} vs X_{2r}	0.34	186	2.57	-1.04	60	2.66	0.01	62	2.66
Y_{2d} vs Y_{2r}	0.15	186	2.57	-0.01	60	2.66	-0.12	62	2.66

X_1 = Side 1 X coordinates

X_2 = Side 2 X coordinates

Y_1 = Side 1 Y coordinates

Y_2 = Side 2 Y coordinates

r = radial end point

d = diameter end point

Table 4.10 Variation in selected quantification parameters - Repeatability and objectivity

Parameter	REPEATABILITY									OBJECTIVITY					
	Repeated digitising			Repeated tracing and digitising			Differing frames in one cardiac cycle			*Equivalent frame in different cardiac cycles			Naive subjects repeated digitising		
	$\bar{X}$	SD	CV	$\bar{X}$	SD	CV	$\bar{X}$	SD	CV	$\bar{X}$	SD	CV	$\bar{X}$	SD	CV
Average maximal diameter (mm)	3.09	0.06	1.9	3.63	0.16	4.4	4.60	0.24	5.2	5.04	0.25	5.0	4.45	0.21	4.7
Minimal diameter (mm)	0.89	0.08	9.1	1.25	0.17	14.0	0.89	0.15	16.8	1.94	0.22	11.4	1.25	0.15	12.1
Percent stenosis (%)	71.05	2.78	3.9	65.70	4.63	7.0	80.60	2.90	3.6	61.5	3.23	5.2	71.93	2.62	3.6
Segment length (mm)	26.65	0.20	7.6	24.10	0.49	2.0	14.40	1.07	7.4	13.13	2.25	17.1	13.73	0.44	3.2
Eccentricity at the minimum diameter (%)	46.4	4.1	8.8	54.2	5.42	10.0	20.56	18.94	92.1	51.08	7.95	15.5	7.83	2.69	34.4
Maximal eccentricity (%)	50.35	1.50	7.3	80.0	8.08	10.1	44.38	16.30	36.7	24.69	10.14	16.2	23.21	5.54	23.8
Mean eccentricity (%)	25.80	1.57	5.8	26.40	2.01	7.6	22.48	14.76	65.70	21.58	2.96	13.7	9.89	2.27	23.0
Atheroma area (mm^2)	24.1	0.70	2.6	22.1	1.76	7.0	43.39	62.14	143.1	8.32	1.75	9.6	15.08	1.88	12.3

8 repeats, 1 artery
* 4 repeats, 1 artery (due to contrast washout)

diameter being the most variable. The act of retracing the same stenosis prior to digitization introduces more error into the quantification procedure, but not enough so as to make the information useless in a clinical situation. The digitization of differing frames within the same cardiac cycle adds yet more variability to dimensions which are not location specific, ie. diameters and lengths but renders spatial information useless (eg. maximal eccentricity) which in turn corrupts data which depends upon its accuracy (eg. atheroma area). When equivalent frames from different cardiac cycles are digitized, eg. at end diastole, variability in all parameters is on the whole, reduced, although the spatial data have variability above that in the straight repeat digitization trials.

Smeas, calculated from repeat digitizing of eight arteries (table 4.11) are all very good, average maximal diameter especially so. Average coordinate number per file by this experienced user (MJ) was also relatively low, thus facilitating rapid computation.

4.3.2 Objectivity

Diameter and length data are repeated well by naive users (table 4.10) but spatial data suffers from the lack of experience.

This trend was negated when the same subjects were involved in the Smeas trial which immediately followed. Smeas values (table 4.11) were on the whole comparable with those of the experienced user, and indeed, results for the spatial data were better.

4.3.3 Validity

When variability in the dimension of crosswire separation for each catheter room and image intensifier size was examined from two randomly chosen locations (one vertical, one horizontal) within the projected field, the data

Table 4.11 Standard errors of measurement on selected quantification parameters - Repeatability and objectivity.

Parameter	REPEATABILITY	OBJECTIVITY
	Repeat digitising	Naive subjects repeat digitising
Average maximal diameter (mm)	0.015	0.14
Minimal diameter (mm)	0.10	0.09
Percent stenosis (%)	3.66	3.40
Segment length (mm)	0.20	0.32
Eccentricity at the minimum diameter (%)	4.30	3.47
Maximal eccentricity (%)	0.99	2.39
Mean eccentricity (%)		
Atheroma Area (mm^2)	0.90	0.69
Average number of co-ordinates/file	352.7	831.6

2 repeats, 8 arteries

presented in table 4.12 was recorded. CVs are all equal to or less than 1.5% affirming that dimensions can be repeated accurately from projected X-ray images.

In order to examine the validity of these dimensions the crosswire separation had to be measured using vernier calipers. Due to the small size of the separation, it was only possible to measure each crosswire separation at three locations without repetition of measurement at the same site. This inhibited the matching of dimensions if independence of samples was to be preserved. Hence an unrelated t test was employed which was essentially reduced to a criterion t test as the differences in the measured dimensions were very small.

Table 4.12 presents the results to these tests. All fail to reach statistical significance confirming that measurements from within a projected image accurately represent their dimensions in real life.

The averaged data presented in table 4.12 was also subjected to correlation analysis. The correlation coefficient between true and computed wire separation stands at 0.98 with SEE +/- 0.026mm.

Mechanisms underlying the magnitude and significance of all these results are discussed in the following chapter.

Table 4.12 Variability and accuracy (using a two tailed unrelated t test, = 0.05) of digitised crosswire separation dimensions - Validity

df = 11, t crit = 2.262

Room	Image Intensifier	Plane	Average Criterion (mm)	$\bar{X}$ (mm)	SD (mm)	CV (%)	t obs
A	SMALL	V	5.42	5.44	0.074	1.3	0.88
		H	5.61	5.61	0.063	1.1	-0.06
	LARGE	V	5.68	5.69	0.080	1.4	0.53
		H	5.74	5.74	0.075	1.3	0.61
B	SMALL	V	5.39	5.42	0.081	1.5	-0.99
		H	5.50	5.45	0.062	1.1	0.78
	LARGE	V	5.41	5.40	0.062	1.1	0.65
		H	5.60	5.59	0.071	1.3	-0.09

Correlation coefficient, true vs computed = 0.98
Standard error of estimate = 0.026mm

V = Vertical
H = Horizontal

Computed dimension 8 repeats
Measured dimension 3 repeats

CHAPTER FIVE

DISCUSSION

5.1 System Characterization

5.1.1 Hand Tracing Tolerance

Pooling of all user and test condition SD results from the experiment described in section 3.6.1 gave a final result of 11.02 g.t.u. This was doubled to 22.04 g.t.u. (0.056cm) to give 95% confidence.

This parameter was then employed in two distinct and differing situations. Firstly, it was used as a criterion by which decisions about the integrity of the raw data could be made (PROGRAM PNTED) and secondly as an "error band" within which the average maximal diameter was computed (PROGRAM ANALYZ). Addressing this latter application in more detail, obviously the larger the tolerance factor and the more uniform (or "unstenosed") the artery, (as non maximal diameters are to some extent included - figure 5.1a) the more inaccurate the estimate of mean maximal diameter. The rationale behind using such an averaging approach was to remove the effects of hand tremor in the tracing which may be manifest as the computation and inclusion into the final data set of unnecessarily large (and unrepresentative) diameters. The fact that this occurs was proven in the early stages of the design of QAMS before such corrections were made. Indeed, hand tremor remains a problem at the onset of tracing and requires certain editing procedures (see PROGRAM PNTED listing). However, one must now address the problem, is the tolerance factor set too larger so as to include an unnecessary amount of diameters less than a true maximum into the calculation of the mean maximal diameter?

In this application, the answer is no. If one considers that the average maximal **projected** dimension on the graphics tablet is approximately 400 g.t.u., 22.04 g.t.u. is 5.5% of

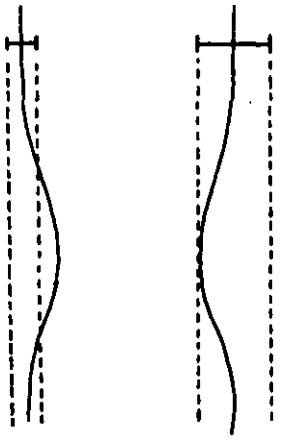

Figure 5.1a Effect of variation in tolerance factor on size of diameters contributing to the average maximum

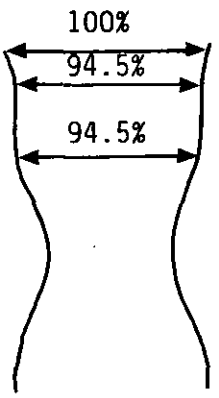

Figure 5.1b Unusual proximal morphology "forces" the inclusion of inappropriately sized diameters into the calculation of the average maximum

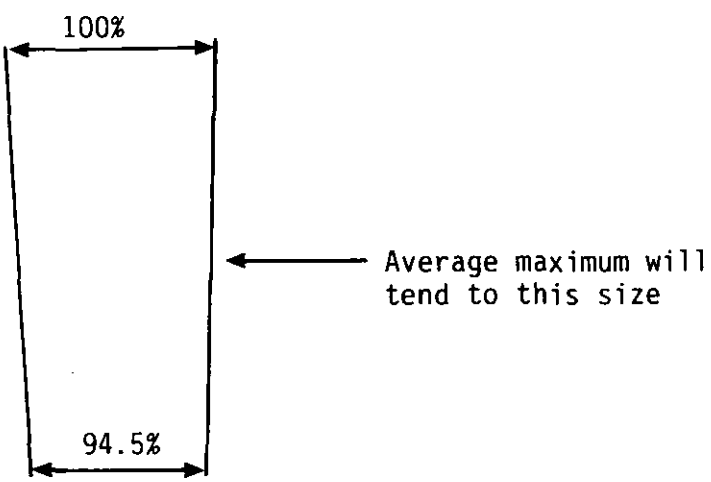

Figure 5.1c Underestimation of the true average maximum on quantification of undiseased coronary arteries

the maximum. At the absolute worst, where natural artery taper above a 50% stenosis for example forces the inclusion of many diameters into the calculation which would not normally have been included (figure 5.1b), the true average maximal diameter would be underestimated by 5.5%. Transferring this to the calculation of percent diameter stenosis:

$$\text{percent diameter stenosis} = \frac{94.5 - 50}{94.5} = 47.1\%$$

results in an underestimation of the true value by 2.9%. This magnitude of error is small in comparison to variabilities in the estimates for the currently most popular method of coronary artery assessment, that of subjective quantification. The above also illustrates the absolute worst case. From experience it is known that such arteries, when diseased, seldom exist, however, if one is to quantify undiseased arteries, this underestimation may become an important factor and must be taken into account (figure 5.1c).

Whilst no error in a system is desirable, it is rarely achievable, more so in a clinical situation. However this **potential** source of error could be diminished using one of two approaches.

1. Reduce the size of the tolerance factor, perhaps to half the current value, giving 68% confidence about the size of the diameters.

2. Increase the size of the image, thereby decreasing the contribution of the tolerance factor to the magnitude of diameter size.

The first suggestion is impractical, for it is essential in the other application of the tolerance factor that all reversals in the raw data are removed in order to allow the following routines to run. The tolerance factor could be

separately adjusted to meet the demands of PROGRAM PNTED and PROGRAM ANALYZ although this would be inconsistent methodology. The answer probably lies in the second suggestion. Provided that the resolution of the standard clinical film could still maintain adequate grey scale separation, without excessive "graininess", the coronary arterial image size could be magnified by perhaps another two times, reducing the error in the percent stenosis estimate to 0.9% (computed value 49.1%). Obviously, the larger the image, the smaller the error, and perhaps larger magnifications are possible without the need for image enhancement.

These practices however, were not employed due to size of the graphics tablet. For the effects of pincushion distortion to be removed, the position of the image centre must be known and stenosis coordinate positions must be considered relative to the centre (section 3.5). This can only be accomplished if the **full** image is projected as a single entity. Possible future enhancements are discussed in chapter 9.

Smeas for the parameter of total coordinate number (TCN - table 4.1a) is very high as a result of the wide variation collected by each individual. This variation is statistically significant for both X constant and Y constant (table 4.1b) but shows no learning effect either on a pooled (table 4.1b) or individual (table 4.1c) level. This large discrepancy in the consistency of total number of coordinates collected is to be expected, as each individual's hand-eye coordination is different, resulting in varying rates of tracing. The question now is, what effect does this variation have on the more important parameters of mean coordinate value (MCV) and SD?

Smeas for MCV and SD are both low, suggesting good repeatability at varying TCN. There are no statistically significant differences for MCV and SD either between users, between test conditions or with interaction between the two

when X is constant (table 4.1b). This is also the case for MCV alone when Y is constant. Interestingly, there is a significant difference for SD at the 1% level for this test condition for between users (subjects) only. This suggests that it is perhaps physically easier to trace vertically than horizontally. When regarding the raw data table (table 4.1a) there appears to be no obvious link with TCN; the highest SD on run 1 has a TCN of 454.2 and the lowest a TCN of 296.0 - this trend is reversed on run 2 with the highest SD having a TCN of 146.2 and the lowest 281.5 coordinates. Whilst this difference is worrying and perhaps should be considered in image selection (i.e. **do not** select purely horizontally orientated stenoses) it is unlikely that stenoses will have direction in one of the frontal planes exclusively.

Individual testing between test conditions yielded no significance difference for either MCV or SD in either digitization direction, again reinforcing the conclusion that their is no training effect in this relatively simple task of tracing a straight line. This gives support to the argument that the calculation of hand tracing tolerance from a pooling of SDs across all users and test conditions will account for variability typical of the digitization process, and that it should **not** be necessary to adjust the magnitude of this value as a users experience with the system grows.

5.1.2. Magnification and Pincushion Distortion Factors

a. Magnification factors. Rates of change of magnification factor (table 4.2 and figure 4.1) for each room at the same image intensifier size are all reasonably comparable, with room A magnification factor being larger throughout. However, there is a considerable discrepancy between the rates calculated for these systems and those quoted by the only reference found to deal with this material, ie. Brown et al 1977. For his small image intensifier, the rate was $0.002cm^{-1}$ and for the larger $0.0037cm^{-1}$. Figures

from the present study are approximately 8 times larger for the small and 6 times larger for the large, although one must bear in mind that the equipment Brown used was different from that used in this study. The results from table 4.2 translate to an approximate error of 1.65% cm^{-1} axial displacement for the small image intensifier and 2.25% cm^{-1} axial displacement for the large image intensifier - not too far removed from the quoted maximum of 1.5% cm^{-1} axial displacement (Brown et al 1986) although Browns original figures are considerably better.

As mentioned in chapter 3, axial displacement in the major application of the QAMS (chapter 7) is likely to be quite small, although the suggestion of view matching discussed earlier and in chapter 9 would allow any possible errors to be removed. Whilst these results have no direct relevance as the system stands, they are useful for the user to know if accurate dimensional measurements are to be gained and aid in the selection of appropriate images for this aim to be met.

b. Pincushion distortion factors. As with the magnification factors, derived pincushion distortion factors for the systems at the Groby Road Hospital differ quite markedly from those values quoted by Brown et al 1977. Brown cites values of $1.25 \times 10^{-4} cm^{-2}$ and $5.0 \times 10^{-4} cm^{-2}$ for the small and large image intensifier size respectively. Values from this study are comparable for the small but some ten times smaller for the large.

Whilst this discrepancy is quite marked, the QAMS performs well when test objects were reduced to true size from arbitrarily chosen positions in the image field (section 4.3.3). Hence differences between present figures and those of Brown are almost certainly a result of differing equipment.

Pincushion distortion is confirmed to be absent in three of the four catheter rooms (chapter 9). The intercept for room B, large image intensifier is significantly different from 1.0. This result may indeed be a reflection of the "optical" characteristics of the equipment in use in that catheter room, but more than likely, it is due to use of inferior material as the calibration grid (industrial mesh).

5.2 **Software Validity**

5.2.1 PROGRAM PNTED

With the present algorithm (figure 3.8), detection rate was 100% for the test file presented as figure 4.3a. On the strength of these results PROGRAM PNTED should be capable of removing all errors inherent in the data due to inconsistent digitization.

5.2.2 PROGRAM DIAMAV

Whilst all t ratios generated from the testing of actual versus computed area are non significant, (table 4.4) it is important to notice that values are larger for the areas of smallest size. This again raises the problem of the effects of hand tracing tolerance magnitude on digitized object size. When digitized area is large, the observed t ratio is low and vice versa (table 4.4). Should a user ever need to digitize very small coronary arteries, for example, those of a child, the magnitude of the hand tracing tolerance may interfere with obtaining accurate results. As previously discussed, the only real answer is to increase the size of the projected image. Unfortunately, this is not possible (from a image distortion correction point of view - the CAP-35B **can** magnify up to 1.6 times) with the present QAMS design. It is therefore important to only select arteries which are within the validated range, or more importantly from the point of this discussion, above the minimum end of the range, ie. $0.5cm^2$. Provided this is the case, the

regression results presented in table 4.5 suggest that the computed area is a highly accurate reflection of true area digitized.

5.2.3 PROGRAM DIAMRS

Variability of mean diameter length in tubes 1 to 5 (table 4.6) is increased above that of tubes 6 to 10. This trend is not apparent in the angle data which shows a consistent result regardless of tube diameter or tube length.

These results suggest that most of the error in the QAMS is directly attributable to the actual digitization procedure (inability of the user to follow desired digitization path exactly) and the raw data resulting, rather than inability of the software to perform the calculations correctly. The criterion diameter for tubes 1 to 5 was 50mm. Experience with digitizing coronary arteries has shown that a **projected** image of an adult coronary artery is seldom likely to be this small, resulting in diminished magnitude of the tracing effect, although less error would have resulted if the original image were larger in the first instance.

When the digitized object is curved, errors are enhanced slightly (table 4.7) probably due to the extra difficulty encountered in trying to trace accurately whilst constantly changing direction. Again smaller objects suffer more, whilst those of a size routinely digitized (curves 1 and 3) have comparable variability.

The choice of correct bubble length for any particular artery is important. A small bubble may produce relatively more diameter lines resulting in higher sampling but variability is magnified, evident from the higher values of CV in table 4.8. Indeed, where profile changes abruptly, employing a small bubble stretching over relatively few coordinates can cause this area to remain unsampled (figure 5.2a). Should the profile be sufficiently complex and the bubble too small, then many areas of the artery may go

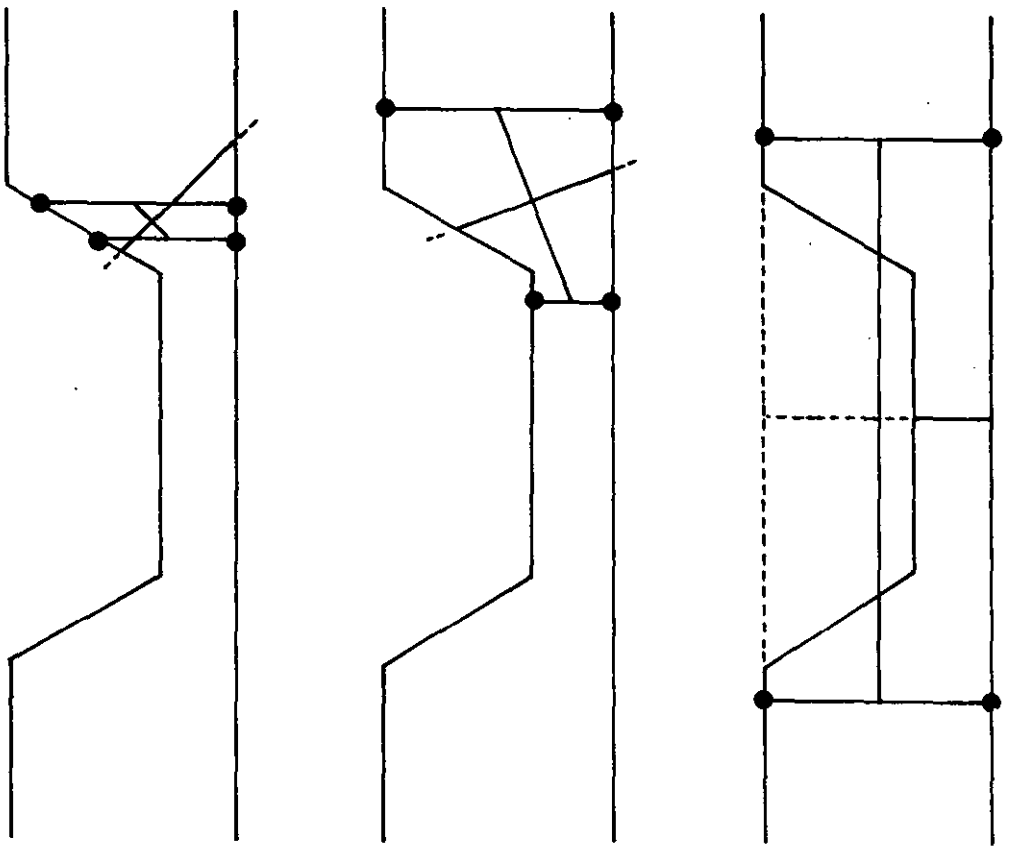

Figure 5.2 Effect of varying bubble length on sampling rate and consistency of diameter lengths

unsampled causing the program to register "too many diameter end points not found", and abort. Clearly then, employing a small bubble length is not recommended. As bubble length increases, variability drops reasonably quickly as the currently employed value of bublen is approached (figure 5.2b) and either settles out or in some cases drops slightly more. So, perhaps the longer the bubble the better? Again, this is not the case. If the bubble length is too long, the movement and positioning of the bubble does not reflect the profile of the artery. The decreasing variability of the diameter lengths is simply reflecting the loss of the true shape of the artery - it approximates to the shape of the bubble, i.e. a tube. In the exaggerated case, it may even be possible for the computed axis to lie outside the margins of the profile data (figure 5.2c). It therefore seems appropriate to use a bubble whose length is sufficiently large enough to **virtually** guarantee the solution a located diameter for each change in position yet sufficiently small enough to accurately reflect arterial morphology. This criterion is adequately provided by stenosis average diameter.

5.2.4 PROGRAM ECCFTR

The magnitude of the observed t ratios confirm excellent agreement between the actual and computed profile positions. The signs of the t ratios are randomly distributed reflecting no consistent differences with respect to position (i.e. above or below) between diameter and radial end points. These results confirm the hypothesis that in the artery with reasonably gentle curvature in one direction only, one may employ previous assumptions regarding shape of the inner surface of the left ventricle and heart in general. This allows computerized reconstruction of arterial morphology prior to the establishment of coronary artery disease.

5.3 **Usability**

5.3.1 Repeatability

CVs (table 4.10) for repeat digitizing are all acceptable, although there is a a tendency for parameters which are location specific ie. those requiring a location to work from (eg. eccentricities), to be more variable. This occurs as a consequence of the slight shape difference in profile digitized on each repeat. Minimal diameter also shows moderate variability, but, as the diameter is so small originally, this has little effect on the percent stenosis estimate. Again this variability exists as a function of original image size, a larger image would reduce the effect of hand tremor on the data (chapter 9). However, it is interesting to note that the magnitude of the SDs for average maximal and minimal diameter, having been corrected for pincushion distortion and magnification are very close to the previously quantified digitizing variability (i.e. 11.02 g.t.u. is the digitization SD on the graphics tablet surface. As the image is projected at approximately two to two and a half times magnification, digitization SD at true size approximates to 0.11mm). This relationship is also true in other test conditions, including the objectivity trial. This fact allows three conclusions to be drawn:

1). Corrections for pincushion distortion and magnification add little error to the processed data.

2). Digitization variability appears to be set at the correct magnitude.

3). Digitization variability is the major source of error in quantification of coronary arteries using QAMS.

Smeas for this test condition are all good (table 4.11), particularly that of average maximal diameter. This reinforces the previously discussed suggestion also implied

by conclusion 3 above, that the coronary arterial image be magnified prior to digitization (chapter 9).

When retracing is added to the redigitizing procedure, errors are enhanced slightly, probably as a result of inability of the hand to re-trace the same path, rather than the brains ability to perceive it.

Results from the digitization of the same lesion at differing stages through the same cardiac cycle show highest variability. This is accountable for in the dramatic morphology changes which occur as a consequence of the variations in pressure both in the coronary artery itself and the ventricles (more so the left), plus, of course, the shape of the latter changes throughout systole and diastole.

Errors in the non spatial data when an equivalent frame from differing cardiac cycles was used are only slightly greater than those in repeat digitizing with the exception of segment length. As mentioned in chapter 3, great care must be taken in applying this parameter, as it is not fixed. Stenosis length, which is the length between the upper and lower 90th percentiles was not used due to artery taper. Hence, high variability in segment length is due to differing starting and/or ending position.

Spatially dependant data show more variability than either repeat digitizing or repeat tracing and digitizing. This may be explained by the fact the the cine film is not gated to the ECG so an equivalent frame may not have been generated from exactly the same portion of the cardiac cycle, ie. we are seeing similar effects to those exhibited when sequential stenoses from differing cardiac cycles were examined, although not to the same extent.

Overall, the system appears repeatable in the clinical situation and is acceptably within routine clinical tolerances. The previous results from chapter 4 confirm that the user is most accurate in selecting a portion of the

cardiac cycle for digitization (eg. end diastole - this usually coincides with when the stenosis appears most severe, - section 3.1) and keeping to it, rather than digitizing images from anywhere within the cardiac cycle, where gross errors can result.

5.3.2 Objectivity

Results arising from this testing regime using naive users suggests that non spatial data can be repeated well with no training, whereas the spatial data may require a familiarization period (table 4.10). Indeed, this hypothesis was borne out by the results from the following Smeas trial (table 4.11) where the same naive users returned lower Smeas for maximal eccentricity and eccentricity at the minimal diameter than the experienced user (MJ). Other standard errors were comparable with the repeatability trial suggesting that objective results are obtainable on the QAMS following **brief** experience. However, new users tend to spend a long time digitizing a stenosis, with the consequent accumulation of a large number of coordinates. This has the disadvantage of labouring processing time (see later) but produces a more accurate picture of morphology. This latter fact may go some way to explaining the lower standard errors of the naive group.

5.3.3 Validity

The system has been shown to produce exceptionally valid measurements from the crosswire separation experiment (table 4.12). It is rather surprising that the results are so good considering that the experiment was carried out using industrial mesh - not the most accurate of equipment. Chapter 9 discusses future work in this area.

In conclusion to this section, the Q.A.M.S. has been shown to be repeatable, objective and valid and is therefore worthy of application and further development.

5.4 **General Discussion**

The introduction and use of a computer in the quantification of coronary stenoses has allowed repeatable, objective and valid measurements to be made. Variability in percent diameter stenosis estimate has been reduced from the order of 12-25% (Koh et al 1979, De Rowen et al 1977) for the commonly employed subjective method to around 4% with the QAMS following some familiarization. The use of the catheter as a scaling device has allowed absolute dimensions to be computed, parameters more physiologically meaningful when one considers myocardial blood supply (section 6.2.1).

The process of quantification is automated, in that selection of dimensions for quantification is under computer control once the data have been entered. This removes subjective bias in the selection of particular maximal and minimal diameters allowing Smeas for absolute dimensions to be lower than those recorded for visually assisted quantification (Smeas QAMS 0.015mm - 0.1mm, 0.08mm Gensini et al 1971 and 0.2mm MacAlpin et al 1973).

Correction for image distortion is a simple matter of applying a previously derived correction for the catheter room and image intensifier size used. This meets the original aim of the system in that no other work is necessary (regarding correction on every occasion - unlike Reibers method) at the time of catheterization.

Validation data for this system compares well with the more complex and expensive techniques of edge detection and videodensitometry. Reiber et al 1978 demonstrated a correlation coefficient of 0.99 and a Smeas of 2.33% when he regressed known object size against the computed values. Nichols et al 1984 did the same with videodensitometry for the parameter of cross-sectional area and showed comparable results (r=0.99, SEE 3.9%). The QAMS had a correlation coefficient of 0.98 and standard error of the estimate (SEE) of 0.026mm (0.75% of a 3.5mm artery) under these validation

conditions. However, it is fair to say that **all** validations (including the QAMS system, section 3.6.3) were performed on objects of greater than 1mm diameter, therefore the correlation between observed and true life may be somewhat poorer in the clinical environment. Certainly, repeatability (using videodensitometry) of relative area measurements from clinical data below this cut off are poor, running at 20-30% (Sandor et al 1979).

Repeatability for the minimal diameter using the original system proposed by Brown et al 1977 stands at +/- 0.027mm and validation results are accurate to +/- 0.08mm. The QAMS in its present form returns 0.09mm and +/- 0.071mm (average SD measurement table 4.12) in direct comparison. Therefore the two systems have equivalent validity yet the Brown - Dodge system is much more repeatable.

What is the secret of Browns accuracy? The answer must surely lie in the fact that the system utilizes images projected at five times normal size. The errors introduced as a consequence of having to retrace the stenosis on the graphics tablet following tracing from the film is negligible in comparison. This reaffirms the earlier suggestion that quantification using the QAMS should utilize larger images (chapter 9).

Browns system is also exceptionally fast in computing the quantification parameters, achieving this in just three minutes, in comparison to twenty minutes using the QAMS. This latter figure can be reduced to around fifteen minutes as the user becomes more experienced and total number of coordinates collected falls (table 4.11). As discussed in chapter 3, it was intended to transfer the system to a computer with a 6 megahertz chip, but this could not be achieved due to breakdown. However, subsequent to completing experiments on QAMS, the quantification software has successfully been transferred to a PC clone, resulting in a reduction of processing time to two and a half minutes on average (chapter 9).

Results from the similar system proposed by Owen et al 1983 agree reasonably well with the QAMS also. Repeatability of 0.05mm, validation of test object correlation coefficient of 0.99, SEE +/- 0.025mm and validation correlation coefficient of artificially induced coronary stenoses (plastic cylinders) in dogs 0.99, with a SEE +/- 0.062mm.

In conclusion, the QAMS is a microcomputer based mensuration system composed of peripherals which all may be used independently. It is capable of being used easily, producing accurate and valuable results from standard clinical coronary arteriography films. It is a prototype, and therefore warrants further development.

The present system meets all the original aims of chapter 2 and is capable of producing results of comparable accuracy to the Brown - Dodge system on which the QAMS was to some extent based. However, the QAMS has certain advantages over this and any other system currently in existence. Primarily, the fact that it is microcomputer based and allows access to the raw data for manipulation into new parameters will see its continued use and improvement throughout the following years.

SECTION 2

APPLICATIONS

CHAPTER SIX

INTRODUCTION TO THE PATHOPHYSIOLOGICAL CONSEQUENCES OF CORONARY ARTERY DISEASE

6.1 Introduction

The ability to provide quantitative information about the nature, severity and morphology of coronary artery disease (CAD) in any particular vessel is perhaps, in itself, interesting, however, what use is it? Are the measurements any better (or worse) at describing disease severity than the methods currently employed? Do the measurements mean anything in terms of the patients ability to live a normal life, coping with the daily demands asked of his body? Can one infer anything about the performance of the heart as a pump now that quantitative information about the state of its blood supply is available? The list of questions is endless.

Clearly then, the QAMS now requires application. It is true to say that there are many avenues in the study of CAD where quantification would complement and increase understanding. However, due to the nature of work carried out at the Groby Road Hospital, Leicester, this thesis will focus on two main applications.

1. The quantification of changes in stenotic dimensions as a result of Percutaneous Transluminal Coronary Angioplasty (PTCA) and their correlation with patient exercise tolerance (chapter 7).

2. The role of quantification of CAD in the evaluation of myocardial function (chapter 8).

In order to introduce and discuss the above two specific applications, it is necessary that the physiological consequences of CAD are understood, along with how the performance of the affected heart may be measured. A

discussion of these two topics forms the basis of this chapter.

6.2 The Pathophysiology of the Ischaemic Heart

Ischaemia is defined as a deficient blood supply and can occur in one of two states.

1. When tissue demand for blood, or more correctly, oxygen, is in excess of the capacity for the **normal** circulation to deliver it.

2. When blood flow (and therefore oxygen supply) to a tissue is restricted in some way despite normal demands.

Ischaemia of the myocardium as a result of CAD is generated according to the latter mechanism and is felt symptomatically as chest pain (angina) by the patient. This section reviews the genesis of this condition and ensuing physiological consequences.

6.2.1 Haemodynamics of Coronary Arterial Stenosis

Pressure loss and flow in the diseased coronary artery are usually related according the general fluid mechanics equation:

$$P = fQ + sQ^2$$

The coefficients f and s can be expanded and modified to meet the biological application thus:

$$P = \left(\frac{8\Pi\mu L}{As} \cdot \frac{1}{As}\right).Q + \left(\frac{\rho K}{2}\left(\frac{1}{As} - \frac{1}{An}\right)^2 \cdot Q^2\right.$$

Where P = Pressure loss across the stenosis.

μ = Absolute blood viscosity.

L = Stenosis length.

An = Cross-sectional area of normal artery (equivalent to d_{max}^2 if measurements are made in one plane only).

As = Cross-sectional area of the stenotic segment (equivalent to d_{min}^2 if measurements are made in plane only).

ρ = Blood density.

K = A constant related to flow profile (varies between 1.0 and 2.0).

Q = Volume flow.

Examining the relationships within the above equation, one must appreciate that pressure loss across a stenosis is a two component mechanism. Losses from the f coefficient are related by Poiseuilles equation to the reciprocal of the cross-sectional area of the stenotic segment and stenotic length, and produce viscous 'resistance' to flow at the stenosis. Losses from the s coefficient are related to the difference in absolute size between the reciprocal of the stenotic cross-sectional area and the normal cross-sectional area, facts important in the genesis of turbulence distal to the stenosis.

When blood is delivered to a coronary artery at aortic pressure, flow occurs due to the pressure gradient between the aorta and the myocardial perfusion bed. However, when the artery is narrowed by a stenosis, this natural gradient is disrupted into zones of varying pressure giving rise to the above pressure loss effects.

Consider the natural pressure gradient to be broken into three stages (figure 6.1).

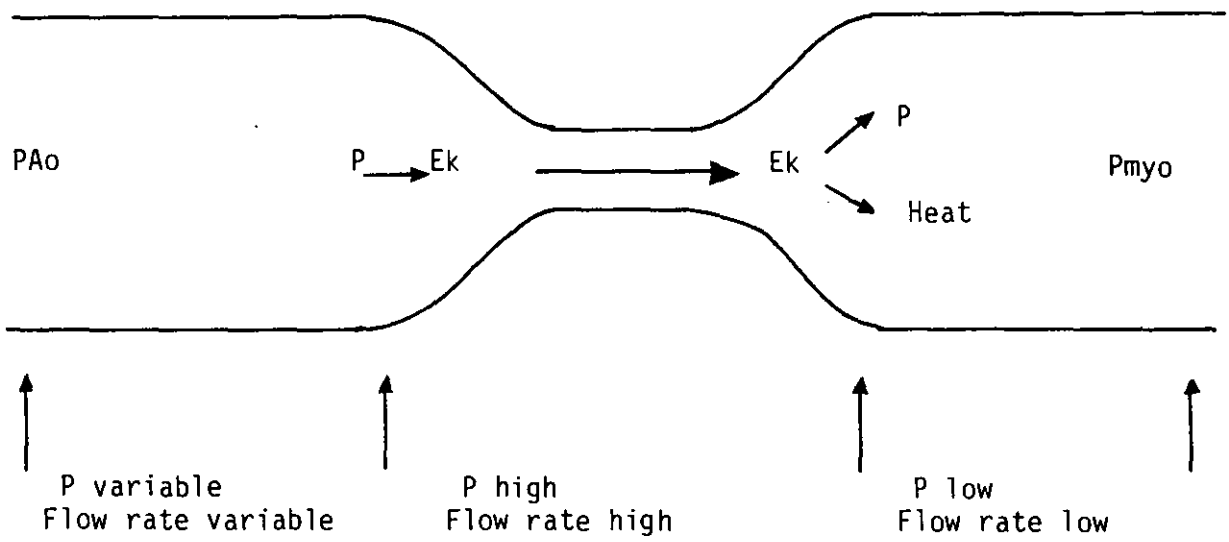

PAo = Aortic pressure
P = Pressure
Ek = Kinetic energy
Pmyo = Pressure of myocardial perfusion bed (varies through cardiac cycle)

Figure 6.1 Variation in pressure and flow in a stenotic coronary artery

1. The pressure gradient established between the aorta and the proximal part of the stenosis.

2. The pressure gradient across the stenosis.

3. The pressure gradient between the distal part of the stenosis and the myocardial perfusion bed.

When laminar flow (higher flow rate in the centre of the arterial stream as compared to the edges) encounters the "entrance" to the stenosis, some of the driving pressure is converted to kinetic energy causing pressure reduction in this region. This loss of pressure due to the viscous resistance of the stenosis is primarily dependant upon the absolute cross-sectional area of the stenosis and is only important at low (resting) rates of flow. Figure 6.2 shows an arbitrary classification of pressure-flow curves for varying stenotic severity. Losses due to viscous resistance are linearly related to pressure gradient (see equation) and are thus demonstrated as the lower straight line portions of each curve. Addressing these areas only, one can see that as stenosis severity increases, the flow rate at which pressure losses begin, and the extent to which the viscous term contributes to total pressure loss gets less and less (Young et al 1977, Gould et al 1978). Obviously, with no stenosis, there is little or no pressure loss, and any loss that is incurred is linearly related to flow due to small differences in size between normal and "stenotic" cross-sectional area (see equation).

This increased kinetic energy causes the flow rate through the stenosis to become enhanced (venturi effect) resulting in more viscous energy losses. Energy losses at this location are compounded by increasing stenotic length (Kindt et al 1969, Lipscomb et al 1978).

On exit from the stenosis, the kinetic energy is in part reconverted back to pressure again, the extent of the reconversion being dependant on absolute cross-sectional

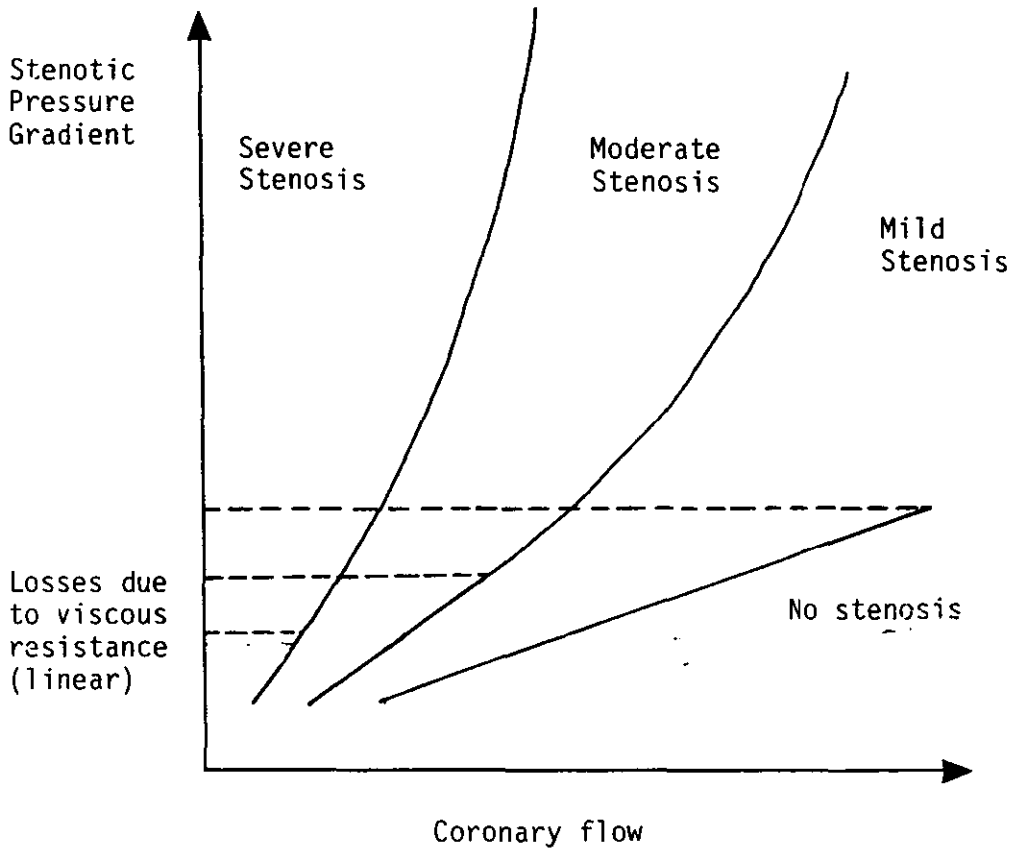

Figure 6.2 Arbitary classification of pressure flow curves for varying stenotic severity

area of stenosis and normal artery, plus flow rate. When the difference between stenotic and normal artery size distal to the stenosis is not great, the flow profile through the stenosis is able to "reattach" itself to the artery wall with little loss of energy and thus pressure (Kloche et al 1980). With higher flow rates however, more pressure is converted to kinetic energy **pre** stenotically and hence intrastenotic blood flow is higher. On exiting from the stenosis, this is decelerated by the slower flowing blood in the distal coronary artery causing loss of energy as heat and turbulence (Lipscomb et al 1978). With high flow rate and severe stenosis, the above losses can be added to losses due to flow profile detachment at the stenosis exit (Kloche et al 1980). Gould et al 1978 demonstrated pressure losses due to viscous and turbulent events of 65% and 35% respectively at rest flow rates, but 33% and 67% respectively at maximal vasodilation. The rate at which the stenosis "opens up" (the exit angle) has also been shown to play a part in pressure loss with variations between 10 and 30 degrees having greatest effect (Gould et al 1982).

This loss of energy causes pressure distal to the stenosis to become reduced, thus enhancing the gradient across the lesion. This promotes further increases in flow through the stenosis until pressure differences and viscous forces are balanced and flow rate steadies out. With pressure distal to the stenosis diminished, a slower flow rate is established between the artery and the myocardium which induces further turbulence until equilibrium is met.

However, pressure within the myocardium is not constant and varies throughout the cardiac cycle affecting the speed and direction of blood flow in the coronary artery. For mild and moderate stenoses, systolic compression of the myocardium increases distal coronary pressure causing stenotic pressure gradient to be diminished or even reversed. This reduces or temporarily halts coronary flow. The exact opposite occurs for myocardial relaxation.

For severe stenoses blood flow in systole is often seen to increase. This is rather paradoxical but may be explained by increased viscous losses due to the stenosis size, causing greater pressure loss at the entrance to the stenosis, thereby establishing a strong gradient for blood flow.

These effects are **not** governed by stenosis geometry or original artery flow rate as they result from pressure changes within the myocardium. Hence changes in coronary blood flow are not fully described by the fluid mechanics equation above.

Many workers have tried to look for a "critical" coronary stenosis, ie. a value of relative size reduction (diameter or cross-sectional area) below which significant haemodynamic effects are seen. May et al 1963 demonstrated that no significant pressure gradient was established across a stenosis until 80% of the cross-sectional area was involved. These values are close to the figure of 75% proposed by Reul et al 1983 using a hydrodynamic model. However, results based on relative size reduction have to be carefully considered as the equation is based on absolute size measurements. Harrison et al 1984 examined the maximal hyperaemic response of patients with CAD during surgery. Hyperaemia is a physiological index related to the ability of coronary arteries to supply the heart with blood on demand. The affected artery was clamped proximal to the stenosis for 20 seconds then released. Coronary flow rate distal to the stenosis was measured using a doppler flowmeter. Maximal flow rate was divided by the previously measured resting levels, quantifying the maximal hyperaemic response. He demonstrated considerable overlap between percent area stenosis measurement from arteriographic image quantification and normal maximal hyperaemic response (percent area stenosis 7-54% with a normal response, 27-94% with abnormal response). However, when the stenoses were considered in terms of absolute size, all normal responses had minimal cross-sectional areas above $3.5mm^2$ and all

abnormal responses below 3.5mm^2. This study exemplifies the need for absolute quantification if the fluid dynamics of coronary arteries are to be understood.

However, should we really consider stenoses and fixed "pipe like" lesions? Various studies have shown that stenosis geometry is **not** fixed, and can vary according to differing physiological conditions. Gould et al 1982 whilst vasodilating dog arteries with induced stenoses demonstrated an increase in the size of their "normal" portions, thus increasing the apparent severity of the lesion under study. Brown 1984 in a review article highlighted this problem with particular reference to eccentric lesions, where part of the stenotic segment wall is normal. Any physiological condition causing vasoconstriction or vasodilation can alter not only the normal artery size but also stenotic dimensions directly. This problem was readdressed by Santamore et al 1985 who experimentally demonstrated that local vasoconstriction around eccentric lesions lead to an increase in stenotic resistance by directly altering stenotic dimensions. So perhaps, measurements made from coronary arteries at rest (ie. normal arteriography) may not reflect stenotic dimensions or general artery morphology on exercise where vasodilation is apparent.

What then, would be a more appropriate measure? Reactive hyperaemia is becoming the favourite parameter in recent literature as it is a combination of information from rest and the investigative condition and therefore more accurately reflects true physiology. Gould et al 1974 observed no change in resting coronary artery blood flow through a stenosis until it reached 85% severity. However by inducing hyperaemia with contrast media the normal response was lost at 30-45% stenosis and the ability to demonstrate hyperaemia at all was obliterated at 88-93% stenosis. White et al 1984 correlated visually assessed percent stenosis with the reactive hyperaemic response and reported very little relationship ($r = 0.25$).

Clearly then, it is not physiologically meaningful to use percent stenosis (diameter or CSA) to characterize coronary disease, as such quantification cannot be extrapolated to the potential effects when demand on the heart increases. The usefulness of absolute dimensions and artery eccentricity have already been discussed in this review and will be evaluated in the forthcoming applications.

In conclusion, the haemodynamic effects of CAD manifest themselves as a decreased perfusion pressure in the distal coronary artery coupled with a decreased flow rate. The next section now investigates the physiological consequences of these phenomena.

6.2.2 The Genesis and Physiological Consequences of Ischaemia

Myocardial perfusion is an autoregulatory process. If flow rate and perfusion pressure distal to a coronary stenosis are reduced, then the myocardium compensates by allowing maximal dilation of precapillary sphincters (as myocardial oxygen extraction is at near maximum even at rest, and therefore blood flow is the limiting factor - Bove 1985). This mechanism preserves an adequate supply of blood and therefore oxygen to the metabolically active myocardial cells but is only sufficient however to compensate for the effects of the stenosis at rest.

On exercise, coronary artery blood flow increases. This further reduces distal perfusion pressure and flow rate (section 6.2.1). The myocardial perfusion bed is already fully dilated and oxygen consumption is elevated as a result of increased cardiac output. Coronary artery flow and artery to myocardium perfusion gradient becomes insufficient to supply oxygen to the deep (subendocardial) layers of the myocardium and ischaemia develops. These ischaemic areas have disordered function (see later) which reduces the pumping efficiency of the ventricle. Mild cardiac failure develops and end diastolic pressure is increased. This in

turn further reduces the perfusion gradient between the distal coronary artery and the myocardium resulting in compounded subendocardial ischaemia.

The key to understanding the physiological consequences of ischaemia finds origin in the development of stiffness of the ventricular wall produced by an abnormal relaxation mechanism. Hypoxia as a direct consequence of the ischaemia results in an insufficient ATP supply to drive the ATPase enzymes in the sarcoplasmic reticulum (SR) of the myocardial cell (Nayler et al 1978). Hence, the normal release of Ca^{2+} ions from the SR and consequent binding with troponin (part of actin filament) initiating muscular contraction (Guyton 1980) occurs, but all Ca^{2+} ions cannot be returned to the SR, and intracellular Ca^{2+} concentration remains higher than normal. This results in the actin - myosin complex of that particular cell remaining partly contracted, ie. not fully relaxed.

This mechanism alters the way in which end diastolic pressure in the ventricle responds to changes in volume (other mechanisms also have an effect, eg. ventricular interaction, the pericardium, etc. - Glantz et al 1978). The relationship is shifted upward and to the left (figure 6.3) such that smaller volume changes are associated with higher chamber pressures and at any given volume the end diastolic pressure within the ventricle is greater. Chamber stiffness, the ratio between pressure changes to volume change, is thus increased (Weber et al 1986).

Visner et al 1985 induced global left ventricular ischaemia in dogs by clamping the left coronary artery. This was associated with a shift in the pressure-volume relationship indicative of increased myocardial stiffness. This change mimics that exactly seen during regional ischaemia suggesting that changes in regional diastolic mechanics are a direct result of the ischaemic process rather than interaction between ischaemic and non-ischaemic segments.

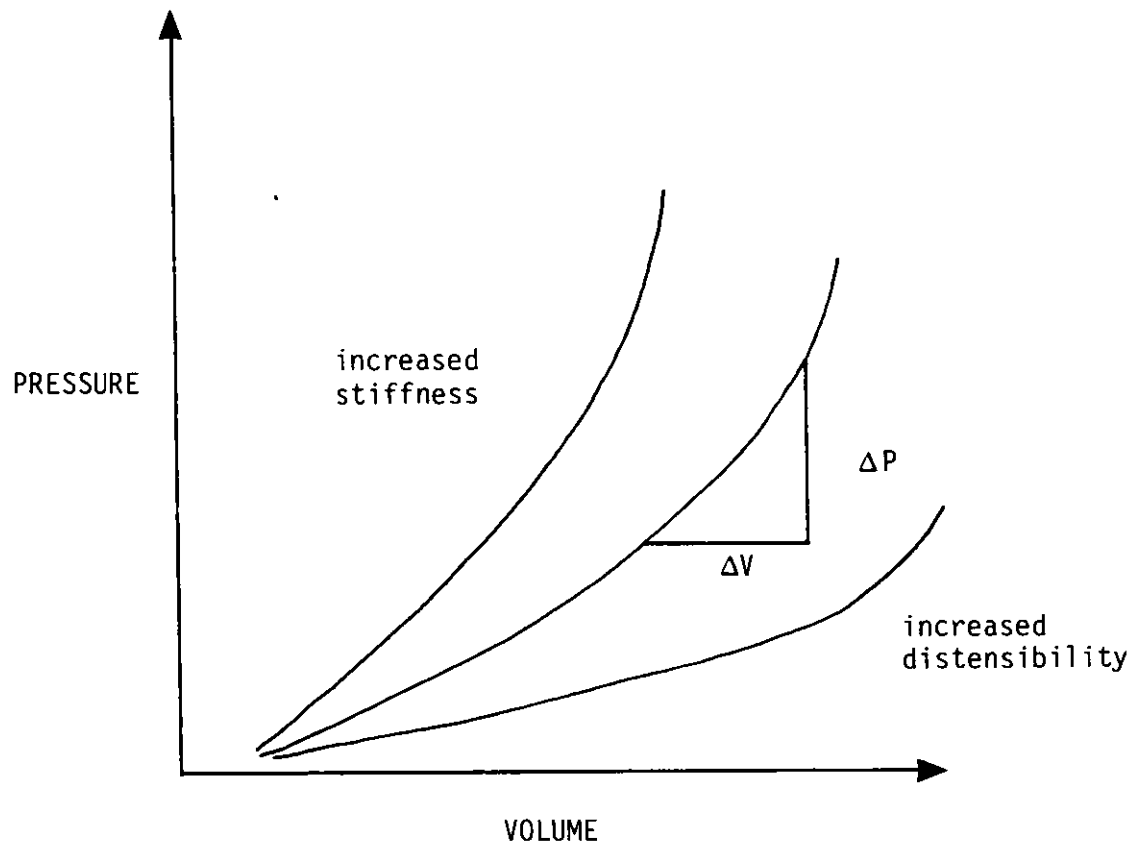

$$\frac{\Delta P}{\Delta V} = \text{Stiffness (solved by monoexponential curve fitting)}$$

$$\frac{\Delta V}{\Delta P} = \text{Distensibility}$$

Figure 6.3 The end diastolic pressure-volume relation for the left ventricle

Tebbe et al 1980 have reported that shifts in the diastolic pressure-volume curve with exercise indicative of ischaemic changes occurred in all patients with angina and in 75% of patients with no symptoms.

Smaller effects in systolic function usually follow changes in the diastolic performance of the ventricle and may be investigated by measuring the maximal rate of pressure increase (+dP/dt) within the ventricle. Tomoike et al 1978 demonstrated significantly reduced +dP/dt changes during strenuous exercise in dogs with limited coronary flow. Peak -dP/dt (diastolic performance) has been shown to fall by 38.4% and peak +dP/dt by 19.9% following one minute coronary occlusions in conscious dogs (Kumada et al 1979). However, Ross 1976 recommends that systolic dysfunction is more accurately reflected by the velocity of circumferential fibre shortening rather than +dP/dt, due to afterload sensitivity.

It has been suggested (Willis-Hurst 1974) that the reduction in function of an ischaemic segment of the heart may serve as a protective mechanism against myocardial infarct. The reduced movement of the segment will not only reduce total myocardial oxygen demand but will also offset the effects of systolic squeeze allowing more uniform perfusion throughout the cardiac cycle. This theory supports that of Ellestad 1980 who suggests that the diminished heart rate response to exercise (and lower heart rate for any given workload) in some patients with CAD serves to improve myocardial perfusion as relatively more of the cardiac cycle is spent in diastole, the interval where myocardial blood flow occurs.

In conclusion, the major effect of ischaemia on the heart is to increase ventricular wall stiffness, which in turn affects its efficiency as a pump.

6.3 **Measuring the Performance of the Ischaemic Heart in the Clinical Environment**

Many of the experiments whose results are described above utilize muscle preparations from animals or the complete animal model combined with sophisticated equipment for the measurement of tensions, velocities etc. Whilst experiments of this kind greatly increase our understanding of the mechanics of ventricular function, they cannot be repeated (without grave ethical problems) in the human. This section then briefly describes what techniques may be applied and clinical data collected in order to infer the performance of the ischaemic heart.

Investigative techniques may be basically subdivided into those which are invasive (requiring entry into the body) and those which are not.

6.3.1 Invasive Techniques

Invasive techniques for the assessment of ventricular function carry with them an increased risk of morbidity and mortality above that encountered with non-invasive techniques. They are also more expensive and involve more discomfort for the patient. Currently, catheterization is the usual method chosen for study of ventricular function.

Catheterization.

Technique (femoral approach only): The femoral artery is treated with local anesthesia and an arterial needle inserted. The needle is then slowly withdrawn until pulsatile blood flow is obtained. At this point the needle is fixed in position and a J tipped guide wire (section 3.2.2) is introduced through it. The guide wire is passed up to the level of the mid-abdominal aorta before the point above the artery is compressed and the needle removed. A No. 5 french Teflon dilator is then passed over the guide wire in order to spread the subcutaneous soft tissues and

the femoral artery wall. The dilator is then removed and an arterial sheath inserted over its introducer which surrounds the guide wire. Once the sheath has passed into the femoral artery, introducer and guide wire may be removed. A pigtail catheter is then passed through the sheath and the guide wire advanced to the mid-abdominal aorta, at which point the catheter is allowed to follow. The system is then passed as a whole up to the lower thoracic aorta before the guidewire is removed. The catheter is then advanced (under fluoroscopic control) around the aortic arch and through the aortic valve into the left ventricle. Contrast media (section 3.2.2) may then be delivered via the catheter to achieve opacification of the left ventricle. Images are recorded on 35mm cine film in exactly the same manner as for coronary arteries (section 1.1) from a variety of views (including biplane), although the 30 degree RAO is most common. Ventricular pressures are also transmitted via the fluid in the catheter and may be recorded in either analogue or digital form.

Analysis: Subsequent analysis of either the cine films or pressure data allows the deviation of various indices of ventricular function.

Simple visual inspection of regional wall motion is carried out routinely in most cardiothoracic units. The angiographer divides the ventricle up into several regions and assigns a semiquantitative grade based upon personal interpretation of the extent of systolic contraction and diastolic relaxation in that region (Diamond et al 1984). However, this subjective technique is rapidly being replaced by computer assisted methods which usually involve the user digitizing the left ventricular outline of each successive frame throughout one cardiac cycle. The degree, direction and rate of movement of the walls may then be objectively quantified by computer. Using such a system Gibson et al 1976 established reversed (inward) movement of the left ventricular wall during isovolumic relaxation in patients with CAD. Shepertycki et al 1983 reported overall

sensitivity of 87.5% and specificity of 97.9% of such a computerized method in comparison to subjective assessment. However, as Diamond et al 1984 explains, subjective assessment of regional wall motion can be adversely biased by knowledge of the patients coronary anatomy, and thus endorses use of the objective methods of computer analysis. Data (shortening of computer generated lengths between the centre of gravity of the LV and the end diastolic and end systolic outlines) from the digitized images were combined with continuous pressure recordings from the LV by Sasayama et al 1984 allowing generation of pressure - length loops thus quantifying myocardial work. Hypofunction, characterised by 30% reduced shortening and a 25% decrease in segmental work was recorded during pacing stress in patients with angina pectoris.

Volumetric data may be derived from ventricular outlines by applying mathematical equations which approximate the shape of the ventricle to various geometric figures (cones, ellipses) or apply integration techniques (Simpsons rule). Many different equations exist and are reviewed in the paper by Beranek et al 1976. Kennedy et al 1966 cite normal values for end diastolic ($70 ml m^{2-1}$) and end systolic ($24 ml m^{2-1}$) volumes, along with stroke volume ($45 ml m^{2-1}$) and ejection fraction (67%). Vogel et al 1973 draw attention to the hazards involved in estimating ejection fraction from a single plane ventriculogram as healthy wall movement in one view does not necessarily indicate well functioning walls in another; underestimation of the true value is common. Cohn et al 1974 enforces this argument and reports that it is not uncommon to see variations in ejection fraction of 10% on repeat angiography. He ascribes these differences to an altered haemodynamic state between the two tests. Volumetric measurements were combined with exercise in normals, and patients with and without angina in a study by Sharma et al 1976. Changes in the volumes immediately following exercise (decrease in normals, no change in non angina and increase in angina) showed clear separation between the three groups. Interestingly, ejection fraction

showed no consistent change. Baan et al 1984 describes an electronic catheter which is capable of measuring the ventricular volumes directly, thus removing the need for mathematical assumptions.

Increased left ventricular end diastolic pressure on exercise in patients with CAD was documented by Lichtlen 1971. He demonstrated good correlation with severity of CAD even in patients with normal LV function.

Knowledge of changes in pressure and volume of the left ventricle allow inferences to be made about the "stiffness" of the ventricle in exactly the same manner as in the animal experiments cited previously. Grossman et al 1976 described an abnormal pressure-volume relationship in the acutely ischaemic ventricle under clinical conditions, leading to increased stiffness. He concludes by explaining that systolic dysfunction generally seen in cardiac failure has genesis in altered diastolic properties of the ventricular chambers. Gradient of the pressure-volume curve at end systole (E_{max}) and the ratio of peak systolic pressure to end systolic volume (P/V_{es}) were examined by El-Tobgi et al 1984 as indices of LV function. He concludes that E_{max} is the only **systolic** pressure volume variable capable of separating normal and abnormal ventricular function.

Rate of change of pressure (positive and/or negative) may also be recorded clinically and used to evaluate myocardial function. Mason 1969 draws caution to using +dP/dt as it is exceptionally sensitive to changes in preload and afterload, recommending that it be used only to evaluate directional changes of contractility in response to intervention in an individual patient rather than using it to evaluate the different contractile properties between patients. Ludbrook et al 1981 demonstrated a lower peak -dP/dt in patients with asynchronous relaxation, reflecting increased chamber stiffness during diastolic filling.

Analysis of the rate of change of ventricular shape with time permits the calculation of the velocity of movement of the ventricular wall. This is commonly employed at the level of the minor equator where the extent of shortening may also be measured. By using these data plus pressure recordings it is possible to calculate (using an ellipsoidal model of varying wall thickness) wall stress at the minor equator and correlate it with the extent of shortening of the circumferential fibres (Ross 1969). Extrapolation of stress-velocity plots to zero stress allows the expression of maximal contractile element velocity (V_{max}). Hugenholtz et al 1970 reports that V_{max} appears to aid significantly in the evaluation of myocardial mechanics in patients with heart disease and "apparently" normal ventricular function (V_{max} is significantly lower than in subjects with normal ventricular mechanics). Yin 1981 reminds us that myocardial wall stress is one of the primary determinants of myocardial oxygen consumption, concluding that we are valid in applying the necessary models in order to enhance understanding of ventricular mechanics in the absence of a technique to measure wall stress directly.

6.3.2 Non Invasive Techniques

Various non-invasive techniques have become popular over recent years. These have allowed the effects of CAD to be evaluated under stress and have proven useful in the determination of the prognosis and severity of disease, the evaluation of medical therapy, screening for latent coronary disease and evaluation of functional capacity (Ellestad 1980).

1. Exercise testing.

Technique: This involves stressing the patients heart by asking him to perform some form of exercise which is usually familiar to him. Exercise is continued until symptoms typical of the patients condition are evoked or the test is completed. Such a process allows investigation of the

patients capacity for exercise. Tests may be single load, or continuous tests with loading changing incrementally or continuously. Differing test also employ a variety of equipment. The protocols of Nalge et al 1971 and Naughton et al 1964 use a step, Bruce 1971 and Balke et al 1959 utilize a treadmill and other workers have used a bicycle ergometer. Each mode of exercise has good and bad points, with cost, ease of performing the exercise (ie. familiarity) muscle groups involved (ie. extent of stress applied) and ease of recording investigative parameters all entering into the argument.

Analysis: Heart rate is a parameter measured on all exercise tests and is usually used as a criterion by which time of termination of a test may be judged. As stressing anyone (CAD or not) to their maximal capacity is very dangerous, achievement of 85% of maximal heart rate is usually taken as successful completion of the test (Ellestad 1980). Wiens et al 1984 evaluated heart rate response to exercise in 172 patients with angiographically documented CAD. He reported that chronotrophic incompetence is a relatively infrequent occurrence in such a test population, however, it may be useful in detecting patients with CAD who have indeterminable exercise test (65 patients had no exercise ECG abnormalities yet failed to reach 85% of maximal heart rate on completion of test).

Twelve lead ECG recording is also very popular in exercise testing. This allows the depolarisation/repolarisation cycle of the heart to be viewed from many "electrical" planes and positions. Significant ST segment depression, taken to be 1mm or more horizontal or downsloping depression below the isoelectric line 0.08 seconds after the J point (Sendoe et al 1984) occurs as a result of myocardial ischaemia. The depression evolves from intracellular potassium loss producing a current flow during diastole from endocardium to epicardium. This current flow in the direction of the recording electrode displaces the baseline of the ECG upward which is offset by the balancing current

produced by ECG equipment. It is only when depolarisation (QRS complex) imbalances the potential of the compensating current that during systole, the shift is manifest as ST segment depression (Ellestad 1980). Hakki et al 1983 reported that a false negative ST segment response is infrequent (10%) amongst patients with CAD and is usually associated with a less extensive disease state. However, the location of the ST segment depression seldom correlates with the anatomical site of the CAD (Fox et al 1984) although it is useful in predicting mortality risk both individually and in large populations (Weiner et al 1984).

Rate of progression of ST segment depression relative to increases in heart rate were studied by Elamin et al 1982. They reported, quite controversially, that ranges of the slope data were all different, with no overlap, in patients with differing numbers of coronary arteries affected by CAD and thus could be used to predict its presence and severity. Fox 1982 in reply to this paper states that he cannot believe the results when one considers coronary collateral supply and variations in coronary anatomy. Quyyumi et al 1984 has tried to reproduce the results of Elamin with little success. The usefulness of the ST/heart rate slope remains unproven even today.

Hakki et al 1984 draws attention to the size of the R wave necessary for ST segment depression to develop. Low R wave amplitude (<11mm) is rarely associated with ST segment depression even in patients with multivessel CAD.

Other electrographic changes coincident with ischaemia have been evaluated. O'Hara et al 1984 described equivalent discriminative capacity of Q wave changes (small in CADs, getting smaller on exercise) to that of ST segment depression.

Blood pressure is also generally recorded during evaluation of exercise tolerance. Amon et al 1984 evaluated an abnormal post exercise response (failure to fall or

increasing) of systolic blood pressure (SBP) in patients with CAD. Expressing results as ratios of early recovery SBP to peak exercise SBP gave greater sensitivity to the SBP changes than exercise electrocardiographic changes. Changes in the rate pressure product (RPP - SBP multiplied by heart rate) bears close correlation with alterations in directly measured myocardial oxygen consumption (Amsterdam et al 1977). Use of beta blocking agents have an improved exercise tolerance time with termination of the exercise test occurring at the same RPP indicative of myocardial oxygen consumption as the limiting factor (Ellestad 1980).

The ability of the heart to circulate blood and the ability of tissues to extract it may be evaluated by measuring one parameter, that of maximal oxygen uptake ($\dot{V}O_2max$). This may be measured directly by collecting samples of expired air from the patient, or estimated indirectly by calculating work done by the patient on the test and applying a factor which describes the oxygen requirement per unit of work (eg. $1.8 ml min^{-1}$ per $1 mkg^{-1}$ of work - Balke et al 1959). Nitroglycerin, in a study by Detry et al 1971 was effective in increasing $\dot{V}O_2max$ in patients with CAD mainly by reducing peripheral vascular tone and the left ventricular pressure-volume relationship. Ehsani et al 1984 documented decreased $\dot{V}O_2max$ in patients with CAD in comparison to age-matched healthy subjects. $\dot{V}O_2max$ correlated well with various indices of LV function ($r = 0.7$ for maximal heart rate and $r = 0.77$ for change in ejection fraction) suggesting that impaired LV function is the limiting factor in attaining normal $\dot{V}O_2max$. As substantial individual variation exists in the normal values for $\dot{V}O_2max$, results may be better quantified as functional aerobic impairment (FAI - Bruce 1971). This is calculated according to the following formula:

$$FAI = \left(\frac{\text{Predicted } \dot{V}O_2 \text{ max} - \text{Observed } \dot{V}O_2 \text{ max}}{\text{Predicted } \dot{V}O_2 \text{ max}} \right) \times 100$$

Phonocardiographic and carotid artery pressure measurements may also be made from the patient at the time of exercise testing. However results tend to be less reproducible than those already described and suffer greatly from motion artifact (Sutton et al 1977).

Exercise testing allows investigation of the incapacitation resulting from the physiological effects of CAD and is routinely carried out in many hospitals across the UK. However, Redwood et al 1972 suggests that the information gained from a stress test can easily be obtained from a patients self reported history, and advocates that only in patients with atypical anginal syndromes is exercise testing of any value.

2. Echocardiography

Technique: Ultrasound (sound above 20,000 hertz) is generated in short pulses by piezoelectric crystals and directed toward the heart. The sound is reflected and received at the crystal from the surface of the heart whenever tissue acoustic impedance changes (function of tissue density), occurring typically at the interface of blood and endocardium, endocardium and myocardium and myocardium with epicardium and pericardium. The reflected sound is then displayed as an image on an oscilloscope in one (or more) of a number of ways.

Analysis: Two dimensional echocardiography (TDE) which allows multiple tomographic - equivalent views of the heart and its internal structures to be obtained is currently the most popular echocardiographic method of studying LV function.

Pictures produced by TDE can be thought of as inverse video images of those produced by angiocardiography. Hence many of the indices of LV function employed by this latter technique can be re-employed for TDE eg. EF (Folland et al 1979) and WMA (Parisi et al 1980).

3. Nuclear Cardiology

Nuclear Cardiology involves injection of a radiolabelled tracer into the patients bloodstream which is then distributed in proportion to the function under investigation. This radiopharmaceutical emits gamma photons with energy sufficient to transverse overlying tissues where they are interact with an imaging device (collimator and gamma camera) which produces electrical signals as an end product. These are then passed on to a computer where they may be quantified, stored and displayed.

In order to evaluate left ventricular function (rather than the effects of coronary disease on myocardial perfusion, where Thallium imaging would be the study of choice), two main types of study may be performed, those of first pass radionuclide angiography (1st RNA) and multiple gated equilibrium (MUGA) RNA.

1st RNA

Technique: Invariably, ^{99m}Tc is used as the radioisotope either as pertechnetate or bound to diethyltriamine pentacetic acid (DTPA) although intravascular tracers may be used if a MUGA study is to be performed in combination.

The radiopharmaceutical is injected as a bolus into the vein of the arm and tracked as it makes its way through the atria and ventricles of the right and left hearts, thus allowing temporal analysis of their function.

Analysis: Apart from the qualitative data achieved from the images, time-activity curves (as emissions are independent of geometry) may be constructed for right and left hearts which then may be analyzed as one would a time-volume curve. Reduto et al 1981 demonstrated reduced filling fraction (35% vs 47%) at rest during the first third of diastole in 68 patients with CAD. Peak filling rate at this time and overall peak filling rate were also lower than normal. He

concludes that at rest, **early** diastolic performance is often abnormal despite normal systolic performance with dysfunction increasing on exercise. Ejection fraction may also be derived from averaging of the peaks of the time activity curve across the course of a few cardiac cycles (Ashburn et al, 1978). Bodenheimer et al 1978 reported excellent correlation of LV ejection fraction with that obtained by contrast angiocardiography (r = 0.82). Incidence of wall motion abnormalities were also in good agreement in a study by Marshall et al 1977 with 59% of abnormal segments detected.

MUGA RNA

Technique: ^{99m}Tc is bound to red blood cells by previous injection of the stannous ion (Strauss et al 1980). The radiopharmaceutical then mixes with the blood pool eventually coming to equilibrium. Once achieved, a 16 frame composite ECG gated image may be built up from several hundred cardiac cycles.

Analysis: Creation of areas of interest by software on the controlling computer can allow quantification of counts within specific areas on certain frames of the image. Hence left ventricular counts may be computed for the end diastolic and end systolic frames which permits the calculation of ejection fraction once background activity has been subtracted. Such values have been shown to correlate well with contrast angiocardiography (r = 0.92, Strauss et al 1971, r=0.92, Green et al 1978, r = 0.74, Albrechtsson et al 1982) and have good interobserver agreement (r=0.95, Green et al 1985). Biello et al 1981 describes a method which removes subjective bias and operator error in deducing the position of the LV regions of interest by employing edge detection algorithms. Intraobserver variability is 0.9+/-0.57 ejection fraction units and interobserver variability 3.0+/-2.5 ejection fraction units using this method.

MUGA RNA may be combined with stress testing (usually bicycle) in order to examine LV responses to exercise. Steingart et al 1984 observed decreased ejection fraction and peak systolic pressure-end systolic **count** relationship in 25 patients with CAD engaged in supine exercise.

MUGA RNA also allows production of the spatial distribution of functional variables (such as regional ejection fraction, extent of contraction (amplitude) or timing of contraction (phase)) as images themselves. These are known as parametric images. These parameters allow quantitative investigation of wall motion (Vos et al 1983) and can increase sensitivity of the MUGA RNA in detection of CAD (Norris et al 1984).

The dynamics of a labelled blood pool may also be investigated by using non imaging scintillation probes (nuclear stethoscopes) which are capable of producing real time quantitative data on a beat by beat basis (Green et al 1981). Resulting time-activity curves may be processed in a manner similar to that of MUGA RNA.

These sections have attempted to provide a framework on which discussions regarding the extent of ischaemia may be evaluated using tests routinely employed in the clinical environment. The following two chapters seek to evaluate the usefulness of data provided by QAMS in combination with some of the tests discussed.

CHAPTER SEVEN

APPLICATION ONE

QUANTIFICATION OF STENOTIC DIMENSIONS AND THEIR RELATIONSHIP WITH EXERCISE PERFORMANCE IN PATIENTS RECEIVING PERCUTANEOUS TRANSLUMINAL CORONARY ANGIOPLASTY (P.T.C.A).

7.1 **Introduction**

It would seem logical that improvement in myocardial blood supply to a dysfunctioning, ischaemic heart following PTCA (sections 1.4.3 and 7.2) should re-normalise its function, resulting in amelioration of exercise tolerance. This chapter aims to investigate whether this is indeed the case, and explore also if stenotic anatomy correlates with the capacity for exercise. In answering these questions, comparisons between subjective and quantitative methods of artery analysis are made along with discussions regarding PTCA success rate and coronary artery morphology.

7.2 **Literature Review**

PTCA was first introduced by Gruentzig et al 1979 following its development from the technique of Dotter and Judkins for the treatment of femoral artery atherosclerotic disease. The basic equipment consists of a guide catheter and a dilating catheter. The guide catheter has normal external diameter (French No 8 or 9) but greater internal diameter when compared with the standard coronary angiographic catheter. Amplatz or Judkins curves of varying size (Przybojewski et al 1984) allow the catheter to be positioned into the affected artery orifice in the manner described previously (section 3.2.2). The dilating catheter runs inside the guide catheter and has a double lumen which communicates with a balloon at its tip. This is made of polyvinyl chloride or irradiated polyolefin and demarcated by two radio-opaque markers. The double lumen also allows pressure measurement and artery contrast injection to take

place as well as inflation of the balloon. Various sizes of dilating catheter are available (French No. 4 - 5, balloon length 1 - 2cm, post inflation diameter 2 - 3.7mm), the choice being dependant on arterial morphology.

The original dilating catheters were headed by a short soft wire, 5mm along which served to direct the catheter into the artery and thus a avoid injury. In 1983 however, a steerable guidewire system was introduced. Wires of this system are teflon coated and have flexible tips. They are unconnected with the enshrouding dilation catheter, allowing independent control from the proximal (operator end) of the catheter system. A unique feature of these guidewires is that their stiffness diminishes gradually toward the distal tip, which is normally gold coated to improve radiopacity.

Using fluoroscopy, first the guidewire is "steered" across the stenosis and into the distal coronary artery. The dilating catheter follows and is carefully positioned across the stenosis (indicated by visual assessment or recording or a pressure gradient) thus temporarily blocking the artery. Expeditious dilation then takes place, accomplished by purging the balloon of all air and inflating it with a solution of 50% contrast medium and 50% saline pumped in at pressure of 3 to 6 atmospheres for 4 to 10 seconds (Gruentzig 1981). Inflation and deflation is repeated at least three times, the pressure being increased with each dilation. Coronary arteriography is then repeated to examine the extent of stenotic change, a successful result being classified as 20% visual improvement in percent diameter stenosis. PTCA may then be repeated until such a change is apparent or the procedure terminated. Improvements in percent diameter stenosis or, more importantly, minimal diameter (section 6.2.1), serve to increase distal myocardial blood supply affecting anginal relief and an improved cardiovascular response to exercise.

The usefulness of dimensional arteriographic criteria for classification of success or failure was questioned by

O'Neill et al 1984. He measured coronary vasodilatory reserve using a digital radiographic technique (time of appearance of injected contrast media) in 15 patients before and after PTCA and correlated his findings with caliper measurements of change in percent stenosis and translesional pressure gradient. The correlation (r = 0.61) was significant for stenosis (reduction from 71% to 34%) and pressure gradient (reduction from 47mmHg to 21mmHg) but more so for pressure gradient and the coronary hyperaemic reserve (r = 0.77). He concludes by suggesting that either of the two latter measurements be routinely adopted for assessing PTCA outcome, as they reflect the altered physiological state and are not subject to the problems that exist in the measurement of coronary arteriograms (section 3.1). Adoption of such criteria would also assist in predicting true outcome in dilation of "dynamic" or "functional" stenoses (section 6.2.1).

Since 1977, there has been much improvement in the PTCA equipment, the most noticeable change being the introduction of a steerable guidewire system as discussed earlier. Gruentzig in a personal communication to Przybojewski et al 1984 states that this has been greatly responsible for the much improved primary success rate of the PTCA technique, as crossing the stenosis is made much easier.

Changes in dilating catheter design have also allowed higher dilation pressures to be applied in PTCA. The effect of higher pressure dilation (up to 10 or 12 atmospheres) on overall outcome were studied by Meier et al 1984. 100 patients processed with the "old, low pressure" catheters were compared with 100 patients receiving PTCA from the "new high pressure" catheter. Both groups were matched for age, sex, artery distribution, initial degree of stenosis and pressure gradient. Following PTCA, primary success, complications and residual degree of stenosis were not different in the two groups. However, residual pressure gradient was significantly lower in the high pressure group (11mmHg +/- 7mmHg vs. 16mmHg +/- 10mmHg). This result

indicates a better haemodynamic outcome without increased risk. These authors now propose to investigate the effects of higher pressures on recurrence rate, but conclude that it is at least "safe" to use the new balloon types. Whilst clinical and angiographic parameters influence successful PTCA, procedural factors (eg. inflation pressure) and PTCA experience appear to be the most important determinants of success (Faxon et al 1982).

Patients suitable for the technique are generally highly selected, with factors such as good overall left ventricular function with objective (if safe and practiced) evidence of myocardial ischaemia (section 6.2.3) and short history of angina (less than one year) unresponsive to maximal medical therapy weighing heavily. Stenotic anatomy is also carefully considered, the ideal patient being the single vessel case, with a short, proximal concentric lesion, easily accessible with no ostial or side branch involvement (Gruentzig 1981). However, increasing experience with the technique has lead to is employment in the multistenotic single vessel case (Katz et al 1982), left main stem stenosis (Stertzer et al 1985), recent and PTCA induced coronary artery occlusion (Holmes et al 1984, Dervan et al 1983, Marquis et al 1984), double and triple vessel disease (Gruentzig et al 1982, Hubner et al 1988) and even in aortocoronary graft stenoses (Ford et al 1981).

Laser angioplasty is now receiving attention in various cardiothoracic centres, particularly in the United States. Work with models which simulate the physiological conditions of the human arterial circulation (Gressman et al 1984, Shelton et al 1986) predict that precise alignment of the laser catheter provides the greatest obstacle for use in human coronary arteries, although such systems have been used in the larger peripheral arteries (Bowker et al 1986).

PTCA has been shown to increase stenotic dimensions in the animal model through intimal fracture combined with stretching of a non involved portion of the vessel rather

than plaque compression (Sanborn et al 1982). Cracking of the intima and separation of it from the media has been histologically demonstrated in various cadaver arteries following postmortem PTCA (Castaneda - Zuniga et al 1980). They propose that the stretched media distends following dilation, carrying with it the intima and atheromatous material. Beyond a certain point, the arterial widening becomes permanent due to overstretching of the muscle fibres. Block 1980 however, describes the mechanism to be made up from some plaque compression combined with endothelial desquamation and shearing of superficial plaque elements. For moderate stenoses, he describes re-endothelialisation and healing of the intima being responsible for an enlarged lumen whereas in more severe stenoses, splitting of the atheromatous plaque may occur, sometimes extending to the internal elastic membrane, causing an immediate increase in lumen size. This mechanism may explain the irregular artery edges or filling defects visualized post PTCA. Fibrosis and healing then occurs, the separated intimal flaps becoming retracted and endothelialised, further enlarging the lumen. It is this latter mechanism proposed by Block that presents the currently favoured hypothesis (Willman 1985).

The National Heart, Lung and Blood Institute (NHLBI, Dorros et al 1983) reported on the initial clinical experience with PTCA from 34 centres within the United States. Of the 1500 patients enrolled, PTCA was deemed successful in 63%. Major complications (MI, emergency CABG or in hospital death) occurred in 9.2%, with non fatal complications being significantly influenced by presence of unstable angina and initial lesion severity greater than 90% (visual assessment). These facts reemphasize the need for careful patient selection but illustrate the relative safety of PTCA as a method of non surgical myocardial revascularisation. Subjective quantification of changes in stenotic morphology as a result of PTCA have been presented as the largest group in the literature. Objective quantification of coronary arteries is usually not practiced, although results of PTCA

tend to be supported by non invasive analyses. Kent et al 1982 affected a change in percent diameter stenosis from 74% to 31% following PTCA, and reports a 64% success rate. Such changes were associated with improved myocardial function as assessed by multiple gated acquisition (MUGA) radionuclide angiography (RNA). At 3 months follow up, 27 of the initially successful 38 patients had sustained improvements as assessed by treadmill stress test. Scholl et al 1982 reports very similar results with stenosis severity being reduced from 78% to 35%. Trans-stenotic pressure gradient was reduced from 46mmHg to 12mmHg. From 36 of the 45 initial successes, 33 were asymptomatic at one month, the number of patients with ST segment depression on exercise was reduced from 20 to 7 and perfusion defects on thallium imaging reduced from 21 to 6. Average treadmill time for the group was significantly increased (448 to 618 seconds) and average ratepressure product (RRP) rose from 19.81×10^3 to 31.35×10^3. They suggest that such non invasive tests may be useful in determining guidelines for repeat arteriography in patients who have had PTCA. Exercise tolerance was also significantly improved in a group of patients reported on by Lewis et al 1983. Mean duration of exercise was improved from an 5.5 to 7.2 minutes and maximal heart rate from 125 to 136 beats min^{-1}. Improved LV function was also apparent as measured by MUGA RNA. Meier et al 1984 documented changes in percent diameter stenosis of 70% to 27% for low pressure balloon inflation and 73 to 31% for high pressure balloon inflation. These changes were associated with pressure reductions from 50mmHg to 16mmHg and 49mmHg to 11mmHg respectively.

Objective assessment of changes on PTCA were investigated in a group of patients with unstable angina by Meyer et al 1981 but were not supported by non invasive tests for presence/absence of ischaemia. Pre PTCA, the stenoses measured 95.5% cross-sectional area stenosis and were reduced to 61.5% immediately after PTCA. On follow up arteriography (4.9 months) the degree of stenosis had risen slightly to 69.2% cross-sectional area stenosis without

recurrence of symptoms. Stenotic severity was assessed from measurement of traced outlines by Cowley et al 1981. PTCA was effective in reducing percent diameter stenosis from 82.2% to 33.9% and pressure gradient from 48mmHg to 8mmHg. When success rate was analyzed according to severity, results were significantly better (12/12 vs 6/12) in patients with less than 90% stenosis. Successful candidates also demonstrated an improved exercise capacity, improved heart rate response (118 beats min^{-1} to 147 beats min^{-1}) and RPP ($20.3x10^3$ to $28.3x10^3$). Exercise thallium scans were normal in 11 of 13 patients and all had improved by at least one functional class of angina. Ischinger et al 1983 noticed that performing PTCA on stenoses with less than 60% severity (as measured by a digital caliper) had primary and long term results similar to those of higher grade stenoses, but the incidence of myocardial infarct was higher in this group, perhaps being a function of lack of sufficient collateral blood flow on complication. They conclude by suggesting that performing PTCA on such lesions may accelerate the disease process and should be avoided. Changes in stenotic severity following PTCA measured using an edge detection system were compared with densitometric measurements in a study by Serruys et al 1984. The coronary lesions were selected prior to PTCA for their extreme severity and symmetry. Single plane edge detection measurements of diameter were converted to percent area stenosis by assuming a circular artery cross-section. Estimates by both methods agreed well pre PTCA, ($r = 0.89$) however, discrepancies enlarged post PTCA, ($r = 0.62$) being explained by asymmetric morphological changes in luminal cross section, incorrectly assessed from diameter measurements in the single plane view. These authors however fail to discuss the limited resolution power of videodensitometry or its inability to provide absolute dimensions (section 2.2.5). The Brown-Dodge system (section 2.2.3) for coronary artery quantification was employed by Johnson et al 1986 in analyzing changes in cross-sectional area of the coronary lumen 6 months post PTCA. Successful PTCA was associated with three fold increase in minimal

cross-sectional area (1.0mm^2 to 3.2mm^2). Interestingly though, the area remains well below normal and less than half the cross-sectional area of the dilating balloon. Follow up arteriography at 7.2 months revealed late increases in 8 of 23 patients (2.7mm^2 - 4.1mm^2). They postulate a possible vasospastic response immediately post PTCA to explain this discrepancy but conclude by stating that angiographic and non invasive analyses performed immediately post PTCA will not define the ultimate adequacy of coronary dilation in many patients undergoing PTCA. Complication rate versus morphology was assessed by Meier et al 1983b when stenoses were categorized as either long or short (measured using digitial calipers) and concentric or eccentric (estimated by visually assessing if the stenotic lumen appeared to lie within one half of an extrapolated normal lumen in at least one projection). Long stenoses did not differ from short stenoses in terms of overall complications or gain in luminal diameter or distal pressure. Eccentric stenoses showed a lower rate of primary success (80% vs. 89%) with inability to cross the stenosis being the major reason. Stenoses which were long and eccentric had the highest complication rate (25%) and short and concentric stenoses the lowest (12%) despite similar improvements in minimal diameter and pressure gradient. These authors highlight eccentricity particularly as a risk factor against successful PTCA and recommend its consideration in patient selection.

Restenosis following PTCA was associated with an increased (8.8mm to 10.4mm) length (measured from tracings) of the original lesion (Jackson et al 1985). Changes in the ST/heart rate slope post PTCA have been investigated by Silverton et al 1984. They demonstrated a fall in the relationship equivalent to single vessel disease change following successful PTCA in 23 of 25 patients. No significant difference was noted in the 2 patients in which PTCA was not successful. At six months follow up, six patients had recurrent chest pain and were retested. The test correctly identified the three patients who were

exhibiting restenosis and three who were not. These authors recommend the tests use in the non invasive evaluation of the results of PTCA, despite the inability of any other centres to repeat their original results (section 6.2.3). Wijns et al 1985a combined edge detection quantitative angiography with stress testing and thallium scintigraphy in order to detect restenosis post PTCA. Percent diameter stenosis for the whole group was reduced from 64% to 30% immediately following PTCA, but had increased to 63% 8.6 months later. The positive predictive value of a thallium scan was 82% compared with 60% for an exercise test, recommending the former for future use in the non invasive evaluation of PTCA results.

In a separate study, Wijns et al 1985b correlated stenotic severity with trans-stenotic pressure gradient and derived a curvilinear relationship which was best normalized by logging the obstructive area measurements ($r = 0.74$). By applying cutoffs of 80% cross-sectional area stenosis and 0.3 mean pressure gradient (normalized for mean aortic pressure) the occurrence of thallium perfusion defects induced by exercise were correctly predicted in 83% of patients.

Non invasive estimation of changes in myocardial performance following PTCA without reference to dimensional changes in stenotic severity has also been popular in the literature. However, most reports have tended to utilize MUGA RNA which is the technique used in the second application of this thesis, hence a discussion of this literature is reserved for chapter 8.

Despite the advent of quantitative coronary arteriography, there has been no definite reports which categorically relate exercise performance with stenotic severity; many workers, with the possible exception of Wijns, have reported improved artery caliber and enhanced exercise tolerance but none have actually investigated the two areas quantitatively and statistically in order to answer the questions:

1. Is PTCA effective in improving exercise performance?

2. Can a patients exercise tolerance be predicted (with any certainty) from arteriographic assessment?

3. Can stress test results infer anything about the state of the coronary circulation?

This application of QAMS was designed to answer these and other questions (section 7.3.4).

7.3 **Method**

7.3.1 Patient Selection and Sequence of Events

Sixty two patients with significant (70% or more visually assessed percent diameter stenosis in at least one vessel) coronary disease (59 one vessel disease, 3 two vessel disease) were retrospectively selected from a current list of all patients who had received PTCA (performed by the same operator) over the period 23rd December 1982 to 10th July 1985. Sex ratio of the total group was preserved in the sample (51 males 11 females) with mean age 52.9 +/- 8.5 years. By reviewing the patients notes, it was possible to obtain cine numbers and stress test data for each of the following events (depending upon PTCA result for that particular patient):

N.B. Initial PTCA is expressed as PTCA1 and second PTCA resulting from restenosis or failed PTCA1 as PTCA2.

Initial arteriogram (10.6 +/- 5.2 weeks prior to PTCA1).

Initial stress test (18.3 +/- 10.7 weeks prior to PTCA1).

PTCA1 procedure.

Initial PTCA1 follow up stress test (8.0 +/- 9.3 weeks

post PTCA1).

Long term follow up stress test (29.9 +/- 12.4 weeks post PTCA1).

Long term follow up arteriogram (performed routinely in all patients until February 1984, then only in problematic cases: 29.8 +/- 9.5 weeks post PTCA1).

Pre PTCA2 stress test, 19.1 +/- 9.9 weeks post PTCA1).

PTCA2 procedure (19.9 +/- 11.6 weeks post PTCA1).

Initial PTCA2 follow up stress test (29.1 +/- 14.2 weeks post PTCA1).

Long term PTCA2 follow up stress test (49.7 +/- 11.7 weeks post PTCA1).

Long term PTCA2 follow up arteriogram (39.4 +/- 13.7 weeks post PTCA1).

7.3.2 Quantification of PTCA Patient Arteriograms

The protocol for individual image quantification is fully described in appendix 1. For each arteriogram, every effort was made to obtain at least two views (one in which stenosis appeared most severe and its complement at 90 degrees) of each affected artery. However, this was not possible (due to poor image quality or overlapping with other structures etc.) in some of the patients films resulting in only one image quantification. In some instances however, quantification was possible from three (the other taken from the next best view) images.

For each cine film, artery, procedure, left ventricular function score and presence of collaterals was recorded from the Radiologists report with subjectively assessed percent stenosis and judgement regarding success or failure of the

PTCA procedure (based on 20% or more visual improvement in percent diameter stenosis). In addition to the normally produced stenotic data (section 3.5), the parameter percent longitudinal area stenosis was computed thus:

$$\text{Longitudinal area stenosis (\%)} = \left(\frac{\text{Undiseased stenotic area} - \text{diseased stenotic area}}{\text{Undiseased stenotic area}} \right) \times 100$$

This parameter allows expression of atheroma area corrected for original artery size.

Regarding sequential arteriograms, care was taken to examine the stenosis from the same view as in previous quantifications (provided images from the same view had been recorded) in order to enable direct comparisons to be made, however for reasons described above, this was not always possible.

7.3.3 Quantification of PTCA Patient Exercise Performance

Treadmill based exercise involves large numbers of muscle groups and has been proved to elicit the highest levels of maximal oxygen consumption ($\dot{V}O_2max$ - Astrand et al 1961). This fact, combined with the familiarity of the exercise to all make it an ideal medium by which the exercise capacity of a patient with CAD may be investigated. The protocol by which work load is progressively increased should include an initial level of work well within the patients anticipated physical capacity and continue to levels expected to produce symptoms.

The Groby Road Hospital achieves this by employing the Sheffield (modified Bruce) protocol (Sheffield et al 1976 - figure 7.1) which utilizes successive three minute exercise loads with incremental belt speed and gradient. Current medication is maintained for patient safety thus reducing the chances of a false positive result, however this

SHEFFIELD (MODIFIED BRUCE) PROTOCOL

NAME AGE DATE HOSPITAL NO. CONSULTANT

Reason for Test Technician

Medication Doctor

Predicted Heart Rate Maximum 85% Maximum =

		LOW LEVEL		SYMPTOM		MAXIMAL						
	Resting	Stage 1	Stage 2	Stage 3	Stage 4	Stage 5	Stage 6		Imm. Att.	3 min.	6 min.	9 min.
Speed mph		1·7	1·7	1·7	2·5	3·4	4·2					
Slope		0	5	10	12	14	16					
Minute per stage		Sheffield's addition			Original Bruce							
Heart Rate												
Blood pressure												
S-T segment ↑or↓												
Chest pain												
Dyspnoea												
Fatigue												
Extrasystoles												

Test stopped at..... minutes..... Seconds of Stage.....

Other Comments:

Reason for Stopping Test:

- ☐ S-T Changes
- ☐ Chest pain
- ☐ Dyspnoea
- ☐ Fatigue
- ☐ Leg pain
- ☐ General appearance
- ☐ Cerebral symptoms
- ☐ Heart rate achieved
- ☐ Arrhythmia
- ☐ Hypotension
- ☐ Hypertension
- ☐ Heart block
- ☐ Completion of Schedule
- ☐ .....
- ☐ .....

Test: POSITIVE/NEGATIVE

Signed.....

Figure 7.1 The Sheffield stress test protocol

practice may mask the true effects of changes in stenotic severity as medication will tend to prevent rises in heart rate and blood pressure (Harrison 1985). The patient is prepared for full 12 lead ECG recording and the test is explained. On exercise, ST segment changes in all twelve leads are noted throughout the test as is the incidence of chest pain, shortness of breath (dyspnoea) extrasystoles and onset (plus grade) of fatigue.

During the final minute of each exercise level, the attending Doctor measures the patients blood pressure and records the heart rate from the ECG monitoring system. The test is terminated when one (or more) of the following conditions is fulfilled:-

1. Development of progressive angina at least as severe as that which would normally cause the patient to stop exercise.

2. A fall in systolic blood pressure or heart rate.

3. Severe dyspnoea or faintness (especially if the patient looks clammy).

4. Ventricular tachycardia or fibrillation.

5. The patient experiences chest pain in the absence of ST changes.

6. The patient becomes/feels unsteady.

7. Marked ST segment depression (>= 5mm)

8. Presence of atrial arrhythmias and/or ventricular extrasystoles.

9. Marked elevation of blood pressure.

10. Development of high grade block.

Depending on the circumstances and cooperation of the patient, the test may also be terminated when severe fatigue is experienced or 85% of maximal predicted heart rate is achieved, although the results from such tests may not adequately reflect true exercise capacity. Experience of the Doctor is also an important factor in encouraging the patient to exercise to a sufficient level and, on repeat testing, ideally the same Doctor should be present. This however, is seldom the case.

On cessation of the test, the patient is monitored for at least nine minutes in order to confirm return of all parameters to rest levels. The Doctor then completes the schedule by recording the reason for stopping the test and deciding (on the basis of ST segment changes, section 6.2.3) whether the test was positive or negative in inducing myocardial ischaemia.

In order to investigate the relationship between exercise capacity and stenotic severity changes resulting from PTCA, the following parameters were recorded from the exercise test data:

Heart rate at rest and maximal exercise.

Systolic and diastolic blood pressure at rest, maximal exercise and three minutes post exercise.

Time to termination of test.

Sum of significant ST segment changes in all leads across all levels of exercise and on recovery.

In addition, age, height and weight were recorded from the patients notes.
From the above data, exercise heart rates and blood pressures were normalized for resting haemodynamic state by expressing each parameter as a percentage of the rest value. In addition, rest and maximal exercise rate pressure

product (heart rate multiplied by systolic blood pressure) plus exercise pulse pressure (systolic - diastolic pressure) were calculated (Amsterdam et al 1977). Systolic blood pressure (SBP) ratio was derived by dividing SBP at 3 minutes recovery by peak SBP (Amon et al 1984).

Power exerted by the patient at rest and maximal exercise was calculated by two methods:

1. Using the simple physical principle that power exerted by the patient will be equal to force multiplied by distance moved divided by time (Sheffield 1980):

$$\text{Power (watts)} = \left[\frac{\text{Body Mass.'g'.Beltspeed.Gradient}}{\text{(kg)} \quad (ms^{-1}) \quad (mmin^{-1}) \quad (\%)} \right]$$

$$6000$$

2. Using the method of Balke et al 1959 which includes a corrective for the metabolic cost of rest and level walking:

$$\text{Power (watts)} = \left[\frac{\text{Body Mass.'g'.Beltspeed.(0.073+Gradient)}}{\text{(kg)} \quad (ms^{-1}) \quad (mmin^{-1}) \quad (\%)} \right]$$

$$6000$$

Acceleration due to gravity ('g') is assumed to be $10ms^{-2}$.

Total work done by the patient was calculated as the sum of all work performed throughout the exercise test.

Symptom limited $\dot{V}O_2max$ and peak estimated $\dot{V}O_2$ may also be calculated from maximal power provided by the above equation by assuming that 1.8ml of oxygen is necessary in order to perform 1 meter kilogram of work in one minute (Balke et al 1959).

$$\dot{V}O_2max \; mlmin^{-1} = 1.8 \times \text{Maximal power (watts)}$$

$$\dot{V}O_2 \text{ mlmin}^{-1} \text{ kg}^{-1} = \frac{1.8 \times \text{maximal power (watts)}}{\text{Body Weight (kg)}}$$

Such an assumption has been shown to return oxygen consumption values to within +/- 10% of values actually measured (Balke 1960) and is often used in order to predict exercise levels necessary to elicit oxygen consumptions in a required experimental range (Nalge et al 1971).

Predicted peak (pp) $\dot{V}O_2$ is calculated for each patient from the regression equations proposed by Bruce et al 1973. This allows estimation of what the oxygen consumption would be in the absence of CAD. The most well known equations of Astrand et al 1954 were avoided as their subject population was composed of well trained people.

Sedentary men:

$$pp\dot{V}O_2 \text{ (mlmin}^{-1}\text{kg}^{-1}) = 57.8 - 0.445 \text{ (Age,yrs)} \quad r = 0.65$$

Sedentary women:

$$pp\dot{V}O_2 \text{ (mlmin}^{-1}\text{kg}^{-1}) = 41.2 - 0.343 \text{ (Age,yrs)} \quad r = 0.72$$

Inspection of daily exercise habits from the patients notes precluded the use of regression equations for active men and women.

From the oxygen consumption data, functional aerobic capacity (FAC) was calculated, with peak estimated $\dot{V}O_2$ replacing peak $\dot{V}O_2$ measured by the usual gaseous techniques.

$$FAC(\%) = \frac{\text{Peak estimated } \dot{V}O_2}{\text{Predicted peak } \dot{V}O_2}$$

Rest and exercise oxygen pulse (the amount of oxygen delivered in one beat of the heart, a relative measure of changes in stroke volume (Astrand and Rodahl, 1977)) was calculated by dividing peak estimated $\dot{V}O_2$ at rest and exercise by respective heart rate.

Height and weight were combined in the calculation of body surface area (Dubois and Dubois, 1916) such that the above data, if necessary, may be corrected for variations in patient body size.

$$\text{Body surface area } (m^2) = \text{Height}_{(cm)}^{0.425} + \text{Weight}_{(kg)}^{0.745} \times 0.007184$$

Although some of the above data is based on predictions from regression equations, it may prove useful in examination of change in exercise performance resulting from PTCA when the whole group is considered. Obviously, such data are useless in evaluating individual changes.

7.3.4 Statistical Analyses

This chapter attempts to answer the following questions:

1. Does PTCA have a significant effect on exercise performance and/or stenotic anatomy? Serial two tailed unrelated t tests between adjacent stages of the PTCA procedure (ie. arteriography vs. pre PTCA1, pre PTCA1 vs. post PTCA1, post PTCA1 vs. follow up, follow up vs. pre PTCA2 and pre PTCA2 vs. post PTCA2) on each data variable will allow this question to be answered.

2. Across all stages of the PTCA procedure, do any parameters of exercise performance correlate significantly with coronary artery morphology? This investigation is best explored by employing linear regression, which will not only produce a correlation coefficient, but also returns standard error of estimate and regression relationship t ratio, thus allowing examination of the correlation in real terms plus the significance and direction of the regression relationship.

3. Using information from the above tests, can the significance of the relationships of the most useful

parameters be improved by analyzing the better matched data from the initial PTCA procedure only? Linear regression again is most useful.

4. Can a combination of significantly correlating exercise parameters be usefully employed in order to predict percent diameter stenosis from data arising from:

   a) the whole set of PTCA percent diameter stenosis results.

   b) percent diameter stenosis data from the initial PTCA procedure.

   The use of stepwise multiple regression, which allows inspection of each parameters contribution to the variance of each relationship, is the test of choice.

5. Can PTCA failure rate be explained by unfavourable stenotic morphology? Hierarchical testing of successful PTCA stenotic data vs. failed PTCA stenotic data using two tailed unrelated t tests is to be used.

6. Does subjective assessment of stenotic severity correlate significantly with the quantified value provided by QAMS? Linear regression, which will allow differences from the line of identity to be evaluated, is the most appropriate test.

As this chapter is intended to illustrate one application of the usefulness of quantified stenotic data, analyses are limited to the above. Undoubtedly data collected from this study may also allow investigation of other facets of the PTCA procedure sometime in the future.

7.4 Results

Statistical analysis for this chapter utilized all exercise tolerance data which was matched with stenotic data for the

same patient (N = 137). Where multiple view quantitative data existed for any artery (the usual case), averages were taken prior to matching. The whole data set includes failed PTCAs as well as the successes. These were not considered separately as interest lies in relationships and changes in the group as a whole. Also, following failure, the patient is usually medically managed and not re-catheterized or exercise tested, and therefore data from the failed cases post PTCA would be absent.

As PTCA patient review is not standardized at the Groby Road Hospital (ie. not all patients received a follow up arteriogram) and the fact that it has regional status (ie. some patients had follow up exercise tolerance tests nearer their homes) it has not been possible to compile a complete data set for each patient so that the patient population is the same for each test at each stage. Rather, the patient population, and the number of patients varies at each stage. Should a definitive study of the effects of PTCA be required, it would be necessary to adopt standard practices into the way in which the PTCA patients are currently reviewed. Such practices would be costly and not necessarily of direct benefit to the patient.

7.4.1 Efficacy of the PTCA Procedure

Significant CAD (greater than or equal to 70% stenosis by visual assessment) was judged to be present in 86 vessels in the 62 patient sample. PTCA was attempted in 65 arteries (46 LAD, 17 RCA and 2Cx). PTCA2 was required by 7 patients, 6 following restenosis, 1 following a failed first attempt.

PTCA results are presented in table 7.1, with primary success defined as greater than or equal to 20% visual improvement in percent diameter stenosis, primary failure defined as either a failure to cross the stenosis with the dilating catheter or less than 20% visual improvement in percent diameter stenosis, and restenosis being defined as an increase in percent diameter stenosis of at least 30% by

Table 7.1 PTCA procedure results

	No of arteries
Primary success, long term success	41
Primary fail, no further intervention	11
Restenosis, successful second PTCA	6
Restenosis, no second PTCA attempted	6
Primary fail, successful second PTCA	1
Total number of arteries	65
Primary success rate (41+6+6)	53 (82%)
Primary failure rate (11+1)	12 (18%)
Overall success rate (41+6+1)	48 (74%)
Overall failure rate (11+6)	17 (26%)

the time of follow up arteriography. Nine patients eventually required CABG (emergency and planned). Overall, 20 complications occurred throughout the PTCA procedure (15 intimal tears, 5 myocardial infarcts) with no deaths.

Grade of angina (table 7.2) based on severity of shortness of breath (NYHA classification) post PTCA was improved by at least one functional class in 46 patients (74%).

Table 7.3 presents results from the inter PTCA stage unrelated t tests. Each t ratio is classified as being either non significant (NS) or significant (numbers 1 - 6), with the number indicating the probability level. Whilst the direction of the mean difference (table 7.4) may well be predicted "a priori" for the pre PTCA1/pre PTCA2 vs. the post PTCA1/post PTCA2 tests (ie. improvement in exercise tolerance and stenotic parameters) this is not so for all other test combinations. Therefore all significant levels relate to two tailed values.

All t ratios (table 7.3) are non significant when initial arteriogram parameter is tested against the same parameter at pre PTCA1, with the exception of summated ST segment change on recovery (figure 7.2a). Whilst the difference in the means between the two groups is marked (table 7.4), the standard deviation of the arteriogram group is large. Also the group is small suggesting unrealistic "weight" contribution from one or two patients resulting in the significant result. Sum of all ST segment change (exercise and recovery) remains non significant for this test combination.

Where pre PTCA is tested against post PTCA1, most parameters show a significant result. Some parameters exceed significance at the 0.01% level, these are longitudinal area stenosis, atheroma area (figure 7.2b), percent diameter stenosis (figure 7.2c), minimal diameter (figure 7.2d), functional aerobic capacity (FAC), peak estimated oxygen consumption ($peV\dot{O}_2$ - figure 7.2e), work done (figure 7.2f),

Table 7.2 Number of patients occupying various grades of angina pre and post PTCA

	angina grade				
	0	1	2	3	4 (unstable)
pre PTCA	0	22	12	9	19 62
post PTCA	39	14	4	3	2 62

Median score pre PTCA = 2

Median score post PTCA = 0

Table 7.3 Inter PTCA stage two tailed unrelated t tests

		Exercise heart rate	Exercise systolic blood pressure	SBP ratio	Exercise rate pressure product	Work done (FXS)	Exercise time (mins)	Exercise ST change	ST change on recovery	Sum of ST change
Initial arteriogram vs pre PTCA1	tobs	-0.83^{NS}	-0.62^{NS}	-0.43^{NS}	-0.75^{NS}	-0.91	-0.82^{NS}	-0.99^{NS}	2.73^{5}	0.73^{NS}
	df	58	58	56	58	57	58	58	58	58
Pre PTCA1 vs post PTCA1	tobs	-5.55^{6}	-1.68^{1}	-1.12^{NS}	-4.36^{6}	-4.07^{6}	-3.48^{5}	3.50^{5}	0.66^{NS}	3.51^{5}
	df	93	93	91	93	91	93	93	93	93
Post PTCA1 vs Follow up	tobs	-0.28^{NS}	-0.02^{NS}	-0.20^{NS}	-0.19^{NS}	1.07^{NS}	0.01^{NS}	1.36^{NS}	0.70^{NS}	1.43^{NS}
	df	61	61	61	61	60	61	61	61	61
Follow up vs pre PTCA2	tobs	2.46^{1}	1.00^{NS}	1.01^{NS}	2.07^{1}	2.01^{1}	2.49^{2}	-4.52^{6}	-2.72^{2}	-4.84
	df	26	26	25	26	26	26	26	26	26
Pre PTCA2 vs post PTCA2	tobs	-1.03^{NS}	-0.83^{NS}	0.32^{NS}	-1.03^{NS}	-4.07^{6}	-2.10^{1}	1.86^{1}	1.39^{NS}	2.06^{1}
	df	11	11	10	11	11	11	11	11	11

Significance levels

1 $0.05 \leqslant p > 0.01$
2 $0.01 \leqslant p > 0.05$
3 $0.005 \leqslant p > 0.001$
4 $0.001 \leqslant p > 0.005$
5 $0.0005 \leqslant p > 0.0001$
6 $p < 0.0001$

Table 7.3 Continued

		Peak estimated VO_2	Functional aerobic capacity	VO_2 max	Average maximal diameter	Minimal diameter	Stenosis	Stenotic length	Segment length	Eccentricit at the minimal diameter
Initial arteriogram vs pre PTCA1	tobs	-0.85^{NS}	-1.19^{NS}	-0.86^{NS}	-0.68^{NS}	-1.31^{NS}	1.02^{NS}	0.55^{NS}	1.27^{NS}	1.08^{NS}
	df	58	58	57	58	58	58	42	58	56
Pre PTCA1 vs post PTCA1	tobs	-4.25^{6}	-4.36^{6}	-3.86^{5}	0.68^{NS}	-12.35^{6}	13.28^{6}	2.41^{2}	1.72^{1}	1.65^{NS}
	df	93	93	91	91	91	93	59	91	91
Post PTCA1 vs Follow up	tobs	0.38^{NS}	-0.36^{NS}	0.90^{NS}	1.24^{NS}	1.96^{1}	-0.91^{NS}	-2.25^{1}	-2.61^{2}	-0.48^{NS}
	df	61	61	60	59	59	61	39	59	58
Follow up vs pre PTCA2	tobs	2.22^{1}	2.54^{2}	1.83^{1}	-0.89^{NS}	2.80^{3}	-2.54^{2}	0.61^{NS}	-1.33^{NS}	-1.86^{1}
	df	26	26	26	25	26	26	23	26	24
Pre PTCA2 vs post PTCA2	tobs	-1.39^{NS}	-2.72^{2}	-2.16^{1}	-0.2^{NS}	-3.27^{3}	1.84^{1}	-1.12^{NS}	0.37^{NS}	0.55^{NS}
	df	11	11	11	10	11	11	8	11	10

Table 7.3 Continued

		Maximal eccentricity	Mean eccentricity	Atheroma area	Longlitudinal area stenosis
Initial arteriogram vs pre PTCA1	tobs	1.19[1]	1.49[NS]	1.51[NS]	0.89[NS]
	df	56	56	55	55
Pre PTCA1 vs post PTCA1	tobs	3.34[4]	2.61[2]	5.22[6]	8.86[6]
	df	91	91	90	90
Post PTCA1 vs Follow up	tobs	-2.36[1]	-1.89[1]	-0.63[NS]	-0.82[NS]
	df	58	58	57	57
Follow up vs pre PTCA2	tobs	0.31[NS]	0.07[NS]	-2.00[1]	-1.63[NS]
	df	24	24	24	24
Pre PTCA2 vs post PTCA2	tobs	0.36[NS]	0.06[NS]	0.42[NS]	1.46[NS]
	df	10	10	10	10

Table 7.3a Inter PTCA stage unrelated t tests, normalised haemodynamic data

	$\frac{\text{exfh - restfh}}{\text{restfh}} \times 100$		$\frac{\text{exSBP - rest SBP}}{\text{rest SBP}} \times 100$	
	tobs	df	tobs	df
Initial arteriogram vs pre PTCA1	-1.20^{NS}	58	0.89^{NS}	58
Pre PTCA1 vs post PTCA1	-1.79^{1}	93	-1.59^{NS}	93
Post PTCA1 vs Follow up	-0.66^{NS}	61	-1.54^{NS}	61
Follow up vs pre PTCA2	2.12^{1}	26	-0.20^{NS}	26
Pre PTCA2 vs post PTCA2	-1.22^{NS}	11	0.89^{NS}	11

1 $0.05 \leqslant p > 0.01$

Table 7.4 Changes in exercise tolerance and stenotic anatomy data at each PTCA stage (Mean +/- one standard deviation)

	Arteriogram	Pre PTCA1	Post PTCA1	Follow up	Pre PTCA2	Post PTCA2
exfh (bpm)	116.7±26.64	125.3±25.46	152.98±22.31	154.71±24.93	124.71±36.36	146.5±40.07
exSBP (mmHg)	148.6±28.53	155.24±26.35	165.83±22.46	163.95±26.25	152.14±29.41	163.33±16.02
sbp ratio	1.12±0.13	1.15±0.17	1.20±0.21	1.21±0.14	1.14±0.17	1.11±0.1
ex RPP	17.84±6.8	19.75±6.24	25.21±5.83	25.5±6.00	19.49±8.46	24.3±8.29
Work (Fs Watts)	712.83±551.1	926.16±584.0	1398.58±518.97	1255.97±451.17	883.14±321.5	1561.08±26.99
extime (min)	11.71±4.27	13.13±4.31	15.88±3.08	15.80±2.53	13.01±2.69	15.98±2.37
exST (mm)	4.57±6.60	4.76±5.02	1.59±3.41	0.52±1.6	5.43±4.28	1.67±2.66
RecST (mm)	2.14±3.45	0.33±1.29	0.167±1.08	0.00±0.00	0.71±1.25	0.00±0.00
SumST (mm)	6.71±7.98	5.09±5.14	1.76±3.78	0.52±1.6	6.14±4.71	1.67±2.66
$PeVO_2$ (ml/min/kg)	26.27±13.02	30.79±13.32	41.53±10.76	40.50±9.17	31.31±10.44	39.15±9.8
FAC (%)	76.92±40.20	95.30±38.33	128.45±34.70	131.91±38.85	93.07±17.05	116.25±12.99
VO_2max (ml/min)	1968.52±1013.8	2323.81±1028.44	3092.83±850.75	2897.78±704.98	2257.43±1058.87	3247.6±393.6
Avmaxd (mm)	3.30±0.59	3.47±0.61	3.38±0.66	3.17±0.57	3.4±0.7	3.50±0.86
Mind (mm)	0.79±0.25	1.01±0.44	2.16±0.43	1.91±0.56	1.27±0.35	2.24±0.69
Stenosis (%)	75.65±8.69	70.29±13.57	36.21±10.81	39.31±16.16	58.09±19.43	40.52±14.01
Stenlen (mm)	10.41±4.0	9.26±4.46	6.70±2.90	9.62±5.2	8.25±2.86	11.42±6.11
Seglen (mm)	16.50±4.44	14.31±4.26	12.86±3.68	15.65±4.46	18.52±6.36	17.33±4.79
Eccmin (%)	31.09±10.7	23.19±17.48	17.46±15.47	19.46±13.38	32.10±20.32	26.13±15.44
Max ecc (%)	57.73±24.78	39.52±21.81	25.34±18.28	46.12±49.88	39.96±21.08	35.68±18.78
Mean ecc (%)	23.15±10.09	16.86±9.80	11.63±9.33	16.93±11.6	16.56±9.6	16.20±9.82
Atharea (mm^2)	16.43±8.49	11.90±6.23	5.93±4.20	6.67±4.37	11.68±8.42	9.82±5.97
Longlit. Area (%)	33.92±10.24	30.72±7.42	16.76±7.57	18.61±8.98	25.03±8.83	18.33±6.16

Table 7.4a Changes in normalised maximal exercise heart rate and systolic blood pressure at each PTCA stage (mean +/- one standard deviation)

	Arteriogram	Pre PTCA1	Post PTCA1	Follow up	Pre PTCA2	Post PTCA2
Normalised exfn	74.18+55.57	95.95+36.47	105.19+33.11	112.25+40.56	77.19+26.68	102.35+46.74
Normalised exSBP	26.36+13.65	20.41+17.02	26.16+18.20	33.17+14.43	34.81+29.02	23.05+14.70

Summated ST segment changes (all leads) on exercise and recovery vs. PTCA stage.

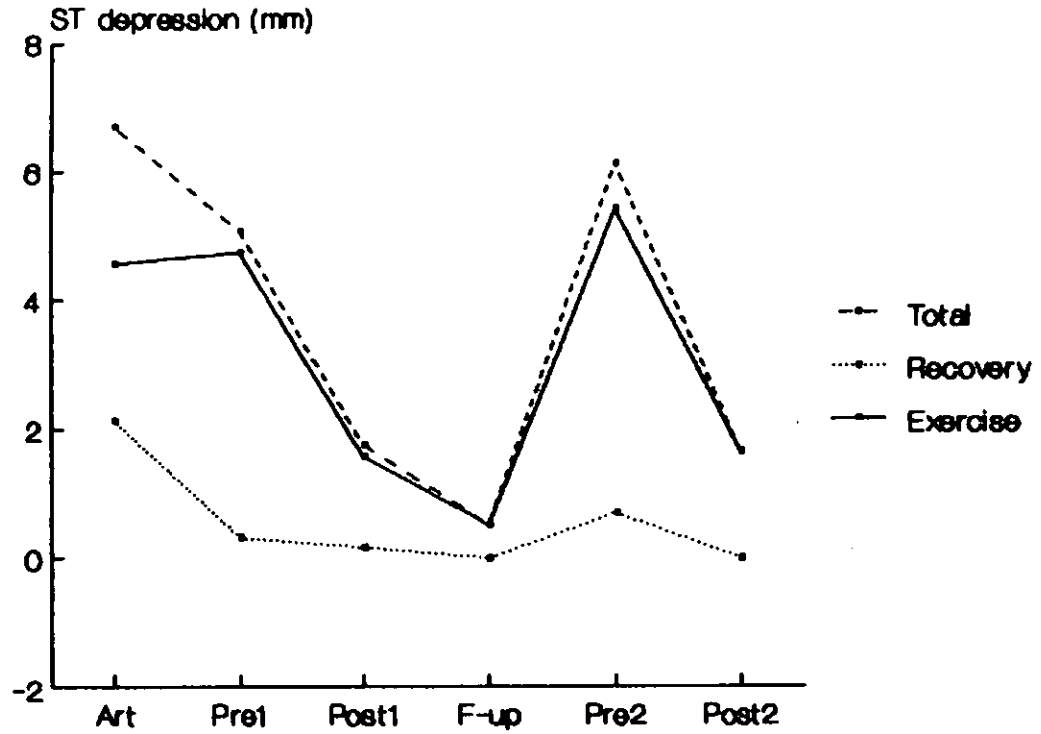

Atheroma area and longitudinal area stenosis vs. PTCA stage.

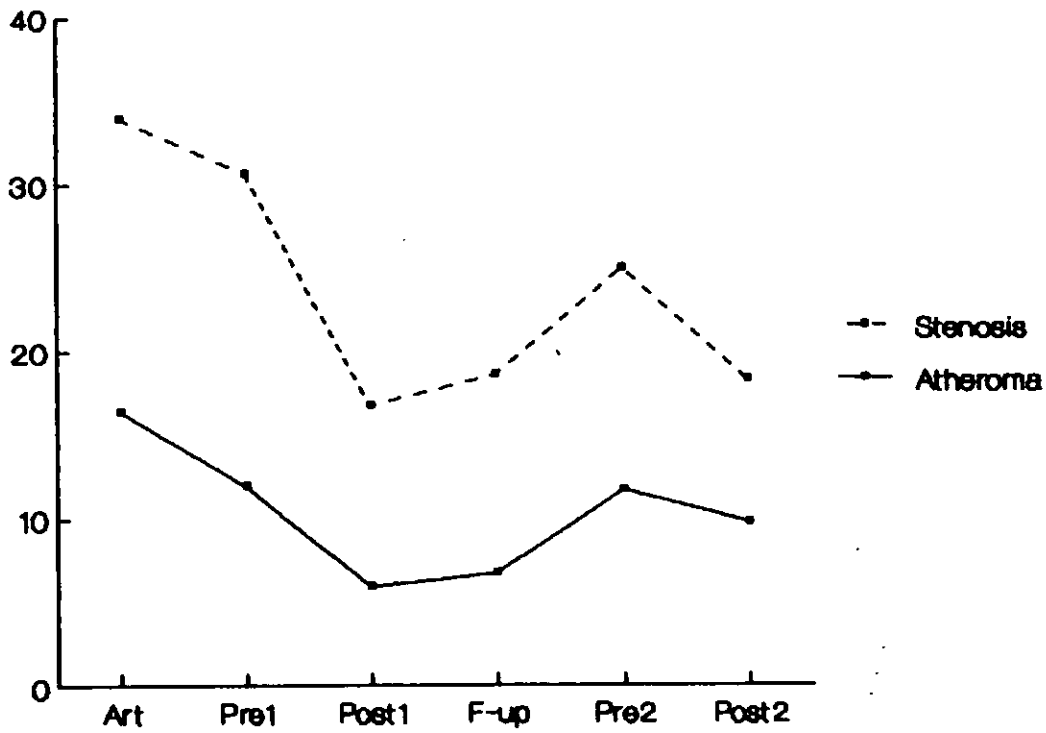

Figures 7.2a and 7.2b

Percent diameter stenosis (Mean +/- 1 SD) vs. PTCA stage.

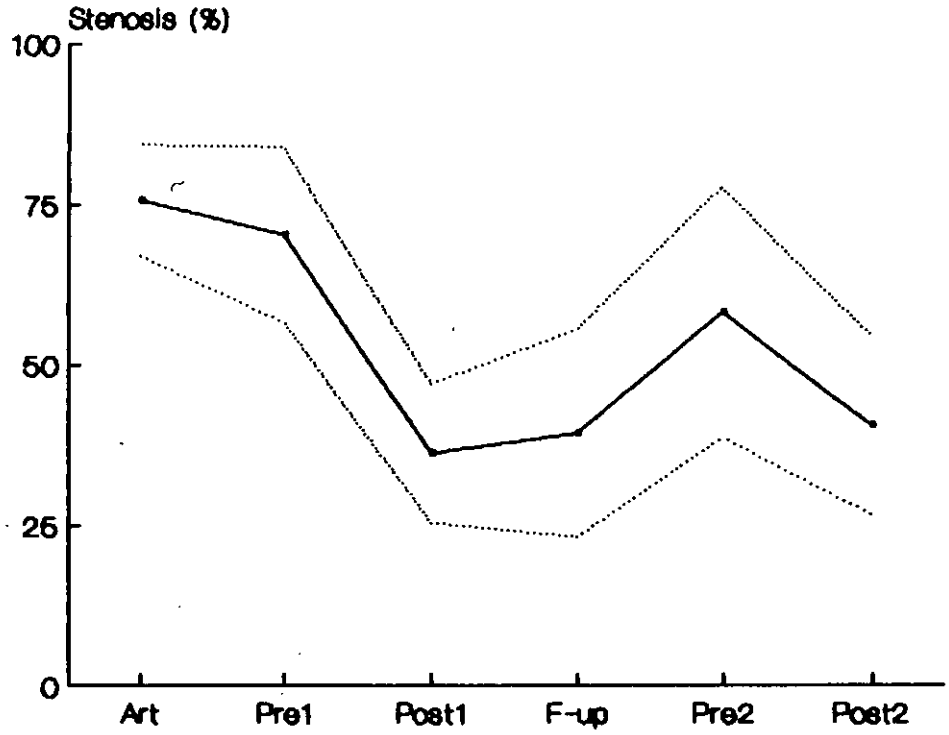

Average maximal diameter and minimal diameter vs. PTCA stage.

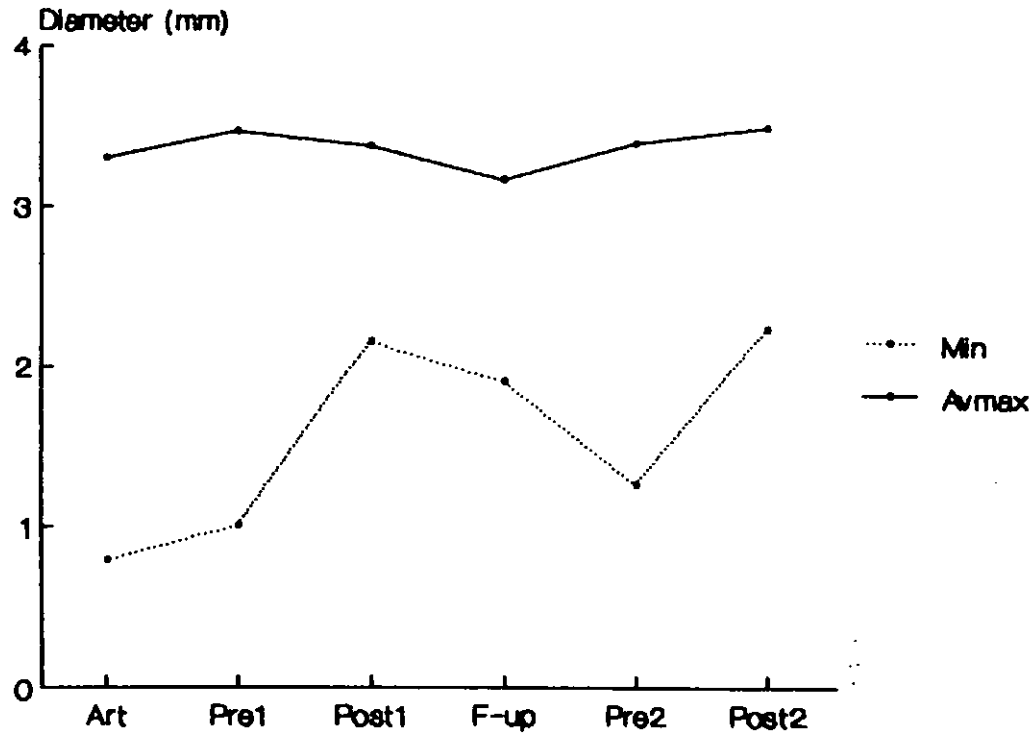

Figures 7.2c and 7.2d

Peak estimated oxygen consumption and functional aerobic capacity vs PTCA stage.

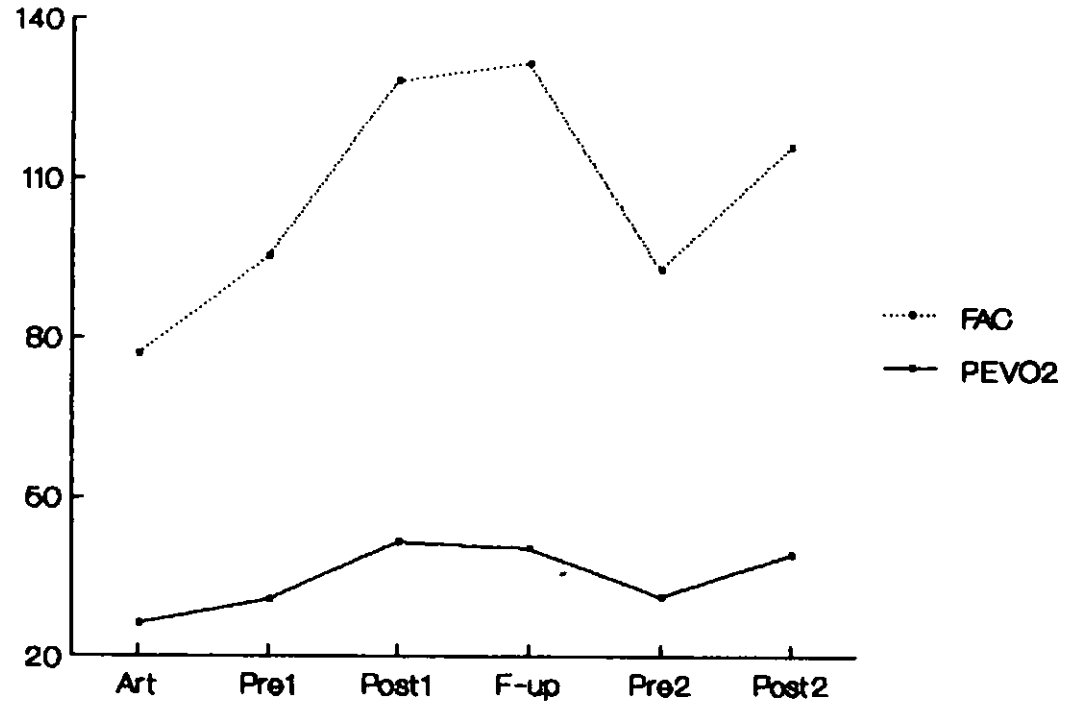

Work done and cumulative exercise time vs. PTCA stage.

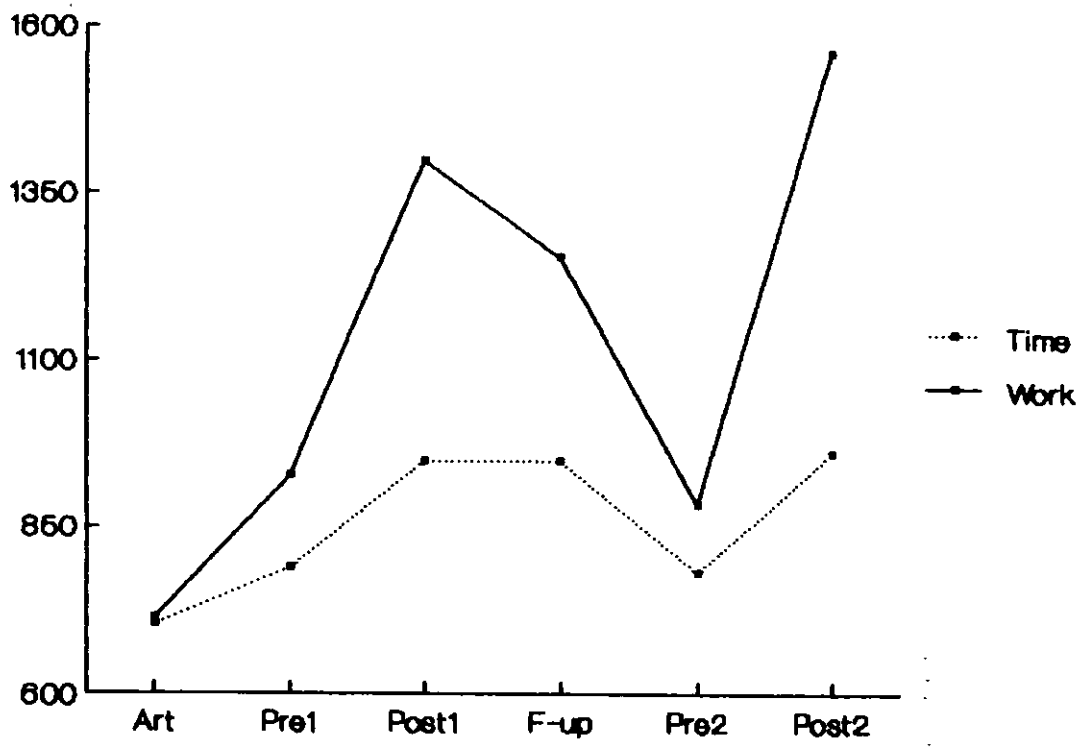

Figures 7.2e and 7.2f

Exercise evoked maximal heart rate, systolic blood pressure and rate pressure product vs. PTCA stage.

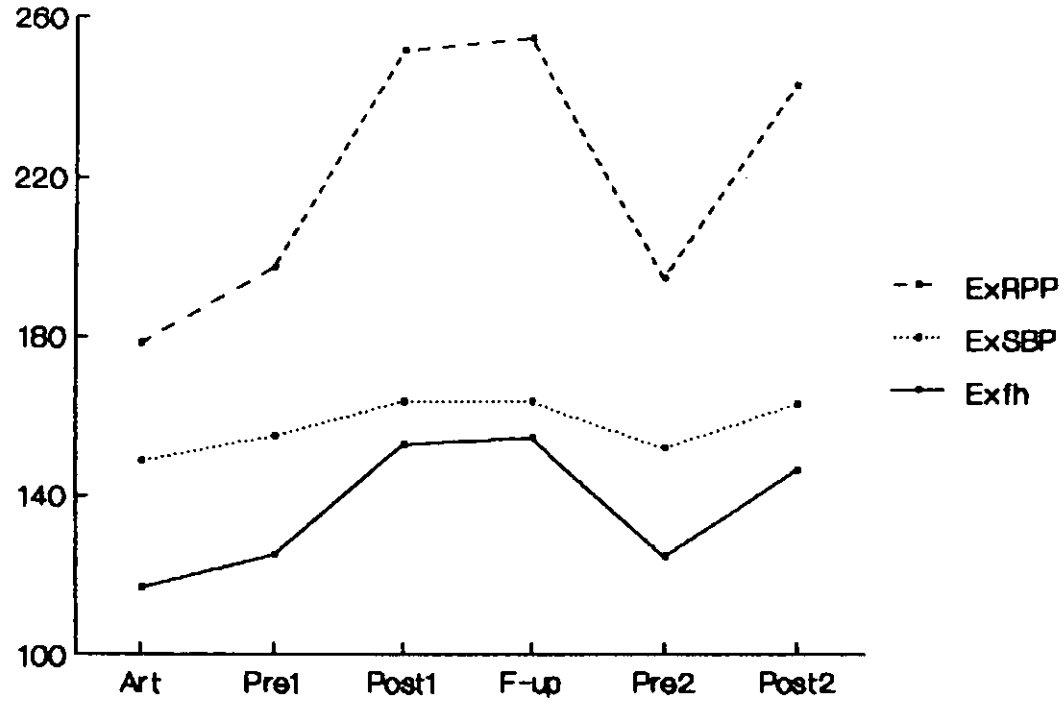

Normalised exercise evoked maximal heart rate and systolic blood pressure vs. PTCA stage.

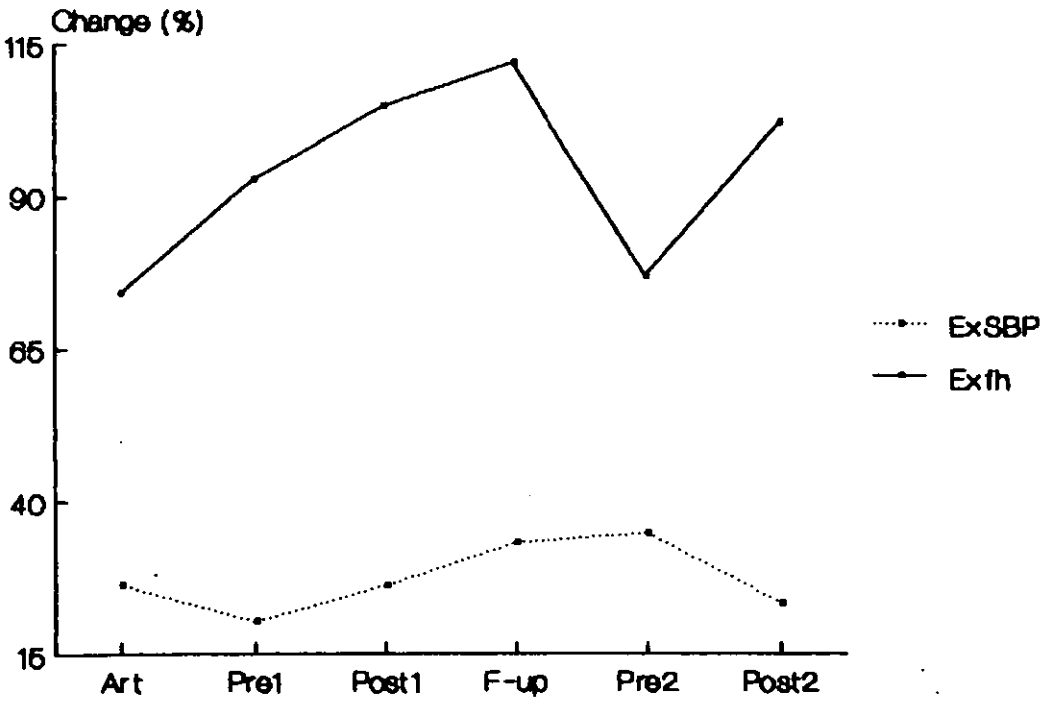

Figures 7.2g and 7.2h

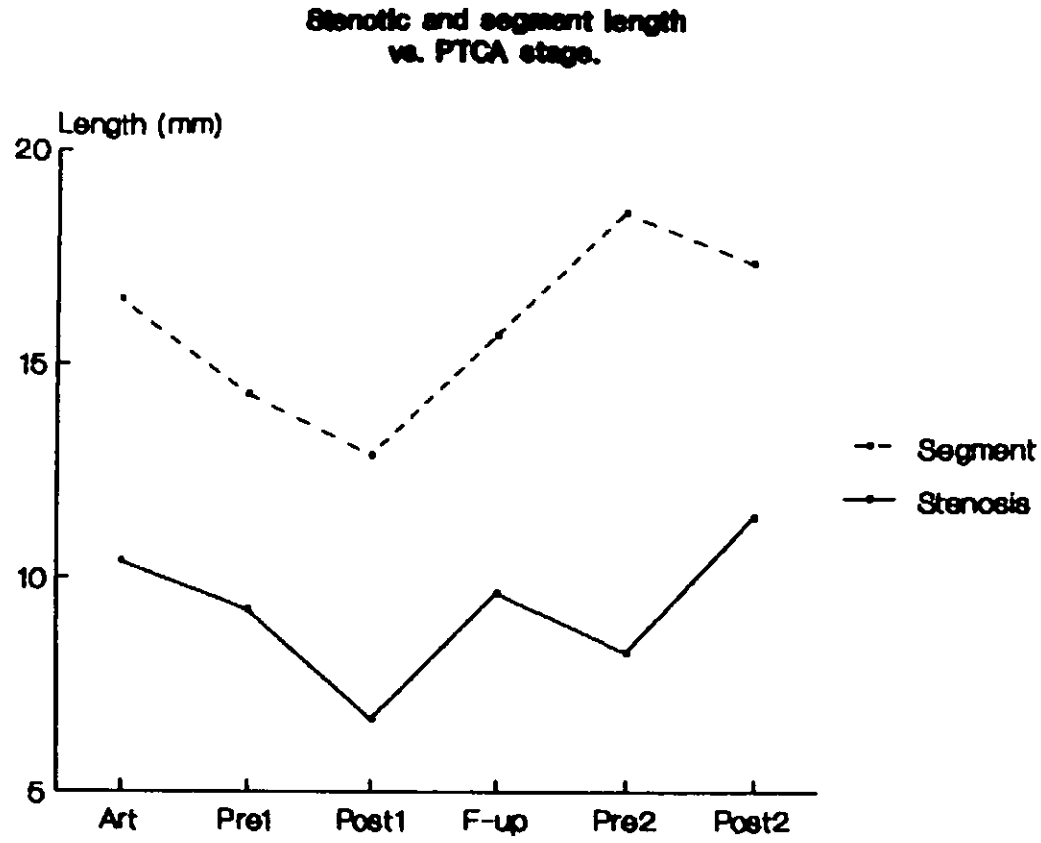

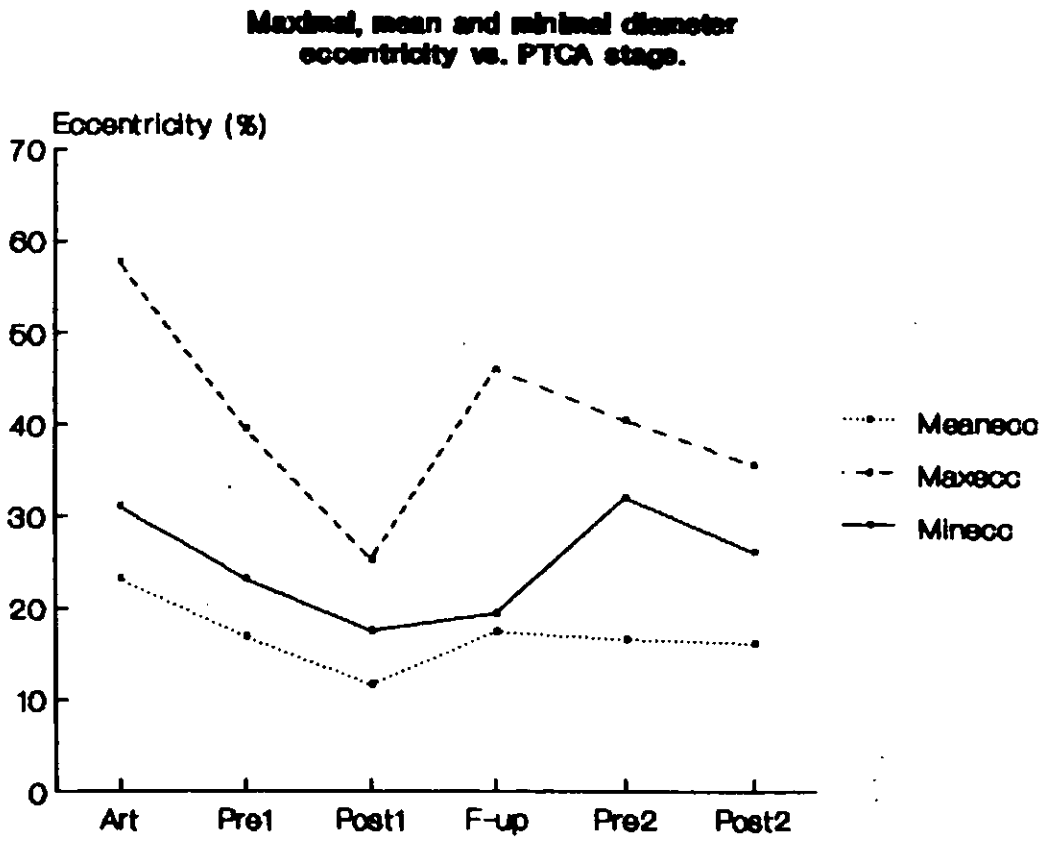

Figures 7.2i and 7.2j

exercise rate pressure product (exRPP) and maximal exercise heart rate (exfh - figure 7.2g). However, the parameters of exfh and exercise systolic blood pressure (exSBP) which contribute to the calculation of exRPP can be markedly affected by changes in drug therapy, particularly changes in the dosage or administration of βblockers (section 1.4.1). Overall, 23 patients (37%) underwent a drug therapy change from treatment involving the use of β blockers to treatment not using βblockers. Hence, exfh and exSBP were reanalyzed expressed as percentage change of their rest values (ie. normalized for resting haemodynamic state - figure 7.2h). Exfh was still significant although much less so (table 7.3a), exSBP was non significant (tables 7.3a and 7.4a).

On the post PTCA1 vs. follow up tests, all exercise tolerance parameters showed non significant differences. Minimal diameter was significant at the 5% level. Inspection of the mean change (table 7.4) suggests reduction of minimal diameter below the post angioplasty dimension. Percent diameter stenosis was non significant. Changes in lesion length (stenotic and segment - figure 7.2i) exhibited significant differences (table 7.3), becoming increased above their post PTCA1 values (table 7.4). Significant changes in stenotic morphology were also evident from maximal and mean eccentricity changes (figure 7.2j) whilst atheroma area and longitudinal area stenosis were non significant (table 7.3).

Comparing follow up to pre PTCA2 (table 7.3) revealed significant differences in most exercise tolerance variables, being particularly strong in parameters relating to ST segment changes. Minimal diameter and percent diameter stenosis were also significant as was atheroma area. However this latter parameter was not significant when normalized for undiseased artery area (longitudinal area stenosis). Normalized exfh was also significant at the 5% level.
The second PTCA procedure significantly affected work done, exercise time, ST changes, FAC and $\dot{V}O_2$max, along with

minimal diameter and percent diameter stenosis. Mean changes (table 7.4) are for the better. Drug therapy was unchanged in all patients receiving PTCA2 and all potentially sensitive parameters are non significant both in absolute (table 7.3) and relative (table 7.3a) terms.

In all cases, significant differences in the stenotic anatomy data are associated with mean differences much larger than those incurred by the errors of digitization (table 4.11).

7.4.2 Relationship between Exercise Performance and Coronary Anatomy - Whole Group

ST segment changes are considered as a whole for the purposes of these analyses.

Minimal diameter, percent diameter stenosis, minimal cross-sectional area and percent cross-sectional area stenosis all have a strongly significant regression relationship with exercise performance. Table 7.5 presents the results to the regression analyses, displaying only those where the t ratio (reflecting whether the gradient is significantly different from zero or not) is significant. Each t ratio is assigned a significance rating as in the previous section. Correlation coefficients are not themselves labelled, as levels of significance are identical to the corresponding t ratio. Minimal diameter correlates the best, followed by percent diameter stenosis and the cross-sectional area based parameters. All standard error of estimates are quite large and the data well spread.

Of the eccentricity variables, eccentricity at the minimal diameter correlates most highly and most often with the exercise parameters. Mean eccentricity is next most useful, with maximal eccentricity relating least well to exercise performance. Atheroma area shows fair correlation with a moderate number of exercise parameters (table 7.5). However, these correlations and t ratios are much enhanced

Table 7.5 Regression analysis - exercise performance vs stenotic parameters, all patients included

DEPENDANT VARIABLE			INDEPENDANT VARIABLE: Exercise heart rate	Exercise systolic blood pressure	SBP ratio	Exercise rate pressure product	Exercise SBP - exercise DBP	Work Done (FxS)	Work Done (Balkes equ)	Exercise time (minutes)
Minimal diameter (mm)		tobs	5.17^{6}	3.19^{4}	2.42^{2}	5.02^{6}	3.69^{5}	4.26^{6}	4.25^{6}	3.99^{6}
		SEE	0.65	0.69	0.70	0.65	0.68	0.67	0.67	0.67
		r	0.41	0.27	0.21	0.40	0.30	0.35	0.35	0.33
		N	135	135	132	135	135	133	133	135
Percent diameter stenosis (%)		tobs	-5.00^{6}	-3.32^{4}	-2.12^{1}	-5.08^{6}	-4.49^{6}	-3.60^{5}	-3.59^{5}	-3.57^{5}
		SEE	19.31	20.21	20.79	19.25	19.60	20.14	20.14	20.09
		r	-0.40	-0.27	-0.18	-0.40	-0.36	-0.30	-0.30	-0.29
		N	137	137	134	137	137	135	135	137
Minimal cross sectional area (mm^2)		tobs	4.81^{6}	2.803^{3}	2.37^{2}	4.60^{6}	3.28^{4}	3.88^{6}	3.88^{6}	3.73^{5}
		SEE	1.74	1.83	1.86	1.75	1.81	1.79	1.79	1.79
		r	0.39	0.24	0.20	0.37	0.27	0.32	0.32	0.31
		N	135	135	132	135	135	133	133	135
Percent cross sectional area stenosis (%)		tobs	-4.62^{6}	-3.13^{4}	-2.39^{2}	-4.86^{6}	-4.55^{6}	-3.19^{4}	-3.18^{4}	-3.33^{4}
		SEE	18.74	19.39	19.87	18.60	18.78	19.53	19.54	19.39
		r	-0.37	-0.27	-0.20	-0.39	-0.36	-0.27	-0.27	-0.28
		N	137	137	134	137	137	135	135	137
Eccentricity at the minimum diameter (%)		tobs	-3.05^{3}	1.71^{1}	-1.70^{1}	-2.81^{3}	-2.37^{2}	-2.14^{1}	-2.11^{1}	
		SEE	15.91	16.30	16.28	16.00	16.13	16.21	16.21	
		r	-0.26	-0.15	-0.15	-0.24	-0.20	-0.19	-0.18	
		N	131	131	128	131	131	129	129	
Maximal eccentricity (%)		tobs		-2.02^{1}		-2.29^{1}	-2.34^{1}			
		SEE		27.33		27.29	27.27			
		r		-0.19		-0.20	-0.20			
		N		131		131	131			
Mean eccentricity (%)		tobs	-2.48^{2}	-1.90^{1}		-2.72^{3}	-2.29^{1}	-1.67^{1}	-1.71^{1}	
		SEE	9.98	10.07		9.93	10.01	10.12	10.11	
		r	-0.21	-0.17		-0.23	-0.20	-0.15	-0.15	
		N	130	131		131	131	129	129	
Atheroma area (mm^2)		tobs	-2.41^{2}	-2.91^{3}		-3.09^{3}	-3.30^{4}	-1.83^{1}	-1.95^{1}	
		SEE	6.20	6.14		6.11	6.08	6.26	6.25	
		r	-0.21	-0.25		-0.26	-0.28	-0.16	-0.17	
		N	129	129		129	129	127	127	
Longlitudinal area stenosis (%)		tobs	-4.22^{6}	-4.46^{6}	-2.45^{2}	-5.17^{6}	-5.14^{6}	-2.75^{3}	-2.79^{3}	-2.71^{3}
		SEE	9.55	9.49	10.00	9.27	9.28	9.93	9.92	9.92
		r	-0.35	-0.37	-0.21	-0.42	-0.41	-0.24	-0.24	-0.23
		N	129	129	126	129	129	127	127	129

All significance tests are 1 tailed

Significance levels

1 $0.05 \leq p > 0.01$
2 $0.01 \leq p > 0.005$
3 $0.005 \leq p > 0.001$
4 $0.001 \leq p > 0.0005$
5 $0.005 \leq p > 0.0001$
6 $p \leq 0.0001$

Table 7.5 Regression analysis - exercise performance vs stenotic parameters, all patients included

continued.

DEPENDANT VARIABLE		INDEPENDANT VARIABLE: ST change (total) on exercise	Total ST change on recovery	Exercise ST change & recovery ST change	Peak estimated VO_2	Functional aerobic capacity	Maximal oxygen consumption
Minimal diameter (mm)	tobs	-3.01[3]	-2.53[2]	-3.54[5]	4.27[6]	4.49[6]	4.24[6]
	SEE	0.69	0.69	0.68	0.67	0.66	0.67
	r	-0.25	-0.21	-0.29	0.35	0.36	0.35
	N	135	135	135	135	135	133
Percent diameter stenosis (%)	tobs	3.09[3]	2.51[2]	3.60[5]	-3.98[6]	-4.39[6]	-3.90[6]
	SEE	20.31	20.54	20.07	19.88	19.66	19.98
	r	0.26	0.21	0.30	-0.32	-0.35	-0.32
	N	137	137	137	137	137	135
Minimal cross sectional area (mm^2)	tobs	-3.27[4]	-2.23[1]	-3.70[5]	3.75[5]	3.86[6]	3.84[6]
	SEE	1.81	1.85	1.79	1.79	1.79	1.79
	r	-0.27	-0.19	-0.31	0.31	0.32	0.32
	N	135	135	135	135	135	133
Percent cross sectional area stenosis (%)	tobs	3.24[4]	2.15[1]	3,63[5]	-3.51[5]	-3.93[6]	-3.56[5]
	SEE	19.43	19.83	19.25	19.31	19.11	19.36
	r	0.27	0.18	0.30	-0.29	-0.32	-0.30
	N	137	137	137	137	137	135
Eccentricity at the minimum diameter (%)	tobs		1.90[1]		-1.74[1]		-2.16[1]
	SEE		16.25		16.30		16.19
	r		0.16		-0.15		-0.19
	N		131		131		129
Maximal eccentricity (%)	tobs						-1.74[1]
	SEE						27.62
	r						-0.15
	N						129
Mean eccentricity (%)	tobs						-1.86[1]
	SEE						10.09
	r						-0.16
	N						129
Atheroma area (mm^2)	tobs		2.49[2]				-2.63[3]
	SEE		6.19				6.18
	r		0.22				-0.23
	N		129				127
Longlitudinal area stenosis (%)	tobs	2.24[1]	3.04[3]	3.01[3]	-2.88[3]	-3.27[4]	-3.15[5]
	SEE	10.00	9.85	9.85	9.88	9.80	9.84
	r	0.20	0.26	0.26	-0.25	-0.28	-0.27
	N	129	129	129	129	129	127

All significance levels 1 tailed.

Significance levels

1 $0.05 \leqslant p > 0.01$

2 $0.01 \leqslant p > 0.005$

3 $0.005 \leqslant p > 0.001$

4 $0.001 \leqslant p > 0.0005$

5 $0.0005 \leqslant p > 0.0001$

6 $p \leqslant 0.0001$

and more frequent being significant with all exercise variables once atheroma area is normalized for undiseased artery size.

As in the previous section, exfh, exSBP and exRPP correlate frequently and in some cases highly with stenotic anatomy. Table 7.5a illustrates the degree of correlation once these variables have been normalized for resting haemodynamic state. Many previously strong regression relationships are now weak or non significant, and therefore not displayed.

Correlations of height, weight and body surface area (regression with percent diameter stenosis, section 7.4.4) with all parameters were non significant (except with those involving these parameters in their deriving equations). Hence all data described above remains uncorrected for body size.

7.4.3 Relationship between Exercise Performance and Coronary Anatomy - Pre/Post PTCA1 Group only

These regression analyses have excluded work done using Balkes equation, all direct reference to exercise systolic blood pressure, exercise pulse pressure, minimal cross-sectional area and percent cross-sectional area stenosis as their interrelationships were less strong than those preserved for study.

Overall, the pattern of significant results is preserved across all parameters (table 7.6) with the possible exception of maximal eccentricity and eccentricity at the minimal diameter, whose positions have been reversed. Generally, all correlation coefficients and t ratios are increased and standard errors of estimate decreased. Once again, exfh and exRPP correlate strongly. Table 7.6a presents the same analyses once normalization has taken place.

Table 7.5a Regression analysis - Normalised haemodynamic data vs stenotic parameters, all patients and PTCA stages included

	Normalised exfh				Normalised exSBP			
	tobs	SEE	r	N	tobs	SEE	r	N
Minimal diameter (mm)	1.71[1]	0.70	0.15	135	2.44[2]	0.70	0.21	135
Percent diameter stenosis (%)					-2.09[1]	20.68	-0.18	137
Minimal cross sectional area (mm^2)					2.31[1]	1.85	0.20	135
Percent cross sectional area stenosis (%)					-2.15[1]	19.83	-0.18	137
Eccentricity at the minimum diameter (%)					-1.90[1]	16.26	-0.17	131
Longlitudinal area stenosis (%)					-2.87[3]	9.88	-0.25	130

Significance levels

1 $0.05 \leqslant p > 0.01$
2 $0.01 \leqslant p > 0.005$
3 $0.005 \leqslant p > 0.001$

Table 7.6 Regression analysis - exercise performance vs stenotic parameters, pre/post PTCAl group only

		INDEPENDANT VARIABLE							
		Exercise heart rate	Exercise rate pressure product	Work Done (IxS)	Exercise time (mins)	Total ST change	Peak estimated VO_2	Functional aerobic capacity	Maximal oxygen consumption
Minimum diameter (mm)	tobs	5.14[6]	4.33[6]	3.78[5]	3.55[5]	-2.22[1]	4.06[6]	4.09[6]	3.68[5]
	SEE	0.64	0.66	0.67	0.68	0.71	0.67	0.67	0.68
	r	0.48	0.42	0.37	0.35	-0.23	0.40	0.40	0.36
	N	90	90	90	90	90	90	90	90
Percent diameter stenosis (%)	tobs	-5.24[6]	-4.94	-3.34[3]	-3.18[3]	2.01[1]	-3.78[5]	-3.81[5]	-3.45[5]
	SEE	18.65	19.24	20.07	20.18	20.82	19.78	19.76	20.01
	r	-0.48	-0.43	-0.33	-0.32	0.21	-0.37	-0.37	-0.34
	N	92	92	92	92	92	92	92	92
Eccentricity at the minimum diameter (%)	tobs	-2.60[2]	-1.93[1]						
	SEE	16.30	16.53						
	r	-0.27	-0.20						
	N	90	90						
Maximal eccentricity (%)	tobs	-3.05[3]	-1.93[1]	-2.42[2]	-1.68[1]		-2.24[1]		-2.40[2]
	SEE	20.56	21.17	20.93	21.27		21.02		20.94
	r	-0.31	-0.20	-0.25	-0.18		-0.23		-0.25
	N	90	90	90	90		90		90
Mean eccentricity (%)	tobs	-2.96[3]	-2.15[3]	-1.86[1]					-1.77[1]
	SEE	9.52	9.72	9.79					9.80
	r	-0.30	-0.22	-0.19					-0.18
	N	90	90	90					90
Atheroma area (mm^2)	tobs	-1.95[1]	-2.47[2]	-1.72[1]					-1.94[1]
	SEE	6.09	6.02	6.12					6.10
	r	-0.20	-0.25	-0.18					-0.20
	N	89	89	89					89
Longlitudinal area stenosis (%)	tobs	-4.06[6]	-4.76[6]	-2.70[3]	-2.62[2]	1.98[1]	-2.97[3]	-3.13[3]	-2.86[3]
	SEE	9.44	9.18	9.89	9.91	10.06	9.81	9.76	9.84
	r	-0.40	-0.45	-0.28	-0.27	0.21	-0.30	-0.32	-0.29
	N	89	89	89	89	89	89	89	89

All significance levels 1 tailed.

Significance levels

1 $0.05 \leqslant p > 0.01$

2 $0.01 \leqslant p > 0.005$

3 $0.005 \leqslant p > 0.001$

4 $0.001 \leqslant p > 0.0005$

5 $0.0005 \leqslant p > 0.0001$

6 $p \leqslant 0.0001$

Table 7.6a Regression analysis - Normalised haemodynamic data vs stenotic parameters, pre/post PTCAl data only

	Normalised exfh				Normalised exSBP			
	tobs	SEE	r	N	tobs	SEE	r	N
Minimal diameter (mm)	1.94[1]	0.71	0.20	93	2.03[1]	0.70	0.23	93
Percent diameter stenosis (%)					-1.84[1]	20.77	-0.19	95
Minimal cross sectional area (mm^2)	1.85[1]	1.83	0.19	93	2.44[2]	20.77	-0.19	93
Minimal cross sectional area stenosis (%)					-2.08[1]	19.63	-0.21	95
Atheroma area (mm)					-1.97[1]	6.03	-0.20	92
Longlitudinal area stenosis (%)					-2.92[3]	9.79	-0.29	93

Significance levels

1 $0.05 \leqslant p > 0.01$

2 $0.01 \leqslant p > 0.005$

3 $0.005 \leqslant p > 0.001$

All data is unrelated to body size and therefore remains uncorrected (regression with percent diameter stenosis, section 7.4.4).

7.4.4 Estimating Percent Diameter Stenosis from Exercise Performance

Employing stepwise multiple regression, and entering all exercise parameters plus age, height, weight, body surface area and body mass index (BMI - related to obesity) as predictor variables, the variables of exfh, sum of ST segment changes and BMI were selected for the whole group (table 7.7a) and exfh, FAC and BMI being selected for the pre/post PTCA1 group (table 7.7b). Correlation coefficients were 0.52 and 0.57, respectively. Both relationships were highly significant ($p <= 0.01\%$). Table 7.7c demonstrates multiple regression analysis results for the pre/post PTCA1 group utilizing the exercise parameters selected for the whole group for comparison. Indeed, correlation coefficient is improved to 0.54, although overall F ratio is reduced from 14.06 to 11.9. It is interesting to note that when used in combination with other parameters, BMI becomes significant, yet, considered alone the regression relationship with percent diameter stenosis is non significant (two tailed) in both groups (table 7.7d and 7.7e).

As exfh accounted for the majority of the variance explained by the above relationships, these stepwise multiple regressions were then repeated with the most drug sensitive parameters removed. For the whole group, FAC and sum of ST segment changes were selected with $peVO_2$ and BMI contributing for the pre/post PTCA1 group. Correlation coefficients are dramatically reduced, SEEs increased only marginally and the significance of the relationships preserved in both cases (table 7.7f and 7.7g). Table 7.7h shows results to regression analysis of those variables contributing significantly to the whole group on the pre/post PTCA1 data set for comparison. This relationship

Table 7.7a Predicting percent diameter stenosis from exercise tolerance data - whole group

Percent diameter stenosis = 1.35 BMI - 0.3lexfh + 0.83 SumST + 60.83

Variable	Regression coefficient	Standard error of coefficient	F df 1,114	Probability	Partial variance (%)
BMI	1.3519	0.07686	3.093	0.08129	2.64
exfh	-0.3109	0.0635	23.982	<0.0001	17.38
SumST	0.8263	0.3694	5.005	0.02722	4.21
CONSTANT	60.8322				

SEE = 18.24, r = 0.52, variance explained = 25.09%

Overall f ratio, df 3,114 = 14.06 $p \leq 0.0001$

Table 7.7b Predicting percent diameter stenosis from exercise tolerance data - pre/post PTCA1 group only

Percent diameter stenosis = 1.87 BMI - 0.32 exfh - 0.12 FAC + 65.58

Variable	Regression coefficient	Standard error of coefficient	F df 1,87	Probability	Partial variance (%)
BMI	1.8709	0.8071	5.373	0.02280	5.82
exfh	-0.3160	0.0715	19.534	0.00003	18.34
FAC	-0.1198	0.0477	6.322	0.01377	6.77
CONSTANT	65.5753				

SEE = 17.43, r = 0.57, variance explained = 29.86%

Overall F ratio, df 3,87 = 13.77, $p \leq 0.0001$

Table 7.7c Predicting percent diameter stenosis in the pre/post PTCAl group using parmeters selected from the whole group

Percent diameter stenosis = 1.97 BMI - 0.34 exfh + 0.58 SumST + 51.63

Variable	Regression coefficient	Standard error of coefficient	F df 1,87	Probability	Partial variance (%)
BMI	1.9734	0.8276	5.688	0.01927	6.13
exfh	-0.3448	0.0717	-23.117	0.00001	21.00
SumST	0.5826	0.3904	2.226	0.13929	2.50
CONSTANT	51.6329				

SEE = 17.83, r = 0.54, variance explained = 26.64%

Overall F ratio, df 3,87 = 11.90 $p \leqslant 0.0001$

Table 7.7d Regression analysis - Percent diameter stenosis vs body size and obesity indices, whole group

Variable	N	tobs (two tailed)	SEE	r
Height	119	-0.88^{NS}	21.01	-0.08^{NS}
Weight	119	0.48^{NS}	21.06	0.04^{NS}
BSA	119	-0.26^{NS}	21.07	-0.02^{NS}
BMI	119	1.85^{NS} (p=0.067)	20.78	0.17

Table 7.7e Regression analysis - Percent diameter stenosis vs body size and obesity indicies, pre/post PTCAl group only

Variable	N	tobs (two tailed)	SEE	r
Height	83	-1.19^{NS}	21.02	-0.13
Weight	93	0.26^{NS}	21.27	0.02
BSA	83	-1.17^{NS}	21.03	-0.13
BMI	83	1.85^{NS} (p=0.069)	20.77	0.20

Table 7.7f Predicting percent diameter stenosis from parameters not directly affected by drug therapy - whole group

Percent diameter stenosis = 1.04 SumST changes - 0.14 FAC + 66.26

Variable	Regression coefficient	Standard error of coefficient	F df 1,129	Probability	Partial variance (%)
SumST	1.0393	0.3592	8.370	0.00448	6.09
FAC	-0.1433	0.0438	10.716	0.00136	7.67
CONSTANT	66.2592				

SEE = 19.1271, r = 0.41, variance explained = 15.82%

Overall F ratio, df 2,129 = 13.3 $p \leqslant 0.0001$

Table 7.7g Predicting percent diameter stenosis from parameters not directly affected by drug therapy - pre/post PTCA1 group only

Percent diameter stenosis = 1.93 BMI - 0.56 $peVO_2$ + 27.03

Variable	Regression coefficient	Standard error of coefficient	F df 1,88	Probability	Partial variance (%)
BMI	1.9346	0.8855	4.773	0.03157	5.14
$peVO_2$	-0.5598	0.1524	13.482	0.00041	13.29
CONSTANT	27.0284				

SEE = 19.1296, r = 0.42, variance explained = 15.54%

Overall F ratio, df 2,88 = 9.28 $p \leqslant 0.0005$

Table 7.7h Predicting percent diameter stenosis in the pre/post PTCA1 group using parameters selected from the whole group

Percent diameter stenosis = 0.64 SumST - 0.17 FAC + 71.54

Variable	Regression coefficient	Standard error of coefficient	F df 1,88	Probability	Partial variance (%)
FAC	-0.1656	0.0521	10.1251	0.00202	10.32
SumST	0.6412	0.4244	2.28	0.13444	2.53
CONSTANT	71.5415				

SEE = 19.4491, r = 0.38, variance explained = 12.69%

Overall F ratio, df 2,88 = 7.54, $p \leqslant 0.001$

is severely affected both in terms of correlation coefficient and strength of significance.

7.4.5 Influence of Stenotic Anatomy on PTCA Failure Rate

PTCA failure rate due to inability to cross the stenosis with the dilating catheter was 29.4% in the RCA group of patients (table 7.8), almost twice the rate for PTCA of LAD arteries (15.2%). PTCA failure in circumflex arteries was also high at 50.0%, however, the data set for this group is very small at two patients and is not considered further. Hierarchical unrelated two tailed t tests were carried out using variables important when assessing PTCA feasibility from the pre PTCA1 and pre PTCA2 stenotic data in order to investigate if RCA failure rate may be explained by unusual stenotic anatomy. The data from these tests is presented as table 7.9.

No significant differences in stenotic morphology existed between arteries in which PTCA was successful and arteries in which it was not (due to inability to cross the stenosis) when LAD and RCA arteries were considered collectively. All parameters remained non significant when all (ie. PTCA1 and PTCA2) LAD successes were tested against all LAD failures. When RCA data were tested in the same manner, differences between average maximal diameter (figure 7.3a) minimal diameter (figure 7.3b) and eccentricity at the minimal diameter (figure 7.3c) proved significant. Mean differences (table 7.9a) demonstrated that the failure group had smaller dimensions and higher eccentricity.

Considering just the pre PTCA1 data and repeating the tests gave no significant differences for the LAD group (table 7.9) and significant differences with larger t ratios in the same parameters for the RCA group. Direction of mean differences are consistent with the above (table 7.9a).

Table 7.8 Overall PTCA success and failure rates (breakdown)

	Success	Failure (all cases)		Failure (inability to cross the stenosis)
LAD	37	9	46	7 (15.2%)
RCA	10	7	17	5 (29.4%)
CX	1	1	2	1 (50.0%)
	48	17		12

Table 7.9 Two tailed unrelated t tests - pre PTCA stenotic data. Primary success PTCA vs primary fail (inability to cross the stenosis) PTCA

Test Condition		All success vs all failure	All LAD success vs all LAD failure	All RCA success vs all RCA failure	PTCAl LAD success vs PTCAl LAD failure	PTCAl RCA success vs PTCAl RCA failure
Parameter						
Average maximal diameter	tobs	1.06^{NS}	0.32^{NS}	2.16^{1}	0.09^{NS}	2.27^{1}
	df	114	80	31	74	29
Minimal diameter	tobs	1.33^{NS}	0.75^{NS}	2.64^{1}	1.12^{NS}	2.72^{1}
	df	114	80	31	73	29
Percent diameter stenosis	tobs	0.70^{NS}	1.19^{NS}	1.97^{NS}	1.32^{NS}	2.00^{NS}
	df	115	81	31	74	29
Stenotic length	tobs	0.67^{NS}	0.46^{NS}	0.42^{NS}	1.20^{NS}	0.42^{NS}
	df	66	45	19	41	18
Segment length	tobs	0.10^{NS}	0.33^{NS}	0.69^{NS}	1.24^{NS}	0.69^{NS}
	df	114	80	31	73	29
Eccentricit... at the minimal diameter	tobs	1.43^{NS}	0.18^{NS}	2.84^{2}	1.17^{NS}	4.26^{3}
	df	98	70	25	64	24
Maximal eccentricity	tobs	1.06^{NS}	0.18^{NS}	1.57^{NS}	0.32^{NS}	1.65^{NS}
	df	98	70	25	64	28
Mean eccentricity	tobs	0.6^{NS}	0.13^{NS}	0.76^{NS}	0.15^{NS}	0.86^{NS}
	df	98	70	25	64	24
Stenotic area	tobs	1.56^{NS}	1.06^{NS}	1.37^{NS}	1.30^{NS}	1.33^{NS}
	df	97	69	25	63	24
Atheroma area	tobs	0.22^{NS}	0.91^{NS}	0.80^{NS}	1.26^{NS}	0.73^{NS}
	df	97	69	25	63	24

Significance levels:

1 $0.05 \leq p > 0.01$

2 $0.01 \leq p > 0.005$

3 $0.005 \leq p > 0.001$

Table 7.9a Descriptive statistics, stenotic morphology, success vs failure (mean +/- 1 standard deviation)

	Average maximal diameter (mm)	Minimal diameter (mm)	Eccentricity at the minimal diameter (%)
All successes	3.52+/-0.65	1.1+/-0.49	23.8+/-18.3
All fails	3.35+/-0.71	0.99+/-0.65	31.7+/-30.1
All LAD successes	3.50+/-0.63	1.10+/-0.46	24.1+/-19.8
All LAD fails	3.56+/-0.76	1.22+/-0.68	22.85+/-18.80
All RCA successes	3.63+/-0.69	1.09+/-0.59	22.0+/-13.3
All RCA fails	3.05+/-0.56	0.52+/-0.28	47.7+/-34.6
PTCAl LAD successes	3.47+/-0.65	1.09+/-0.46	24.1+/-18.5
PTCAl LAD fails	3.55+/-0.61	1.30+/-0.75	16.1+/-13.8
PTCAl RCA successes	3.67+/-0.70	1.09+/-0.56	20.4+/-11.3
PTCAl RCA fails	3.05+/-0.56	0.52+/-0.28	47.7+/-34.7

Average maximal diameter dimension in successful and failed PTCA procedures.

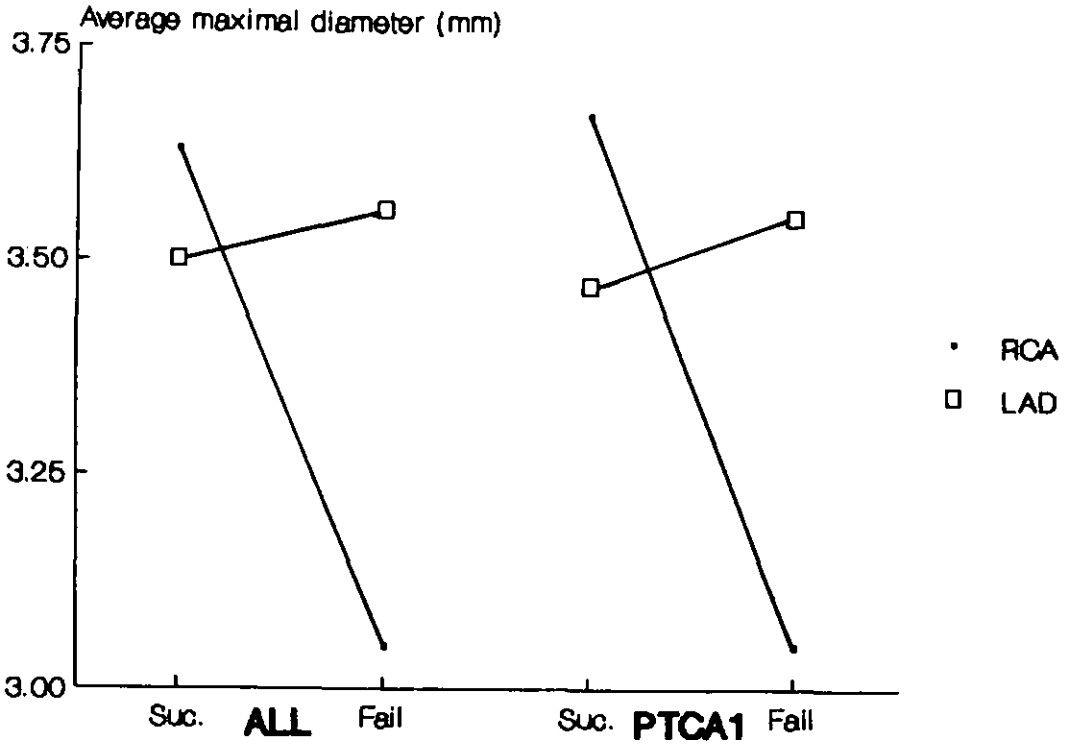

Minimal diameter dimension in successful and failed PTCA procedures.

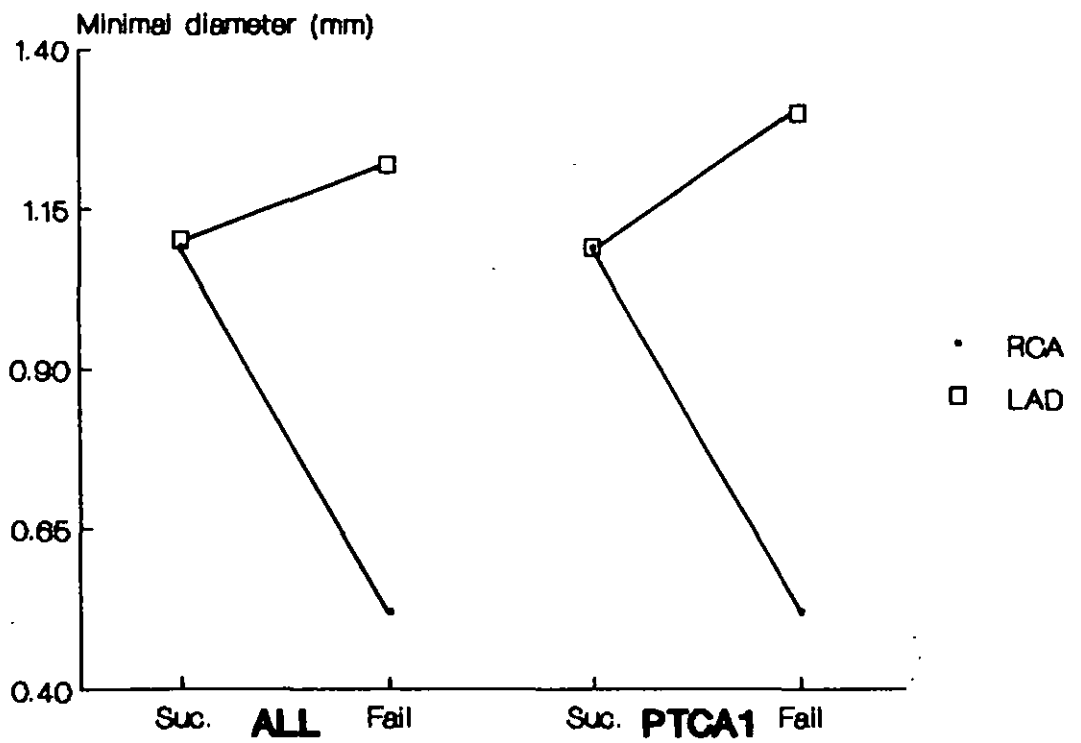

Figures 7.3a and 7.3b

Eccentricity at the minimal diameter in successful and failed PTCA procedures.

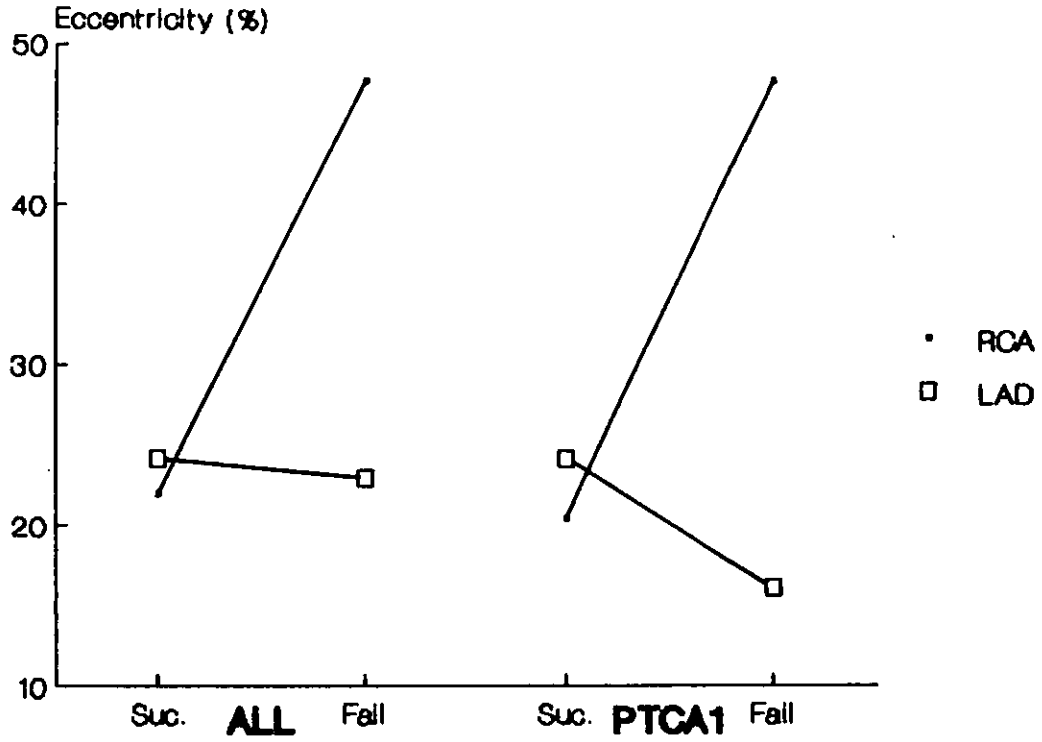

Figure 7.3c

7.4.6 Relationship between Subjective and Quantified Estimation of Percent Diameter Stenosis

QAMS estimation of percent diameter stenosis was regressed against the reviewing Radiologists visual interpretation (averaging of QAMS values from differing views was necessary in order to match the data). Visual interpretation was treated as the independent variable in order to investigate validity of predicting QAMS percent stenosis from the visually assessed values (figure 7.4).

The data correlated remarkably well ($r = 0.79$) yielding a highly significant regression relationship (table 7.10) and a reasonably low SEE at 11.77%. The gradient and constant of the regression relationship were tested against the line of identity (table 7.10) and proved significantly different.

7.5 Discussion

7.5.1 The Efficacy of the PTCA Procedure

The primary success rate (82%) in this group of patients is greater than the primary success rate (73%) of the first 200 PTCA cases (within which these patients are included) undertaken at the Groby Road Hospital, Leicester (Hubner et al, 1988). However, this may be explained by the relatively small sample of this study where each artery accounts for 1.54% of the total. Primary success rate is much greater than that quoted by the NHLBI (Dorros, 1983) and Kent et al 1982 in which only 63% and 64% of PTCAs were initially successful. However, these figures are compiled from PTCAs performed before the introduction of the steerable guide wire system which has contributed greatly to PTCA success (Przybojewski, 1984).

Median (as data are clearly skewed) grade of angina was markedly reduced by the PTCA procedure (table 7.2) with 39 patients becoming asymptomatic on exercise where previously there had been none. PTCA was also beneficial in converting

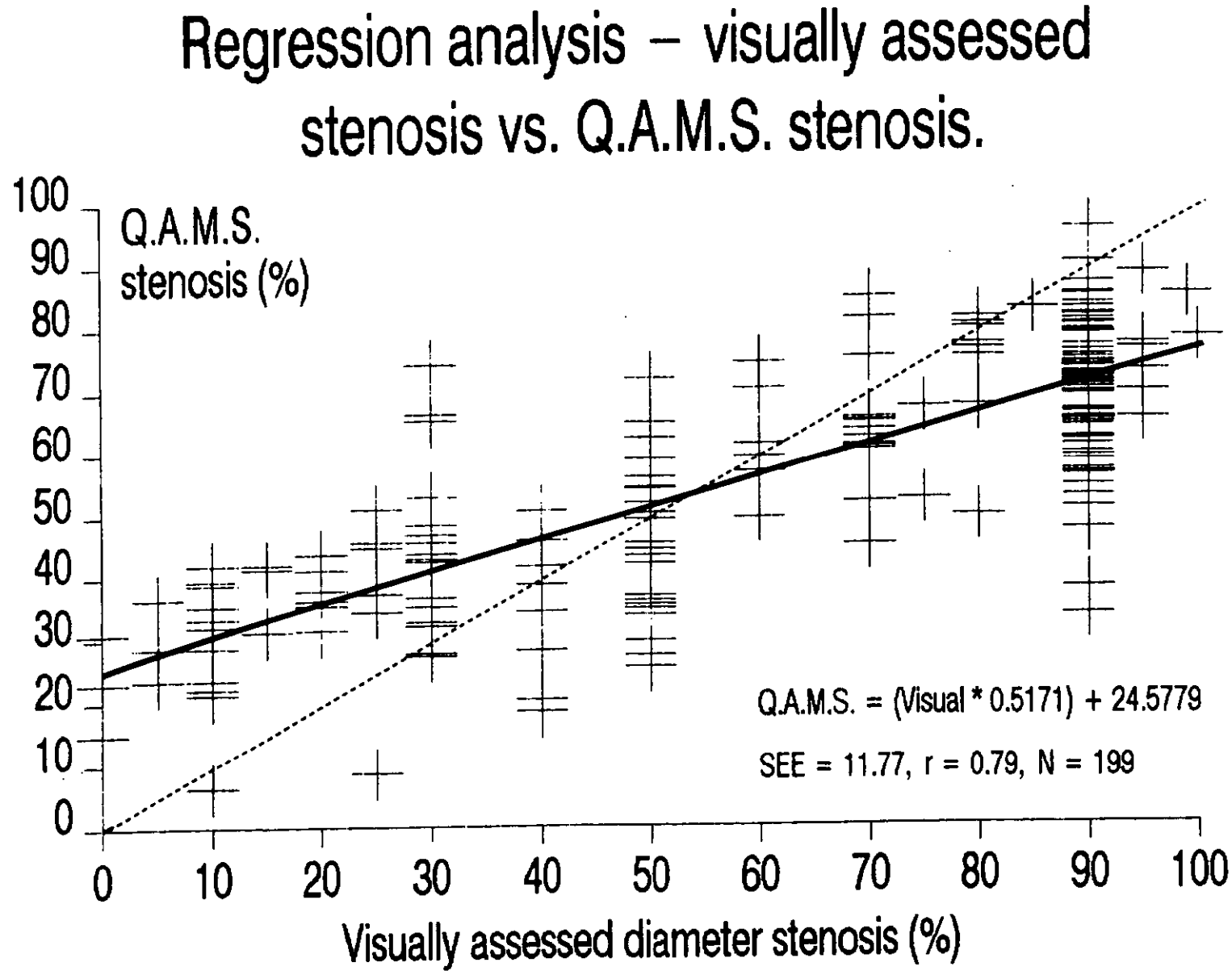
Regression analysis – visually assessed stenosis vs. Q.A.M.S. stenosis.
Q.A.M.S. stenosis (%)
100
90
80
70
60
50
40
30
20
10
0
Q.A.M.S. = (Visual * 0.5171) + 24.5779
SEE = 11.77, r = 0.79, N = 199
0
10
20
30
40
50
60
70
80
90
100
Visually assessed diameter stenosis (%)

Figure 7.4

Table 7.10 Regression analysis - visually assessed stenosis vs Q.A.M.S. stenosis

Q.A.M.S. stenosis = 0.52 visual stenosis + 24.58

Variable	Regression coefficient	Standard error of coefficient	tobs df 197	Probability
Visual stenosis	0.5171	0.0281	18.38	$\leqslant 0.0001$
CONSTANT	24.5779			

SEE = 11.77, r = 0.79, N = 199

Testing against line of identity:

1. Gradient $\quad tobs = \dfrac{0.5171-1.0}{0.0281} = -17.19$, $p \leqslant 0.0001$

2. Constant $\quad tobs = \dfrac{24.5779-0}{11.77-0.0281} = 2.09$, NS

unstable angina (grade 4) to low level stable angina, typically grade 1 or even 0. Such results agree with those of Cowley et al 1981 and Lewis et al 1983 in which obvious improvement was apparent by a change in each patient of one functional class of angina at least.

Of the parameters directly measurable using Q.A.M.S. (area is inferred from a circular model), the most haemodynamically significant is the minimal diameter (Young et al 1977, Gould 1978, section 6.2.1) whilst percent diameter stenosis is widely used clinically. As expected, the PTCA procedure produces markedly significant changes in these two parameters on the first and second attempts, with the extent of dilation of the stenosis (table 7.4) being comparable to other visual (Kent et al 1982, Scholl et al 1982, and Meier et al 1983a) and quantitative (Meyer et al 1981, Serruys et al 1984 and Wijns et al 1985ab) methods of stenotic assessment. Such changes must allow improvement in distal coronary artery blood flow and perfusion pressure (section 6.2.1), thus reversing exercise induced ischaemia and improving myocardial contractility by decreasing ventricular chamber stiffness (section 6.2.2). Such effects are widely manifest in these data set by significant changes in many exercise related parameters as a result of PTCA (table 7.3).

Exfh, exSBP and exRPP show significant changes on PTCA1 but not PTCA2. It is likely that some of the variance in the changes on PTCA1 may be explained by changes in drug therapy although there is still a significant increase in normalized exfh as a result of PTCA1 and a significant decrease in those patients who are classified as restenosed in comparison to the follow up group. Previous studies (Cowley et al 1981 and Scholl et al 1982) with mixed drug therapy report changes in the above parameters of similar magnitude to this study. Interestingly, systolic blood pressure ratio shows no significant differences as a result of PTCA which would have been expected if it were a sensitive predictor of significant CAD (Amon et al 1984, section 6.2.3).

Work done (force multiplied by distance moved equation; Balkes equation is less well related to stenotic morphology, section 7.5.2) by the patient shows large significant differences (table 7.3) as a result of the two PTCA procedures, inspection of group means (table 7.4) suggesting improvement. Work is also significantly affected by restenosis, being reduced. The strongly significant differences observed in percent diameter stenosis and more so, minimal diameter confirm the importance of these parameters in the patients ability to perform work. Whilst myocardial perfusion itself has not been quantified (ST changes however reflect it, see later), changes associated with the above conditions must result from changes in myocardial oxygen supply (section 6.2.1).

Exercise time also shows similar significant changes to work done, although less strongly. On PTCA1, exercise time is improved from 13.13 mins (788 secs) pre PTCA to 15.88 (953 secs) post PTCA1. Whilst the difference shows agreement with the results of Scholl et al 1982 (448 secs improved to 618 secs) absolute treadmill times in this study are considerably higher despite use of a similar exercise protocol. This may reflect better physical conditioning or less severe disease in this PTCA patient group. Scholls study utilized visual assessment of stenotic severity reporting changes of 78% to 35%, comparing well to this group in which PTCA1 affected a reduction from 70.3% to 36.2%. However, visual assessment is prone to high observer variability (Koh et al 1979) which may explain this difference in treadmill times. Kent et al 1982 describes changes in visual percent stenosis on PTCA from 74% to 31%, associated with treadmill time improvement from 7 minutes to 17 minutes, however treadmill protocol was very different for the Sheffield protocol in this case. Lewis et al 1983 showed no statistically significant difference in exercise time (5.5 to 7.2 mins) as a result of PTCA and fails to quote the protocol used.
Significant reduction of coronary narrowing (assessed by either minimal diameter or percent stenosis) significantly

affected exercise induced ischaemia (inferred by ST segment changes) with mean differences (tabled 7.4) indicating better myocardial perfusion with PTCA. Such ST changes have been demonstrated by Scholl et al 1982, however without the aid of significance testing.

Surprisingly, changes in predicted exercise parameters (peVO_2, FAC and VO_2max) are significant as a result of PTCA. Whilst these parameters are more than likely useless when compared to their equivalents derived from respiratory gas analysis (eg. FAC averages around 100% from pre PTCA1 onwards (table 7.4), suggesting that this parameter is **not** reflecting true FAC), they may be useful in determining whether disease state is haemodynamically significant and/or allow group comparisons between normals and cardiac patients to be made.

Broadly speaking, it is evident from these results that exercise performance is not affected one way or the other in the time between initial arteriographic assessment and pre PTCA1. All parameters (except SBP ratio) are then improved by the significant reduction in stenotic severity which (presumably) has allowed orderly myocardial function to be restored. These changes are retained throughout the time period to follow up, despite a significant change (decrease) in minimal diameter which is unlikely to be haemodynamically significant (2.16mm to 1.91mm). Most exercise parameters are then detremented as follow up exercise performance is compared to exercise performance of patients visually judged to have restenosed (and typically presenting with anginal symptoms). Changes are less significant than those of the reverse process (pre PTCA1 to post PTCA1) in keeping with the relatively larger minimal diameter of the pre PTCA2 group. Work, exercise time, ST changes and some predicted exercise parameters are then significantly affected again by the PTCA2 procedure, although to a smaller extent than on PTCA1 as secondary stenotic narrowing is less severe. The parameters of exfh, exSBP and exRPP show no significant

differences as drug therapy in all patients receiving PTCA2 is constant.

PTCA produces no significant effect on average maximal diameter of the artery at any of the review stages, although there is a tendency (non significant) for it to become smaller both at post PTCA and on follow up. These changes may relate to an immediate vasospastic response (Johnson et al 1986) and a local late remodeling process within the arterial vessel wall following the barotrauma of PTCA (Serruys et al 1988). However, these tendencies may simply be a function of differing patient population in the three samples.

Length of stenosis (both stenotic and segment), which may have a minor haemodynamic effect (section 6.2.1) show significant differences at post PTCA1 and follow up. These changes are explained by PTCA making the top and bottom of the stenosis a normal caliber again, hence 90% of the maximal diameter becomes closer to the minimal diameter both proximally and distally, resulting in a shorter stenotic segment (figure 7.5). For this reason, segment length is also reduced as the user perceives what was previously abnormal artery to be normal, and consequently begins tracing closer to the minimal diameter then on the post PTCA1 arteriogram (figure 7.5). On follow up, the significant difference in the minimal diameter demonstrates that restenosis is occurring to some extent, but this effect is masked by the tendency of the average maximal diameter to become smaller too, preserving current percent diameter stenosis (non significant). However, this minimal diameter reduction has affected a "pulling in" of the proximal and distal margins of the stenosis, thus increasing stenotic and segment length (figure 7.5). However, these changes in length do not adversely affect exercise performance confirming their weak contribution to the haemodynamic effect of coronary stenosis (section 6.2.1).
Eccentricity at the minimal diameter, a parameter perhaps more important in assessing technical difficulty of the PTCA

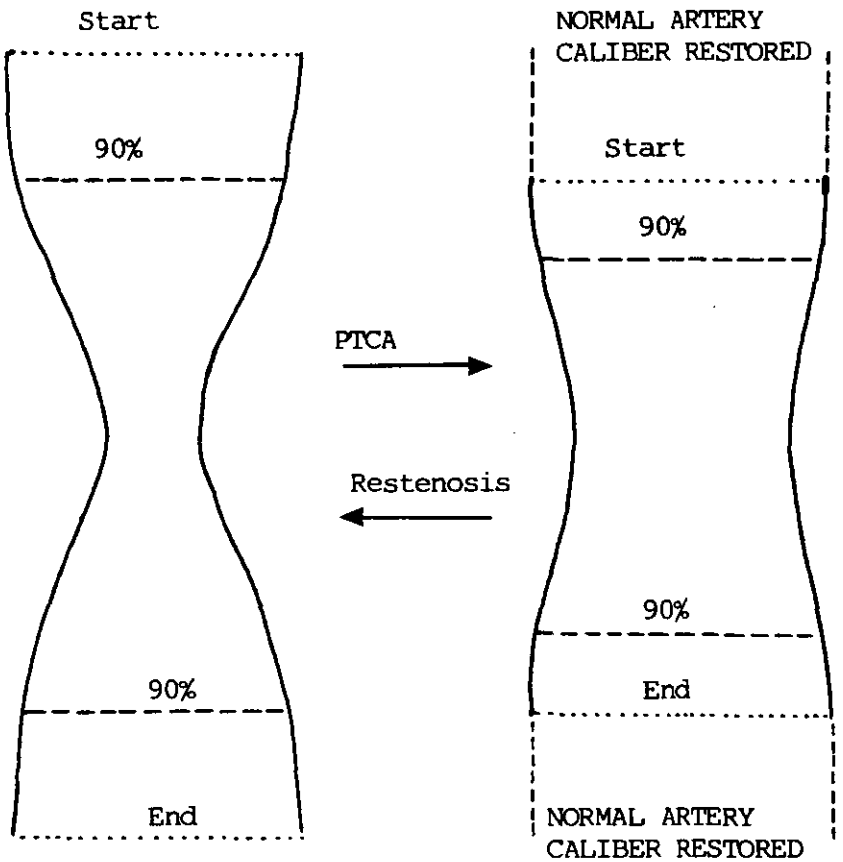

Figure 7.5 Changes in stenotic and segment length as a result of PTCA and restenosis

procedure (see later) shows only a significant difference at follow up vs. pre PTCA2. This is more than likely due to patient population differences. However, where population difference is relatively constant (pre PTCA1 vs. post PTCA1) this parameter is non significant, reflecting that changes in minimal diameter appear concentric around the balloon catheter. Maximal eccentricity and mean eccentricity are both significantly affected by PTCA1, a change reversed on follow up. This indicates the immediate effect of PTCA on vessel tortuousity (maximal and mean) is to "smooth it out", an effect which is reversed following remodeling and healing.

The current theory of the effect of PTCA on the stenosis supports atheromal compression rather than spreading in low grade stenoses and medial stretching plus splitting in high grade stenoses (Block, 1980 - figure 7.6). Assuming that stenoses receiving PTCA1 fall into the latter category, the morphological changes revealed by QAMS support this theory. Consider the stylized situation presented as figure 7.7. PTCA is effective in reducing stenotic severity concentrically around the minimal diameter. Maximal eccentricity is reduced as is stenotic length (not shown, see figure 7.5) and, to a small non significant extent, average maximal diameter. With time, the minimal diameter becomes reduced rather than enlarged. This fact refutes the observation of Johnson et al 1986 where late increases were apparent, explained by a reversal of the vasospastic response. However, the above describes the trend in the whole group. Should the data be separated according to eccentricity, this late increase may well be exhibited. Percent diameter stenosis however, is preserved by the reduction in average maximal diameter. Decreases in minimal diameter occur concentrically again allowing maximal eccentricity to become reestablished, on average being more severe in relative terms than previously as maximal diameter is reduced. As atheromal area remains constant (Block, 1980, Castaneda-Zuniga et al, 1980) and the medial layers heal, tension in them increases causing the atheroma to be

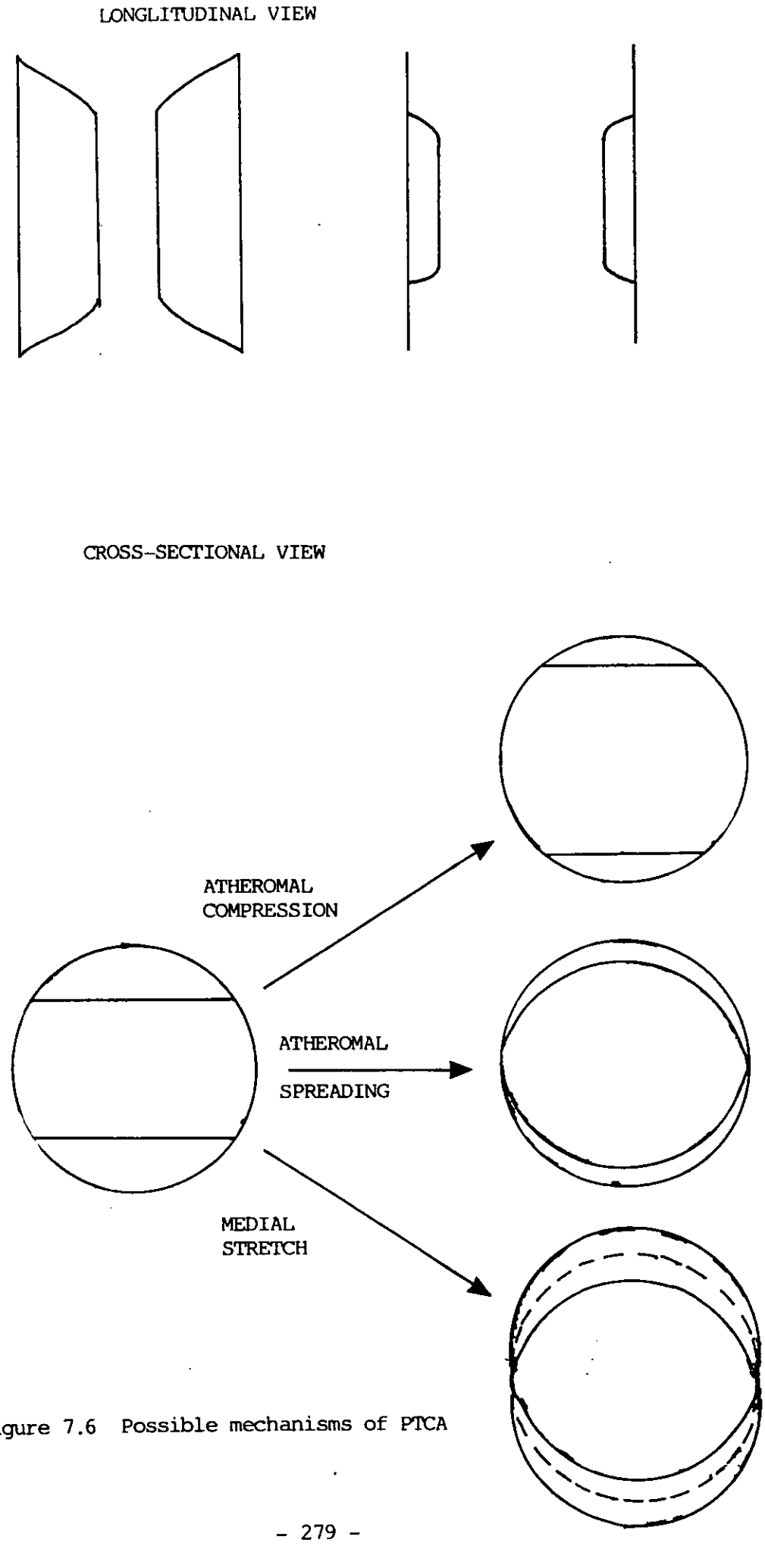

Figure 7.6 Possible mechanisms of PTCA

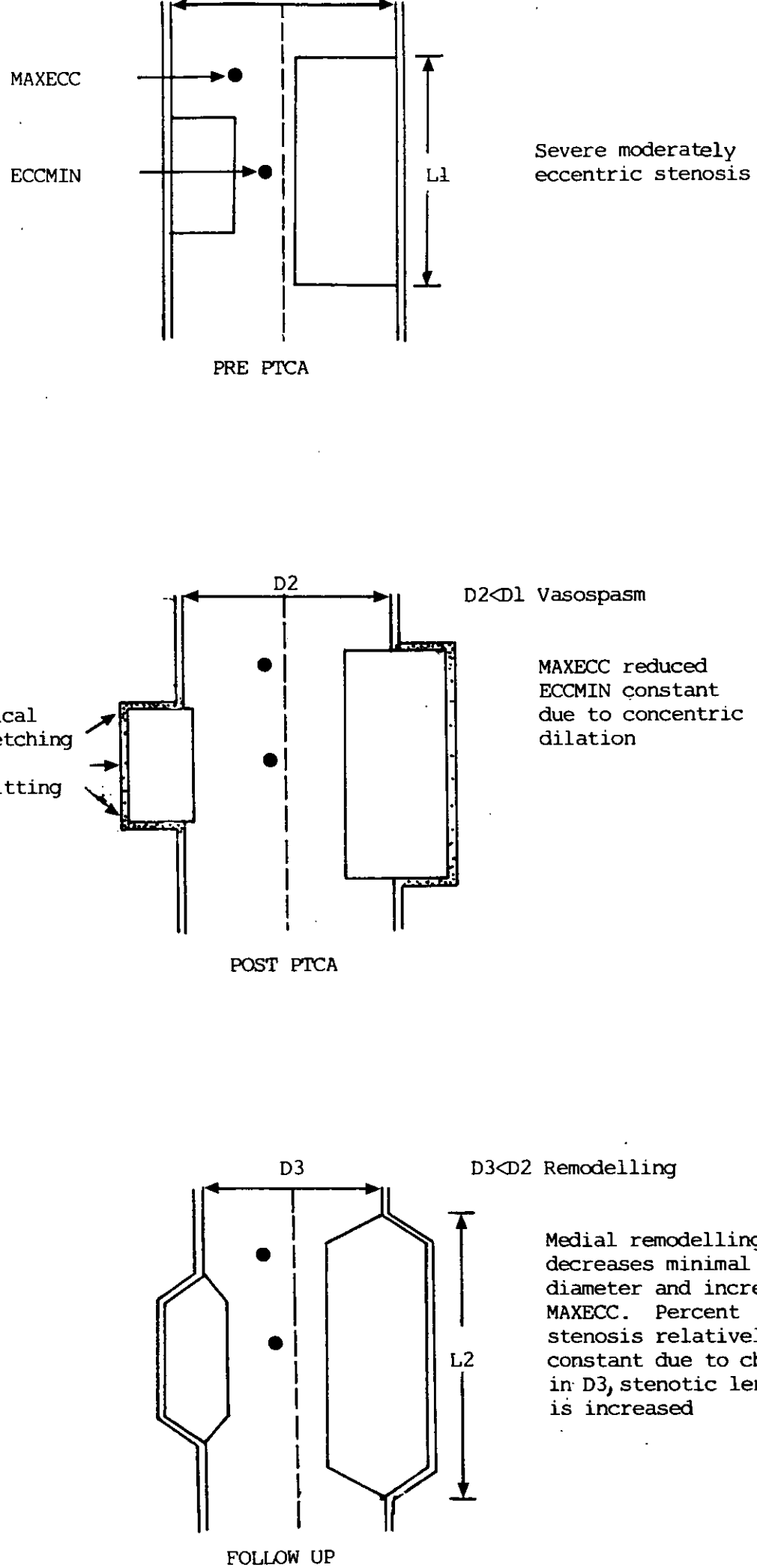

Figure 7.7 Changes in stenotic morphology following PTCA

pushed back towards the centre. Restenosis is not complete so the atheroma appears to spread, causing the stenosis to increase in length.

Atheromal area and longitudinal area stenosis (a parameter combining atheromal area and stenosis length) are both significantly affected by PTCA1. Current theories (above) suggest that changes in the atheroma are due to medial effects rather than compression. PTCA2 in the lower grade stenoses show no significant differences in the atheromal parameters. This category would normally be classified as mild disease and therefore normally demonstrate atheromal compression (Block, 1980). However, histological changes resulting from a second PTCA have not been documented. It may be that changes in exercise performance may result from a spreading of the atheroma (figure 7.6) to previously non involved portions of the vessel not quantifiable by the two dimensional nature of QAMS. Atheromal area is significantly changed also between follow up and pre PTCA2. However, this change fails to be significant once normalized for artery area reflecting that patient population change is the probable cause of this result.

In conclusion, these tests have demonstrated that PTCA is effective not only in improving exercise performance but also in considerably altering stenotic morphology. Additionally, quantification of stenotic parameters has allowed insight to be gained in the possible mechanism of PTCA.

7.5.2 Relationship between Exercise Performance and Coronary Anatomy - Whole Group

Regressing exercise performance against stenotic anatomy in a large group of patients who are subject to changes in drug therapy which may affect effort tolerance would never yield perfect results. Drawing data from a relatively uncontrolled (ie. clinical) environment will always enhance variability. However, the aim of these studies was to use Q.A.M.S. as a tool by which the effects of varying stenotic

morphology may be related to exercise performance, and, should significant results be gleaned then hopefully this would pave the way for the use of Q.A.M.S. in similar studies under more rigorous conditions.

On the whole, all the above considered, the results are encouraging. The regression analyses have been carried out with stenotic anatomy as the dependant variable such that SEEs reflect degree of error in predicting these variables from the respective parameters of exercise performance.

Minimal diameter has the strongest relationship of all stenotic variables confirming its importance in the haemodynamic effects of arterial narrowing (Young et al, 1977, Gould et al, 1978). Interestingly, minimal cross-sectional area, on which the fluid dynamic equations are actually based, correlates less well than minimal diameter or percent diameter stenosis. This may well be due to the circular cross-section assumption made for calculation of this parameter which is known not to be correct. This is an area where the future development of view matching may see a reversal in the above (chapter 9).

Many t ratios for the parameters of minimal diameter, percent diameter stenosis and their cross-sectional area equivalents show very high statistical significance confirming the validity of comparing exercise performance with stenotic anatomy. Standard errors of estimate for each relationship are very high however, suggesting that using the regression equations (not presented) from such analyses would not be useful in predicting individual stenotic dimensions. There may be of some use though in predicting whether coronary disease is likely to be haemodynamically significant or not in a similar patient population where arteriographic information is perhaps not available. Eccentricity variables are weak correlators as they have little to do with the equations of fluid dynamics. However, high values of eccentricity (ie. the maximal eccentricity) may be important in reducing distal myocardial perfusion

pressure by inducing friction and turbulence, thus increasing energy loss of stenotic blood flow. Unfortunately, this is not true of this set of data, instead, eccentricity at the minimum diameter, correlates best and most often. It would be most interesting to develop QAMS further, incorporating immediate graphical representation with location of these parameters, thus allowing comparison of their relative positions to be made. If, for example, the position of maximal eccentricity were proximal to that of eccentricity at the minimal diameter (figure 7.8a), then all turbulence effects would occur at the mouth of the stenosis, and would be streamed at the minimal diameter and perhaps recover for exit from the stenosis, the position where turbulence is most important (section 6.2.2). Should eccentricity at the minimal diameter be proximal to maximal eccentricity, then the position would be reversed (figure 7.8b). Mean eccentricity, may also have some bearing on generation of turbulence, however, the problem with this variable (at the moment anyway) is there is no way of telling if the returned value is composed of a continued gradual deviation of stenotic artery axis from diseased artery axis, or violent departure at only one or two sites. It would seem logical to assume that these two conditions would have differing physiological effects.

Absolute atheroma area correlates rather poorly with exercise performance. However, atheroma area is a two dimensional parameter. It is possible for a high grade stenosis to have the same atheroma area as a low grade stenosis, with consequently differing effects on exercise performance. Hence, once atheroma area is normalized for undiseased artery area, all correlations and t ratios are much improved.

Exercise parameters correlating most strongly with stenotic anatomy include exfh, exSBP and exRPP. As discussed in the previous section, some of the explained variance may be due to changes in drug therapy. Repeating the analyses with

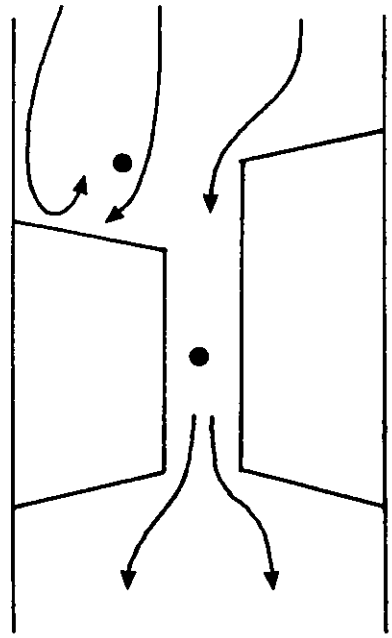

MAXECC preceeding minimal diameter

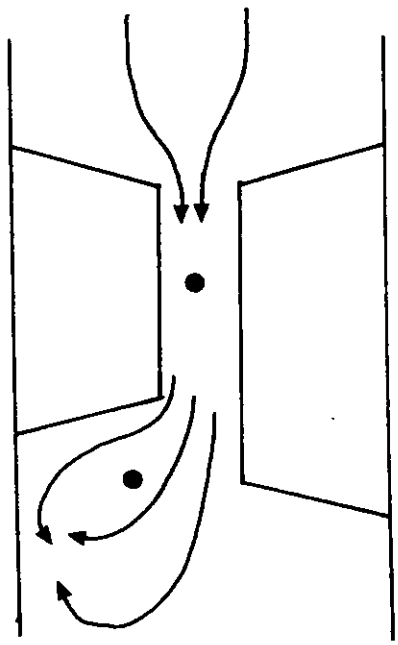

MAXECC following minimal diameter

Figure 7.8 "Possible" physiological consequences of differing maximal eccentricity positioning

normalized data confirms this suspicion. However, the parameters of work, exercise time, sum of ST changes and the predicted exercise parameters ($peV\dot{O}_2$, FAC and $\dot{V}O_2max$) all correlate significantly with variables shown to be important in resistance to stenotic blood blow.

7.5.3 Relationship between Exercise Performance and Coronary Anatomy - Pre/Post PTCA1 Group only

Results to these analyses are perhaps more meaningful as the matching rate was quite high (ie. the group was composed of a pre and post result from each patient in many cases). However, drug therapy is still very variable again contributing to the relationships involving exfh, exSBP and exRPP.

Minimal diameter remains the strongest correlator above percent diameter stenosis. Cross-sectional areas were not considered as they had proved inferior to diameter measurements in the section above.

Eccentricity at the minimum diameter has become less important in this more homogeneous data set whereas maximal eccentricity is increased in significance and correlating reasonably highly with work and $\dot{V}O_2max$. This effect may well be due to turbulence pre PTCA1 which is removed post PTCA1, although location of this variable in relation to the minimal diameter may be important (section 7.5.1) and is unknown. However, this effect is not preserved and eccentricity tends to reestablish itself with time (section 7.5.1).

Changes in atheroma area follow the previous pattern, except that correlation coefficients are, on the whole slightly lower in this group. However, these are improved beyond those previously shown when normalized, clearly demonstrating that it is important to consider artery size in deriving quantitative relationships.

Work and exercise time continue to be highly significant variables when related to minimal diameter, however, the predicted exercise parameters all have more significant relationships. $Pe\dot{V}O_2$ is basically a reflection of stage reached on the stress test (section 7.3.3), $\dot{V}O_2max$ adds to this the effect of body weight (see next section for body size correlations) to $pe\dot{V}O_2$s detriment while FAC compares $pe\dot{V}O_2$ to standards based on the performance cardiac patients (Bruce et al, 1973). Therefore, aside from the potentially drug affectable parameters, the most powerful predictor of stenotic anatomy may well be the exercise stage reached and completed.

7.5.4 Estimating Percent Diameter Stenosis from Exercise Performance

As already demonstrated, equations using one predictor variable leave much of the variance unexplained. Therefore, stepwise multiple regression was used to examine to what extent more of the variance could be accounted for by using more predictors. Number of predictors was never allowed to exceed three, as equations became increasingly cumbersome to use and variance explained obeys the law of diminishing returns.

For the whole group, it was possible to explain 25.1% of the variance from the three predictors of exfh, sum of ST changes and body mass index (BMI). Standard error of estimate was high at 18.24% diameter stenosis. Exfh contributed most significantly accounting for 17.4% of the variance explained. The overall correlation coefficient of 0.52, whilst highly significant still confirms the use of this equation for group work only.

This situation was improved for the pre/post PTCA1 group with 29.9% of the variance explained from the predictors of exfh, FAC and BMI. Once again, exfh accounted for the majority of the variance at 18.3%. With a correlation coefficient of 0.57 and SEE 17.43%, this equation (table

7.7b) would prove marginally more useful than that above in predicting percent diameter stenosis from variables of exercise performance and obesity in a group of PTCA patients. Using the same parameters as those selected from the previous analysis on data from the pre/post PTCA1 group, variance explained was increased to 26.6%, correlation coefficient to 0.54 and SEE reduced to 17.83%. However the variables of BMI and sum of ST changes were not contributing significantly to the relationship, with exfh accounts for 21% of the explained variance (table 7.7c).

Clearly, exfh is very powerful in these relationships, but as proved already, much of the changes resulting from PTCA are due to changes in drug therapy. These tests were thus repeated without exfh, exSBP and exRPP being allowed to enter the equations. For the whole group, just the two parameters of FAC and sum of ST changes were selected. Variance explained was reduced below the previous analysis to 15.8%. Correlation coefficient was reduced to 0.41 and SEE increased to 19.13%. Both variables contributed approximately equally to the explained variance.

For the pre/post PTCA1 group, the results were again made worse, with explained variance from the parameter of $peVO_2$ and BMI being 15.5%, less than the whole group value. Correlation coefficient was slightly better at 0.42 and SEE the same at 19.13%. $PeVO_2$ contributed two and a half times more to the explained variance than BMI. Using the same parameters as before, variance explained was very low at 12.7%, lower than using a simple linear relationship in some cases. SEE and correlation coefficient were also adversely affected (19.45% and 0.38 respectively).

This work confirms that it is impossible to predict with any real accuracy percent diameter stenosis from any combination of exercise parameters. However, as with the simple linear equations, they may prove useful in comparative work or assessing presence of significant disease in groups of PTCA patients.

It is also interesting to note that BMI, a widely used index of obesity, correlates significantly with percent diameter stenosis when the direction of the coefficient can be predicted ($p = 0.3\%$), in both in the whole group and in the pre/post PTCA1 group. However, assuming direction may not be valid as there is no supporting evidence confirming that in a population of patients with CAD, the more obese subject will demonstrate the more severe disease. Whether this is a chance finding or an actual effect warrants a further, more controlled study.

7.5.5 Influence of Stenotic Anatomy on PTCA Failure

The NHLBI (Dorros et al, 1983) have reported that the chances of a successful PTCA can be enhanced by choosing the right sort of candidate, ie. one with a short, discrete concentric stenosis, proximally located etc. (sections 1.4.3 and 7.2). These analyses set out to establish if there was anything about the stenotic morphology as measured by QAMS which predisposed to failure.

Within the data available, it was noticed that failure due to inability to cross the stenosis at pre PTCA with the dilating catheter was relatively high in the RCA group.

In order to exclude the effect of all failures having different morphology from all successes, tests were conducted in a hierarchical manner for the whole group, down through the individual arteries, ending at considering only pre PTCA1 data.

No significant differences were noted when all successful pre PTCA stenotic data were tested against all failed pre PTCA stenotic data, ruling out a general failure morphology. This was also the case when the LAD artery was considered separately, giving rise to the conclusion that the failures associated with the LAD group must be attributable to other aspects of morphology not taken into account or other unmeasured physiological and/or anatomical indices.

On considering the RCA group alone, significant differences were present in average maximal diameter, minimal diameter and eccentricity at the minimal diameter. Inspection of group means (figures 7.3a to 7.3c) proved that artery dimensions were indeed smaller in the RCA fail group and eccentricity at the minimum diameter was larger. These are important factors when considering technical feasibility of the PTCA procedure. A small average maximal diameter and small minimal diameter increase the problem in gaining entry into the artery with the catheter, and more importantly, getting the dilating catheter across the stenosis once located. The high eccentricity at the minimum diameter will further complicate the crossing procedure as careful manipulation (ie. steering) to one side of the artery or another will be required in order to bridge the stenosis. Visually assessed eccentricity has previously been shown to complicate the PTCA procedure and reduce the rate of primary success (Meier et al 1983b).

Data from just the pre PTCA1 procedure were then considered for each artery as minimal diameter is smaller in this group, thus representing the "worst case" scenario (section 7.4.1). No significant differences were recorded for the LAD artery, but the three parameters proving significant previously were all significant again, eccentricity at the minimum diameter more so.
In conclusion, it would seem likely that the high failure rate of the RCA group may indeed be attributed, in part at least (as all aspects of stenotic morphology have not been measured), to small pre-angioplasty dimensions and high eccentricity at the minimal diameter. Without quantification capabilities, these differences would not have come to light.

7.5.6 Relationship between Subjective and Quantified Estimation of Percent Diameter Stenosis

Visually assessed percent diameter stenosis correlates very highly with that produced by the QAMS with 63.2% of the

variance explained. The regression relationship is highly significant (t = 18.4). The standard error of estimate, at 11.77% is considerably better than those reported in predicting percent diameter stenosis from simple linear or multiple regression of stenosis vs. exercise performance (section 7.5.2, 7.5.3 and 7.5.4). Indeed, the equation presented in table 7.10 may well be useful for removing bias in the visual estimation of percent diameter stenosis for clinicians not having access to quantification equipment.

The regression line differs significantly from the line of identity, enforcing the need for correction of bias. Underestimation of true stenosis with mild stenoses and overestimation of true stenosis with severe stenoses is evident from the position of data above and below this line. This observation confirms the data of Koh et al 1979. Grouping of data around the commonly used grades of 90% and 50% by visual assessment is also evident. It may well be that the relationship may be improved by adoption of a more continuous scale for visual stenotic assessment by the clinicians.

In conclusion, visually assessed stenosis, at this centre at least, agrees well with that measured by QAMS. The regression relationship derived may be useful in redressing the effects of under and overestimation.
In overall conclusion, study of data arising from this group of PTCA patients has proved that the availability of quantified material (particularly absolute measurements) relating to stenotic morphology can greatly enhance the understanding of the mechanism of PTCA and its physiological consequences. Data from the QAMS agree well with that reported in the literature and has proven useful both clinically and in a research capacity. With continued improvement, uses of the QAMS can only increase our knowledge of the effects of this treatment of CAD.

CHAPTER EIGHT

APPLICATION TWO

THE RELATIONSHIP BETWEEN MYOCARDIAL FUNCTION AND SEVERITY OF CAD IN PATIENTS RECEIVING CORONARY ARTERIOGRAPHY OR P.T.C.A.

8.1 Introduction

Whole body exercise performance is ultimately governed by quality of myocardial function, which in turn is dependant upon resistance to myocardial blood flow. Whilst the previous chapter demonstrated the usefulness of using QAMS in investigating exercise tolerance, this chapter focuses on its application in evaluating the extent of myocardial function. In doing so, various indices of left ventricular performance (quantified using a non-invasive radioisotope test) at rest and exercise are related to, and tested against stenotic morphology, both in a sample of patients undergoing routine arteriography for disease management assessment and in a smaller group of patients receiving PTCA.

8.2 Literature Review

As discussed in section 6.2.3, there are two radioisotope techniques available for studying myocardial function, those of first pass radionuclide angiography (1st RNA) and multiple gated acquisition radionuclide angiography (MUGA RNA). Perfusion techniques, eg. Thallium imaging, do not provide quantitative information regarding ventricular performance, rather, they pictorially reflect the physiological consequences of the anatomical disease. For this reason, this review concentrates on the two former quantitative methods.

Ejection fraction (EF - section 6.3) has long been utilized by many workers as an index of myocardial performance. The advent of radiopharmaceuticals and radiation counting

devices assisted by computers (section 6.3) which have the capability to measure rate of radiation emission from user specified areas in captured images, has continued this tradition. Berger et al 1979 using 1st RNA (section 6.3.2) demonstrated increased EF (67% to 82%) in 13 normals and decrease or failure to change in 44 of 60 patients with CAD when subjected to vigorous cycle ergometery. Using the same test and type of exercise, Upton et al 1980 demonstrated decreased or a failure to increase EF by more than 5% in 18 of 25 patients with angiographically demonstrated CAD **prior** to onset of anginal symptoms or electrocardiographic evidence of myocardial ischaemia. Abnormal EF response was presented in all patients on manifestation of ST segment depression. He concludes that 1st RNA provides an early sensitive technique by which patients suspected of having CAD may be tested. A much larger study was conducted by Gibbons et al 1982. He evaluated EF response to upright cycle exercise using 1st RNA in 281 patients with chest pain, significant CAD and normal resting ventricular function. EF response to exercise varied widely (range -36% to +26%). Changes were related to 28 clinical catheterization (including visually assessed percent diameter stenosis) and 1st RNA variables. Several of the variables, not related to extent of the disease (eg. resting pulse pressure) were significant independent predictors of changes in EF. Interestingly, percent diameter stenosis was **not** amongst any of the significant variables, although number of diseased vessels was. However, Gibbons observations indicated that change in EF is a complex response influenced by many pathophysiological variables, not necessarily directly linked with disease state and as such is perhaps not the best indicator of extent of CAD. Changes in MUGA RNA EF on treadmill exercise with simultaneously measured $\dot{V}O_2$ up to $\dot{V}O_2max$ was undertaken in a group of asymptomatic patients by Ehsani et al 1984. In those patients with an abnormal (lower than rest) peak exercise EF (51% rest to 47% on exercise), $\dot{V}O_2max$ was 21 +/- 4ml $kg^{-1}min^{-1}$ compared with patients in whom EF response was normal (55% to 60%) where $\dot{V}O_2max$ was 27 +/- 4ml $kg^{-1}min^{-1}$.

Seemingly, impaired LV function can limit ability to perform exercise (as measured by $\dot{V}O_2max$) even in patients not limited by angina. Angiographic extent (number of vessels) of CAD was compared to EF response on exercise using 1st RNA in a group of patients exhibiting LV dysfunction at rest by Higginbotham et al 1984. Exercise induced decreases of 5% or greater were highly prevalent in those patients with multivessel CAD who were later to demonstrate high mortality rate during long term follow up on medical therapy. The test may therefore be useful in highlighting prognostic outcome in patient exhibiting severe CAD if course of therapy is monitored.

A reversal in exercise induced EF response in patients receiving PTCA has often been reported in the literature. Sigwart et al 1982 using 1st RNA demonstrated a decrease from 66% to 46% on exercise pre PTCA which was reversed to an increase from 64% to 69% 6 months post PTCA in 7 patients. No quantitative data on disease severity is reported. De Puey et al 1983 demonstrated changes in percent diameter stenosis of 90 +/- 9% to 12 +/- 9% from traced caliper measurements following PTCA in 44 patients. This was associated with an increase in peak exercise EF (MUGA RNA) from 61% pre PTCA to 66% post PTCA. Whilst this change is very significant ($p<0.001$), pre PTCA LV function was still adequate on exercise (rest 58%) demonstrating selectivity of PTCA patients. On follow up angiography in 19 patients, 6 had restenosed, 4 of whom demonstrated abnormal EF response (failure to increase by 5%). De Puey concludes by stating that MUGA RNA is useful in documenting changes in functional reserve in patients receiving PTCA. Unfortunately, no quantitative relationships are drawn between stenotic severity and EF. This is also true of the study by Kent et al 1982 in which MUGA RNA EF was improved from 51% pre PTCA to 62% post PTCA, associated with change in percent diameter stenosis from 74% to 31%. Using atrial pacing, changes in regional EF resulting from PTCA (5 segments in LAO position) were investigated by Weiss et al 1984. PTCA affected a reduction in percent diameter

stenosis from 90% to 31%. This was associated with a change in involved (ie. supplied by artery receiving PTCA) segment regional EF from a decrease of 36% pre PTCA to no change following PTCA at the same heart rate. Again however, no exploration of the relationship between disease severity and ventricular function is made. Global and regional EF changes (3 segments, LAO position) were also improved following PTCA in the study by Lewis et al 1985. With PTCA reducing percent diameter stenosis from 70% to 25%, MUGA RNA global EF was improved from 59% to 67% on peak exercise. Changes in regional EF were most apparent in the septal region (59% to 79%) with moderate increases in the apical segment (50% to 61%). The ability of MUGA RNA to detect degree of restenosis following PTCA was investigated by De Puey et al 1984. Patients receiving late follow up arteriography after successful PTCA were categorized as less than 20% restenosis, more than 20%, but less than 50% and more than 50%. All arteriographic measurements were made with calipers from tracings. MUGA RNA correctly predicted presence of greater than 50% restenosis in 77% of patients. In the above centre, like the Groby Road Hospital where routine recatheterization is not undertaken, MUGA RNA may be useful in predicting the long term outcome of PTCA, allowing more careful management of patients with an unsuccessful long term result.

Whilst EF is routinely used to indicate myocardial performance in many centres, it computation is sensitive to methodology. Slutsky et al 1980 investigated the correlation between EF on angiography and MUGA RNA EF using various differing methodologies. Correlation was highest with a user defined LV area of interest (AOI) in conjunction with a computer assigned background region beyond the lower left quadrant of the ventricle, or a manually drawn ring around the end diastolic image. However the latter method increased inter and intraobserver variability. Using a fixed AOI and computer generated background decreased variability but was not always associated with the best correlation with angiography. Sorenson et al 1981 employed

fixed AOI (end diastolic image only) and variable AOI (end diastolic and end systolic images) to measure exercise MUGA RNA EF in 8 normal subjects. Abnormal (failure to increase by 5%) EF response was noted in 5 of the 8 subjects using the fixed method, and zero using the variable method. Therefore, false abnormal EF responses to exercise MUGA RNA may occur due to method of region of interest selection even in subjects whose ventricular function is normal.

Wall motion analysis, which highlights disordered ventricular relaxation and contraction (section 6.3) resulting from myocardial ischaemia was employed by Berger et al 1979. New or exaggerated regional wall motion abnormalities (RWMA) were detected in 28 of 60 patients in the 10 degree RAO view using 1st RNA with cycle ergometry. Interobserver variability in assessing RWMA on exercise is low (80% complete agreement in 3 observers) and compares well with contrast ventriculography (78% complete agreement - Brady et al 1980a). Indeed, RWMAs often precede the more classic indicants of ischaemia (angina, ST changes) when performing work (Upton et al 1980). MUGA RNA has previously been proven to be of equivalent sensitivity to the more expensive and invasive method of intravenous digital ventriculography in detecting RWMAs on exercise, where atrial pacing was used to increase heart rate (Wasserman et al 1984). However, because of technical factors, the investigating views used by the two techniques are not equivalent leading to differences in the location of the RWMAs. Perhaps 1st RNA would have been the better technique to use for comparison.

Amelioration of RWMAs following PTCA has been demonstrated by Kent et al 1982 in which 94% of patients exhibited at least one RWMA pre PTCA, being reduced to just 8% following successful PTCA.

MUGA RNA allows evaluation of regional ventricular abnormalities without the involvement of wall motion assessment by the production of parametric images (section

6.2.3). Mathematical analysis of time - activity curves from individual pixels in the image reveal phasic fluctuations in differing cardiac chambers. This so called phase image, can not only distinguish atria from ventricles but also, within the ventricles (most often the left), regions with delayed or paradoxical emptying may be defined. Phase imaging was employed in 70 patients with suspected CAD by Walton et al 1981, and the results compared to findings at catheterization. Regions of abnormally high phase (late emptying) were detected in 42 of 61 patients with CAD. These results were often associated with total occlusion of a coronary artery, low EF and extensive RWMAs. Quantification of the phase image by calculating mean and standard deviation of phase value was reported on by Ratib et al 1982. By comparing with normals, he detected an abnormal phase response (mean greater than two standard deviations above normal mean) in 95% of patients during exercise while only 86% had abnormal EF and/or RWMA. Phase analysis was also employed in a group of patients with valvular disease where abnormal EF and RWMAs are common. Phase was abnormal in only 18% of patients despite RWMAs in 45% and abnormal EF response in all. Therefore quantitative phase imaging is a highly sensitive and specific indicator of regional myocardial ischaemia and is therefore specific to CAD unlike EF and RWMA. Quantification of the phase image was taken a step further by Gerber et al 1983 who not only computed SD but skewness also. In healthy subjects, SD was low reflecting ventricular synchrony and skew slightly negative. Exercise changed this profile little. In patients with CAD, resting phase profile showed larger SD and positive skewness reflecting ventricular asynchrony. On exercise, SD was further increased (16.5 degrees to 27.4 degrees) as was skewness (0.35 to 0.75), demonstrating increased asynchrony and tardokinesis. Phase SD has been shown to be improved by administration of nitrates in patients exhibiting angina at rest (Marzullo et al 1984). Phase SD was changed from 14.5 degrees with no symptoms to 22.8 degrees during the ischaemic episode. Intravenous

injection of isosorbide dinitrate returned phase SD to the control level (14.2 degrees).

Changes in rate of fall and rise of ventricular pressure have often been reported as a sensitive indicator of myocardial dysfunction both in the animal model (Weisfeldt et al 1978, Kay et al 1979) and in the human (Tebbe et al 1980 - section 6.2.2). Whilst pressure is not measurable using MUGA RNA, volume or more correctly, count rate being proportional to volume, is. Boyles law states that pressure is inversely proportional to volume, therefore, using MUGA RNA, it is possible to examine myocardial function by computing the rate of change of counts within a LV AOI. Results may then be corrected for end diastolic counts allowing expression of rate of change of volume with time (in units of end diastolic volumes).

Evidence was presented in section 6.2.2 that ischaemia tends to alter the dynamics of diastole prior to its effects on systolic function. This fact was confirmed by Hirakawa et al 1977 who demonstrated that diastolic rate of volume change (+dv/dt) was the most sensitive indicator in separating ischaemic patients from normals and hypertensives. Poliner et al 1984 compared normals and patients with CAD on exercise using MUGA RNA. Both groups exhibited the same peak diastolic filling rate (measured in the first half of diastole, as atrial systole which occurs late in diastole can increase filling rate dramatically, and is unrelated to disease state - Benchimol et al 1969) at rest (2.3 end diastolic volume (EDVs) per second). This parameter was increased on exercise in the normals to 3.1 EDV sec^{-1} and decreased in the CAD patients to 1.7 EDV sec^{-1}. Peak systolic ejection rate (PER) was not significantly affected in the normals but fell in the patients from 2.5 EDV sec^{-1} to 1.9 EDV sec^{-1}. However, sensitivity of changes in chamber volumes were markedly different; for PER 67%, and for PFR 98%. Interestingly, PFR exercise/rest ratio was always greater than 1 for

patients with normal arteries (and normals) and 1 or less in patients with significantly disease.

Impaired LV diastolic filling appears to be reversed following successful PTCA. Bonow et al 1982 described a group of patients in which LV diastolic filling at rest was improved from 2.3 EDV sec^{-1} to 2.8 EDV sec^{-1} concordant with a change in percent diameter stenosis (calipers) from 76% to 30%. Similar results were reported in another paper by Bonow 1985 where LV diastolic filling was improved from 2.5 EDV sec^{-1} to 3.0 EDV sec^{-1}. This was associated with improved intersection (20 sectors) phase differences from 6.0 degrees to 5.1 degrees reflecting more homogenous resting diastolic function. PFR at rest was unchanged (2.4 EDV sec^{-1} to 2.5 EDV sec^{-1}) by PTCA in the study by Lewis et al 1985. During exercise however, PFR was improved from 2.1 EDV sec^{-1} to 2.5 EDV sec^{-1} highlighting the beneficial effects of PTCA in improving diastolic function on exercise.

Differences in time (in comparison to normal) to various events in the cardiac cycle may also highlight disordered cardiac function. Time to PER occurred significantly later in systole in a group of patients with CAD in comparison to normals (Slutsky et al 1983). Arterial occlusion in dogs significantly delayed time to minimum count in the region of LV supplied by that artery reflecting inability of the ventricle to relax (section 6.2.2 - Green et al 1984).

It is evident from this literature review, that, as with the previous chapter, no work has yet related extent of myocardial dysfunction to severity of coronary disease. However, parameters which may demonstrate a relationship have been presented.

Remembering that coronary collateral supply is not quantified by QAMS (greater than 75% diameter stenosis coincided with the development of coronary collaterals in dogs - Tomoike et al 1983) it would still seem logical that

the extent of CAD may relate to the hearts ability to perform normally. It is along this aspect that the experiments presented in this chapter were conducted. Changes in myocardial function and disease state are also investigated in a small group of patients receiving PTCA.

8.3 **Method**

8.3.1 Patient Selection

Over the period 8th August 1984 to 9th January 1986 45 patients were subjected to an exercise radioisotope test (section 8.3.3a) at a rate of one per week. Due to excessive patient and/or heart movement (see later), poor count statistics (particularly of the exercise images), large R-R interval variability (see later) or insufficient level of exercise, the final group consisted of just 28 patients. All were to receive coronary arteriography the following day, the majority (68%) either for assessment for suitability for PTCA or for PTCA itself. All patients had a recent exercise test. Following successful PTCA of the LAD artery (mean 28.8+/-9.3 weeks) exercise MUGA RNA was repeated in 5 patients the day prior to follow up arteriography. Current medication was preserved in all patients.

Group details:

Group 1. N = 23, 21 male, 2 female. Mean age 53.7+/-8.6 years.

Group 2. N = 5, 4 male, 1 female. Mean age 52.8+/-6.8 years.

8.3.2 Quantification of Arteriograms

For each patient, the following days arteriograms were quantified using QAMS in the manner described in appendix 1. For each diseased artery, efforts were made to obtain data

from at least two orthogonal views, however, this was not always possible for reasons discussed in section 7.3.2. Blocked arteries were awarded a figure of 100% for percent diameter stenosis. Obviously, no other quantifiable data are obtainable in such cases.

Stenotic morphology data were then averaged for each affected artery as described previously. For the analysis of global function, percent diameter stenosis in the 3 supplying arteries was weighted according to the average blood flow carried in each thus:

LAD 47% weighting
RCA 33% weighting
Cx 20% weighting

These figures are those quoted for right dominant coronary circulation (Brandt et al 1977).

Group details:

Group 1. 15 patients with single vessel disease (11 LAD, 4 RCA), 4 with double vessel disease (2 LAD/RCA, 2 LAD/Cx) and 4 with triple vessel disease.

Group 2. All patients had right dominant coronary circulation with single vessel disease of the LAD artery.

8.3.3 Quantification of Myocardial Function

Coronary arteriography indicates areas of potential ischaemia by defining anatomical lesions in the coronary arteries. Myocardial perfusion (eg. ^{201}Tl imaging) complements this by providing information about coronary blood flow. Neither of these methods however, permits assessment of the consequences of coronary disease on myocardial function. Contrast ventriculography could be used, but is most often performed at rest. Thus, patients

with CAD often exhibit (apparently) normal regional and global LV function at rest when investigated by this method. Therefore, there exists a need for a method which is non invasive, safe and repeatable which permits global and regional LV function to be assessed during stress.

8.3.3a Development of a New Radioisotope Test Exercise Protocol

RNA allows investigation of myocardial function (section 6.2.3). Whilst 1st RNA allows any chamber view to be used (no overlap due to bolus injection) timing of the injection to coincide with symptoms is critical. Also, count rate for adults using this technique is very high, thus scintillation counter deadtime may become a problem. Therefore MUGA RNA was chosen as the technique around which the act of exercise whilst imaging was to be introduced.

On beginning this work, exercise MUGA RNA was not practiced at the radioisotope imaging unit, Groby Road Hospital. At some time previously, however, it had been, with supine ergometry being used as the mode of exercise. However this was soon abandoned as patient movement resulted in much deterioration of the acquired images.

Apart from treadmill testing, erect cycling would most closely match everyday exercise stress and has been proven to elicit VO_2max to within 5% of that evoked by treadmill testing (Astrand et al 1961), thereby proving its use as a good modality of exercise in terms of extent of fat free mass involved. Also, should erect exercise be used in preference to supine, cardiac haemodynamics (ie venous return) would more closely represent the normal situation. Therefore it was decided that erect cycling exercise would be adopted as the mode of stress to combine with MUGA RNA.

A cycle ergometer was borrowed from the Department of Human Sciences, Loughborough University. The ergometer was fitted with a magnetic mechanism which allowed the work rate to be

selected in the range zero to 450 Watts at various pedal revolution rates (prr - figure 8.1). Maximal efficiency has been proved to be evoked at a prr of 50 revs min^{-1} (Astrand and Rodahl 1977), however, this frequency was not supported on this model of ergometer, thus 60 revs min^{-1} was used instead. Prr was communicated to the patient by means of a digital display which could be mounted anywhere around the imaging equipment so as to always be in view (figure 8.2a).

A wooden base was constructed for the ergometer to rest upon (figure 8.2a). This was necessary in order that the ergometer could be brought close enough to the imaging equipment so that the patient was in contact (figure 8.2b). A velcro strip was used to strap the patient to the collimator face in order to minimize movement during exercise. Foam wedges positioned between the patients chest and the collimator allowed the correct view to be maintained during image acquisition (figure 8.2b).

As recent exercise test (treadmill) data were available, and therefore patient tolerance was well known, the exercise MUGA RNA protocol was designed to elicit symptoms in the shortest time possible. Therefore, the maximal work rate performed on the treadmill was calculated using Balkes equation (section 7.3.3) and work rate on the bicycle adjusted such that the maximal work rate would be elicited by 6 minutes of exercise. Each exercise stage was to be 3 minutes long, therefore the initial 6 minutes were to be at two lower but incrementally increasing work loads in order to give the patients cardiovascular system time to adapt to the exercise stress. Following this third stage (between minute 6 and minute 9), if no symptoms were evoked, work rate could be increased further. Patient heart rate (fh) and blood pressure (BP) were recorded at each stage using the Critikon exercise monitor (figure 8.3a), the microphone within the cuff (figure 8.3b) being placed over the brachial artery of the right arm. Occurrence of stress induced ECG abnormalities were monitored at the V6 position using Cardiac Recorders equipment (figure 8.4a). Upper electrodes

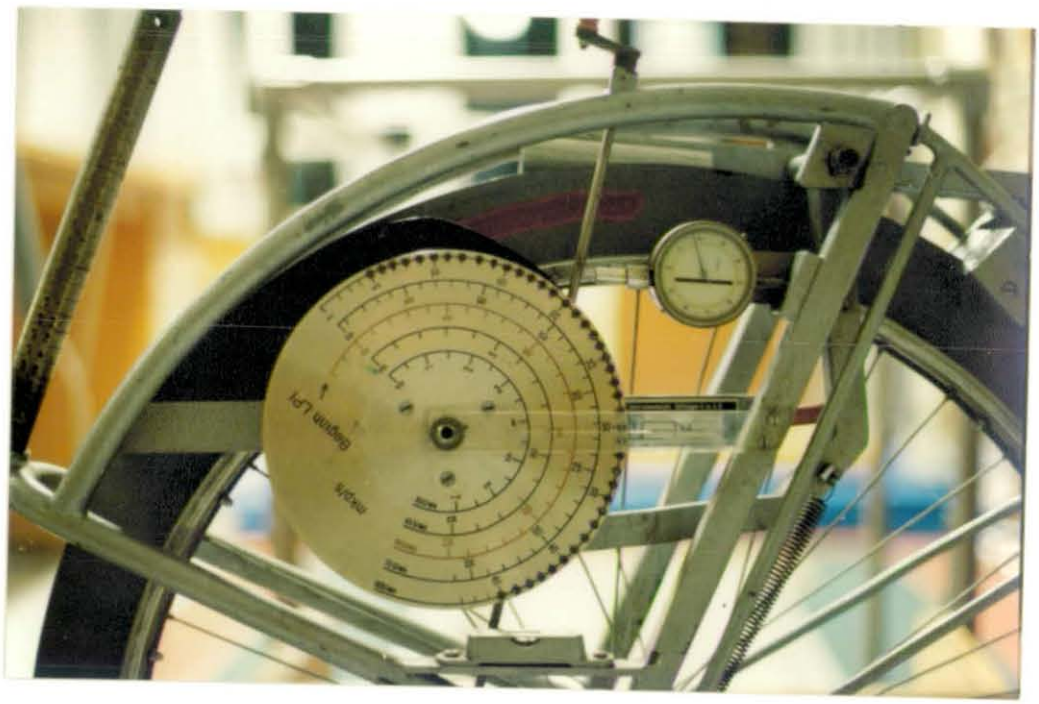

Figure 8.1 Work rate adjustment mechanism on cycle ergometer

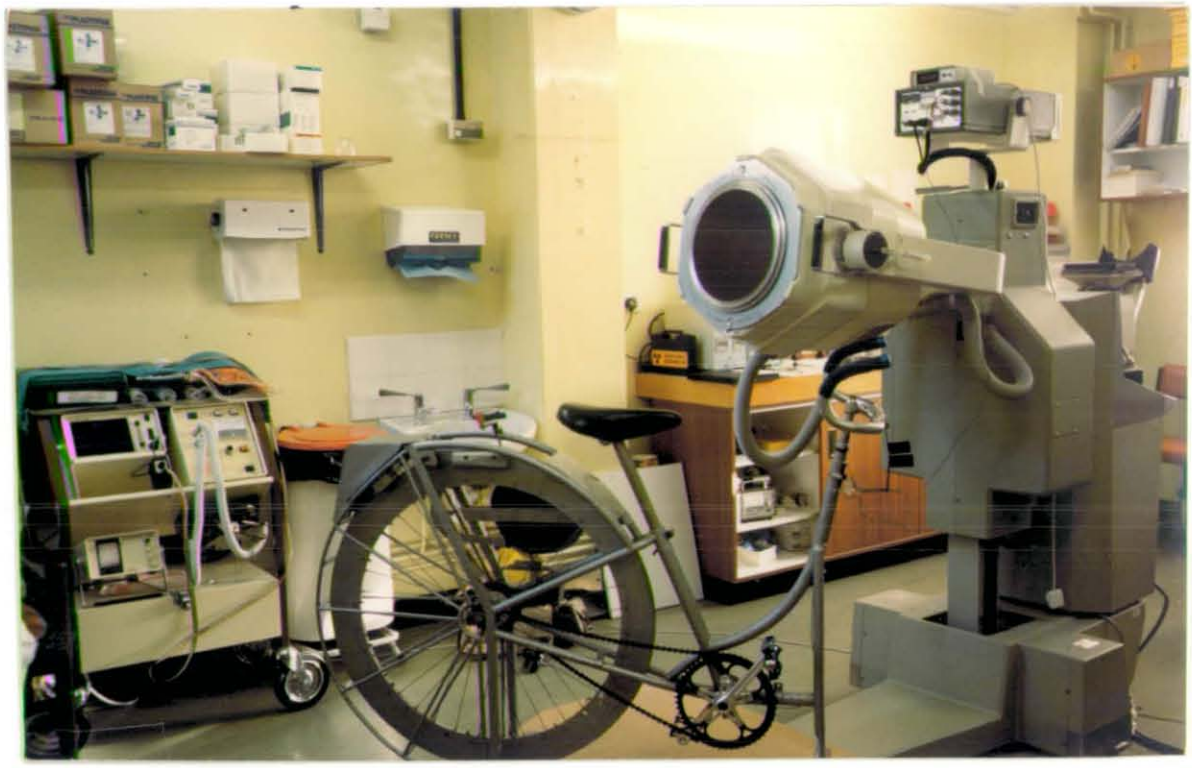

Figure 8.2a Equipment set up prior to MUGA RNA. Notice the defibrillator, bicycle ergometer, gamma camera and pedal revolution rate monitor (mounted on top of persistence monitor, top right hand corner)

Figure 8.2b MUGA RNA in progress. Notice use of velcro strip and wedges for patient positioning

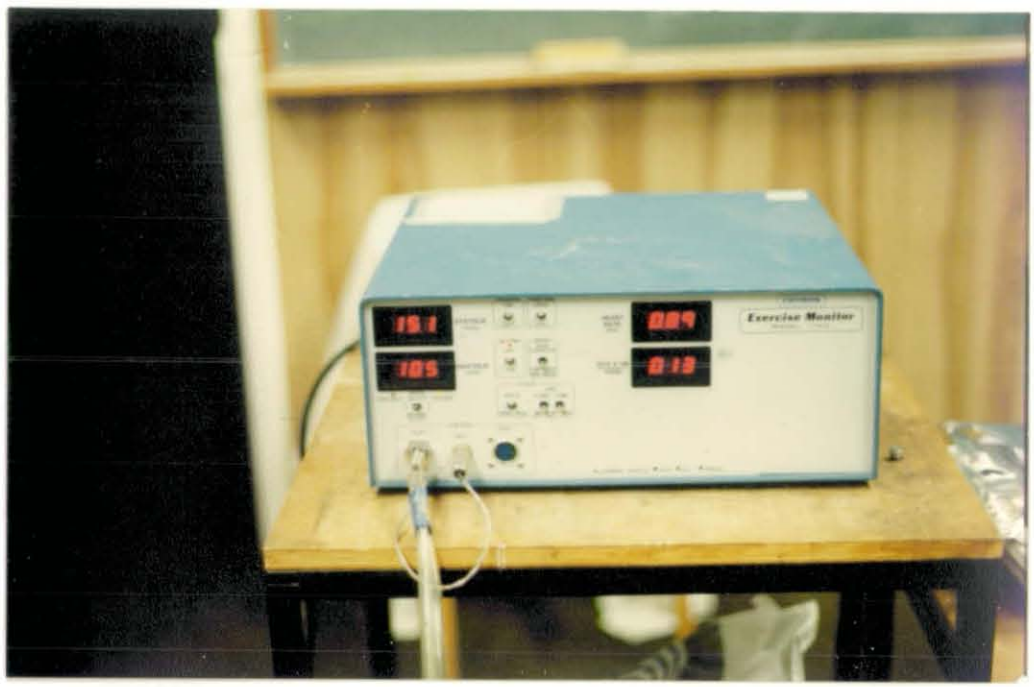

Figure 8.3a The Critikon exercise monitor

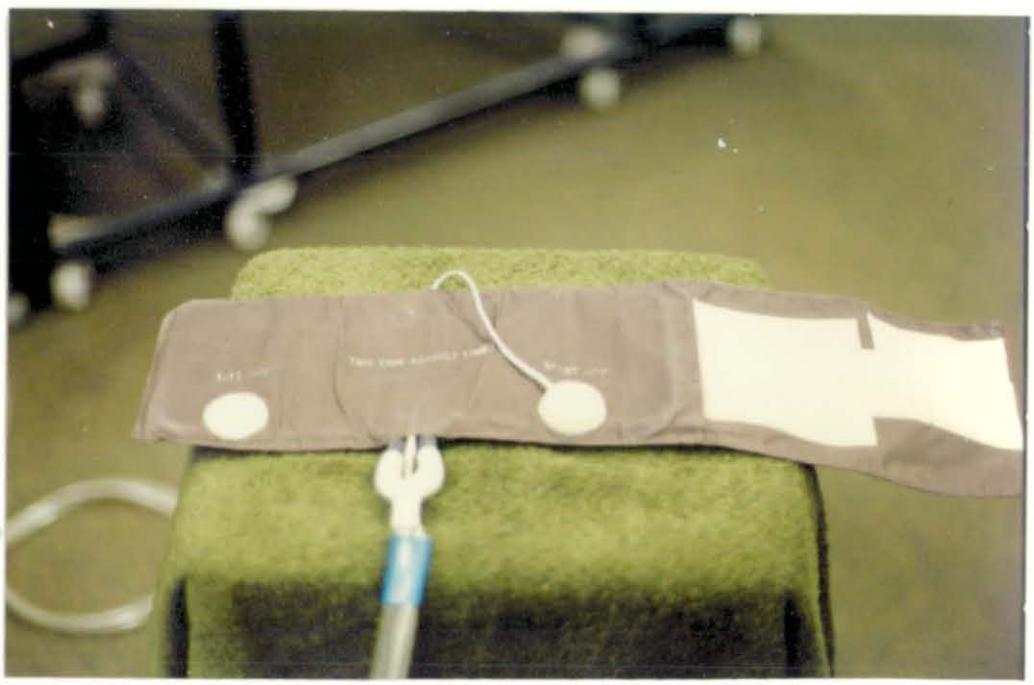

Figure 8.3b Blood pressure cuff with brachial artery microphone

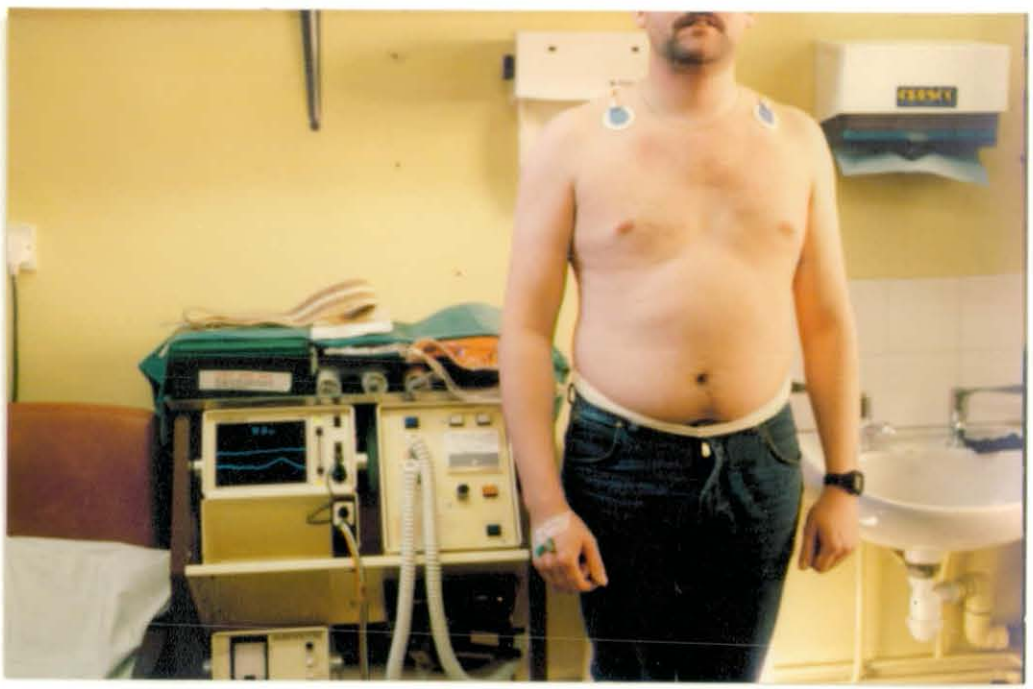

8.4a ECG electrode positioning, anterior view

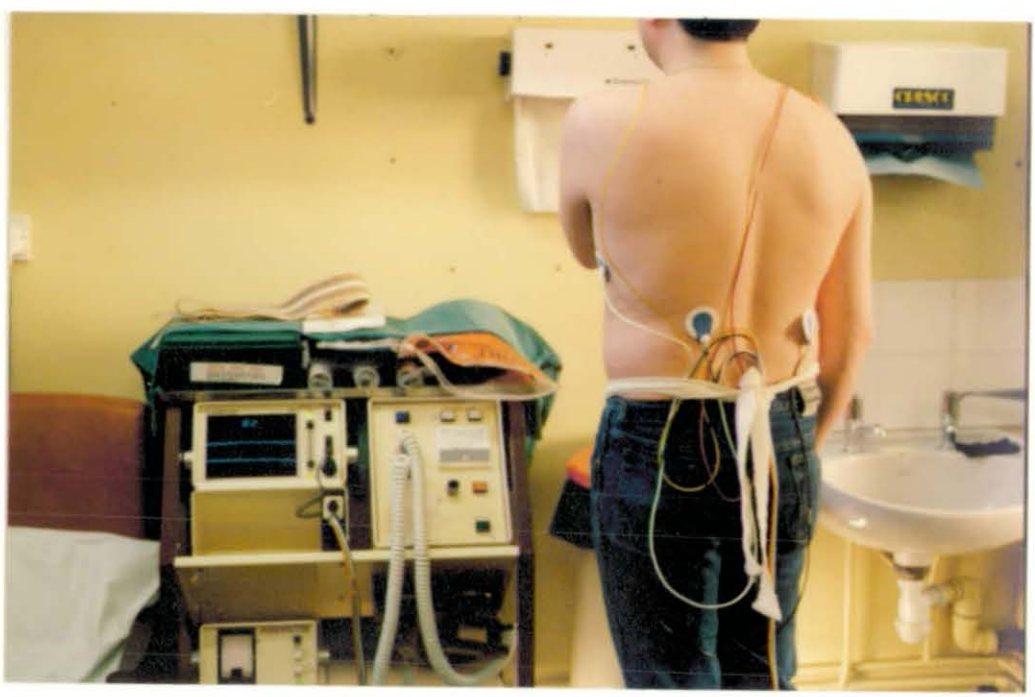

8.4b ECG electrode positioning, posterior view

were placed on the clavicles and the lower electrodes on the patients back in order to minimize muscular interference from the respiratory muscles (figures 8.4a and 8.4b). Exercise was terminated on fulfillment of the conditions presented in section 7.3.3. Much motivation of the patient was provided by the team in order to encourage achievement of an adequate level of exercise such that symptoms would be evoked (sensitivity 94% vs 62% in those patients who developed chest pain and/or ST changes and/or RPP greater than 250 x 10^3 - Brady et al 1980b).

8.3.3.b Exercise MUGA RNA Procedure

^{99m}Tc eluted that day as sodium pertechnetate from a ^{99}Molybdenum generator at the regional radiopharmacy, Leicester Royal Infirmary, Leicester is delivered to the radioisotope room each morning. The patient receiving the test, who has previously been selected and given verbal consent, is collected from the Ward and the test explained. A small venflon butterfly needle is then inserted into the dorsal venous network of the patients hand through which is administered 0.2mg/kg stannous pyrophosphate reconstituted with 5ml of bacteriostatic free 0.9% saline. This completes the first stage of the in vivo labelling of the red blood cells described by Pavel et al 1977. During the time between administration of the stannous ion and injection of the ^{99m}Tc (typically 20 minutes) the patients height and weight are recorded, ECG electrodes are positioned for recording in the 3 standard leads, the augmented leads and the V6 position and the computer (ADAC Ltd.) is prepared for the study.

The protocol used is that recommended in the IMAC handbook, reference No. DD 7605 A/A. Briefly, heart rate varying window widths are not selected as it is important to collect as much data as possible once the patient is exercising. The additional time take for frequent R-R interval calculation during acquisition would result in much loss of data, and is therefore overridden. However, as heart rate

in cardiac patients shows a slower response to reaching the steady state in comparison to normals, then significant variation in R-R interval may occur once acquisition has started. This was always checked by recording heart rate at 15 second intervals throughout the exercise period and checking its variability. R-R interval has inherent +/- 20% variability within the acquiring software; unacceptable variability (arbitrarily selected as +/- 10% original R-R interval) resulted in the test not being used in further analyses. The protocol was set for imaging of 90% of the cardiac cycle thus maximizing the number of counts per unit of examination time. Rollover protection (count saturation) is turned off as a stress study is too short for rollover to occur. This is necessary to remove interrupts in data collection which check for approaching rollover.

Following the 20 minute period within which the stannous - RBC complex has been formed and excess stannous pyrophosphate has cleared from the vascular pool, 20 milli curies (740 megaBq.) Of ^{99m}Tc (whole body dose 400 millirads) are injected intravenously via the venflon needle. An additional five minute delay allows up to 95% ^{99m}Tc labelling of the RBCs to occur (Pavel et al 1977). The patient is then connected to the ECG recorder which in turn provides R-R interval information to the computer.

Imaging of the patient requires positioning of their heart at the 30cm diameter gamma camera face (figure 8.2b). Gamma radiation is emitted from the intravascular tracer at an energy of 140 KeV as the ^{99m}Tc (half life 6 hours) decays to ^{99}Tc (half life $2.1x10^5$ years). A high sensitivity collimator (figure 8.2a) focuses the gamma radiation onto a Sodium Iodide (NaI) crystal converting the radiation into photons of visible light. The NaI crystal is in direct contact with 37 photomultiplier tubes arranged hexagonally allowing the light to be converted and amplified into spatial electrical pulses. An x,y coordinate system is then employed to process all signals from the photomultiplier tubes yielding the position of each gamma radiation event in

the NaI crystal. The summed output (energy) or brightness signal is input to the single channel analyzer (SCA) which functions as an electronic window, in this case tuned to 140KeV. This serves to remove events detected by the crystal resulting from Compton scattering which, if left unchecked, would result in blurring of the image.

Pulses accepted by the SCA are recorded and displayed in real time on the persistence monitor attached to the camera (figure 8.2a and 8.2b). The x,y coordinates are also transmitted to the computer via an analogue to digital converter where they are stored in a 64 x 64 matrix.

However, whilst each gamma emission is being processed, the hearts cyclic function is altering the temporal relationship between activity at various positions in the camera field of view. For this reason, the image is subdivided into 16 frames which are gated from the R wave (end diastole) supplied by the ECG monitor. Provided that heart rate is reasonably constant, several hundred cardiac cycles may then be acquired in this manner, such that each frame represents a sixteenth of 90% of a composite cardiac cycle. Such an image may then be displayed or analyzed allowing separate appreciation of systolic end diastolic function.

The patient is first imaged whilst standing at the gamma camera face in the 10 degree RAO position. This image is collected only for routine clinical assessment and is not considered further in this work. The patient is then asked to sit astride the cycle ergometer and then positioned close to the camera in a 45 degree LAO view with 10 degree cranial tilt (figure 8.2b). This view was chosen so as to give maximum separation between left and right ventricles whilst allowing the LV to be examined from a modified, "end on" position (figure 8.5). The usefulness of this view becomes apparent in the following section. Using the persistence monitor to check, minor modifications of this view were made in some cases to accommodate different patient anatomy. Once the position is set, foam wedges and the velcro strip

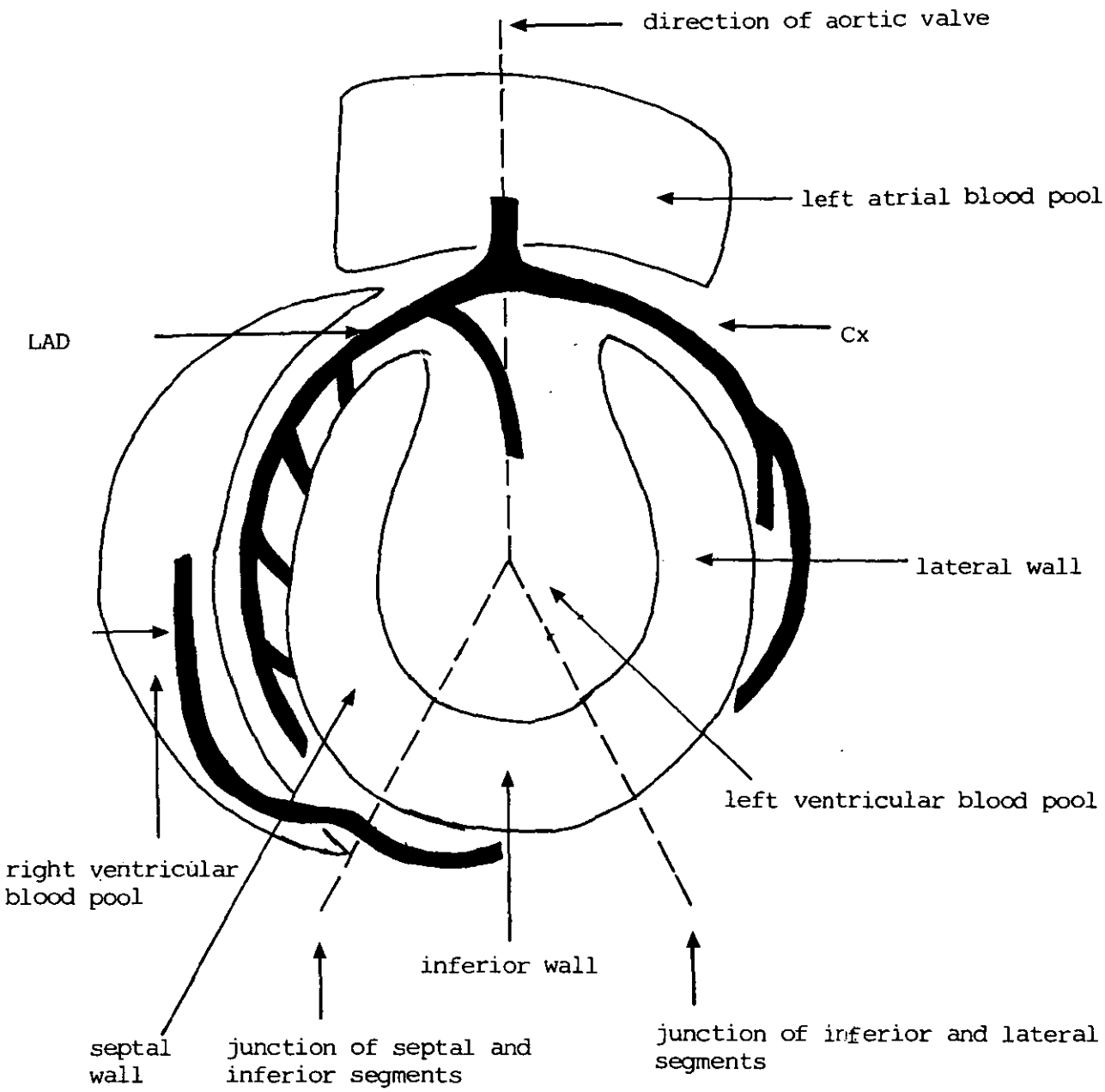

Figure 8.5 Left ventricular blood pool and superimposed segmental divisions in the 45 degree LAO 10 degree cranial tilt view

prevent the patient moving further (figure 8.2b). A rest image of 4 to 5 minutes duration was collected from this view.

Following this, the Critikon cuff was fitted to the patient and rest fh and BP recorded. The machine was then programmed to actuate at 3 minute intervals one minute out of phase with the exercise, such that fh and BP were recorded during the second minute. Initial work load was set and one minute allowed to elapse for the phase difference to become established.

The supervising team consisted of a Doctor, computer operator, coordinator/timekeeper (MJ), technician and nurse. The Doctor was responsible for patient well-being whilst the technician provided encouragement to the patient. The nurse monitored the ECG. On commencing the exercise, the patient was encouraged to reach the 60 revs min^{-1} prr required for the set work rate as quickly as possible in order to establish a steady physiological state. A one minute period was allowed in order for this to be achieved before a fresh calculation of R-R interval was made (pressing 'do not store' key) and the acquisition began in earnest. Acquisition is continued for the following two minutes within which fh and BP are measured. At the end of the 2 minutes the study is accepted and normalized prior to commencement of the next level of the exercise or termination of the test. In this way, should a patient be genuinely unable to complete a stage, the previous complete stage is still available for analysis where symptoms may have been evident.

Following termination of the test, the patient rests in the acquisition position until recovered enough to dismount the cycle. Fh, BP and ST changes continue to be monitored until they have returned to base line. The Venflon is then removed and the patient escorted back to the Ward.

8.3.3c Image Processing and Quantification

The raw rest and exercise MUGA RNA images are firstly processed using resident software. This involves production of a complementary 13 frame smoothed and background subtracted (SB) study to the raw 16 frame study in addition to various parametric images, including a global amplitude and phase image. These images are used in the normal clinical assessment of the patient.

Quantification of a study (ie. rest or exercise, using the LAO modified view only) begins by displaying the SB images in cine loop format and outlining the LV diastolic and systolic AOIs directly onto the computers monitor using a chinagraph pencil. The SB images are chosen in preference to the raw images due to zero background activity interference. Once the outlines are judged to fit the AOIs adequately (figure 8.6), the ADAC systems' 2 AOI ejection fraction program is run. During this, the operator digitizes the two contours using a light pen and applies these AOIs to the raw data. In addition, the program constructs a horseshoe background AOI from two digitized points around the inferior surface of the LV. This serves to subtract from the EF calculation activity due to blood contained within structures above and below the LV (figure 8.6). The final result if expressed according to the following formula:

$$\text{Ejection Fraction (\%)} = \left[\frac{\text{End diastolic counts} - \text{End systolic counts}}{\text{End diastolic counts}}\right] \times 100$$

This method closely follows that of Green et al 1978.

As disease in any one coronary artery will tend to affect LV function in the region it supplies, a program was written which allowed the LV to be divided up into 3 anatomical regions which corresponded to the position of the 3 major coronary arteries, thus allowing individual regional

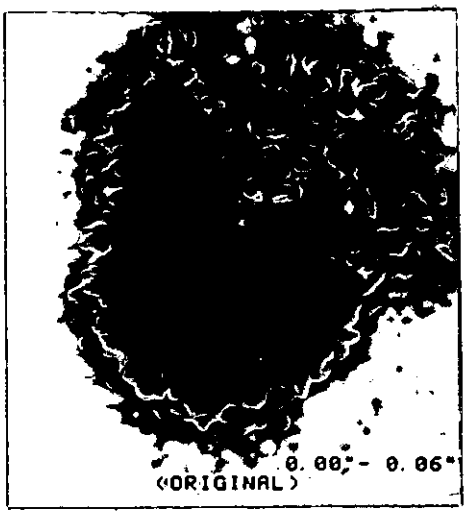

Original image

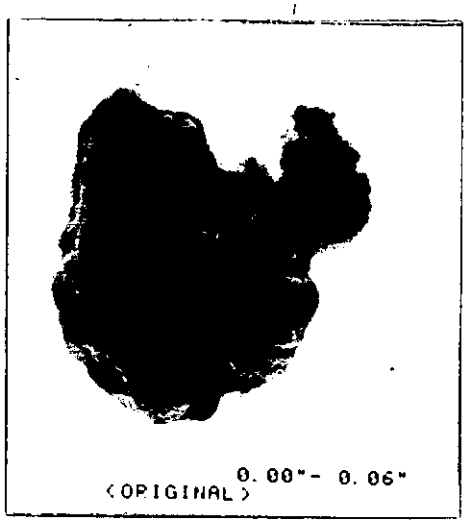

Smoothed and background subtracted image

Original image with end diastolic overlay

Original image with end systolic and background overlays

Figure 8.6 Calculation of two area of interest ejection fraction

analysis. PROGRAM MUGA (appendix 2), written in Fortran 66 requires that the user creates a new end diastolic overlay, to which is added the position of the aortic valve plane, the position of the inferior junction of the right and left ventricles, and the position where inferior wall becomes lateral wall (figure 8.7). The first two points are always well defined, with the third coming with experience. Employing the 45 degree LAO 10 degree cranial tilt view, the LV is essentially being viewed end on, allowing such anatomical separation (see later for discussion of atrial superimposition). In addition, a user rather than computer generated background area is drawn for later correction (figure 8.7). Other images, eg. phase and amplitude are also used at this stage such that the final outline is correctly positioned. Once complete, the overlays are written to a file containing the five named areas, ie. global, septal, inferior, lateral and background.

Phasic differences are then examined in each region by first subjecting the SB image data (fitted with new overlay) to Fourier analysis. This process fits (by least squares analysis) the volume curve in each pixel of the AOI (ie. global and segments) in question with the first harmonic of a cosine curve. This necessitates altering the curve's amplitude and angular phase in order to obtain the closest fit. As a matter of course, the program displays an amplitude image (reflecting stroke volume) a phase image (reflecting timing of contraction) and a phase histogram (reflecting number of pixels contracting a each instant ie. synchrony) for each region. The phase image is particularly useful as it serves as a check by which atrial superimposition can be excluded. Presence of very light or very dark pixels at the the top of the phase image (ie. global, septal, and lateral AOIs) confirm atrial superimposition, and the original outlines must be redrawn such that these are excluded. If left unchecked, resulting numeric data would not reflect **ventricular** activity. However, it must be stressed that phase differences may exist due to ventricular dysfunction, and it is important

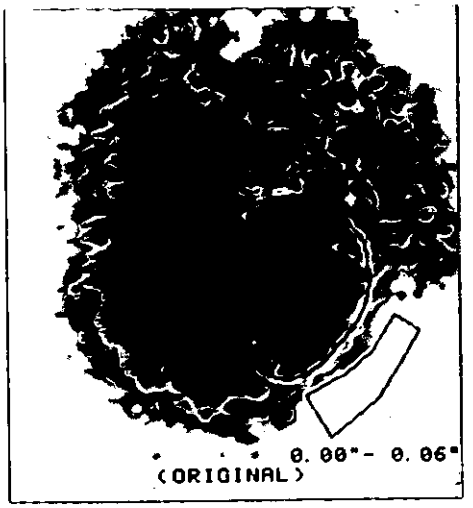

Original image

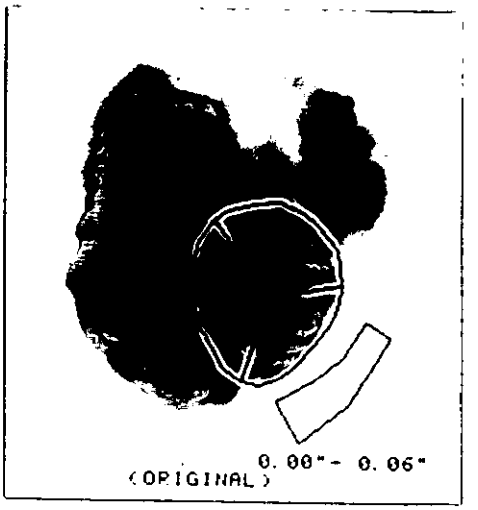

Smoothed and background subtracted image

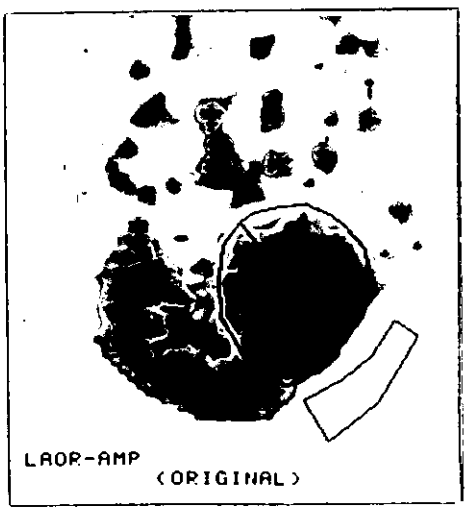

Amplitude image

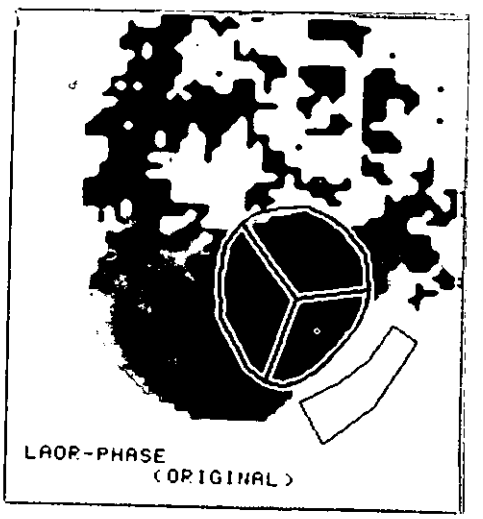

Phase image

Figure 8.7 Segmented end diastolic overlay (with user defined background) fitted to the original image, the smoothed and background subtracted image, the amplitude image and the phase image

that these areas be included. Experience and common sense usually make this distinction possible. The phase value of each pixel, together with the images are then written to disk.

PROGRAM MJHIST (appendix 2) then reads these data, and displays it as a phase histogram (figures 8.8a and 8.8b). The user then selects the range within which calculations are to be made. Normally this is the total data set, however, the range provision is made such that the odd one or two atrial pixels can be excluded from phase calculations without the need for redrawing the overlays. The program then proceeds to calculate mean phase, standard deviation and skew value (Kurtosis - Snedecor 1946) for that particular AOI. All other AOIs within the overlay are processed in the same manner.

Normal numeric data (count information) are then created from the raw data for each AOI in the overlay using the established ADAC software. The result is a time activity curve for each segment. This is then written to disk.

PROGRAM EFDVDT (appendix 2) reads this numeric data for the global and segmental areas. Patient age is included as input to be used by the program to calculate maximal obtainable heart rate. For each study (rest or exercise) heart rate achieved is then calculated from the frame time information. Counts and size of the background area are then computed and the raw data background subtracted according to its size. The normally produced SB data are **not** used for these analyses as the study is composed of 13 images only. The 16 frame time activity curve is then fitted by a cubic spline routine which results in the generation of a 100 point interpolated time activity curve with corresponding values of the first derivative (figures 8.9a and 8.9b). By using this interpolative method, it was hoped that the inadequacy in framing rate capabilities of the 16 frame system would be overcome, allowing investigation of LV ejection and filling rates. Normally,

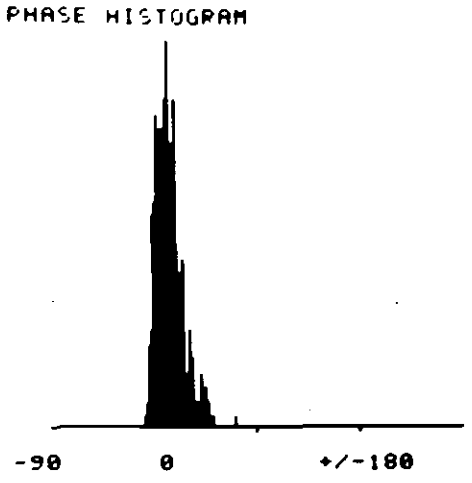

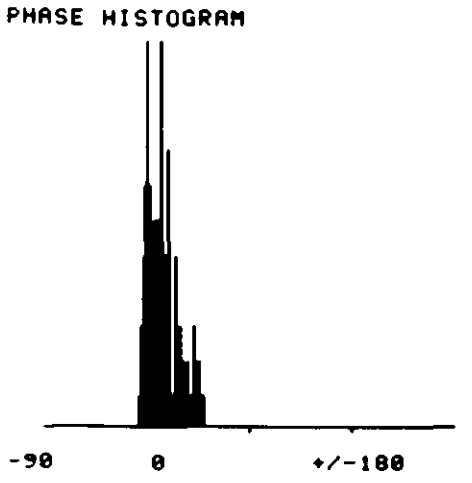

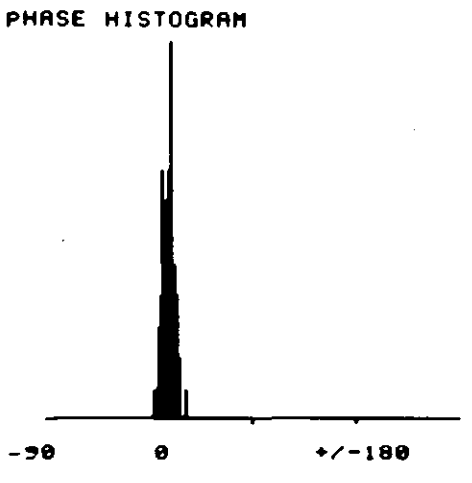

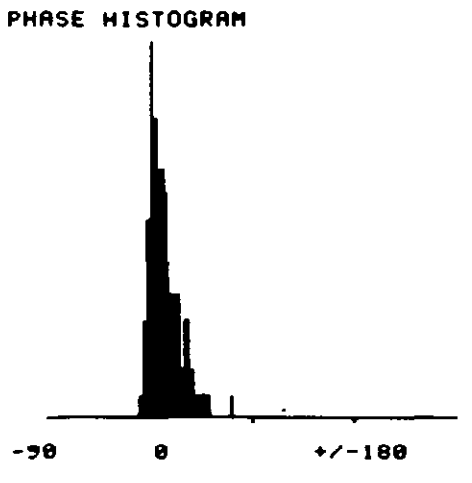

Figure 8.8a Resting global and segmental phase histograms

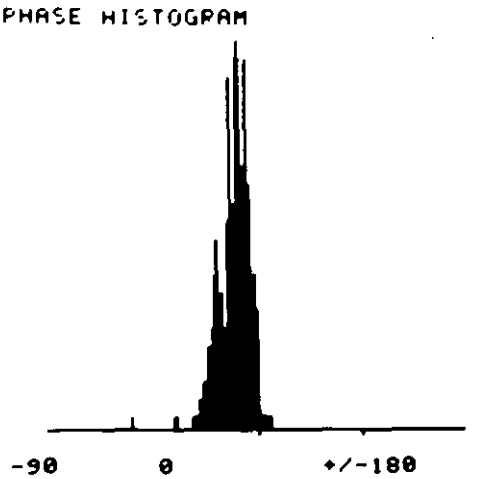

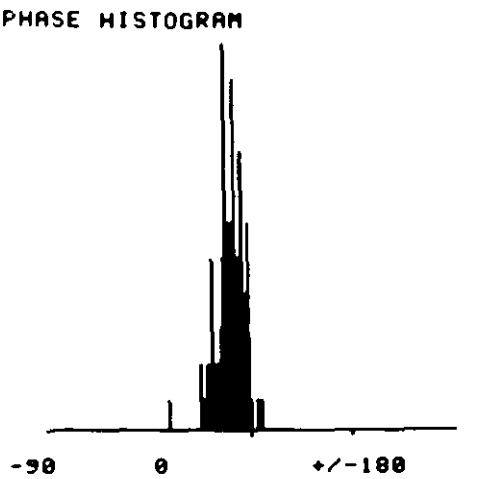

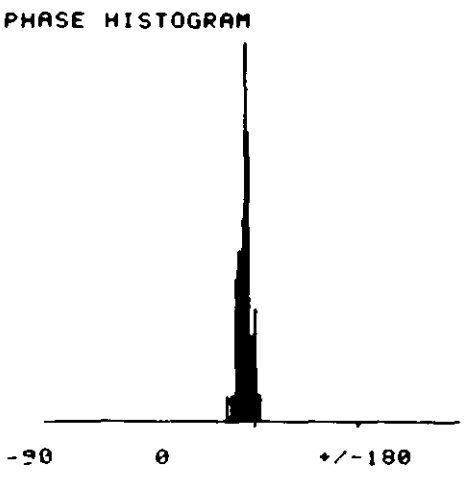

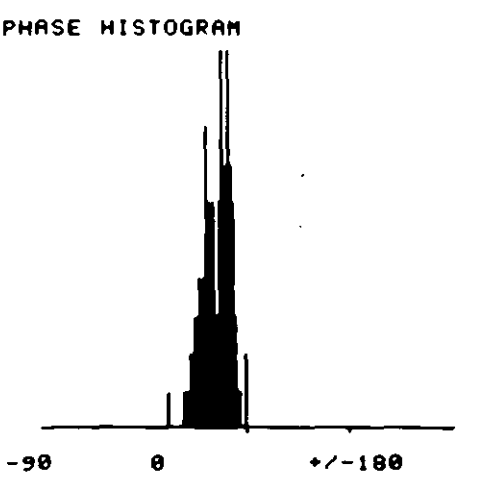

Figure 8.8b Exercise global and segmental phase histograms. Notice the change in mean phase, standard deviation of phase and histogram skewness

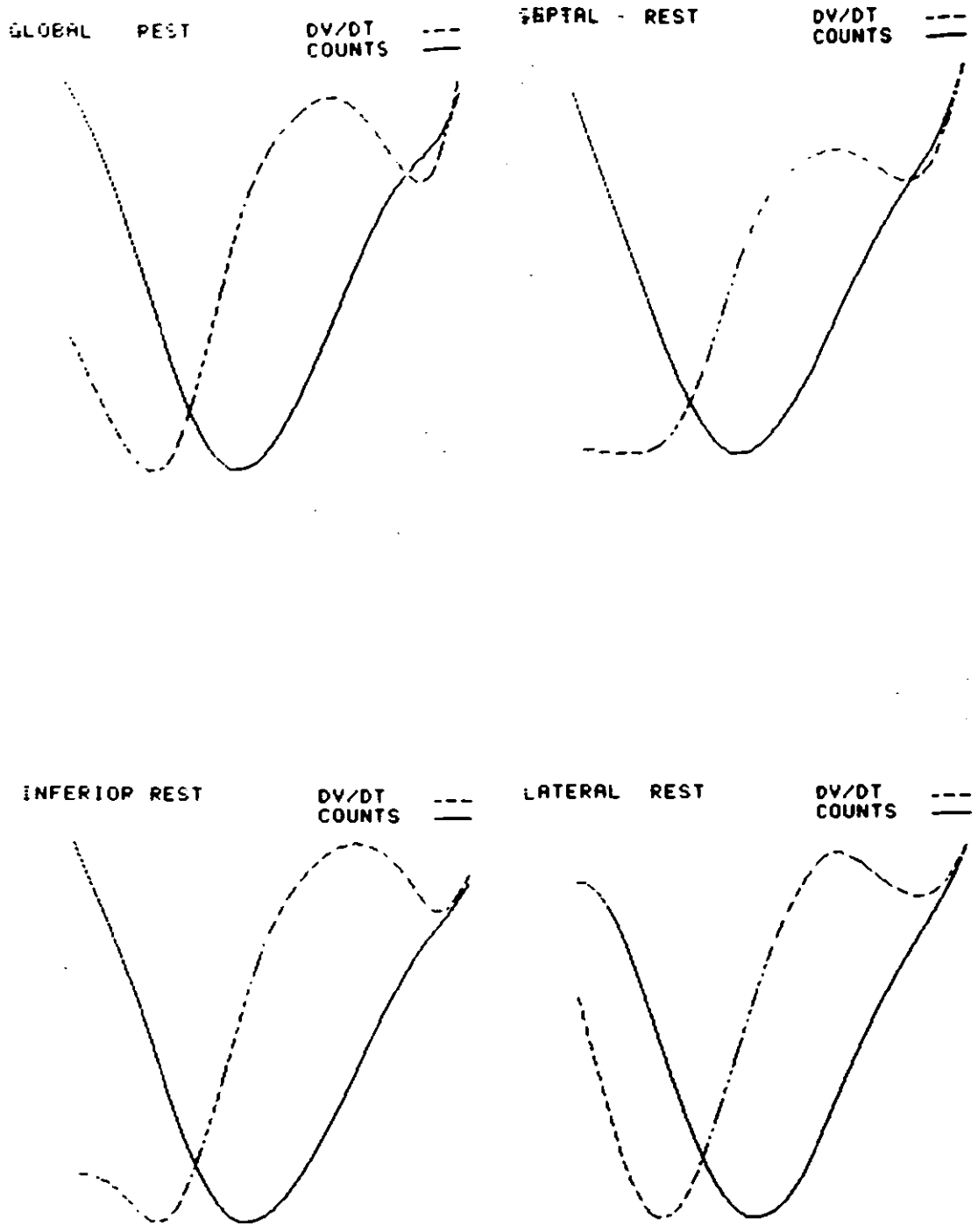

Figure 8.9a 100 point interpolated time-activity and first derivative curves for global area and segments at rest

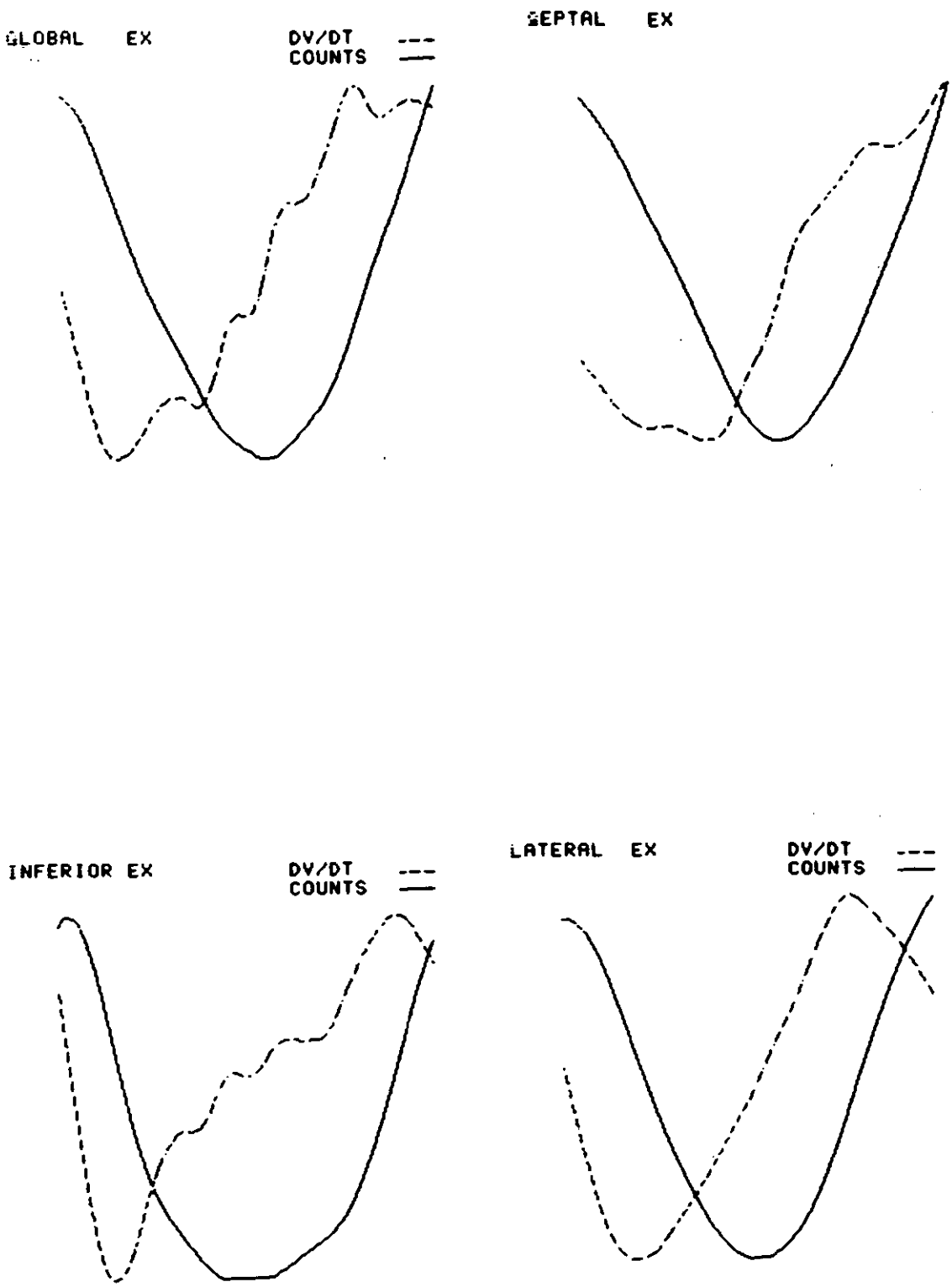

Figure 8.9b. 100 point interpolated time-activity and first derivative curves for global area and segments on exercise. Notice increased proportion of systole and reduced filling rate in the first half of diastole

frame lengths of 20 milliseconds are required for measurement of such parameters during exercise (Bacharach et al 1979) translating to heart rates of 160 beats per minute. In order to perform this interpolation, the routine must be provided with a value which reflects the variation in the count data due to normal statistical fluctuation and physiological variation on a beat to beat basis, ie. error introduced from variation other than the cyclic nature of the heart in each frame must be quantified.

Briefly, this figure is calculated from the mean count of the time activity curve according to the following formula:

$$\text{Smoothing factor (counts)} = 1.25 \times \left(\sqrt{\frac{\text{Mean count} \times 9750}{121.8 \times \text{Mean Count}}} \right)$$

Where: 1.25 = Coefficient of variation from static radioisotope emission.
9750 = Mean normalized count.
121.8 = Standard deviation of normalized count.

This formula was derived from an experiment involving collection of five 16 frame studies from a phantom filled with ^{99m}Tc, gated by a cardiac simulator. The figures above correct for statistical variation in count rate for non physiological data (ie. where mean is constant) whilst the form of the equation applies a correction for cyclic variation based on standard deviation of a proportion theory (Snedecor 1946).

From the 100 point time activity curve, the following parameters are then calculated:

Stroke Volume.

Ejection Fraction (essentially the 1 AOI method, Slutsky et al 1980).

Cardiac Output (Stroke volume x heart rate).

Peak ejection period (PEP - time from end diastole to maximum count in the first half of cardiac cycle).

Systolic time interval (STI - time from PEP to minimum counts).

Diastolic time interval (time from STI to PEP).

Peak ejection rate (PER - maximum first derivative value in STI).

Peak filling rate (PFR - maximum first derivative value in DTI).

Peak filling rate in 1st half of diastole (PFR/2 - maximum first derivative value in first half of diastole. Division of diastole made on calculation of ventricular fullness achieved by application of smoothing factor to latter frames of study).

Rate ratio 1 (PER/PFR).

Rate ratio 2 (PER/PFR2).

Time to PER (expressed as a percentage of R-R interval, ie. normalized).

Time to PFR (normalized for R-R interval).

Time to PFR/2 (normalized for R-R interval).

Time to PER (normalized for STI).

Time to PFR (normalized for DTI).

Time to PFR/2 (normalized for DTI).

In addition to the above, results for septal, inferior and lateral AOIs are normalized for global size. A hardcopy of

all of these results is obtained at the printer. The 100 point time activity curve with superimposed first derivative were plotted to the computer monitor for producing microdot copies if required (figure 8.9).

Obviously, as all calculations are ultimately derived from the global end diastolic AOI, this program relies on the LV contracting more or less concentrically around its centre of gravity. In order to check that this was indeed a valid assumption, PROGRAM MOVCEN (appendix 2) was written to quantify movements of the centre of gravity between the diastolic and systolic outlines. The program utilized the overlays submitted for 2 AOI EF calculation. Centres of gravity were calculated for each outline as the mean of the digitized points contained within. The shift between the two centroids was calculated relative to the end diastolic diameter. Direction of shift is returned as left, right up or down (figure 8.10). Centroids with much movement reflected a non concentric contraction, leading to potential errors in the EFDVDT program. Such tests were not considered in the final analysis.

The single image count information provided by existing software was used to examine regional contraction or stroke volume from the global and segmental amplitude images, achieved by fitting the amplitude image with the segmental overlays.

For the 5 PTCA patients, exercise MUGA RNA was performed again 28.8 weeks later. In order that everything except of course, myocardial function was kept constant, PROGRAM AOICOP (appendix 2) was written such that the segmental AOI applied to the pre PTCA exercise MUGA RNA could be reutilized post PTCA, thus keeping segmental spatial relationships intact (figure 8.11). The program allows that the overlay be translocated (as the LV is unlikely to be in the same position on the monitor screen post PTCA), rotated (some patient rotation may have taken place on the second exercise MUGA RNA, ie. the old overlay is located relative

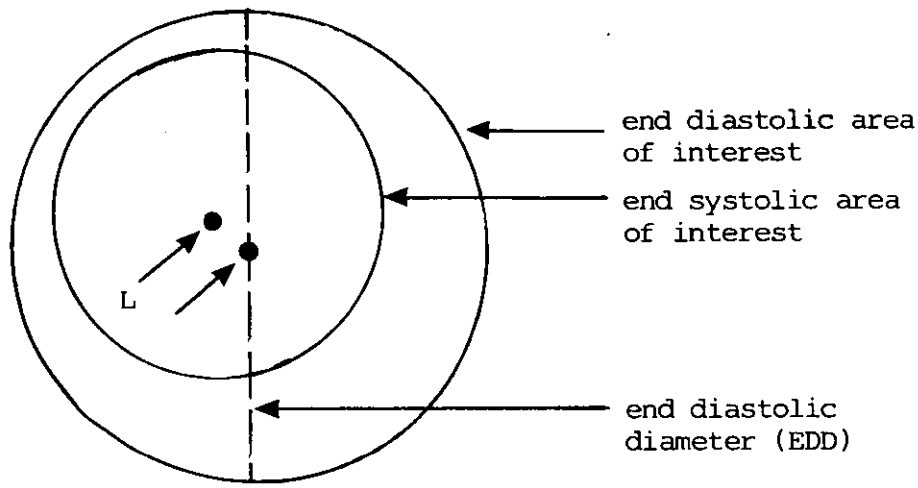

$$\text{Centroid movement (\%)} = \frac{L}{EDD} \times 100$$

Direction of movement is Up (example)

Direction of movement is left (example)

Figure 8.10 Principle of the program MOVCEN

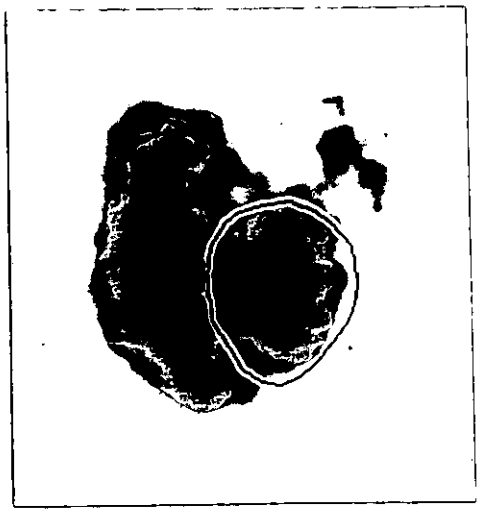

Fitted

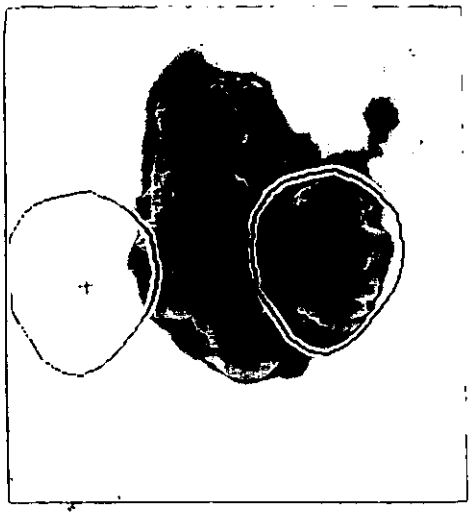

Translocated

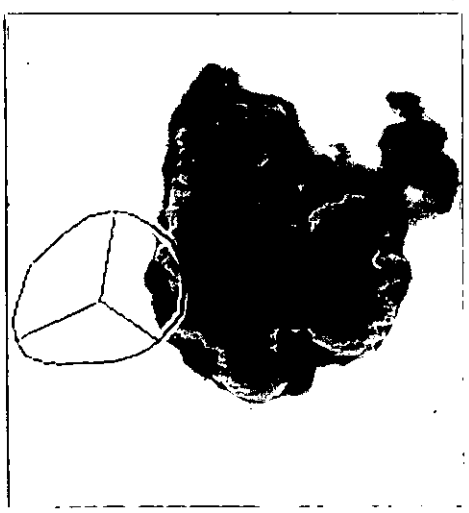

Rotated

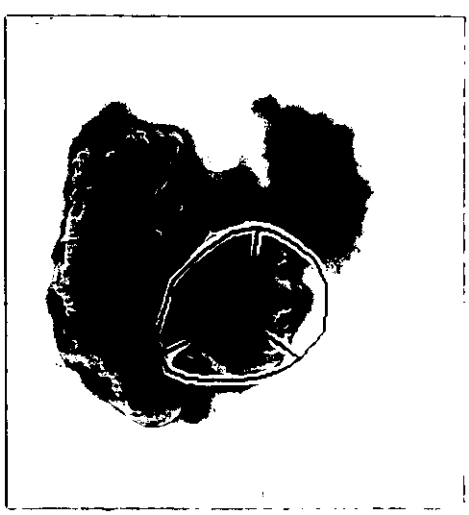

Superimposed

Figure 8.11 Use of the program AOICOP

to a new aortic valve plane position) and edited (as view angle may be slightly different), although efforts were made to reduce the latter. In practice, translocation and rotation were often required whilst editing was not. Application of the old overlay to the new test results ensured the myocardial function was the only true variable.

All above programs were run on rest and exercise MUGA RNA tests for all AOIs (global, septal, inferior and lateral) both before and after PTCA in the 5 patients mentioned.

8.3.4 Statistical Analyses

Investigations regarding evaluation of the relationship between myocardial function and stenotic morphology are best explored using linear regression analysis, with stenotic parameters being utilized as the dependent variable such that error introduced from predictions based on myocardial function may be examined. This technique will serve for investigating both global and segmental function, although for the former, only percent diameter stenosis is available as an indicant of stenotic severity (section 8.3.2).

For the 5 PTCA patients, two tailed related t tests will be performed on indices of myocardial function and stenotic anatomy between the pre PTCA and the post PTCA conditions for both rest and exercise.

8.4 **Results**

8.4.1 The Relationship Between Myocardial Function and Stenotic Morphology

Table 8.1 presents all significant results obtained when global myocardial function was regressed against a weighted value (proportional to average blood flow in each artery) of percent diameter stenosis. All t ratios are given a significance number as in the previous chapter which also serves the correlation coefficient.

Table 8.1 Regression analysis, global MUGA RNA vs weighted percent diameter stenosis

		t obs	SEE	r	N
	2AOIEF	-2.538[1]	18.96	-0.48	23
	SD Phase	2.615[1]	18.83	0.50	23
REST	SV/BSA	-2.254[1]	19.45	-0.44	23
	PERSTI%	2.992[2]	18.15	0.55	23
	2AOIEF	-2.997[2]	18.14	-0.55	23
	XPhase	-2.743[1]	18.60	-0.51	23
	Skew Phase	2.461[1]	19.10	0.47	23
	1AOIEF	-2.508[1]	19.02	-0.48	23
	STI	-2.082[1]	19.74	-0.41	23
EXERCISE	DTI	2.236[1]	19.48	0.44	23
	PER	2.236[1]	19.26	0.46	23
	PFR/2	-2.262[1]	19.44	-0.44	23
	time to PER/2	-3.278[3]	17.63	-0.58	23
	PFRDTI%	-2.446[1]	19.12	-0.47	23
	R-R interval	2.296[1]	19.38	0.45	23

Significance levels

1 $0.05 \leqslant p > 0.01$
2 $0.01 \leqslant p > 0.005$
3 $0.005 \leqslant p > 0.001$

Only four parameters from a possible 32 have a significant regression relationship with weighted percent diameter stenosis at rest. Levels of significance are low and SEEs approximately equal to those demonstrated in the previous chapter.

There is a greater frequency of significant relationships when exercise global myocardial function is regressed against weighted percent diameter stenosis. Correlation coefficients and t ratios remain low in all but one case, when time to PRF/2 is considered ($r = 0.58$). SEEs are generally akin to those experienced in the previous chapter. Means and standard deviations (SDs) of all parameters presented in table 8.1 are cited in table 8.2. Note the negative sign for PER signifies that blood is leaving the left ventricle.

When segmental myocardial function was regressed against percent diameter stenosis present in the artery supplying that segment, and the data considered collectively, there were **no** significant observations recorded (table 8.3). When each segment was considered separately, significant relationships occurred with little frequency and the significantly relating parameters differed between segments. Levels of significance are no higher than those tests considering global function, although t ratios, correlation coefficients and SEEs are higher and lower respectively, reflecting the smaller group size. Percent diameter stenosis in the three groups of septal, inferior and lateral segments are reasonably homogenous (table 8.4), ranging from 70.9% to 80.5%, although higher than those encountered with the PTCA patients of the previous chapter. These values reflect the inclusion of some patients with blocked (ie. 100% stenosis) arteries.

Parameters correlating significantly with percent diameter stenosis in the previous analysis were then regressed against other parameters of stenotic morphology (table 8.5). Amongst those parameters which correlated significantly,

Figure 8.2 Descriptive statistics, global MUGA RNA and weighted percent diameter stenosis

		Mean	Standard deviation
REST	2AOIEF(%)	62.0	8.14
	SD Phase (^{o})	16.31	6.16
	SV/BSA (counts/m^2)	3114.08	951.27
	PERSTI(%STI).	47.77	16.76
EXERCISE	2AOIEF(%)	63.74	9.54
	X Phase (^{o})	55.36	16.43
	Skew Phase	-0.99	0.74
	1AOIEF(%)	36.27	11.65
	STI(%R-R)	44.39	7.27
	DTI(%R-R)	49.14	6.79
	PER(EDV/sec)	-3.56	1.86
	PFR/2(EDV/sec)	3.47	2.03
	time to PFR/2(%R-R)	76.90	9.79
	PFRDTI(%DTI)	53.44	16.87
	R-R interval	0.5175	0.1206
	% diameter stenosis(%) (weighted)	45.01	21.18

Table 8.3 Regression analysis, segmental exercise MUGA RNA vs percent diameter stenosis

Pooled segmental data - no significant observations

		tobs	SEE	r	N
	SD Phase	2.126[1]	15.48	0.47	18
SEPTAL	lAOIEF	-2.651[1]	14.61	-0.55	18
	Amplitude	-3.033[2]	13.97	-0.60	18
INFERIOR	STI	-3.021[1]	13.99	-0.73	10
	DTI	3.947[3]	11.93	0.81	10
LATERAL	time to PFR	-2.792[1]	14.41	-0.75	8

Significance levels

1 $0.05 \leqslant p > 0.01$

2. $0.01 \leqslant p > 0.005$

3 $0.005 \leqslant p > 0.001$

Table 8.4 Descriptive statistics, segmental exercise MUGA RNA and percent diameter stenosis

		Mean	Standard deviation
	SD Phase (^{o})	28.67	16.31
SEPTAL	lAOIEF(%)	29.78	12.32
	Amplitude (count)	107.39	22.52
	% diameter stenosis (%)	76.87	17.00
	STI (%R-R)	43.37	7.28
INFERIOR	DTI (%R-R)	49.49	7.50
	% diameter stenosis (%)	80.45	19.30
	time to PFR (%R-R)	72.28	10.24
LATERAL	% diameter stenosis (%)	70.68	20.23

Table 8.5 Regression analysis, segmental exercise MUGA RNA vs stenotic morphology

		t obs	SEE	r	N
SEPTAL	lAOIEF vs minimal diameter	2.528[1]	0.53	0.53	18
	STI vs minimal diameter	2.574[1]	0.57	0.70	9
INFERIOR					
	DTI vs minimal diameter	-3.547[3]	0.48	-0.80	9
	time to PFR vs minimal diameter	2.654[1]	0.35	0.76	7
	time to PFR vs segment length	-2.671[1]	2.74	-0.77	7
LATERAL	time to PFR vs atheroma area	-4.731[2]	3.08	-0.90	7
	time to PFR vs longlitudinal area stenosis	-5.700[3]	4.25	-0.93	7

Significance levels

1 $0.05 \leqslant p > 0.01$

2 $0.01 \leqslant p > 0.005$

3 $0.005 \leqslant p > 0.001$

minimal diameter was a frequent dependant variable. Levels of significance were generally at the lowest level in all but the relationship with DTI in the inferior segment where it reached less than 0.5%. Myocardial performance in the lateral segment was the only region to correlate significantly with parameters other than percent diameter stenosis and minimal diameter. Segment length, atheroma area and percent longitudinal stenosis (section 7.3.2) demonstrated their importance, the latter particularly so ($p < 0.5\%$). Generally, variability of the quantitative information for the three groups is higher than that previously encountered reflecting the small group size (table 8.6).

Global exercise myocardial performance once corrected for resting myocardial function (by its subtraction from the exercise values) showed very poor relationship with weighted percent diameter stenosis (table 8.7) with only the one parameter of mean phase proving significant at the 5% level. Descriptive information about this relationship is presented in the same table.

8.4.2 The Effects of PTCA on Myocardial Function and Stenotic Morphology

Due to the nature of this work, repeatability of myocardial function could not be investigated. Therefore, significant differences discussed may well be within the degree of error introduced by repeating the test.

As all 5 PTCA patients had disease of the LAD artery only, changes in function (rest and exercise) of the global area and septal segment could be investigated using related t tests. All tests are two tailed due to inability to predict the direction of difference "a priori".

For the global area, only the 3 parameters of exercise PFR/2, exercise PER/PFR ratio and time to PER on exercise demonstrated significant changes as a result of PTCA (table

Table 8.6 Descriptive statistics, segmental exercise MUGA RNA and stenotic morphology

		Mean	Standard deviation
SEPTAL	lAOIEF (%)	29.78	12.32
	Minimal diameter (mm)	0.82	0.61
INFERIOR	STI (%R-R)	44.06	7.36
	DTI (%R-R)	49.09	7.84
	Minimal diameter (mm)	0.81	0.75
LATERAL	time to PFR (%R-R)	72.64	11.00
	Minimal diameter (mm)	1.07	0.50
	Segment length (mm)	17.72	3.90
	Atheroma area (mm^2)	11.81	6.59
	% longlitudinal stenosis (%)	27.33	10.57

Table 8.7 Regression analysis, exercise global MUGA RNA corrected for resting function vs weighted percent diameter stenosis

	t obs	SEE	r	N
$\overline{X}$ Phase	-2.364[1]	19.27	-0.46	23

	Mean	Standard deviation
$\overline{X}$ Phase (^{o})	31.76	17.57
% diameter stenosis (%)	45.01	21.18

8.8). Whilst all significance levels were below 5%, PFR/2 demonstrated the largest t ratio. This was associated with an approximate improvement of 1.6 EDV sec^{-1} following PTCA (table 8.10).

For the septal segment, only mean phase at rest and skew phase on exercise proved significantly different following PTCA. Again, all significance levels were around the 5% mark. Mean changes as a result of PTCA are presented in table 8.10.

Larger significant differences were associated with changes in minimal diameter, percent diameter stenosis, maximal eccentricity and mean eccentricity following PTCA (table 8.9). Degree of stenosis reflected by minimal diameter and percent diameter stenosis show good agreement with the mean of the PTCA group from the previous chapter. However, length, eccentricities and area variables tend to be greater, reflecting the inclusion of a patient with a very long and offset stenosis into this small group (table 8.10).

8.5 **Discussion**

8.5.1 <u>The Relationship Between Myocardial Function and Stenotic Morphology</u>

In investigating global LV function, it was necessary to weight the contribution each artery makes to perfusing the LV in order to arrive at a figure which reflected the global effects of the disease state (section 8.3.2). Whilst there is likely to be much individual variation around the values adopted for this work (Brandt et al 1977) the correction appears to serve its purpose, in that myocardial function parameters previously reported in the literature to be affected by percent diameter stenosis (although no actual relationships have been established) show significant results.

Table 8.8 2 tailed related t tests, rest and exercise MUGA RNA results, pre PTCA vs post PTCA

		t obs	N
GLOBAL AREA	exercise PFR/2	-3.125[1]	5
	exercise PER/PFR	-2.680[1]	5
	exercise, time to PER	-2.585[1]	5
SEPTAL SEGMENT	resting mean phase	-2.296[1]	5
	exercise skew phase	-2.694[1]	5
	exercise STI	2.541[1]	5

Significance level 1: $0.05 \leqslant p > 0.01$

Table 8.9 2 tailed related t tests, Q.A.M.S. stenotic morphology results, pre PTCA vs post PTCA

	t obs	N
Minimal diameter (mm)	-5.138^{3}	5
Percent diameter stenosis (%)	10.046^{5}	5
Segment length (mm)	2.846^{1}	5
Eccentricity at the minimal diameter (%)	2.167^{1}	5
Maximal eccentricity (%)	4.239^{2}	5
Mean eccentricity (%)	5.608^{3}	5
Atheromal area (mm^2)	2.472^{1}	5
Percent longlitudinal stenosis (%)	2.515^{1}	5

Significance levels

1 $0.05 \leqslant p > 0.01$
2 $0.01 \leqslant p > 0.05$
3 $0.005 \leqslant p > 0.001$
4 $0.001 \leqslant p > 0.005$
5 $0.0005 \leqslant p > 0.0001$

Table 8.10 Descriptive statistics, MUGA RNA (rest and exercise) and Q.A.M.S. stenotic morphology results, pre and post PTCA

		PRE PTCA		POST PTCA	
		Mean	Standard deviation	Mean	Standard deviation
	Exercise PFR/2(EDV/sec)	3.62	0.57	5.27	1.19
GLOBAL	Exercise PER/PFR	-1.19	0.37	-0.83	0.14
AREA	Exercise time to PER(%R-R)	14.69	5.61	30.42	13.42
	Resting mean phase(^{o})	24.58	10.32	31.85	9.75
SEPTAL	Exercise skew phase	-0.70	0.39	-0.39	0.19
SEGMENT	Exercise STI(%R-R)	45.56	2.98	36.79	5.99
	Minimal diameter(mm)	1.07	0.32	2.35	0.43
	% diameter stenosis (%)	70.45	12.31	39.17	7.28
	Segment length(mm)	15.27	5.60	13.76	4.79
Q.A.M.S.	Eccentricity at the				
DATA	minimal diameter (%)	32.66	26.21	26.41	23.73
	Maximal eccentricity (%)	45.63	24.74	30.63	26.66
	Mean eccentricity (%)	22.49	16.61	16.50	15.80
	Atheromal area (mm^2)	17.83	11.83	7.05	7.66
	% longlitudinal stenosis (%)	33.48	10.65	20.41	15.21

Relationships involving resting global LV function with percent diameter stenosis are most often non significant, demonstrating that in this group of patients at least, resting function is reasonably good. However, EF measured using a 2 AOI method and stroke volume (SV) corrected for body surface area (BSA) both show significant negative regression relationships with percent diameter stenosis, inferring that EF and SV are lower at higher degrees of stenosis, thus indicating compromised cardiac function at rest (Ellestad 1980). Resting ventricular function increases in asynchrony (Ratib et al 1982) and time to PER gets longer (in terms of STI) as disease severity is increased confirming the above.

On exercise, many more parameters of myocardial function show significant relationships with percent diameter stenosis, indicative of the increased haemodynamic effect at larger coronary artery flow rates (section 6.2.1). Of particular interest is the significantly positive relation with R-R interval, indicating that patients with more severe disease achieve a lower maximal heart rate on exercise. This occurs because the diastolic period (the portion of the cardiac cycle where coronary blood flow and therefore myocardial perfusion occurs - section 6.2.2) becomes the limiting factor as heart rate rises, ie. patients with more severe disease cannot tolerate much shortening of the diastolic component, as their ability to perfuse the LV is already reduced. However, this relationship is weak reflecting the heterogeneity in strength and frequency of anti-anginal preparations being taken by these patients. As with rest, EF demonstrates a negative regression relationship with percent diameter stenosis. This occurs as a result of the generation of ischaemia in the LV and the development of wall stiffness (section 6.2.2). This stiffness increases end diastolic pressure which in turn increases end diastolic volume leading to decreased EF. Interestingly mean EF by the two methods shows great disparity (table 8.2), a fact previously reported by Slutsky et al 1980.

In this group most of the parameters based on systolic function (mean phase, STI and PER) show a response which reflects the limiting factor of heart rate. Using STI as the example, patients with the more severe disease are unable to achieve the higher heart rates, therefore the proportion of the cardiac cycle occupied by systole is relatively less, as diastole has been shown to shorten in preference to systole with reducing R-R interval (Slutsky et al 1983). Patients with less severe disease are able to exercise to higher heart rates (Ellestad 1980) explaining the increased proportion of the cardiac cycle attributable to systole. However, as R-R interval decreases, both components (systole and diastole) obviously show a reduction in real terms (Van Der Hoeven et al 1977). Changes in mean phase parallel the explanation for STI whereas for PER, the reverse argument applies (Bianco et al 1979). These results could have been corrected for heart rate by using analysis of covariance, but the weak association with heart rate resulting from heterogeneous drug therapy precluded this. At face value then, these results contrast with those cited in the literature, where mean phase is seen to increase and therefore STI increases on exercise (Walton et al 1981, Ratib et al 1982, Slutsky et al 1983). These differences are for the most part explained by the covariance of heart rate and the fact that these studies have **not** related changes to disease severity. However, there are gross differences in patient population between this study and those above. Of Waltons group, 69% of patients had at least one major coronary artery blocked. Ratib has 43% of patients with triple vessel disease (76% double and triple vessel disease combined) whilst Slutsky has 56% of patients with triple vessel disease. This contrasts with this study where only 17% of patients have triple vessel disease (35% double and triple combined) and 17% one blocked coronary artery.

The inability of this study to correct for heart rate covariance precludes making direct comparisons of phase and ejection rates with the above work.

PFR/2 demonstrates a negative regression relationship with percent diameter stenosis, initially indicating that diastolic dysfunction is evident (Poliner et al 1984) as a shift of the pressure volume curve resulting in reduced ventricular compliance (section 6.2.2). Again, with heart rate as the covariate, PFR/2 may actually be increasing in real terms. By comparing gradients of the regression relationship however (-1.21 STI and -4.61 PFR/2), it is unlikely that this is the case, as gradients should be approximately equal if correction for heart rate is all that is needed. The larger negative value for PFR/2 would lead to suggest true diastolic dysfunction. Accompanying this fall, the timing of this event appears to occur significantly earlier both in terms of R-R interval (gradient -0.63) and DTI (gradient -0.59). These small gradients would tend to suggest that the direction of these relationships would reverse following heart rate correction, demonstrating additional diastolic compromise. DTI is prolonged reflecting the limiting factor of diastolic component reduction with increasing heart rate.

Concentrating just on exercise, and examining the myocardial performance of each segment of the LV individually but considering the data collectively, returned little in the way of significant results. This fact suggests that each segment is either not demonstrating the effects of ischaemia or that the responses in each segment are different, and therefore masked when considered as a whole. Accordingly, each segment was then considered separately. Very few parameters in comparison to the global area showed significant results, probably as a result of the poorer count statistics in these smaller areas. Moreover, of those parameters being significant, the number was related to the sample size. The septal region demonstrated increased asynchrony of segmental ventricular contraction, reduced EF (1 AOI method) and reduced amplitude with increasing stenotic severity, changes indicative of the effects of ischaemia (Ellestad 1980, Ratib et al 1982). The inferior segment, exhibiting the greatest degree of stenosis,

demonstrated significant changes in the timing of systole and diastole akin to those in the global area, again reflecting heart rate covariance. A decrease in time to PFR with increasing stenotic severity was evident in the lateral segment. Gradient of the regression relationship at -1.49 is low suggesting correction for heart rate covariance would reverse this relationship.

Using minimal diameter in place of percent diameter stenosis as the dependant variable and repeating the analyses tended to reduced the significance of the relationships, and in the case of the septal region, failed to achieve significance with phase standard deviation and amplitude of contraction. This is in direct contrast to the results presented in Chapter 7 where minimal diameter was always a stronger predictor. Inadequacy in view matching in this smaller group leading to variability in artery average maximal diameter may account for the better correlation demonstrated with percent diameter stenosis. Morphological parameters based on area however demonstrated a greater degree of significance, reflecting the addition of length to the dimensional measurements, a parameter of some influence in the equations of fluid dynamics (section 6.2.1). This parameter is also important when considered alone, correlating significantly although less strongly than percent diameter stenosis. The direction of these relationships is opposite to expected as with the data above. Regression relationship gradients are all less than 1 demonstrating the influence of heart rate as a covariate.

Correcting the exercise data for resting myocardial performance by considering **change** in function in comparison to weighted percent diameter stenosis, yielded only one significant result, the direction of the relationship indicating preserved diastolic function by limiting heart rate achieved. The failure of any other parameters to correlate significantly points to variable resting function in this group of patients, perhaps reflecting the heterogeneity of their disease and/or drug therapy state.

Overall, the better count statistics of the global area have allowed investigation of the effects of exercise on the LV with a compromised blood supply. Several parameters correlate significantly with degree of stenosis on exercise, although overall, the relationships are not that strong. The inability to wholly relate myocardial performance to stenotic anatomy as measured by QAMS is not surprising however, as QAMS does not include any beneficial effects gained in LV perfusion by the coronary collateral circulation.

The effects of dynamic or functional stenoses previously described by Gould et al 1982, Brown et al 1984 and Santamore 1985 (section 6.2.1) may also aid in producing a variable global exercise response in the light of apparently severe disease. Unfortunately, relating the parameters of eccentricity to global LV function is not possible, as the contribution each artery makes to LV perfusion must be taken into account, which means the adoption of some form of weighting system (section 8.2.3). The probable diversity of stenosis eccentricity in two or more arteries would tend to make such a calculation useless globally. Also, in order to weight absolute dimensional parameters eg. minimal diameter, disease must be present in all three arteries. How one would weight minimal diameter for the presence of disease in just two arteries remains a problem for contemplation.

In dividing the ventricle up into segments and analyzing each relative to the supplying artery allows the above to be achieved but suffers at the hands of poor count statistics and non concentric LV contraction. Whilst the latter was quantified, with movement of the systolic AOI relative to the diastolic AOI at rest being 9.9% and exercise 8.5% of end diastolic length, this movement could not be removed and therefore adds to errors in quantitative calculations.

In overall conclusion, QAMS has proved useful in quantifying percent diameter stenosis which correlates significantly with some variables of global myocardial performance at rest

and during exercise. The testing of patients free from the effects of drugs would also allow better investigation of myocardial function with disease severity. By using a higher ^{99m}Tc dose a more thorough investigation of segmental function may be possible, although movement of the heart in the chest will always remain a problem. In the light of these findings, QAMS seems better suited to use in the PTCA and perhaps CABG environment.

8.5.2 Effect of PTCA on Myocardial Function and Stenotic Morphology

Improvement in diastolic function post PTCA is apparent even in this small group highlighted by the significant difference in the PFR/2 parameter (Lewis et al 1985, Bonow et al 1985), which exhibits the highest t ratio. R-R interval showed no significant differences in this group and therefore it is not necessary to consider this as a covariate. Size of improvement approximates to that reported by Lewis et al 1985. This increase in PFR/2 highlights the effect of the significantly improved state of the coronary lesion (table 8.9) allowing restoration of myocardial perfusion pressure and removal of LV stiffness (section 6.2.2). PER/PFR ratio is also significantly affected, with PFR exceeding PER on average, implying better diastolic function post PTCA. Systolic function also becomes less laboured in that PER occurs significantly later post PTCA, indicant of normal function (Slutsky et al 1980). However, initiation of PER so early in systole pre PTCA seems spurious.

Resting mean phase of the septal segment occurs significantly later post PTCA, probably as a result of drug regime changes. On exercise, there is a significant change in the phase histogram in that skewness is reduced and the distribution appears more normal (symmetrical). This indicates better segmental synchrony post PTCA (Gerber et al 1983, Ratib et al 1982). However pre PTCA, exercise skew phase was the opposite of that expected. For this, there

are two possible explanations. Firstly, tardokinesis is not evident, or secondly, most of the ventricle is tardokinetic. The first proposal would seem most tenable considering that all of these patients had been selected to receive PTCA and therefore have good LV function. From these results then, it seems unlikely that patients with single vessel disease exhibit the phase changes on exercise documented by Walton et al 1981 and Ratib et al 1982. However, the group size is really too small to serve as conclusive proof.

Overall however, the number of significant parameters and level of significance is low, for both the global and septal regions, reflecting the fact that subtle changes in myocardial function as a result of PTCA either cannot be detected by using our "in-house" software, the exercise level attained was not sufficient to evoke symptoms pre PTCA or myocardial dysfunction in this **small** group of patients with single vessel disease is not great. A repeat study, with more patients is required in order to investigate fully altered myocardial performance following PTCA. Backing this up with a computer capable of acquiring at a higher framing rate, plus utilization of a larger dose of ^{99m}Tc would enhance success of the study.

As with the data presented in chapter 7, large significant differences exist in parameters reflecting stenotic morphology as measured by QAMS post PTCA. Interestingly, percent diameter stenosis shows the largest difference, a reversal of the trend of chapter 7, probably being explained by differences in view as discussed earlier. Mean eccentricity is also highly affected, the tortuousity being significantly reduced as a result of PTCA.

In conclusion, significant differences in stenotic morphology are reciprocated by significant improvement in a few parameters which reflect global diastolic function on exercise post PTCA.

CHAPTER NINE

CONCLUSIONS AND PROPOSALS FOR FURTHER WORK

9.1 Conclusions

A system capable of quantifying stenotic morphology in both relative (percent diameter stenosis, eccentricity etc.) and absolute (minimal diameter, atheroma area etc.) terms has successfully been developed. The system is microcomputer based and reasonably easy to use (section 9.2) utilizing standard clinical coronary arteriographic film without the need for special images or processing. The QAMS software has been written in a portable high level language for longevity and easy access for future development. The system has employed standard cardiovascular unit equipment (eg cine projector) combined with commonly available peripherals (graphics, tablet, printer, etc). It is estimated that such a system could be assembled for less than £5,000 (£1,500 computer and printer, £ 2,500 graphics tablet, provided the current software were available).

Each facet of the image quantification procedure has been validated and demonstrated competence of its theory in the practical situation. Overall, results produced by the QAMS have proved repeatable, objective and valid.

On application, changes in stenotic morphology following PTCA have demonstrated significant relationships with parameters characterizing patient exercise tolerance. Generally, associations involving absolute measurements (particularly minimal diameter) proved the stronger reinforcing current opinion in recent literature. New parameters based on arterial eccentricity have proved particularly interesting in examination of the long term PTCA effect. Relationships between stenotic morphology and ventricular (global and regional) function correlated less strongly than those above probably reflecting the present inability (section 9.2) of QAMS to quantify contribution

from the collateral circulation. However, significant relations were demonstrated between percent diameter stenosis and global diastolic function in a sample of patients with a mixed number of arteries affected by CAD. Compromised diastolic function was ameliorated following PTCA in a small number of patients with CAD of the LAD artery.

In overall conclusion, whilst the system in its present form has several shortcomings (section 9.2) results produced have proved worthwhile and valuable in practical application. The QAMS system therefore warrants further development leading to regular application.

9.2 **Proposals for Further Work**

Should the opportunity ever arise for further development of the QAMS, attention to the following aspects would enhance its usability and quality of produced results.

Short term developments (ie. those changes which would bring a quick return in QAMS performance):

1. Transfer of complete system to a new host microcomputer. This development is, in part, complete as the **quantification** software is now resident on a IBM PC clone. This has successfully reduced run time once the coordinates have been collected from fifteen minutes to two and a half minutes on average. The next logical step is to transfer the graphics tablet interface to the IBM PC clone such that coordinates may be collected directly into the new microcomputers memory.

2. Writing a PROGRAM ARTDR equivalent for the new host microcomputer. IBM PC clones have adequate graphics capabilities for on screen representation of coordinate files produced by QAMS. A hardcopy facility would also prove valuable for inclusion into the patients notes. This capability may also aid in examination of the

nature and the relative positions of artery eccentricity variables (section 7.5.2).

3. Use of complementary view (orthogonal) data to reconstruct a three dimensional representation of the artery in space. Diseased diameters from two views at 90 degrees may be matched according to the algorithm presented in appendix 1. Representation of the artery in this form would allow:

   a. An elliptical model for artery cross section to be used, giving an accurate estimate of true artery cross-sectional area.

   b. The effects of magnification due to axial displacement between stenosis and catheter positions to be removed.

   c. Computation of atheromal volume.

   d. More accurate representation of artery eccentricity.

4. Increasing the size of the image being quantified. There are two ways of achieving this:

   a. Purchase a larger graphics tablet.

   b. Develop software to allow the digitization of an image to become a two stage process thus: Project image at normal size and digitize margins for calculation of pincushion distortion. Then, increase the size of the stenotic image (with catheter in view), digitize, and transform stenotic coordinates to original (unmagnified) position.

Such a facility would greatly improve repeatability and objectivity of results in the digitizing of coronary stenosis.

5. Provision of a better user interface. Now that the QAMS have proved useful, more attention needs to be directed at making it as "user friendly" as possible, thus minimizing the possibility of making mistakes and losing data. The provision of a new host microcomputer with hard disk would easily afford this, allowing automatic implementation (ie. no floppy system disks) and the storing of results.

6. Complete software upgrade to Fortran 1977 standards. This would enhance run time and program readability, removing the necessity for cumbersome error trapping.

7. Repetition of the validity experiments in catheter room A, with the small image intensifier selected (section 3.6.1), using an accurate calibration grid rather than industrial mesh. This would allow accurate investigation of the "optical" characteristics of this equipment which, on the basis of previous validation results are not normal (section 5.1.2).

8. Histological validation of the quantification of coronary stenoses using QAMS. Whilst this would be a costly and difficult experiment to perform (section 3.6.3.) it is necessary that QAMS be validated against other objective measures of coronary anatomy prior to continued use. Perhaps this would be better achieved by performing the X-ray filming elsewhere, having previously quantified magnification and pincushion distortion factors in a manner similar to that cited in section 3.6.1. This would overcome the ethical problems and allow the work to be completed at relative leisure. Histological quantification however still remains a problem. Perhaps the work could be done

collaboratively with a local firm familiar with histology, eg. Fisons plc, Loughborough.

9. Provision of new algorithms and software for the calculation of artery eccentricity, capable of quantification in arteries whose directional changes are acute and in more than one direction.

Long terms developments (ie. those improvements which would be "nice" to have, but are not ultimately necessary).

1. Combination of the individual quantification programs into a single functional unit. This would reduce runtime as it would not be necessary to re-read the original data for each programs execution. However, as IBM PC clones are much faster than the Vector 3, the absolute time incurred in the above is very small and consequently the improvement gained by providing this facility would also be small. There are also practical difficulties. Most modern compilers have a 64K maximum limit for source code size. The present size of QAMS source code would dictate combination of perhaps three of the six programs into two combined units, this concurrent implementation would still be required. Perhaps while the original data is being used, it could be temporarily located on a RAM disk (effectively a portion of computer memory) to improve access speed to the full.

2. Combine QAMS with videodensitometry such that the myocardial "blush", evident with significant collateral circulation may be quantified. This would allow more accurate representation of functional significance of a coronary stenosis for use in examination of ventricular function (chapter 8).

As QAMS continues to develop, no doubt other enhancements will become evident. It is perhaps pertinent to state that the software provided may also be of use in the

quantification of any structure which resembles a tube, and therefore is perhaps better **not** considered as being specific to the quantification of CAD.

APPENDIX 1

1. Making a Measurement

Sections 3.4.2 and 3.5 have described in detail what the software does, how it does it and what files are produced as a consequence. This section deals with what the user has to do in order to produce a result. Detailed description of the Vector3 operating system is avoided. The user is referred to the manufacturers manuals or any CP/M handbook.

1. Power up Vector3, graphics tablet and peripherals. The Vector3 requires approximately 10 minutes warm up in order to achieeve a successful "boot" from any system disk. The graphics tablet emits a four tone signal (three short - one long) following a self check if everything is alright. If this tone is not obtained, refer to manufacturers handbook.

2. Select frame exhibiting the stenosis to be digitized according to the criteria laid down in section 3.1. Ensure also that the complete frame is within the active area of the graphics tablet. This may be checked by running the cursor around the margins of the frame. A continuous red light displayed on the cursor with absence of the continuous alarm signal indicates acceptability.

3. Mark the edges of the cine frame using a fine nibbed water soluble pen (figure APP1). These marks when digitized will be used to calculate the image centre. Since the image is usually circular or a "squared off" circle it does not matter where the marks are placed as connecting diagonals will always cross at the centre. However, taking reference from the embedded graphics tablet wires is recommended for extra certainty, forming what would be a square should the marks be connected in series.

Figure APP1. A stenotic segment prepared for quantification. Notice the 4 frame margin marks in the corners, the traced catheter width and artery contour. NB. The pen used here is rather thicker than the one normally employed in order for the marks to be visible in the photograph. Also, shading has been omitted in order to demonstrate the stenosis.

4. Mark a section of catheter with four points, two either side, evenly spaced and parallel (figure APP1). Four points are necessary in order to compute a reasonable diameter from the catheter (PROGRAM ANALYZ). Choose a portion of any catheter in the frame as long as its external diameter is known. Ensure that the section chosen is unforshortened and as close to the stenosis as possible, this minimizing the effects of axial displacement.

5. Trace the stenosis with the water soluble pen (figure APP1). It beneficial (in terms of repeatability and ease of use) to have a definite edge to trace to when digitizing a stenosis. It is therefore advised that stenosis "preparation" for the final tracing be considered as two separate actions.

   a. Cortical integration of differing grey levels across the stenotic edge producing a minds eye map of where the tracing with lie.

   b. Application of the tracing to the graphics tablet surface. Due to the finite width of the pen nib, it is impossible to trace exactly the desired path. For this reason, the practice of shading the lines on the inside edge, towards the centre of the stenosis, should be adopted, such that the outside edge of the tracing demonstrates the path to be digitized.

6. Insert a QAMS system disk into drive A and boot up. Displaying the directory reveals all the programs and files necessary for a full stenosis evaluation (system disk creation is covered elsewhere in appendix 1). It is important to remember that all files produced by the programs are stored on this disk. Therefore it will become necessary to copy these to another disk should the user wish to store any of the digitized information.

7. Run BITPAD.SUB. The collection program BITPADB is first loaded up and presents the user with a coordinate accumulation screen displaying some simple operating instructions as well as the number of point mode coordinates and stream mode coordinates collected and remaining. All should be zeroed.

8. Begin digitization - POINT MODE. The following data is to be collected in point mode:

   a. the cine frame margins - 4 points
   b. the diameter of the catheter - 4 points.

   Point mode is activated by pressing button 1 of the cursor when in the active area, ensuring that the green light is off. If this light is on when powered up, it may be deactivated by pressing button 5. The accumulation screen should then inform the user that point mode is active by displaying the words POINT MODE in inverse video. Before digitization can proceed therefore, point mode must be active. Failure to ensure activity prior to starting will upset the structure of the resultant data file and invalidate the results.

   The user may now digitize the marked points by administering a single press to button 1 for every coordinate in the following order:

   a. Cine frame - Top left hand corner, bottom left hand corner, bottom right hand corner, top right hand corner.

   b. Catheter diameter - Starting side is irrelevant. Side 1 top point, bottom point. Side 2 top point, bottom point.

Point mode collection is now complete. The user should ensure that eight points have been collected by reference to the accumulation screen.

9. Continue digitization - STREAM MODE. Activate stream mode by pressing button 5. This is confirmed by illumination of the green light on the cursor. However, POINT MODE remains in inverse video and STREAM MODE is normal video on the accumulation screen. This is because a full switch to stream mode cannot take place until the first coordinate of stream mode has been entered. Unlike with point mode, it is exceptionally difficult to enter just one coordinate of stream mode to complete the switch when the entry rate is 25 coordinates per second. Therefore the user is advised **not** to try. Place the cursor at the top of either traced side of the stenosis. Press button 2 of the cursor and keep depressed as the artery side is traced as carefully as possible. Release button 2 when the end of the side is reached. Stream mode will have become active and highlighted accordingly when the program receives the first stream mode coordinate. Immediate continued collection of successive coordinates in this way ensures minimal error, although the routine is prone to some data corruption on switching (see PROGRAM PNTED). The accumulation screen reveals the collection of X number of coordinate pairs. The user must now instruct the program that he/she is ready to digitize the second side of the stenosis. This is achieved by pressing button 3. The routine responds by asking the question at the bottom of the screen: collect second array (Y/N)? If the pressing of push button 3 was intentional, the user replies Y at the keyboard and proceeds to trace side 2 from the top downwards in exactly the same manner as side 1. On finishing, the accumulation screen reveals the total number of coordinates collected, both in point and stream mode.

Forty seconds are allowed (2000 coordinate pairs) for total stream mode digitization time. With practice this may be reduced to around 20 seconds with little loss of data integrity.

10. End digitization. This is achieved by pressing button 4. The accumulation screen disappears and is replaced by the message: DATA TRANSFERRING TO DISK. The program BITPADB finishes when all data has been transferred to the file DATA.DAT.

11. Data conversion. The program BITPADD is automatically loaded from the submit file and asks the user to supply a specific filename. If the system is to be used in concurrent collection-evaluation mode with no desire to store the raw data then the response should be BITPDCOO.RDS as character handling is very poor in this version of Fortran (as explained in section 3.3.3). If the system is to be used in multi-collection mode for later evaluation then the filename supplied may be anything of the users choice (maximum eleven characters).

    The program then proceeds to convert the hexadecimal data in the file DATA.DAT to ASCII storing it on disk under the user supplied filename. The program terminates by informing the user of the number of points collected in each section of the datafile and erasing the hexadecimal file automatically.

12. Run STEN.SUB. This concatenates the programs PNTED, DIAMAV, DIAMRS, ANALYZ and ECCFTR requiring only that the data filename and catheter room be supplied as user input for PNTED and the external diameter of the catheter digitized for ANALYZ. Hence the system runs almost without user interaction once the stenosis has been digitized producing two sheets of quantified information at the printer (programs ANALYZ and ECCFTR). If multi-collection mode has been opted for

on digitization then the submit file STEN.SUB must be supplemented to either rename (data lost) or copy to another disk (data preserved), then rename the datafile from the user supplied name to BITPDCOO.RDS before running the quantification programs. An example of such a submit file can be found elsewhere in appendix 1.

Should graphical representation of the artery diameters etc. be desired, then the necessary datafiles must be transferred to the Prime System using MOVE - IT and GETFILE communication software packages (example elsewhere in appendix 1).

2. Typical datafile structure

```
1        Start Point Mode
9        Start Stream Mode - Side 1
252      Start Stream Mode - Side 2
243      No. Coordinates Side 1
178      No. Coordinates Side 2
8        No. Coordinates Point Mode
429      Total No. Coordinates
0
1
1        System Flags (ignore)
1
1
----------------------------------------------
1183  ---- X Coordinate   PAIR 1
10050 ---- Y Coordinate
1063                                          P
1788                           FRAME          O
10561                          MARGINS        I
1351                                          N
10590                 PAIR 4                  T
10293
----------------------------------------------
2947                  PAIR 5
10297                                         M
2913                           CATHETER       O
10141                          DIMENSION      D
3172                                          E
10281
3154                  PAIR 8
10136
______________________________________________
4139                  PAIR 9                  S
9330                                          T
4151                    .                     R
9223                                          E
.                       .                     A
.                                             M
.
                                           MODE
```

3. Creating a Q.A.M.S. system disk under CP/M.

a. Creating the system disk.

BOOT UP
Ensure the system disk (in Drive A) has the programs FORMAT.COM and SYS.COM present.
Place blank disk in Drive B.

From the A prompt, type:

A> FORMAT B: (Return)

Disk is formatted. Then type:

A> SYS B: (Return)

System tracks will now be transferred to disk B making it a "bootable" system disk.

b. Transferring the QAMS system.

Insert the QAMS system disk in Drive A, new disk in Drive B. Copy over the following files using the syntax below.

Syntax: PIP B:=A: File.Extension

eg.1 PIP B:=A: PNTED.COM
transfers program PNTED from A to B.

eg. 2 PIP B:=A *.COM
transfer all files with extension COM from A to B.

QAMS System files: SUBMIT.COM, PNTED.COM, DIAMAV.COM, DIAMRS.COM, ANALYZ.COM, ECCFTR.COM, SIDE1POI.NTS, SIDE2POI.NTS, AXPTS, POINTMAG.NIF, BITPDCOO.RDS, ARCRADII.EPS DIAMETER.EPS, AVERAGED.IAM. PIP.COM is a useful addition, though not part of the system.

4. Creating a submit file.

A submit file allows programs to run concurrently.

Place the QAMS system disk in Drive A.

Type from the A prompt:

A> PIP original submit file name.SUB = CON:

Program names to run concurrently (as they would be typed normally).

CONTROL Z (keyed in by holding control key down and typing Z).

```
eg  PIP BITPAD.SUB = CON:
        BITPADB
        BITPADD
        ^Z
```

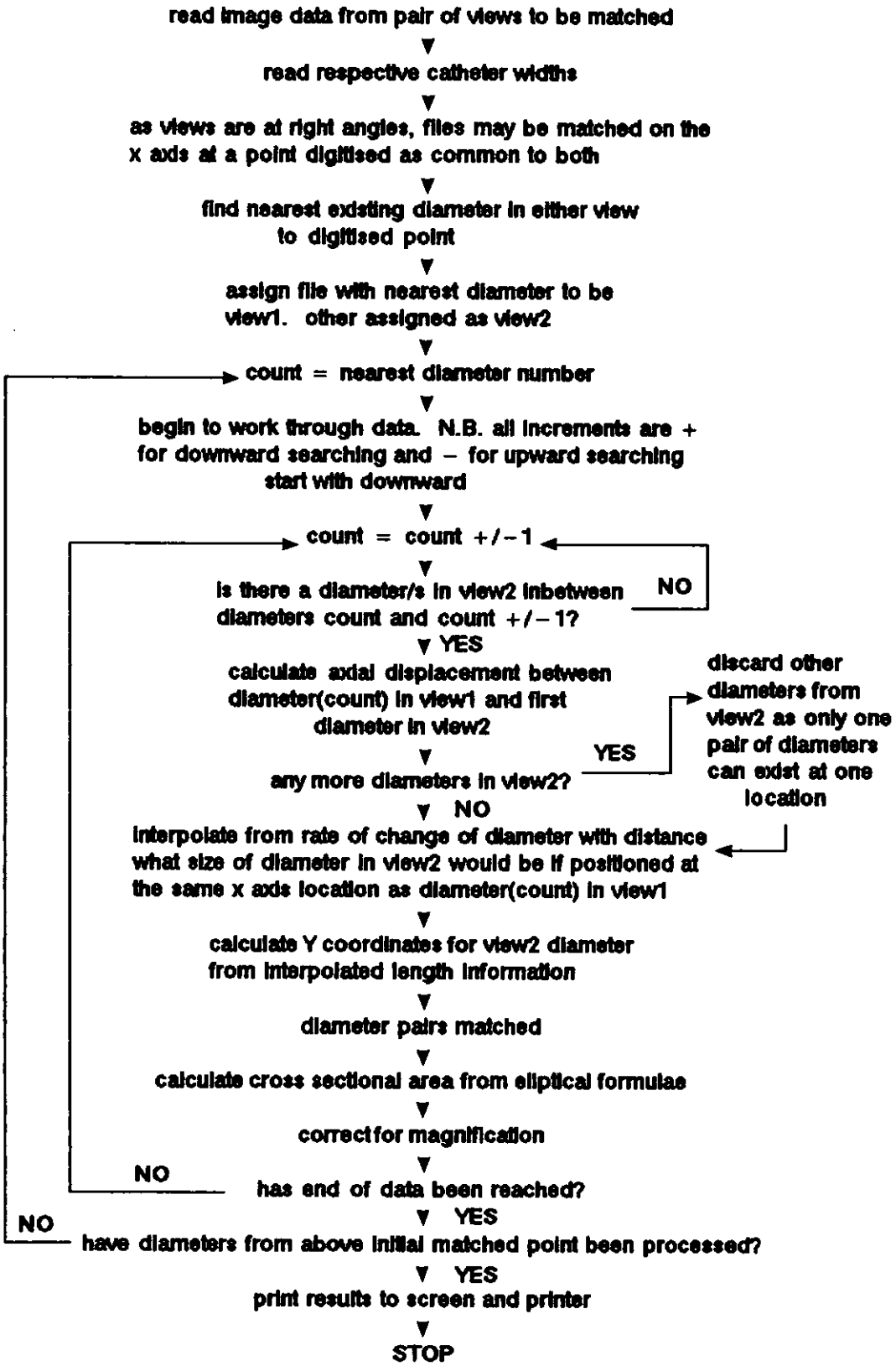

5. view matching algorithm

```
      PROGRAM PNTED
C
      INTEGER FILDES(12),START1,START2,N1,N2,N3,NT,N,STARTP,ENDP,END1
      INTEGER END2,CHECK1,CHECK2,CHECK3,J,P,S,DUMX,DUMY,CATHRM,MAGVAL
      INTEGER XSIDE(2000),YSIDE(2000),N1OR2,F,R,PPSIDE,F1,F2,K,F3
      INTEGER I2,YI2,XI3,YI3,XI1,YI1,XI4,YI4,Z1,Z2,Z3,Z4,Z5,N4,F4,Q
C
      DOUBLE PRECISION TOL,X1,Y1,X2,Y2,X3,Y3,X4,Y4,DIST1,DIST2,DIST
      DOUBLE PRECISION X(100),Y(100),XA,YA,XB,YB,XC,YC
C
C
      COMMON/SET1/XSIDE,YSIDE/SET2/S,N1OR2/SET3/TOL/SET4/X1,Y1
      COMMON/SET5/X2,Y2/SET6/XC,YC,CATHRM,MAGVAL/SET7/XI2,YI2,F,J
C
C
C     ------------------------------------------------------------------
C     PUT HAND-TRACING TOLERANCE IN DIGITISER UNITS INTO TOL
C
      TOL =22.04
C
C
C     ------------------------------------------------------------------
C     PROGRAM PNTED IS A GENERAL POINT EDITING PROGRAM WHICH HAS BEEN
C     EMPLOYED HERE SPECIFICALLY TO AID IN THE CALCULATION OF
C     SERIAL DIAMETERS ALONG THE LENGTH OF AN ARTERY INTERIOR
C     WALL TRACED FROM X-RAY ON A TRANSPARENT DIGITISING TABLET.  THE
C     TABLET DELIVERS EITHER POINT MODE OR STREAM MODE CO-ORDINATES
C     (WHICH ARE INTEGERS UP TO 5 DIGITS) ACCORDING TO WHICH OF THE
C     CURSOR BUTTONS IS PRESSED.  POINT MODE DELIVERS ONE CO-ORDINATE
C     PAIR PER PRESS OF ITS BUTTON WHILE STREAM MODE WILL DELIVER A
C     CONSTANT STREAM OF UP TO 200 CO-ORDINATE PAIRS PER SECOND (DEPENDING
C     UPON BAUD RATE) WHILE ITS BUTTON REMAINS PRESSED.
C
C     THE PROGRAMS WHICH INTERFACE THE DIGITISING TABLET WITH THE COMPUTER
C     ARE DESIGNED TO WRITE CO-ORDINATES FOR BOTH SIDES DIRECTLY INTO
C     MEMORY SO THAT THE COMPUTER CAN RECEIVE STREAM MODE CO-ORDINATES
C     AS FAST AS POSSIBLE.  THEN ANOTHER OF THESE PROGRAMS CONVERTS
C     THE STORED INFORMATION TO ASCII AND WRITES IT TO DISK UNDER THE
C     NAME BITPDCOORDS (ABBREVIATION FOR BITPAD-COORDINATES).  THIS
C     FILE HAS THE FOLLOWING STRUCTURE:
C
C     FILE DESCRIPTORS, 12 SINGLE VALUES, 1 PER LINE
C     POINT-MODE CO-ORDINATES
C     SIDE1 STREAM-MODE CO-ORDINATES
C     SIDE2 STREAM-MODE CO-ORDINATES
C     ALL CO-ORDINATE DATA IS SINGLE ALTERNATE X,Y VALUES, 1 PER LINE.
C
C     FILE DESCRIPTORS ARE NUMBERS OF COORDINATE PAIRS CONTAINED IN EACH
C     SECTION. IN DETAIL THEY ARE:
C
C     START OF POINT MODE
C     START OF SIDE1
C     START OF SIDE2
C     NUMBER OF SIDE1 CO-ORDINATE PAIRS
C     NUMBER OF SIDE2 CO-ORDINATE PAIRS
C     NUMBER OF POINT-MODE CO-ORDINATE PAIRS
C     TOTAL NUMBER OF CO-ORDINATE PAIRS
C     DESCRIPTORS 8 TO 12 ARE DUMMIES.
C
C     INFORMATION IS STORED THIS WAY TO OPTIMISE USE OF MEMORY AND
C     SPEED OF OPERATION.
C
C     ------------------------------------------------------------------
C
C     THIS PROGRAM EDITS THE CO-ORDINATE FILE WHICH RESULTS FROM THE
```

```
C     TRACING TO ENSURE THAT EVERY CONSECUTIVE SET OF 3 POINTS
C     IS DISTINCT AND THAT THE EFFECTS OF HAND TREMOR ARE FILTERED
C     OUT.  HAND TREMOR ARISES BECAUSE THE HUMAN OPERATOR IS UNABLE TO
C     FOLLOW A LINE WITH THE CURSOR TO THE RESOLUTION ACCURACY OF
C     THE DIGITISING TABLET.  THE EFFECTS ARE REMOVED BY DEFINING A TOLERANCE
C     (DETERMINED FROM TRIALS) FOR HAND TRACING ACCURACY
C     AND USING THIS TO DEFINE A CIRCLE AROUND THE LAST POINT
C     ACCEPTABLE FOR INCLUSION.  THE NEXT POINT BECOMES ACCEPTABLE IF IT
C     LIES OUTSIDE THE CIRCLE, OR, IF ITS POSITION DOES NOT IMPLY A
C     DIRECTION REVERSAL. IF ONE OF THE FOLLOWING POINTS LIES INSIDE THE
C     CIRCLE BUT HAS A POSITION WHICH IMPLIES THAT THE REVERSAL HAS OCCURED,
C     THEN THIS IS CONSIDERED TO REPRESENT HAND TREMOR OR A GLITCH. POINTS
C     IN THE TREMOR ARE ALL THOSE COMPOSING THIS REVERSAL AND ARE FILTERED
C     OUT BY RESETTING A COUNTER WHICH OMITS THEM AS ACCEPTABLE CO-ORDINATES
C     AS THEY ARE WRITTEN TO FILE.
C
C     ------------------------------------------------------------------
C     DETERMINE WHICH ROOM WAS USED FOR THE ARTERIOGRAPHY.
C
      WRITE(1,1)
 1    FORMAT(' WHICH CATHETER ROOM 1=ROOM A:2=ROOM B:')
C
      READ(1,2) CATHRM
 2    FORMAT(I2)
C
      WRITE(1,25)
 25   FORMAT('WHAT LEVEL OF MAGNIFICATION 1=SMALL:2=BIG:')
C
      READ(1,26) MAGVAL
 26   FORMAT(I2)
C     ------------------------------------------------------------------
C     READ FILE DESCRIPTORS (GIVEN IN FIRST 12 LINES OF FILE BITPDCOORDS)
C     INTO FILDES( ).  NOTE 0 = DRIVE NUMBER.  FIRST ITEM OF ANY SECTION
C     HAS A SEPARATE READ STATEMENT TO FACILITATE CODING OF ERROR MESSAGES.
C     FILE DESCRIPTORS ARE INITIALLY READ INTO A VECTOR FOR THE SAME
C     REASON.
C
C
C     OPEN FILES.
C
      CALL OPEN(6,'BITPDCOORDS',0)
      CALL OPEN(7,'SIDE1POINTS',0)
      CALL OPEN(8,'SIDE2POINTS',0)
      CALL OPEN(9,'POINTMAGNIF',0)
C
      READ(6,20,ERR=30,END=50) FILDES(1)
      READ(6,20,ERR=70,END=90)(FILDES(J),J=2,12)
C
C
C     ------------------------------------------------------------------
C     PUT START OF SIDE1 INTO START1
C         START OF SIDE2 INTO START2
C         NUMBER OF SIDE1 CO-ORDINATE PAIRS INTO N1
C         NUMBER OF SIDE2 CO-ORDINATE PAIRS INTO N2
C         NUMBER OF POINT MODE CO-ORDINATE PAIRS INTO NP
C         TOTAL NUMBER OF CO-ORDINATE PAIRS INTO NT
C         TOTAL NUMBER OF CO-ORDINATE PAIRS IN SIDES ONLY INTO N
C         DUMMIES INTO Z1 TO Z5
C
          STARTP=FILDES(1)
          START1 = FILDES(2)
          START2 = FILDES(3)
          N1 = FILDES(4)
          N2 = FILDES(5)
          NP = FILDES(6)
```

```
          NT = FILDES(7)
          Z1 = FILDES(8)
          Z2 = FILDES(9)
          Z3 = FILDES(10)
          Z4 = FILDES(11)
          Z5 = FILDES(12)
           N = N1 + N2
C
C
C     ------------------------------------------------------------------
C     PUT START OF POINT MODE INTO STARTP
C         END OF POINT MODE INTO ENDP
C         END OF SIDE1 INTO END1
C         END   OF SIDE2 INTO END2
C         NUMBER OF POINT MODE CO-ORDINATES INTO NP
C
      ENDP   = START1 - 1
      END1   = START2 - 1
      IF(STARTP.EQ.0) END2=NT
      IF(STARTP.NE.0) END2=STARTP+NT-1
C
C
C     ------------------------------------------------------------------
C     CHECK THAT START1, START2, N1, N2, NP, NT CORRECTLY RELATE AND THAT
C     N1 AND N2 ARE GREATER THAN THE MINIMUM REQUIRED.
C
      IF(STARTP.EQ.0) CHECK1=1
      IF(STARTP.NE.0) CHECK1=STARTP+NP
      CHECK2=N1+START1
      IF(STARTP.EQ.0) CHECK3=NT
      IF(STARTP.NE.0) CHECK3=STARTP+NT-1
C
      IF(START1.NE.CHECK1) GOTO 110
      IF(START2.NE.CHECK2) GOTO 130
      IF(END2.NE.CHECK3)   GOTO 150
      IF(N1.LT.3)          GOTO 170
      IF(N2.LT.3)          GOTO 190
C
C
C     ------------------------------------------------------------------
C     READ POINT MODE CO-ORDINATES INTO X(P),Y(P). 4 POINTS MUST BE PRESENT
C     WHICH INDICATE THE POSITIONS OF THE MARGINS OF THE CINE FRAME. IF NO
C     OTHER POINTS HAVE BEEN COLLECTED, WRITE -1,-1 TO THE FILE POINTMAGNIF
C     FLAGGING THE ABSENCE OF MAGNIFICATION INFORMATION.
C
      DO 3 J=1,NP
        READ(6,20,ERR=250,END=270) XSIDE(J)
        READ(6,20,ERR=250,END=270) YSIDE(J)
 3    CONTINUE
C
C     COMPUTE IMAGE CENTRE.
C
      XA = (XSIDE(1)+XSIDE(3))/2.0
      YA = (YSIDE(1)+YSIDE(3))/2.0
C
      XB = (XSIDE(2)+XSIDE(4))/2.0
      YB = (YSIDE(2)+YSIDE(4))/2.0
C
      XC = (XA+XB)/2.0
      YC = (YA+YB)/2.0
C
C     ASSIGN DUMMY VARIABLES TO -1.
C
      DUMX = -1
      DUMY = -1
C
```

```
C     IF NO FURTHER POINT MODE DATA EXISTS, WRITE DUMX,DUMY TO FILE.
C
      IF(NP.EQ.4) REWIND 9
      IF(NP.EQ.4) WRITE(9,9) DUMX,DUMY
      IF(NP.EQ.4) GOTO 5
C
C     IF FURTHER POINT MODE DATA DOES EXIST, CORRECT IT FOR PINCUSHION
C     MAGNIFICATION. WRITE THE DATA TO POINTMAGNIF.
C
      S = 5
      N1OR2 = NP
      CALL PCUSH
C
      DO 4 J=1,NP
        WRITE(9,9) XSIDE(J),YSIDE(J)
 4    CONTINUE
C
C     READ STREAM MODE CO-ORDINATES INTO ARRAY XSIDE( ),YSIDE( )
C
C     SIDE1:
C
 5    J = 1
      READ(6,20,ERR=290,END=310) XSIDE(J)
      READ(6,20,ERR=290,END=310) YSIDE(J)
      DO 6 J=2,N1
        READ(6,20,ERR=330,END=350) XSIDE(J)
        READ(6,20,ERR=330,END=350) YSIDE(J)
 6    CONTINUE
C
C     CORRECT ALL SIDE1 DATA FOR PINCUSHION MAGNIFICATION. OMIT THE FIRST
C     COORDINATE OF STREAM MODE DUE TO ITS POSSIBLE SPURIOUS NATURE AS A
C     RESULTS OF THE SWITCHING BETWEEN POINT AND STREAM MODE.
C
      S = 2
      N1OR2 = N1
      CALL PCUSH
C
C     WRITE SIDE1 CO-ORDINATE PAIRS TO FILE SIDE1POINTS, BYPASSING ANY
C     CO-ORDINATE PAIR DUPLICATED IN THE FOLLOWING TWO CO-ORDINATE
C     PAIRS TO ENSURE THAT EVERY CONSECUTIVE SET OF 3 POINTS IS
C     DISTINCT. OMIT ALSO COORDINATES WHICH ARE NEGATIVE OR MORE THAN
C     11000 IN VALUE. THESE MAY BE PRESENT AS AN ARTIFACT OF THE
C     COORDINATE COLLECTION PROGRAM.
C
      N3 = N1-1
      DO 14 J=2,N1
        IF((J.LE.N1-1).AND.(IABS(XSIDE(J)).GT.11000).OR.(IABS(YSIDE(J))
     &.GT.11000)) GOTO 8
        IF((J.LE.N1-1).AND.(XSIDE(J).EQ.XSIDE(J+1)).AND.
     &(YSIDE(J).EQ.(YSIDE(J+1)))) GOTO 8
        IF((J.LE.N1-2).AND.(XSIDE(J).EQ.XSIDE(J+2)).AND.
     &(YSIDE(J).EQ.(YSIDE(J+2)))) GOTO 8
        IF(J.LE.N1-1) WRITE(7,9,ERR=430) XSIDE(J),YSIDE(J)
        IF(J.EQ.N1) WRITE(7,9,ERR=430) XSIDE(J),YSIDE(J)
 9    FORMAT(2I7)
      GOTO 14
 8      N3 = N3-1
 14   CONTINUE
C     PRIOR TO WRITING NEW TOTAL FOR N1 TO N3, PASS VALUE TO N4 FOR SIDE2
C
        N4 = N1
        N1 = N3
C
```

```
C     SIDE2:
C
C     ALLOW N4 TO REPRESENT THE START OF SIDE2
      N4 = N4+1
      J = N4
C
      READ (6,20,ERR=370,END=390) XSIDE(J)
      READ (6,20,ERR=370,END=390) YSIDE(J)
      N4 = N4+1
      DO 10 J = N4,N
        READ (6,20,ERR=410,END=15) XSIDE(J)
        READ (6,20,ERR=410,END=15) YSIDE(J)
 10    CONTINUE
 15   N4=N4-1
C
C     CORRECT ALL SIDE2 DATA FOR PINCUSHION MAGNIFICATION. OMIT THE FIRST
C     COORDINATE OF STREAM MODE DUE TO POSSIBLE SPURIOUS NATURE AS A
C     RESULT OF THE SWITCHING BETWEEN SIDE1 AND SIDE2.
C
      S = N4+2
      N1OR2 = N
      CALL PCUSH
C
C     WRITE SIDE2 CO-ORDINATE PAIRS TO FILE SIDE2POINTS, BYPASSING ANY
C     CO-ORDINATE PAIR DUPLICATED IN THE FOLLOWING TWO CO-ORDINATE
C     PAIRS TO ENSURE THAT EVERY CONSECUTIVE SET OF 3 POINTS IS
C     DISTINCT. OMIT ALSO COORDINATES WHICH ARE NEGATIVE OR MORE THAN
C     11000 IN VALUE. THESE MAY BE PRESENT AS AN ARTIFACT OF THE
C     COORDINATE COLLECTION PROGRAM.
C
      N3 = N2-1
      N4 = N4+2
      DO 700  J=N4,N
        IF((J.LE.N).AND.(IABS(XSIDE(J)).GT.11000).OR.(IABS(YSIDE(J))
     &.GT.11000)) GOTO 11
        IF((J.LE.N-1).AND.(XSIDE(J).EQ.XSIDE(J+1)).AND.
     &(YSIDE(J).EQ.(YSIDE(J+1)))) GOTO 11
        IF((J.LE.N-2).AND.(XSIDE(J).EQ.XSIDE(J+2)).AND.
     &(YSIDE(J).EQ.(YSIDE(J+2)))) GOTO 11
        IF(J.LE.N-1) WRITE(8,600,ERR=450) XSIDE(J),YSIDE(J)
        IF(J.EQ.N) WRITE(8,600,ERR=450) XSIDE(J),YSIDE(J)
 600    FORMAT(2I7)
        GOTO 700
 11    N3 = N3-1
 700    CONTINUE
        N2 = N3
C
      GOTO 800
C
C
C     ------------------------------------------------------------------
C     FILE READ FORMAT STATEMENTS
C
 20   FORMAT(I7)
C     ------------------------------------------------------------------
C     ERROR MESSAGES
C
 30   WRITE(1,40)
 40   FORMAT('FILE BITPDCOORDS READ ERROR, ITEM 1')
      GOTO 9999
C
 50   WRITE(1,60)
 60   FORMAT('FILE BITPDCOORDS ERROR, END AT ITEM 1')
```

```
      GOTO 9999
C
 70   WRITE(1,80) FILDES(J-1),J
 80   FORMAT('FILE BITPDCOORDS READ ERROR, FILE DESCRIPTOR SECTION, ITEM
     & BELOW ',I5,' POSITION ',I5)
      GOTO 9999
C
 90   WRITE(1,100)
 100  FORMAT('FILE BITPDCOORDS ERROR, END IN FILE DESCRIPTOR SECTION, NO
     &STREAM MODE CO-ORDINATES READ')
      GOTO 9999
C
 110  WRITE(1,120) START1,CHECK1
 120  FORMAT('FILE BITPDCOORDS DESCRIPTOR RELATIONSHIP ERROR, START1.NE.
     &CHECK1, START1 = ',I5,'CHECK1 = ',I5,'SEE PROGRAM AND FILE')
      GOTO 9999
C
 130  WRITE(1,140) START2,CHECK2
 140  FORMAT('FILE BITPDCOORDS DESCRIPTOR RELATIONSHIP ERROR, START2.NE.
     &CHECK2, START2 = ',I5,' CHECK2 = ',I5,' SEE PROGRAM AND FILE')
      GOTO 9999
C
 150  WRITE(1,160) END2,CHECK3
 160  FORMAT('FILE BITPDCOORDS DESCRIPTOR RELATIONSHIP ERROR, END2.NE.CH
     &ECK3, END2 = ',I5,' CHECK3 = ',I5,' SEE PROGRAM AND FILE')
      GOTO 9999
C
 170  WRITE(1,180)
 180  FORMAT('FILE BITPDCOORDS ERROR, FEWER THAN 3 CO-ORDINATE PAIRS IN
     &STREAM MODE SECTION FOR SIDE1')
      GOTO 9999
C
 190  WRITE(1,200)
 200  FORMAT('FILE BITPDCOORDS ERROR, FEWER THAN 3 CO-ORDINATE PAIRS IN
     &STREAM MODE SECTION FOR SIDE2')
      GOTO 9999
C
 250  P=STARTP + J - 1
      WRITE(1,260) XSIDE(J-1),YSIDE(J-1),P
 260  FORMAT('FILE BIPDCOORDS READ ERROR, POINT MODE SECTION, ITEM BELOW
     & ',I5,' ',I5,' POSITION ',I5)
      GOTO 9999
C
 270  P = STARTP + J - 1
      WRITE(1,280) XSIDE(J-1),YSIDE(J-1),P
 280  FORMAT('FILE BITPDCOORDS ERROR IN POINT MODE SECTION, END BELOW IT
     &EM ',I5,' ',I5,' POSITION ',I5)
      GOTO 9999
C
 290  WRITE(1,300) START1
 300  FORMAT('FILE BITPDCOORDS READ ERROR, STREAM MODE SECTION, AT FIRST
     &ITEM POSITION',I5)
      GOTO 9999
C
 310  P = START1 + J - 1
      WRITE(1,320) START1
 320  FORMAT('FILE BITPDCOORDS ERROR, END IN STREAM MODE SECTION AT FIRS
     &T ITEM  POSITION ',I5)
      GOTO 9999
C
 330  P = START1 + J - 1
      WRITE(1,340) XSIDE(J-1),YSIDE(J-1),P
 340  FORMAT('FILE BITPDCOORDS READ ERROR, STREAM MODE SECTION, ITEM BEL
```

```
     &OW ',I5,' ',I5,' POSITION ',I5)
      GOTO 9999
C
 350  P=START1+J-1
      WRITE(1,360) XSIDE(J-1),YSIDE(J-1),P
 360  FORMAT('FILE BITPDCOORDS ERROR END SIDE 1, STREAM MODE SECTION
     &AT ITEM BELOW ',I5,' ',I5,' POSITION ',I5)
C
 370  WRITE(1,380) XSIDE(N1),YSIDE(N1),START2
 380  FORMAT('FILE BITPDCOORDS READ ERROR, STREAM MODE SECTION AT
     &FIRST ITEM FOR SIDE 2, ITEM BELOW ',I5,' ',I5,' POSITION ',I5)
C
 390  WRITE(1,400) START2
 400  FORMAT('FILE BITPDCOORDS ERROR, END IN STREAM MODE SECTION AT
     &FIRST ITEM FOR SIDE 2, POSITION ',I5)
C
 410  P=START2+J-1
      WRITE(1,420) XSIDE(J-1),YSIDE(J-1),P
 420  FORMAT('FILE BITPDCOORDS READ ERROR,SIDE 2, STREAM MODE
     &SECTION AT ITEM BELOW ',I5,' ',I5,' POSITION ',I5)
C
 430  WRITE(1,440) J
 440  FORMAT('WRITE ERROR-SIDE1POINTS;COINCIDENT POINT TEST:ITEM',I5)
      GOTO 9999
C
 450  WRITE(1,460) J
 460  FORMAT('WRITE ERROR-SIDE2POINTS;COINCIDENT POINT TEST:ITEM',I5)
      GOTO 9999
C
C
C     ------------------------------------------------------------------
C
 800  ENDFILE 6
      ENDFILE 7
      ENDFILE 8
      ENDFILE 9
C
C
C     ------------------------------------------------------------------
C     REMOVE GLITCHES DUE TO HAND TREMOR.  THESE ARE DEFINED TO BE DOUBLE
C     REVERSALS OF TRACING DIRECTION WITHIN A CIRCLE OF RADIUS EQUAL TO
C     HAND-TRACING TOLERANCE.  THE CIRCLE IS CENTRED ON THE MIDDLE OF
C     EACH CONSECUTIVE SET OF THREE DISTINCT POINTS.  THE PRECEEDING POINT
C     AND CENTRE POINT DEFINE CURRENT DIRECTION WHILE THE LAST POINT OF
C     THE SET IS USED TO INDICATE ANY CHANGE IN CURRENT DIRECTION.  THE
DIAMETER
C     OF THE CIRCLE PERPENDICULAR TO CURRENT DIRECTION GIVES THE BOUNDARY
C     ACROSS WHICH TESTS FOR REVERSAL ARE MADE.  A FIRST REVERSAL OCCURS
C     IF THE LAST POINT OF THE SET OF 3 LIES WITHIN THE CIRCLE AND ON
C     THE SAME SIDE OF THE BOUNDARY AS THE FIRST POINT OF THE SET OF 3.
C     A SECOND REVERSAL OCCURS IF THERE HAS BEEN A FIRST REVERSAL, AND ANY
C     POINT FOLLOWING THE LAST OF THE SET OF 3 LIES WITHIN THE CIRCLE
C     WHILE BEING ON THE OPPOSITE SIDE OF THE BOUNDARY TO THE FIRST POINT
C     OF THE SET OF 3. WHENEVER A DOUBLE REVERSAL OCCURS, ALL POINT LYING
C     WITHIN THE CIRCLE ARE CONSIDERED TO BE SPURIOUS AND ARE OMITTED FROM
C     THE TOTAL SET.
C     ------------------------------------------------------------------
C
      F = -1
 825  F = F+1
C
      IF(F.EQ.0) N1OR2 = N1
      IF(F.EQ.1) N1OR2 = N2
C
C     SIDE1:
```

```
C     READ POINTS FROM FILE SIDE1POINTS INTO XSIDE( ),YSIDE( )
C
      IF(F.EQ.0) CALL OPEN(7,'SIDE1POINTS',0)
C
C     SIDE2:
C     READ POINTS FROM FILE SIDE2POINTS INTO XSIDE( ),YSIDE( )
C
      IF(F.EQ.1) CALL OPEN(8,'SIDE2POINTS',0)
C
      DO 900 J = 1,N1OR2
      IF(F.EQ.0) READ(7,850,END=900) XSIDE(J),YSIDE(J)
      IF(F.EQ.1) READ(8,850,END=900) XSIDE(J),YSIDE(J)
 850  FORMAT(2I7)
 900  CONTINUE
C
C     REWIND FILES.
C
      IF(F.EQ.0) REWIND 7
      IF(F.EQ.1) REWIND 8
C
C     WRITE FIRST COORDINATE TO FILE.
C
      J = 1
      IF(F.EQ.0) WRITE(7,1000,ERR=5000) XSIDE(J),YSIDE(J)
      IF(F.EQ.1) WRITE(8,1000,ERR=5200) XSIDE(J),YSIDE(J)
C
C     SINCE HAND TREMOR IS MOST PREVALANT AT THE ONSET OF TRACING, NO
C     SUCCESSIVE CO-ORDINATES ARE WRITTEN TO FILE UNTIL INITIAL TOLERANCE
C     BOUNDRY IS EXCEEDED. THIS ENSURES ALSO THAT CORRECT DIRECTION
C     OF VECTOR IS ESTABLISHED. INTEGER VALUES ARE CONVERTED TO DOUBLE
C     PRECISION TO ALLOW ACCURATE COMPUTATION OF DISTANCE.
C
C     FINDING FIRST CO-ORDINATE PAIR OUTSIDE TOLERANCE LIMIT.
C
      X(J) = (XSIDE(J))
      Y(J) = (YSIDE(J))
C
 950  J = J+1
      X(J) = (XSIDE(J))
      Y(J) = (YSIDE(J))
C
      DIST=DSQRT((X(J)*X(J)+X(1)*X(1)+Y(J)*Y(J)+Y(1)*Y(1))
     &-2*(X(J)*X(1)+Y(J)*Y(1)))
      IF(DIST.LE.TOL) GOTO 950
C
C     FILE FORMAT STATEMENT
 1000 FORMAT(2I7)
C
C     PUT COORDINATES OF FIRST THREE POINTS INTO1,Y1 X2,Y2 X3,Y3
RESPECTIVELY.
C
      X1 = XSIDE(1)
      Y1 = YSIDE(1)
C
      X2 = XSIDE(J)
      Y2 = YSIDE(J)
C
      X3 = XSIDE(J+1)
      Y3 = YSIDE(J+1)
C
C
C     INITIALISE F3 FOR EXISTENCE OF COORDINATE PAIR X4,Y4
C
```

```
      F3 = 0
C
C     SET F4 FOR SUBROUTINE FILLIN.
C
      F4 = 0
C
      GOTO 2600
C
C
C     FOLLOWING THE FIRST PASS, FILL STORES WITH EDITED POINTS.
C
 2000 J = J+1
      IF(J.GE.N1OR2) GOTO 4000
C
      IF(Q.EQ.0) X1 = X2
      IF(Q.EQ.0) Y1 = Y2
C
      IF(F3.EQ.0) X2 = X3
      IF(F3.EQ.0) Y2 = Y3
      IF(F3.EQ.1) X2 = X4
      IF(F3.EQ.1) Y2 = Y4
C
C     RESET F3
      F3 = 0
C
C
      X3 = XSIDE(J+1)
      Y3 = YSIDE(J+1)
C
C     CHECK DATA FOR SEGMENTS FORMING RIGHT ANGLES SINCE THESE ARE TRUE
C     ERRORS WHICH MAY GO UNDETECTED USING THIS SYSTEM.
C
 2600 P = 0
      Q = 0
C
C
C     CONVERT X1,Y1,X2,Y2,X3,Y3 TO INTEGERS TO FACILITATE RIGHT ANGLE
C     CHECK AND WRITE COMMANDS.
C
      XI1 = X1
      YI1 = Y1
      XI2 = X2
      YI2 = Y2
      XI3 = X3
      YI3 = Y3
C
      IF((XI2.EQ.XI3).AND.(YI2.EQ.YSIDE(J-1))) P = 1
      IF((YI2.EQ.YI3).AND.(XI2.EQ.XSIDE(J-1))) P = 1
C
C     BYPASS BELOW COMPUTATIONS IF X1,Y1=X2,Y2 OR X2,Y2=X3,Y3. THIS CAN
C     OCCUR FOLLOWING REVERSAL ERADICATION WHICH TEMPORARILY UPSETS THE
C     'CLEANLYNESS' OF EVERY THREE COORDINATE PAIRS. THE FLAG Q DETECTS
C     THIS AND IF RAISED PREVENTS PROBLEMS REGARDING FOLLOWING NEARBY
C     REVERSALS.
C
      IF((XI1.EQ.XI2).AND.(YI1.EQ.YI2)) Q = 1
      IF((XI2.EQ.XI3).AND.(YI2.EQ.YI3)) Q = 1
      IF(Q.EQ.1) GOTO 2000
      Q = 0
C
      IF((P.EQ.1).AND.(J.LE.N1OR2-3))  X2 = XSIDE(J+2)
      IF((P.EQ.1).AND.(J.LE.N1OR2-3))  Y2 = YSIDE(J+2)
      IF((P.EQ.1).AND.(J.LE.N1OR2-3))  XI2 = XSIDE(J+2)
```

```
      IF((P.EQ.1).AND.(J.LE.N1OR2-3))  YI2 = YSIDE(J+2)
C
      IF((P.EQ.1).AND.(J.LE.N1OR2-3))  X3 = XSIDE(J+3)
      IF((P.EQ.1).AND.(J.LE.N1OR2-3))  Y3 = YSIDE(J+3)
      IF((P.EQ.1).AND.(J.LE.N1OR2-3))  XI3 = XSIDE(J+3)
      IF((P.EQ.1).AND.(J.LE.N1OR2-3))  YI3 = YSIDE(J+3)
C
C     CHECK FOR THE EQUIVALENCE OF X2,Y2 X3,Y3 AND X1,Y1 X2,Y2. THIS
C     WILL OCCUR ON THE SECOND PASS FOLLOWING RIGHT ANGLE DETECTION.
C     IF FULFILLED A NEW SET OF COORDINATES ARE PICKED UP BY INCREMENTING J.
C
      IF((XI1.EQ.XI2).AND.(YI1.EQ.YI2)) GOTO 2000
      IF((XI2.EQ.XI3).AND.(YI2.EQ.YI3)) GOTO 2000
C
C     PUT DISTANCE BETWEEN X2,Y2 AND X3,Y3 INTO DIST1
C
C     CLEAR DIST1
C
      DIST1 = 0.0
C
      DIST1 = DSQRT((X3*X3 + X2*X2 + Y3*Y3 + Y2*Y2) - 2*(X3*X2 + Y3*Y2))
C
C     IF A FIRST REVERSAL HAS OCURRED, SET REVERSAL FLAG R TO 1
C
      R = 0
      IF((PPSIDE(X3,Y3).EQ.PPSIDE(X1,Y1)).AND.(DIST1.LE.TOL)) R = 1
      IF((PPSIDE(X3,Y3).EQ.0).AND.(DIST1.LE.TOL)) R = 1
C
C     IF A REVERSAL HAS NOT OCCURED AND F4 = 0, FILL IN MISSING DATA.
C
      IF((F4.EQ.0).AND.(R.EQ.0)) CALL FILLIN
      F4 = 1
C
C     IF A FIRST REVERSAL HAS NOT OCCURRED, WRITE X2,Y2 TO FILE AND
C     TEST NEXT SET OF 3 CONSECUTIVE POINTS
C
      IF((R.EQ.0).AND.(F.EQ.0)) WRITE(7,1000,ERR=5400) XI2,YI2
      IF((R.EQ.0).AND.(F.EQ.1)) WRITE(8,1000,ERR=5600) XI2,YI2
C
C     WRITE XI3,YI3 TO FILE IF THEY ARE THE LAST POINTS IN THE VECTOR.
C
      IF((J.EQ.N1OR2-1).AND.(R.EQ.0).AND.(F.EQ.0)) WRITE(7,1000,ERR=
     &5400) XI3,YI3
      IF((J.EQ.N1OR2-1).AND.(R.EQ.0).AND.(F.EQ.1)) WRITE(8,1000,ERR=
     &5600) XI3,YI3
      IF(R.EQ.0) GOTO 2000
C
C     IF A FIRST REVERSAL HAS OCCURRED, LOOK FOR A SECOND REVERSAL
C     WITHIN THE TOLERANCE CIRCLE CENTRED ON X2,Y2. SET FLAG F1 TO
C     1 IF POINT TESTED IS WITHIN CIRCLE; SET FLAG F2 TO 1 IF POINT
C     TESTED IS ON SAME SIDE OF BOUNDARY AS THAT GIVING FIRST REVERSAL.
C     IF BOTH CONDITIONS HOLD, CONTINUE TESTING POINTS FORWARD OF X3,Y3
C
      K = J
C
 3000 K = K + 1
C
C
C     IF THE END OF THE VECTOR IS REACHED AS K INCREMENTS (i.e. A
C     REVERSAL HAS BEEN DETECTED BUT IT IS THE LAST POINT) WRITE
C     XI2,YI2 TO FILE.
C
      IF((K.GE.N1OR2).AND.(F.EQ.0)) WRITE(7,1000,ERR=5400) XI2,YI2
```

```
      IF((K.GE.N1OR2).AND.(F.EQ.1)) WRITE(8,1000,ERR=5600) XI2,YI2
C
      IF(K.GE.N1OR2) GOTO 4000
C
      F1 = 0
      F2 = 0
      F3 = 1
C
      X4 = XSIDE(K+1)
      Y4 = YSIDE(K+1)
      XI4 = X4
      YI4 = Y4
C
C     IF XI2,YI2 AND XI4,YI4 ARE EQUIVALENT, INCREMENT K FOR ANOTHER
C     XI4,YI4 COORDINATE PAIR
C
      IF((XI2.EQ.XI4).AND.(YI2.EQ.YI4)) GOTO 3000
C
C     PUT DISTANCE OF POINT UNDER TEST FROM X2,Y2 INTO DIST2
C
C     CLEAR DIST2
C
      DIST2 = 0.0
C
      DIST2 = DSQRT((X4*X4 + X2*X2 + Y4*Y4 + Y2*Y2) - 2*(X4*X2 + Y4*Y2))
C
      IF(DIST2.LE.TOL) F1 = 1
      IF((PPSIDE(X4,Y4)).EQ.(PPSIDE(X1,Y1))) F2 = 1
      IF(PPSIDE(X4,Y4).EQ.0) F2 = 1
C
      IF((F1.EQ.1).AND.(F2.EQ.1)) GOTO 3000
C
C     FORWARD TESTING STOPS IF POINT UNDER TEST IS EITHER OUTSIDE
C     CIRCLE OR IF IT IS ON OPPOSITE SIDE OF BOUNDARY TO X3,Y3 GIVING A
C     FIRST REVERSAL.
C
      J = K
C
C     ONCE A SATISFACTORY POINT HAS BEEN FOUND FOLLOWING A REVERSAL,
C     WRITE XI2,YI2 TO FILE.
C
      IF(F.EQ.0) WRITE(7,1000,ERR=5400) XI2,YI2
      IF(F.EQ.1) WRITE(8,1000,ERR=5600) XI2,YI2
C
C     IF X4,Y4 REPRESENTS THE LAST COORDINATE OF THE VECTOR, WRITE
C     XI4,YI4 TO FILE.
C
      IF((J.EQ.N1OR2-1).AND.(F.EQ.0)) WRITE(7,1000,ERR=5400) XI4,YI4
      IF((J.EQ.N1OR2-1).AND.(F.EQ.1)) WRITE(8,1000,ERR=5600) XI4,YI4
C
C
C
C     TEST NEXT SET OF 3 CONSECUTIVE POINTS
C
      GOTO 2000
C
 4000 IF(F.EQ.0) GOTO 825
C
      GOTO 9999
C
C     ---------------------------------------------------------------
C     ERROR MESSAGES
C
```

```
 5000 WRITE(1,5100)
 5100 FORMAT('WRITE ERROR-SIDE1POINTS:REVERSAL TESTING:ITEM1')
      GOTO 9999
C
 5200 WRITE(1,5300)
 5300 FORMAT('WRITE ERROR-SIDE2POINTS:REVERSAL TESTING:ITEM1')
      GOTO 9999
C
 5400 WRITE(1,5500)
 5500 FORMAT('WRITE ERROR-SIDE1POINTS:REVERSAL TESTING:')
      GOTO 9999
C
 5600 WRITE(1,5700)
 5700 FORMAT('WRITE ERROR-SIDE2POINTS:REVERSAL TESTING:')
      GOTO 9999
C
C     ------------------------------------------------------------------
C
 9999 ENDFILE 7
      ENDFILE 8
C
      STOP
C
      END
C     ************************************************************************
C
      SUBROUTINE PCUSH
C
      INTEGER XSIDE(2000),YSIDE(2000),X,Y,S,CATHRM,MAGVAL
C
      DOUBLE PRECISION A,B,C,R,K,XDISP,YDISP,XC,YC
C
      COMMON/SET1/XSIDE,YSIDE/SET2/S,N1OR2/SET6/XC,YC,CATHRM,MAGVAL
C     ------------------------------------------------------------------
C
C     THIS ROUTINE CORRECTS FOR SELECTIVE MAGNIFICATION OF OBJECTS NEAR
C     TO THE EDGES OF THE CINE FRAME (AS COMPARED WITH THEIR SIZE AT THE
C     CENTRE OF THE FIELD: THE PINCUSHION DISTORTION EFFECT).
C     THIS OCCURS AS A DIRECT RESULT OF THE CONVEX-CURVED NATURE OF THE
C     INPUT PHOSPHOR VACUUM TUBE.
C
C     C IS AN EMPIRICALLY DERIVED CONSTANT SPECIFIC TO THE CATHETER ROOM
C     USED WHICH IS A COMPONENT OF THE EQUATION WHICH CHARACTERISES THE
C     DISTORTION:
C                    DELTA R' = DELTA R/(1 + C(R*R))
C
C         WHERE:     DELTA R' = THE GRID INTERVAL THAT WOULD BE MEASURED
C                               WITHOUT PINCUSHION DISTORTION.
C                     DELTA R = THE MEASURED GRID INTERVAL
C                           C = EMPIRICALLY DERIVED CONSTANT
C                           R = RADIAL DISTANCE FROM CENTRE OF FIELD TO
C                               POINT OF INTEREST.
C
C     ------------------------------------------------------------------
C
      IF((CATHRM.EQ.1).AND.(MAGVAL.EQ.1)) C = 0.0020136
      IF((CATHRM.EQ.1).AND.(MAGVAL.EQ.2)) C = 0.00062484
      IF((CATHRM.EQ.2).AND.(MAGVAL.EQ.1)) C = 0.00065315
      IF((CATHRM.EQ.2).AND.(MAGVAL.EQ.2)) C = 0.00053700
C
      A = DSQRT(C)
      B = 1/A
C
C     USE XC,YC AS THE IMAGE CENTRE AS CALCULATED IN THE MAIN PROGRAM.
```

```
C     CALCULATE THE RADIAL DISTANCE FROM THIS POINT TO THE POINT OF
C     INTEREST. OBTAIN PINCUSHION CORRECTED VALUES FROM SUBSTITUTION
C     INTO THE EQUATION. DISPLACEMENTS ARE INITIALLY CORRECTED TO CENTIMETERS
C     SINCE THE CONSTANT C IS EXPRESSED IN CM-2.
C
      DO 10 J=S,N1OR2
        IF((X.EQ.XSIDE(J)).AND.(Y.EQ.YSIDE(J))) GOTO 10
        XDISP = XC-XSIDE(J)
        YDISP = YC-YSIDE(J)
        IF((DABS(XDISP).LE.1.0D-36).AND.(DABS(YDISP).LE.1.0D-36))
     &GOTO 10
        XDISP = XDISP/393.7
        YDISP = YDISP/393.7
        R = DSQRT(XDISP*XDISP+YDISP*YDISP)
        K = (B*DATAN(R*A))/R
        XSIDE(J) = IDINT((K*XSIDE(J))+0.5)
        YSIDE(J) = IDINT((K*YSIDE(J))+0.5)
 10   CONTINUE
C
      RETURN
C
      END
C     ********************************************************************************
      FUNCTION PPSIDE(X,Y)
C
      INTEGER PPSIDE
      DOUBLE PRECISION R,SINGRA,COSGRA,XPERP1,YPERP1,XPERP2,YPERP2
      DOUBLE PRECISION PERPLN,X1,Y1,X2,Y2,TOL,X,Y
C
      COMMON/SET3/TOL/SET4/X1,Y1/SET5/X2,Y2
C
C     ------------------------------------------------------------------------
C     THIS SUBROUTINE DETECTS THE DIRECTION OF THE DATA VECTOR. EQUAL VALUES
C     OF PPSIDE REFLECT REVERSALS WHERAS UNEQUAL VALUES IMPLY A CONSTANT
C     DIRECTION.
C     ------------------------------------------------------------------------
C     PUT SINE AND COSINE OF X1,Y1 TO X2,Y2 GRADIENT ANGLE INTO
C     SINGRA, COSGRA RESPECTIVELY
C
      R = DSQRT((X2*X2 + X1*X1 + Y2*Y2 + Y1*Y1) - 2*(X2*X1 + Y2*Y1))
      SINGRA = (Y2 - Y1)/R
      COSGRA = (X2 - X1)/R
C
C     PUT END POINTS OF TOLERANCE CIRCLE DIAMETER PERPENDICULAR TO X1,Y1
C     X2,Y2 INTO XPERP1,YPERP1 AND XPERP2,YPERP2.
C
      XPERP1 = X2 + SINGRA*TOL
      YPERP1 = Y2 - COSGRA*TOL
C
      XPERP2 = X2 - SINGRA*TOL
      YPERP2 = Y2 + COSGRA*TOL
C
C     PUT REGION DEFINITION OF X,Y IN RELATION TO DIAMETER AS BOUNDARY
C     INTO PERPLN.
C
      PERPLN = 0.0
      PERPLN = (YPERP2 - YPERP1)*X + (XPERP1 - XPERP2)*Y + (XPERP2*Y2 +
     &YPERP1*X2) - (XPERP1*Y2 + YPERP2*X2)
C
C     SET PPSIDE TO 1 OR -1 ACCORDING TO REGION OF X,Y OR SET PPSIDE
C     TO 0 IF X,Y IS IN BOUNDARY LINE, ALLOWING FOR LIMITS OF COMPUTING
C     ACCURACY.
C
```

```
      IF(PERPLN.LE.-1.0D-36) PPSIDE = -1
      IF(PERPLN.GE. 1.0D-36) PPSIDE =  1
      IF((PERPLN.GT.-1.0D-36).AND.(PERPLN.LT.1.0D-36)) PPSIDE = 0
C
      RETURN
      END
C     ***************************************************************************
C
      SUBROUTINE FILLIN
C
      INTEGER F,XSIDE(2000),YSIDE(2000),XI2,YI2,MPX1,MPY1,MPX2,MPY2
      INTEGER MPX3,MPY3,J
C
      COMMON/SET1/XSIDE,YSIDE/SET7/XI2,YI2,F,J
C     ---------------------------------------------------------------------
C     DUE TO THE FACT THAT THE MAIN PROGRAM OMITS INITIAL COORDINATES
C     UNTIL THE TOLERANCE LIMIT IS EXCEEDED IN ORDER TO ESTABLISH THE
C     VECTOR DIRECTION CORRECTLY, THIS GAP MUST BE 'FILLED IN' SO AS TO
C     OBTAIN REASONABLY SPACED SEQUENTIAL DIAMETER LINES. THIS IS ACHEIVED
C     BY CALCULATING THE MIDPOINT OF THE SEGMENT JOINING THE FIRST AND
C     SECOND COORDINATES FOLLOWED BY THE MIDPOINTS OF THE SEGMENTS CREATED
C     BY THE CALCULATION OF THIS POINT. THESE VALUES ARE THEN WRITTEN
C     TO THEIR RESPECTIVE FILES DEPENDING ON THE VALUE OF F.
C     ---------------------------------------------------------------------
C
      MPX2 = ((XSIDE(1) + XSIDE(J))/2)+1
      MPY2 = ((YSIDE(1) + YSIDE(J))/2)+1
C
      MPX1 = (XSIDE(1)+MPX2)/2
      MPY1 = (YSIDE(1)+MPY2)/2
C
      MPX3 = (MPX2+XSIDE(J))/2
      MPY3 = (MPY2+YSIDE(J))/2
C
      IF(F.EQ.0) WRITE(7,10) MPX1,MPY1
      IF(F.EQ.0) WRITE(7,10) MPX2,MPY2
      IF(F.EQ.0) WRITE(7,10) MPX3,MPY3
C
      IF(F.EQ.1) WRITE(8,10) MPX1,MPY1
      IF(F.EQ.1) WRITE(8,10) MPX2,MPY2
      IF(F.EQ.1) WRITE(8,10) MPX3,MPY3
C
 10   FORMAT(2I7)
C
      RETURN
      END
C
C     ***************************************************************************
```

```
      PROGRAM DIAMAV
C
      INTEGER K,J,N1,N2,N,C,X(2000),Y(2000),A(2000),B(2000)
C
      REAL TRIARS(2000)
C
      DOUBLE PRECISION XSUM,YSUM,XC,YC,XA,YA,XB,YB,AREA,AVLEN,LEN
C
C
C     ------------------------------------------------------------------
C     PROGRAM DIAMAV IS THE FIRST OF THREE CHAINED PROGRAMS DESIGNED TO
C     CALCULATE DIAMETERS ALONG THE LENGTH OF AN ARTERY INTERIOR
C     WALL TRACED FROM X-RAY ON A TRANSPARENT DIGITISING TABLET.
C     THIS PROGRAM READS THE TWO ERROR FREE FILES PRODUCED BY THE
C     PROGRAM PNTED AND CALCULATES THE AREA ENCLOSED BY THE TWO
C     VECTORS, ALONG WITH THEIR AVERAGE LENGTH AND SEPARATION.
C     THE VALUE FOR THE AVERAGE SEPARATION OR DIAMETER IS THEN WRITTEN
C     TO FILE (AVERAGEDIAM) READY TO BE REFERENCED BY THE SECOND OF
C     THE THREE PROGRAMS (PROGRAM DIAMRS). HERE IT IS USED AS THE LENGTH
C     OF A MATHEMATICAL BUBBLE WHICH IS USED IN THE CALCULATION OF
C     THE ARTERY DIAMETERS.
C     TO FORM A CONTINUOUS LOOP, DATA FROM SIDE2POINTS IS READ INTO THE
C     VECTORS X(J),Y(J) IN REVERSE ORDER JOINING THE NORMALLY ARRANGED
C     DATA FROM SIDE1POINTS. THE LOOP IS THEN COMPLETED BY JOINING
C     THE THE FIRST COORDINATE IN SIDE1POINTS BY AN IMAGINARY LINE WITH
C     WHAT IS NOW THE LAST COORDINATE IN SIDE2POINTS, AND THE LAST
C     COORDINATE IN SIDE1POINTS WITH WHAT IS NOW THE FIRST COORDINATE
C     OF SIDE2POINTS. TO EVALUATE THE AREA ENCLOSED BY THE LOOP, THE
C     CENTROID OF THE POINTS DEFINING THE LOOP IS CALCULATED AND USED
C     AS A CENTRE AROUND WHICH A RADIAL VECTOR TO EACH POINT SWEEPS.
C     STARTING AT THE FIRST POINT ENTERED, THE AREA OF THE TRIANGLE
C     BETWEEN THE CENTROID, FIRST POINT AND THE SECOND POINT IS
C     OBTAINED AND STORED IN A VECTOR. THIS IS REPEATED FOR THE SECOND
C     TRIANGLE FORMED BETWEEN THE CENTROID, SECOND AND THIRD POINTS.
C     THIS PROCESS CONTINUES UNTIL THE WHOLE LOOP HAS BEEN TRAVERSED,
C     THE LAST TRIANGLE BEING THAT BETWEEN THE CENTROID, THE NTH POINT
C     AND THE FIRST POINT (WHICH IS WRITTEN TO THE Nth+1 POSITION OF
C     THE LOOP TO ENABLE THIS LAST TRIANGLE TO BE REFERENCED). THE TOTAL
C     AREA ENCLOSED BY THE LOOP IS OBTAINED BY SUMMING THE CONTENTS
C     OF THE VECTOR TRIARS( ).
C     EACH OF THE TRIANGLES FORMED WITH THE CENTROID HAS A BASE DEFINED
C     TO BE THE DIRECTED LINE FROM THE CENTROID TO THE FIRST TRACED
C     POINT OF THE TRIANGLE. ANY POINT IN THE PLANE WILL BE EITHER
C     TO THE LEFT, RIGHT OR ON THIS LINE. THE FUNCTION USED TO CALCULATE
C     TRIANGLE AREA GIVES AN AREA WHICH IS EITHER NEGATIVE OR POSITIVE
C     ACCORDING TO WHETHER THE SECOND POINT IS TO THE RIGHT OR LEFT
C     OF ITS BASE RESPECTIVLY. BY TAKING THE ABSOLUTE VALUE FOR AREA
C     NEGATIVE AND POSITIVE AREAS GIVEN BY THIS FUNCTION COMBINE
C     IN A MANNER WHICH ALLOWS FOR THE CALCULATION OF AREA FROM THE

C     INFOLDING OF ANY LOOP TRACED IN EITHER DIRECTION.
C
C     THE AVERAGE DIAMETER IS CALCULATED AS THE AREA DIVIDED BY THE
C     MEAN OF THE SIDE LENGTHS AND PUT INTO VARIABLE AVERAGEDIAM.
C
C
C     ------------------------------------------------------------------
C     READ 'SIDE1POINTS' INTO X( ),Y( ) THEN 'SIDE2POINTS' (IN REVERSE

C     ORDER INTO X( ), Y( ).
C
      CALL OPEN(6,'SIDE1POINTS',0)
C
      N1 = 1
      J = 1
```

```
C
      READ(6,20) X(J),Y(J)
 4    J = J+1
      READ(6,20,END=5) X(J),Y(J)
      N1 = N1+1
      GOTO 4
C
 5    CALL OPEN(7,'SIDE2POINTS',0)
C
      N2 = 1
      J = N1+1
C
      READ(7,20) A(J),B(J)
 6    J = J+1
      READ(7,20,END=7) A(J),B(J)
      N2 = N2+1
      GOTO 6
C
C     OBTAIN TOTAL.
C
 7    N = N1+N2
C
C     IN ORDER TO FORM A CONTINUOUS LOOP, THE DIRECTION OF COORDINATES
C     FROM SIDE2POINTS MUST BE REVERSED.
C
      J = N+1
      N1 = N1+1
      DO 10 C=N1,N
        J = J-1
        X(J) = A(C)
        Y(J) = B(C)
 10   CONTINUE
      N1 = N1-1
C
      GOTO 430
C
C     ------------------------------------------------------------------
C     FILE READ FORMAT STATEMENT
C
 20   FORMAT(2I7)
C
C     ------------------------------------------------------------------
C     CLOSE THE LOOP
C
 430  X(N+1) = X(1)
      Y(N+1) = Y(1)
C
C     PUT LOOP CENTROID COORDINATES INTO XC,YC ENSURING THAT THE FIRST/
C     LAST POINT CONTRIBUTES TO THE CENTROID CALCULATIONS ONCE ONLY.
C
      XSUM = 0.0
      YSUM = 0.0
C
      DO 440 J = 1,N
        XSUM = XSUM+X(J)
        YSUM = YSUM+Y(J)
 440  CONTINUE
C
      XC = XSUM/N
      YC = YSUM/N
C
C     ROTATE BASE VECTOR ROUND LOOP, ACCUMULATE SEGMENT LENGTHS AND PUT
C     SIGNED TRIANGLE AREAS INTO VECTOR TRIARS( ). ACCUMULATE TRIARS( )
C     INTO AREA.
```

```
C
      LEN = 0.0
      AREA = 0.0
C
      DO 450 J = 1,N
        XA = X(J)
        YA = Y(J)
        XB = X(J+1)
        YB = Y(J+1)
C
        LEN = (LEN+(DSQRT((XA*XA+XB*XB+YA*YA+YB*YB)-2*(XA*XB+YA*YB))))
C
        TRIARS(J) = ((YB*XA+YC*XB+YA*XC)-(YB*XC+YC*XA+YA*XB))/2.0
C
        AREA = AREA + TRIARS(J)
C
 450  CONTINUE
C
C     TAKE ABSOLUTE VALUE OF AREA THEREBY MAKING CALCULATIONS INDEPENDANT
C     OF DIRECTION OF TRACE.
C
      AREA = DABS(AREA)
C
C     CALCULATE THE AVERAGE ARTERY SIDE LENGTH AND ITS DIAMETER.
C
      AVLEN = 0.0
      AVDIAM = 0.0
C
      AVLEN = LEN/2.0
      AVDIAM = AREA/AVLEN
C
C     DISPLAY RESULTS.
C
      WRITE(1,470) AREA,AVLEN,AVDIAM
 470  FORMAT( ' AREA = ',F16.5,' AVLEN = ',F16.5,' AVDIAM = ',F16.5)
C
C     WRITE THE AVERAGE DIAMETER (WHICH BECOMES THE BUBBLE LENGTH IN THE
C     FOLLOWING PROGRAM) TO DISK.
C
      CALL OPEN(8,'AVERAGEDIAM',0)
      WRITE(8,480) AVDIAM
 480  FORMAT(F16.5)
C
C     CLOSE FILES AND END PROGRAM
C
 9999 ENDFILE 6
      ENDFILE 7
      ENDFILE 8
C
      STOP
C
      END
C
C     ***************************************************************************
```

```
      PROGRAM DIAMRS
C
      INTEGER XSIDE1(1000),YSIDE1(1000),XSIDE2(1000),YSIDE2(1000)
      INTEGER F1,F2,DISUB,STBUB1,STBUB2,BUBAVP,N1,N2,J,S,ENDERR,BUBPTS
      INTEGER SCAN1,ENBUB1,SCAN2,ENBUB2,SUMPT1,SUMPT2,AVPTS1,AVPTS2
      INTEGER BEGIN1,BEGIN2,START1,END1,START2,END2,STAGE
C
      DOUBLE PRECISION BUBLEN,LEN1,LEN2,MINANG,LENA,LENB,LENC,LEND
      DOUBLE PRECISION LENTHI,PI
C
      COMMON/SET1/N1,N2/SET2/MINANG/SET3/BEGIN1,BEGIN2/SET4/ENDERR
      COMMON/SET5/XSIDE1,YSIDE1,XSIDE2,YSIDE2
      COMMON/SET6/STBUB1,ENBUB1,STBUB2,ENBUB2/SET7/PI/SET8/DISUB
      COMMON/SET9/START1,END1,START2,END2/SET10/STAGE
C     ------------------------------------------------------------------
C
C     PROGRAM DIAMRS FOLLOWS PROGRAM DIAMAV AS THE SECOND OF THREE CHAINED
C     PROGRAMS DESIGNED TO CALCULATE ARTERY DIAMETERS. PROGRAM DIAMRS
C     READS THE COORDINATE FILES PRODUCED BY THE PROGRAM PNTED
C     FOLLOWING AREA CALCULATION BY THE PROGRAM DIAMAV INTO THE VECTORS
C     XSIDE1( ),YSIDE1( ) AND XSIDE2( ),YSIDE2( ).
C
C     BECAUSE THE DISTRIBUTION OF POINTS IN SIDE1 AND SIDE2 ARE UNEVEN, AND
THE
C     INTERNAL SHAPE AND BENDING OF THE ARTERY CAN VARY, IT IS DIFFICULT
C     TO IDENTIFY PAIRS OF POINTS(ONE IN SIDE1, THE OTHER IN SIDE2)
C     THAT CAN BE SAID TO BE OPPOSITE ENDS OF A DIAMETER. USE OF MINIMUM
C     ANGLES OF INTERSECTION AND MINIMUM DISTANCE BETWEEN SIDES TEND TO
C     BE VUNERABLE TO UNFORTUNATE COMBINATIONS OF INTERNAL SHAPE, BENDING
C     OR DISTRIBUTION. THIS ALGORITHM IS AN ATTEMPT TO OVERCOME THESE
C     PROBLEMS. IT RESTS UPON TWO ASSUMPTIONS:  1). THAT BENDING CAN BE
TRACKED
C     WITH REASONABLE ACCURACY OVER A DISTANCE EQUAL TO ITS AVERAGE
C     INTERNAL DIAMETER(WHICH IS THE VALUE SUPPLIED BY THE PROGRAM DIAMAV).
C     THIS ASSUMPTION IS GIVEN EFFECT BY PASSING A MATHEMATICAL BUBBLE
C     DOWN THE ARTERY SUCH THAT THE LENGTH OF THE BUBBLE IS EQUAL TO THE
C     AVERAGE DIAMETER. THE BUBBLE STARTS AT THE TOP(LOW SUBSCRIPT) ENDS
C     OF THE SIDES, EXPANDS TO FULL LENGTH, MOVES DOWN THE ARTERY(IN
C     ONE POINT INCREMENTS ON EITHER SIDE) AND CONTRACTS AGAINST THE BOTTOM
C     END. WITHIN EACH EXPANDING, MOVING AND CONTRACTING BUBBLE, ONE AXIS
C     POINT AND TWO DIAMETER END POINTS ARE DEFINED:THE CO-ORDINATES
C     OF THESE ARE CALCULATED. 2).  THAT THE MID-POINT OF LINES CONNECTING
C      THE TOP AND BOTTOM OF A BUBBLE GIVES A REASONABLE FIRST
C      APPROXIMATION TO AN AXIS POINT. THE DIAMETER THROUGH THE AXIS
C     POINT IS THEN DEFINED AS THE LINE PERPENDICULAR TO THE LINE BISECTED
C     BY THE AXIS POINT. DIAMETER END POINTS ARE ESTABLISHED BY SEARCHING
EACH
C      SIDE FOR THE SEGMENT WHICH INTERSECTS THE DIAMETER LINE AND
C     CALCULATING THE POINTS OF INTERSECTION. FOR SPEED, THE SEARCH
C     ALWAYS STARTS FROM THE LAST COORDINATE FOUND AND REVERSES
C     WHEN DISTANCE OF TESTED SEGMENTS FROM THE DIAMETER LINE APPEARS TO
C     INCREASE. ONCE LOCATED, DIAMETER END POINTS ARE WRITTEN TO FILE.
C     ------------------------------------------------------------------
C     PUT INTO MINANG A CONSTANT REFLECTING THE MINIMAL ANGLE
C     OBTAINABLE BETWEEN ANY DIAMETER LINE AND ANY ARTERY SIDE. THIS IS
C     USED IN DETERMINING ERRORS OF INTERSECTION.
C
      MINANG = 3.33333321D-4
C
C     SET PI
      PI = 3.141592654
C
C
```

```
C     READ 'SIDE1POINTS' INTO XSIDE1( ),YSIDE1( ) AND 'SIDE2POINTS' INTO
C     XSIDE2( ), YSIDE2( ).
C
      CALL OPEN(6,'SIDE1POINTS',0)
C
      N1 = 1
      J = 1
C
      READ(6,20,ERR=290) XSIDE1(J),YSIDE1(J)
 4    J = J+1
      READ(6,20,ERR=290,END=5) XSIDE1(J),YSIDE1(J)
      N1 = N1+1
      GOTO 4
C
 5    CALL OPEN(7,'SIDE2POINTS',0)
C
      N2 = 1
      J = 1
C
      READ(7,20,ERR=290) XSIDE2(J),YSIDE2(J)
 6    J = J+1
      READ(7,20,ERR=290,END=7) XSIDE2(J),YSIDE2(J)
      N2 = N2+1
      GOTO 6
C
C     READ AVERAGE ARTERY DIAMETER FROM FILE AVERAGEDIAM INTO BUBLEN
C     WHICH IS THE LENGTH OF THE BUBBLE PASSED DOWN THE SIDES FOR
C     CALCULATING AXIS POINT CO-ORDINATES
C
 7    CALL OPEN(8,'AVERAGEDIAM',0)
      READ(8,25,ERR=310) BUBLEN
C
      ENDFILE 8
C
C     ------------------------------------------------------------------
C     FILE READ FORMAT STATEMENTS
C
 20   FORMAT(2I7)
 25   FORMAT(F16.3)
C
C     ------------------------------------------------------------------
      GOTO 6010
C     ------------------------------------------------------------------
C     ERROR MESSAGES
C
 290  WRITE(1,300)
 300  FORMAT('FILE BITPDCOORDS READ ERROR, STREAM MODE SECTION')
      GOTO 9999
C
 310  WRITE(1,320)
 320  FORMAT('FILE AVERAGEDIAM READ ERROR')
      GOTO 9999
C
C     ------------------------------------------------------------------
C
C     OPEN NEW FILE FOR DIAMETER POINTS OF INTERSECTION
C
 6010 CALL OPEN(8,'DIAMETEREPS',0)
C
C     EXPAND BUBBLE FROM LOWEST SIDE SUBSCRIPTS DOWNWARDS (IN DIRECTION
C     OF SUBSCRIPT INCREASING)
C     SCAN1,SCAN2 ARE SIDE1,SIDE2 SUBSCRIPTS
C     STBUB1,STBUB2 ARE START-OF-BUBBLE SIDE1,SIDE2 SUBSCRIPTS
```

```
C     ENBUB1,ENBUB2 ARE   END-OF-BUBBLE SIDE1,SIDE2 SUBSCRIPTS
C     LEN1,LEN2 ARE LENGTH-OF-BUBBLE ON SIDE1,SIDE2 AS MEASURED FROM
C     STBUB1,STBUB2.
C
C     THIS SECTION TO EXPAND THE BUBBLE AND THE FOLLOWING TWO SECTIONS
C     TO MOVE AND CONTRACT IT AND ARE DESIGNED TO SET VALUES FOR
C     STBUB1,STBUB2,ENBUB1,ENBUB2 WHICH ARE USED TO SET THE LOCATION
C     OF THE AXIS POINTS ACCORDING TO THE BUBBLE LENGTH. THESE VALUES
C     ARE THEN TEMPORARILY ADJUSTED BY THE SUBROUTINE ADJBUB IN ORDER
C     TO MINIMISE THE POSSIBILITY OF DIAMETER END POINTS NOT FOUND.
C     THE ADJUSTED VALUES ARE THEN USED BY THE SUBROUTINE AXDIAS TO
C     COMPUTE DIAMETER END COORDINATES.
C
C     F1,F2 ARE FLAGS WHICH DETECT WHEN SIDE1,SIDE2 HAVE REACHED
C     FULL BUBBLE LENGTH. ONCE BOTH SIDES HAVE ACHIEVED THIS, THE BUBBLE
C     MAY THEN BE MOVED DOWN THE ARTERY.
C
C     IN ORDER TO AVOID DIAMETER END NOT FOUND ERRORS (WHICH OCCUR WHEN
C     THE SIDES OF THE BUBBLE DO NOT LINE UP WITH EACH OTHER) THE BUBBLE
C     MUST START FROM  COMPLEMENTARY POSITIONS IN THE TWO VECTORS. THIS IS
C     ACHEIVED USING PYTHAGORAS THEOREM, WHEREBY LENGTHC IS FIXED(THE
C     LENGTH BETWEEN THE FIRST COORDINATE PAIRS OF THE TWO SIDES),
C     AND LENGTHS A AND B CHANGE UNTIL LENGTHC IS EXCEEDED. J IS
C     RESET TO THE PREVIOUS COORDINATE PAIR(TO ALLOW FOR PERFECT ALIGNMENT
C     OF THE VECTORS) AND THEN ASSIGNED TO STBUB2. THE PROCESS IS REPEATED
C     FOR SIDE1.
C
C     CALCULATING LENGTH BETWEEN FIRST TWO COORDINATE PAIRS.
C
      S = 1
      LENC = 0.0
C
      LENC = LENTHI(XSIDE1(S),YSIDE1(S),XSIDE2(S),YSIDE2(S))
C
C     SEARCHING SIDE2 FROM SIDE1:
C
C     CALCULATING LENGTHS A AND B
C
      J = 1
      LENA = 0.0
      LENB = 0.0
C
 6100 J = J+1
      LENA = LENTHI(XSIDE2(S),YSIDE2(S),XSIDE2(J),YSIDE2(J))
      LENB = LENTHI(XSIDE1(S),YSIDE1(S),XSIDE2(J),YSIDE2(J))
      LEND = DSQRT(LENA*LENA+LENB*LENB)
C
      IF(LEND.LT.LENC) GOTO 6100
      IF(LEND.GE.LENC) STBUB2 = J-1
C
C     SEARCHING SIDE1 FROM SIDE2:
C
C     CALCULATING LENGTHS A AND B
C
      J = 1
      LENA = 0.0
      LENB = 0.0
C
 6200 J = J+1
      LENA = LENTHI(XSIDE1(S),YSIDE1(S),XSIDE1(J),YSIDE1(J))
      LENB = LENTHI(XSIDE2(S),YSIDE2(S),XSIDE1(J),YSIDE1(J))
      LEND = DSQRT(LENA*LENA+LENB*LENB)
C
```

```
      IF(LEND.LT.LENC) GOTO 6200
      IF(LEND.GE.LENC) STBUB1 = J-1
C
      F1 = 0
      F2 = 0
C
C     INITIALISE START1,START2,END1,END2 WHICH STORE SIDE1 AND SIDE2
C     ALTERED BUBBLE SUBSCRIPTS ONCE THE AXIS HAS BEEN ESTABLISHED.
C     THIS SAVES UNNECESSARY SEARCHING FROM ONE CALL TO ANOTHER.
C
      START1 = 1
      END1 = 1
C
      START2 = 1
      END2 = 1
C
C     INITIALISE BEGIN1 AND BEGIN2 WHICH STORE SIDE1,SIDE2 SUBSCRIPTS
C     GIVING CURRENT POSITION FROM WHICH SEARCH TAKES PLACE FOR
C     SIDE SEGMENT WHICH INTERSECTS WITH DIAMETER.
C
      BEGIN1 = 0
      BEGIN2 = 0
C
      DISUB = 1
C
C     INITIALISE ENDERR FOR ERROR ACCUMULATION.
C
      ENDERR = 0
C
C     SET PROGRAM STAGE.
C
      STAGE = 1
C
C     SET BUBPTS TO 2. THIS AVOIDS A POSSIBLE ERROR IN AXDIAS.
C
      BUBPTS = 2
C
C     BUBBLE EXPANDS BY 1 POINT EACH SIDE PER CYCLE IN THIS SECTION.
C     COUNT NUMBER OF POINTS PER SIDE INTO BUBPTS.
C
 600  BUBPTS = BUBPTS + 1
C
C     SIDE1
C     COUNT NUMBER OF POINTS INTO SCAN1 UNTIL SCAN1 EQUALS BUBPTS.
C     MEASURE LENGTH FROM STBUB1 INTO LEN1 AND SET FLAG F1 TO 1 IF LEN1
C     EQUALS OR EXCEEDS BUBLEN.  BYPASS SIDE1 EXPANSION IF F1 IS ALREADY
C     SET
C
      IF(F1.EQ.1) GOTO 800
      LEN1 = 0.0
      SCAN1 = STBUB1
 700  LEN1=LEN1 + LENTHI(XSIDE1(SCAN1),YSIDE1(SCAN1),XSIDE1(SCAN1+1),YS
     &IDE1(SCAN1+1))
        SCAN1 = SCAN1 + 1
        IF((SCAN1-STBUB1.LE.BUBPTS).AND.(SCAN1-STBUB1.LE.N1)) GOTO 700
C
C     RESET SCAN1 TO LAST VALUE USED BY LENTHI( ) FUNCTION
C
      SCAN1 = SCAN1 - 1
C
C     IF END OF SIDE1 HAS BEEN REACHED BY EXPANSION ALONG SIDE1, ABORT
C     PROGRAM WITH ERROR MESSAGE.  IF EXPANSION ALONG SIDE1 IS COMPLETE,
C     SET FLAG F1
```

```
C
      IF(SCAN1-STBUB1+1.GE.N1) GOTO 1800
      IF(LEN1.GE.BUBLEN) F1 = 1
C
C     SET VALUE OF ENBUB1 ACCORDING TO WHETHER LEN1 IS SLIGHTLY LESS THAN,
C     EQUAL TO OR SLIGHTLY GREATER THAN BUBLEN
C
      IF(LEN1.LE.BUBLEN) ENBUB1 = SCAN1
      IF(LEN1.GT.BUBLEN) ENBUB1 = SCAN1 - 1
C
C     ENSURE THAT FOLLOWING ALIGNMENT OF THE TOP OF THE VECTORS, THE
C     FIRST BUBBLE CONTAINS AT LEAST TWO POINTS OF SIDE1.
C
      IF(STBUB1.GE.ENBUB1) ENBUB1 = STBUB1+1
C
C
C
C     ------------------------------------------------------------------
C     SIDE2
C     COUNT NUMBER OF POINTS INTO SCAN2 UNTIL SCAN2 EQUALS BUBPTS.
C     MEASURE LENGTH FROM STBUB1 INTO LEN1 AND SET FLAG F2 TO 1 IF LEN2
C     EQUALS OR EXCEEDS BUBLEN.  BYPASS SIDE2 EXPANSION IF F2 IS ALREADY
C     SET
C
 800  IF(F2.EQ.1) GOTO 1100
      LEN2 = 0.0
      SCAN2 = STBUB2
 900  LEN2 = LEN2 + LENTHI(XSIDE2(SCAN2),YSIDE2(SCAN2),XSIDE2(SCAN2+1),Y
     &SIDE2(SCAN2+1))
        SCAN2 = SCAN2 + 1
        IF((SCAN2.LE.BUBPTS).AND.(SCAN2-STBUB2.LE.N2-STBUB2)) GOTO 900
C
C     RESET SCAN2 TO LAST VALUE USED BY THE LENTHI( ) FUNCTION.
C
      SCAN2 = SCAN2 - 1
C
C     IF END OF SIDE2 HAS BEEN REACHED BY EXPANSION ALONG SIDE2, ABORT
C     PROGRAM WITH ERROR MESSAGE.
C     IF EXPANSION ALONG SIDE1 IS COMPLETE, SET FLAG F1.
C
      IF(SCAN2-STBUB2+1.GE.N2) GOTO 2000
      IF(LEN2.GE.BUBLEN) F2 = 1
C
C     SET VALUE OF ENBUB2 ACCORDING TO WHETHER LEN2 IS SLIGHTLY LESS THAN,
C     EQUAL TO OR SLIGHTLY GREATER THAN BUBLEN.
C
      IF(LEN2.LE.BUBLEN) ENBUB2 = SCAN2
      IF(LEN2.GT.BUBLEN) ENBUB2 = SCAN2 - 1
C
C     ENSURE THAT FOLLOWING ALIGNMENT OF THE TOP OF THE VECTORS, THE
C     FIRST BUBBLE CONTAINS AT LEAST TWO POINTS OF SIDE2.
C
      IF(STBUB2.GE.ENBUB2) ENBUB2 = STBUB2+1
C
C     NOW AXIS ESTABLISHED, ALTER BUBBLE SUBSCRIPTS TO ALLOW MAXIMUM
C     POSSIBILITY OF FINDING DIAMETER END POINTS.
C
 1100 CALL ADJBUB
C
C     PUT AXIS POINT CO-ORDINATES CALCULATED FROM CURRENT BUBBLE INTO
C     XAXIS( ),YAXIS( ) AND ENDS OF DIAMETER THROUGH THE AXIS POINT INTO
C     XDEND1( ),YDEND1( ) FOR SIDE1 AND XDEND2( ),YDEND2( ) FOR SIDE2.
C     END POINTS ARE THEN WRITTEN TO FILE.
C
```

```
      CALL AXDIAS
C
C     CONTINUE EXPANSION UNTIL BOTH FLAGS ARE SET.
C
 1100 IF((F1.EQ.0).OR.(F2.EQ.0)) GOTO 600
C
C
C     ------------------------------------------------------------------
C     MOVE BUBBLE DOWN ARTERY
C
C     SUMPT1,SUMPT2 ARE STORES INTO WHICH THE TOTAL NUMBER OF POINTS
C     IN EACH FULL-SIZED BUBBLE FOR SIDE1,SIDE2 ARE ACCUMULATED SO
C     THAT THE AVERAGE NUMBER IN EACH SIDE OF A BUBBLE CAN BE CALCULATED.
C     F1,F2 ARE FLAGS WHICH ARE SET WHEN END OF BUBBLE REACHES END OF
C     SIDE1,SIDE2.  IF BUBBLE REACHES THE END OF ONE SIDE BEFORE IT
C     REACHES THE END OF THE OTHER, THE FORMER SIDE OF THE BUBBLE IS
C     HELD CONSTANT WHILE THE LATTER SIDE IS ALLOWED TO REACH THE END
C     OF ITS SIDE OF THE ARTERY.
C
      SUMPT1 = 0
      SUMPT2 = 0
C
      F1 = 0
      F2 = 0
C
C     SET PROGRAM STAGE.
C
      STAGE = 2
C
C     SIDE1:
C     MOVE SIDE1 OF BUBBLE ALONG BY INCREMENTING STBUB1.  PUT NEW STARTING
C     VALUE INTO SCAN1 AND SET LEN1 TO ZERO FOR START OF NEW LENGTH
C     CALCULATIONS.
C
 1200 IF(F1.EQ.1) GOTO 1350
      STBUB1 = STBUB1 + 1
      SCAN1  = STBUB1
       LEN1  = 0.0
C
C     MEASURE SIDE1 LENGTH OF BUBBLE FROM STBUB1 INTO LEN1 UNTIL LENGTH
C     EQUALS BUBLEN.
C
 1300 LEN1 = LEN1 + LENTHI(XSIDE1(SCAN1),YSIDE1(SCAN1),XSIDE1(SCAN1+1),Y
     &SIDE1(SCAN1+1))
        SCAN1 = SCAN1 + 1
        IF((LEN1.LE.BUBLEN).AND.(SCAN1.LT.N1)) GOTO 1300
C
C     RESET SCAN1 TO VALUE LAST USED BY LENTHI( ) FUNCTION.
C
      SCAN1 = SCAN1 - 1
C
C     SET FLAG F1 IF HIGHEST SUBSCRIPT USED IN LENTHI( ) FUNCTION REACHED
C     BOTTOM OF SIDE1.
C
      IF(SCAN1 + 1.GE.N1) F1 = 1
C
C     SET ENBUB1 ACCORDING TO WHETHER LEN1 IS SLIGHTLY LESS THAN, EQUAL
C     TO OR SLIGHTLY GREATER THAN BUBLEN.
C
      IF(LEN1.LE.BUBLEN) ENBUB1 = SCAN1
      IF(LEN1.GT.BUBLEN) ENBUB1 = SCAN1 - 1
C
C     ADD NUMBER OF POINTS IN CURRENT SIDE1 INTO SUMPT1
C     SO THAT MEAN CAN BE CALCULATED.
```

```
C
      SUMPT1 = SUMPT1 + ENBUB1 - STBUB1 + 1
C
C     IF THERE IS NOT AT LEAST 1 POINT IN BUBLEN FOLLOWING STBUB1,
C     WRITE ERROR MESSAGE TO SCREEN AND ABORT PROGRAM.
C
      IF(STBUB1.GE.ENBUB1) GOTO 2200
C
C     ------------------------------------------------------------------
C     SIDE2:
C     MOVE SIDE2 OF BUBBLE ALONG BY INCREMENTING STBUB2.  PUT NEW STARTING
C     VALUE INTO SCAN2 AND SET LEN2 TO ZERO FOR START OF NEW LENGTH
C     CALCULATIONS.
C
 1350 IF(F2.EQ.1) GOTO 1500
      STBUB2 = STBUB2 + 1
       SCAN2 = STBUB2
        LEN2 = 0.0
C
C     MEASURE SIDE2 LENGTH OF BUBBLE FROM STBUB2 INTO LEN2 UNTIL LENGTH
C     EQUALS BUBLEN.
C
 1400 LEN2 = LEN2 + LENTHI(XSIDE2(SCAN2),YSIDE2(SCAN2),XSIDE2(SCAN2+1),Y
     &SIDE2(SCAN2+1))
        SCAN2 = SCAN2 + 1
        IF((LEN2.LE.BUBLEN).AND.(SCAN2.LT.N2)) GOTO 1400
C
C     RESET SCAN2 TO VALUE LAST USED BY LENTHI( ) FUNCTION.
C
      SCAN2 = SCAN2 - 1
C
C     SET FLAG F2 IF HIGHEST SUBSCRIPT USED IN LENTHI( ) FUNCTION REACHED
C     BOTTOM OF SIDE2.
C
      IF(SCAN2+1.GE.N2) F2 = 1
C
C     SET ENBUB2 ACCORDING TO WHETHER LEN2 IS SLIGHTLY LESS THAN, EQUAL
C     TO OR SLIGHTLY GREATER THAN BUBLEN.
C
      IF(LEN2.LE.BUBLEN) ENBUB2 = SCAN2
      IF(LEN2.GT.BUBLEN) ENBUB2 = SCAN2 - 1
C
C     ADD NUMBER OF POINTS IN CURRENT SIDE2 INTO SUMPT2 SO THAT MEAN
C     CAN BE CALCULATED.
C
      SUMPT2 = SUMPT2 + ENBUB2 - STBUB2 +1
C
C     IF THERE IS NOT AT LEAST 1 POINT IN BUBLEN FOLLOWING STBUB2,
C     WRITE ERROR MESSAGE TO SCREEN AND ABORT PROGRAM.
C
      IF(STBUB2.GE.ENBUB2) GOTO 2400
C
C     NOW AXIS ESTABLISHED, ALTER BUBBLE SUBSCRIPTS TO ALLOW MAXIMUM
C     POSSIBILITY OF FINDING DIAMETER END POINTS.
C
 1500 CALL ADJBUB
C
C     PUT AXIS POINT CO-ORDINATES CALCULATED FROM CURRENT BUBBLE INTO
C     XAXIS( ),YAXIS( ) AND ENDS OF DIAMETER THROUGH THE AXIS POINT INTO
C     XDEND1( ),YDEND1( ) FOR SIDE1 AND XDEND2( ),YDEND2( ) FOR SIDE2.
C     END POINTS ARE THEN WRITTEN TO FILE.
C
      CALL AXDIAS
```

```
C
C     CONTINUE MOVEMENT OF BUBBLE UNTIL FLAGS FOR BOTH SIDES SET
C
 1500 IF((F1.EQ.0).OR.(F2.EQ.0)) GOTO 1200
C
C     ------------------------------------------------------------------
C     USE INTEGER DIVISION TO PUT A CLOSE APPROXIMATION TO THE AVERAGE
C     NUMBER OF POINTS IN LENGTH BUBLEN FOR SIDE1,SIDE2 INTO AVPTS1,AVPTS2
C     AND MEAN OF NUMBER OF POINTS IN A BUBBLE INTO BUBAVP.
C
      AVPTS1 = SUMPT1/STBUB1
      AVPTS2 = SUMPT2/STBUB2
      BUBAVP = (AVPTS1+AVPTS2)/2
C
C     COMPARE THE VALUE OF BUBAVP WITH ENDERR:THE ACCUMULATION OF
C     TOO MANY NON-INTERSECTING DIAMETER LINES RESULTS IN INCOMPLETE
C     DATA-THEREFORE THE PROGRAM ABORTS.
C
      IF(ENDERR.GT.BUBAVP) WRITE(1,550)
  550 FORMAT('TOO MANY DIAMETER END POINTS NOT FOUND, PROGRAM ABORTS')
      IF(ENDERR.GT.BUBAVP) GOTO 9999
C
C     ------------------------------------------------------------------
C     CONTRACT BUBBLE
C
C     SET PROGRAM STAGE.
C
      STAGE = 3
C
      ENBUB1 = N1
      ENBUB2 = N2
C
C     LET TOP OF LAST FULL SIZED BUBBLE APPROACH ITS BOTTOM.
C     LENGTH CALCULATIONS FOR DETECTING ATTAINMENT OF BUBLEN
C     ARE NO LONGER NEEDED.
C
 1600 IF(STBUB1.LE.N1-2) STBUB1 = STBUB1 + 1
      IF(STBUB2.LE.N2-2) STBUB2 = STBUB2 + 1
C
C     NOW AXIS ESTABLISHED, ALTER BUBBLE SUBSCRIPTS TO ALLOW MAXIMUM
C     POSSIBILITY OF FINDING DIAMETER END POINTS.
C
      CALL ADJBUB
C
C     PUT AXIS POINT CO-ORDINATES CALCULATED FROM CURRENT BUBBLE INTO
C     XAXIS( ),YAXIS( ) AND ENDS OF DIAMETER THROUGH THE AXIS POINT INTO
C     XDEND1( ),YDEND1( ) FOR SIDE1 AND XDEND2( ),YDEND2( ) FOR SIDE2.
C     END POINTS ARE THEN WRITTEN TO FILE.
C
      CALL AXDIAS
C
C
C     CONTINUE CONTRACTION UNTIL BOTTOM OF BOTH SIDES HAS BEEN REACHED.
C
      IF((STBUB1.LE.N1-2).OR.(STBUB2.LE.N2-2)) GOTO 1600
C
C     PRESENT ERROR INFORMATION.
C
      WRITE(1,1760) ENDERR
 1760 FORMAT( 'No. DIAMETER END POINTS NOT FOUND = ',I5)
C
C     ------------------------------------------------------------------
      GOTO 9999
```

```
C
C     ERROR MESSAGES
C
 1800 WRITE(1,1900)
 1900 FORMAT('FIRST-TRACED SIDE HAS INSUFFICIENT POINTS')
      GOTO 9999
C
 2000 WRITE(1,2100)
 2100 FORMAT('SECOND-TRACED SIDE HAS INSUFFICIENT POINTS')
      GOTO 9999
C
 2200 STORE1 = STBUB1 + 1
      WRITE(1,2300) STBUB1,STORE1
 2300 FORMAT('POINT DENSITY TOO LOW ON FIRST-TRACED SIDE BETWEEN POINT
     &NUMBER' ,I5,' AND ',I5)
      GOTO 9999
C
 2400 STORE2 = STBUB2 +1
      WRITE(1,2500) STBUB2,STORE2
 2500 FORMAT('POINT DENSITY TOO LOW ON SECOND-TRACED SIDE BETWEEN POINT
     &NUMBER ',I5,' AND ',I5)
      GOTO 9999
C
C
C     CLOSE FILES AND END PROGRAM
C
 9999 ENDFILE 6
      ENDFILE 7
      ENDFILE 8
C
      STOP
C
      END
C     ***************************************************************************
      FUNCTION LENTHI(XDUM1,YDUM1,XDUM2,YDUM2)
C
      INTEGER XDUM1,YDUM1,XDUM2,YDUM2
      DOUBLE PRECISION XDISP,YDISP,LENTHI
C
      XDISP = XDUM2 - XDUM1
      YDISP = YDUM2 - YDUM1
C
      LENTHI = DSQRT(XDISP*XDISP + YDISP*YDISP)
C
      RETURN
      END
C
C     ***************************************************************************
      FUNCTION LENGTH(XDUM1,YDUM1,XDUM2,YDUM2)
C
      DOUBLE PRECISION XDUM1,YDUM1,XDUM2,YDUM2,XDISP,YDISP,LENGTH
C
      XDISP = XDUM2 - XDUM1
      YDISP = YDUM2 - YDUM1
C
      LENGTH = DSQRT(XDISP*XDISP + YDISP*YDISP)
C
      RETURN
      END
C
C     ***************************************************************************
      SUBROUTINE ADJBUB
C
```

```
      INTEGER XSIDE1(1000),YSIDE1(1000),XSIDE2(1000),YSIDE2(1000)
      INTEGER START1,START2,END1,END2,DISUB,F1,F2,F3,F4,F5,I
      INTEGER SCAN1,BEGIN1,DISIDE,NEXT,SCAN2,BEGIN2,ENDERR,F6,SETSUB
      INTEGER STBUB1,STBUB2,ENBUB1,ENBUB2,STAGE,N1,N2
C
      INTEGER*4 X1S1,Y1S1,X2S1,Y2S1,X1S2,Y1S2,X2S2,Y2S2,X3S1,Y3S1
      INTEGER*4 X3S2,Y3S2
C
      DOUBLE PRECISION XMIDTP,YMIDTP,XMIDBM,YMIDBM,XAX,YAX,CAX
      DOUBLE PRECISION LINEA,LINEB,LINEC,LINED
      DOUBLE PRECISION XCOEFT,YCOEFT,CONSTT
      DOUBLE PRECISION XCOEFB,YCOEFB,CONSTB
C
      COMMON/SET1/N1,N2/SET5/XSIDE1,YSIDE1,XSIDE2,YSIDE2
      COMMON/SET6/STBUB1,ENBUB1,STBUB2,ENBUB2
      COMMON/SET9/START1,END1,START2,END2/SET11/XCOEFT,YCOEFT,CONST
      COMMON/SET12/XMIDTP,YMIDTP,XMIDBM,YMIDBM/SET10/STAGE
C
C
C     ------------------------------------------------------------------
C     THIS SUBROUTINE EFFECTIVLY ALTERS THE VALUE OF STBUB1,ENBUB1 AND STBUB2
C     ENBUB2 IN ORDER TO PRODUCE A BUBBLE WHOSE MARGINS ARE AT APPROXIMATLY
C     90 DEGREES TO THE AXIS LINE. THIS ALLOWS FOR MAXIMUM POSSIBILITY
C     IN THE LOCATION OF DIAMETER LINES.
C
C     THIS IS ACHEIVED BY RUNNING LINES AT 90 DEGREES TO THE TOP AND
C     BOTTOM OF THE AXIS LINE IN QUESTION AND COMPUTING THE NEAREST
C     EXISTING COORDINATE TO ITS INTERSECTING POINT ON BOTH SIDES OF
C     THE ARTERY. IN THIS WAY BUBBLE GROWTH AND MOVEMENT ARE LEFT
C     UNDISTURBED AND THE AXIS LINE IS CORRECTLY PROVIDED BY THE MAIN
C     PROGRAM.
C     ------------------------------------------------------------------
C
C     SET SETSUB TO 0 TO INFORM THE FUNCTION DISIDE THAT THIS IS
C     SUBROUTINE ADJBUB.
C
      SETSUB = 0
C
C     IN THE FINAL STAGE OF THE PROGRAM, END1 AND END2 MUST BE FIXED
C     AS THE ENDS OF THEIR RESPECTIVE VECTORS.
C
      IF(STAGE.EQ.3) END1 = N1
      IF(STAGE.EQ.3) END2 = N2
C
C     COMPUTE EQUATION OF THE AXIS LINE.
C
      XMIDTP = (XSIDE1(STBUB1)+XSIDE2(STBUB2))/2.0
      YMIDTP = (YSIDE1(STBUB1)+YSIDE2(STBUB2))/2.0
C
      XMIDBM = (XSIDE1(ENBUB1)+XSIDE2(ENBUB2))/2.0
      YMIDBM = (YSIDE1(ENBUB1)+YSIDE2(ENBUB2))/2.0
C
      XAX = YMIDTP-YMIDBM
      YAX = XMIDBM-XMIDTP
      CAX = (YMIDBM*XMIDTP)-(YMIDTP*XMIDBM)
C
C     COMPUTE EQUATIONS OF LINES AT 90 DEGREES TO TOP AND BOTTOM
C     OF CURRENT AXIS LINE.
C
C     TOP
C
      XCOEFT = XMIDTP-XMIDBM
      YCOEFT = YMIDTP-YMIDBM
      CONSTT=(YMIDBM*YMIDTP+XMIDBM*XMIDBM)-(YMIDTP*YMIDBM+XMIDTP*
```

```
     &XMIDTP)
C
C      BOTTOM
C
       XCOEFB = XCOEFT
       YCOEFB = YCOEFT
       CONSTB=(YMIDBM*YMIDBM+XMIDBM*XMIDBM)-(YMIDTP*YMIDBM+XMIDTP*
     &XMIDBM)
C
C      LOCATING THE NEAREST COORDINATES.
C
C      SIDE1
C
       F1 = 0
       F2 = 0
       F3 = 0
       F5 = 0
        I = 1
C
 50    IF(F5.EQ.0) SCAN1 = START1 - 1
       IF(F5.EQ.1) SCAN1 = END1-1
       IF(F5.EQ.0) CONST = CONSTT
       IF(F5.EQ.1) CONST = CONSTB
C
 100   SCAN1 = SCAN1 + I
       IF((F5.EQ.0).AND.(I.EQ.1).AND.(SCAN1.GE.N1-2)) GOTO 260
       IF((F5.EQ.1).AND.(I.EQ.1).AND.(SCAN1.GE.N1-2)) GOTO 300
       IF((F5.EQ.0).AND.(I.EQ.-1).AND.(SCAN1.LE.3)) GOTO 260
       IF((F5.EQ.1).AND.(I.EQ.-1).AND.(SCAN1.LE.3)) GOTO 300
C
       X1S1 = XSIDE1(SCAN1)
       Y1S1 = YSIDE1(SCAN1)
       SCAN1 = SCAN1+I
       X2S1 = XSIDE1(SCAN1)
       Y2S1 = YSIDE1(SCAN1)
       SCAN1 = SCAN1+I
       X3S1 = XSIDE1(SCAN1)
       Y3S1 = YSIDE1(SCAN1)
       SCAN1 = SCAN1-(I+I)
C
       IF(DISIDE(X1S1,Y1S1).EQ.0) F1 = 1
       IF(DISIDE(X2S1,Y2S1).EQ.0) F2 = 1
       IF(DISIDE(X1S1,Y1S1).NE.DISIDE(X2S1,Y2S1)) F3 = 1
       IF(F1.EQ.1) GOTO 200
       IF(F2.EQ.1) GOTO 200
C
       LINEA = DABS(X1S1*XCOEFD + Y1S1*YCOEFD + CONSTD)
       LINEB = DABS(X2S1*XCOEFD + Y2S1*YCOEFD + CONSTD)
       LINEC = DABS(X3S1*XCOEFD + Y3S1*YCOEFD + CONSTD)
C
C      'STICKING' OF THE SEARCHING PROCESS CAN OCCUR WHEN COORDINATE
C      DENSITY IS HIGH AND ARTERY PROFILE IS CHANGING RELATIVLY QUICKLY.
C      THIS IS OVERCOME BY OBSERVING NO CHANGE IN THE LINE FUNCTION,
C      WHICH PROMOTES A ONE UNIT INCREMENT OF THE PREVIOUS BUBBLE MARGIN
C      BEFORE BEING PASSED TO AXDIAS.
C
       IF(LINED.EQ.LINEB) POINT1 = SCAN1 + 1
       IF(LINED.EQ.LINEB) GOTO 250
C
       LINED = LINEB
C
C      BECAUSE THE VALUE OF THE LINE TEST REFLECTS NOT ONLY THE PLACEMENT
C      OF COORDINATES RELATIVE TO THE DIAMETER LINE (i.e. ABOVE OR BELOW)
```

```
C     BUT ALSO THE LINEAR DISTANCE FROM IT, THERE ARE OCCASIONS WHERE
C     THE TEST REVEALS AN APPARENT REVERSAL IN THE DATA EVEN THOUGH IT
C     IS CLEAN (REFER TO THESIS FOR DETAILS). HENCE THE FOLLOWING CODE
C     CHECKS FOR THE CONVERGENCE OR DIVERGENCE OF LINE AS THE DIAMETER
C     LINE IS APPROACHED OR LEFT, PLUS ALLOWS FOR THE CASE WHERE VALUES
C     OF LINE ARE CONTRADICTORY REFLECTING AN APPARENT REVERSAL.
C
      F4 = 0
      F6 = 0
      IF((F3.EQ.1).AND.(LINEA.LE.LINEB)) POINT1 = SCAN1
      IF((F3.EQ.1).AND.(LINEA.GT.LINEB)) POINT1 = SCAN1 + I
      IF(F3.EQ.1) GOTO 250
      IF((I.EQ.1).AND.(LINEB.LE.LINEA)) F4 = 1
      IF((I.EQ.-1).AND.(LINEA.GE.LINEB)) GOTO 100
      IF((F4.EQ.1).AND.(SCAN1.LE.N1-3)) GOTO 100
      IF((LINEA.LE.LINEB).AND.(LINEC.LE.LINEB)) F6 = 1
      IF(DISIDE(X2S1,Y2S1).NE.DISIDE(X3S1,Y3S1)) F6 = 1
      IF(F6.EQ.1) GOTO 100
      IF((F4.EQ.1).AND.(SCAN1.GT.N1-3)) GOTO 300
C
      SCAN1 = SCAN1+1
      I = -1
      GOTO 100
C
 200  IF(F1.EQ.1) POINT1 = SCAN1
      IF(F2.EQ.1) POINT1 = SCAN1 + I
C
 250  IF(F5.EQ.0) START1 = POINT1
      IF(F5.EQ.1) GOTO 275
C
 260  F3 = 0
      F5 = 1
      GOTO 50
 275  END1 = POINT1
C
C     SIDE2
C
 300  F1 = 0
      F2 = 0
      F3 = 0
      F5 = 0
       I = 1
C
 450  IF(F5.EQ.0) SCAN2 = START2 -1
      IF(F5.EQ.1) SCAN2 = END2 - 1
      IF(F5.EQ.0) CONST = CONSTT
      IF(F5.EQ.1) CONST = CONSTB
C
 500  SCAN2 = SCAN2 + I
      IF((F5.EQ.0).AND.(I.EQ.1).AND.(SCAN2.GE.N2-2)) GOTO 660
      IF((F5.EQ.1).AND.(I.EQ.1).AND.(SCAN2.GE.N2-2)) GOTO 800
      IF((F5.EQ.0).AND.(I.EQ.-1).AND.(SCAN2.LE.3)) GOTO 660
      IF((F5.EQ.1).AND.(I.EQ.-1).AND.(SCAN2.LE.3)) GOTO 800
C
      X1S2 = XSIDE2(SCAN2)
      Y1S2 = YSIDE2(SCAN2)
      SCAN2 = SCAN2+I
      X2S2 = XSIDE2(SCAN2)
      Y2S2 = YSIDE2(SCAN2)
      SCAN2 = SCAN2+I
      X3S2 = XSIDE2(SCAN2)
      Y3S2 = YSIDE2(SCAN2)
      SCAN2 = SCAN2-(I+I)
```

```
C
      IF(DISIDE(X1S2,Y1S2).EQ.0) F1 = 1
      IF(DISIDE(X2S2,Y2S2).EQ.0) F2 = 1
      IF(DISIDE(X1S2,Y1S2).NE.DISIDE(X2S2,Y2S2)) F3 = 1
      IF(F1.EQ.1) GOTO 600
      IF(F2.EQ.1) GOTO 600
C
      LINEA = DABS(X1S2*XCOEFD + Y1S2*YCOEFD + CONSTD)
      LINEB = DABS(X2S2*XCOEFD + Y2S2*YCOEFD + CONSTD)
      LINEC = DABS(X3S2*XCOEFD + Y3S2*YCOEFD + CONSTD)
C
C     CHECK FOR STICKING.
C
      IF(LINED.EQ.LINEB) POINT2 = SCAN2 + 1
      IF(LINED.EQ.LINEB) GOTO 650
      LINED = LINEB
C
C     SEE PREVIOUS SOFTWARE EXPLANATION.
C
      F4 = 0
      F6 = 0
      IF((F3.EQ.1).AND.(LINEA.LE.LINEB)) POINT2 = SCAN2
      IF((F3.EQ.1).AND.(LINEA.GT.LINEB)) POINT2 = SCAN2 + I
      IF(F3.EQ.1) GOTO 650
      IF((I.EQ.1).AND.(LINEB.LE.LINEA)) F4 = 1
      IF((I.EQ.-1).AND.(LINEA.GE.LINEB)) GOTO 500
      IF((F4.EQ.1).AND.(SCAN2.LE.N2-3)) GOTO 500
      IF((LINEA.LE.LINEB).AND.(LINEC.LE.LINEB)) F6 = 1
      IF(DISIDE(X2S2,Y2S2).NE.DISIDE(X3S2,Y3S2)) F6 = 1
      IF(F6.EQ.1) GOTO 500
      IF((F4.EQ.1).AND.(SCAN2.GT.N2-3)) GOTO 800
C
      SCAN2 = SCAN2+1
      I = -1
      GOTO 500
C
 600  IF(F1.EQ.1) POINT2 = SCAN2
      IF(F2.EQ.1) POINT2 = SCAN2 + I
C
 650  IF(F5.EQ.0) START2 = POINT2
      IF(F5.EQ.1) GOTO 675
C
 660  F3 = 0
      F5 = 1
      I = 1
      GOTO 450
 675  END2 = POINT2
C
 800  RETURN
      END
C     ********************************************************************************
      SUBROUTINE AXDIAS
C
      INTEGER XSIDE1(1000),YSIDE1(1000),XSIDE2(1000),YSIDE2(1000)
      INTEGER START1,START2,END1,END2,DISUB,F,F1,F2,F3,F4,F5,I
      INTEGER SCAN1,BEGIN1,DISIDE,NEXT,SCAN2,BEGIN2,ENDERR,F6,SETSUB
C
      INTEGER*4 X1S1,Y1S1,X2S1,Y2S1,X1S2,Y1S2,X2S2,Y2S2,X3S1,Y3S1
      INTEGER*4 X3S2,Y3S2
C
      DOUBLE PRECISION XMIDTP,YMIDTP,XMIDBM,YMIDBM,XCNTRE,YCNTRE
      DOUBLE PRECISION LINEA,LINEB,XDEND1,PI,XDEND2,YDEND2
      DOUBLE PRECISION YDEND1,XCOEF1,YCOEF1,CONST1,GRADET,ANGDIF
```

```
      DOUBLE PRECISION ANGLE,XCOEF2,YCOEF2,CONST2,MINANG,XCOEFD
      DOUBLE PRECISION YCOEFD,CONSTD,LINEC
C
      COMMON/SET1/N1,N2/SET2/MINANG/SET3/BEGIN1,BEGIN2/SET4/ENDERR
      COMMON/SET5/XSIDE1,YSIDE1,XSIDE2,YSIDE2
      COMMON/SET9/START1,END1,START2,END2/SET7/PI/SET8/DISUB
      COMMON/SET12/XMIDTP,YMIDTP,XMIDBM,YMIDBM
      COMMON/SET13/XCOEFD,YCOEFD,CONSTD
C     ------------------------------------------------------------------
C
C     THIS SUBROUTINE COMPUTES A CENTRAL AXIS FOR THE ARTERY FROM WHICH
C     DIAMETER LINES ARE TAKEN. THE CO-ORDINATES OF THESE AXIS POINTS
C     ARE WRITTEN TO XAXIS( ),YAXIS( ) WITH SUBSCRIPT DISUB. DIAMETER END
C     CO-ORDINATES ARE WRITTEN TO XDEND1( ),YDEND1( ) FOR SIDE1, AND
C     XDEND2( ),YDEND2( ) FOR SIDE2. THESE ARE THEN WRITTEN TO FILE.
C     ------------------------------------------------------------------
C
C     SET F TO 1 TO ALLOW FOR DIAMETER END NOT FOUND.
      F = 1
C
C     SET SETSUB TO 1 TO INFORM THE FUNCTION DISIDE THAT THIS IS
C     SUBROUTINE AXDIAS.
C
      SETSUB = 1
C
C     USE MID-POINT OF LINE BETWEEN ABOVE TWO MID-POINTS PROVIDED BY
C     ADJBUB AS AXIS POINT AND PUT INTO XCNTRE,YCNTRE.
C
      XCNTRE = (XMIDTP+XMIDBM)/2.0
      YCNTRE = (YMIDTP+YMIDBM)/2.0
C
      DISUB = DISUB+1
C
C
C     THE DIAMETER LINE IS CONSIDERED TO BE A LINE THROUGH XCNTRE,YCNTRE
C     PERPENDICULAR TO THE LINE BETWEEN XMIDTP,YMIDTP AND XMIDBM,YMIDBM.
C     PUT THE COEFFICIENTS OF THE DIAMETER LINE INTO XCOEFD,YCOEFD,CONSTD
C
      XCOEFD = XMIDTP-XMIDBM
      YCOEFD = YMIDTP-YMIDBM
      CONSTD=(YMIDBM*YCNTRE+XMIDBM*XCNTRE)-(YMIDTP*YCNTRE+XMIDTP*
     &XCNTRE)
C
C     SIDE1: SEARCH FOR THE SEGMENT THROUGH WHICH THE DIAMETER LINE
C     RUNS.
C
      F1 = 0
      F2 = 0
      F3 = 0
      F5 = 0
       I = 1
      SCAN1 = BEGIN1
C
  100 SCAN1 = SCAN1 + I
      IF((I.EQ.1).AND.(SCAN1.GE.N1-2)) GOTO 800
      IF((I.EQ.-1).AND.(SCAN1.LE.START1+1)) GOTO 800
C
      X1S1 = XSIDE1(SCAN1)
      Y1S1 = YSIDE1(SCAN1)
      SCAN1 = SCAN1+I
      X2S1 = XSIDE1(SCAN1)
      Y2S1 = YSIDE1(SCAN1)
      SCAN1 = SCAN1+I
```

```
      X3S1 = XSIDE1(SCAN1)
      Y3S1 = YSIDE1(SCAN1)
      SCAN1 = SCAN1-(I+I)
C
      IF(DISIDE(X1S1,Y1S1).EQ.0) F1 = 1
      IF(DISIDE(X2S1,Y2S1).EQ.0) F2 = 1
      IF(DISIDE(X1S1,Y1S1).NE.DISIDE(X2S1,Y2S1)) F3 = 1
      IF(F1.EQ.1) GOTO 200
      IF(F2.EQ.1) GOTO 200
      IF(F3.EQ.1) GOTO 200
C
      LINEA = DABS(X1S1*XCOEFD + Y1S1*YCOEFD + CONSTD)
      LINEB = DABS(X2S1*XCOEFD + Y2S1*YCOEFD + CONSTD)
      LINEC = DABS(X3S1*XCOEFD + Y3S1*YCOEFD + CONSTD)
C
C     REFER TO SOFTWARE EXPLANATION IN PREVIOUS SUBROUTINE FOR LINE TEST
C     COMMENTS.
C
      F4 = 0
      F6 = 0
      IF((I.EQ.1).AND.(LINEB.LE.LINEA)) F4 = 1
      IF((I.EQ.-1).AND.(LINEA.GE.LINEB)) GOTO 100
      IF((F4.EQ.1).AND.(SCAN1.LE.END1-3)) GOTO 100
      IF((LINEA.LE.LINEB).AND.(LINEC.LE.LINEB)) F6 = 1
      IF(DISIDE(X2S1,Y2S1).NE.DISIDE(X3S1,Y3S1)) F6 = 1
      IF(F6.EQ.1) GOTO 100
      IF((F4.EQ.1).AND.(SCAN1.GT.END1-3)) GOTO 400
C
      SCAN1 = SCAN1+1
      I = -1
      GOTO 100
C
 200  BEGIN1 = SCAN1
C
      IF(F1.EQ.1) XDEND1=X1S1
      IF(F1.EQ.1) YDEND1=Y1S1
      IF(F2.EQ.1) XDEND1=X2S1
      IF(F2.EQ.1) YDEND1=Y2S1
      IF((F1.EQ.1).OR.(F2.EQ.1)) GOTO 400
C
      XCOEF1 = Y1S1 - Y2S1
      YCOEF1 = X2S1 - X1S1
      CONST1 = Y2S1*X1S1-Y1S1*X2S1
C
      GRADET = XCOEFD*YCOEF1 - XCOEF1*YCOEFD
C
      ANGDIF = DABS(ANGLE(XCOEFD,-YCOEFD) - ANGLE(XCOEF1,-YCOEF1))
C
      NEXT = BEGIN1 + 1
C
      IF(ANGDIF.LE.MINANG) WRITE(1,300) BEGIN1,NEXT
 300  FORMAT(' SEGMENT OF SIDE1 BETWEEN POINT NUMBERS ',I5,' AND ',I5,'
     & TOO NEAR PARALLEL WITH DIAMETER')
      IF(ANGDIF.LE.MINANG) DISUB = DISUB-1
      IF(ANGDIF.LE.MINANG) GOTO 1100
C
      XDEND1 = (YCOEFD*CONST1 - YCOEF1*CONSTD)/GRADET
      YDEND1 = (XCOEF1*CONSTD - XCOEFD*CONST1)/GRADET
C
 400  F1 = 0
      F2 = 0
      F3 = 0
      F5 = 0
```

```
       I = 1
      SCAN2 = BEGIN2
C
 500  SCAN2 = SCAN2 + I
      IF((I.EQ.1).AND.(SCAN2.GE.N2-2)) GOTO 800
      IF((I.EQ.-1).AND.(SCAN2.LE.START2+1)) GOTO 800
C
      X1S2 = XSIDE2(SCAN2)
      Y1S2 = YSIDE2(SCAN2)
      SCAN2 = SCAN2+I
      X2S2 = XSIDE2(SCAN2)
      Y2S2 = YSIDE2(SCAN2)
      SCAN2 = SCAN2+I
      X3S2 = XSIDE2(SCAN2)
      Y3S2 = YSIDE2(SCAN2)
      SCAN2 = SCAN2-(I+I)
C
      IF(DISIDE(X1S2,Y1S2).EQ.0) F1 = 1
      IF(DISIDE(X2S2,Y2S2).EQ.0) F2 = 1
      IF(DISIDE(X1S2,Y1S2).NE.DISIDE(X2S2,Y2S2)) F3 = 1
      IF(F1.EQ.1) GOTO 600
      IF(F2.EQ.1) GOTO 600
      IF(F3.EQ.1) GOTO 600
C
      LINEA = DABS(X1S2*XCOEFD + Y1S2*YCOEFD + CONSTD)
      LINEB = DABS(X2S2*XCOEFD + Y2S2*YCOEFD + CONSTD)
      LINEC = DABS(X3S2*XCOEFD + Y3S2*YCOEFD + CONSTD)
C
C     REFER TO SOFTWARE EXPLANATION IN PREVIOUS SUBROUTINE FOR LINE TEST
C     COMMENTS.
C
      F4 = 0
      F6 = 0
      IF((I.EQ.1).AND.(LINEB.LE.LINEA)) F4 = 1
      IF((I.EQ.-1).AND.(LINEA.GE.LINEB)) GOTO 500
      IF((F4.EQ.1).AND.(SCAN2.LE.END2-3)) GOTO 500
      IF((LINEA.LE.LINEB).AND.(LINEC.LE.LINEB)) F6 = 1
      IF(DISIDE(X2S2,Y2S2).NE.DISIDE(X3S2,Y3S2)) F6 = 1
      IF(F6.EQ.1) GOTO 500
      IF((F4.EQ.1).AND.(SCAN2.GT.END2-3)) GOTO 800
C
      SCAN2 = SCAN2+1
      I = -1
      GOTO 500
C
 600  BEGIN2 = SCAN2
C
      IF(F1.EQ.1) XDEND2 = X1S2
      IF(F1.EQ.1) YDEND2 = Y1S2
      IF(F2.EQ.1) XDEND2 = X2S2
      IF(F2.EQ.1) YDEND2 = Y2S2
C
      IF((F1.EQ.1).OR.(F2.EQ.1)) GOTO 750
C
C
      XCOEF2 = Y1S2 - Y2S2
      YCOEF2 = X2S2 - X1S2
      CONST2 = Y2S2*X1S2-Y1S2*X2S2
C
      GRADET = XCOEFD*YCOEF2 - XCOEF2*YCOEFD
C
      ANGDIF = DABS(ANGLE(XCOEFD,-YCOEFD) - ANGLE(XCOEF2,-YCOEF2))
C
```

```
      NEXT = BEGIN2 + 1
C
      IF(ANGDIF.LE.MINANG) WRITE(1,700) BEGIN2,NEXT
 700  FORMAT(' SEGMENT OF SIDE2 BETWEEN POINT NUMBERS ',I5,' AND ',I5,'
     & TOO NEAR PARALLEL WITH DIAMETER')
      IF(ANGDIF.LE.MINANG) DISUB = DISUB-1
      IF(ANGDIF.LE.MINANG) GOTO 1100
C
      XDEND2 = (YCOEFD*CONST2 - YCOEF2*CONSTD)/GRADET
      YDEND2 = (XCOEF2*CONSTD - XCOEFD*CONST2)/GRADET
C
C     WRITE DIAMETER END POINTS TO FILE.
C
 750  WRITE(8,780) XDEND1,YDEND1
      WRITE(8,780) XDEND2,YDEND2
C
C     FILE FORMAT STATEMENT.
C
 780  FORMAT(2F11.4)
C
      F = 0
 800  IF(F.NE.0) F = 1
        IF(F.EQ.1) ENDERR = ENDERR + 1
        IF(F.EQ.1) DISUB = DISUB - 1
C
 1100 RETURN
C
      END
C
C     ***************************************************************************
      FUNCTION DISIDE(X,Y)
C
      INTEGER DISIDE,DISUB,SETSUB
C
      INTEGER*4 X,Y
C
      DOUBLE PRECISION XCOEF,YCOEF,CONSNT,LINE,XCOEFT,YCOEFT,CONST
      DOUBLE PRECISION XCOEFD,YCOEFD,CONSTD
C
      COMMON/SET8/DISUB/SET11/XCOEFT,YCOEFT,CONST
      COMMON/SET13/XCOEFD,YCOEFD,CONSTD/SET14/SETSUB
C
C     ---------------------------------------------------------------------
C     DISIDE DETECTS WHICH SIDE OF THE CALCULATED DIAMETER LINE POINT WITH
C     CO-ORDINATES X,Y IS POSITIONED. THE LINE EXPRESSION IS POSITIVE
C     FOR ALL POINTS ABOVE IT, ZERO FOR ALL POINTS IN IT AND NEGATIVE
C     FOR ALL POINTS BELOW IT IN THE CARTESIAN PLANE. DISIDE IS MADE 1,0
C     OR -1 RESPECTIVELY ACCORDING TO WHICH OF THESE CONDITIONS APPLIES.
C     SETSUB IS THE SWITCH WHICH TELLS THE FUNCTION WHICH EQUATION IS
C     APPROPRIATE FOR THE CURRENT CALL.
C     ---------------------------------------------------------------------
C
      IF(SETSUB.EQ.0) XCOEF = XCOEFT
      IF(SETSUB.EQ.0) YCOEF = YCOEFT
      IF(SETSUB.EQ.0) CONSNT = CONST
C
      IF(SETSUB.EQ.1) XCOEF = XCOEFD
      IF(SETSUB.EQ.1) YCOEF = YCOEFD
      IF(SETSUB.EQ.1) CONSNT = CONSTD
C
      LINE = X*XCOEF + Y*YCOEF + CONSNT
      IF(LINE.LE.-1.0D-36) DISIDE = -1
      IF(LINE.GE.1.0D-36) DISIDE = 1
```

```
      IF((LINE.GT.-1.0D-36).AND.(LINE.LT.1.0D-36)) DISIDE = 0
C
      RETURN
      END
C
C     ***************************************************************************
      FUNCTION ANGLE(A,B)
C
      INTEGER F1,F2,F
C
      DOUBLE PRECISION R2,S2,C2,A,B,PI,ANGLE,S1,C1
C
      COMMON/SET7/PI
C
C     ---------------------------------------------------------------
C
C     PUT SQUARES OF HYPOTENUSE INTO R2,SINE INTO S2,COSINE INTO C2.
C
      R2 = A*A + B*B
      IF(R2.LT.2.0E-4) WRITE(1,10)A,B
 10   FORMAT( 'ERROR-PARAMETERS ',F7.5,' AND ',F7.5,' PASSED TO ANGLE
     & FUNCTION TOO SMALL')
      IF(R2.LT.2.0E-4) GOTO 400
C
      S2 = A*A/R2
      C2 = B*B/R2
C
C     ENSURE THAT NUMERICAL ACCURACY PROBLEMS DO NOT PREVENT CORRECT
C     WORKING OF OCTANT TRAPS.
C
      IF(S2.LT.1.0E-4) S2 = 0.0
      IF(C2.LT.1.0E-4) C2 = 0.0
C
      IF(S2.GT.1.0-1.0E-4) S2 = 1.0
      IF(C2.GT.1.0-1.0E-4) C2 = 1.0
C
      F = 0
      IF(DABS(S2-C2).LT.1.0E-4) F = 1
      IF(F.EQ.1) S2 = 0.5
      IF(F.EQ.1) C2 = 0.5
C
      IF(C2.LT.S2) S2 = 1.0 - C2
      IF(S2.LT.C2) C2 = 1.0 - S2
C
      S1 = DSIGN(DSQRT(S2),A)
      C1 = DSIGN(DSQRT(C2),B)
C
C     ---------------------------------------------------------------
C
C     ARCSINE AND ARCCOS ARE NOT INTRINSIC FUNCTIONS IN THIS VERSION
C     OF FORTRAN. THIS PROBLEM IS OVERCOME BY USING ARCTAN.
C
C     ---------------------------------------------------------------
C
      IF((A.LT.0.0).OR.(B.LE.0.0)) GOTO 100
        F1=0
        F2=0
        IF((0.0.LE.S2).AND.(S2.LE.0.5)) F1=1
        IF((0.5.LE.C2).AND.(C2.LE.1.0)) F2=1
        IF((F1.EQ.1).AND.(F2.EQ.1)) ANGLE = DATAN(S/DSQRT(1.0-S*S))
C
        F1=0
        F2=0
```

```
        IF((0.5.LE.S2).AND.(S2.LE.1.0)) F1=1
        IF((0.0.LE.C2).AND.(C2.LE.0.5)) F2=1
        IF((F1.EQ.1).AND.(F2.EQ.1)) ANGLE = DATAN(DSQRT(1.0-C*C)/C)
        GOTO 400
C
C     ---------------------------------------------------------------
C
 100  IF((A.LE.0.0).OR.(B.GT.0.0)) GOTO 200
        F1=0
        F2=0
        IF((0.5.LE.S2).AND.(S2.LE.1.0)) F1=1
        IF((0.0.LE.C2).AND.(C2.LE.0.5)) F2=1
        IF((F1.EQ.1).AND.(F2.EQ.1)) ANGLE = DATAN(DSQRT(1.0-C*C)/C)
C
        F1=0
        F2=0
        IF((0.0.LE.S2).AND.(S2.LE.0.5)) F1=1
        IF((0.5.LE.C2).AND.(C2.LE.1.0)) F2=1
        IF((F1.EQ.1).AND.(F2.EQ.1)) ANGLE = PI-(DATAN(S/DSQRT(1.0-S*S)))
        GOTO 400
C
C     ---------------------------------------------------------------
C
 200  IF((A.GT.0.0).OR.(B.GE.0.0)) GOTO 300
        F1=0
        F2=0
        IF((0.0.LE.S2).AND.(S2.LE.0.5)) F1=1
        IF((0.5.LE.C2).AND.(C2.LE.1.0)) F2=1
        IF((F1.EQ.1).AND.(F2.EQ.1)) ANGLE = PI-(DATAN(S/DSQRT(1.0-S*S)))
C
        F1=0
        F2=0
        IF((0.5.LE.S2).AND.(S2.LE.1.0)) F1=1
        IF((0.0.LE.C2).AND.(C2.LE.0.5)) F2=1
        IF((F1.EQ.1).AND.(F2.EQ.1)) ANGLE = 2*PI-(DATAN(DSQRT(1.0-C*C)
     &/C))
        GOTO 400
C
C     ---------------------------------------------------------------
C
 300  IF((A.GE.0.0).OR.(B.LT.0.0)) GOTO 400
        F1=0
        F2=0
        IF((0.5.LE.S2).AND.(S2.LE.1.0)) F1=1
        IF((0.0.LE.C2).AND.(C2.LE.0.5)) F2=1
        IF((F1.EQ.1).AND.(F2.EQ.1)) ANGLE = 2*PI-(DATAN(DSQRT(1.0-C*C)
     &/C))
C
        F1=0
        F2=0
        IF((0.0.LE.S2).AND.(S2.LE.0.5)) F1=1
        IF((0.5.LE.C2).AND.(C2.LE.1.0)) F2=1
        IF((F1.EQ.1).AND.(F2.EQ.1)) ANGLE = 2*PI+(DATAN(S/DSQRT(1.0
     &-S*S)))
        GOTO 400
C
C     ---------------------------------------------------------------
C
 400  RETURN
      END
C     ***************************************************************************
```

```
      PROGRAM ANALYZ
C
      INTEGER MAXSUB,NMAX,POSMAX(750),MINCEN,HISUB,LOSUB,F1,F2
      INTEGER DISUB,J,COUNT,DIF,NPM,FCF
C
      INTEGER*4 XP(10),YP(10)
C
      REAL MAXLEN(750),DILENS(750),CSA(750),XCOEFD,YCOEFD,CONSTD,TOLEN
      REAL MAXSUM,AVMAXD,LENGTH,MINDIA,PI,HIDIST,LODIST,TODIST,LEN
      REAL AVMX90,HILEN,LOLEN,XAXIS(750),YAXIS(750),MINCSA,MAXCSA
      REAL AVCSA,CSA90,DIASTS,CSASTS
C
      DOUBLE PRECISION CWORIG,CF,XDEND1,YDEND1,XDEND2,YDEND2
C
      COMMON/SET1/XP,YP/SET2/CWORIG/SET3/CF/SET4/SCALE
C
C
C     ------------------------------------------------------------------
C
C     PROGRAM ANALYZ FOLLOWS PROGRAM DIAMRS AS THE THIRD OF THREE
C     CHAINED PROGRAMS DESIGNED TO CALCULATE ARTERY DIAMETERS. IT
C     CONCERNS ITSELF WITH THE ANALYSIS OF DIAMETER LENGTHS WHICH
C     ARE CALCULATED FROM THE POINTS OF INTERSECTION CONTAINED IN
C     THE FILE DIAMETER.EPS.
C
C     THE FACILITY EXISTS WHEREBY RELATIVE RESULTS (i.e. %STENOSIS etc)
C     MAY BE CONVERTED TO ABSOLUTE MEASURES BY THE APPLICATION OF A
C     MAGNIFICATION CORRECTION FACTOR.
C     ------------------------------------------------------------------
C
C     PUT THE NUMBER OF DIGITISER UNITS IN 1mm INTO SCALE AND AN
C     ESTIMATE OF THE USERS HAND TRACING TOLERANCE INTO TOL.
C
      SCALE = 39.37
      TOL = 22.04
C
C     SET PI
      PI = 3.141592654
C
C     ------------------------------------------------------------------
C     READ THE CONTENTS OF POINTMAG.NIF. IF MAGNIFICATION CORRECTION IS
C     REQUIRED ACTUAL DATA WILL BE PRESENT. IF NOT REQUIRED, THEN XP(1)
C     YP(1) WILL BE -1,-1. THE FLAG FCF DETECTS THIS CONDITION CAUSING
C     A WARNING TO BE PRINTED WITH THE RESULTS. IF THE NUMBER OF POINT
C     MODE COORDINATES IS NOT EQUAL TO FOUR(THE REQUIRED NUMBER), THEN
C     ABSOLUTE MEASUREMENTS CANNOT BE DERIVED AND THE PROGRAM REVERTS TO
C     PRODUCING ONLY RELATIVE ONES.
C
      FCF = 0
C
      CALL OPEN(6,'POINTMAGNIF',0)
      J = 0
      NPM = 0
C
  1   J = J+1
      READ(6,5,END=2) XP(J),YP(J)
      NPM = NPM+1
      GOTO 1
C
  2   IF((XP(1).EQ.-1).AND.(YP(1).EQ.-1)) FCF = 1
      IF((XP(1).EQ.-1).AND.(YP(1).EQ.-1)) CF = 1.0
      IF((XP(1).EQ.-1).AND.(YP(1).EQ.-1)) REWIND 6
      IF((XP(1).EQ.-1).AND.(YP(1).EQ.-1)) WRITE(6,40) CF
      IF((XP(1).NE.-1).AND.(YP(1).NE.-1).AND.(NPM.NE.4)) WRITE(1,30)
```

```
      IF(NPM.NE.4) XP(1) = -1
      IF(NPM.NE.4) YP(1) = -1
      IF((XP(1).EQ.-1).AND.(YP(1).EQ.-1)) GOTO 3
C
      WRITE(1,35)
      READ(1,40) CWORIG
      CALL MAGNIF
C
C     ------------------------------------------------------------------
C
C     OPEN DIAMETER END POINTS FILE.
C
 3    CALL OPEN(7,'DIAMETEREPS',0)
C
C     OPEN A FILE FOR STORING THE ARTERY AXIS POINTS (FOR PLOTTING).
C
      CALL OPEN(8,'AXIS-POINTS',0)
C
C     READ DIAMETER END POINTS, CALCULATE DIAMETER LENGTHS, CROSS-
C     SECTIONAL AREAS, AXIS POINTS AND OBTAIN N (NDIAMS).
C
      NDIAMS = 0
      J = 0
 10   J = J+1
      READ(7,100,END=20) XDEND1,YDEND1
      READ(7,100) XDEND2,YDEND2
      DILENS(J) = DSQRT((XDEND1*XDEND1+XDEND2*XDEND2+YDEND1*YDEND1+
     &YDEND2*YDEND2)-2*(XDEND1*XDEND2+YDEND1*YDEND2))
      CSA(J) = PI*((DILENS(J)/2.0)*(DILENS(J)/2.0))
      XAXIS(J) = (XDEND1+XDEND2)/2.0
      YAXIS(J) = (YDEND1+YDEND2)/2.0
      WRITE(8,100) XAXIS(J),YAXIS(J)
      WRITE(8,100) XAXIS(J),YAXIS(J)
      NDIAMS = NDIAMS+1
      GOTO 10
C
C     ------------------------------------------------------------------
C
C     FILE FORMAT STATEMENT.
C
 5    FORMAT(2I7)
 30   FORMAT(' INCORRECT NUMBER OF POINT MODE COORDINATES-PROGRAM
     &  REVERTING TO CALCULATION OF RELATIVE MEASURES ONLY')
 35   FORMAT(' ENTER CATHETER WIDTH IN MM (e.g. 2.0) ')
 40   FORMAT(F7.2)
 100  FORMAT(2F11.4)
C
C     ------------------------------------------------------------------
C
C     PUT MINIMUM DIAMETER LENGTH INTO MINDIA AND MAXIMUM DIAMETER LENGTH
C     INTO MAXDIA:PUT MINIMUM CSA INTO MINCSA AND MAXIMUM CSA INTO MAXCSA
C     PUT LOCATION OF MINIMAL C.S.A. INTO MINCEN.
C
 20   F1 = 0
      MINDIA = DILENS(1)
      MAXDIA = DILENS(1)
      MINCSA = CSA(1)
      MAXCSA = CSA(1)
      MINCEN = 1
C
      DO 3500 DISUB = 1,NDIAMS
        IF(DILENS(DISUB).LT.MINDIA) MINDIA = DILENS(DISUB)
        IF(DILENS(DISUB).GT.MAXDIA) MAXDIA = DILENS(DISUB)
```

```
        IF(CSA(DISUB).LT.MINCSA) F1 = 1
        IF(F1.EQ.1) MINCSA = CSA(DISUB)
        IF(F1.EQ.1) MINCEN = DISUB
        F1 = 0
C
        IF(CSA(DISUB).GT.MAXCSA) MAXCSA = CSA(DISUB)
 3500   CONTINUE
C
C
C     ------------------------------------------------------------------
C     THERE MAY BE SEVERAL DIAMETER LENGTH MAXIMA WITHIN THE LIMITS OF HAND
C     TRACING TOLERANCE. PUT MAXIMA INTO MAXLEN( ) WITH SUBSCRIPT MAXSUB.
C     PUT DILENS( ) SUBSCRIPTS OF MAXIMA IN POSMAX( ).
C
      MAXSUB = 0
      DO 3600 DISUB = 1,NDIAMS
        F1 = 0
        IF(DILENS(DISUB).GT.MAXDIA-TOL) F1 = 1
C
        IF(F1.EQ.1) MAXSUB = MAXSUB + 1
        IF(F1.EQ.1) MAXLEN(MAXSUB) = DILENS(DISUB)
        IF(F1.EQ.1) POSMAX(MAXSUB) = DISUB
 3600   CONTINUE
C
C
C     ------------------------------------------------------------------
C     PUT NUMBER OF MAXIMA INTO NMAX
C
      NMAX = MAXSUB
C
C
C     PUT AVERAGE OF MAXIMUM DIAMETERS INTO AVMAXD AND 90% OF THIS VALUE
C     INTO AVMX90
C
      MAXSUM = 0.0
      DO 3700 MAXSUB = 1,NMAX
        MAXSUM = MAXSUM + MAXLEN(MAXSUB)
 3700   CONTINUE
        AVMAXD = MAXSUM/NMAX
        AVMX90 = 0.9*AVMAXD
C
C     CONVERT AVERAGE MAXIMAL AND 90% OF AVERAGE MAXIMAL DIAMETER
C     INTO CROSS SECTIONAL AREAS(CIRCULAR ASSUMPTION,SINGLE PLANE).
C
      AVCSA = PI*((AVMAXD/2.0)*(AVMAXD/2.0))
      CSA90 = 0.9*AVCSA
C
C
C     ------------------------------------------------------------------
C     PUT DISTANCE ALONG AXIS FROM TOP OF AXIS TO CENTRE OF MINIMA INTO
C     HILEN.  PUT DISTANCE ALONG AXIS FROM CENTRE OF MINIMA TO BOTTOM OF
C     AXIS INTO LOLEN
C
      LEN = 0.0
      NDIAMS = NDIAMS-1
      DO 3800 DISUB = 1,NDIAMS
        LEN = LEN + LENGTH(XAXIS(DISUB),YAXIS(DISUB),XAXIS(DISUB+1),YAXI
     &S(DISUB+1))
        IF(DISUB.EQ.MINCEN-1) HILEN = LEN
        IF(DISUB.EQ.MINCEN-1) LEN = 0.0
 3800 CONTINUE
      NDIAMS = NDIAMS+1
        LOLEN = LEN
        TOLEN = HILEN + LOLEN
C
C
C     ------------------------------------------------------------------
```

```
C
C     STARTING AT CENTRAL MINIMUM, MOVE UP AND DOWN TO LOCATE FIRST
C     OCCURANCE OF A CROSS SECTIONAL AREA GREATER THAN OR EQUAL TO
C     CSA90. PUT CSA( ) SUBSCRIPTS INTO HISUB,LOSUB RESPECTIVELY.
C     IF HISUB OR LOSUB ARE NOT FOUND, SET FLAGS F1,F2 RESPECTIVELY
C
      F1 = 0
      DISUB = MINCEN+1
      DO 3900  COUNT = 1,MINCEN
        DISUB = DISUB-1
        IF(CSA(DISUB).GE.CSA90) GOTO 3950
 3900   CONTINUE
        F1 = 1
 3950   HISUB = DISUB
C
      F2 = 0
      DO 4000 DISUB = MINCEN,NDIAMS
        IF(CSA(DISUB).GE.CSA90) GOTO 4500
 4000   CONTINUE
        F2 = 1

 4500   LOSUB = DISUB
C
C
C     PUT DISTANCE FROM UPPER 90% MAX CSA TO CENTRE INTO HIDIST AND
C     DISTANCE FROM LOWER 90% MAX CSA INTO LODIST.
C     INITIALISE HIDIST AND LODIST TO 0.0 TO ACT AS FLAG FOR NON-EXISTENCE
C     OF ONE OR THE OTHER.
C
      IF(F1.EQ.1) TODIST = 0.0
      IF(F1.EQ.1) GOTO 4650
C
      DIF = MINCEN - HISUB
      IF(DIF.EQ.0) HIDIST = 0.0
      IF(DIF.EQ.0) GOTO 4650
C
      LEN = 0.0
      MINCEN = MINCEN-1
      DO 4600 DISUB = HISUB,MINCEN
        LEN = LEN + LENGTH(XAXIS(DISUB),YAXIS(DISUB),XAXIS(DISUB+1),YAXI
     &S(DISUB+1))
 4600 CONTINUE
      MINCEN = MINCEN+1
      HIDIST = LEN
C
 4650 IF(F2.EQ.1) TODIST = 0.0
      IF(F2.EQ.1) GOTO 4800
C
      DIF = MINCEN - LOSUB
      IF(DIF.EQ.0) LODIST = 0.0
      IF(DIF.EQ.0) GOTO 4750
C
      LEN = 0.0
      LOSUB = LOSUB-1
      DO 4700 DISUB=MINCEN,LOSUB
        LEN = LEN + LENGTH(XAXIS(DISUB),YAXIS(DISUB),XAXIS(DISUB+1),
     &YAXIS(DISUB+1))
 4700 CONTINUE
      LOSUB = LOSUB+1
      LODIST = LEN
C
 4750 TODIST = HIDIST+LODIST
C
```

```
C
C
C     ------------------------------------------------------------------
C     PUT PERCENTAGE DIAMETER CONSTRICTION INTO DIASTS, PERCENTAGE CROSS
C     SECTIONAL AREA INTO CSASTS.
C
 4800 DIASTS = 100*((AVMAXD-MINDIA)/AVMAXD)
      CSASTS = 100*((AVCSA-MINCSA)/AVCSA)
C
C     ------------------------------------------------------------------
C
C     OUTPUT BASIC INFORMATION TO PRINTER AT THE START OF A NEW PAGE.
C
      WRITE(2,5800)
 5800 FORMAT(1H1, ' ')
      IF(FCF.EQ.1) WRITE(2,5900)
 5900 FORMAT(' NOTE-ABSOLUTE MEASUREMENTS BELOW REFER TO THE PROJECTED
     & DIMENSIONS TAKEN FROM ')
      IF(FCF.EQ.1) WRITE(2,5925)
 5925 FORMAT(' ==========================================================
     &========== ')
      IF(FCF.EQ.1) WRITE(2,5950)
 5950 FORMAT(' THE BITPAD. i.e. THEY ARE NOT CORRECTED FOR MAGNIFICATI
     &ON ')
      IF(FCF.EQ.1) WRITE(2,5975)
 5975 FORMAT(' ==========================================================
     &== ')
      WRITE(2,6100)
 6100 FORMAT('                SINGLE PLANE OUTPUT')
      WRITE(2,6200)
 6200 FORMAT('                **********************')
C
      WRITE(2,6300)
 6300 FORMAT( ' ')
      WRITE(2,6400)
 6400 FORMAT('       DIAMETER RESULTS')
      WRITE(2,6500)
 6500 FORMAT('       ----------------')
C
      AVMAXD = ((100*AVMAXD/SCALE+0.5)/100)*CF
      WRITE (2,6600) AVMAXD
 6600 FORMAT('       MEAN MAXIMAL DIAMETER          = ',F6.2,' mm')
C
      AVMX90 = ((100*AVMX90/SCALE+0.5)/100)*CF
      WRITE (2,6700) AVMX90
 6700 FORMAT('       90% OF MAXIMAL DIAMETER        = ',F6.2,' mm')
C
      MINDIA = ((100*MINDIA/SCALE+0.5)/100)*CF
      WRITE (2,6800) MINDIA
 6800 FORMAT('       MINIMUM DIAMETER               = ',F6.2,' mm')
C
      DIASTS = (100*DIASTS+0.5)/100
      WRITE (2,6900) DIASTS
 6900 FORMAT('       % DIAMETER STENOSIS            = ',F6.2,' %')
C
      WRITE(2,7000)
 7000 FORMAT(' ')
      WRITE(2,7100)
 7100 FORMAT('       CROSS-SECTIONAL AREA RESULTS')
      WRITE(2,7200)
 7200 FORMAT('       ---------------------------')
C
      AVCSA = ((100*AVCSA/(SCALE*SCALE)+0.5)/100)*CF
      WRITE (2,7300) AVCSA
```

```
 7300 FORMAT('       MEAN MAXIMAL C.S.A.            = ',F6.2,' sq.mm')
C
      CSA90 = ((100*CSA90/(SCALE*SCALE)+0.5)/100)*CF
      WRITE (2,7400) CSA90
 7400 FORMAT('       90% OF MAXIMAL C.S.A.          = ',F6.2,' sq.mm')
C
      MINCSA = ((100*MINCSA/(SCALE*SCALE)+0.5)/100)*CF
      WRITE (2,7500) MINCSA
 7500 FORMAT('       MINIMUM C.S.A.                 = ',F6.2,' sq.mm')
C
      CSASTS = (100*CSASTS+0.5)/100
      WRITE (2,7600) CSASTS
 7600 FORMAT('       % C.S.A. STENOSIS              = ',F6.2,' %')
C
      WRITE(2,7700)
 7700 FORMAT( ' ')
      WRITE(2,7800)
 7800 FORMAT('       LENGTH RESULTS')
      WRITE(2,7900)
 7900 FORMAT('       --------------')
C
      HIDIST = ((100*HIDIST/SCALE+0.5)/100)*CF
      IF(F1.EQ.0) WRITE (2,8000) HIDIST
 8000 FORMAT('       DISTANCE TO UPPER 90th CENTILE = ',F6.2,' mm')
C
      IF(F1.NE.0) WRITE (2,8100)
 8100 FORMAT('              NO UPPER 90th CENTILE DETECTED')
C
      LODIST = ((100*LODIST/SCALE+0.5)/100)*CF
      IF(F2.EQ.0) WRITE (2,8200) LODIST
 8200 FORMAT('       DISTANCE TO LOWER 90th CENTILE = ',F6.2,' mm')
C
      IF(F2.NE.0) WRITE (2,8300)
 8300 FORMAT('              NO LOWER 90th CENTILE DETECTED')
C
      TODIST = ((100*TODIST/SCALE+0.5)/100)*CF
      WRITE (2,8400) TODIST
 8400 FORMAT('       STENOTIC LENGTH                = ',F6.2,' mm')
C
      TOLEN = ((100*TOLEN/SCALE+0.5)/100)*CF
      WRITE (2,8500) TOLEN
 8500 FORMAT('       SEGMENT LENGTH                 = ',F6.2,' mm')
C
C     ------------------------------------------------------------------
C
C     CLOSE FILE AND END PROGRAM
C
      ENDFILE 6
      ENDFILE 7
      ENDFILE 8
C
      STOP
C
      END
C     ******************************************************************************
      FUNCTION LENGTH(XDUM1,YDUM1,XDUM2,YDUM2)
C
      REAL XDUM1,YDUM1,XDUM2,YDUM2,XDISP,YDISP,LENGTH
C
      XDISP = XDUM2 - XDUM1
      YDISP = YDUM2 - YDUM1
C
      LENGTH = SQRT(XDISP*XDISP + YDISP*YDISP)
```

```
C
      RETURN
      END
C
C     ************************************************************************
      SUBROUTINE MAGNIF
C
      INTEGER*4 XP(10),YP(10)
C
      DOUBLE PRECISION XT,YT,XB,YB,CWPROJ,CWORIG,CF
      DOUBLE PRECISION DCOEFX,DCOEFY,DCONST,COEFX1,COEFY1
      DOUBLE PRECISION CON1,COEFX2,COEFY2,CON2,GRAD1,GRAD2,XINT1,YINT1
      DOUBLE PRECISION XINT2,YINT2,TWO
C
      COMMON/SET1/XP,YP/SET2/CWORIG/SET3/CF/SET4/SCALE
C     ------------------------------------------------------------------------
C
C     THIS SUBROUTINE CALCULATES A MAGNIFICATION CORRECTION FACTOR FOR
C     SINGLE PLANE VIEWS. IT IS BASED ON THE RATIO OF KNOWN CATHETER
C     WIDTH TO PROJECTED CATHETER WIDTH WHICH IS DIGITISED ALONG WITH
C     THE STENOSIS. EMPLOYMENT OF SUCH A CORRECTION FACTOR ALLOWS
C     EXPRESSION OF RESULTS IN ABSOLUTE TERMS RATHER THAN ONLY RELATIVE
C     ONES.
C
C     USING THE FOUR POINTS WHICH DESCRIBE THE CATHETER WIDTH, CALCULATE
C     THE MIDPOINTS OF LINES JOINING THE TOP POINTS AND THE BOTTOM POINTS
C     OF EACH SIDE.
C
C     INTEGER*4 VARIABLES CANNOT BE DIVIDED BY REAL NUMBERS. HENCE ASSIGN
C     THE VARIABLE TWO AS A DOUBLE PRECISION VALUE 2.0
C
C     ------------------------------------------------------------------------
C

      TWO = 2.0
C
      XT = (XP(1)+XP(3))/TWO
      YT = (YP(1)+YP(3))/TWO
C
      XB = (XP(2)+XP(4))/TWO
      YB = (YP(2)+YP(4))/TWO
C
C     CALCULATE THE MIDPOINT OF THE LINE BETWEEN THE ABOVE TWO MIDPOINTS
C     AS AN AXIS POINT. PUT INTO XMID,YMID.
C
      XMID = (XT+XB)/TWO
      YMID = (YT+YB)/TWO
C
C     THE CATHETER DIAMETER LINE IS CONSIDERED TO BE A LINE THROUGH XMID,
C     YMID PERPENDICULAR TO THE LINE JOINING THE TOP AND BOTTOM LINES.
C     PUT THE COEFFICIENTS OF THE DIAMETER INTO DCOEFX,DCOEFY,DCONST.
C
      DCOEFX = XT-XB
      DCOEFY = YT-YB
      DCONST = (YB*YMID+XB*XMID)-(YT*YMID+XT*XMID)
C
C     CALCULATE THE EQUATIONS OF THE LINES JOINING POINTS 1 WITH 2 AND
C     POINTS 3 WITH 4.
C
      COEFX1 = YP(1)-YP(2)
      COEFY1 = XP(2)-XP(1)
      CON1 = YP(2)*XP(1)-YP(1)*XP(2)
C
      COEFX2 = YP(3)-YP(4)
```

```
      COEFY2 = XP(4)-XP(3)
      CON2 = YP(4)*XP(3)-YP(3)*XP(4)
C
C     CALCULATE GRADIENTS OF THESE LINES.
C
      GRAD1 = DCOEFX*COEFY1-COEFX1*DCOEFY
      GRAD2 = DCOEFX*COEFY2-COEFX2*DCOEFY
C
C     CALCULATE THE POINTS OF INTERSECTION OF THE DIAMETER LINE WITH
C     THE ABOVE EQUATIONS.
C
      XINT1 = (DCOEFY*CON1-COEFY1*DCONST)/GRAD1
      YINT1 = (COEFX1*DCONST-DCOEFX*CON1)/GRAD1
C
      XINT2 = (DCOEFY*CON2-COEFY2*DCONST)/GRAD2
      YINT2 = (COEFX2*DCONST-DCOEFX*CON2)/GRAD2
C
C     CALCULATE THE DIAMETER OF THE CATHETER.
C
      CWPROJ = DSQRT((XINT1*XINT1+XINT2*XINT2+YINT1*YINT1+YINT2*YINT2)
     &-2*(XINT1*XINT2+YINT1*YINT2))
C
C     CONVERT DIAMETER TO mm.
C
      CWPROJ = CWPROJ/SCALE
C
C     CALCULATE MAGNIFICATION CORRECTION FACTOR (CF).
C
      CF = CWORIG/CWPROJ
C
      RETURN
C
      END
C
C     ***************************************************************************
```

```
      PROGRAM ECCFTR
C
      INTEGER N,J,POSMIN,DISUB,MAXSUB,F1,F2,LOSUB,HISUB,E,STEP
C
      REAL X1(2000),Y1(2000),X2(2000),Y2(2000),MINDIA,MAXDIA
      REAL MAXSUM,AVMAXD,X1P,Y1P,X2P,Y2P,X1D,Y1D,X2D,Y2D,CF,SCALE
      REAL XCENTR,YCENTR,DET,AREA1,AREA2,DIFAR,PAXX,PAXY
      REAL LPIX(1000),LPIY(1000),UPIX(1000),UPIY(1000),MPX,MPY,DIAM
      REAL AVECC,DILENS(1000),XAXIS(1000),YAXIS(1000),LENGTH,STORE
      REAL LDIFF,LRATE,UDIFF,URATE,PLRAD,DLRAD,MAXECC,PURAD,DURAD
      REAL SHIFT,ECCENT,MINECC
C
      DOUBLE PRECISION MINANG,ANGDIF,DELTAL,DELTAU,LRAD,URAD,AP,BP,CP
      DOUBLE PRECISION AD,BD,CD,A(2000),B(2000),C(2000),DIFANG,PRXANG
      DOUBLE PRECISION CURANG,XTRAN,YTRAN
C
      COMMON/SET1/MINDIA/SET2/DILENS,DISUB/SET3/XAXIS,YAXIS
      COMMON/SET4/X1P,Y1P,X2P,Y2P,X1D,Y1D,X2D,Y2D
      COMMON/SET5/X1,Y1,X2,Y2/SET6/POSMIN/SET7/MINECC,MAXECC,AVECC
C
C
C
C     THIS PROGRAM READS THE FILE OF DIAMETER END POINTS PRODUCED BY THE
C     PROGRAM DIAMRS AND CALCULATES THE MEAN ECCENTRICITY OF THE ARTERY
C     SEGMENT ALONG WITH THE MAXIMAL ECCENTRICITY AND THE ECCENTRICITY AT
C     THE MINIMAL DIAMETER. IN THE PAST MANY ASSUMPTIONS HAVE BEEN MADE
C     ABOUT THE INTERNAL SHAPE OF THE LEFT VENTRICLE, THE MOST COMMON ONE
C     BEING ITS APPROXIMATION TO AN ELLIPSOID. THIS PROGRAM IS BASED ON
C     THE ASSUMPTION THAT ONE MAY EXTRAPOLATE THIS SHAPE TO THE EXTERNAL
C     SURFACE AND CONSIDER IT TO BE A PORTION OF THE ARC OF A CIRCLE.
C     HENCE THE PROGRAM WORKS BY FIRST FITTING THE DISEASED ARTERY WITH
C     AN INTERPOLATED NORMAL PORTION BASED ON THE CALCULATIONS FOR THE
C     ARC OF A CIRCLE. ONCE ESTABLISHED, THE POINTS OF INTERSECTION OF
C     THE EXISTING DIAMETER LINES WITH THE 'UNDISEASED ARTERY' CAN BE
C     COMPUTED AND HENCE ECCENTRICITY CALCULATED.
C
C     HOWEVER, THIS ALGORITHM IS ONLY SUITABLE FOR ARTERIES WHICH ARE
C     EITHER STRAIGHT OR CURVED IN ONE DIRECTION. MULTIPLE CURVES IN
C     ALTERNATE DIRECTIONS WILL RESULT IN AN ANOMOLOUS FIT OF THE ARC
C     TO THE ARTERY, THUS GENERATING SPURIOUS RESULTS.
C
C
C
C     SET HAND TRACING TOLERANCE INTO TOL AND THE NUMBER OF BITPAD UNITS
C     IN 1mm INTO SCALE.
C
      TOL = 22.04
      SCALE = 39.37
C
C
C
C     READ THE FILE DIAMETER.EPS CONTAINING THE DIAMETER END POINT
C     INFORMATION, CALCULATE DIAMETER LENGTHS, AXIS POINTS AND OBTAIN N.
C
      CALL OPEN(6,'DIAMETER.EPS',0)
C
C     OPEN A FILE FOR THE RESULTANT 'UNDISEASED' DIAMETER END POINTS.
C
      CALL OPEN(7,'ARCRADII.EPS',0)
C
C     OPEN THE FILE POINTMAG.NIF AND OBTAIN THE MAGNIFICATION CORRECTION
C     FACTOR.
C
```

```
      CALL OPEN(8,'POINTMAG.NIF',0)
C
      READ(8,5) CF
 5    FORMAT(F7.2)
C
      N = 0
      J = 0
 10   J = J+1
C
      READ(6,20,END=30) X1(J),Y1(J)
      READ(6,20) X2(J),Y2(J)
      DILENS(J) = LENGTH(X1(J),Y1(J),X2(J),Y2(J))
      XAXIS(J) = (X1(J)+X2(J))/2.0
      YAXIS(J) = (Y1(J)+Y2(J))/2.0
      N = N+1
      GOTO 10
C
 20   FORMAT(2F11.4)
C
C     PUT MINIMUM DIAMETER LENGTH INTO MINDIA AND MAXIMUM DIAMETER LENGTH
C     INTO MAXDIA:PUT LOCATION OF MINIMAL DIAMETER INTO POSMIN.
C
 30   MINDIA = DILENS(1)
      MAXDIA = DILENS(1)
      POSMIN = 0
C
      DO 40 DISUB = 1,N
        IF(DILENS(DISUB).LT.MINDIA) POSMIN = DISUB
        IF(DILENS(DISUB).LT.MINDIA) MINDIA = DILENS(DISUB)
        IF(DILENS(DISUB).GE.MAXDIA) MAXDIA = DILENS(DISUB)
 40   CONTINUE
C
C     ------------------------------------------------------------------
C     THERE MAY BE SEVERAL DIAMETER LENGTH MAXIMA WITHIN THE LIMITS OF HAND
C     TRACING TOLERANCE. PUT SUCCESSIVE MAXIMA INTO MAXSUM AND COUNT
C     INTO MAXSUB. OBTAIN THE AVERAGE MAXIMA BY DIVISION OF MAXSUM BY
C     MAXSUB.
C
      MAXSUM = 0.0
      MAXSUB = 0
C
      DO 50 DISUB = 1,N
        F1 = 0
        IF(DILENS(DISUB).GT.MAXDIA-TOL) F1 = 1
        IF(F1.EQ.1) MAXSUB = MAXSUB + 1
        IF(F1.EQ.1) MAXSUM = MAXSUM + DILENS(DISUB)
 50   CONTINUE
C
      AVMAXD = MAXSUM/MAXSUB
C     ------------------------------------------------------------------
C
C     STARTING AT CENTRAL MINIMUM, MOVE UP AND DOWN TO LOCATE FIRST
C     OCCURANCE OF A DIAMETER GREATER THAN OR EQUAL TO AVMAXD. PUT
C     DIAMETER SUBSCRIPTS INTO HISUB,LOSUB . IF NOT LOCATED, SET FLAG
C     F1 AND/OR F2.
C
      F1 = 0
      E = 1
      STEP = -1
C
      DO 60 DISUB = POSMIN,E,STEP
        IF(DILENS(DISUB).GE.AVMAXD) GOTO 70
 60   CONTINUE
```

```
        F1 = 1
        IF(F1.EQ.1) CALL LOCMAX(E,STEP)
 70     HISUB = DISUB
C
      F2 = 0
      E = N
      STEP = 1
C
      DO 80DISUB = POSMIN,E,STEP
        IF(DILENS(DISUB).GE.AVMAXD) GOTO 90
 80   CONTINUE
        F2 = 1
        IF(F2.EQ.1) CALL LOCMAX(E,STEP)
 90     LOSUB = DISUB
C
C     ASSIGN LOCATED DIAMETER END POINTS TO PROXIMAL AND DISTAL
C     REFERENCE POINTS.
C
      X1P = X1(HISUB)
      Y1P = Y1(HISUB)
      X2P = X2(HISUB)
      Y2P = Y2(HISUB)
C
      X1D = X1(LOSUB)
      Y1D = Y1(LOSUB)
      X2D = X2(LOSUB)
      Y2D = Y2(LOSUB)
C
C     CALCULATE DISEASED AREA.
C
      CALL AREAS(X1,Y1,X2,Y2,HISUB,LOSUB,AREA1)
C
C     COMPUTE COEFFICIENTS OF DIAMETER LINES.
C
      AP = Y1P-Y1P
      BP = X2P-X1P
      CP = X1P*Y2P-X2P*Y1P
C
      AD = Y1D-Y2D
      BD = X2D-X1D
      CD = X1D*Y2D-X2D*Y1D
C
C     CHECK DIAMETER LINES FOR PARALLELILITY USING THE FUNCTION ANGLE.
C     PARALLELILITY IS JUDGED TO BE PRESENT IF THE DIFFERENCE IN THE
C     ANGLES BETWEEN THE TWO DIAMETER LINES IS LESS THAN THE MINIMAL
C     OBTAINABLE ON THE BITPAD(MINANG).
C
      MINANG = 3.33333321E-4
C
      ANGDIF = (ANGLE(AD,-BD)-ANGLE(AP,-BP))
C
      IF(ABS(ANGDIF).LE.MINANG) CALL LINFIT(HISUB,LOSUB)
      IF(ABS(ANGDIF).LE.MINANG) GOTO 135
C
C     CALCULATE THE POINTS OF INTERSECTION BETWEEN THE TWO DIAMETER LINES.
C     THIS REPRESENTS THE CENTRE OF THE CIRCLE FROM WHICH THE ARCS ARE
C     FITTED.
C
      DET = AP*BD-AD*BP
      XCENTR = (BP*CD-BD*CP)/DET
      YCENTR = (AD*CP-AP*CD)/DET
C
C     CALCULATE RADII FOR UPPER AND LOWER BOUND ARCS AT PROXIMAL AND
```

```
C     DISTAL ENDS.
C
      PLRAD = SQRT((X1P*X1P+XCENTR*XCENTR+Y1P*Y1P+YCENTR*YCENTR)-2*
     &(X1P*XCENTR+Y1P*YCENTR))
      DLRAD = SQRT((X1D*X1D+XCENTR*XCENTR+Y1D*Y1D+YCENTR*YCENTR)-2*
     &(X1D*XCENTR+Y1D*YCENTR))
C
      PURAD = SQRT((X2P*X2P+XCENTR*XCENTR+Y2P*Y2P+YCENTR*YCENTR)-2*
     &(X2P*XCENTR+Y2P*YCENTR))
      DURAD = SQRT((X2D*X2D+XCENTR*XCENTR+Y2D*Y2D+YCENTR*YCENTR)-2*
     &(X2D*XCENTR+Y2D*YCENTR))
C
C     CALCULATE THE ANGULAR RATE OF CHANGE OF RADIUS FOR UPPER AND LOWER
C     BOUNDS.
C
      LDIFF = DLRAD - PLRAD
      LRATE = LDIFF/ANGDIF
C
      UDIFF = DURAD - PURAD
      URATE = UDIFF/ANGDIF
C
C     BEGIN TO WORK THROUGH DIAMETER LINES BETWEEN PROXIMAL AND DISTAL
C     ENDS CALCULATING FIRST THE EQUATION OF THE LINE IN TERMS OF A,B
C     AND C. SOLVE THE POINTS OF INTERSECTION WITH UPPER AND LOWER ARCS,
C     THEN CALCULATE MIDPOINTS, SHIFT AND ECCENTRICITY. STORE AND PROGRESS.
C
      MAXECC = 0.0
      MINECC = 0.0
      STORE = 0.0
C
C     CALCULATE THE AXIS POINT OF THE PROXIMAL DIAMETER LINE AND THE
C     ANGLE BETWEEN THIS POINT AND THE RIGHT DIRECTED HORIZONTAL.
C
      PAXX = (X1P+X2P)/2.0
      PAXY = (Y1P+Y2P)/2.0
C
      XTRAN = PAXX - XCENTR
      YTRAN = PAXY - YCENTR
C
      PRXANG = ANGLE(YTRAN,XTRAN)
C
      HISUB = HISUB+1
      LOSUB = LOSUB-1
C
      DO 110 J = HISUB,LOSUB
        A(J) = YCENTR-YAXIS(J)
        B(J) = XAXIS(J)-XCENTR
        C(J) = XCENTR*YAXIS(J) - XAXIS(J)*YCENTR
C
C     CALCULATE THE ANGULAR CHANGE BETWEEN CURRENT AXIS POINT AND THE
C     PROXIMAL AXIS POINT USING THE COORDINATE APPROACH.
C
      XTRAN = XAXIS(J) - XCENTR
      YTRAN = YAXIS(J) - YCENTR
C
      CURANG = ANGLE(YTRAN,XTRAN)
C
      DIFANG = CURANG - PRXANG
C
C     COMPUTE THE CHANGE IN RADIUS FOR THE CHANGE IN ANGLE AND ADJUST
C     LRAD AND URAD ACCORDINGLY.
C
      DELTAL = LRATE*DIFANG
```

```
      DELTAU = URATE*DIFANG
C
      LRAD = PLRAD + DELTAL
      URAD = PURAD + DELTAU
C
C     CALCULATE THE COORDINATES OF THE POINTS AT THE ENDS OF THE RADII.
C
      LPIX(J) = ((LRAD/PLRAD)*((X1P-XCENTR)*COS(DIFANG)-(Y1P-YCENTR)
     &*SIN(DIFANG)))+XCENTR
      LPIY(J) = ((LRAD/PLRAD)*((Y1P-XCENTR)*COS(DIFANG)+(X1P-YCENTR)
     &*SIN(DIFANG)))+XCENTR
      UPIX(J) = ((URAD/PURAD)*((X2P-XCENTR)*COS(DIFANG)-(Y2P-YCENTR)
     &*SIN(DIFANG)))+XCENTR
      UPIY(J) = ((URAD/PURAD)*((Y2P-XCENTR)*COS(DIFANG)+(X2P-YCENTR)
     &*SIN(DIFANG)))+XCENTR
C
C     CALCULATE THE ECCENTRICITY FACTORS AS THE SHIFT IN MIDPOINTS BETWEEN
C     THE DISEASED AND UNDISEASED SEGMENTS DIVIDED BY THE UNDISEASED
C     DIAMETER.
C
      MPX = (LPIX(J)+UPIX(J))/2.0
      MPY = (LPIY(J)+UPIY(J))/2.0
      DIAM = LENGTH(LPIX(J),LPIY(J),UPIX(J),UPIY(J))
      WRITE(7,132) LPIX(J),LPIY(J)
      WRITE(7,132) UPIX(J),UPIY(J)
 132  FORMAT(2F11.4)
C
      SHIFT = LENGTH(XAXIS(J),YAXIS(J),MPX,MPY)
C
      ECCENT = (SHIFT/(DIAM/2.0))*100
C
      IF(ECCENT.GE.MAXECC) MAXECC = ECCENT
      IF(J.EQ.POSMIN) MINECC = ECCENT
      STORE = STORE+ECCENT
C
 110  CONTINUE
C
      HISUB = HISUB-1
      LOSUB = LOSUB+1
C
      AVECC = STORE/(LOSUB-1-HISUB-1)
C
C     CALCULATE UNDISEASED AREA.
C
      LPIX(HISUB) = X1P
      LPIY(HISUB) = Y1P
      UPIX(HISUB) = X2P
      UPIY(HISUB) = Y2P
C
      LPIX(LOSUB) = X1D
      LPIY(LOSUB) = Y1D
      UPIX(LOSUB) = X2D
      UPIY(LOSUB) = Y2D
C
      CALL AREAS(LPIX,LPIY,UPIX,UPIY,HISUB,LOSUB,AREA2)
C
      DIFAR = AREA2 - AREA1
C
C     DISPLAY RESULTS.
C
 135  WRITE(1,140)
 140  FORMAT('       ECCENTRICITY RESULTS.')
C
```

```
      WRITE(1,150)
 150  FORMAT('        _____')
C
      WRITE(1,175)
 175  FORMAT(' ')
C
      WRITE(1,200) MINECC
 200  FORMAT(' ECCENTRICITY FACTOR AT MINIMUM DIAMETER = ',F8.2,'%')
C
      WRITE(1,175)
C
      WRITE(1,300) MAXECC
 300  FORMAT('              MAXIMAL ECCENTRICITY FACTOR = ',F8.2,'%')
C
      WRITE(1,175)
C
      WRITE(1,400) AVECC
 400  FORMAT('                  MEAN ECCENTRICITY FACTOR = ',F8.2,'%')
C
      WRITE(1,175)
      WRITE(1,175)
C
      WRITE(1,500)
 500  FORMAT('        AREA RESULTS.')
C
      WRITE(1,550)
 550  FORMAT('        _____')
C
      WRITE(1,175)
C
      AREA1 = ((100*AREA1)/((SCALE*SCALE)+0.5)/100)*CF*CF
      WRITE(1,600) AREA1
 600  FORMAT('                              STENOTIC AREA = ',F8.2,'sq.mm')
C
      WRITE(1,175)
C
      AREA2 = ((100*AREA2)/((SCALE*SCALE)+0.5)/100)*CF*CF
      WRITE(1,650) AREA2
 650  FORMAT('                            UNDISEASED AREA = ',F8.2,'sq.mm')
C
      WRITE(1,175)
C
      DIFAR = ((100*DIFAR)/((SCALE*SCALE)+0.5)/100)*CF*CF
      WRITE(1,700) DIFAR
 700  FORMAT('                              ATHEROMA AREA = ',F8.2,'sq.mm')
C
C     CLOSE FILES AND END.
C
      ENDFILE 6
      ENDFILE 7
      ENDFILE 8
C
      STOP
C
      END
C
C     ******************************************************************************
      FUNCTION ANGLE(A,B)
C
      INTEGER F1,F2,F
C
      DOUBLE PRECISION R2,S2,C2,A,B,PI,ANGLE,S1,C1
C
```

```
      COMMON/SET7/PI
C
C     ---------------------------------------------------------------
C
C     PUT SQUARES OF HYPOTENUSE INTO R2,SINE INTO S2,COSINE INTO C2.
C
      R2 = A*A + B*B
      IF(R2.LT.2.0E-4) WRITE(1,10)A,B
 10   FORMAT( 'ERROR-PARAMETERS ',F7.5,' AND ',F7.5,' PASSED TO ANGLE
     & FUNCTION TOO SMALL')
      IF(R2.LT.2.0E-4) GOTO 400
C
      S2 = A*A/R2
      C2 = B*B/R2
C
C     ENSURE THAT NUMERICAL ACCURACY PROBLEMS DO NOT PREVENT CORRECT
C     WORKING OF OCTANT TRAPS.
C
      IF(S2.LT.1.0E-4) S2 = 0.0
      IF(C2.LT.1.0E-4) C2 = 0.0
C
      IF(S2.GT.1.0-1.0E-4) S2 = 1.0
      IF(C2.GT.1.0-1.0E-4) C2 = 1.0
C
      F = 0
      IF(DABS(S2-C2).LT.1.0E-4) F = 1
      IF(F.EQ.1) S2 = 0.5
      IF(F.EQ.1) C2 = 0.5
C
      IF(C2.LT.S2) S2 = 1.0 - C2
      IF(S2.LT.C2) C2 = 1.0 - S2
C
      S1 = DSIGN(DSQRT(S2),A)
      C1 = DSIGN(DSQRT(C2),B)
C
C     ---------------------------------------------------------------
C
C     ARCSINE AND ARCCOS ARE NOT INTRINSIC FUNCTIONS IN THIS VERSION
C     OF FORTRAN. THIS PROBLEM IS OVERCOME BY USING ARCTAN.
C
C     ---------------------------------------------------------------
C
      IF((A.LT.0.0).OR.(B.LE.0.0)) GOTO 100
        F1=0
        F2=0
        IF((0.0.LE.S2).AND.(S2.LE.0.5)) F1=1
        IF((0.5.LE.C2).AND.(C2.LE.1.0)) F2=1
        IF((F1.EQ.1).AND.(F2.EQ.1)) ANGLE = DATAN(S/DSQRT(1.0-S*S))
C
        F1=0
        F2=0
        IF((0.5.LE.S2).AND.(S2.LE.1.0)) F1=1
        IF((0.0.LE.C2).AND.(C2.LE.0.5)) F2=1
        IF((F1.EQ.1).AND.(F2.EQ.1)) ANGLE = DATAN(DSQRT(1.0-C*C)/C)
        GOTO 400
C
C     ---------------------------------------------------------------
C
 100  IF((A.LE.0.0).OR.(B.GT.0.0)) GOTO 200
        F1=0
        F2=0
        IF((0.5.LE.S2).AND.(S2.LE.1.0)) F1=1
        IF((0.0.LE.C2).AND.(C2.LE.0.5)) F2=1
```

```
        IF((F1.EQ.1).AND.(F2.EQ.1)) ANGLE = DATAN(DSQRT(1.0-C*C)/C)
C
        F1=0
        F2=0
        IF((0.0.LE.S2).AND.(S2.LE.0.5)) F1=1
        IF((0.5.LE.C2).AND.(C2.LE.1.0)) F2=1
        IF((F1.EQ.1).AND.(F2.EQ.1)) ANGLE = PI-(DATAN(S/DSQRT(1.0-S*S)))
        GOTO 400
C
C     ------------------------------------------------------------------
C
 200  IF((A.GT.0.0).OR.(B.GE.0.0)) GOTO 300
        F1=0
        F2=0
        IF((0.0.LE.S2).AND.(S2.LE.0.5)) F1=1
        IF((0.5.LE.C2).AND.(C2.LE.1.0)) F2=1
        IF((F1.EQ.1).AND.(F2.EQ.1)) ANGLE = PI-(DATAN(S/DSQRT(1.0-S*S)))
C
        F1=0
        F2=0
        IF((0.5.LE.S2).AND.(S2.LE.1.0)) F1=1
        IF((0.0.LE.C2).AND.(C2.LE.0.5)) F2=1
        IF((F1.EQ.1).AND.(F2.EQ.1)) ANGLE = 2*PI-(DATAN(DSQRT(1.0-C*C)
     &/C))
        GOTO 400
C
C     ------------------------------------------------------------------
C
 300  IF((A.GE.0.0).OR.(B.LT.0.0)) GOTO 400
        F1=0
        F2=0
        IF((0.5.LE.S2).AND.(S2.LE.1.0)) F1=1
        IF((0.0.LE.C2).AND.(C2.LE.0.5)) F2=1
        IF((F1.EQ.1).AND.(F2.EQ.1)) ANGLE = 2*PI-(DATAN(DSQRT(1.0-C*C)
     &/C))
C
        F1=0
        F2=0
        IF((0.0.LE.S2).AND.(S2.LE.0.5)) F1=1
        IF((0.5.LE.C2).AND.(C2.LE.1.0)) F2=1
        IF((F1.EQ.1).AND.(F2.EQ.1)) ANGLE = 2*PI+(DATAN(S/DSQRT(1.0
     &-S*S)))
        GOTO 400
C
C     ------------------------------------------------------------------
C
 400  RETURN
      END
C     ********************************************************************************
C
      SUBROUTINE LOCMAX
C
      INTEGER J,E,STEP,POSMIN,DISUB
C
      REAL MINDIA,MAX,DILENS
C
      COMMON/SET1/MINDIA/SET2/DILENS,DISUB/SET7/POSMIN
C
C     ------------------------------------------------------------------
C
C     THIS SUBROUTINE LOCATES THE MAXIMAL DIAMETER EITHER ABOVE OR
C     BELOW THE MINIMUM IN THE ABSENCE OF A DIAMETER IN EXCESS OF THE
C     AVERAGE MAXIMUM.
```

```
C
C
C     ------------------------------------------------------------------
C
      MAX = MINDIA
C
      DO 10 J = POSMIN,E,STEP
        IF(DILENS(J).GE.MAX) DISUB = J
        IF(DILENS(J).GE.MAX) MAX = DILENS(J)
 10   CONTINUE
C
      RETURN
C
      END
C
C     ******************************************************************************
C
      SUBROUTINE LINFIT
C
      INTEGER POSMIN,J,HISUB,LOSUB
C
      REAL COEFX1,COEFY1,COEFC1,COEFX2,COEFY2,COEFC2,MAXECC,MINECC
      REAL STORE,XCOEFD,YCOEFD,CONSTD,GRAD1,LPIX(1000),LPIY(1000)
      REAL UPIX(1000),UPIY(1000),MPX,MPY,DIAM,SHIFT,ECCENT,AVECC,GRAD2
      REAL XAXIS(1000),YAXIS(1000),X1(2000),Y1(2000),X2(2000),Y2(2000)
C
      COMMON/SET5/X1P,Y1P,X2P,Y2P,X1D,Y1D,X2D,Y2D/SET3/XAXIS,YAXIS
      COMMON/SET6/X1,Y1,X2,Y2/SET7/POSMIN/SET8/MINECC,MAXECC,AVECC
C
C     ------------------------------------------------------------------
C
C     THIS SUBROUTINE FITS A STRAIGHT LINE BETWEEN THE PROXIMAL AND
C     DISTAL DIAMETER LINES WHEN THEY HAVE BEEN JUDGED TO BE PARALLEL
C     TO EACH OTHER. THE SUBROUTINE GOES ON TO CALCULATE MAXIMAL AND MEAN
C     ECCENTRICITY AND ECCENTRICITY AT THE MINIMUM DIAMETER.
C
C     ------------------------------------------------------------------
C
C     DETERMINE THE EQUATIONS OF THE FITTED STRAIGHT LINES.
C
C     LOWER BOUND.
C
      COEFX1 = Y1P-Y1D
      COEFY1 = X1D-X1P
      COEFC1 = Y1D*X1P-Y1P*X1D
C
C     UPPER BOUND.
C
      COEFX2 = Y2P-Y2D
      COEFY2 = X2D-X2P
      COEFC2 = Y2D*X2P-Y2P*X2D
C
C     CALCULATE THE DIAMETER EQUATION, THE POINTS OF INTERSECTION WITH
C     THE FITTED STRAIGHT LINES AND THE ECCENTRICITY FACTOR. OBTAIN THE
C     MAXIMUM, THE FACTOR AT THE MINIMUM DIAMETER AND THE MEAN.
C
      MAXECC = 0.0
      MINECC = 0.0
      STORE = 0.0
C
      HISUB = HISUB+1
      LOSUB = LOSUB-1
C
      HISUB = HISUB+1
```

```
      LOSUB = LOSUB-1
C
      DO 10 J=HISUB,LOSUB
        XCOEFD = Y1(J)-Y2(J)
        YCOEFD = X2(J)-X1(J)
        CONSTD = Y2(J)*X1(J)-Y1(J)*X2(J)
C
C       LOWER BOUND.
C
        GRAD1 = XCOEFD*COEFY1-COEFX1*YCOEFD
        LPIX(J) = YCOEFD*COEFC1-COEFY1*CONSTD/GRAD1
        LPIY(J) = COEFX1*CONSTD-XCOEFD*COEFC1/GRAD1
C
C       UPPER BOUND.
C
        GRAD2 = XCOEFD*COEFY2-COEFX2*YCOEFD
        UPIX(J) = YCOEFD*COEFC2-COEFY2*CONSTD/GRAD2
        UPIY(J) = COEFX2*CONSTD-XCOEFD*COEFC2/GRAD2
C
        MPX = (LPIX(J)+UPIX(J))/2.0
        MPY = (LPIY(J)+UPIY(J))/2.0
        DIAM = LENGTH(LPIX(J),LPIY(J),UPIX(J),UPIY(J))
        WRITE(7,132) LPIX(J),LPIY(J)
        WRITE(7,132) UPIX(J),UPIY(J)
 132    FORMAT(2F11.4)
C
        SHIFT = LENGTH(XAXIS(J),YAXIS(J),MPX,MPY)
C
        ECCENT = (SHIFT/(DIAM/2.0))*100
C
        IF(ECCENT.GE.MAXECC) MAXECC = ECCENT
        IF(J.EQ.POSMIN) MINECC = ECCENT
        STORE = STORE+ECCENT
C
 10   CONTINUE
C
      HISUB = HISUB-1
      LOSUB = LOSUB+1
C
      AVECC = STORE/(LOSUB-1-HISUB-1)
C
      RETURN
C
      END
C
C     ******************************************************************************
C
      FUNCTION LENGTH(XDUM1,YDUM1,XDUM2,YDUM2)
C
      REAL XDUM1,YDUM1,XDUM2,YDUM2,XDISP,YDISP,LENGTH
C
      XDISP = XDUM2 - XDUM1
      YDISP = YDUM2 - YDUM1
C
      LENGTH = SQRT(XDISP*XDISP+YDISP*YDISP)
C
      RETURN
C
      END
C
C     ******************************************************************************
C
      SUBROUTINE AREAS(X1,Y1,X2,Y2,HISUB,LOSUB,AREA)
```

```
C
      INTEGER J,HISUB,LOSUB
C
      REAL XSUM,YSUM,XA,TA,XB,YB,XC,YC,XD,YD,XE,YE,TRIAR1(500)
      REAL TRIAR2(500),TRIAR3,TRIAR4,TRIAR5,AREA,X1(1000),Y1(1000)
      REAL X2(1000),Y2(1000),X1P,Y1P,X2P,Y2P,X1D,Y1D,Y2D,Y2D
C
      COMMON/SET5/X1P,Y1P,X2P,Y2P,X1D,Y1D,X2D,Y2D
C
C     ------------------------------------------------------------------
C
C     THIS SUBROUTINE CALCULATES THE AREA OF THE STENOSIS AND ITS
C     'UNDISEASED' AREA.
C
C     ------------------------------------------------------------------
C
      XSUM = 0.0
      YSUM = 0.0
C
      DO 10 J = HISUB,LOSUB
        XSUM = XSUM + X1(J)
        YSUM = YSUM + Y1(J)
        XSUM = XSUM + X2(J)
        YSUM = YSUM + Y2(J)
 10   CONTINUE
C
      TRIAR3 = 0.0
C
C     COMPUTE THE CENTROID OF THE DATA.
C
      XC = XSUM/((LOSUB-HISUB)*2)
      YC = YSUM/((LOSUB-HISUB)*2)
C
C     CALCULATE THE LEFT HAND AREA.
C
      LOSUB = LOSUB-1
C
      DO 20 J = HISUB,LOSUB
        XA = X1(J)
        YA = Y1(J)
        XB = X1(J+1)
        YB = Y1(J+1)
C
        TRIAR1(J) = ((YB*XA+YC*XB+YA*XC)-(YB*XC+YC*XA+YA*XB))/2.0
        TRIAR3 = TRIAR3 + TRIAR1(J)
C
 20   CONTINUE
C
      LOSUB = LOSUB+1
C
C     CALCULATE THE RIGHT HAND AREA.
C
      HISUB = HISUB+1
C
      DO 30 J = HISUB,LOSUB
        XD = X2(J)
        YD = Y2(J)
        XE = X2(J+1)
        YE = Y2(J+1)
C
        TRIAR2(J) = ((YE*XD+YC*XE+YD*XC)-(YE*XC+YC*XD+YD*XE))/2.0
        TRIAR3 = TRIAR3 + TRIAR2(J)
C
```

```
 30   CONTINUE
C
      HISUB = HISUB-1
      TRIAR3 = ABS(TRIAR3)
C
C     CALCULATE REMAINING AREAS.
C
      TRIAR4 = ((Y2D*X1D+YC*X2D+Y1D*XC)-(Y2D*XC+YC*X1D+Y1D*X2D))/2.0
      TRIAR5 = ((Y1P*X2P+YC*X1P+Y2P*XC)-(Y1P*XC+YC*X2P+Y2P*X1P))/2.0
C
      AREA = ABS(TRIAR3 + TRIAR4 + TRIAR5)
C
      RETURN
C
      END
C
C     ******************************************************************************
```

```
C     ------------------------------------------------------------------
      LIBRARY 'GINOGRAF'
      LIBRARY 'GINO'
      LIBRARY 'VAPPLB'
      LIBRARY 'LUSUBV'
C
      PROGRAM ARTDR
C
      INTEGER L1,L2,L3,J,NX,NY,N1,K,F,NPLOT,N2,N3,NT,C
C
      REAL X1(1000),Y1(1000),XMIN,XMAX,YMIN,YMAX,X(10),Y(10)
      REAL XTITLE,YTITLE,XVAL1(1000),YVAL1(1000),MAX,MIN,X2(1000)
      REAL Y2(1000),XVAL2(1000),YVAL2(1000),X3(1000),Y3(1000)
      REAL XVAL3(1000),YVAL3(1000)
C
      CHARACTER*1 REPLY,REPLY1
      CHARACTER*32 XLAB,YLAB,FILE1,FILE2,FILE3
      CHARACTER*64 TITLE
C
      COMMON/SET1/NPLOT
C     ------------------------------------------------------------------
C
C     PROGRAM ARTDR IS A GRAPHICS ROUTINE WHICH ALLOWS THE PLOTTING OF
C     COORDINATE INFORMATION PRODUCED BY THE SUITE OF QUANTITATIVE
C     ANGIOGRAPHIC MENSURATION PROGRAMS.  A MAXIMUM OF 3 FILES MAY BE
C     PLOTTED AT ANY ONE TIME, AND MUST BE ENTERED IN THE FOLLOWING ORDER:
C
C             1). THE DISEASED DIAMETER END POINTS (PRODUCED BY DIAMRS).
C             2). THE UNDISEASED DIAMETER END POINTS (PRODUCED BY ECCFTR).
C             3). THE ARTERY AXIS POINTS (PRODUCED BY DIAMRS).
C
C     THE PROGRAM HARNESSES GINO ROUTINES AND IS ONLY THEREFORE RUNABLE ON
C     SYSTEMS WHICH HOST THIS PACKAGE (IN THIS CASE THE PRIME MAINFRAME).
C
C     ------------------------------------------------------------------
C
 1    CALL COUA('HOW MANY FILES DO YOU WISH TO PLOT(1-3) ')
      READ(1,5) NPLOT
 5    FORMAT(I2)
C
      WRITE(1,20)
 20   FORMAT(' ')
C
      IF(NPLOT.GE.2) WRITE(1,10)
 10   FORMAT('PLEASE OBSERVE YOU ENTER THE FILES IN THE CORRECT ORDER')
C
      WRITE(1,20)
C
      IF(NPLOT.GE.1) CALL COUA('DISEASED DIAMETER END POINT FILE IS ')
      IF(NPLOT.GE.1) READ(*,'(A)') FILE1
      IF(NPLOT.GE.1) CALL STRLEN(FILE1,L1)
C
      WRITE(1,20)
C
      IF(NPLOT.GE.2) CALL COUA('UNDISEASED DIAMETER END POINT FILE IS ')
      IF(NPLOT.GE.2) READ(*,'(A)') FILE2
      IF(NPLOT.GE.2) CALL STRLEN(FILE2,L2)
C
      IF(NPLOT.EQ.3) CALL COUA('AXIS POINT FILE IS ')
      IF(NPLOT.EQ.3) READ(*,'(A)') FILE3
      IF(NPLOT.EQ.3) CALL STRLEN(FILE3,L3)
C
      WRITE(1,20)
```

```
C
      CALL COUA('XAXIS LABEL WILL BE ')
      READ(*,'(A)') XLAB
      CALL STRLEN(XLAB,NX)
C
      WRITE(1,20)
C
      CALL COUA('YAXIS LABEL WILL BE ')
      READ(*,'(A)') YLAB
      CALL STRLEN(YLAB,NY)
C
      WRITE(1,20)
C
      CALL COUA('GRAPH TITLE WILL BE ')
      READ(*,'(A)') TITLE
C
      IF(NPLOT.GE.1) OPEN(6,FILE=FILE1(1:L1),STATUS='OLD',ACCESS=
     &'SEQUENTIAL')
      IF(NPLOT.GE.1) CALL TOTAL(X1,Y1,6,N1)
      IF(NPLOT.GE.2) OPEN(7,FILE=FILE2(1:L2),STATUS='OLD',ACCESS=
     &'SEQUENTIAL')
      IF(NPLOT.GE.2) CALL TOTAL(X2,Y2,7,N2)
      IF(NPLOT.EQ.3) OPEN(8,FILE=FILE3(1:L3),STATUS='OLD',ACCESS =
      IF(NPLOT.EQ.3) CALL TOTAL(X3,Y3,8,N3)
C
      F = 0
C
C     OBTAIN RELATIVE CORRECTION FACTORS FROM DISEASED
      DIAMETER END POINT DATA.
C
      XMIN = 99999
      YMIN = 99999
      XMAX = -99999
      YMAX = -99999
C
      DO 300 J = 1,N1
        IF(X1(J).LT.XMIN) XMIN = X1(J)
        IF(Y1(J).LT.YMIN) YMIN = Y1(J)
        IF(X1(J).GE.XMAX) XMAX = X1(J)
        IF(Y1(J).GE.YMAX) YMAX = Y1(J)
      CONTINUE
C
      DIFFX = XMAX - XMIN
      DIFFY = YMAX - YMIN
C
      IF(DIFFX.GE.DIFFY) MIN = XMIN
      IF(DIFFX.GE.DIFFY) MAX = XMAX
      IF(DIFFY.GT.DIFFX) MIN = YMIN
      IF(DIFFY.GT.DIFFX) MAX = YMAX
C
      C = 1
C
 310  IF(C.EQ.1) NT = N1
      IF(C.EQ.2) NT = N2
      IF(C.EQ.3) NT = N3
C
      DO 320 J = 1,NT
        IF(C.EQ.1) XVAL1(J) = ((X1(J)-XMIN)/(MAX-MIN))*100
        IF(C.EQ.1) YVAL1(J) = ((Y1(J)-YMIN)/(MAX-MIN))*100
        IF(C.EQ.2) XVAL2(J) = ((X2(J)-XMIN)/(MAX-MIN))*100
        IF(C.EQ.2) YVAL2(J) = ((Y2(J)-YMIN)/(MAX-MIN))*100
        IF(C.EQ.3) XVAL3(J) = ((X3(J)-XMIN)/(MAX-MIN))*100
        IF(C.EQ.3) YVAL3(J) = ((Y3(J)-YMIN)/(MAX-MIN))*100
```

```
 320 CONTINUE
C
      C = C+1
      IF(C.NE.NPLOT+1) GOTO 310
C
C     OBTAIN THE NUMBER OF DATA PAIRS BY INTEGER DIVISION.
C
      IF(NPLOT.GE.1) N1 = N1/2
      IF(NPLOT.GE.2) N2 = N2/2
      IF(NPLOT.EQ.3) N3 = N3/2
C
      CALL GINO
C
C     CALL GRAPHICS TERMINAL
C
      IF(F.EQ.0) CALL S5664
C
C     CALL LASER PRINTER
C
 350  IF(F.EQ.1) CALL CNA2
C
C     SELECT BLACK PEN.
      CALL PENSEL(1,0.0,0)
C
C     SET UP AXES (AXES TYPE,OPTIMUM WINDOW,LINEAR,LINEAR,DIVISIONS
C     PER AXIS,MINX,MAXX,MINY,MAXY,XLABEL,YLABEL)
C
      CALL AXIPLO(0,160.0,,160.0,3,3,7,7,-20.0,120.0,-20,120.0
     &XLAB,NX,YLAB,NY)
C
      CALL SPAGRA(10.0,5.0,XTITLE,YTITLE)
      CALL GRAMOV(XTITLE,YTITLE)
      CALL CHASTR(TITLE)
C
      C = 1
C
 375  IF(C.EQ.1) NT = N1
      IF(C.EQ.2) NT = N2
      IF(C.EQ.3) NT = N3
C
      DO 400 J = 1,NT,4
        K = 2*J-1
        IF(C.EQ.1) X(1) = XVAL1(K)
        IF(C.EQ.1) Y(1) = YVAL1(K)
        IF(C.EQ.1) X(2) = XVAL1(K+1)
        IF(C.EQ.1) Y(2) = YVAL1(K+1)
C
        IF(C.EQ.2) X(1) = XVAL2(K)
        IF(C.EQ.2) Y(1) = YVAL2(K)
        IF(C.EQ.2) X(2) = XVAL2(K+1)
        IF(C.EQ.2) Y(2) = YVAL2(K+1)
C
        IF(C.EQ.3) X(1) = XVAL3(K)
        IF(C.EQ.3) Y(1) = YVAL3(K)
        IF(C.EQ.3) X(2) = XVAL3(K+1)
        IF(C.EQ.3) Y(2) = YVAL3(K+1)
C
C       SET UP SYMBOL AND NUMBER OF POINTS PER GRAPH (DATA,No.,SYMBOL).
C
        CALL GRASYM(X,Y,2,C,0)
C
C       PLOT POINTS AND JOIN BY LINES.
C
```

```
        CALL GRAPOL(X,Y,2)
C
 400  CONTINUE
C
      C = C+1
      IF(C.NE.NPLOT+1) GOTO 375
C
      CALL GINEND
C
C     HARD COPY OPTION.
C
      F = 0
      WRITE(1,600)
 600  FORMAT('DO YOU REQUIRE A HARD COPY (Y/N) ')
      READ(*,'(A)') REPLY
      IF(REPLY.EQ.'Y') F = 1
      IF(F.EQ.1) GOTO 350
C
C     RE-RUN OPTION.
C
      WRITE(1,700)
 700  FORMAT('DO YOU REQUIRE A RE-RUN (Y/N) ')
      READ(*,'(A)') REPLY1
      IF(REPLY1.EQ.'Y') GOTO 1
C
      CALL EXIT
C
      END
C
C     ********************************************************************
C
      SUBROUTINE STRLEN(CHRVAL.L)
C
      INTEGER L,J
      CHARACTER*32,CHRVAR
C
C     ------------------------------------------------------------------
C
      J = 0
 100  J = J+1
C
      IF(CHRVAR(J:J).NE.' ') GOTO 100
      L = J-1
C
      RETURN
      END
C
C     ********************************************************************
C
      SUBROUTINE TOTAL(X,Y,CN,N)
C
      INTEGER J,NPLOT N,CN
C
      REAL X(1000),Y(1000)
C
      COMMON/SET1/NPLOT
C
C     ------------------------------------------------------------------
C
C     THIS SUBROUTINE CALCULATES THE TOTALS OF THE DATA FILES
C     ------------------------------------------------------------------
C
      J = 0
```

```
 100  J = J+1
C
      IF(CN.LE.8) READ(CN,300,END=200) X(J),Y(J)
      GOTO 100
      N = J-1
C
 300  FORMAT(2F11.4)
C
      RETURN
      END
C
C     ***************************************************************************
```

```
10 GOTO 260
20 REM X AXIS VARIATION SUBROUTINE
30 FOR J=ST1 TO SUM1
40 INPUT£1,NO(J),X(J),Y(J)
50 X1=X1+X(J):X2=(X2+(X(J)*Y(J)))
60 NEXT J
70 X3=((X1*X1)/SUM1)
80 XM=(X1/SUM1):SDX=SQR((X2-X3)/(SUM1-1))
90 CVX=((SDX/XM)*100)
100 LPRINT "X AXIS DEVIATION-RESULTS"
110 LPRINT"No. COORDINATES=";SUM1"        MEAN=";XM
120 LPRINT"STANDARD DEVIATION=";SDX"    COEFFICIENT OF VARIATION=";CV
130 RETURN
140 REM Y AXIS VARIATION SUBROUTINE
150 FOR J=ST2 TO GT
160 INPUT£1,NO(J),X(J),Y(J)
170 Y1=Y1+Y(J):Y2=(Y2+(Y(J)*Y(J)))
180 NEXT J
190 Y3=((Y1*Y1)/SUM2)
200 YM=(Y1/SUM2):SDY=SQR((Y2-Y3)/(SUM2-1))
210 CVY=((SDY/YM)*100)
220 LPRINT"Y AXIS DEVIATION RESULTS"
230 LPRINT"No. COORDINATES=";SUM2"        MEAN=";YM
240 LPRINT"STANDARD DEVIATION=";SDY"    COEFFICIENT OF VARIATION=";CV
250 RETURN
```

```
260 DIM X(300):DIM Y(300) :DIM NO(300)
270 PRINT CHR$(4): INPUT "ENTER FILENAME";A$
280 LPRINT "FILENAME=";A$:LPRINT:LPRINT
290 OPEN"I",£1,"B:"+A$
300 IF EOF(1) THEN GOTO 430
310 FOR I= 1 TO 12
320 INPUT£1,N
330 IF I=2 THEN ST1=N
340 IF I=3 THEN ST2=N
350 IF I=4 THEN SUM1=N
360 IF I=5 THEN SUM2=N
370 IF I=7 THEN GT=N
380 NEXT I
390 PRINT:PRINT:PRINT
400 INPUT"ENTER ORDER OF RUN e.g.YX";A$
410 IF LEFT$(A$,1)="X" THEN GOSUB 30:LPRINT:GOSUB 150
420 IF LEFT$(A$,1)="Y" THEN GOSUB 150:LPRINT:GOSUB 30
430 CLOSE£1
440 END
```

```
C     8.  PROGRAM CUSHCALC .FOR
C
      INTEGER X(30),Y(30),FILDES(12)
C
      DOUBLE PRECISION LENGTH,MPX(20),MPY(20),LEN(20),RADLEN(20)
      DOUBLE PRECISION ORIG,LENTHI,L1,L2,VERT,HORI,VMF,HMF,MF
C
C     ------------------------------------------------------------
C     PROGRAM CUSHCALC COMPUTES CHANGES IN MAGNIFICATION FACTORS
C     INCREASING HEIGHT AND RADIAL DISTANCE FROM THE CENTRE OF THE
C     INTENSIFIER.
C     ------------------------------------------------------------
C     READ FILE DESCRIPTORS (GIVEN IN FIRST 6 LINES OF FILE BITPDC
C     INTO FILDES( ).  NOTE 1 = DRIVE NUMBER.  FIRST ITEM OF ANY
C     SECTION HAS A SEPARATE READ STATEMENT TO FACILITATE CODING OF ERROR
C     MESSAGES.
C     FILE DESCRIPTORS ARE INITIALLY READ INTO A VECTOR FOR THE
C     SAME REASON.
C
C
C     OPEN FILES.
C
      CALL OPEN(6,'BITPDCOORDS',0)
      READ(6,20)(FILDES(J),J=1,12)
C
C     ------------------------------------------------------------
C     READ DATA FROM FIRST SQUARE
C
      DO 10 J = 1,5
         READ(6,20) X(J)
         READ(6,20) Y(J)
 10   CONTINUE
C
 20   FORMAT(I7)
C
```

```
C
      VERT = 0.568
      HORI = 0.562
C
C     CALCULATE LENGTHS
      L1 = 0.0
      L2 = 0.0
      VMF = 0.0


      HMF = 0.0
      MF = 0.0
C
      L1 = (LENTHI(X(2),Y(2),X(3),Y(3))/393.7)
      L2 = (LENTHI(X(3),Y(3),X(4),Y(4))/393.7)
C
C     CALCULTE MAG FACTORS
C
      VMF = L1/VERT
      HMF = L2/HORI
      MF = (VMF+HMF)/2.0
C
      WRITE(1,30) L1,VMF
      WRITE(1,30) L2,HMF
      WRITE(1,35) MF
 30   FORMAT(2F12.5)
 35   FORMAT(' OVERALL MF = ',F12.5)
C
C     READ OUTER FIELD DATA
C
      DO 40 J = 6,28,2
C
```

```
      LEN(J) = 0.0
      RADLEN(J) = 0.0
C
C     READ ORIGINAL DIMENSION
C
      WRITE(1,45)
 45   FORMAT(' INPUT ORIGINAL DIMENSION IN CMS')
C
C
         READ(1,60)ORIG
         READ(6,20) X(J)
         READ(6,20) Y(J)
         READ(6,20) X(J+1)
         READ(6,20) Y(J+1)
         LEN(J) = ((LENTHI(X(J),Y(J),X(J+1),Y(J+1))/393.7)/ORIG)/M
         MPX(J) = (X(J)+X(J+1))/2.0
         MPY(J) = (Y(J)+Y(J+1))/2.0
         RADLEN(J) = (LENGTH(X(1),Y(1),MPX(J),MPY(J))/393.7)
         WRITE(1,50) LEN(J),RADLEN(J)
 50      FORMAT(2F12.5)
 40   CONTINUE
 60   FORMAT(F7.5)
C
C
C
      STOP
      END
C     ***************************************************************
      FUNCTION LENTHI(XDUM1,YDUM1,XDUM2,YDUM2)
C
      INTEGER XDUM1,YDUM1,XDUM2,YDUM2
      DOUBLE PRECISION XDISP,YDISP,LENTHI
C
```

```
      XDISP = XDUM2 - XDUM1
      YDISP = YDUM2 - YDUM1
C
      LENTHI = DSQRT(XDISP*XDISP + YDISP*YDISP)
C
      RETURN
      END
C
C     ****************************************************************
      FUNCTION LENGTH(XDUM1,YDUM1,XDUM2,YDUM2)
C
      INTEGER XDUM1,YDUM1
      DOUBLE PRECISION XDUM2,YDUM2,XDISP,YDISP,LENGTH
C
      XDISP = XDUM2 - XDUM1
      YDISP = YDUM2 - YDUM1
C
      LENGTH = DSQRT(XDISP*XDISP + YDISP*YDISP)
C
      RETURN
      END
C
C     ****************************************************************
```

9. Transferring files between the Vector 3 and the Prime System.

In order to allow the transfer of ASCII data between two computers, each must have a program which allows each computer to act as a transmission and/or reception device. These are GETFILE for the Prime and MOVE-IT for the Vector 3 (held on the MOVE-IT disk, PDP11 room, Department of Human Sciences, Loughborough University).

eg. Transferring the file AXPTS from the Vector 3 to the Prime.

Machine	Command/Prompts	Meaning
VECTOR3	A>MOVE-IT	Boot up and run program
PRIME	LOGIN etc. OK, A *>ARTDR	Login and attach to subdirectory you want data to be sent to eg. ARTDR
VECTOR3	TA	Select option which allows Vector to TA(1k) to Prime. NB. Vector must be attached to Prime through the Cambridge ring. Terminal emulator mode now active.
VECTOR 3 (acting as a Prime terminal)	GETFILE Filename (to be produced in in Prime subdir.) OK, READY FOR FILE	Call up GETFILE and create output file.

	TRANSFER	
	Type ESC then S	Return to CP/M level
	Filename to be sent to remote computer: eg. B:AXPTS.	Enter filename to send to Prime.
VECTOR 3 (acting as a Prime terminal)	Protocol to use? X	Use fastest transfer protocol.
	TRANSMISSION COMPLETE	Data sent.
	Type ESC then ESC	Close file at CP/M end.
	OK, CLOSE ALL	Close file at Prime end.

File AXPTS will now be resident in the ARTDR subdirectory.

```
C       PROGRAM "MUGA.FOR/OBJ/SAV"    WRITTEN AT
C       RADIOISOTOPE IMAGING UNIT, GROBY ROAD HOSPITAL, LEICESTER
C       TO DRAW SEGMENTAL REGIONS PROCESSABLE UNDER NEW SOFTAWARE
C
        COMMON/OVLADR/IOVL /IMBUF/IMBUF1(256) /VDMAP/MAP(256)
        COMMON/IMODE/MODE /IMGBLK/NBLK /EXT/IEXT(32) /TEXT/ITEXT(4)
        COMMON/FRAME/IFRM /COUNT/ICNT /MASHST/MASRES(32)
        COMMON/IOPAC/LIT(36),FLOT(10) /WORK/IWORK(256)
        COMMON/FILE/IFILE(6)
        COMMON/AREA1/IAREAG(2,50) /AREA2/IAREAS(2,50) /AREA3/IAREAI(2,50)
        COMMON/AREA4/IAREAL(2,50) /AREAB/IAREAB(2,50)
        COMMON/ACNT/IGPT,ISPT,IIPT,ILPT,IBPT
        DIMENSION IPTS(3)
        TYPE 500
        CALL SETDAT
        CALL VIDSET
        CALL FETCH()
        CALL FNDOV3(1)
        CALL DISP
100     CALL DRWSEG(IPTS)
        TYPE 505
        GO TO (110,120,900),NOYES()
110     CALL FETCH(1)
        CALL DISP
        TYPE 510
        GO TO (100,120,900),NOYES()
120     CALL STOROI(IPTS)
        CALL IVIDCO(0)
        STOP'PROCESSING COMPLETE'
900     STOP'PROGRAM ERROR'
500     FORMAT(///15X,'RADIOISOTOPE IMAGING UNIT'//
     1  20X,'GROBY ROAD HOSPITAL'////
     2  15X'SEGMENTAL AREA DRAWING PROGRAM'////)
505     FORMAT('0CHECK WITH NEW IMAGE (Y OR N) ? '$)
510     FORMAT('0REDRAW AREAS (Y OR N) ? '$)
        END



        SUBROUTINE SETDAT
        COMMON/EXT/IEXT(32)
        COMMON/TEXT/ITEXT(4)
        COMMON/WORK/IWORK(256)
        COMMON/FILE/IFILE(6)
        COMMON/AREA1/IAREAG(2,50) /AREA2/IAREAS(2,50) /AREA3/IAREAI(2,50)
        COMMON/AREA4/IAREAL(2,50) /AREAB/IAREAB(2,50)
C
        DATA IEXT/'00','01','02','03','04','05','06','07','08','09',
     1  '0A','0B','0C','0D','0E','0F','0G','0H','0I','0J','0K',
     2  '0L','0M','0N','0O','0P','0Q','0R','0S','0T','0U','0V'/
        DATA ITEXT/'.R','.M','01','00'/
        DATA IFILE/'AD','1:','NA','ME','.M','01'/
        DATA IAREAG/100*0/
        DATA IAREAS/100*0/
        DATA IAREAI/100*0/
        DATA IAREAL/100*0/
        DATA IAREAB/100*0/
        J=0
        DO 10 I=1,256
        J=J+I-1
        IWORK(I)=J
10      CONTINUE
        RETURN
        END
```

```
      SUBROUTINE VIDSET
      COMMON/VDMAP/MAP(256)
      COMMON/OVLADR/IOVL
      COMMON/IMGBLK/NBLK
      COMMON/IMODE/MODE
      DO 100 I=1,256
      MAP(I)=INT((I-1)*63./255)
100   CONTINUE
      MODE=4
      NBLK=256
      CALL REFALL(0,0,3)
      CALL VDINIT()
      CALL OVCLR
      CALL ZEROC(NBLK,MODE)
      CALL IVIDCO(6,MODE,NBLK)
      RETURN
      END
```

```
      SUBROUTINE FETCH(IFLAG)
      COMMON/MASHST/MASRES(32)
      COMMON/FILE/IFILE(6)
      COMMON/EXT/IEXT(32)
      COMMON/TEXT/ITEXT(4)
      IF (IFLAG.EQ.1)GO TO 100
      TYPE 500
      ACCEPT 10,IFILE(3),IFILE(4)
100   CALL NEWINV
      RETURN
10    FORMAT(2A2)
500   FORMAT('0ENTER PATIENT I.D.  (4 CHARS.) '$)
      END
```

```
      SUBROUTINE NEWINV
C     SUB. NEWINV TO READ MASTER FILE AND LIST IMAGES
C     FOR NEW SOFTWARE DISCS
C     NEWINV VERSION 2 MODIFIED 4-JUL-85
C     STOPS AFTER 16 IMAGES, PROMPTS TO CONTINUE
C
      COMMON/COUNT/ICNT
      COMMON/FILE/IFILE(6)
      COMMON/TEXT/ITEXT(4)
      COMMON/MASHST/MASRES(32)
      DIMENSION ICHARS(5)
      IFILE(5)=ITEXT(2)
      IFILE(6)=ITEXT(3)
      IBLK=IFILTH(IFILE)
      IF(IBLK.NE.-2)GO TO 50
      IFILE(6)=ITEXT(4)
      IBLK=IFILTH(IFILE)
      IF(IBLK.EQ.-2)GO TO 900
      ICNT=0
50    TYPE 500
      CALL CLOSE(2)
      CALL ASSIGN (2,IFILE,12,OLD)
      DEFINE FILE 2(32,32,U,IV)
      DO 100 I=1,32
      IF(ICNT.EQ.17)PAUSE'HIT <RETURN> TO CONTINUE LIST'
      READ(2'I)MASRES
      IF(MASRES(1).EQ.0)GO TO 100
      ICNT=ICNT+1
      DO 110 J=1,5
      ICHARS(J)=MASRES(J)
110   CONTINUE
      TYPE 505,I,ICHARS
100   CONTINUE
120   RETURN
900   TYPE 510,IFILE(3),IFILE(4)
      STOP'PROGRAM STOPPED --- NO PATIENTS FOUND'
500   FORMAT(/10X,'IMAGE LIST:')
505   FORMAT(10X,I3,1X,5A2)
510   FORMAT(//10X,'PATIENT ',2A2,'  NOT FOUND'//)
      END
```

```
      SUBROUTINE FNDOV3(IIN)
C
C     TO FIND OVERLAY DIRECTORY AND CHECK IF IT EITHER
C     FULL OR EMPTY
C     IF FULL PROMPT TO RECOPY PATIENT WITH LESS OVERLAYS.
C     IF EMPTY PROMPT TO DO STANDARD MUGA PROCESSING FIRST
C     BOTH FULL AND EMPTY GIVE A STOP CONDITION, OTHERWISE
C     RETURN TO CALLING ROUTINE
C
      COMMON/IMBUF/IMBUF1(256)
      COMMON/OVLADR/IOVL
      COMMON/IOPAC/LIT(36),FLOT(10)
      COMMON/FILE/IFILE(6)
      DIMENSION IEND(4)
      DIMENSION IDATA(16)
      DATA IEND/'.0','ZZ','  ','  '/
50    IF(IIN.EQ.0)TYPE 500
      IF(IIN.EQ.0)ACCEPT 10,IFILE(3),IFILE(4)
      CALL CLOSE(2)
      IEND(3)=IFILE(5)
      IEND(4)=IFILE(6)
      IFILE(5)=IEND(1)
      IFILE(6)=IEND(2)
      IBLK=IFILTH(IFILE)
      IF(IBLK.EQ.-2)GO TO 920
      CALL ASSIGN(2,IFILE,12,OLD)
      DEFINE FILE 2(16,16,U,IV)
      IZCNT=0
      DO 100 I=1,16
      READ(2'I)IDATA
      IF(IDATA(1).EQ.0)IZCNT=IZCNT+1
100   CONTINUE
      IF(IZCNT.EQ.17)GO TO 910
      IF(IZCNT.EQ.0)GO TO 900
      CALL CLOSE(2)
      IFILE(5)=IEND(3)
      IFILE(6)=IEND(4)
      CALL ASSIGN(2,IFILE,12,OLD)
      DEFINE FILE 2(32,32,U,IV)
      RETURN
10    FORMAT(2A2)
900   STOP'OVERLAY FILE FULL - - RECOPY WITH LESS OVERLAYS'
910   STOP'NO OVERLAYS - PROCESSING REQUIRED'
920   STOP'PATIENT NOT FOUND - - CHECK STUDY NAME AND RE-RUN'
500   FORMAT(/10X,'ENTER 4 CHARACTER PATIENT I.D. '$)
      END
```

```
      SUBROUTINE DISP
      COMMON/VDMAP/MAP(256)
      COMMON/MASHST/MASRES(32)
      COMMON/COUNT/ICNT
      COMMON/TEXT/ITEXT(4)
      COMMON/FILE/IFILE(6)
      COMMON/EXT/IEXT(32)
      COMMON/FRAME/IFRM
      DIMENSION IVIEW(5)
100   TYPE 500
      ACCEPT 10,MREC
      IF(MREC.LT.1.OR.MREC.GT.ICNT)GOTO 100
      READ(2'MREC)MASRES
      IFRM=MASRES(20)
      MODE=MASRES(8)
      IFILE(5)=ITEXT(1)
      IFILE(6)=IEXT(MREC)
      DO 110 I=1,5
110   IVIEW(I)=MASRES(I)
      CALL DISPIM
      CALL CHRGEN(IVIEW,10,22,10)
      CALL IVIDCO(6,MODE,MAP,256)
      RETURN
500   FORMAT('0SELECT IMAGE FROM LIST')
10    FORMAT(I5)
      END



      SUBROUTINE DISPIM
C
C     TO DECIDE ON IMAGE TYPE, RETRIEVE FROM DISC
C
      COMMON/IMODE/MODE
      COMMON/FILE/IFILE(6) /IMGBLK/NBLK
      COMMON/FRAME/IFRM
      IMTYPE=1
      IF(IFRM.GT.1)GO TO 200
      GO TO 250
200   IMTYPE=2
      TYPE 500,IFRM
      ACCEPT 10,IFRAME
250   CALL IMGRW(IFILE,IMTYPE,IFRAME,MODE,256,2)
      RETURN
500   FORMAT(10X,'WHICH DYNAMIC FRAME  (1 - ',I5,') ? '$)
10    FORMAT(I5)
      END
```

```
      SUBROUTINE DRWSEG(IPTS)
C
C     DRWSEG VERSION 2
C     INCLUDES VERIFICATION/ALTERATION OF SEGMENT LINE POSITION
C
      COMMON/IMBUF/IMBUF1(256)
      COMMON/FILE/IFILE(6)
      COMMON/OVLADR/IOVL
      COMMON/IOPAC/LIT(36),FLOT(10)
      COMMON/AREA1/IAREAG(2,50)
      COMMON/AREA2/IAREAS(2,50)
      COMMON/AREA3/IAREAI(2,50)
      COMMON/AREA4/IAREAL(2,50)
      COMMON/AREAB/IAREAB(2,50)
      COMMON/ACNT/IGPT,ISPT,IIPT,ILPT,IBPT
      DIMENSION IPTS(3)
100   CALL OVCLR
      TYPE 500
      CALL AOIDRW(IAREAG,IGPT)
      CALL COFG(IAREAG,IGPT,IX,IY)
105   TYPE 505
      CALL LIGHTP(IX1,IY1)
      CALL GETNP(IAREAG,IGPT,IX1,IY1,ICNT)
      CALL LINE(IAREAG(1,ICNT),IAREAG(2,ICNT),IX,IY,4)
110   TYPE 507
      GO TO (120,115,110),NOYES()
115   CALL LINE(IAREAG(1,ICNT),IAREAG(2,ICNT),IX,IY,0)
      GO TO 105
120   TYPE 510
      CALL LIGHTP(IX2,IY2)
      CALL GETNP(IAREAG,IGPT,IX2,IY2,ICNT2)
      CALL LINE(IAREAG(1,ICNT2),IAREAG(2,ICNT2),IX,IY,4)
130   TYPE 507
      GO TO (140,135,130),NOYES()
135   CALL LINE(IAREAG(1,ICNT2),IAREAG(2,ICNT2),IX,IY,0)
      GO TO 120
140   TYPE 515
      CALL LIGHTP(IX3,IY3)
      CALL GETNP(IAREAG,IGPT,IX3,IY3,ICNT3)
      CALL LINE(IAREAG(1,ICNT3),IAREAG(2,ICNT3),IX,IY,4)
145   TYPE 507
      GO TO (155,150,145),NOYES()
150   CALL LINE(IAREAG(1,ICNT3),IAREAG(2,ICNT3),IX,IY,0)
      GO TO 140
155   TYPE 520
      CALL AOIDRW(IAREAB,IBPT)
      CALL CWCCW(IAREAG,IGPT,IX,IY,ICW)
      CALL SEGMNT(IAREAG,IAREAI,IGPT,IX,IY,ICNT2,ICNT3,ICW,IIPT)
      CALL SEGMNT(IAREAG,IAREAL,IGPT,IX,IY,ICNT3,ICNT,ICW,ILPT)
      CALL SEGMNT(IAREAG,IAREAS,IGPT,IX,IY,ICNT,ICNT2,ICW,ISPT)
      CALL OVCLR
      PAUSE'HIT <RETURN> TO DISPLAY SEGMENT 1'
      CALL AOIDSP(IAREAS,ISPT,0)
      PAUSE'HIT <RETURN> TO DISPLAY SEGMENT 2'
      CALL OVCLR
      CALL AOIDSP(IAREAI,IIPT,0)
      PAUSE'HIT <RETURN> TO DISPLAY SEGMENT 3'
      CALL OVCLR
      CALL AOIDSP(IAREAL,ILPT,0)
      PAUSE'HIT <RETURN> TO DISPLAY BACKGROUND AREA'
      CALL OVCLR
      CALL AOIDSP(IAREAB,IBPT,0)
      PAUSE'HIT <RETURN> TO CONTINUE'
```

```
      SUBROUTINE GETNP(AOIBND,IPOINT,IPX,IPY,ICNT)
      INTEGER AOIBND(2,50)
      INTEGER DIST(50)
C
      DO 100 I=1,IPOINT-1
      IDISTA=(IPX-AOIBND(1,I))**2+(IPY-AOIBND(2,I))**2
      DISTA=SQRT(IDISTA*1.)
      DIST(I)=INT(DISTA)
100   CONTINUE
C
C     FIND MIN DIST
C
      ICNT=1
      MIN=DIST(1)
      DO 110 I=2,IPOINT-1
      IF(DIST(I).GT.MIN)GO TO 110
      ICNT=I
      MIN=DIST(I)
110   CONTINUE
      RETURN
      END
```

```
      SUBROUTINE CWCCW(AOIBND,IPOINT,ICX,ICY,ICW)
      INTEGER AOIBND(2,50)
      DIMENSION IXDF(50)
      DIMENSION IYDF(50)
      DIMENSION IYDF2(50)
      DO 100 I=1,IPOINT
      IXDF(I)=ICX-AOIBND(1,I)
      IYDF(I)=ICY-AOIBND(2,I)
      IYDF2(I)=IYDF(I)**2
100   CONTINUE
      IYMIN=255
      IMARK=0
      DO 110 I=1,IPOINT
      IF(IYDF2(I).GT.IYMIN.OR.IXDF(I).LT.0)GO TO 110
      IYMIN=IYDF2(I)
      IMARK=I
110   CONTINUE
      ICW=1
      IF((ICY-AOIBND(2,(IMARK+1))).LT.(ICY-AOIBND(2,IMARK)))ICW=-1
      RETURN
      END
```

```
      INTEGER AOIBND(2,50)
      INTEGER AOIX(2,50)
      IF(ICNTA.GT.ICNTB.AND.ICW.EQ.-1)GO TO 200
      IF(ICNTB.GT.ICNTA.AND.ICW.EQ.1)GO TO 215
      LOOP=0
      DO 100 I=ICNTB,ICNTA,ICW
      LOOP=LOOP+1
      AOIX(1,LOOP)=AOIBND(1,I)
      AOIX(2,LOOP)=AOIBND(2,I)
100   CONTINUE
      GO TO 220
200   LOOP=0
      DO 110 I=ICNTA,IPOINT
      LOOP=LOOP+1
      AOIX(1,LOOP)=AOIBND(1,I)
      AOIX(2,LOOP)=AOIBND(2,I)
110   CONTINUE
      DO 120 I=2,ICNTB
      LOOP=LOOP+1
      AOIX(1,LOOP)=AOIBND(1,I)
      AOIX(2,LOOP)=AOIBND(2,I)
120   CONTINUE
      GO TO 220
215   LOOP=0
      DO 130 I=ICNTB,IPOINT
      AOIX(1,LOOP)=AOIBND(1,I)
      AOIX(2,LOOP)=AOIBND(2,I)
130   CONTINUE
      DO 140 I=1,ICNTA
      LOOP=LOOP+1
      AOIX(1,LOOP)=AOIBND(1,I)
      AOIX(2,LOOP)=AOIBND(2,I)
140   CONTINUE
220   CONTINUE
      LOOP=LOOP+1
      AOIX(1,LOOP)=ICX
      AOIX(2,LOOP)=ICY
      LOOP=LOOP+1
      AOIX(1,LOOP)=AOIX(1,1)
      AOIX(2,LOOP)=AOIX(2,1)
      RETURN
      END


      TYPE 525
      GO TO (100,300,900),NOYES()
300   CALL OVCLR
      CALL AOIDSP(IAREAS,ISPT,0)
      CALL AOIDSP(IAREAI,IIPT,0)
      CALL AOIDSP(IAREAL,ILPT,0)
      CALL AOIDSP(IAREAB,IBPT,0)
      CALL CLOSE(2)
      IPTS(1)=ICNT
      IPTS(2)=ICNT2
      IPTS(3)=ICNT3
      RETURN
900   STOP'ERROR IN ROUTINE DRWSEG. PROGRAM TERMINATED'
500   FORMAT('0DRAW LV OUTLINE WITH LIGHT PEN')
505   FORMAT('0MARK TOP OF SEPTUM WITH LIGHT PEN')
507   FORMAT(/'0IS THIS O.K.? (Y OR N) '$)
510   FORMAT('0MARK BOTTOM OF SEPTUM WITH LIGHT PEN')
515   FORMAT('0MARK JUNCTION OF INFERIOR AND
     1  LATERAL WALLS WITH LIGHT PEN')
520   FORMAT('0DRAW BACKGROUND AREA WITH LIGHT PEN')
525   FORMAT('0REDRAW AREAS ? (Y OR N) '$)
      END
```

```
      SUBROUTINE STOAOI
      COMMON /FILE/IFILE(6)
      COMMON/AREA1/IAREAG(2,50)
      COMMON/AREA2/IAREAS(2,50)
      COMMON/AREA3/IAREAI(2,50)
      COMMON/AREA4/IAREAL(2,50)
      COMMON/AREAB/IAREAB(2,50)
      COMMON/ACNT/IGPT,ISPT,IIPT,ILPT,IBPT
      DIMENSION IPACK(100)
      DIMENSION IPK(128)
      DIMENSION IODT(16)
      DIMENSION IOVLXT(2)
      DIMENSION IOVNAM(8)
      DIMENSION INAM(30)
      DATA IPACK/100*0/
      DATA IPK/128*0/
      DATA IOVLXT/'.O','ZZ'/
      DATA IOVNAM/'SE','GM','EN','TA','L ','AR','EA','S '/
      DATA INAM/'GL','OB','AL','  ','AR','EA','SE','PT','AL','  ',
     1 'AR','EA','IN','FE','RI','OR','  ','  ','LA','TE','RA','L ',
     2 'AR','EA','BA','CK','GR','OU','ND','  '/
C
      IFILE(5)=IOVLXT(1)
      IFILE(6)=IOVLXT(2)
      CALL CLOSE(2)
      I=IFILTH(IFILE)
      IF(I.EQ.-2)GO TO 920
      CALL ASSIGN (2,IFILE,12,OLD)
      DEFINE FILE 2(16,16,U,IV)
      DO 100 IOVREC=1,16
      READ(2'IOVREC,ERR=900)IODT
      IF(IODT(1).EQ.0)GO TO 110
100   CONTINUE
      TYPE 500
      GO TO 910
110   CONTINUE
      IF(IOVREC.EQ.1)GO TO 920
      DO 115 I=1,8
      IODT(I)=IOVNAM(I)
115   CONTINUE
      IODT(9)=8
      WRITE(2'IOVREC)IODT
      IFILE(6)=IODT(10)
      CALL AOIPAK(IAREAG,IGPT,IPACK)
      CALL CLOSE(2)
      CALL ASSIGN (2,IFILE,12,NEW)
      DEFINE FILE 2(8,128,U,IV)
      IPK(1)=IGPT
      DO 120 I=1,100
      IPK(I+1)=IPACK(I)
120   CONTINUE
      IPK(116)=0
      IPK(117)=0
      DO 125 I=1,6
      IPK(122+I)=INAM(I)
125   CONTINUE
      WRITE(2'1)IPK
      DO 130 I=1,100
130   IPACK(I)=0
      CALL AOIPAK(IAREAS,ISPT,IPACK)
      IPK(1)=ISPT
      DO 140 I=1,100
      IPK(I+1)=IPACK(I)
140   CONTINUE
```

```
      DO 145 I=1,6
      IPK(122+I)=INAM(I+6)
145   CONTINUE
      WRITE(2'2)IPK
      DO 150 I=1,100
150   IPACK(I)=0
      CALL AOIPAK(IAREAI,IIPT,IPACK)
      IPK(1)=IIPT
      DO 155 I=1,100
      IPK(I+1)=IPACK(I)
155   CONTINUE
      DO 160 I=1,6
      IPK(122+I)=INAM(I+12)
160   CONTINUE
      WRITE(2'3)IPK
      DO 165 I=1,100
165   IPACK(I)=0
      CALL AOIPAK(IAREAL,ILPT,IPACK)
      IPK(1)=ILPT
      DO 170 I=1,100
      IPK(I+1)=IPACK(I)
170   CONTINUE
      DO 175 I=1,6
      IPK(122+I)=INAM(I+18)
175   CONTINUE
      WRITE(2'4)IPK
      DO 180 I=1,100
180   IPACK(I)=0
      CALL AOIPAK(IAREAB,IBPT,IPACK)
      IPK(1)=IBPT
      DO 185 I=1,100
      IPK(I+1)=IPACK(I)
185   CONTINUE
      DO 190 I=1,6
      IPK(122+I)=INAM(I+24)
190   CONTINUE
      WRITE(2'5)IPK
      CALL CLOSE(2)
      RETURN
500   FORMAT(10X,'OVERLAY FILE FULL')
900   STOP'READ ERROR FOR OVERLAY DIRECTORY'
910   STOP'RECOPY PATIENT FILES WITH LESS THAN 16 OVERLAYS'
920   STOP'DO NORMAL MUGA PROCESSING FIRST'
      END
```

```
C       PROGRAM ASHIST.FOR/OBJ/SHA  18-JUN-85 SOLE PROPERTY
C       OF T.J.HEARD, MEDICAL PHYSICS,G.R.H
C       AND M.JACKSON, LOUGHBOROUGH UNIVERSITY OF TECHNOLOGY
C
C       TO ANALYSE DATA FILES GENERATED FROM PHASE HISTOGRAMS
C       BY PROGRAM FOURAN
C
C
        COMMON/ARRAY/ARR1(180,2) /MXSMNS/XMAX,XMIN,YMAX,YMIN
        COMMON/IMBUF/IMBUF1(256) /YDMAP/MAP(256)
        COMMON/OVLADR/IOVL /IMGBLK/NBLK /IMODE/MODE
        DIMENSION ILIT(62)
        DIMENSION AREA(8)
        DIMENSION NFRAME(10)
        DIMENSION RATE(10)
        DIMENSION COUNTS(8)
        DIMENSION IFILE(6)
        DIMENSION IEXT(3)
        DIMENSION ITEXT(8)
        DATA IEXT/'.N','.T','DF'/
        DATA IFILE/'AD','1:','NA','ME','.N','DF'/
        CALL VIDSET
        TYPE 500
C
C       CALL FOR PT. NAME
C
1       PAUSE'INSERT PATIENT DISC, HIT <RETURN> TO CONTINUE'
        TYPE 505
        ACCEPT 10,IFILE(3),IFILE(4)
C
C       OPEN DIRECTORY AND READ, AND TYPE
C
2       IFILE(5)=IEXT(1)
        IFILE(6)=IEXT(3)
        CALL ASSIGN (2,IFILE,12,OLD)
        DEFINE FILE 2(32,8,U,IV)
5       TYPE 510
        DO 100 I=1,32
        READ(2'I)ITEXT
        IF(ITEXT(1).EQ.0)GO TO 110
        TYPE 515,I,ITEXT(1),ITEXT(2),ITEXT(3),ITEXT(4),
     1  ITEXT(5),ITEXT(6)
100     CONTINUE
110     CONTINUE
C
C       SELECT N.D. FILE
C
        TYPE 520
        ACCEPT 15,IND
        IF(IND.EQ.0) GO TO 910
        IF(IND.LT.1.OR.IND.GT.(I-1))GO TO 5
        READ(2'IND)ITEXT
        CALL CLOSE(2)
        IFILE(5)=IEXT(2)
        IFILE(6)=ITEXT(7)
C
C       OPEN SELECTED FILE
C
        CALL ASSIGN(2,IFILE,12,OLD)
        CALL NDHEAD(2,NRCHAN,ILIT,IFIRST,OEXT,IAREA,AREA,NFRAME,RATE,IERR)
        J=0
        DO 155 I=1,NFRAME(1),2
        J=J+1
        CALL NDREAD(2,0,0,2,NRCHAN,IFIRST,ISEQ,TIME,COUNTS,IERR)
        ARR1(J,1)=COUNTS(1)
        ARR1(J,2)=I*1.+1.
155     CONTINUE
```

```
      DO 165 I=1,180
      IF(ARR1(I,2).LE.270.)ARR1(I,2)=ARR1(I,2)-90.
      IF(ARR1(I,2).GT.270.)ARR1(I,2)=ARR1(I,2)-450.
165   CONTINUE
      CALL OVCLR
      CALL MAXMNH
      CALL AXISH
      CALL POINTH
170   TYPE 525
      CALL LIGHTP(IX1,IY1)
      TYPE 530
      CALL LIGHTP(IX2,IY2)
      IF(IX2.LT.IX1)GO TO 170
      CALL LINE(IX1,220,IX1,120,6)
      CALL LINE(IX2,220,IX2,120,6)
171   TYPE 535
      GO TO (173,172,171),NOYES()
172   CALL LINE(IX1,220,IX1,120,0)
      CALL LINE(IX2,220,IX2,120,0)
      GO TO 170
173   IS=IX1-40
      IF=IX2-40
      DO 174 I=IS,IF
      IF(ARR1(I,1).GT.0.0)GO TO 175
174   CONTINUE
175   NS=I
      DO 176 I=IF,IS,-1
      IF(ARR1(I,1).GT.0.0)GO TO 177
176   CONTINUE
177   NF=I
      TOTCNT=0.0
      PHPTOT=0.0
      PIXTOT=0.0
C     TYPE 700,NS,NF
      DO 178 I=NS,NF
      PHPTOT=PHPTOT+(ARR1(I,1)*ARR1(I,2))
      PIXTOT=PIXTOT+ARR1(I,1)
178   CONTINUE
      IF(PIXTOT.EQ.0.0)GO TO 172
      AMEAN=PHPTOT/PIXTOT
      SDIFF2=0.0
      SDIFF3=0.0
      DO 180 I=NS,NF
      K=IFIX(ARR1(I,1))
      IF(K.EQ.0)GO TO 180
      DIFF=ARR1(I,2)-AMEAN
      DO 181 J=1,K
C     DIFF=ARR1(I,2)-AMEAN
      SDIFF2=SDIFF2+DIFF**2
      SDIFF3=SDIFF3+DIFF**3
181   CONTINUE
180   CONTINUE
      SDIFF2=SDIFF2/(PIXTOT-1)
      SDIFF2=SQRT(SDIFF2)
      SDIFF3=SDIFF3/(PIXTOT*SDIFF2**3)
      N=5
185   WRITE(N,555)PIXTOT,AMEAN,SDIFF2,SDIFF3
      IF(SDIFF3.GE.0.5.OR.SDIFF3.LE.-0.5)WRITE(N,560)
      IF(SDIFF3.LT.0.5.AND.SDIFF3.GT.-0.5)WRITE(N,565)
      IF(N.EQ.6)GO TO 190
      TYPE 590
      GO TO (186,190,900),NOYES()
186   N=6
      GO TO 185
190   CALL CLOSE(N)
```

```
      TYPE 595
      ACCEPT 15,I
      IF(I.EQ.0)GO TO 900
      CALL OVCLR
      IF(I.EQ.1)GO TO 2
      IF(I.EQ.2)GO TO 1
      GO TO 190
900   CALL IVIDCO(0)
      STOP'MJHIST COMPLETED'
910   CALL IVIDCO(0)
      STOP'NO DATA SELECTED - - MJHIST TERMINATED'
10    FORMAT(2A2)
15    FORMAT(I5)
500   FORMAT('0PROGRAM MJHIST TO ANALYSE PHASE HISTOGRAMS')
505   FORMAT('0ENTER 4 CHAR PT. I.D. : '$)
510   FORMAT(14X,'SELECT PHASE DATA FROM LIST : ')
515   FORMAT(10X,I5,1X,6A2)
520   FORMAT(14X,'0 NO SELECTION DESIRED'/
     1  14X$)
525   FORMAT('0MARK LOWER PHASE LIMIT WITH L.P.')
527   FORMAT('0IFLAG = ',I5,' I = ',I5,' COUNTS(I) = ',F8.0)
530   FORMAT('0MARK UPPER PHASE LIMIT WITH L.P.')
535   FORMAT('0ARE THESE LIMITS OK ? (Y OR N)')
555   FORMAT(1X,'TOTAL NUMBER OF PIXELS = ',F8.0/
     1  1X,'MEAN PHASE VALUE = ',F15.10/
     2  1X,'STANDARD DEVIATION = ',F15.10/
     3  1X,'SKEW VALUE = ',F15.10//)
560   FORMAT(1X,'SKEW VALUE SIGNIFICANT')
565   FORMAT(1X,'SKEW VALUE NOT SIGNIFICANT')
590   FORMAT(1X'DO YOU WANT THIS PRINTED ? (Y OR N) '$)
595   FORMAT(1X,'SELECT:'/
     1  1X,'1. ANALYZE MORE DATA FROM THIS PATIENT'/
     2  1X,'2. ANALYZE ANOTHER PATIENT'/
     3  1X,'0. STOP THE PROGRAM'/
     4  1X$)
700   FORMAT('0NS=',I5,' NF=',I5)
      END
```

```
C
      COMMON/ARRAY/ARR1(180,2) /MXSMNS/XMAX,XMIN,YMAX,YMIN
C
      XMIN=9998.
      XMAX=-9999.
      YMIN=9999.
      YMAX=-9998.
      DO 100 I=1,180
      IF(ARR1(I,1).LT.YMIN)YMIN=ARR1(I,1)
      IF(ARR1(I,1).GT.YMAX)YMAX=ARR1(I,1)
      IF(ARR1(I,2).LT.XMIN)XMIN=ARR1(I,2)
      IF(ARR1(I,2).GT.XMAX)XMAX=ARR1(I,2)
100   CONTINUE
C     TYPE 500,XMIN,XMAX,YMIN,YMAX
500   FORMAT('0XMIN=',F10.3,'XMAX=',F10.3,'YMIN=',F10.3,'YMAX=',F10.3)
      RETURN
      END
```

```
      SUBROUTINE AXISH
C
      COMMON /MAXMNS/XMAX,XMIN,YMAX,YMIN
C
      CALL OVCLR
      CALL LINE(85,40,85,220,2)
105   IF(YMIN.LT.0)GO TO 110
      CALL LINE(40,220,220,220,2)
      GO TO 115
110   IY=240-INT(-180*YMIN/(YMAX-YMIN))
      CALL LINE(40,IY,220,IY,2)
115   CONTINUE
      RETURN
      END
```

```
      SUBROUTINE POINTH
C
      COMMON/ARRAY/ARR1(180,2) /MXSMNS/XMAX,XMIN,YMAX,YMIN
C
      IX1=40
      IY1=220-INT(180*(ARR1(1,1)-YMIN)/(YMAX-YMIN))
      DO 100 I=2,180
      IX=40+I
      IY=220-INT(180*(ARR1(I,1)-YMIN)/(YMAX-YMIN))
      CALL LINE(IX1,IY1,IX,IY,1)
      IX1=IX
      IY1=IY
100   CONTINUE
      RETURN
      END
```

```
C       PROGRAM "EFDVDT" TO CALCULATE GLOBAL AND SEGMENTAL
C       EJECTION FRACTION AND DV/DT USING NUMERIC DATA
C       GENERATED BY "NEW SOFTWARE" BASED
C       ON SEGMENTAL AREAS PRODUCED BY "MUGA".
C
C       PROGRAM SET UP ON 1-FEB-85
C
C       PROPERTY OF T.J.HEARD, DISTRICT DEPARTMENT OF MEDICAL PHYSICS
C       RADIOISOTOPE IMAGING UNIT, GROBY ROAD HOSPITAL, LEICESTER.
C
        COMMON/REST/IREST(2)
        COMMON/IMGBLK/NBLK
        COMMON/IMODE/MODE
        COMMON/OVLADR/IOVL
        COMMON/ARRATE/F(4)
        COMMON/ARR1/BY(100,9)
        COMMON/MAXMIN/AMAXS(4),IMXMN(4,2)
        COMMON/VARS/Y(32,5),T,IPR
        DIMENSION INAME(10)
        DIMENSION INM(2)
        DIMENSION IDATE(5)
        DIMENSION INUM(3)
        DIMENSION IREFER(15)
        DATA Y/160*0.0/
        CALL SETVID
100     CALL OVCLR
        TYPE 500
        ACCEPT 10,IPRINT
        IF(IPRINT.EQ.1)GO TO 105
        IF(IPRINT.EQ.2)GO TO 110
        GO TO 100
105     IPR=5
        GO TO 115
110     IPR=6
115     TYPE 505
        ACCEPT 15,INAME
        TYPE 506
        ACCEPT 16,IAGE
        INM(1)=INAME(1)
        INM(2)=INAME(2)
        IF(IPR.EQ.5)GOTO 120
        TYPE 510
        ACCEPT 20,INUM
        TYPE 515
        ACCEPT 25,IDATE
        TYPE 520
        ACCEPT 30,IREFER
        IF(IPR.EQ.5)GO TO 120
        PRINT 525,INAME,INUM,IDATE
        PRINT 530,IREFER
120     CALL OVCLR
        CALL NDGET2(INM,IAGE)
        CALL DVDTMJ(N)
        CALL MXRATE(N)
        CALL PLOT
        CALL CLOSE(IPR)
125     TYPE 535
        ACCEPT 10,IGO
        GO TO (120,100,900),IGO
        IF(IGO.LT.1.OR.IGO.GT.3)GO TO 125
900     CALL IVIDCO(0)
```

```
10      FORMAT(I5)
15      FORMAT(10A2)
16      FORMAT(I5)
20      FORMAT(3A2)
25      FORMAT(5A2)
30      FORMAT(15A2)
500     FORMAT(10X,'PROGRAM "EFDVDT". THIS VERSION IS FOR USE'/
     1  10X,'WITH DATA FROM PATIENT DISCS ONLY.'/
     +  18X,'DO YOU WANT RESULTS :-'/
     2  18X,'1. LISTED ON TERMINAL'/
     3  18X,'2. LISTED ON PRINTER'/
     4  20X$)
505     FORMAT('0SURNAME & INITIAL      (20 CHARS.MAX):'$)
506     FORMAT('0ENTER AGE OF PATIENT (YRS.): '$)
510     FORMAT('0HOSPITAL NUMBER         (6 CHARS.MAX):'$)
515     FORMAT('0DATE OF TEST (DD-MMM-YY)(9 CHARS.MAX):'$)
520     FORMAT(1X,'REASON FOR TEST        (30 CHARS.MAX):'$)
525     FORMAT(1X,10A2,5X,3A2,5X,5A2/)
530     FORMAT(1X,15A2//)
535     FORMAT('0DO YOU WANT TO:'/
     1  5X,'1. DO ANOTHER RUN ON THIS PATIENT'/
     2  5X,'2. DO ANOTHER RUN ON ANOTHER PATIENT'/
     3  5X,'3. TERMINATE PROGRAM'/
     4  5X$)
        STOP'PROGRAM "EFDVDT" TERMINATED'
        END
```

```
        SUBROUTINE SETVID
        COMMON/OVLADR/IOVL
        COMMON/IMGBLK/NBLK
        COMMON/IMODE/MODE
        DIMENSION MAP(256)
        DO 100 I=1,256
        MAP(I)=INT((I-1)*63./255)
100     CONTINUE
        MODE=2
        NBLK=256
        CALL REFALL(0,0,3)
        CALL VDINIT()
        CALL OVCLR
        CALL ZEROC(NBLK,MODE)
        CALL IVIDCO(6,MODE,MAP,NBLK)
        RETURN
        END
```

```
      SUBROUTINE NDGET2(INM,IAGE)
C     SUB. NDGET2 TO RETRIEVE DATA FROM DISC,LOAD TO ARRAY
C     NEW VERSION FOR USE WITH EFDYDT
C
C     INPUT/OUTPUT PARAMETERS
C               IFRAME = NUMBER OF FRAMES
C                    T = FRAME TIME
C                    Y = DATA ARRAY (DIMENSION Y(32,5)
C                  IPR = PRINT/TYPE FLAG
C                    F = AREA FACTORS
C                  INM = PATIENT'S NAME
C
C
      COMMON/REST/IREST(2)
      COMMON/ARRATE/F(4)
      COMMON/VARS/Y(32,5),T,IPR
      DIMENSION INM(2)
      DIMENSION ILIT(62)
      DIMENSION AREA(8)
      DIMENSION NFRAME(10)
      DIMENSION RATE(10)
      DIMENSION COUNTS(8)
      DIMENSION IFILE(6)
      DIMENSION IEXT(2)
      DIMENSION ITEXT(8)
      DATA IEXT/'.N','.T'/
      DATA IFILE/'AD','1:','NA','ME','.N','DF'/
C
C
      IFILE(3)=INM(1)
      IFILE(4)=INM(2)
C     CHECK N.D. DIRECTORY ON DISC
C
      IBLK=IFILTH(IFILE)
      IF(IBLK.EQ.-2) GO TO 910
C
C     OPEN DIRECTORY AND READ, AND TYPE
C
      CALL CLOSE(2)
      CALL ASSIGN (2,IFILE,12,OLD)
      DEFINE FILE 2(32,8,U,IV)
5     TYPE 505
      DO 100 I=1,32
      READ(2'I)ITEXT
      IF(ITEXT(1).EQ.0)GO TO 110
      TYPE 510,I,ITEXT(1),ITEXT(2),ITEXT(3),ITEXT(4),
     1 ITEXT(5),ITEXT(6)
100   CONTINUE
110   CONTINUE
C
C     SELECT N.D. FILE
C
      TYPE 515
      ACCEPT 15,IND
      IF(IND.EQ.0) GO TO 900
      IF(IND.LT.1.OR.IND.GT.(I-1))GO TO 5
      READ(2'IND)ITEXT
      WRITE(IPR,516)ITEXT(1),ITEXT(2),ITEXT(3),
     1 ITEXT(4),ITEXT(5),ITEXT(6)
      CALL CLOSE(2)
      IREST(1)=ITEXT(5)
      IREST(2)=ITEXT(6)
      IFILE(5)=IEXT(2)
      IFILE(6)=ITEXT(7)
C     CHECK SELECTED N.D.FILE IS ON DISC
```

```
C
      IBLK=IFILTH(IFILE)
      IF(IBLK.EQ.-2)GO TO 920
C
C     OPEN SELECTED FILE
C
      CALL ASSIGN(2,IFILE,12,OLD)
      CALL NDHEAD(2,NRCHAN,ILIT,IFIRST,OEXT,IAREA,AREA,NFRAME,RATE,IERR)
C     WRITE(IPR,517)AREA(1),AREA(2),AREA(3),AREA(4),AREA(5)
      DO 120 IFLAG=1,NFRAME(1)
      CALL NDREAD(2,0,0,1,NRCHAN,IFIRST,ISEQ,TIME,COUNTS,IERR)
      Y(IFLAG,1)=COUNTS(1)
      Y(IFLAG,2)=COUNTS(2)
      Y(IFLAG,3)=COUNTS(3)
      Y(IFLAG,4)=COUNTS(4)
      Y(IFLAG,5)=COUNTS(5)
120   CONTINUE
C
C     CALC. HR, PREDICTED MAX HR & % ACHIEVED
C
      T=RATE(1)
      H=3.375/T
      FHM=216-(IAGE*0.8)
      PMFH=100*H/FHM
      IFRAME=NFRAME(1)
      WRITE(IPR,525)IAGE,FHM,H,PMFH
      WRITE(IPR,530)
      DO 125 I=1,IFRAME
      WRITE(IPR,535)Y(I,1),Y(I,2),Y(I,3),Y(I,4),Y(I,5)
125   CONTINUE
C
C     CALC. BACKGROUND WEIGHTING FACTORS (AREA(I)/AREA(BGD))
C
      DO 130 I=1,4
      F(I)=AREA(I)/AREA(5)
130   CONTINUE
      WRITE(IPR,517)AREA(1),F(1),AREA(2),F(2),AREA(3),F(3),
     1 AREA(4),F(4),AREA(5)
      CALL CLOSE(2)
C
C     BGD SUB DATA
C
      DO 135 I=1,IFRAME
      DO 140 J=1,4
      Y(I,J)=Y(I,J)-(Y(I,5)*F(J))
140   CONTINUE
      Y(I,5)=0.0
135   CONTINUE
      WRITE(IPR,540)
      DO 145 I=1,IFRAME
      WRITE(IPR,545)Y(I,1),Y(I,2),Y(I,3),Y(I,4)
145   CONTINUE
      RETURN
```

```
900       STOP'MANUAL STOP IN "NDGET2"'
910       STOP'NO N.D. DIRECTORY ON DISC - DO MUGA PROCESSING'
920       STOP'SELECTED N.D. FILE IS NOT ON DISC'
15        FORMAT(I5)
500       FORMAT('0ENTER PATIENTS AGE (YRS.): '$)
505       FORMAT(14X,'SELECT NUMERIC DATA : ')
510       FORMAT(10X,I5,1X,6A2)
515       FORMAT(14X,'0 NO SELECTION DESIRED'/
     1    14X$)
516       FORMAT(1X,'DATA NAME : ',6A2/)
517       FORMAT(//1X,'NAME',10X,'AREA (PIXELS)',10X,' FACTOR '/
     1    1X,'GLOBAL    ',5X,F8.4,13X,F8.4/
     2    1X,'SEPTAL    ',5X,F8.4,13X,F8.4/
     3    1X,'INFERIOR  ',5X,F8.4,13X,F8.4/
     4    1X,'LATERAL   ',5X,F8.4,13X,F8.4/
     5    1X,'BACKGROUND  ',3X,F8.4//)
525       FORMAT(1X,'PREDICTED MAX. HEART RATE FOR AGE ',I5,' IS ',F8.3/
     1    1X,'PATIENT ACHIEVED ',F8.3,' (',F8.3,' % OF MAXIMIUM)'//)
530       FORMAT(1X,'ORIGINAL DATA'//
     1    1X,'GLOBAL   SEPTAL  INFERIOR LATERAL  BACKGROUND'/
     2    1X,'=========================================='//)
535       FORMAT(5F8.0)
540       FORMAT(//1X,'AREA NORMALISED, BACKGROUND SUBTRACTED DATA'//
     1    1X,'GLOBAL   SEPTAL  INFERIOR  LATERAL'/
     2    1X,'================================='//)
545       FORMAT(1X,4F8.0)
          END
```

```
C       SUB. DVDTMJ.FOR/OBJ    TRANSLATION OF PROGRAM
C       SUPPLIED BY MARK JACKSON FROM LOUGHBOROUGH UNIVERSITY
C       MODIFIED TO USE REAL*4 ARRAYS RATHER THAN DOUBLE PRECISION
C
C       THIS VERSION IS MODIFIED TO OPERATE WITH COUNTS
C       AFTER AREA NORMALISED BACKGROUND SUBTRACTION
C       INPUT PARAMETER.  TO BE USED WITH PROGRAM EFDVDT
C
C       PROGRAM SET UP 31-JAN-85
C       LAST MODIFIED 29-APR-86
C
        COMMON/VARS/Y(32,5),T,IPR
        COMMON/ARR1/BY(100,9)
        DIMENSION CCX(101,4)
        DIMENSION AK(101)
        DIMENSION AY(101)
        DIMENSION AKX(101)
        DIMENSION X(101)
        DIMENSION DX(101)
        DIMENSION SPX(3)
C
C       CALCULATE N
C
        N=16
        IF(Y(17,1).GT.0)N=32
        DO 12 I=1,N
        AK(I)=T*I
12      CONTINUE
        DO 15 ILOOP=1,4
C
        AMAX=-99999.
        AMIN=99999.
C
C       LOAD DATA
C
        DO 20 ILOAD=1,N
        AY(ILOAD)=Y(ILOAD,ILOOP)
20      CONTINUE
C
C
C       CALCULATE SMOOTHING FACTOR
C
        COUNT=0.0
        DO 21 I=1,N
        COUNT=COUNT+AY(I)
21      CONTINUE
        CMEAN=COUNT/N*1.0
        CMRT=SQRT(CMEAN)
        SF=1.25*CMRT*9750./CMEAN/121.8
        SF=SF*CMEAN/100.
        TYPE 500,SF
C
C
        X(1)=8*AY(1)-11*AY(2)+4*AY(3)
        X(2)=5.5*AY(1)-7*AY(2)+2.5*AY(3)
        X(3)=3*AY(1)-3*AY(2)+AY(3)
C
        DO 30 I=4,N+3
        X(I)=AY(I-3)
        AKX(I)=AK(I-3)
30      CONTINUE
C
        X(N+6)=8*X(N+3)-11*X(N+2)+4*X(N+1)
        X(N+5)=5.5*X(N+3)-7*X(N+2)+2.5*X(N+1)
        X(N+4)=3*X(N+3)-3*X(N+2)+X(N+1)
```

```
      AKX(3)=2*AKX(4)-AKX(5)
      AKX(2)=2*AKX(3)-AKX(4)
      AKX(1)=2*AKX(2)-AKX(3)
C
      AKX(N+4)=2*AKX(N+3)-AKX(N+2)
      AKX(N+5)=2*AKX(N+4)-AKX(N+3)
      AKX(N+6)=2*AKX(N+5)-AKX(N+4)
C
      DO 40 I=1,N+6
      DX(I)=SF
40    CONTINUE
C
      S=0.9*(N+6)
      CALL REINSH(CCX,(N+6),AKX,X,DX,S)
C
C     IF(ILOOP.EQ.1)WRITE(IPR,510)
C     IF(ILOOP.EQ.2)WRITE(IPR,511)
C     IF(ILOOP.EQ.3)WRITE(IPR,512)
C     IF(ILOOP.EQ.4)WRITE(IPR,513)
C
C     WRITE(IPR,520)
C     DO 50 I=1,N
C     CALL VALC3(SPX,AK(I),CCX,(N+6),AKX,IPR)
C     WRITE(IPR,25)AK(I),AY(I),SPX(1),SPX(2)
C     Y(I,ILOOP)=SPX(2)
C50   CONTINUE
C     WRITE(IPR,530)
      ATT=(AK(N)-AK(1))/100.
      DO 51 I=1,100
      AT=AK(1)+(I-1)*ATT
      CALL VALC3(SPX,AT,CCX,(N+6),AKX,IPR)
C     WRITE(IPR,535)AT,SPX(1),SPX(2),SPX(3)
      BY(I,ILOOP)=SPX(1)
      BY(I,(ILOOP+4))=SPX(2)
      BY(I,9)=AT
51    CONTINUE
15    CONTINUE
      RETURN
25    FORMAT(F8.6,3(5X,F8.0))
500   FORMAT(/1X,'SF = ',F8.2)
505   FORMAT(1X,'PREDICTED HEART RATE FOR AGE ',I5,' IS ',F8.2,' BPM'/
     1  1X'PATIENT ACHIEVED ',F8.3,' % OF MAXIMUM ')
510   FORMAT(/1X,'GLOBAL AREA'//)
511   FORMAT(/1X,'SEPTAL AREA'//)
512   FORMAT(/1X,'INFERIOR AREA'//)
513   FORMAT(/1X,'LATERAL AREA'//)
520   FORMAT(1X,'   TIME       COUNTS       CORR          DERIV'/
     1  1X,'=============================================='//)
525   FORMAT(//1X'MAXIMUM RATE OF EMPTYING = ',F8.0/
     1  1X,'MAXIMUM RATE OF FILLING = ',F8.0//
     2  1X,'J1 = ',I5,'  J2 = ',I5)
530   FORMAT(1X,'   TIME   CORR. COUNTS  1ST DERIV.   2ND DERIV.'/
     1  1X'=============================================='//)
535   FORMAT(1X,F8.6,3(F10.0))
551   FORMAT(//1X,'RR=',F8.4,' J=',I5,' J1=',I5,' J2=',I5//)
553   FORMAT(1X,'% SEGMENTAL COUNT')
555   FORMAT(1X,'PER = ',F8.0,' PFR = ',F8.0,' PFR/2 = ',F8.0)
560   FORMAT(1X,'% GLOBAL COUNT')
565   FORMAT(1X,'% R-R INTERVAL TIMES TO:'/
     1  1X,' PER     PFR      PFR/2'/
     2  1X,3F8.0)
570   FORMAT(1X,'TIME TO PER(%STI) = ',F8.0/
     1  1X,'TIME TO PFR(%DTI) = ',F8.0/
     2  1X,'TIME TO PFR/2(%DTI) = ',F8.0)
575   FORMAT(1X,'PER/PFR = ',F8.0,' PER/(PFR/2) = ',F8.0)
      END
```

```
      SUBROUTINE VALC3(SP,T,CC,N,AK,IPR)
C*****************************************************************************
C*
C*      VALC3 EVALUATES A CUBIC SPLINE AND ITS FIRST TWO DERIVATIVES
C*
C*****************************************************************************
C
      DIMENSION CC(101,4),AK(101),SP(3)
C
      N1=N-1
      DO 10 I=1,N1
      I1=I+1
      IF(T.LT.AK(1))GO TO 18
      IF(T.GT.AK(N))GO TO 14
      IF(T.GE.AK(I).AND.T.LT.AK(I1))GO TO 20
      IF(T.EQ.AK(N))GO TO 16
10    CONTINUE
14    WRITE(IPR,500)T,AK(N)
16    I=N-1
      GO TO 20
18    WRITE(IPR,505)T,AK(1)
C
20    A=CC(I,1)
      B=CC(I,2)
      C=CC(I,3)
      D=CC(I,4)
C
      H=T-AK(I)
      SP(1)=A+B*H+C*H**2+D*H**3
      SP(2)=B+2.0*C*H+3.0*D*H**2
      SP(3)=2.0*C+6.0*D*H
C
      RETURN
500   FORMAT(1X,'T > AK(N)     T = ',F8.4,' AK(N) = ',F8.4)
505   FORMAT(1X,'T < AK(1)     T = ',F8.4,' AK(1) = ',F8.4)
      END
```

```
      SUBROUTINE REINSH(CC,N2,AK,Y,DY,S)
C
C     SUB. REINSH  - - -  FITS SMOOTHEST CUBIC SPLINE !!!
C
C     PARAMETERS:
C             CC - SPLINE COEFFICIENTS
C             N2 - NUMBER OF DATA POINTS
C             AK - ARRAY OF INDEPENDENT VARIABLES
C                - FRAME NUMBER WHEN SPLINING TIME VALUES
C              Y - ARRAYOF DEPENDENT VARIABLE
C             DY - ARRAY OF ESTIMATE OF ERROR IN Y
C              S - CONSTANT DETERMINING OF FIT
C
C*********************************************************************
C
      DIMENSION A(101)
      DIMENSION B(101)
      DIMENSION C(101)
      DIMENSION D(101)
      DIMENSION CC(101,4)
      DIMENSION AK(101)
      DIMENSION Y(101)
      DIMENSION DY(101)
      DIMENSION R(101),R1(101),R2(101),T(101),T1(101),U(101),V(101)
C
      N1=1
C
      M1=N1-1
      M2=N2+1
C
      R(M1)=0.0
      R(N1)=0.0
      R1(N2)=0.0
      R2(N2)=0.0
      R2(M2)=0.0
      U(M1)=0.0
      U(N1)=0.0
      U(N2)=0.0
      U(M2)=0.0
      P=0.0
C
      M1=N1+1
      M2=N2-1
      H=AK(M1)-AK(N1)
C
      F=(Y(M1)-Y(N1))/H
C
      DO 10 I=M1,M2
      I1=I+1
      IN1=I-1
      G=H
      H=AK(I1)-AK(I)
      E=F
      F=(Y(I1)-Y(I))/H
      A(I)=F-E
      T(I)=2.0*(G+H)/3.0
      T1(I)=H/3.0
C
      R2(I)=DY(IN1)/G
      R(I)=DY(I1)/H
      R1(I)=-DY(I)/G-DY(I)/H
10    CONTINUE
C
      DO 20 I=M1,M2
      I1=I+1
      I2=I+2
```

```
C(I)=R(I)*R1(I1)*R1(I)*R2(I1)
      D(I)=R(I)*R2(I2)
20    CONTINUE
C
      F2=-S
25    CONTINUE
C
      DO 30 I=M1,M2
      IN1=I-1
      IN2=I-2
C
      R1(IN1)=F*R(IN1)
      R2(IN2)=G*R(IN2)
      R(I)=1.0/(P*B(I)+T(I)-F*R1(IN1)-G*R2(IN2))
      U(I)=A(I)-R1(IN1)*U(IN1)-R2(IN2)*U(IN2)
C
      F=P*C(I)+T1(I)-H*R1(IN1)
      G=H
      H=D(I)*P
30    CONTINUE
C
      DO 40 I=M2,M1,-1
      I1=I+1
      I2=I+2
C
      U(I)=R(I)*U(I)-R1(I)*U(I1)-R2(I)*U(I2)
40    CONTINUE
      E=0.0
      H=0.0
C
      DO 50 I=N1,M2
      I1=I+1
      G=H
      H=(U(I1)-U(I))/(AK(I1)-AK(I))
      V(I)=(H-G)*DY(I)**2
      E=E+V(I)*(H-G)
50    CONTINUE
C
      V(N2)=-H*DY(N2)**2
      G=V(N2)
      E=E-G*H
      G=F2
      F2=E*P**2
C
      IF(F2.GE.S.OR.F2.LE.G) GO TO 65
C
      F=0.0
      H=(V(M1)-V(N1))/(AK(M1)-AK(N1))
C
      DO 60 I=M1,M2
      I1=I+1
      IN1=I-1
      IN2=I-2
C
      G=H
      H=(V(I1)-V(I))/(AK(I1)-AK(I))
      G=H-G-R1(IN1)*R(IN1)-R2(IN2)*R(IN2)
      F=F+G*R(I)*G
      R(I)=G
60    CONTINUE
C
      H=E-P*F
      IF(H.LE.0.0) GO TO 65
C
      P=P+(S-F2)/((SQRT(S/E)+P)*H)
      GO TO 25
C
65    CONTINUE
```

```
C
      DO 70 I=N1,N2
      A(I)=Y(I)-P*Y(I)
      C(I)=U(I)
      CC(I,1)=A(I)
      CC(I,3)=C(I)
70    CONTINUE
C
      DO 80 I=N1,M2
      I1=I+1
      H=AK(I1)-AK(I)
      D(I)=(C(I1)-C(I))/H/3.0
      B(I)=(A(I1)-A(I))/H-(H*D(I)+C(I))*H
      CC(I,4)=D(I)
      CC(I,2)=B(I)
80    CONTINUE
      RETURN
      END
```

```
C
      COMMON/ARR1/BY(100,9)
      COMMON/VARS/Y(16,5),T,IPR
C
      DIMENSION IT(4,2)
      DIMENSION CMAXS(4)
      DIMENSION IDT(4,2)
      DIMENSION IDT2(4)
C
      FH=3.375/T
C
      DO 100 I=1,4
C
C     CALCULATE LIMITS OF VARIATION
C     CV1 IS UPPER LIMIT
C     CV2 IS LOWER LIMIT
C
      COUNT=0.0
      DO 50 J=1,100
      COUNT=COUNT+BY(J,I)
50    CONTINUE
      COUNT=SQRT(COUNT/100)
      CV=2.00156/COUNT
      CV2=1-CV
      CV1=1+CV
C
C     FIND FIRST MAX.  (ED FRAME)
C
      YMAX=-9999.
      YMIN=99999.
      DO 105 J=1,30
      IF(BY(J,I).GT.YMAX)IT(I,1)=J
      IF(BY(J,I).GT.YMAX)YMAX=BY(J,I)
105   CONTINUE
C
C     FIND MIN
C
      DO 110 J=25,75
      IF(BY(J,I).LT.YMIN)IT(I,2)=J
      IF(BY(J,I).LT.YMIN)YMIN=BY(J,I)
110   CONTINUE
C
      CMAXS(I)=YMAX
      SV=YMAX-YMIN
      EF=(YMAX-YMIN)*100./YMAX
      Q=SV*FH
      RR=N*T/0.9
      PEP=BY(IT(I,1),9)*100./RR
      STI=(BY(IT(I,2),9)-BY(IT(I,1),9))*100./RR
      DTI=100.-STI-PEP
      IF(I.EQ.1)WRITE(IPR,500)
      IF(I.EQ.2)WRITE(IPR,505)
      IF(I.EQ.3)WRITE(IPR,510)
      IF(I.EQ.4)WRITE(IPR,515)
      WRITE(IPR,520)SV,EF,Q
      WRITE(IPR,525)RR,PEP,STI,DTI
C
      DVMAX=-9999.
      DVMIN=99999.
C
C     FIND MAX,MIN DV/DT
C
      DO 115 J=IT(I,1)+1,100
      IF(BY(J,(I+4)).GT.DVMAX)IDT(I,1)=J
      IF(BY(J,(I+4)).GT.DVMAX)DVMAX=BY(J,(I+4))
      IF(BY(J,(I+4)).LT.DVMIN)IDT(I,2)=J
      IF(BY(J,(I+4)).LT.DVMIN)DVMIN=BY(J,(I+4))
115   CONTINUE
```

```
  500     FORMAT(///1X,'GLOBAL DATA'//)
  505     FORMAT(///1X,'SEPTAL DATA'//)
  510     FORMAT(///1X,'INFERIOR DATA'//)
  515     FORMAT(///1X,'LATERAL DATA'//)
  520     FORMAT(1X,'SV = ',F8.3,' EF = ',F8.3,' CARD. OUTPUT = ',E12.6/)
  525     FORMAT(1X,'R-R INTERVAL (MSEC) = ',F8.6/
     1    1X,'PEP = ',F8.2,' STI = ',F8.2,' DTI = ',F8.2,' (% R-R)'/)
  530     FORMAT(1X,'RESULTS RELATIVE TO THIS AREA'/
     +    1X,'============================='//
     1    1X,'PER = ',F8.4,' PFR = ',F8.4,' PFR/2 = ',F8.4/)
  535     FORMAT(1X,'PER/PFR = ',F8.4,' PER/(PFR/2) = ',F8.4/)
  540     FORMAT(1X,'RESULTS RELATIVE TO GLOBAL AREA'/
     +    1X,'============================='//
     1    1X,'PER = ',F8.4,' PFR = ',F8.4,' PFR/2 = ',F8.4/)
  545     FORMAT(1X,'PER/PFR = ',F8.4,' PER/(PFR/2) = ',F8.4/)
  550     FORMAT(/1X,'TIME TO PER (% R-R) = ',F8.4/
     1    1X,'TIME TO PFR (% R-R) = ',F8.4/
     2    1X,'TIME TO PFR/2 (% R-R) = ',F8.4/
     3    1X,'TIME TO PER (% STI) = ',F8.4/
     4    1X,'TIME TO PFR (% DTI) = ',F8.4/
     5    1X,'TIME TO PFR/2 (% DTI) = ',F8.4///)
  600     FORMAT(1X,'ILIM = ',I5)
          END
```

```
C
C       FIND IF FULL BY END OF FRAMES
C
        PCNT1=BY(IT(I,1),I)*CV1
        PCNT2=BY(IT(I,1),I)*CV2
        DO 120 J=60,100
        IF(BY(J,I).GE.PCNT1)GO TO 125
120     CONTINUE
        GO TO 135
125     ILIM=J
        CTMAX=BY(J,I)
        DO 130 J2=(J+1),100
        IF(BY(J2,I).LT.PCNT1)GO TO 130
        IF(BY(J2,I).LT.CTMAX)GO TO 130
        CTMAX=BY(J2,I)
        ILIM=J2
130     CONTINUE
        GO TO 140
135     ILIM=111
140     ILIM=INT(0.5+IT(I,2)+(ILIM-IT(I,2))/2.)
        TYPE 600,ILIM
C
C       FIND AND STORE FRAME FOR PFR/2
C
        DVMAX=-9999.
        DO 145 J=IT(I,2),ILIM
        IF(BY(J,(I+4)).GT.DVMAX)ICNT=J
        IF(BY(J,(I+4)).GT.DVMAX)DVMAX=BY(J,(I+4))
145     CONTINUE
        IDT2(I)=ICNT
C
        PER=BY(IDT(I,2),(I+4))/CMAXS(I)
        PFR=BY(IDT(I,1),(I+4))/CMAXS(I)
        PFR2=BY(IDT2(I),(I+4))/CMAXS(I)
C
        RATE1=PER/PFR
        RATE2=PER/PFR2
C
        IF(I.EQ.1)GO TO 150
        PERG=BY(IDT(I,2),(I+4))/CMAXS(1)
        PFRG=BY(IDT(I,1),(I+4))/CMAXS(1)
        PFR2G=BY(IDT2(I),(I+4))/CMAXS(1)
C
        RATE1G=PERG/PFRG
        RATE2G=PERG/PFR2G
C
150     TIME1=BY(IDT(I,2),9)*100./RR
        TIME2=BY(IDT(I,1),9)*100./RR
        TIME3=BY(IDT2(I),9)*100./RR
        TIME4=(BY(IDT(I,2),9)-BY(IT(I,1),9))*100./
     1  (BY(IT(I,2),9)-BY(IT(I,1),9))
        TIME5=(BY(IDT(I,1),9)-BY(IT(I,2),9))*100./(RR-BY(IT(I,2),9))
        TIME6=(BY(IDT2(I),9)-BY(IT(I,2),9))*100./(RR-BY(IT(I,2),9))
C
        WRITE(IPR,530)PER,PFR,PFR2
        WRITE(IPR,535)RATE1,RATE2
        IF(I.EQ.1)GO TO 155
        WRITE(IPR,540)PERG,PFRG,PFR2G
        WRITE(IPR,545)RATE1G,RATE2G
155     WRITE(IPR,550)TIME1,TIME2,TIME3,TIME4,TIME5,TIME6
100     CONTINUE
        CALL CLOSE(IPR)
        RETURN
```

```
      COMMON/OVLADR/IOVL
      COMMON/REST/IREST(2)
      DIMENSION ICHAR1(4)
      DIMENSION ICHAR2(4)
      DIMENSION ICHAR3(4)
      DIMENSION ICHAR4(4)
      DIMENSION ILEG1(3)
      DIMENSION ILEG2(3)
      DATA ICHAR1/'GL','OB','AL','  '/
      DATA ICHAR2/'SE','PT','AL','  '/
      DATA ICHAR3/'IN','FE','RI','OR'/
      DATA ICHAR4/'LA','TE','RA','L '/
      DATA ILEG1/'CO','UN','TS'/
      DATA ILEG2/'DV','/D','T '/
      CALL CHRGEN(IREST,10,0,4)
      IF(I.EQ.1)CALL CHRGEN(ICHAR1,1,0,8)
      IF(I.EQ.2)CALL CHRGEN(ICHAR2,1,0,8)
      IF(I.EQ.3)CALL CHRGEN(ICHAR3,1,0,8)
      IF(I.EQ.4)CALL CHRGEN(ICHAR4,1,0,8)
      CALL CHRGEN(ILEG2,22,0,6)
      CALL CHRGEN(ILEG1,22,1,6)
      CALL LINE(220,18,240,18,4)
      CALL LINE(220,27,240,27,1)
      RETURN
      END
```

```
      SUBROUTINE PLOT
      COMMON/REST/IREST(2)
      COMMON/IMGBLK/NBLK
      COMMON/IMODE/MODE
      COMMON/OVLADR/IOVL
      COMMON/ARR1/BY(100,9)
      COMMON/VARS/Y(16,5),T,IPR
      DO 80 L=1,4
      CALL OVCLR
      J=L
      CALL TITLE(L)
50    YMAX=-9999.
      YMIN=99999.
      DO 100 I=1,100
      IF(BY(I,J).LT.YMIN)YMIN=BY(I,J)
      IF(BY(I,J).GT.YMAX)YMAX=BY(I,J)
100   CONTINUE
      YR=(YMAX-YMIN)
      DO 110 I=1,99
      IX1=40+(I-1)*2
      IY1=240-INT(200*(BY(I,J)-YMIN)/YR)
      IX2=40+I*2
      IY2=240-INT(200*(BY((I+1),J)-YMIN)/YR)
      IF(J.LT.5)K=1
      IF(J.GE.5)K=4
      CALL LINE(IX1,IY1,IX2,IY2,K)
110   CONTINUE
      IF(J.GE.5)GO TO 120
      J=J+4
      GO TO 50
120   CONTINUE
      CALL ITTOUR(7)
      PAUSE'TAKE PHOTO OF CURVES - - HIT <RETURN> TO CONTINUE'
80    CONTINUE
      RETURN
      END
```

```
C       PROGRAM "MOVCEN" TO CALCULATE MOVEMENT OF CENTROID OF
C       VENTRICLE FROM DIASTOLE TO SYSTOLE RELATIVE TO DIASTOLIC
C       DIAMETER AND TO GIVE DIRECTION OF MOVEMENT
C
        COMMON/VDMAP/MAP(256) /OVLADR/IOVL /IMGBLK/NBLK /IMODE/MODE
        DIMENSION DIFF(50),IPTS(2),IPACK(100),IPK(128)
        DIMENSION IBIT(4)
        DIMENSION IADIAS(2,50),IASYST(2,50),IODT(16)
        DIMENSION IFILE(6)
C
        DATA IBIT/'  ','- ','.0','ZZ'/
        DATA IFILE/'IP','1:','NA','ME','.0','ZZ'/
C
C
C       SET VIDEO
C
        MODE=2
        NBLK=256
        CALL LINMAP(MAP,0)
        CALL REFALL(0,0,3)
        CALL VDINIT()
        CALL OVCLR
        CALL ZEROC(NBLK,MODE)
        CALL IVIDCO(6,MODE,MAP,NBLK)
C
C       ENTER PATIENT I.D. AND OPEN,READ AND LIST OVERLAY DIRECTORY
C
5       IFILE(5)=IBIT(3)
        IFILE(6)=IBIT(4)
        CALL ASSIGN(1,'AD0:SCRTCH.FIL',14,SCR)
        DEFINE FILE 1(1,1,U,IV)
        CALL CLOSE(1)
        TYPE 500
        ACCEPT 10,IFILE(3),IFILE(4)
        IF(IFILE(3).EQ.IBIT(1).OR.IFILE(3).EQ.IBIT(2))GO TO 900
        CALL ASSIGN(2,IFILE,12,OLD)
        DEFINE FILE 2(16,16,U,IV)
200     TYPE 505
        DO 100 I=1,16
        READ(2'I)IODT
        IF(IODT(1).NE.0)TYPE 510,I,IODT(1),IODT(2),IODT(3),IODT(4),
     1  IODT(5),IODT(6),IODT(7),IODT(8)
100     CONTINUE
        TYPE 515
        ACCEPT 15,IREC
        IF(IREC.EQ.0)STOP'NO OUTLINES EQUALS NO RESULTS !!!'
        READ(2'IREC)IODT
        IF(IODT(1).EQ.0)GO TO 200
        IFILE(6)=IODT(10)
        CALL CLOSE(2)
C
C       OPEN AND READ OVERLAY FILE,READ FIRST TWO RECORDS ONLY,
C       DISPLAY AREAS.
C
        CALL OVCLR
        CALL ASSIGN(2,IFILE,12,OLD)
        DEFINE FILE 2(8,128,U,IV)
        READ(2'1)IPK
        DO 110 I=1,100
        IPACK(I)=IPK(I+1)
110     CONTINUE
        IPTS(1)=IPK(1)
        CALL AOIUPK(IPACK,IPK(1),IADIAS)
        CALL AOIDSP(IADIAS,IPK(1),0)
        READ(2'2)IPK
        DO 115 I=1,100
        IPACK(I)=IPK(I+1)
115     CONTINUE
```

```
      CALL AOIUPK(IPACK,IPK(1),IASYST)
      CALL AOIDSP(IASYST,IPK(1),0)
      CALL CLOSE(2)
C
C     FIND AND MARK CENTROIDS
C
      CALL COFG(IADIAS,IPTS(1),IX1,IY1)
      CALL COFG(IASYST,IPTS(2),IX2,IY2)
      CALL LINE((IX1+3),IY1,(IX1-3),IY1,1)
      CALL LINE(IX1,(IY1+3),IX1,(IY1-3),1)
      CALL LINE((IX2-3),(IY2-3),(IX2+3),(IY2+3),1)
      CALL LINE((IX2-3),(IY2+3),(IX2+3),(IY2-3),1)
C
C     CALCULATE EQUATION OF LINE JOINING CENTROIDS
C
      IYDIFF=IY2-IY1
      IXDIFF=IX2-IX1
      IF(IXDIFF.EQ.0)IXDIFF=1
      IF(IYDIFF.EQ.0)IYDIFF=1
      AM=1.*IYDIFF/IXDIFF
      C=IY1-AM*IX1
C
C     CALCULATE NEARNESS OF EACH POINT TO LINE
C
      DO 120 I=1,IPTS(1)
      DIFF(I)=ABS(AM-(1.0*IADIAS(2,I)-C)/IADIAS(1,I))
120   CONTINUE
C
C     FIND ONE END OF DIASTOLIC DIAMETER
C
      ICT1=0
      ICT2=0
      AMIN1=999.
      AMIN2=999.
      DO 125 I=1,IPTS(1)
      IF(DIFF(I).GT.AMIN1)GO TO 125
      DIST1=SQRT((IADIAS(1,I)-IX1)**2+(IADIAS(2,I)-IY1)**2)
      DIST2=SQRT((IADIAS(1,I)-IX2)**2+(IADIAS(2,I)-IY2)**2)
      IF(DIST2.GT.DIST1)GO TO 125
      AMIN1=DIFF(I)
      ICT1=I
125   CONTINUE
C
C     FIND OTHER END OF DIASTOLIC DIAMETER
C
      DO 130 I=1,IPTS(1)
      IF(DIFF(I).GT.AMIN2)GO TO 130
      DIST1=SQRT((IADIAS(1,I)-IX1)**2+(IADIAS(2,I)-IY1)**2)
      DIST2=SQRT((IADIAS(1,I)-IX2)**2+(IADIAS(2,I)-IY2)**2)
      IF(DIST1.GT.DIST2)GO TO 130
      AMIN2=DIFF(I)
      ICT2=I
130   CONTINUE
C
C     FIND DISTANCE BETWEEN CENTROIDS,DIASTOLIC DIAMETER AND
C     CALCULATE MOVEMENT OF CENTROIDS AS PERCENT OF DIASTOLIC
C     DIAMETER AND CALCULATE DIRECTION OF MOVEMENT
C
      IXDIFF=IADIAS(1,ICT2)-IADIAS(1,ICT1)
      IYDIFF=IADIAS(2,ICT2)-IADIAS(2,ICT1)
      CALL LINE(IADIAS(1,ICT1),IADIAS(2,ICT1),IADIAS(1,ICT2),
     1  IADIAS(2,ICT2),4)
      DLEN=SQRT(1.0*(IXDIFF**2+IYDIFF**2))
      IF(DLEN.EQ.0.0)STOP'WHAT? NO DIASTOLIC DIAMETER??!!'
      COFGD=SQRT(1.0*((IY2-IY1)**2+(IX2-IX1)**2))
      RELM=100.*COFGD/DLEN
      IYDIR=IY1-IY2
      IXDIR=IX1-IX2
```

```
C
C       TYPE RESULTS
C
        TYPE 520,IFILE(3),IFILE(4),RELM,COFGD,DLEN
        PRINT 520,IFILE(3),IFILE(4),RELM,COFGD,DLEN
        IF(IYDIR.GT.0)PRINT 525
        IF(IYDIR.LT.0)PRINT 530
        IF(IXDIR.GT.0)PRINT 535
        IF(IXDIR.LT.0)PRINT 540
        IF(IXDIR.EQ.0.AND.IYDIR.EQ.0)PRINT 545
        IF(IYDIR.GT.0)TYPE 525
        IF(IYDIR.LT.0)TYPE 530
        IF(IXDIR.GT.0)TYPE 535
        IF(IXDIR.LT.0)TYPE 540
        IF(IXDIR.EQ.0.AND.IYDIR.EQ.0)TYPE 545
        GO TO 5
900     CALL IVIDCO(0)
        STOP'FIRST I WILL FINISH PRINTING, THEN ITS "GOODBYE!!"'
10      FORMAT(2A2)
15      FORMAT(I5)
500     FORMAT(//10X,'MOVEMENT OF CENTROID PROGRAM'//
     +  15X,'INSERT (OR CHANGE) PATIENT DISC IN DRIVE # 1 ,THEN'/
     1  15X,'ENTER PATIENT NAME (4 CHARS.)'/
     2  15X,'OR ENTER DASH (-) TO STOP:'$)
505     FORMAT(14X,'SELECT OVERLAY')
510     FORMAT(10X,I5,1X,8A2)
515     FORMAT(14X,'0 NO OVERLAY DESIRED'/
     1  15X$)
520     FORMAT(//1X,'PATIENT ',2A2,' RELATIVE MOVEMENT =',F10.5,' %'/
     1  10X,'COFGD = ',F10.5/
     2  10X,'DLEN  = ',F10.5/)
525     FORMAT(10X,'MOVEMENT IS UP')
530     FORMAT(10X,'MOVEMENT IS DOWN')
535     FORMAT(10X,'MOVEMENT IS LEFT')
540     FORMAT(10X,'MOVEMENT IS RIGHT')
545     FORMAT(10X,'NO MOVEMENT AT ALL !!!!')
        END
```

```
C       PROGRAM "AOICOP.FOR/OBJ/SAV"  WRITTEN AT
C       RADIOISOTOPE IMAGING UNIT, GROBY ROAD HOSPITAL, LEICESTER
C       TO COPY AREAS FROM ONE PATIENT DISC TO ANOTHER, TRANSLATE
C       AND ROTATE THE AREA TO ALLOW FOR DIFFERENCE IN POSITIONING
C       RE-CALCULATE THE SEGMENTS AND STORE
C
        COMMON/OVLADR/IOVL /IMBUF/IMBUF1(256) /VDMAP/MAP(256)
        COMMON/IMODE/MODE /IMGBLK/NBLK /EXT/IEXT(32) /TEXT/ITEXT(4)
        COMMON/FRAME/IFRM /COUNT/ICNT /MASHST/MASRES(32)
        COMMON/IOPAC/LIT(36),FLOT(10) /WORK/IWORK(256)
        COMMON/FILE/IFILE(6)
        COMMON/AREA1/IAREAG(2,50) /AREA2/IAREAS(2,50) /AREA3/IAREAI(2,50)
        COMMON/AREA4/IAREAL(2,50) /AREAB/IAREAB(2,50)
        COMMON/ACNT/IGPT,ISPT,IIPT,ILPT,IBPT
        COMMON/SEGBND/ICNT1,ICNT2,ICNT3
        DIMENSION IREST(2)
        DIMENSION IEND(4)
        DATA IEND/'.P','NT','  ','  '/
        TYPE 500
        CALL SETDAT
        CALL VIDSET
        PAUSE'INSERT PATIENT DISC TO COPY FROM <HIT RETURN TO CONTINUE>'
        CALL FNDOV3(0)
        IEND(3)=IFILE(5)
        IEND(4)=IFILE(6)
        CALL OVFIND(IREST)
        IFILE(5)=IEND(3)
        IFILE(6)=IEND(4)
        CALL CLOSE(1)
        PAUSE'CHANGE TO NEW PATIENT DISC <HIT RETURN TO CONTINUE>'
100     TYPE 505,IFILE(3),IFILE(4)
        GO TO (105,110,100),NOYES()
105     I=1
        GO TO 115
110     I=0
115     IFILE(5)=ITEXT(2)
        IFILE(6)=ITEXT(3)
        CALL FETCH(I)
        CALL DISP
        CALL OVTRAN
120     TYPE 510
        GO TO (125,900,120),NOYES()
125     CALL STAOI2(IREST)
        CALL IVIDCO(0)
        STOP'PROCESSING COMPLETE - - OUTLINES STORED'
900     CALL IVIDCO(0)
        STOP'PROGRAM TERMINATED - - OUTLINES NOT STORED'
500     FORMAT(///15X,'RADIOISOTOPE IMAGING UNIT'//
     1  20X,'GROBY ROAD HOSPITAL'////
     2  15X'SEGMENTAL AREA COPYING PROGRAM'////)
505     FORMAT('0IS NEW PATIENT NAME ',2A2,' (Y OR N) '$)
510     FORMAT('0STORE THESE AREAS (Y OR N) ? '$)
        END
```

```
      SUBROUTINE OVFIND(IREST)
      COMMON/IMBUF/IMBUF1(256)
      COMMON/OVLADR/IOVL
      COMMON/IOPAC/LIT(36),FLOT(10)
      COMMON /FILE/IFILE(6)
      COMMON/AREA1/IAREAG(2,50)
      COMMON/ACNT/IGPT,ISPT,IIPT,ILPT,IBPT
      COMMON/SEGBND/ICNT1,ICNT2,ICNT3
      DIMENSION IREST(2)
      DIMENSION IPACK(100)
      DIMENSION IPK(128)
      DIMENSION IODT(16)
      DIMENSION IOVLXT(4)
      DIMENSION IOEXT(2)
      DATA IPACK/100*0/
      DATA IPK/128*0/
      DATA IOVLXT/'.O','ZZ','  ','  '/
      DATA IOEXT/'.Q','  '/
      IOVLXT(3)=IFILE(5)
      IOVLXT(4)=IFILE(6)
      IFILE(5)=IOVLXT(1)
      IFILE(6)=IOVLXT(2)
      CALL CLOSE(2)
      CALL ASSIGN (2,IFILE,12,OLD)
      DEFINE FILE 2(16,16,U,IV)
200   TYPE 500
      DO 100 I=1,16
      READ(2'I)IODT
      IF(IODT(1).NE.0)TYPE 505,I,IODT(1),IODT(2),IODT(3),
     1 IODT(4),IODT(5),IODT(6),IODT(7),IODT(8)
100   CONTINUE
      TYPE 510
      ACCEPT 10,IREC
      IF(IREC.EQ.0)GO TO 900
      READ(2'IREC)IODT
      IF(IODT(1).EQ.0)GO TO 200
      IFILE(6)=IODT(10)
      CALL CLOSE(2)
      CALL ASSIGN (2,IFILE,12,OLD)
      DEFINE FILE 2(8,128,U,IV)
      READ(2'1)IPK
      CALL CLOSE(2)
      DO 120 I=1,100
      IPACK(I)=IPK(I+1)
120   CONTINUE
      CALL AOIUPK(IPACK,IPK(1),IAREAG)
      IREST(1)=IODT(5)
      IREST(2)=IODT(6)
      IGPT=IPK(1)
      IFILE(5)=IOEXT(1)
      IFILE(6)=IODT(5)
      IBLK=IFILTH(IFILE)
      IF(IBLK.EQ.-2)GO TO 910
      CALL ASSIGN (2,IFILE,12,OLD)
      DEFINE FILE 2(1,3,U,IV)
      READ(2'1)ICNT1,ICNT2,ICNT3
      CALL CLOSE(2)
      RETURN
10    FORMAT(I5)
500   FORMAT(14X,'SELECT OVERLAY')
505   FORMAT(10X,I5,1X,8A2)
510   FORMAT(14X,'0 NO OVERLAY DESIRED'/
     1 15X$)
900   STOP'OPERATOR TERMINATION IN ROUTINE "OVFIND"'
910   STOP'NO POINT FILE FOUND !!!!!'
      END
```

```
      SUBROUTINE OVTRAN
      COMMON/FILE/IFILE(6)
      COMMON/SEGBND/ICNT1,ICNT2,ICNT3
      COMMON/AREA1/IAREAG(2,50)
      COMMON/AREA2/IAREAS(2,50)
      COMMON/AREA3/IAREAI(2,50)
      COMMON/AREA4/IAREAL(2,50)
      COMMON/AREAB/IAREAB(2,50)
      COMMON/ACNT/IGPT,ISPT,IIPT,ILPT,IBPT
      INTEGER AOIBND(2,50)
C
100   CALL OVCLR
      CALL COFG(IAREAG,IGPT,IX,IY)
      CALL AOIDSP(IAREAG,IGPT,0)
      CALL LINE((IX-3),(IY+3),(IX+3),(IY-3),1)
      CALL LINE((IX-3),(IY-3),(IX+3),(IY+3),1)
      TYPE 500
      CALL LIGHTP(IX1,IY1)
      CALL LINE(IX1,(IY1+4),IX1,(IY1-4),1)
      CALL LINE((IX1-4),IY1,(IX1+4),IY1,1)
      TYPE 505
      GO TO (105,100,100),NOYES()
105   DO 110 I=1,IGPT
      AOIBND(1,I)=IAREAG(1,I)-(IX-IX1)
      AOIBND(2,I)=IAREAG(2,I)-(IY-IY1)
110   CONTINUE
      CALL AOIDSP(AOIBND,IGPT,0)
      TYPE 510
      GO TO (120,100,100),NOYES()
120   CALL AOIERS(IAREAG,IGPT,1)
      DO 125 I=1,IGPT
      IAREAG(1,I)=AOIBND(1,I)
      IAREAG(2,I)=AOIBND(2,I)
125   CONTINUE
      CALL OVCLR
      CALL AOIDSP(IAREAG,IGPT,0)
126   TYPE 511
      GO TO (127,129,125),NOYES()
127   TYPE 512
      CALL LIGHTP(IMX,IMY)
      CALL LIGHTP(INX,INY)
      CALL GETNP(IAREAG,IGPT,IMX,IMY,IPOS)
      IAREAG(1,IPOS)=INX
      IAREAG(2,IPOS)=INY
      CALL OVCLR
      CALL AOIDSP(IAREAG,IGPT,0)
      GO TO 126
129   CALL COFG(IAREAG,IGPT,IX,IY)
      CALL CWCCW(IAREAG,IGPT,IX,IY,ICW)
      CALL SEGMNT(IAREAG,IAREAS,IGPT,IX,IY,ICNT1,ICNT2,ICW,ISPT)
      CALL SEGMNT(IAREAG,IAREAI,IGPT,IX,IY,ICNT2,ICNT3,ICW,IIPT)
      CALL SEGMNT(IAREAG,IAREAL,IGPT,IX,IY,ICNT3,ICNT1,ICW,ILPT)
      ICHAR=ITTOUR(7)
      PAUSE'HIT RETURN TO DISPLAY SEGMENTS'
      CALL OVCLR
      CALL AOIDSP(IAREAS,ISPT,0)
      CALL AOIDSP(IAREAI,IIPT,0)
      CALL AOIDSP(IAREAL,ILPT,0)
```

```
130     TYPE 515
        GO TO (135,140,130),NOYES()
135     CALL OVROT(IX,IY)
        CALL OVCLR
        GO TO 125
140     TYPE 520
        GO TO (100,145,140),NOYES()
145     TYPE 530
        CALL AOIDRW(IAREAB,IBPT)
        RETURN
10      FORMAT(I5)
500     FORMAT('0MARK NEW POSITON OF CENTRE OF VENTRICLE
     1  WITH LIGHT PEN'/)
505     FORMAT('0IS THIS ACCEPTABLE (Y OR N)'$)
510     FORMAT('0 DOES THIS FIT ? (Y OR N) '$)
511     FORMAT('0EDIT AREA POINTS (Y OR N) ? '$)
512     FORMAT('0MARK THE POINT TO BE MOVED AND ITS NEW POSITION'/
     1  1X,'WITH THE LIGHT PEN')
515     FORMAT('0DO THESE AREAS NEED ROTATION (Y OR N)'$)
520     FORMAT('0TRANSLATE AREAS (Y OR N) ? '$)
530     FORMAT('0DRAW BACKGROUND AREA WITH L.P.')
        END
```

```
      SUBROUTINE STAOI2(IREST)
      COMMON /FILE/IFILE(6)
      COMMON/AREA1/IAREAG(2,50)
      COMMON/AREA2/IAREAS(2,50)
      COMMON/AREA3/IAREAI(2,50)
      COMMON/AREA4/IAREAL(2,50)
      COMMON/AREAB/IAREAB(2,50)
      COMMON/ACNT/IGPT,ISPT,IIPT,ILPT,IBPT
      DIMENSION IREST(2)
      DIMENSION IPACK(100)
      DIMENSION IOVLXT(2)
      DIMENSION IPK(128)
      DIMENSION IODT(16)
      DIMENSION IOVNAM(8)
      DIMENSION INAM(30)
      DATA IOVLXT/'.O','ZZ'/
      DATA IPACK/100*0/
      DATA IPK/128*0/
      DATA IOVNAM/'SE','GM','EN','T ','  ','  ',' 2','  '/
      DATA INAM/'GL','OB','AL','  ','  ','  ','SE','PT','AL','  ',
     1  '  ','  ','IN','FE','RI','OR','  ','  ','LA','TE','RA','L ',
     2  '  ','  ','BK','G ','  ','  ','  ','  ','  ','  '/
C
      IOVNAM(5)=IREST(1)
      IOVNAM(6)=IREST(2)
      IFILE(5)=IOVLXT(1)
      IFILE(6)=IOVLXT(2)
      CALL CLOSE(2)
      I=IFILTH(IFILE)
      IF(I.EQ.-2)GO TO 920
      CALL ASSIGN (2,IFILE,12,OLD)
      DEFINE FILE 2(16,16,U,IV)
      DO 100 IOVREC=1,16
      READ(2'IOVREC,ERR=900)IODT
      IF(IODT(1).EQ.0)GO TO 110
100   CONTINUE
      TYPE 500
      GO TO 910
110   CONTINUE
      IF(IOVREC.EQ.1)GO TO 920
      DO 115 I=1,8
      IODT(I)=IOVNAM(I)
115   CONTINUE
      IODT(9)=8
      WRITE(2'IOVREC)IODT
      IFILE(6)=IODT(10)
      CALL AOIPAK(IAREAG,IGPT,IPACK)
      CALL CLOSE(2)
      CALL ASSIGN (2,IFILE,12,NEW)
      DEFINE FILE 2(8,128,U,IV)
      IPK(1)=IGPT
      DO 120 I=1,100
      IPK(I+1)=IPACK(I)
120   CONTINUE
      IPK(116)=0
      IPK(117)=0
      DO 125 I=1,6
      IPK(122+I)=INAM(I)
125   CONTINUE
      WRITE(2'1)IPK
      DO 130 I=1,100
130   IPACK(I)=0
      CALL AOIPAK(IAREAS,ISPT,IPACK)
      IPK(1)=ISPT
      DO 140 I=1,100
      IPK(I+1)=IPACK(I)
140   CONTINUE
```

```
      DO 145 I=1,6
      IPK(122+I)=INAM(I+6)
145   CONTINUE
      WRITE(2'2)IPK
      DO 150 I=1,100
150   IPACK(I)=0
      CALL AOIPAK(IAREAI,IIPT,IPACK)
      IPK(1)=IIPT
      DO 155 I=1,100
      IPK(I+1)=IPACK(I)
155   CONTINUE
      DO 160 I=1,6
      IPK(122+I)=INAM(I+12)
160   CONTINUE
      WRITE(2'3)IPK
      DO 165 I=1,100
165   IPACK(I)=0
      CALL AOIPAK(IAREAL,ILPT,IPACK)
      IPK(1)=ILPT
      DO 170 I=1,100
      IPK(I+1)=IPACK(I)
170   CONTINUE
      DO 175 I=1,6
      IPK(122+I)=INAM(I+18)
175   CONTINUE
      WRITE(2'4)IPK
      DO 180 I=1,100
180   IPACK(I)=0
      CALL AOIPAK(IAREAB,IBPT,IPACK)
      IPK(1)=IBPT
      DO 185 I=1,100
      IPK(I+1)=IPACK(I)
185   CONTINUE
      DO 190 I=1,6
      IPK(122+I)=INAM(I+24)
190   CONTINUE
      WRITE(2'5)IPK
      DO 195 I=1,128
195   IPK(I)=0
      WRITE(2'6)IPK
      WRITE(2'7)IPK
      WRITE(2'8)IPK
      CALL CLOSE(2)
      RETURN
500   FORMAT(10X,'OVERLAY FILE FULL')
900   STOP'READ ERROR FOR OVERLAY DIRECTORY'
910   STOP'RECOPY PATIENT FILES WITH LESS THAN 16 OVERLAYS'
920   STOP'DO NORMAL MUGA PROCESSING FIRST'
      END
```

```
      SUBROUTINE OVROT(IX,IY)
C     TO ROTATE AN OUTLINE BY AN AMOUNT
C
      COMMON/AREA1/IAREAG(2,50)
      COMMON/ACNT/IGPT,ISPT,IIPT,ILPT,IBPT
      COMMON/SEGBND/ICNT1,ICNT2,ICNT3
      TYPE 500
      CALL LIGHTP(IPX,IPY)
C
C     REDUCE AREA TO 0,0
C
      DO 100 I=1,IGPT
      IAREAG(1,I)=IAREAG(1,I)-IX
      IAREAG(2,I)=IAREAG(2,I)-IY
      IF(IAREAG(1,I).EQ.0)IAREAG(1,I)=1
      IF(IAREAG(2,I).EQ.0)IAREAG(2,I)=1
100   CONTINUE
C
C     REDUCE L.P. POINTS
C
      IPX=IPX-IX
      IPY=IPY-IY
C
C     CALCULATE ANGLE OF ROTATION
C
      PY=FLOAT(IPY)
      PX=FLOAT(IPX)
      AX=FLOAT(IAREAG(1,ICNT1))
      AY=FLOAT(IAREAG(2,ICNT1))
      IF(AY.EQ.0.0.AND.AX.LT.0.0)A=0.0
      IF(AY.EQ.0.0.AND.AX.GT.0.0)A=1.570796327
      IF(AX.EQ.0.0.AND.AY.GT.0.0)A=0.785398163
      IF(AX.EQ.0.0.AND.AY.LT.0.0)A=2.35619449
      IF(AX.NE.0.0.AND.AY.NE.0.0)A=ATAN2(AY,AX)
      IF(PY.EQ.0.0.AND.PX.GT.0.0)B=0.0
      IF(PY.EQ.0.0.AND.PX.LT.0.0)B=1.570796327
      IF(PX.EQ.0.0.AND.PY.GT.0.0)B=0.785398163
      IF(PX.EQ.0.0.AND.PY.LT.0.0)B=2.35619449
      IF(PX.NE.0.0.AND.PY.NE.0.0)B=ATAN2(PY,PX)
      ALPHA=A-B
C
C     SHIFT POINTS
C
      DO 110 I=1,IGPT
      IF(IAREAG(1,I).EQ.0)BETA=2.35619449+ALPHA
      IF(IAREAG(2,I).EQ.0)BETA=ALPHA
      IF(IAREAG(2,I).EQ.0.OR.IAREAG(1,I).EQ.0)GO TO 50
      AX=FLOAT(IAREAG(1,I))
      AY=FLOAT(IAREAG(2,I))
      BETA=ATAN2(AY,AX)-ALPHA
      R=SQRT(AX**2+AY**2)
      GO TO 55
50    R=SQRT((1.*IAREAG(2,I)**2)+(1.*IAREAG(1,I)**2))
55    IAREAG(1,I)=INT(R*COS(BETA))
      IAREAG(2,I)=INT(R*SIN(BETA))
110   CONTINUE
C
C     RELOCATE POINTS
C
      DO 115 I=1,IGPT
      IAREAG(1,I)=IAREAG(1,I)+IX
      IAREAG(2,I)=IAREAG(2,I)+IY
115   CONTINUE
      RETURN
500   FORMAT('0ENTER NEW POSITION OF TOP OF SEPTUM WITH L.P.')
      END
```

BIBLIOGRAPHY

Albrechtsson, J., Eskilsson, J., Lomsky, M., Stubbe, I., Svensson., S.E., and Tylen., U. 1982. Comparision of Left Ventricular Ejection Fraction Assessed by Radionuclide Angiocardiography. Acta. Med. Scand., 211, 147-152.

Amon, K.W., Kent, B.S., Richards, L., and Crawford, M.H. 1984. Usefulness of the Postexercise Response of Systolic Blood Pressure in the Diagnosis of Coronary Artery Disease. Circulation, 70, 6, 951-956.

Amsterdam, E.A., Price, J.E., Berman, D., Hughes, J.L., Riggs, K., DeMaria, A.N., Miller, R.R., and Mason, D.T. 1977. Exercise Testing in the Indirect Assessment of Myocardial Oxygen Consumption: Application for Evaluation of Mechanisms and Therapy of Angina Pectoris. From Exercise in Cardiovascular Health and Disease. Editors Amsterdam, E.A., Wilmore, J.H., DeMaria, A.N., New York Medical Books.

Ashburn, W.L., Schelbert, H.R., and Verba, J.W. 1978. Left Ventricular Ejection Fraction - A Review of Several Radionuclide Angiographic Approaches using the Scintillation Camera. Prog. Cardiovasc. Dis., 20, 4, 267-283.

Astrand, P.O., and Rodahl, K. 1977. Textbook of Work Physiology: Physiological Bases of Exercise. McGraw-Hill Book Company.

Astrand, P.O., and Ryhming, I. 1954. A Nomogram for Calculation of Aerobic Capacity (Physical Fitness) from Pulse Rate during Submaximal Work. J. Appl. Physiol., 7, 218-221.

Astrand, P.O., and Saltin, B. 1961. Maximal Oxygen Uptake and Heart Rate in Various Types of Muscular Activity. J. Appl. Physiol., 16, 6, 977-981.

Baan, J., Van Der Velde, E.T., De Bruin, H.G., Smeenk, G.J., Koops, J., Van Dijk, A.D., Temmerman, D., Senden, J., Buis, B. 1984. Continuous Measurement of Left Ventricular Volume in Animals and Humans by Conductance Catheter. Circulation, 70, 5, 812-823.

Bacharach, S.L., Green, M.V., Borer, J.S., Hyde, J.E., Farkas, S.P., and Johnston, G.S. 1979. Left-Ventricular Peak Ejection Rate, Filling Rate, and Ejection Fraction - Frame Rate Requirements at Rest and Exercise: Concise Communication. J. Nucl. Med., 20, 189-193.

Balke, B. 1960. Biodynamics: Human. From Medical Physics Volume 3, Editor Otto Glasser, 50.

Balke, B., and Ware, R.W. 1959. An Experimental Study of "Physical Fitness" of Air Force Personnel. U.S. Armed Forces Medical Journal, 10, 6, 675-688.

Benchimol, A. 1969. Significance of the Contribution of Atrial Systole to Cardiac Function in Man. Am. J. Cardiol., 23, 568-571.

Beranek, I., Moore, R., Kim, S., Formanek, A., and Amplatz K. 1976. Comparision of Ejection Fraction Calculated by Nine Different Volume Calculation Methods. Radiology, 120, 553-556.

Berger, H.J., Reduto, L.A., Johnstone, D.E., Borkowski, H., Sands, J.M., Conhen, L.S., Langou, R.A., Gottschalk, A., Zaret, B.L., and Pytlik, L. 1979. Global and Regional Left Ventricular Response to Bicycle Exericse in Coronary Artery Disease. Am. J. Med., 66, 13-21.

Bianco, J.A., Makey, D.G., Laskey, W.K., and Shafter, R.B. 1979. Radionuclide Left Ventricular dv/dt for the Assessment of Cardiac Function in Patients with Coronary Disease. J. Nucl. Med., 20, 1-6.

Biello, D.R., Sampathkumaran, K.S., Geltman, E.M., Britson, W.A., Scott, D.J., and Grbac, R.T. 1981. Determination of Left Ventricular Ejection Fraction: A New Method That Requires Minimal Operator Training. Journal of Nuclear Medicine Technology, 9, 2, 77-80.

Black, A.J.R., and King, S.B. 1987. Coronary Angioplasty. Current Opinion in Cardiology, 2, 949-960.

Block, P.C. 1980. Percutaneous Transluminal Coronary Angioplasty. Am. J. Radiol., 135, 955-959.

Bodenheimer, M.M., Banka, V.S., Fooshee, C.M., Hermann, G.A., Helfant, R.H. 1978. Quantitative Radionuclide Angiography in the Right Anterior Oblique View: Comparision With Contrast Ventriculography. Am. J. Cardiol., 41, 718-725.

Bonoron-Adele, S., Sicart, M, Ohayon, J., Colle, J.P., Ledain, L., Tariosse, L., and Besse, P. 1984. Effects of Contrast Media used in Angiocardiography on the Mechanical Performance and the Relaxation of Normal and Ichaemic Myocardium. European Heart Journal, 5, 146-157.

Bonow, R.O., Kent, K.M., Rosing, D.R., Lipson, L.C., Bacharach, S.L., Green, M.V., and Epstien, S.E. 1982. Improved Left Ventricular Diastolic Filling in Patients with Coronary Artery Disease After Percutaneous Transluminal Coronary Angioplasty. Circulation, 66, 6, 1159-1167.

Bonow, R.O., Vitale, D.F., Bacharach, S.L., Frederick, T.M., Kent, K.M., and Green, M.V. 1985. Asynchronous Left Ventricular Regional Function and Impaired Global

Diastolic Filling in Patients with Coronary Artery Disease: Reversal After Coronary Angioplasty. Circulation, 2, 297-307.

Booman, F., Reiber, J.H.C., Gerbrands, J.J., Slager, C.J., Schuurbiers, J.C.H., and Meester, G.T. 1979. Quantitative Analysis of Coronary Occlusions from Coronary Cine-Angiograms. Computers In Cardiology, 177-180.

Bove, A.A. 1985. Effects of Strenuous Exercise on Myocardial Blood Flow. Med. Sci. Sports Exerc., 17, 5, 517-521.

Bowker, T.J. 1986. Laser Angioplasty. Current Opinion in Cardiology, 1, 474-482.

Brady, T.J., Thrall, J.H., Keyes, J.W., Brymer, J.F., Walton, J.A., and Pitt, B. 1980a. Segmental Wall-Motion Analysis in the Right Anterior Oblique Projection: Comparision of Exercise Equilibrium Radiouclide Ventriculography and Exercise Contrast Ventriculography. J. Nucl. Med., 21, 617-621.

Brady, T.J., Thrall, J.H., Lo, K., and Pitt, B. 1980b. The Importance of Adequate Exercise in the Detection of Coronary Heart Disease by Radionuclide Ventriculography. J. Nucl. Med., 21, 1125-1130.

Brandt, P.W.T., Partridge, J.B., and Wattie, W.J. 1977. Coronary Arteriography: Method of Presentation of the Arteriogram Report and a Scoring System. Clin. Radiol., 28, 361-365.

Brown, B.G., Bolson, E.L., and Dodge, H.T. 1982. Arteriographic Assessment of Coronary Atherosclerosis. Arteriosclerosis, 2, 2-15.

Brown, B.G., Bolson, E.L., Dodge, H.T. 1984. Dynamic Mechanisms in Human Coronary Stenosis. Circulation, 70, 6, 917-922.

Brown, B.G., Bolson, E.L., Dodge, H.T. 1986. Quantitative Computer Techniques for Analyzing Coronary Arteriograms. Prog. Cardiovasc. Dis., 28, 6, 403-418.

Brown, B.G., Bolson, E., Frimer, M., and Dodge, H.T. 1977. Quantiative Coronary Arteriography. Circulation, 55, 2, 329-337.

Bruce, R.A. 1971. Exercise Testing of Patients with Coronary Heart Disease: Principles and Normal Standards for Evaluation. Ann. Clin. Res., 3. 323-332.

Bruce, R.A., Kusumi, F., and Hosmer, D. 1973. Maximal Oxygen Uptake and Nomographic Assessment of Functional Aerobic Impairment in Cardiovascular Disease. Am. Heart J., 85, 4, 546-562.

Castaneda-Zuniga, W.R., Fromanek, A., Tadavarthy, M., Viodaver, Z., Edwards, J.E., Zollikofter, C., and Amplatz, K. 1980. The Mechanism of Balloon Angioplasty. Radiology, 135, 565-571.

Cohn, P.F., Levine, J.A., Bergeron, G.A., and Gorlin, R. 1974. Reproducibility of the Angiographic Left Ventricular Ejection Fraction in Patients with Coronary Artery Disease. Am. Heart J., 88, 6, 713-720.

Cook, D.G., Shaper, A.G., Pocock, S.J., Kussick, S.J. 1986. Giving Up Smoking And The Risk Of Heart Attacks: A Report From The British Regional Study. Lancet, ii, 1376-1379.

Cowley, M.J., Vetrovec, G.W., and Wolfgang, T.C. 1981. Efficacy of Percutaneous Transluminal Coronary Angioplasty: Technique, Patient Selection, Salutary Results, Limitations and Complication. Am. Heart J., 101, 272-280.

DePuey, E.G., Boskovic, D., Krajcer, Z., Leatherman, L., Angelini, P., Sonnemaker, R.E., Burdine, J.A., and Springer, A. 1983. Exercise Radiounclide Ventriculography in Evaluating Successful Transluminal Coronary Angioplasty. Cathet. Cardiovasc. Diagn., 9, 153-166.

DePuey, E.G., Leatherman, L.L., Leachman, R.D., Dear, W.E., Masskin, K.M., Mathur, V.S., and Burdine, J.A. 1984. Restenosis After Transluminal Coronary Angioplasty Detected With Exercise-Gated Radionuclide Ventriculography. J. Am. Coll. Cardiol., 4, 6, 1103-1113.

De Rowen, T.A., Murray, J.A., Owen, W. 1977. Variability in the Analysis of Coronary Arteriograms. Circulation, 55, 324-328.

Dervan, J.P., Baim, D.S., Chernile, J., and Grossman, W. 1983. Transluminal Angioplasty of Occluded Coronary Arteries: Use of a Movable Guide Wire System. Circulation, 68, 4, 776-784.

Detry, J.M.R., Bruce, R.A. 1971. Effects of Nitroglycerin of "Maximal" Oxygen Intake and Exercise Electrocardiogram in Coronary Heart Disease. Circulation, 43, 155-163.

Diamond, G.A., Vas, R., Forrester, J.S., Xiange, H.Z., Whiting, J., Pfaff, M., and Swan, H.J.C. 1984. The Influence of Bias on the Subjective Interpretation of Cardiac Angiograms. Am. Heart J., 107, 1, 68-74.

Doorey, A.J., Mehmel, H.C., Schwarz, F.X., and Kubler, W. 1985. Amerlioration by Nitroglycerin of Left Ventricular Ischemia Induced by Percutaneous Transluminal Coronary Angioplasty: Assessment by

Hemodynamic Variables and Left Ventriculography. J. Am. Coll. Cardiol., 6, 2, 267-274.

Dorros, G., Cowley, M.J., Simpson, J., Bentivoglio, L.G., Block, P.C., Bourassa, M., Detre, K., Gosselin, A.J., Gruentzig, A.R., Kelsey, S.F., Kent, K.M., Mock, M.B., Mullin, S.M., Myler, R.K., Passamani, E.R., Stertzer, S.H., Williams, D.O. 1983. Percutaneous Transluminal Coronary Angioplasty: Report of Complications from the National Heart, Lung and Blood Institute PTCA Registry. Circulation, 67, 4, 723-730.

Dubois, D., and Dubois, E.F. 1916. Clinical Calorimetry. A Formula to Estimate the Approximate Surface Area if Height and Weight be Known. Arch Int Med 17, 863-871.

Ehsani, A.A., Biello, D., Seals, D.R., Austin, M.B., Schultz, J. 1984. The Effect of Left Ventricular Systolic Function on Maximal Aerobic Exercise Capacity in Asymptomatic Patients with Coronary Artery Disease. Circulation, 70, 4, 552-560.

Elamin, M.S., Boyle, R., Kardash, M.M., Smith, D.R., Stoker, J.B., Whitaker, W., Mary, D.A.S.G., Linden, R.J. 1982. Accurate Detection of Coronary Heart Disease by New Exercise Test. Br. Heart J., 48, 311-320.

Ellestad, M.H. 1980. Stress Testing: Principles and Practice. F.A. Davis Company.

Ellis, S.G., Roubin, G.S., King, S.B., Douglas, J.S., Weintraub, W.S., Thomas, R.G., and Cox, W.R. 1988. Angiographic and Clinical Predictors of Acute Closure after Native Vessel Coronary Angioplasty. Circulation, 77, 2, 372-379.

El-Tobgi, S., Fouad, F.M., Kramer, J.R., Rincon, G., Sheldon, W.C., and Tarazi, R.C. 1984. Left Ventricular Function in Coronary Artery Disease. Evaluation of Slope of End-Systolic Pressure-Volume Line (E_{max}) and Ratio of Peak Systolic Pressure to End-Systolic Volume (P/V_{es}). J. Am. Coll. Cardiol., 3, 3, 781-788.

Faxon, D.P., Ryan, T.J., McCabe, C.H., Kelsey, S.F., Detre, K. 1982. Determinants of a Successful Percutaneous Transluminal Coronary Angioplasty (NHLBI - PTCA Registry). Am. J. Cardiol., 49, 905.

Folland, E.D., Parisi, A.F., Moynihan, P.F., Jones, D.R., Feldman, C.L., Tow, D.E. 1979. Assessment of Left Ventricular Ejection Fraction and Volumes of Real-time, Two-Dimensional Echocardiography. Circulation, 4, 760-766.

Ford, W.B., Wholey, M.H., Zikria, E.A., Somadani, S.R., and Sullivan, M.E. 1981. Percutaneious Transluminal Dilation of Aortocoronary Saphenous Vein Bypass Grafts. Chest, 79, 5, 529-535.

Fox, K.M., and Ilskey, C. 1982. The Essentials of Exercise Electrocardiography. (Pharmaceutical Company Literature).

Fox, R.M., Hakki, A.H., Iskandrain, A.S. 1984. Relation Between Electrocardiographic and Scintigraphic Location of Myocardial Ischemia During Exercise in One-Vessel Coronary Artery Disease. Am. J. Cardiol., 53, 1529-1531.

Gensini, G.G., Kelly, A.E., DaCosta, B.C.B., Huntington, P.P. 1971. Quantitative Angiography: The Measurement of Coronary Vasomobility in the Intact Animal and Man. Chest, 60, 522-530.

Gerber, K.H., Norris, S.L., Slutsky, R.A., Ashburn, W.L., Higgins, C.B. 1983. Quantitative Phase Analysis of Exercise Radionuclide Left Ventriculography in Normals and Patients with Coronary Artery Disease. Computers and Biomedical Research, 16, 88-98.

Gessman, L., Reno, C., and Maranhao, V. 1984. Transcatheter Laser Dissolution of Human Atherosclerotic Plaques: A Model for Testing Catheters and Techniques. Cathet. Cardiovasc. Diagn., 10, 47-54.

Gibbons, R.J., Lee, K.L., Cobb, R.R., Coleman, R.E., Jones, R.H. 1982. Ejection Fraction Response to Exercise in Patients with Chest Pain, Coronary Artery Disease and Normal Resting Ventricular Function. Circulation, 66, 3, 643-648.

Gibson, D.G., Prewitt, T.A., and Brown, D.J. 1976. Analysis of Left Ventricular Wall Movement During Isovolumic Relaxation and its Relation to Coronary Artery Disease. Br. Heart J., 38, 1010-1019.

Glantz, S.A., and Parmley, W.W. 1978. Factors Which Affect the Diastolic Pressure-Volume Curve. Circ. Res., 42, 2, 171-180.

Golding, L.A.R., Loop, F.D., Holliman, J.L., Franco, I., Borsh, J., Stewart, R.W., Lytle, B.W. 1986. Early Results in Emergency Surgery After Coronary Angioplasty. Circulation, 74, Suppl. III, 26-29.

Gould, K.L. 1978. Pressure-Flow Characteristics of Coronary Stenoses in Unsedated Dogs at Rest and during Coronary Vasodilation. Circ. Res., 43, 2, 242-253.

Gould, K.L., Kelley, K.O., Bolson, E.L. 1982. Experimental Validation of Quantitative Coronary Arteriography for Determining Pressure-Flow Characteristics of Coronary Stenosis. Circulation, 66, 5, 930-937.

Gould, K.L., Lipscomb, K., Hamilton, G.W. 1974. Physiologic Basis for Assessing Critical Coronary Stenosis. Am. J. Cardiol., 33, 87-94.

Green, M.V., Brody, W.R., Douglas, M.A., Borer, J.S., Ostrow, H.G., Line, B.R., Bacharach, S.L., and Johnston, G.S. 1978. Ejection Fraction by Count Rate from Gates Images. J. Nucl. Med., 19, 880-883.

Green, M.V., Jones-Collins, B.A., Bacharach, S.L., Findley, S.L., Patterson, R.E., Larson, S.M. 1984. Scintigraphic Quantification of Asynchronous Myocardial Motion During the Left Ventricular Isovolumic Relaxation Period: A Study in the Dog During Acute Ischemia. J. Am. Coll. Cardiol., 4, 1, 72-79.

Green, M.V., Ostrow, H.G., Bacharach, S.L., Allen, S.I., Bonrow, R.O., and Johnston, G.S. 1981. Real-Time Scintillation Probe Measurement of Left Ventricular Function. Nucl. Med., 20, 3, 116-123.

Gregg, D.E., and Bedynek, J.L. 1984. Compensatory Changes in the Heart During Progressive Coronary Artery Stenosis. From Primary and Secondary Angina Pectoris. Editors Maseri A., Classen. G.A., and Lesch, M. Grune and Stratton Inc.

Grossman, W., and McLaurin, L.P. 1976. Diastolic Properties of the Left Ventricle. Ann. Int. Med., 84, 316-362.

Gruentzig, A.R. 1981. Percutaneous Transluminal Angioplasty in Coronary Occlusion. Hospital Practice, Nov., 129-136.

Gruentzig, A.R., and Collins, J.J. 1982. Angioplasty should be utilized in Double-Vessel and Triple-Vessel Coronary Dsease, a Proposal. Hospital Practice, Sept., 143-155.

Gruentzig, A.R., Senning, A., Siegenthaler, W.E. 1979. Nonoperative Dilation of Coronary-artery Stenosis. New Eng. J. Med., 301, 2, 61-68.

Guyton, A.C. 1980. Textbook of Medical Physiology. W.B. Saunders Company.

Hakki, A.H., DePace, N.L., Colby, J., Iskandrian, A.S. 1983. Implication of Normal Exercise Electrocardiographic Results in Patients with Angiographically Documented Coronary Artery Disease: Correlation with Left Ventricular Function and Myocardial Perfusion. Am. J. Med., 75, 439-444.

Hakki, A.H., Iskandrain, A.S., Kutalek, S., Hare, T.W., Sokoloff, N.M. 1984a. R Wave Amplitude: A New Determinant of Failure of Patients With Coronary Heart Disease to Manifest ST Segment Depression During Exercise. J. Am. Coll. Cardiol., 3, 5, 1155-1160.

Harrison, D.C. 1985. Beta Blockers and Exercise: Physiologic and Biochemical Definitions and New Concepts. Am. J. Cardiol., 55, 29-33.

Harrison, D.G., White, C.W., Hiratzka, L.F., Doty, D.B., Barnes, D.H., Eastham, C.L., and Marcus, M.L. 1984. The Value of Lesion Cross-Sectional Area Determined by Quantitative Coronary Angiography in Assessing the Physiologic Significance of Proximal Left Anterior Descending Coronary Arterial Stenoses. Circulation, 69, 6, 1111-1119.

Higginbotham, M.B., Coleman, R.E., Jones, R.H., and Cobb, F.R. 1984. Mechanism and Significance of a Decrease in Ejection Fraction During Exercise in Patients With Coronary Artery Disease and Left Ventricular Dysfunction at Rest. J. Am. Coll. Cardiol., 3, 1, 88-97.

Hirakawa, A., Saito, M., Motohara, S., Matsumura, T., Sakurai, T., Kadota, K, Yamada, N., Hara, A., Ogino, K., Kawai, C., and Kuwahara, M. 1977. Decreased Early Diastolic dV/dt in Ischemic Heart Disease Observed by ECG-gated Radiocardiography. Japanese Circulation Journal, 41, 507-514.

Holmes, D.R., Vliestra, R.E., Mock, M.B., Smith, H.C., Dorros, G., Cowley, M.J., Kent, K.M., Hammes, L.N., Janke, L., Elveback, L.R., and Vetrovec, G.W. 1983. Employment and Recreation Patterns in Patients Treated by Percutaneous Transluminal Coroanry Angioplasty: A Multicenter Study. Am. J. Cardiol., 52, 710-713.

Holmes, D.R., Vliestra, R.E., Reeder, G.S., Bresnahan, J.F., Smith, H.C., Bove, A.A., and Schaff, H.V. 1984. Angioplasty in Total Coronary Artery Occlusion. J. Am. Coll. Cardiol., 3, 3, 845-849.

Hubner, P.J.B., Walker, J.K., Cook, C., Madden, S. 1988. Results of the First 200 Percutaneous Transluminal Coronary Angioplasties in a Regional Cardiac Unit. In Press.

Hugenholtz, P.G., Ellison, R.C., Urschel, C.W., Mirskey, I., and Sonnenblick, E.H. 1970. Myocardial Force-Velocity Relationships in Clinical Heart Disease. Circulation, 41, 191-202.

Ischinger, T., Gruentzig, A.R., Hollman, J., King, S., Douglas, J., Meier, B., Bradford, J., and Tankersley, R. 1983. Should Coronary Arteries with less than 60% Diameter Stenosis be Treated by Angioplasty? Circulation, 68, 1, 148-154.

Jackson, N.C., Silverton, N.P., Nelson, G.I.C. 1985. Stenosis Recurrence Following Coronary Angioplasty: Changes in Stenosis Length. Proceedings of the Cardiac Society, 14.

Johnson, M.R., Brayden, G.P., Ericksen, E.E., Collins, S.M., Skorton, D.J., Harrison, D.G., Marcus, M.L., and White, C.W. 1986. Changes in Cross-Sectional Area of the Coronary Lumen in the Six Months after Angioplasty:

A Quantitative Analysis of the Variable Response to Percutaneous Transluminal Angioplasty. Circulation, 73, 3, 467-475.

Johnson, M.R., McPherson, D.D., Fleagle, S.R., Hunt, M.M., Hiratzka, L.F., Kerber, R.E., Marcus, M.L., Collins, S.M., and Skorton, D.J. 1988. Videodensitometric Analysis of Human Coronary Stenoses: Validation in vivo by Intraoperative High-Frequency Epicardial Echocardiography. Circulation, 77, 2, 328-336.

Kannel, W.B., Belanger, A., D'Agostino, R., Israel, I. 1986. Physical Activity And Physical Demand On The Job And Risk Of Cardiovascular Disease And Death: The Framingham Study. Am. Heart J., 112, 820-824.

Katz, R.J., Leiboff, R.H., Aaron, B.L., Mills, M., Wasserman, A.G., and Ross, A.M. 1982. Intraoperative Retrograde Balloon Angioplasty of the Left Anterior Descending Coronary Artery for Reperfusion of Jeopardized Proximal Branches. Circulation, 66, Suppl. I, 30-34.

Kay, H.R., Levin, F.H., Grotte, G.J., Rosenthal, S., Austen, G., and Buckley, M.J. 1979. Isovolumic Relaxation As A Critical Determinant of Postischemic Ventricular Function. J. Surg. Res., 26, 659-662.

Kelly, M.E., Taylor, G.J., Moses, H.W., Mikell, F.L., Dove, J.T., Batchelder, J.E., Wellons, H.A., and Schneider, J.A. 1985. Comparative Cost of Myocardial Revascularization: Percutaneous Transluminal Angioplasty and Coronary Artery Bypass Surgery. J. Am. Coll. Cardiol., 5, 16-20.

Kennedy, J.W., Baxley, W.A., Figley, M.M., Dodge, H.T., and Blackmon, J.R. 1966. The Normal Left Ventricle in Man. Circulation, 34, 272-278.

Kent, K.M., Bonow, R.O., Rosing, D.R., Ewels, C.J., Lipson, L.C., McIntosh, C.L., Bacharach, S., Green, M., and Epstein, S.E. 1982. Improved Myocardial Function During Exercise After Successful Percutaneous Transluminal Coronary Angioplasty. New Eng. J. Med., 306, 8, 441-446.

Keys, A. 1970. The Seven Countries Prospective Study. Circulation, Suppl. 1, 41, 199.

Kindt, G.W., and Youmans, J.R. 1969. The Effect of Stricture Length on Critical Arterial Stenosis. Surgery, Gynecology and Obstetrics, April, 729-734.

Klocke, F.J. et al. 1980. Special Problems in Ischemic Heart Disease caused by Coronary Atherosclerosis. Ann. Rev. Med., 31, 489-505.

Koh, D., Mitten, S., Stewart, D., Bolson, E., and Dodge, H. 1979. Comparision Between Computerized Quantitative Coronary Angiography and Clinical Interpretatation. Circulation, 59/60, Suppl. II, 160.

Kumada, T., Karliner, J.S., Pouleur, H., Gallagher, K.P., Shirato, K., and Ross, J. 1979. Effects of Coronary Occlusion on Early Ventricular Diastolic Events in Conscious Dogs. Am. J. Physiol., 237, 542-549.

Lewis, B.S., Halon, D.A., Weiss, A.T., Rosing, D.R., and Gotsman, M.S. 1983. Nonsurgical Myocardial Revascularization: Initial Experience with Percutaneous Transluminal Coronary Angioplasty. Isr. J. Med. Sci., 19, 325-331.

Lewis, J.F., Verani, M.S., Poliner, L.R., Lewis, J.M., Raizner, A.E. 1985. Effects of Transluminal Coronary Angioplasty on Left Ventricular Systolic and Diastolic Function at Rest and During Exercise. Am. Heart J., 109, 792-798.

Lichtlen, P. 1971. The Hemodynamics of Clinical Ischemic Heart Disease. Ann. Clin. Res. 3, 333.

Lipscomb, K., Hooten, S. 1978. Effect of Stenotic Dimensions and Blood Flow on the Hemodynamic Significance of Model Coronary Arterial Stenoses. Am. J. Cardiol., 42, 781-792.

Ludbrook, P.A., Byrne, J.D., Tiefenbrunn, A.J. 1981. Association of Asynchronous Protodiastolic Segmental Wall Motion with Impaired Left Ventricular Relaxation. Circulation, 64, 6, 1201-1211.

MacAlpin, R.N., Abbasi, A.S., Grollman, J.H., and Eber, L. 1973. Human Coronary Artery Size During Life. Radiology, 108, 567-576.

Marquis, J.F., Schwartz, L., Alderidge, H., Majid, P., Henderson, M., Matushinsky, E. 1984. Acute Coronary Artery Occlusion During Percutaneous Transluminal Coronary Angioplasty Treated by Redilation of the Occluded Segment. J. Am. Coll. Cardiol., 4, 6, 1268-1271.

Marshall, R.C., Berger, H.J., Costin, J.C., Freedman, G.S., Wolberg, J., Cohen, L.S., Gottschalk, A., and Zaret, B.L. 1977. Assessment of Cardiac Performance with Quantitative Radionuclide Angiocardiography. Circulation, 56, 5, 820-829.

Marzullo, P., Parodi, O., Schelbert, H.R., L'Abbate, A. 1984. Regional Myocardial Dysfunction in Patients with Angina at Rest and Response to Isosorbide Dinitrate Assessed by Phase Analysis of Radionuclide Ventriculograms. J. Am. Coll. Cardiol., 36, 1357-1366.

Mason, D.T. 1969. Usefulness and Limitations of the Rate of Rise of Intraventricular Pressure (dp/dt) in the Evaluation of Myocardial Contractility in Man. Am. J. Cardiol., 23, 516-527.

May, A.G., DeWeese, J.A., Rob, C.G. 1963. Hemodynamic effects of arterial stenosis. Surgery, April, 513-524.

McMahon, M.M., Brown, B.G., Cukingnan, R., Rolett, E.L., Bolson, E., Frimer, M., and Dodge, H.T. 1979. Quantitative Coronary Angiography: measurement of the "Critical" Stenosis in Patients with Unstable Angina and Single-Vessel Disease without Collaterals. Circulation, 60, 1, 106-113.

Meier, B., Gruentzig, A.R., Goebel, N., Pyle, R., Gosslar, W., and Schlumpf, M. 1983a. Assessment of Stenoses in Coronary Angioplasty. Inter - and intraobserver variability. International Journal of Cardiology, 3, 159-169.

Meier, B., Gruentzig, A.R., Hollman, J., Ischinger, T., and Bradford, J.M. 1983b. Does Length or Eccentricity of Coronary Stenoses Influence the Outcome of Transluminal Dilation? Circulation, 67, 3, 497-499.

Meier, B., Gruentzig, A.R., King, S.B., Douglas, J.S., Hollman, J., Ischinger, T., and Galan, K. 1984. Higher Balloon Dilation Pressure in Coronary Angioplasty. Am. Heart J., 107, 4, 619-622.

Meyer, J., Schmitz, H., Erbel, R., Kiesslich, T., Bocker-Josephs, B., Kerbs, W., Braun, P.C., Bardos, P., Minale, C., Messmer, B.J., and Effert, S. 1981. Treatment of Unstable Angina Pectoris with Percutaneous Transluminal Coronary Angioplasty (PTCA). Cathet. Cardiovasc. Diagn., 7, 361-371.

Nagle, F., Balke, B., Baptista, G., Alleyia, J., and Howley, E. 1971. Compatibility of Progressive Treadmill, Bicycle and Step Tests Based on Oxygen Uptake Reponses. Medicine and Science in Sports, 3, 4, 149-154.

Naughton, J., Balke, B., and Nagle, F. !964. Refinements in Method of Evaluation and Physical Conditioning Before and After Myocardial Infarcation. Am. J. Cardiol., 14, 837-843.

Nayler, W.G., and Williams, A. 1978. Relaxation in Heart Muscle: Some Morphological and Biochemical Considerations. European Journal of Cardiology, 7, 35-50.

Nichols, A.B., Gabrieli, C.F.O., Fenoglio, J.J., and Esser, P.D. 1984. Quantification of Relative Coronary Arterial Stenosis by Cinevideodensitometric Analysis of Coronary Arteriograms. Circulation, 69, 3, 512-522.

Norris, S.L., Slutsky, R.A., Gerber, K.H., Geiss, K.R., Ashburn, W.L., and Higgins, C.B. 1984. Sensitivity and Specificity of Nuclear Phase Analysis Versus Ejection Fraction in Coronary Artery Disease. Am. J. Cardiol., 53, 1547-1552.

O'Hara, M.J., Subramanian, V.B., Davies, A.B., and Raftery, E.B. 1984. Changes of Q Wave Amplitude During Exercise for the Prediction of Coronary Artery Disease. International Journal of Cardiology, 6, 35-45.

O'Neill, W.W., Wlaton, J.A., Bates, E.R., Colfer, H.T., Aueron, F.M., DeFree, M.T., Pitt, B., Vogel, R.A. 1984. Criteria for Successful Coronary Angioplasty as Assessed by Alterations in Coronary Vasodilatory Reserve. J. Am. Coll. Cardiol., 3, 6, 1382-1390.

Owen, R.M., Dewey, J.D., Bove, A.A. 1983. Evaluation of Dimensions and Steady-state Hydraulic Properties of Coronary Arteries. ISA, 43-46.

Paffenberger, R.S., Hyde, R.T., Hsieh, C.C., Wing, A.L. 1986. Physical Activity, Other Lifestyle Patterns, Cardiovascular Disease And Longevity. Acta. Med. Scand., 711, 85-91.

Parisi, A.F., Moynihan, P.F., Folland, E.D., Strauss, W.E., Sharma, G.V.R.K., Sasahara, A.A. 1980. Echocardiography in Actue and Remote Myocardial Infarcation. Am. J. Cardiol., 46, 1205-1214.

Pavel, D.G., Zimmer, A.M., Patterson, V.N. 1977. In Vivo Labeling of Red Blood Cells with ^{99m}Tc: A New Approach to Blood Pool Visualization. J. Nucl. Med., 18, 305-308.

Poliner, L.R., Farber, S.H., Glaeser, D.H., Nylann, L., Verani, M.S., and Roberts, R. 1984. Alteration of Diastolic Filling Rate During Exercise Radionuclide Angiography: A Highly Sensitive Technique for Detection of Coronary Artery Disease. Circulation, 70, 6, 942-950.

Przybojewski, J.Z., Weich, H.F.H. 1984. Percutaneous Transluminal Coronary Angioplasty. A Review of the Literature. South African Medical Journal, January, 1-22.

Quyyumi, A.A., Raphael, M.J., Wright, C., Bealing, L., Fox, K.M. 1984. Inability of the ST Segment/Heart Rate Slope to Predict Accurately the Severity of Coronary Artery Disease. Br. Heart J., 51, 395-398.

Raess, D.H., Mahomed, Y., Brown, J.W., and King, R.D. 1986. Lesser Saphenous Vein as an Alterative Conduit of Choice in Coronary Bypass Operations. Ann. Thorac. Surg., 41, 334-336.

Ratib, O., Henze, E., Schon, H., and Schelber, H.R. 1982. Phase Analysis of Radiouclide Ventriculograms For the Detection of Coronary Artery Disease. Am. Heart J., 104, 1, 1-12.

Reduto, L.A., Wickemeyer, W.J., Young, J.B., Del Ventura, L.A., Reid, J.W., Glaeser, D.H., Quinones, M.A., and Miller, R.R. 1981. Left Ventricular Diastolic Performance At Rest and During Exercise in Patients With Coronary Artery Disease. Circulation, 63, 6, 1228-1237.

Redwood, D.R., and Epstein, S.E. 1972. Uses and Limitations of Stress Testing in the Evaluation of Ischemic Heart Disease. Circulation, 46, 1115-1131.

Reiber, J.H.C., Booman, F., Tan, H.S., Gerbrands, J.J., Slager, C.J., Schuurbiers, J.C.H., and Meester, G.T. 1979. Computer Processing of Coronary Occlusions from X-Ray Arteriograms. Inserm, 88, 79-92.

Reiber, J.H.C., Booman, F., Tan, H.S., Slager, C.J., Schuurbiers, J.C.H., Gerbrands, J.J. 1978. A Cardiac Image Analysis System: Objective Processing of Angiocardiograms. Computers in Cardiology, 239-242.

Reul, H. 1983. Influence of the Degree of Stenoses on Pressure-Loss Energy-Dissipation and Flow in Coronary Arteries. Adv. Cardiovasc. Phys., 5, 1, 185-194.

Rosenman, R.H., Brand, R.J., Jenkins, C.D., Friedman, M., Straus, R., Wurm, M. 1975. Coronary Heart Disease in the Western Collaborative Group Study. JAMA, 233, 8, 872-877.

Ross, J. 1969. The Assessment of Myocardial Performance in Man by Hemodynamic and Cineangiographic Technics. Am. J. Cardiol., 23, 511-515.

Ross, J. 1976. Afterload Mismatch and Preload Reserve: A Conceptual Framework for the Analysis of Ventricular Function. Prog. Cardiovasc. Dis., 18, 4, 255-264.

Sanborn, T.A., Faxon, D.P., Waugh, D., Small, D.M., Haudenschild, C., Gottsman, S.B., and Ryan, T.J. 1982. Transluminal Angioplasty in Experimental Atherosclerosis: Analysis for Embolization Using an In Vivo Perfusion System. Circulation, 66, 5, 917-922.

Sandor, T., Als, A.V., Paulin, S. 1979. Cini-Densitometric Measurement of Coronary Arterial Stenoses. Cathet Cardiovasc Diagn, 5, 229-245.

Santamore, W.P. 1985. Haemodynamics of Coronary Arterial Stenosis. European Journal of Cardiology, 178-192.

Sasayama, S., Nonogi, H., Fujita, M., Sakurai, T., Wakabayashi, A., Kawai, C., Eiho, S., Kuwahara, M. 1984. Analysis of Asynchronous Wall Motion by Regional Pressure-Length Loops in Patients With Coronary Artery Disease. J. Am. Coll. Cardiol., 4, 2, 259-267.

Scholl, J.M., Chaitman, B.R., David, P.R., Dupras, G., Brevers, G., Val, P.G., Crepeau, J., Lesperance, J., and Bourassa., M.G. 1982. Exercise Electrocardiography and Myocardial Scinitigraphy in the Serial Evaluation of the Results of Percutaneous Transluminal Coronary Angioplasty. Circulation, 66, 2, 380-390.

Sendoe, E., and Sigurd, B. 1984. Arrhythimia - Diagnosis and Management.

Serruys, P.W. 1980. Can Unstable Angina Perctoris be Due to Increased Coronary Vasomotor tone? European Heart Journal, Suppl B, 71-85.

Serruys, P.W., Luijten, H.E., Beatt, K.J., Geuskens, R., De Feyter, P.J., Van Den Brand, M., Reiber, J.H.C., Katen, H.J., and Hugenholtz, P.G. 1988. Incidence of Restenosis after Successful Coronary Angioplasty: A Time-Related Phenomenon. Circulation, 77, 2, 361-371.

Serruys, P.W., Reiber, J.H.C., Wijns, W., Van Den Brand, M., Kooijman, C.J., Katen, H.J., and Hugenholtz, P.G. 1984. Assessment of Percutaneous Transluminal Coronary Angioplasty by Quantitative Coronary Angiography: Diameter Versus Densitometric Area Measurements. Am. J. Cardiol., 54, 482-488.

Shaper, A.G. 1987. Epidemiology and Prevention of Ischaemic Heart Disease. Current Opinion in Cardiology, 2, 571-585.

Sharma, B., Goodwin, J.F., Raphael, M.J., Steiner, R.E., Rainbow, R.G., and Taylor, S.H. 1976. Left Ventricular Angiography on Exercise. A New Method of Assessing Left Ventricular Function in Ischaemic Heart Disease. Br. Heart J., 38, 59-70.

Shearn, D.L., Brent, B.N. 1986. Coronary Artery Bypass Surgery in Patients with Left Ventricular Dysfunction. Am. J. Med., 80, 405-411.

Sheffield, L.T., and Roitman, D. 1976. Stress Testing Methodology. Prog. Cardiovasc. Dis., 19, 1, 33-49.

Shelton, M.E., Hoxworth, B., Shelton, J.A., Virmani, R., Fresinger, G.C. 1986. A New Model to Study Quantitative Effects of Laser Angioplasty on Human Atherosclerotic Plaque. J. Am. Coll. Cardiol., 7, 4, 909-915.

Sheffield, L.T., 1980. Exercise stress testing. In Textbook of Cardiovascular Medicine. Editor Braunwald E. W.B. Saunders and Company.

Shepertycki, T.H., and Morton, B.C. 1983. A Computer Graphic-Based Angiographic Model for Normal Left Ventricular Contraction in Man and its Application to the Detection of Abnormalities in Regional Wall Motion. Circulation, 68, 6, 1222-1230.

Shub, C., Vlietstra, R.E., Smith, H.C., Fulton, R.E., Eleveback, L.R. 1981. The Unpredictable Progression of Symptomatic Coronary Artery Disease. Mayo Clin. Proc., 56, 155-160.

Sigwart, U., Grbic, M., Essinger, A., Bischof-Delaloye, A., Sadeghi, H., Rivier, J.L. 1982. Improvement of Left Ventricular Function After Percutaneous Transluminal Coronary Angioplasty. Am. J. Cardiol., 49, 651-657.

Silverton, N.P., Elamin, M.S., Smith, D.R., Ionesuc, M.I., Kardash, M., Whitaker, W., Mary, D.A.S.G., Linden, R.J. 1984. Use of the Exercise Maximal ST Segment/Heart Rate Slope in Assessing the Results of Coronary Angioplasty. Br. Heart J., 51, 379-385.

Slutsky, R.A., Mancini, G.B.J., Gerber, K.H., Carey, P.H., Ashburn, W.L., Higgins, C.B. 1983. Radionuclide Analysis of Ejection Time, Peak Ejection Rate, and Time to Peak Ejection Rate: Response to Supine Bicycle Exercise in Normal Subjects and In Patients with Coronary Heart Disease. Am. Heart J., 105, 802-810.

Slutsky, R., Pfisterer, M., Verba, J., Battler, A., Ashburn, W. 1980. Influence of Different Background and Left-Ventricular Assignments on the Ejection Fraction in Equilibrium Radionuclide Angiography. Radiology, 135, 725-730.

Sorensen, S.G., Caldwell, J., Ritchie, J., and Hamilton, G. 1981. "Abnormal" Responses of Ejection Fraction to Exercise, in Healthy Subjects, Caused by Region-of-Interest Selection. J. Nucl. Med., 22, 1-7.

Steingart, R.M., Wexler, J., Slagle, S., and Scheuer, J. 1984. Radionuclide Ventriculographic Respones to Graded Supine and Upright Exercise: Critical Role of the Frank-Starling Mechanism at Submaximal Exercise. Am. J. Cardiol., 53, 1671-1677.

Stertzer, S.H., Myler, R.K., Insel, H., Wallsh, E., and Rossi, P. 1985. Percutaneous Transluminal Coronary Angioplasty in Left Main Stem Coronary Stenosis: a Five-Year Appraisal. International Journal of Cardiology, 9, 149-159.

Strauss, H.W., McKusick, K.A., Bingham, J.B., 1980. Cardiac Nuclear Imaging: Principles, Instrumentation and Pitfalls. Am. J. Cardiol., 46, 1109-1116.

Strauss, H.W., Zaret, B.L., Hurley, P.J., Natarajan, T.K., Pitt, B. 1971. A Scintiphotographic Method for Measuring Left Ventricular Ejection Fraction in Man without Cardiac Catheterization. Am. J. Cardiol., 28, 575-580.

Sutton, R., Hood, W.P., Koch, G.G. 1977. Noninvasive Assessment of Left Ventricular Function in Chronic Heart Disease. Am. Heart J., 93, 3, 289-297.

Tebbe, U., Hoffmeister, N., Sauer, G., Neuhaus, K.L., Kreuzer, H. 1980. Changes in Left Ventricular Diastolic Function in Coronary Artery Disease With and Without Angina Pectoris Assessed from Exercise Ventriculography. Clin. Cardiol., 3, 19-25.

Tobis, J.M., Nalcioglu, O., and Henry, W.L. 1983. Digital Subraction Angiography. Chest, 84, 1, 69-75.

Tobis, J.M., Nalcioglu, O., Iseri, L., Johnston, W.D., Roeck, W., Castleman, E., Bauer, B., Montelli, S., and Henry, W.L 1984. Detection and Quantitation of Coronary Artery Stenoses from Digital Subtraction Angiograms Compared with 35-Millimeter Film Cineangiograms. Am. J. Cardiol., 54, 489-496.

Tomoike, H., Franklin, D., McKown, D., Kemper, W.S., Guberek, M., and Ross, J. 1978. Regional Myocardial Dysfunction and Hemodynamic Abnormalities During Strenuous Exercise in Dogs with Limited Coronary Flow. Circ. Res., 42, 4, 487-496.

Tomoike, H., Inou, T., Watanabe, K., Mizukami, M., Kikuchi, Y., and Nakamura, M. 1983. Functional Significance of Collaterals During Ameroid-Induced Coronary Stenosis in Conscious Dogs. Circulation, 67, 5, 1001-1008.

Trask, N., Califf, R.M., Conley, M.J., Kong, Y., Peter, R., Lee, L.L., Hackel, D.B., and Wagner, G.S. 1984. Accuracy and Interobserver Variability of Coronary Cineangiography: A Comparison with Postmortem Evaluation. J. Am. Coll. Cardiol., 3, 5, 1145-1154.

Upton, M.T., Rerych, S.K., Newman, G.E., Port, S., Cobb, F.R. and Jones, R.H. 1980. Detecting Abnormalities in Left Ventricular Function During Exercise Before Angina and ST-segment Depression. Circulation, 62, 2, 341-349.

Van Der Hoeven, G.M.A., Clerens, P.J.A., Donders, J.J.H., Beneken, J.E.W., and Vonk, J.T.C. 1977. A Study of Systolic Time Intervals During Uninterrupted Exercise. Br. Heart J., 39, 242-254.

Visner, M.S., Arentzen, C.E., Parrish, D.G., Larson, E.V., O'Connor, M.J., Crumbley, A.J., Bache, R.J., and Anderson, R.W. 1985. Effects of Global Ischemia on

the Diastolic Properties of the Left Ventricle in the Conscious Dog. Circulation, 71, 3, 610-619.

Vogel, J.H.K., Cornish, D., and McFadden, R.B. 1973. Underestimation of Ejection Fraction with Singleplane Angiography in Coronary Artery Disease: Role of Biplane Angiography. Chest, 64, 2, 217-221.

Vos, P.H., Vossepoel, A.M., and Pauwels, E.K.J. 1983. Quantitative Assessment of Wall Motion in Multiple-Gated Studies Using Temporal Fourier Analysis. J. Nucl. Med., 24, 388-396.

Walton, S., Yiannikas, J., Jarrit, P.H., Brown, N.J.G., Swanton, R.H., Ell, P.J. 1981. Phasic Abnormalities of Left Ventricular Emptying in Coronary Artery Disease. Br. Heart J., 46, 245-253.

Wasserman, A.G., Johnson, R.A., Katz, R.J., Leiboff, R.H., Bren, G.B., Varghese, P.J., and Ross, A.M. 1984. Detection of Left Ventricular Wall Motion Abnormalities for the Diagnosis of Coronary Artery Disease: A Comparision of Exercise Radionuclide and Pacing Intravenous Digital Ventriculography. Am. J. Cardiol., 54, 497-501.

Weber, K.T., and Janicki, J.S. 1986. Exercise Testing: Physiologic Principles and Clinical Applications. W.B. Saunders Company.

Weiner, D.A., Ryan, T.J., McCabe, C.H., Chaitman, B.R., Sheffield, T., Ferguson, J.C., Fisher, L.D., Tristain, F. 1984. Prognostic Importance of a Clinical Profile and Exercise Test in Medically Treated Patients With Coronary Artery Disease. J. Am. Coll. Cardiol., 3, 3, 772-779.

Weisfeldt, M.L., Frederiksen, J.W., Yin, F.C.P. and Weiss, J.L. 1978. Evidence of Incomplete Left Ventricular Relaxation in the Dog. J. Clin. Invest., 62, 1296-1302.

Weiss, A.T., Gotsman, M.S., Shefer, A., Halon, D.A., and Lewis, B.S. 1984. Improvement in Regional Ventricular Function After Percutaneous Transluminal Coronary Angioplasty. International Journal of Cardiology, 5, 299-311.

Wharton, C.F.P., and Archer, A.R. 1986. Cardiology. MTP Press Limited.

White, C.W., Wright, C.B., Doty, D.B., Hiratza, L.F., Eastham, C.L., Harrison, D.G., and Marcus, M.L. 1984. Does Visual Interpretation of the Coronary Arteriogram Predict the Physiologic Importance of a Coronary Stenosis? New Eng. J. Med., 310, 13, 819-823.

Wiens, R.D., Lafia, P., Marder, C.M., Evans, R.G., and Kennedy,. H.L. 1984. Chronotropic Incompetence in Clinical Exercise Testing. Am. J. Cardiol., 54, 74-78.

Wijns, W., Serruys, P.W., Reiber, J.H.C., Van Den Brand, M., Simoons, M.L., Kooijman, C.J., Balakumaran, K., and Hugenholtz, P.G. 1985a. Quantitative Angiography of the Left Anterior Descending Coronary Aıtery: Correlations With Pressure Gradient and Results of Exercise Thallium Scintigraphy. Circulation, 71, 2, 273-279.

Wijns, W., Serruys, P.W., Simoons, M.L., Van Den Brand, M., De Feijter, P., Reiber, J.H.C., Hugenholtz, P.G. 1985b. Predictive Value of Early Maximal Exercise Test and Thallium Scintigraphy After Successful Percutaneous Transluminal Coronary Angioplasty. Br. Heart J., 53, 194-200.

Willis-Hurst, J. 1974. The Heart, Arteries and Veins. McGraw-Hill Kogakusha, Ltd.

Willman, V.L. 1985. Percutaneous Transluminal Coronary Angioplasty, A 1985 Perspective. Circulation, 71, 2, 189-192.

Wilson, R.F., Holida, M.D., White, C.W. 1986. Quantitative Angiographic Morphology of Coronary Stenoses Leading to Myocardial Infarction or Unstable Angina. Circulation, 73, 2, 286-293.

Yin, F.C.P. 1981. Ventricular Wall Stess. Circ. Res., 49, 4, 829-842.

Young, D.F., Cholvin, N.R., Kirkeeide, R.L., and Roth, A.C. 1977. Hemodynamics of Arterial Stenoses at Elevated Flow Rates. Circ. Res., 41, 1, 99-107.